Caractérisation des anticorps anti-CASPR2 de patients atteints d'encéphalite limbique auto-immune et impact sur le complexe CASPR2/TAG-1/Kv1.2

Margaux Saint-Martin

N°d'ordre NNT :

THESE de **DOCTORAT DE**

L'UNIVERSITE DE LYON

opérée au sein de

l'Université Claude Bernard Lyon 1

Ecole Doctorale N° 476

(Neurosciences et cognition)

Spécialité de doctorat : Neurosciences

Discipline : Neuroimmunologie

Soutenue publiquement le 11/12/2018, par :

Margaux SAINT-MARTIN

Caractérisation des anticorps anti-CASPR2 de patients atteints d'encéphalite limbique auto-immune et impact sur le complexe CASPR2/TAG-1/Kv1.2

Devant le jury composé de :

	Etablissement/entreprise	
		Président **: M. HONNORAT Jérôme**
M. BAGNARD, Dominique	MC, Inserm Strasbourg	Rapporteur
M. NAVARRO, Vincent	PU-PH, Sorbonne Université (Paris VI)	Rapporteur
Mme. FAIVRE-SARRAILH, Catherine	Professeur, Université Aix Marseille	Examinatrice
M. HONNORAT, Jérôme	PU-PH, Université Lyon 1	Examinateur
Mme. NORAZ, Nelly	Chargé de recherche, INSERM Lyon	Directrice de thèse
Mme. PELLIER-MONNIN, Véronique	MC, Université de Lyon 1	Co-directrice

Résumé

Les encéphalites limbiques à auto-anticorps anti-CASPR2 sont des atteintes du système nerveux central caractérisées par des troubles de la mémoire et des crises d'épilepsie. La protéine CASPR2 (Contactin-associated protein-like 2), avec son partenaire TAG-1 (Transient axonal glycoprotein 1), est connue pour son rôle dans le rassemblement des canaux potassiques voltage-dépendants (Kv1.1 et Kv1.2) dans la région juxtaparanodale des nœuds de Ranvier ; une organisation essentielle pour la conduction rapide de l'influx nerveux. Par ailleurs, un nombre croissant d'études suggère un rôle de CASPR2 dans la plasticité synaptique et l'excitabilité neuronale. La perturbation de ces fonctions pourrait expliquer les symptômes observés chez les patients présentant des anticorps anti-CASPR2. Cependant, la question du rôle pathogénique des anticorps anti-CASPR2 dans les encéphalites limbiques demeure entière. Les travaux de ma thèse ont porté sur la compréhension des mécanismes pathologiques des anticorps anti-CASPR2 de patient dans l'encéphalite limbique auto-immune. Pour ce faire, j'ai déterminé initialement les caractéristiques biologiques des anticorps anti-CASPR2. Ces derniers sont majoritairement de la sous-classe IgG4 et ciblent les domaines N-terminaux discoidine et laminine G1 de la protéine. Puis, j'ai identifié deux mécanismes d'action potentiels des anticorps anti-CASPR2 : (1) la perturbation de l'interaction entre CASPR2 et TAG-1 et (2) l'augmentation de l'expression des canaux Kv1.2 à la membrane. L'ensemble de ces travaux met en avant la pathogénicité des anticorps anti-CASPR2 dans les encéphalites limbiques auto-immunes.

Mots clés : CASPR2, encéphalites limbiques auto-immunes, Kv1, TAG-1, interactions

Institut NeuroMyoGene, U1217, UMR3510, Equipe Synapthopathies et Autoanticorps
Faculté de médecine, 8 Avenue Rockefeller, 69008 Lyon.

Characterization of anti-CASPR2 antibodies in patients presenting with auto-immune limbic encephalitis and impact on the CASPR2/TAG-1/Kv1.2 complex

Abstract

Anti-CASPR2 autoimmune limbic encephalitis is a central nervous system disorder characterized by memory disorders and epilepsy. CASPR2 (Contactin-associated protein-like 2) with its partner TAG-1 (Transient axonal glycoprotein 1), is known for its role in the clustering of voltage-dependent potassium channels (Kv1.1 and Kv1.2) in the juxtaparanodal region of node of Ranvier; an organization essential for the rapid conduction of nerve influx. In addition, an increasing number of studies suggest a role of CASPR2 in synaptic plasticity and neuronal excitability. The perturbation of these functions could explain the symptoms observed in patients with anti-CASPR2 antibodies. However, the pathogenic role of anti-CASPR2 antibodies in limbic encephalitis remains open. During my thesis, I wished to understand the pathogenic mechanisms of anti-CASPR2 antibodies in limbic encephalitis. To this end, I determined the biological characteristics of anti-CASPR2 antibodies. These antibodies are mainly of the IgG4 subclass and directed against the N-terminal discoidin and laminin G1 domains of CASPR2. Furthermore, I identified two potential mechanisms of anti-CASPR2 antibodies: (1) the perturbation of CASPR2/TAG-1 interactions and (2) the increase of Kv1.2 membrane expression. Together, these data bring into evidence a pathogenic role of anti-CASPR2 antibodies in autoimmune limbic encephalitis.

Key word : CASPR2, autoimmune limbic encephalitis, Kv1, TAG-1, interactions

Remerciements

Je remercie tout d'abord les membres de mon jury, les professeurs Dominique BAGNARD, Vincent NAVARRO et Catherine FAIVRE-SARRAILH qui ont accepté de lire et d'évaluer ce travail de thèse et qui m'honorent de leur présence.

Merci au Pr. HONNORAT de m'avoir permis de travailler au sein de son équipe et pour ses nombreux conseils tout au long du projet. J'espère avoir été à la hauteur de vos attentes.

Je remercie également ma directrice de thèse, Nelly, pour tout ce qu'elle m'a appris. Le projet n'a pas toujours été facile mais j'ai été très heureuse de travailler à tes côtés tout au long de ces quatre années. Je remercie ma co-directrice de thèse, Véro, toujours de très bon conseil et très attentive aux personnes qui l'entourent.

Merci aux collègues de Neuro avec lesquels toute cette histoire a commencé et plus particulièrement Véronique R qui m'a beaucoup appris dans mes débuts.

Je tiens également à remercier tous les membres de l'équipe pour leurs conseils, leur bonne humeur et leur soutien au quotidien. Parce qu'avoir un bon projet de thèse c'est bien, mais avec une super équipe, c'est mieux ! Merci Olivier pour tes lumières en électrophy ; Claire pour toutes tes questions ; Virginie, pour toutes tes suggestions et Roger pour ta passion de l'enseignement. Merci Céline et Marie-Eve, piliers de l'équipe, pour votre bonne humeur et tout l'investissement que vous donnez. Merci Fabrice et Do pour vos conseils et votre humour. Merci Chantal et Naura, toujours à la rescousse, pour votre gentillesse. Merci Delphine, pour toutes les discussions constructives sur CASPR2. Merci à Benoît, avec qui ça a été un plaisir de travailler durant cette dernière année ! Je souhaite également plein de super résultats à Kassandre et Pauline qui commencent tout juste leur thèse dans l'équipe !

Merci à tous les co-thésards pour le soutien, les rires partagés, la bonne compagnie et tous vos conseils. Chloé R, avec qui l'entente est tout de suite passée ; Laurent, pour tous ces moments partagés à la paillasse ; Bastien, pour toutes les bières studieuses et moins studieuses ; Elodie S, pour ton humour ; Aude, pour ton soutien ; Chloé B, pour ta bonne humeur contagieuse ; Ines, pour son énergie pétillante ; Alanah, pour la relève du flambeau et à Elodie F, ma complice pour délit de sociabilité ^^.

Je remercie mes amis qui ont été avec moi du début à la fin et qui je sais seront là pour la suite. Merci pour les voyages, les soirées, les rires, les repas, votre folie et votre soutien dans les moments difficiles, chacun a votre façon. Surtout, merci Mathieu pour ta patience et ton soutien indéfectible ces trois dernières années. Ce sont trois années de bons souvenirs et je sens que la suite ne nous décevra pas non plus !

Enfin, merci à ma famille pour sa confiance et sa présence durant toutes ces années. Merci à ma super maman pharmacienne pour tous les colis remplis de médicaments, vitamines et gâteaux qui m'ont aidé à faire face aux petits coups de mou durant ces trois années.

« Je ne crois pas qu'il y ait de bonnes ou de mauvaises situations.
Moi, si je devais résumer ma vie, aujourd'hui avec vous, je dirais que c'est d´abord des rencontres, des gens qui m'ont tendu la main peut-être à un moment où je ne pouvais pas, où j'étais seul chez moi.
Et c'est assez curieux de se dire que les hasards, les rencontres forgent une destinée. Parce que quand on a le goût de la chose, quand on a le goût de la chose bien faite, le beau geste, parfois on ne trouve pas l'interlocuteur en face, je dirais le miroir qui vous aide à avancer.
Alors ce n'est pas mon cas, comme je disais là, puisque moi au contraire j'ai pu, et je dis merci à la vie, je lui dis merci, je chante la vie, je danse la vie, je ne suis qu'amour.
Et finalement quand beaucoup de gens aujourd'hui me disent : "Mais comment fais-tu pour avoir cette humanité ?" eh bien je leur réponds très simplement, je leur dis : "C'est ce goût de l´amour", ce goût donc, qui m'a poussé aujourd'hui à entreprendre une construction mécanique, mais demain qui sait ? Peut-être simplement à me mettre au service de la communauté, à faire le don, le don de soi. »

Otis

Préface

Les encéphalites limbiques sont des atteintes du système nerveux central caractérisées par des troubles de la mémoire, des crises d'épilepsie et des troubles du comportement (Tüzün & Dalmau 2007). Il y a plusieurs années, un groupe d'encéphalites limbiques auto-immunes avec des anticorps dirigés contre des protéines ou des récepteurs synaptiques a été découvert (Tüzün & Dalmau 2007). Ces protéines jouent un rôle dans l'excitabilité neuronale ainsi que dans la formation et la maturation des synapses, essentielles aux processus de mémorisation. Depuis leur découverte, un nombre croissant d'études *in vitro* et *in vivo* suggèrent un rôle pathologique de ces anticorps dans la maladie (revue, Dalmau et al., 2017). En fonction des caractéristiques de ces anticorps, plusieurs modes d'actions sont possibles, rendant l'étude de ces derniers essentielle à la compréhension de la pathologie.

Les anticorps anti-CASPR2, ont été découverts il y a moins de dix ans chez des patients présentant des troubles du système nerveux central (encéphalite limbique) et des troubles du système nerveux périphérique (neuromyotonie et syndrome de Morvan) (Irani et al., 2010 ; Lai et al., 2010). Sur le plan clinique, le faible nombre de patients rapportés rend la caractérisation de la pathologie difficile. De plus, les raisons pour lesquelles les anticorps dirigés contre une même cible antigénique sont associés à un tel éventail clinique restent à clarifier. Enfin, sur le plan mécanistique, le rôle pathologique des anticorps anti-CASPR2 est encore loin d'être compris.

Mon travail de thèse a eu pour but **la caractérisation des anticorps anti-CASPR2 et l'étude de leur rôle pathologique dans l'encéphalite limbique**. La compréhension des mécanismes pathologiques associés aux anticorps anti-CASPR2 devrait permettre de mieux comprendre le rôle physiologique de CASPR2 dans le système nerveux mature et son implication dans de nombreuses autres pathologies.

Table des matières

Abbréviations

ADAM-22 : Disintegrin and metalloproteinase domain-containing protein 22
ADAM-23 : Disintegrin and metalloproteinase domain-containing protein 23
AIS : Segment initial
AMPA : acide α-amino-3-hydroxy-5-methyl-4-isoxazolepropionic
CA1 : Cornu Ammonis 1
CA3 : Cornu Ammonis 3
CASK : Calcium/calmodulin dependant serine protein kinase 3
CASPR2 : Contactin associated protein-like 2
DIV : Jours in vitro
DNER : delta/notch-like epidermal growth factor-related receptor
DPPX : dipeptidyl-peptidase-like protein-6
GABA : acide γ-aminobutyric
GAD-65 : Glutamic acid decarboxylase 65
GluA1 : Glutamate receptor subunit A1
GPI : Glycosylphosphatidylinositol
HEK : Human embryonic kidney
JXP : Juxtaparanode
KO : Knockout
LCR : liquide céphalorachidien
LE : Encéphalite limbique
LGI1 : Leucine-rich glioma inactivated 1
mGluR : metabotropic glutamate receptor
MoS : Syndrome de Morvan
MPP : Membrane palmitoylated protein
NMDA : *N*-methyl-D-aspartate
NMT : Neuromyotonie
PA : Potentiel d'action
PSD-93: Post-synaptic density-93
PSD-95: Post-synaptic density-95
TAG-1 : Transient axonal glycoprotein-1
VGAT : Vesicular GABA transporter
VGCC : voltage-gated calcium channel
VGKC : Voltage gated potassium channel
VLGUT : Vesicular glutamate transporter

INTRODUCTION

I. Les encéphalites limbiques auto-immunes

A. L'encéphalite limbique, tableau clinique

L'encéphalite est une inflammation de l'encéphale associée à des troubles neurologiques (Venkatesan et al., 2013). Elle peut être d'origine infectieuse comme l'encéphalite herpétique (Whitley et al., 1982) ou encore auto-immune comme l'encéphalite à autoanticorps anti-récepteur N-méthyl-D-aspartate (NMDAr) (Dalmau et al., 2007). Les encéphalites sont à différencier des encéphalopathies qui ne sont pas nécessairement associées à une inflammation. Ces dernières peuvent être d'origine métabolique, toxique ou encore associées à certains agents infectieux comme le virus de la grippe (Venkatesan et al., 2013).

Les encéphalites limbiques (EL) se caractérisent par l'apparition aigüe ou subaigüe de troubles de la mémoire antérograde (le patient n'est plus capable de mémoriser de nouvelles informations), de troubles du comportement et/ou de l'humeur (syndrome dépressif, irritabilité) ainsi que de crises d'épilepsie temporale (impliquant notamment l'hippocampe) ou généralisées (Tüzün & Dalmau 2007; Didelot et Honnorat 2009). Elles ont été nommées ainsi car les symptômes suggèrent une atteinte du système limbique, composé entre autres de l'hippocampe, impliqué dans les processus de mémorisation et de l'amygdale, impliquée dans les émotions (Figure 1).

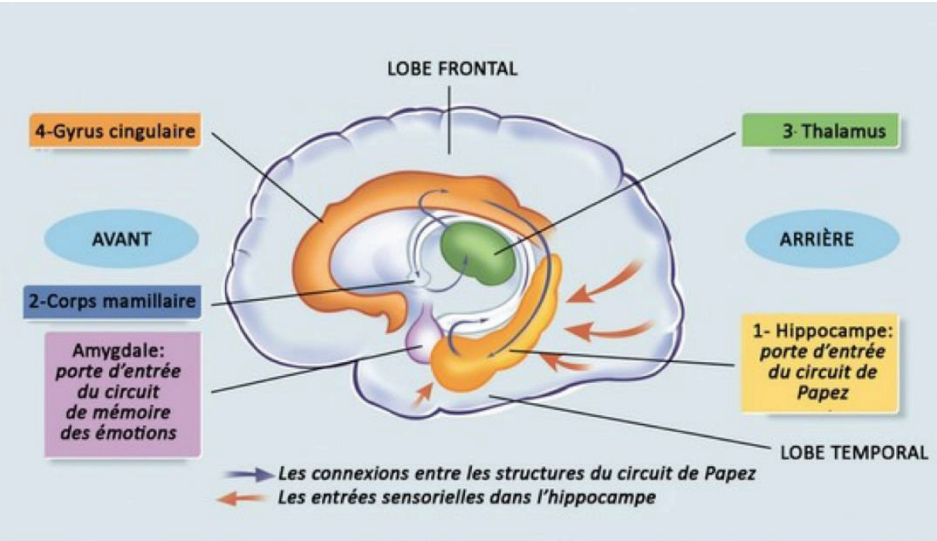

Figure 1 : Schéma du système limbique au sein du cerveau. Le système limbique joue un rôle important dans le comportement et en particulier les émotions et la mémoire. Celui-ci est composé entre autres de l'hippocampe, impliqué dans les processus de mémorisation et de l'amygdale, impliquée dans les émotions.

B. Sémiologie et diagnostic différentiel de l'encéphalite limbique auto-immune

Le diagnostic de l'encéphalite limbique est loin d'être simple. La présentation des symptômes peut en effet varier en fonction de l'origine et du stade d'évolution de l'encéphalite. Lors d'une première consultation, il n'est pas rare que les crises d'épilepsie ainsi que les troubles psychiatriques comprenant délires et hallucinations se révèlent prédominants par rapport aux troubles de la mémoire, élément pourtant majeur du diagnostic pouvant se révéler plus tardivement (Tüzün & Dalmau 2007). Par exemple, dans le cas de l'encéphalite à auto-anticorps anti-NMDAr, une première phase clinique dominée par des troubles psychiatriques peut mener à un diagnostic de maladie psychiatrique non auto-immune et à un traitement inapproprié pouvant s'avérer fatal pour le patient (Dalmau et al., 2007).

En complément de la symptomatologie, des techniques d'imagerie cérébrale couplées à l'analyse du liquide céphalorachidien (LCR) vont permettre de confirmer le diagnostic. Ainsi, un électroencéphalogramme pourra souvent mettre en évidence une activité épileptique temporale ou généralisée (Lawn et al., 2003 ; Tüzün & Dalmau 2007); l'imagerie par résonance magnétique (IRM) pourra révéler des anomalies au niveau des lobes temporaux, souvent de façon asymétrique (hypersignaux FLAIR ou T2) (Figure 2) ; enfin le LCR pourra présenter des signes d'inflammation (augmentation du nombre de lymphocytes, de protéines et d'IgGs) (Tüzün & Dalmau 2007).

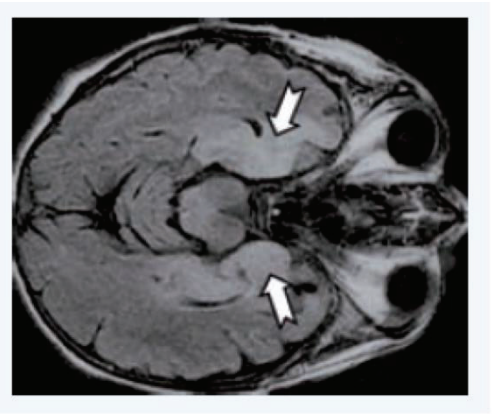

Figure 2 : IRM évocateur d'une encéphalite limbique (Didelot et Honnorat, 2009). IRM encéphalique en FLAIR (Fluid Attenuated Inversion Recovery) en coupe transversale révélant l'existence d'un hypersignal hippocampique bilatéral (flèches).

Une fois les symptômes de l'encéphalite limbique identifiés, il est important de déterminer son origine afin d'adapter au mieux le traitement. Les encéphalites virales sont les plus fréquentes et peuvent évoluer très rapidement. Ainsi, le patient sera traité contre une potentielle infection en première intention en attendant les résultats d'analyses plus poussées (Tuzun et Dalmau 2007). Une fois la cause virale exclue, la présence d'anticorps spécifiques dans le sang et/ou le LCR permettra de mettre en évidence une encéphalite auto-immune.

L'encéphalite limbique auto-immune peut être d'origine paranéoplasique, c'est à dire associée à un cancer. Le diagnostic de l'EL précédant souvent la découverte d'un cancer, la détection d'anticorps associés à une EL paranéoplasique doit conduire à la recherche d'une tumeur (Table 1). L'ablation de la tumeur, si tumeur il y a, et un traitement immunomodulateur (corticoïdes, immunoglobulines intraveineuses et échanges plasmatiques) permettent, dans une partie des cas, le rétablissement du patient (Table 1). Les différences de réponses aux traitements en fonction de la cible antigénique seront évoquées dans le chapitre « cible antigéniques ».

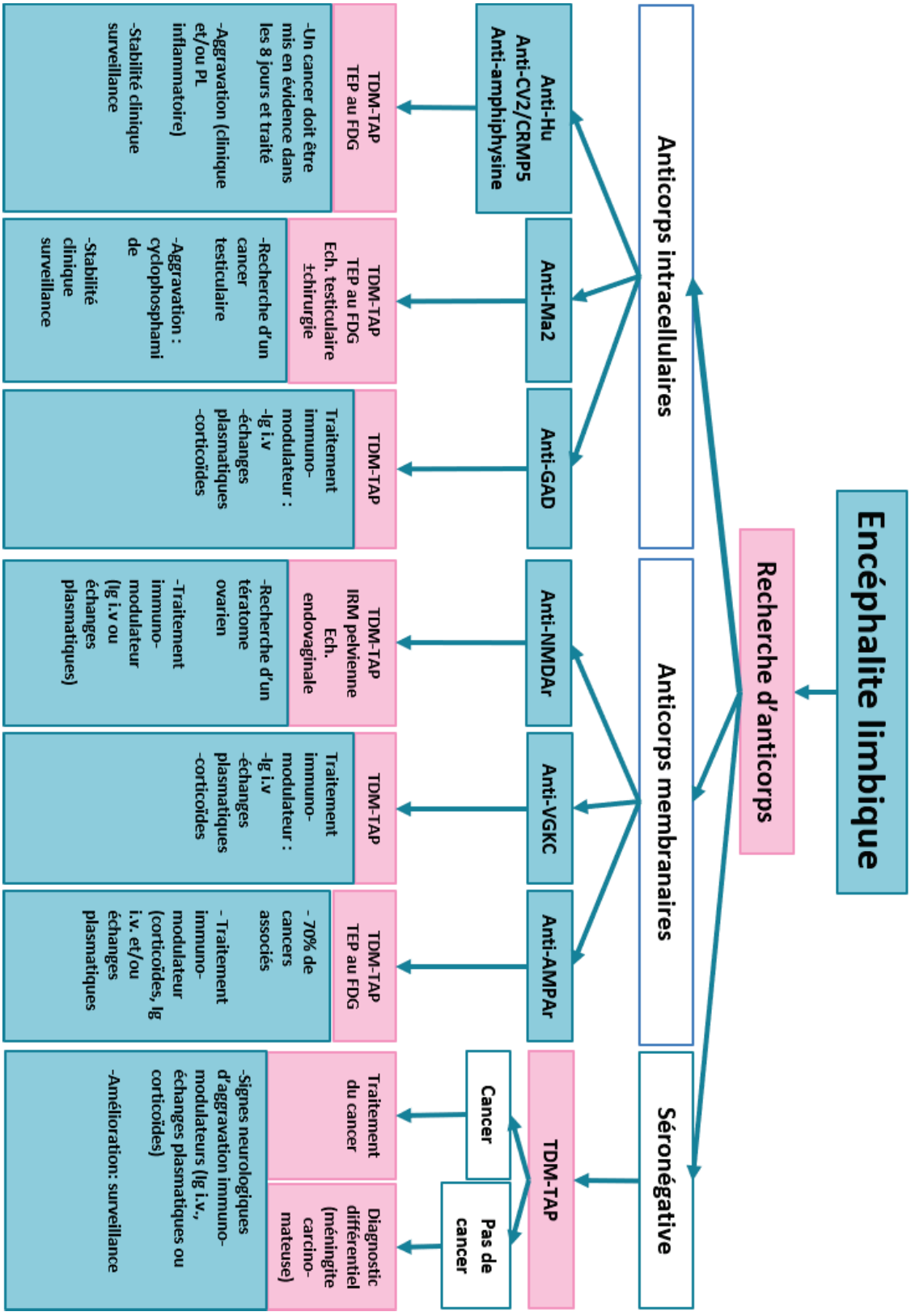

Table 1 : Prise en charge d'une encéphalite limbique (repris de Didelot & Honnorat, 2009).
TDM-TAP : tomodensitométrie thoroco-abdomino-pelvienne; TEP au FDG: tomographie par émission de positons au déoxyglucose; PL: ponction lombaire; Ech : échographie; Ig i.v. : Immunoglobulines intraveineuses; IRM : Imagerie par résonance magnétique.

C. Origines des anticorps dans l'encéphalite limbique auto-immune

Les encéphalites limbiques auto-immunes peuvent être d'origine post-infectieuses ou tumorales. En dehors de ces cas, l'origine des anticorps reste encore largement inconnue (Figure 3).

1. Origine post-infectieuse

Certaines encéphalites, comme l'encéphalite anti-NMDAr peuvent se déclarer quelques semaines après une encéphalite virale telle que l'encéphalite herpétique (Armangue et al., 2014). Un mécanisme possible serait que les antigènes libérés suite à la mort cellulaire induite par le virus, soient captés par les cellules dendritiques, transportés aux ganglions lymphatiques (Figure 3A et C) puis présentés aux cellules B naïves et aux cellules T CD4+ provoquant ainsi une auto-immunité (Figure 3C) (Dalmau et al., 2017).

2. Origine tumorale

Dans les encéphalites limbiques associées à un cancer, la présence de protéines du système nerveux dans les tumeurs peut s'expliquer de deux façons. D'une part, les cellules cancéreuses peuvent exprimer de façon ectopique des protéines neuronales (DeLuca et al., 2009) d'autre part, les tumeurs peuvent contenir des tissus nerveux (Dalmau et al., 2007, Tüzün et al., 2009). Il est possible que la présence de ces protéines neuronales dans les tumeurs soit la cause de la rupture de tolérance (production d'un anticorps contre un antigène du soi). Des évidences suggèrent que les antigènes relargués par les cellules tumorales en apoptose seraient captés par les cellules dendritiques et présentés au système immunitaire au niveau des ganglions lymphatiques induisant ainsi une réponse immunitaire des cellules T cytotoxiques (Figure 3B et C) (Albert et al., 1998). Les patients développent alors des anticorps contre des protéines du système nerveux central, susceptibles de perturber leur fonction. La réponse auto-immune peut également mener à des infiltrats de cellules T cytotoxiques et à une mort neuronale dans le cerveau (Blumenthal et al., 2006 ; Bien et al., 2012).

3. Prédisposition génétique

Il est également possible que certains patients présentent des prédispositions génétiques à l'auto-immunité. Par exemple, des mutations des gènes HLA ont été identifiées chez des patients avec des anticorps anti-LGI1 ou anti-IgLON5 (Gelpi et al., 2016; Van Sonderen et al., 2017). Cette piste reste cependant peu explorée à l'heure actuelle.

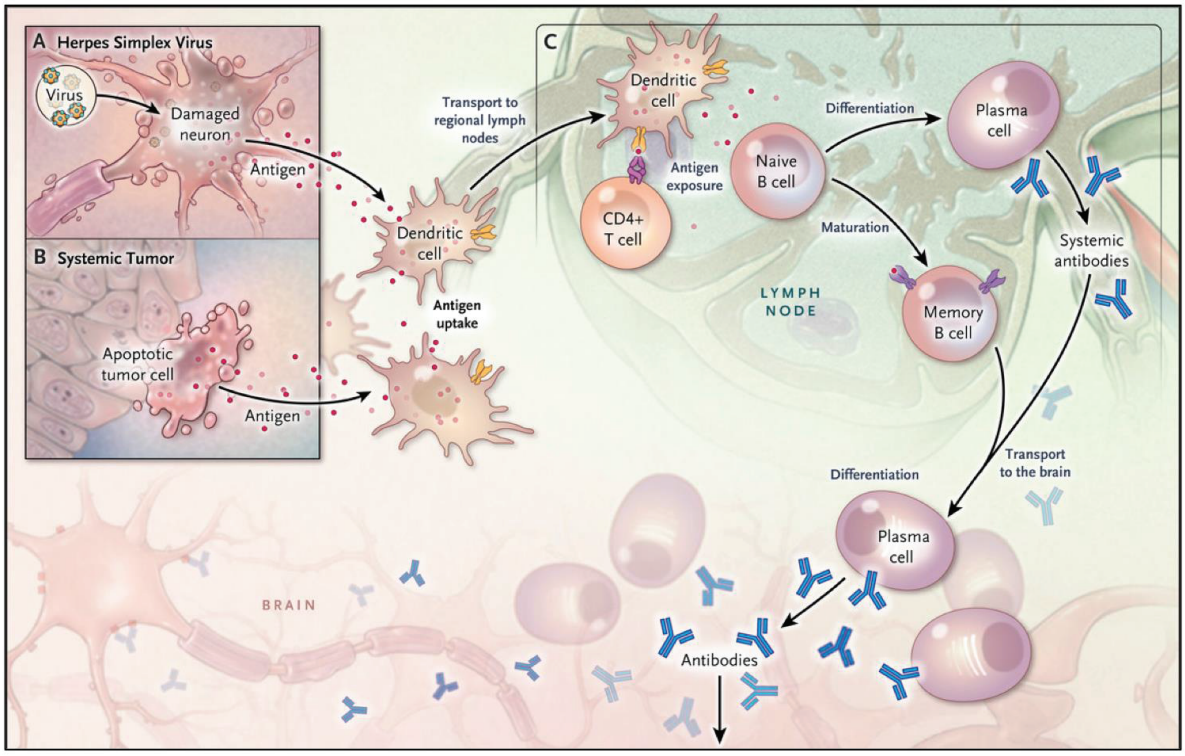

Figure 3 : Mécanismes d'induction de la synthèse des auto-anticorps (Dalmau et Graus, 2018). Deux mécanismes déclencheurs de l'encéphalite limbique sont représentés : le virus de l'Herpès **(A)** et les tumeurs **(B)**. Les antigènes émis par des cellules endommagées à la suite d'une inflammation virale ou des cellules tumorales en apoptose pourraient être captés par les cellules présentatrices d'antigène (cellules dendritiques) puis transportés aux ganglions lymphatiques. Ensuite, les antigènes seraient présentés aux cellules T CD4+ et aux cellules B naïves se différenciant alors en cellules productrices d'anticorps (plasmocyte) **(C)**.

4. Synthèse des anticorps périphérique ou centrale

Le site de production des anticorps reste également matière à débat et il existe actuellement deux hypothèses possibles (Revue Diamond et al., 2009 ; Platt et al., 2017).

La première, est celle d'une synthèse périphérique des anticorps, en accord avec un déclencheur périphérique de la pathologie comme une tumeur, avec un passage des anticorps à travers la barrière hémato-encéphalique (BHE). La BHE, constituée de cellules endothéliales, de péricytes et d'astrocytes, limite le passage des cellules et des protéines sanguines vers le tissu cérébral (Diamond et al., 2009). Ainsi, en conditions physiologiques, le passage des anticorps est possible mais en quantités très faibles ne pouvant pas expliquer pas le taux élevé d'anticorps retrouvés dans le LCR des patients. Pour cela, une rupture de la BHE semble nécessaire. En effet, en l'absence d'une telle rupture, la présence d'anticorps dirigés contre des protéines du cerveau dans le sérum n'induit aucun trouble cérébral

(Diamond et al., 2009). Différents mécanismes ont été ainsi proposés pour expliquer le passage des anticorps à travers la BHE : (1) par activation endothéliale qui augmenterait la perméabilité de la BHE (Figure 4A), (2) sans activation endothéliale par l'intermédiaire de transporteurs (Figure 4B) et (3) par le biais du récepteur Fc néonatal (FcRn) qui permettrait aux anticorps présents dans le cerveau d'être efflués vers la circulation sanguine (Figure 4C) (Diamond et al., 2009).

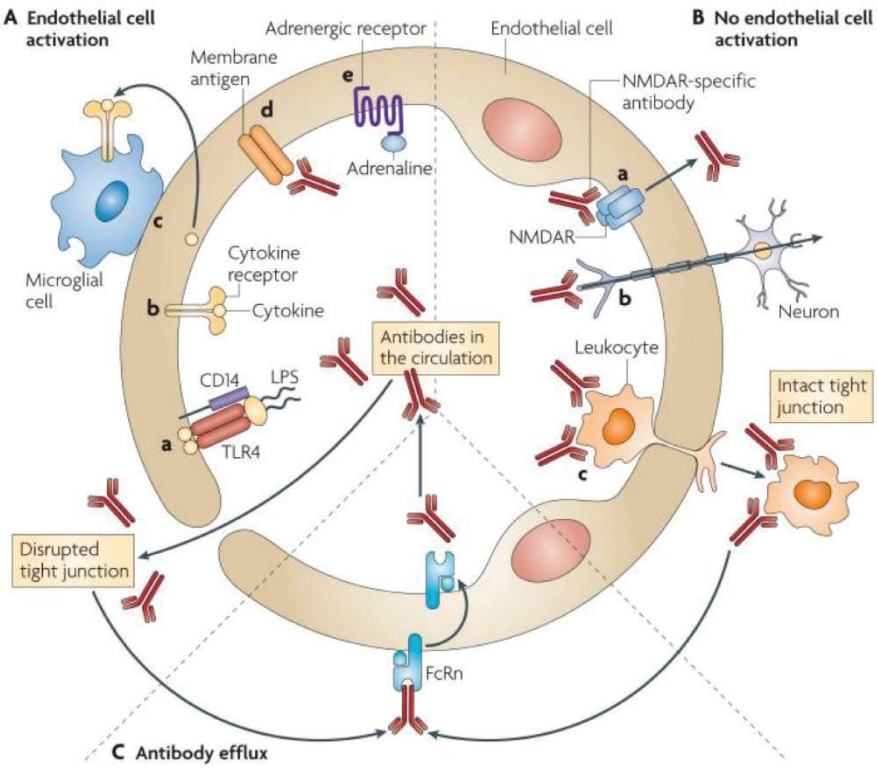

Figure 4 : Schéma des mécanismes de passage des anticorps à travers la BHE (Diamond et al., 2009). A) passage des anticorps par activation endothéliale. (a) brèche induite par des substances microbiennes (LPS), (b) activation des cellules endothéliales par des cytokines pro-inflammatoires, (c) induction d'une réponse immunitaire locale par des cytokines qui favorise la dysfonction de la BHE, (d) altération de la BHE directement par les anticorps, (e) facteurs externes fragilisant la BHE (stress, exercice extrême ou nicotine). **B)** Passage des anticorps en l'absence d'activation endothéliale. (a) endocytose de l'anticorps par un récepteur spécifique, (b) transport axonal rétrograde dans un neurone faisant protrusion à l'intérieur de la lumière des capillaires de la BHE, (c) migration trans-endothéliale d'un leucocyte porteur de l'anticorps au niveau des veinules post-capillaires. **C)** Efflux des anticorps vers la circulation par transport actif médié par le récepteur Fc néonatal (FcRn).

La seconde hypothèse est celle d'une synthèse centrale des anticorps par des plasmocytes. En faveur de cette hypothèse, une étude a montré des infiltrats de plasmocytes dans le système nerveux central de patients présentant une encéphalite limbique anti-NMDAr (Martinez-Hernandez et al., 2011). Cette hypothèse reste cependant peu explorée à l'heure actuelle.

D. Différentes sous-classes et modes d'action des anticorps

La plupart des anticorps présents dans les EL auto-immunes sont des immunoglobulines de type G, principalement de sous-classe IgG1 et IgG4. Une certaine sous-classe d'IgG peut être associée à un certain type d'anticorps ; par exemple les anti-NMDAr sont majoritairement de la sous-classe IgG1. Les deux sous-classes possèdent des caractéristiques biologiques bien différentes (Table 2) et présentent un grand intérêt par rapport à l'étude du mécanisme pathogénique des auto-anticorps.

1. Les anticorps de sous-classe IgG1

Les IgG1 sont la sous-classe majoritaire dans le sérum (60% des IgG totales) (Vidarsson et al., 2014) et sont retrouvées dans la plupart des EL auto-immunes. Ces anticorps sont capables de lier leurs cibles antigéniques entre-elles (*cross-link*) et de provoquer ainsi leur internalisation (Figure 5A) (Dalmau et al., 2008). De plus, les IgG1 sont capables de fixer fortement les récepteurs Fcγ (Table 2), induisant la phagocytose ou la réponse cytotoxique, et d'activer le complément permettant ainsi de faire le lien entre les réponses immunitaires innée et adaptative (Figure 5A).

2. Les anticorps de sous-classe IgG4

Les IgG4 se trouvent habituellement en faible proportion dans le sérum (4% des IgG totales). Cette sous-classe est majoritaire dans les EL à auto-anticorps anti-CASPR2 et anti-LGI1. Les IgG4 ont une faible affinité pour le récepteur Fcγ et n'activent pas le complément (Table 2) (Vidarsson et al., 2014). De plus, une caractéristique unique des IgG4 est leur capacité à échanger des moitiés de molécules pour former des IgG4 bispécifiques monovalentes (Figure 5B) (Rispens et al., 2011), les rendant incapables de lier deux antigènes identiques entre eux ou d'induire leur internalisation (Figure 5C) (Huijbers et al., 2015).

Les IgG4 n'agiraient donc pas par la voie cytotoxique mais plutôt en interférant avec la fonction de leur cible par exemple, en bloquant son interaction avec ses partenaires. Pour cette raison, ces anticorps sont considérés comme « bloquants » (Huijbers et al., 2015 ; Ohkawa et al., 2013).

Table 1 | Properties of human IgG subclasses.

	IgG1		IgG4	
General				
Molecular mass (kD)	146		146	
Amino acids in hinge region	15		12	
Inter-heavy chain disulfide bonds	2		2	
Mean adult serum level (g/l)	6.98		0.56	
Relative abundance (%)	60		4	
Half-life (days)	21		21	
Placental transfer	++++		+++	
Antibody response to:				
Proteins	++		++[e]	
Polysaccharides	+		+/−	
Allergens	+		++	
Complement activation				
C1q binding	++		−	
Fc receptors				
FcγRI	+++[c]	65[d]	++	34
$Fc\gamma RIIa_{H131}$	+++	5.2	++	0.17
$Fc\gamma RIIa_{R131}$	+++	3.5	++	0.21
FcγRIIb/c	+	0.12	+	0.20
$Fc\gamma RIIIa_{F158}$	++	1.2	−	0.20
$Fc\gamma RIIIa_{V158}$	+++	2.0	++	0.25
FcγRIIIb	+++	0.2	−	−
FcRn (at pH < 6.5)	+++		+++	

[a] *Depends on allotype.*
[b] *For A/A isomer.*
[c] *Multivalent binding to transfected cells. Adapted from Bruhns et al. (2).*
[d] *Association constant ($\times 10^6$ M^{-1}) for monovalent binding (2).*
[e] *After repeated encounters with protein antigens, often allergens.*

Table 2 : Propriétés des sous-classes IgG1 et IgG4 humaines (Vidarsson et al, 2014).

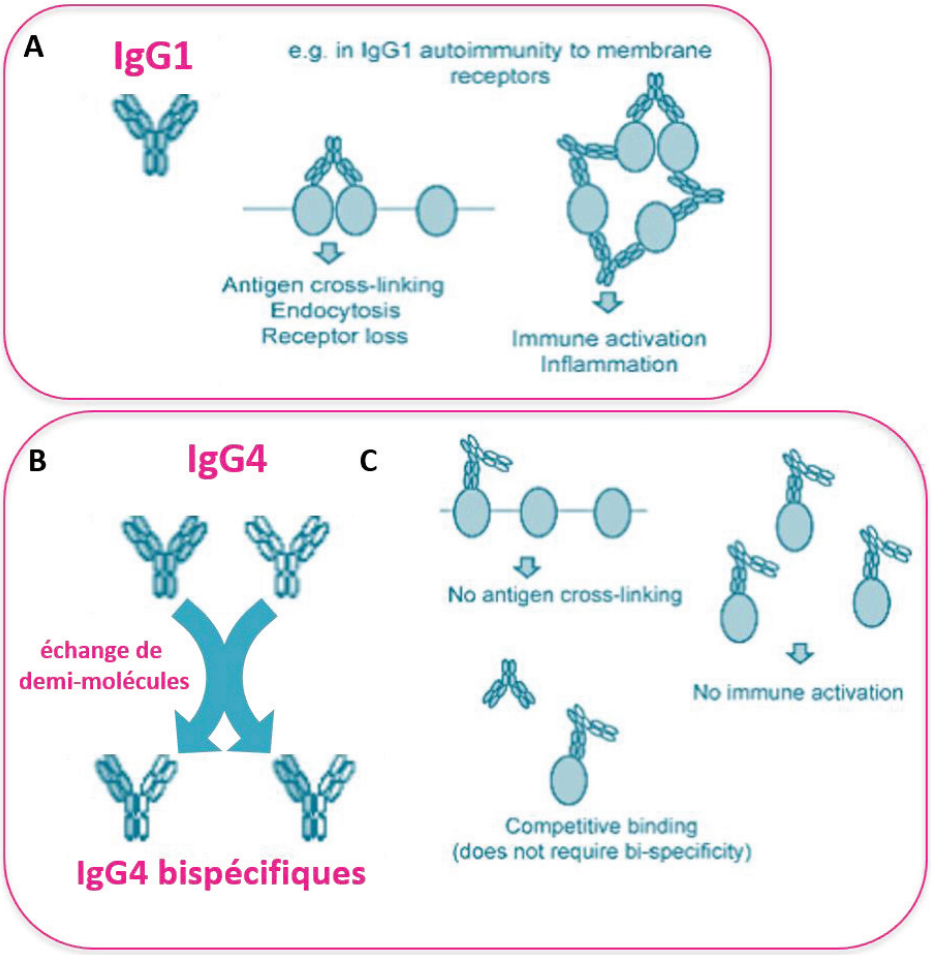

Figure 5 : Fonction des sous-classes IgG1 et IgG4. A) Les IgG1 sont bivalents, ils possèdent deux sites de liaison à l'antigène. Ils sont capables de lier plusieurs antigènes entre eux et d'induire leur internalisation. Ils sont également capables de former de larges complexes avec leur cible et d'activer le complément et la réponse cytotoxique. **B)** Les IgG4 sont capables d'échanger des moitiés de molécule les rendant ainsi bispécifiques ; ils possèdent deux sites de liaison à l'antigène, chacun dirigé contre un antigène ou épitope différent. **C)** Les IgG4 bispécifiques ne sont pas capables de lier deux antigènes identiques entre eux ou de former de larges complexes anticorps-antigène. De plus, ils n'activent pas la voie du complément. Cependant, ils sont capables de se lier à leur cible de façon compétitive perturbant ainsi sa fonction.

E. Différentes cibles antigéniques

Les encéphalites limbiques auto-immunes peuvent être classées en deux groupes selon la cible antigénique : les antigènes intracellulaires et les antigènes membranaires. Chaque groupe présente des marquages immunohistochimiques, des mécanismes pathologiques et une réponse au traitement différents (Figure 6).

1. Antigènes intracellulaires

Les anticorps dirigés contre des antigènes faisant partie de cette catégorie sont les anti-Hu (Figure 6A,B) (Graus et al., 1987), les anti-Ma1/2 (Dalmau et al., 2004), les anti-CV2/CRMP5 (Honnorat et al., 2009), les anti-Yo (Rojas et al., 2000), les anti-Ri (Shams'ili et al., 2003), les anti-Sox1 (Titulaer et al., 2009) et les anti-ZIc4 (Bataller et al., 2004). Dans cette même catégorie, sont également retrouvés des anticorps contre des antigènes intracellulaires synaptiques tel que les anti-amphiphysine (De Camilli et al., 1993), les anti-GAD65 (Honnorat et al., 2001) et les anti-AK5 (Tünzün et al., 2007).

Cette catégorie d'anticorps est majoritairement associée à un cancer et leur détection doit conduire à la recherche d'une tumeur. En fonction de la cible antigénique, un certain type de tumeur peut être associé, permettant d'orienter la recherche (Table 1). De plus, les mécanismes pathologiques chez ces patients ne semblent pas impliquer une action directe des anticorps sur leur cible mais plutôt des mécanismes impliquant les cellules T cytotoxiques et une forte perte neuronale (Figure 6C) (Dalmau et Rosental, 2008 ; Bien et al., 2012). Les patients présentant ces anticorps répondent peu au traitement immunomodulateur, ce qui coïncide avec un rôle mineur des anticorps dans la pathologie et l'aspect irréversible des atteintes.

2. Antigènes membranaires

Les anticorps de cette catégorie sont majoritairement dirigés contre des antigènes synaptiques et correspondent aux : anti-NMDAr (Figure 6D,E) (Dalmau et al., 2007), anti-AMPAr (Lai et al., 2009), anti-GABAr (Lancaster et al., 2010 ; Petit-Pedrol et al., 2014), anti-DPPX (Boronat et al., 2013), anti-mGluR1/5 (Sillevis Smitt et al., 2000, Lancaster et al., 2011), anti-P/Q-type VGCC (Mason et al., 1997), anti-récepteur à la glycine (Hutchinson et al., 2008), anti-récepteur à la dopamine-2 (Dale et al., 2002), anti-DNER (De Graaf et al., 2012), anti-IgLON5, anti-neurexin-3α et anti-LGI1, anti-CASPR2, anti-contactine2 et anti-Kv1 (anciennement connus sous le nom d'anti-VGKC) (Irani et al., 2010 ; Lai et al., 2010 ; for review see Dalmau et al., 2017).

L'association d'une tumeur avec ces anticorps est beaucoup moins fréquente que pour les cibles intracellulaires et dépend généralement de la cible. Le plus souvent, l'ablation de la tumeur, le cas échéant, et un traitement immunosuppresseur permettent le rétablissement des patients, suggérant une action directe et réversible des anticorps sur leur cible sans mort cellulaire (Figure 6F).

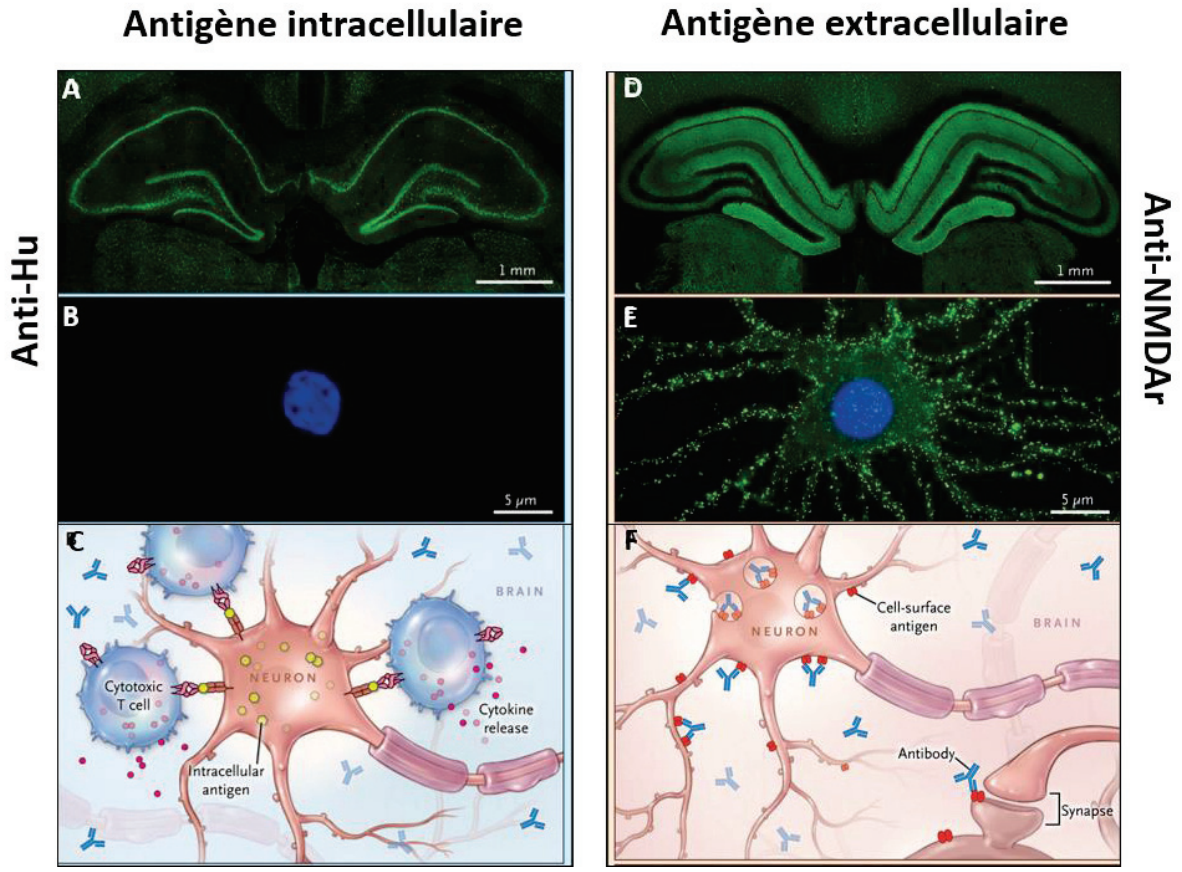

Figure 6 : Cibles antigéniques (Dalmau & Graus, 2018). A) Le marquage sur coupe de cerveau avec les anti-Hu montre un marquage cellulaire. **B)** En cellules vivantes sur cultures de neurones, les anti-Hu ne sont pas capables d'accéder à leur cible intracellulaire. **C)** Les mécanismes pathologiques associés aux antigènes intracellulaires sont majoritairement des mécanismes cytotoxiques puisque les anticorps ne peuvent atteindre leur cible à l'intérieur de la cellule. **D)** Le marquage sur coupe de cerveau avec les anti-NMDAr montre un marquage des prolongements cellulaires. **E)** En cellules vivantes sur cultures de neurones, les anti-NMDAr sont capables d'accéder à leur cible à la surface des cellules et présentent un marquage du corps cellulaire et de ses prolongements. **F)** Les mécanismes pathologiques associés aux antigènes membranaires passent principalement par la liaison des anticorps à leur cible, perturbant leur fonction.

F. L'encéphalite limbique à auto-anticorps anti-CASPR2

Au sein du laboratoire nous nous intéressons plus particulièrement aux encéphalites limbiques à auto-anticorps anti-CASPR2 (Figure 7) dont la découverte est étroitement liée à celle des anticorps anti-VGKC.

1. Origine des anti-CASPR2, les anti-VGKC

Les anti-VGKC (voltage gated potassium channels) ont été initialement identifiés chez des patients présentant un syndrome d'hyperexcitabilité des nerfs périphériques aussi connu sous le nom de neuromyotonie (NMT) (Shillito et al., 1995). Ces patients présentent des troubles purement périphériques avec des rigidités et crampes musculaires accompagnées de fasciculations (contractions involontaires) et d'une légère dysautonomie (Figure 7) (Song et al., 2017). Ultérieurement, les anti-VGKC ont été identifiés chez des patients présentant une encéphalite limbique (Figure 7) (Buckley et al., 2001) ainsi que chez des patients atteints du syndrome de Morvan (MoS), qui combine une NMT et des troubles centraux tel que l'insomnie, des confusions et des hallucinations (Figure 7) (Liguori et al., 2001; review Newsom-Davis et al., 2003).

Les premières expériences d'identification de la cible antigénique ont révélé que les anticorps anti-VGKC étaient dirigés contre les canaux potassiques Kv1.1, Kv1.2 et Kv1.6. Ces canaux ont été mis en évidence par immunoprécipitation à l'aide d'anticorps de patients sur des lysats de cerveaux et révélés par une dendrotoxine marquée à l'iode 125, capable de se lier spécifiquement aux Kv1.1, Kv1.2 et Kv1.6 (Shillito et al., 1995). Cependant, il s'est avéré par la suite que la plupart de ces anticorps ne ciblaient pas directement les canaux potassiques mais des protéines leur étant étroitement associées : CASPR2, TAG-1 et LGI-1 (Irani et al., 2010 ; Lai et al., 2010).

2. Tableau clinique de l'encéphalite limbique anti-CASPR2

Les patients présentant des encéphalites limbiques à auto-anticorps anti-CASPR2 sont majoritairement des hommes (94,4%) âgés en moyenne de 64,5 ans (Joubert et al., 2016). Ils présentent des symptômes de dysfonctionnement du système limbique comprenant des troubles de la mémoire antérograde, des crises d'épilepsie temporale ainsi que des troubles du comportement. A ces troubles, peuvent s'ajouter, une ataxie cérébelleuse (troubles de la coordination) (33%), des douleurs neuropathiques (18%) et une NMT (10%) (Figure 7) (Joubert et al., 2016). Dans quelques cas, des symptômes paroxystiques ont été décrits comme les myoclonies orthostatiques (secousses irrégulières des membres inférieurs) (Van Gerpen et al., 2016 ; Gövert et al., 2016), des troubles du mouvement hyperkinétique (mouvements involontaires) (Bien et al., 2017) et des ataxies cérébelleuses paroxysmales (Joubert et al., 2017). Contrairement aux NMT et MoS, les EL

anti-CASPR2 sont rarement associées à un cancer (16,7%) ou d'autres troubles auto-immuns (5,6%) (Figure 7) (Joubert et al., 2016 ; Van Sonderen et al., 2016).

3. Caractéristiques des anticorps anti-CASPR2

Jusqu'à récemment, les caractéristiques des auto-anticorps anti-CASPR2 étaient inconnues ; ils ont fait l'objet d'une partie de mon travail de thèse ainsi que de publications qui seront plus amplement décrites dans la partie résultats (Pinatel et al., 2015 ; Joubert et al., 2016 ; Joubert et al., 2017). En résumé, nous avons pu montrer que les anticorps anti-CASPR2 sont présents dans le sérum et le LCR des patients atteints d'encéphalite limbique. Ceux-ci sont majoritairement de la sous-classe IgG4 et ciblent principalement les domaines N-terminaux discoidine et laminine G1 de CASPR2 (Figure 7) (Pinatel et al., 2015 ; Joubert et al., 2016 ; Joubert et al., 2017). D'autres équipes travaillant sur les encéphalites limbiques auto-immunes ont publié également des résultats similaires (Olsen et al., 2015 ; van Sonderen et al., 2016).

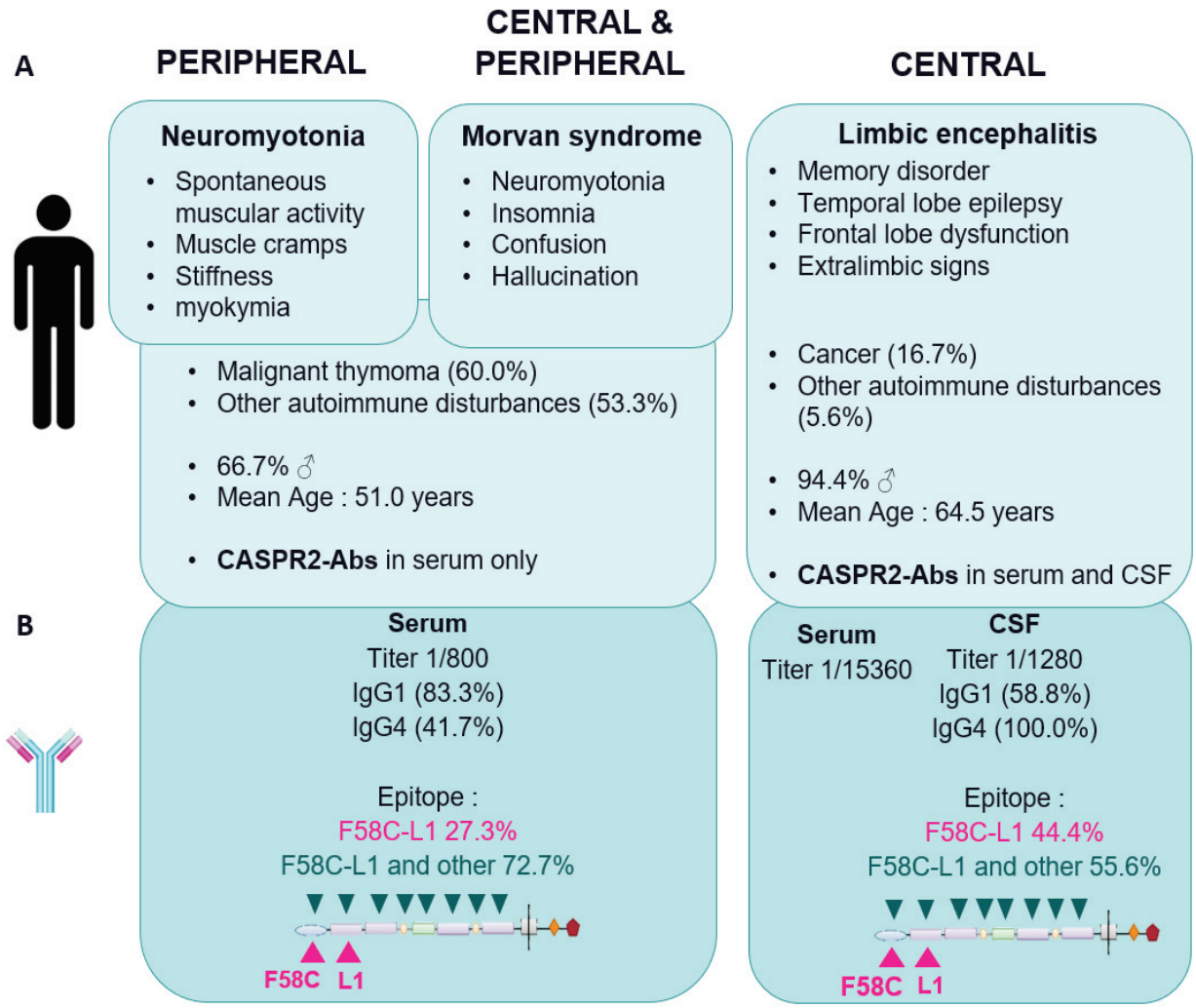

Figure 7 : Maladies auto-immunes à auto-anticorps anti-CASPR2 (Saint-Martin et al., 2018). **A)** Les anticorps anti-CASPR2 sont associés à des troubles du système nerveux périphérique (neuromyotonie et syndrome de Morvan) et central (encéphalite limbique). Les patients sont majoritairement des hommes âgés d'environ 60 ans. Bien que le syndrome de Morvan soit majoritairement associé à des troubles du système nerveux périphérique, les patients présentent également des atteintes centrales telles que de l'insomnie, des confusions et des hallucinations. **B)** Les patients présentant une neuromyotonie et un syndrome de Morvan ont uniquement des anti-CASPR2 dans le sérum alors que les patients présentant une encéphalite limbique présentent des anticorps dans le sérum et le LCR. Tous les patients présentant une encéphalite limbique possèdent des anticorps de la sous-classe IgG4 qui reconnaissent les domaines discoidine (F58C) et laminine G1 (L1) de CASPR2.

II. La protéine CASPR2 (Contactin-associated protein-like 2)

CASPR2 est une protéine d'adhésion cellulaire appartenant avec CASPR1, CASPR3, CASPR4 et CASPR5 à un sous-groupe de la superfamille des neurexines. Les neurexines, localisées dans le compartiment pré-synaptique, jouent un rôle dans la différentiation et la fonction des synapses (Missler et al., 2003 ; Graf et al., 2004 ; Gokce & Südhof, 2013). Elles induisent la formation de synapses excitatrices ou inhibitrices en interagissant avec des partenaires post-synaptiques comme les neuroligines, les LRRTM (Leucin rich repeat transmembrane) ou la cérébelline (Graf et al., 2004). Chez la souris, l'invalidation d'un ou plusieurs gènes codant pour les neurexines (neurexine-1α, 2α et 3α) provoque de sévères dysfonctionnements synaptiques pouvant conduire à leur mort précoce (Südhof, 2017). Chez l'homme, des mutations des gènes codant pour les neurexines ont été identifiées chez des patients atteints d'autisme (Reichelt et al., 2012), d'épilepsie (Møller et al., 2013), de déficience intellectuelle (Schaaf et al., 2012), de schizophrénie (Kirov et al., 2009) et de syndrome de Gilles de la Tourette (Huang et al., 2017). En particulier, la neurexine-3α a été associée aux encéphalites limbiques auto-immunes et les anticorps anti-neurexine-3α seraient capables d'altérer le développement des synapses *in vitro* (Gresa-Arribas et al., 2016).

A. Structure de la protéine CASPR2

CASPR2 est une protéine transmembranaire avec une région C-terminale intracellulaire contenant un motif de liaison aux protéines 4.1B (4.1Bb) également connu sous le nom de motif Glycophorine-NeurexinIV-Paranodine (GNP) (Poliak et al., 1999). Ce

motif permet son interaction avec les protéines du cytosquelette contenant un domaine FERM (Four-point-one, Ezrin, Radixin, Moesin) (Denisenko-Nehrbass et al., 2003). Elle contient également dans sa région intracellulaire un motif de liaison PDZ de type II (PDZb) permettant son interaction avec des protéines d'échafaudage (Figure 8A) (Horresh et al., 2008 et 2010). La partie extracellulaire de CASPR2 est composée d'un domaine de type discoidine (F58C ou D), de quatres domaines de type laminine G (L1-L4), de deux domaines de type EGF (Epidermal growth factor) (E1-E2) et d'un domaine de type fibrinogène (F) (Figure 8A) (Poliak et al., 1999).

CASPR2 possède des similitudes avec la neurexine-1α. Elles possèdent toutes deux des domaines de liaison 4.1B et PDZ intracellulaires ainsi que des domaines laminine G et EGF extracellulaires. Néanmoins, les domaines discoidine et fibrinogène sont une particularité de la protéine CASPR2 (Figure 8A) (Poliak et al., 1999). Des différences entre leur structure 3D ont été également mises en évidence par des études en microscopie électronique. Celles-ci montrent que CASPR2 possède une structure compacte composée de trois lobes (Figure 8B) (Lu et al., 2016 ; Rubio-Marrero et al., 2016) tandis que la neurexine-1α possède une structure allongée. Ces trois lobes flexibles entre eux permettraient à CASPR2 d'arborer deux orientations : verticale ou horizontale (Figure 8B). Cette flexibilité pourrait entre autres moduler la capacité de CASPR2 à interagir avec différents partenaires ou encore impacter sa localisation dans différents compartiments neuronaux (Figure 8B) (Lu et al., 2016). Par exemple, seule CASPR2 dans son orientation horizontale avec une hauteur de 90Å pourrait pénétrer dans la fente synaptique inhibitrice estimée entre 100 et 120Å de large (High et al., 2015 ; Lu et al., 2016).

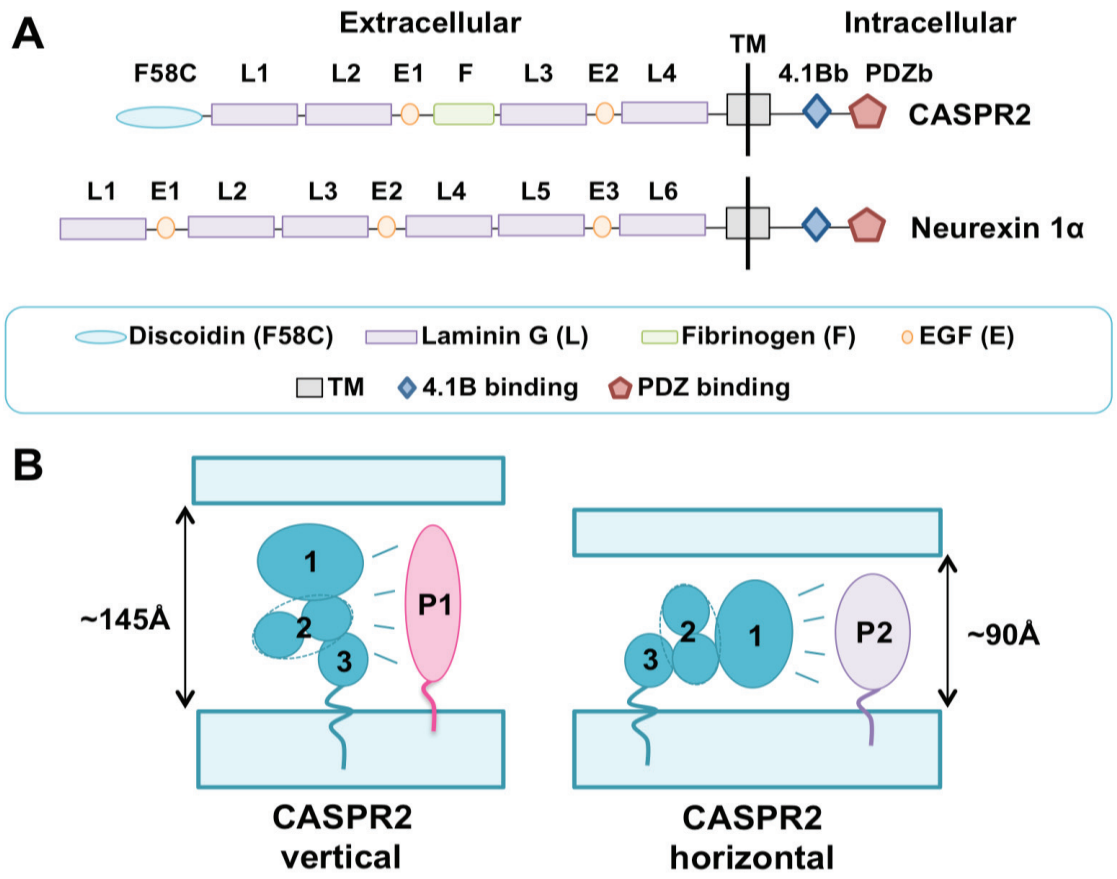

Figure 8 : Structure de CASPR2 et de la neurexine-1α (Saint-Martin et al., 2018). A) CASPR2 et la neurexine-1α possèdent toutes deux des domaines de type laminine G et EGF extracellulaires ainsi qu'un domaine transmembranaire et des domaines de liaison 4.1B et PDZ intracellulaires. CASPR2 possède également un domaine de type discoidine et fibrinogène qui lui sont propres. **B)** Structure de CASPR2 proposée par Lu et al., (2016). CASPR2 est une protéine d'environ ~145Å de long, ~90Å- de large et ~50Å d'épaisseur. Elle se compose de 3 lobes (1, 2 et 3) flexibles entre eux, permettant l'orientation de CASPR2 en vertical ou en horizontal. Une telle flexibilité pourrait révéler différents domaines de la protéine et ainsi moduler la capacité de CASPR2 à interagir avec ses partenaires (P1 et P2). Enfin, la localisation de CASPR2 dans différents compartiments neuronaux pourrait varier en fonction de son orientation.

B. Expression de CASPR2 dans le système nerveux

CASPR2 est fortement exprimée dans le système nerveux, incluant la moelle épinière et le cerveau et faiblement dans l'ovaire et la prostate (Poliak et al., 1999). Son patron d'expression spatio-temporel suggère un rôle dans la mise en place des réseaux neuronaux ainsi que dans les fonctions sensorielles et cognitives chez l'adulte.

1. Au niveau tissulaire

Chez la souris adulte, CASPR2 est fortement exprimée dans le cortex, dans des régions reliées aux fonctions motrices telles que les ganglions de la base ou le noyau pontique mais également dans des régions du système limbique, comprenant l'hippocampe, l'amygdale, le noyau interpédonculaire et les corps mamillaires (Gordon et al., 2016). CASPR2 est également exprimée dans des structures nerveuses impliquées dans les voies sensorielles visuelles, olfactives, auditives, gustatives et somatosensorielles. Pour l'ensemble de ces voies, CASPR2 est exprimée dans les organes sensoriels primaires puis dans le tronc cérébral et les noyaux thalamiques et enfin dans les régions corticales correspondantes (Gordon et al., 2016). Au cours du développement, CASPR2 est détectée à partir du 14^{ième} jour embryonnaire (E14) et son expression augmente graduellement selon un axe postéro-antérieur (Figure 9A et B) (Poliak et al., 1999 ; Peñagarikano et al., 2011 ; Gordon et al., 2016). Dans l'hippocampe, CASPR2 est initialement exprimée dans le Gyrus Denté à E18 puis son expression dans cette structure diminue au 7^{ième} jour post-natal (P7) (Figure 9C). L'expression de CASPR2 débute ensuite vers P7 dans les aires CA3 et CA1 de la corne d'Ammon où elle augmente jusqu'à l'âge adulte (Figure 9C) (Gordon et al., 2016). Concernant le cortex en développement, CASPR2 est initialement détectée, dans la zone marginale à E14 (Peñagarikano et al., 2011). A des stades plus tardifs, son expression s'étend graduellement dans les couches plus profondes de telle façon que chez l'adulte, CASPR2 est présente dans toutes les couches du cortex (Figure 9D) (Bakkaloglu et al., 2008 ; Gordon et al., 2016).

Dans le cerveau humain, le patron d'expression de CASPR2 est similaire à celui décrit pour les rongeurs (Poliak et al., 1999). Néanmoins au niveau du cortex, durant les stades précoces de développement, CASPR2 apparait particulièrement enrichie dans le cortex antérieur temporal et préfrontal chez l'humain (Abrahams et al., 2007). Cet enrichissement suggère un rôle de CASPR2 dans des fonctions cognitives supérieures telles que l'apprentissage du langage (Abrahams et al., 2007).

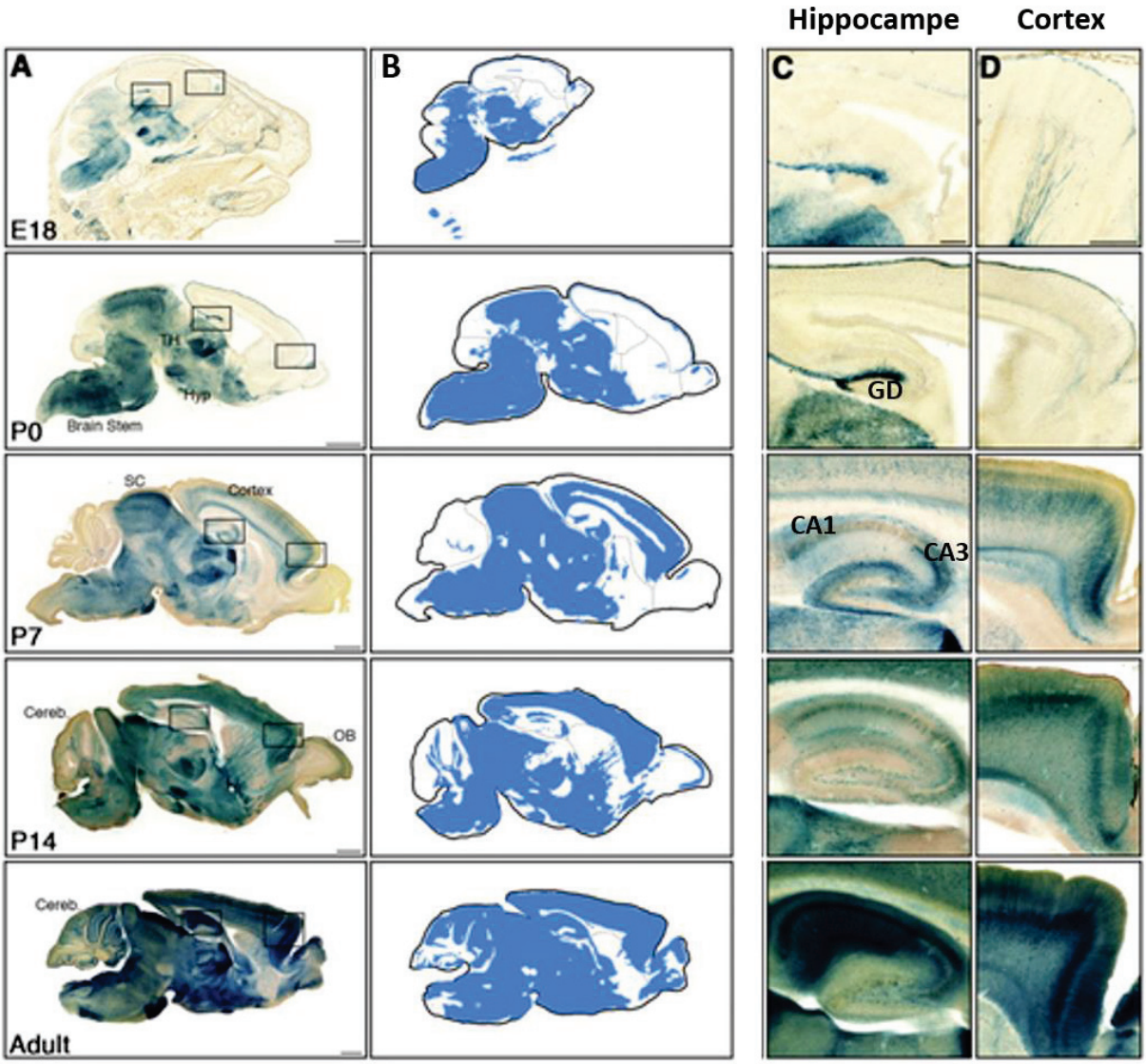

Figure 9 : Expression de CASPR2 durant le développement (Gordon et al., 2016). A) Expression de CASPR2 dans un encéphale de souris à partir du stade embryonnaire jour 18 (E18) au stade adulte. **B)** Représentation schématique de l'expression de CASPR2 dans un encéphale de souris de E18 au stade adulte. **C)** Grossissement de l'hippocampe. L'expression de CASPR2 débute dans le Gyrus Denté (GD) à E18 et évolue graduellement vers les régions CA3 et CA1 de l'hippocampe à l'âge adulte. **D)** Grossissement du cortex. L'expression de CASPR2 débute dans les couches superficielles puis évolue vers les couches profondes du cortex. TH : thalamus, Hyp : Hypothalamus, SC :Superior Colliculus, Cereb : cerebellum, OB : olfactory bulb. Echelle : 1mm (A), 200um (C) et 500um (D).

2. Au niveau cellulaire

In situ dans le cerveau de rat adulte, CASPR2 est exprimée dans une large variété de neurones (Figure 10) (Poliak et al., 1999). Par ailleurs, dans les neurones hippocampiques en culture (DIV4), 58% des neurones inhibiteurs (GAD65-positifs) expriment CASPR2 contre seulement 4% des neurones excitateurs (GAD65-négatifs) (Pinatel et al., 2015). Ces résutats

suggèrent que CASPR2 serait majoritairement associée à une sous-population de neurones inhibiteurs.

Concernant les compartiments neuronaux, CASPR2 est principalement localisée au niveau des dendrites et du corps cellulaire des neurones *in vivo* (Figure 10) (Poliak et al., 1999). *In vitro*, dans les neurones hippocampiques cultivés pendant 4 jours (DIV4), CASPR2 est exprimée dans la plupart des compartiments neuronaux, somato-dendritique mais aussi axonal. Néanmoins, à des stades plus tardifs (DIV7-8), une diminution de l'expression de CASPR2 est observée à la membrane au niveau du compartiment somato-dendritique. Cette diminution serait associée à un processus d'endocytose qui à terme conduirait à une polarisation de CASPR2 le long de l'axone (Bel et al., 2009 ; Pinatel et al., 2015).

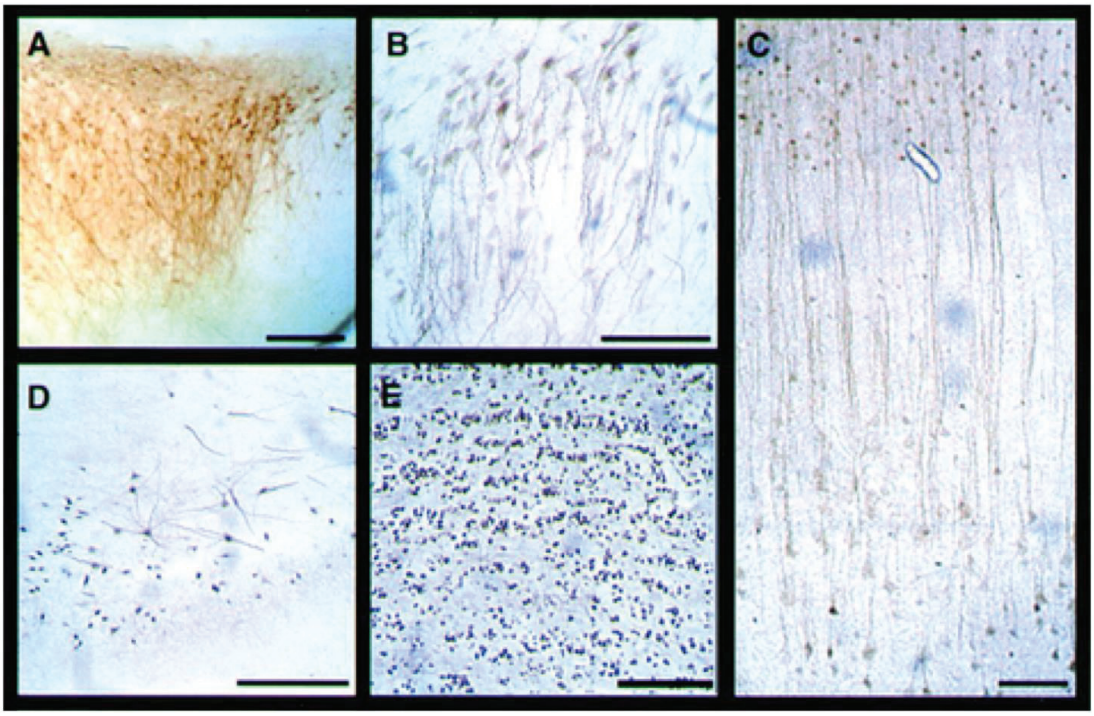

Figure 10 : Expression de CASPR2 dans les neurones (Poliak et al., 1999). Marquage de CASPR2 sur des tranches de cerveau de rat. CASPR2 est exprimée au niveau des corps cellulaires et des dendrites. **A)** Dans l'amygdale. **B)** Dans l'hippocampe. **C)** Dans la cinquième couche de neurones pyramidaux du cortex cérébral. D) Dans le Gyrus Denté. **E)** Dans les cellules granulaires du bulbe olfactif.

Dans les axones myélinisés du système nerveux central et périphérique, CASPR2 est enrichie au niveau du segment initial (AIS) et de la région juxtaparanodale (JXP) des nœuds de Ranvier (NOR) (Figure 11) (Poliak et al., 1999 ; Inda et al., 2006 ; Ogawa et al., 2008 ; Scott et al., 2017). Le segment initial, est une région située dans la région proximale de l'axone,

juste après le corps cellulaire (Figure 11A et B). Au niveau de cette région, riche en molécules d'adhésion et en canaux ioniques voltage-dépendants, sont générés les potentiels d'action (Leterrier, 2018). Les nœuds de Ranvier, quant à eux, se caractérisent par l'absence de myéline et une forte densité de canaux sodiques ; ils permettent la conduction rapide (saltatoire) des potentiels d'action le long de l'axone (Figure 11A et C). Ils sont flanqués de chaque côté par les régions paranodales, zones d'ancrage de la myéline sur l'axone, et les régions juxtaparanodales, situées sous la gaine de myéline (Rasband & Peles, 2015).

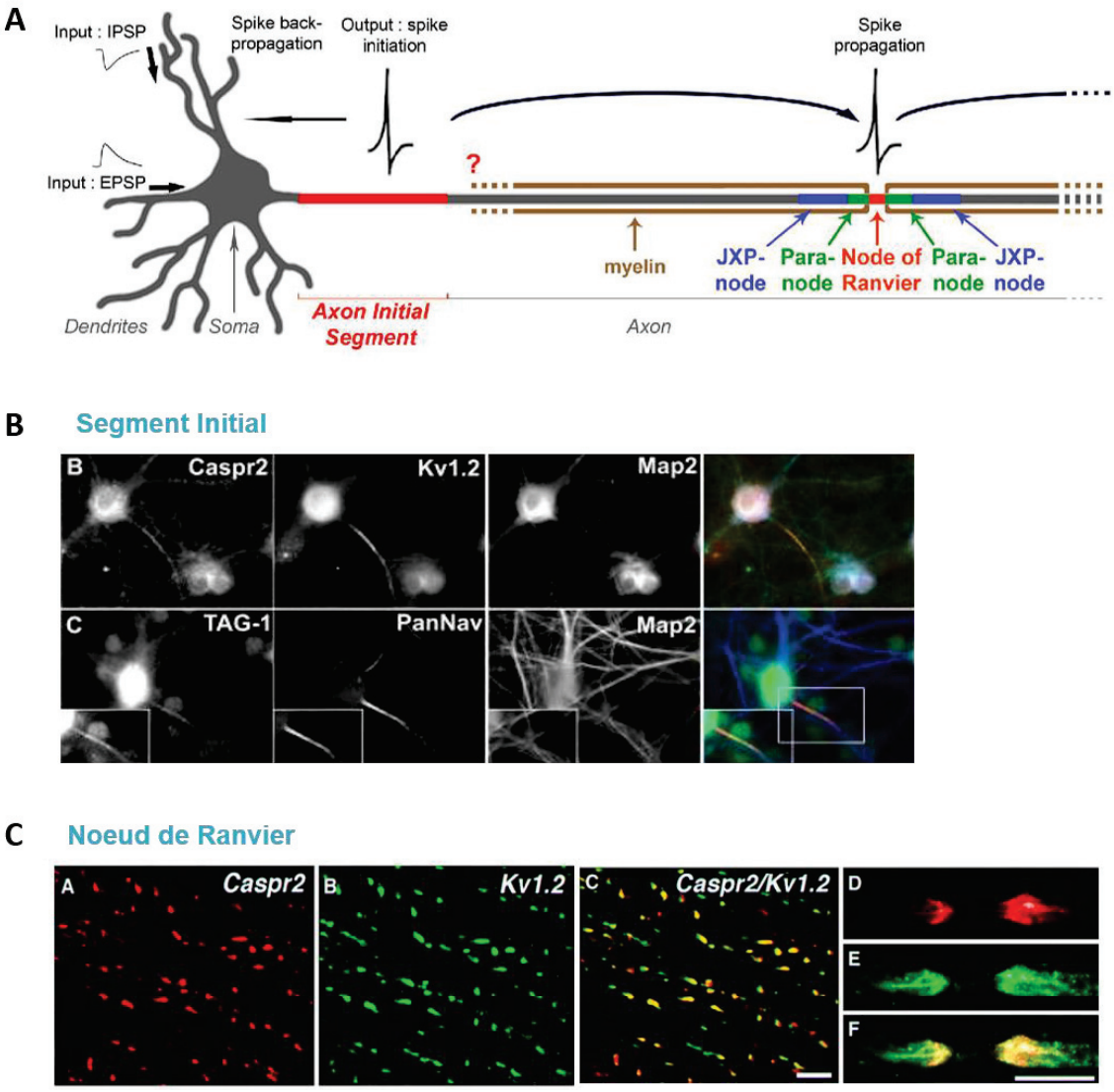

Figure 11 : Expression de CASPR2 dans les neurones (Poliak et al., 1999 ; Ogawa et al., 2008). A) Schéma d'un neurone myélinisé avec le segment initial et le nœud de Ranvier. Le nœud de Ranvier est entouré des régions paranodales et juxtaparanodales. **B)** Marquages de CASPR2, Kv1.2 et TAG-1 au segment initial sur des neurones hippocampiques en culture. **C)** Marquages de CASPR2 et Kv1.2 aux nœuds de Ranvier sur des coupes de nerf optique de rat.

Enfin, de nombreuses études ont suggéré une expression synaptique de CASPR2 mais les résultats sont divergents ou incomplets. Des études biochimiques ont montré la présence de CASPR2 dans des fractions enrichies en membranes synaptiques (Bakkaloglu et al., 2008) ou en synaptosomes (Chen et al., 2015). Cependant, si ces techniques apportent des éléments de réponse à la question, elles sont souvent insuffisantes car contaminés par d'autres compartiments. Ainsi, dans le cas des synaptosomes, la présence de compartiments membranaires non synaptiques peuvent biaiser les résultats.

Les techniques d'immunomarquage montrent également des résultats discordants. En utilisant un marquage post-fixation sur des cultures de neurones corticaux, une faible partie de CASPR2 co-localise avec la sous-unité GluA1 des récepteurs AMPA, post-synaptiques avec un coefficient de colocalisation de Mander de 0.35 (Varea et al., 2015). Notons qu'un coefficient de cet ordre n'est pas un argument fort pour la co-localisation de CASPR2 avec les récepteurs AMPA synaptiques. D'autre part, en utilisant les anticorps de patients, CASPR2 semble partiellement co-localiser avec des marqueurs pré-synaptiques excitateurs et inhibiteurs, respectivement, VGLUT1 et VGAT mais leur co-localisation n'a pas été quantifiée (Figure 12) (Pinatel et al., 2015). De plus, une forte co-localisation est observée avec les terminaisons pré-synaptiques GAD65-positives, apposées à des clusters géphyrine, caractéristiques du compartiment post-synaptique inhibiteur (Pinatel et al., 2015). L'ensemble de ces résultats tendent vers une localisation de CASPR2 au niveau du compartiment pré-synaptique inhibiteur. Cependant, des études plus approfondies sont nécessaires afin de confirmer cette hypothèse.

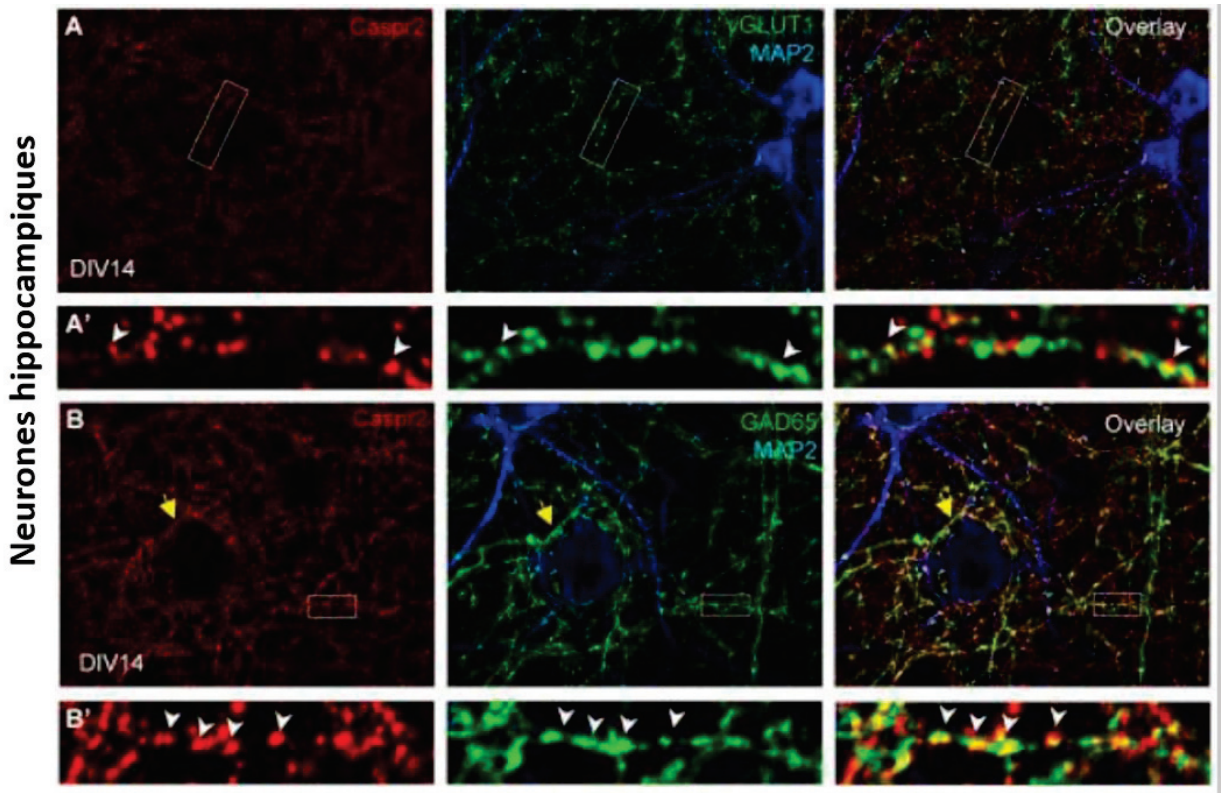

Figure 12 : CASPR2 à la synapse (Pinatel et al., 2015). Marquage de CASPR2 avec les anticorps de patients dans des cultures de neurones hippocampiques à DIV14. **A)** CASPR2 co-localise partiellement avec le marqueur du compartiment pré-synaptique excitateur VGLUT1. **B)** CASPR2 co-localise partiellement avec le marqueur du compartiment pré-synaptique inhibiteur GAD-65.

C. Rôle de CASPR2 dans le développement du système nerveux

En accord avec la présence de CASPR2 durant le développement du système nerveux et plus particulièrement dans les neurones inhibiteurs, de nombreux résultats suggèrent un rôle majeur de CASPR2 dans la mise en place du réseau neuronal inhibiteur.

1. A l'échelle du réseau neuronal

Les souris invalidées pour le gène *Cntnap2* codant pour CASPR2 présentent des défauts de migration des neurones corticaux avec la présence notamment de neurones ectopiques dans le corps calleux (Figure 13A) ainsi que des défauts de projection des neurones corticaux dans le cortex somato-sensoriel (Peñagarikano et al., 2011). Associés à ces défauts, les souris présentent une activité neuronale asynchrone qui résulterait probablement d'un dysfonctionnement du réseau plutôt que d'une activité neuronale anormale *per se* (Peñagarikano et al., 2011).

Un autre paramètre observé chez ces souris KO de 14 à 30 jours est un déficit de certaines sous-populations d'interneurones GABAergiques inhibiteurs dans le striatum, l'hippocampe et le cortex somato-sensoriel (Figure 13B). Ce déficit ne serait pas dû à un défaut de production/migration ou survie mais plutôt à un défaut de différenciation ou d'activité de ces neurones (Peñagarikano et al., 2011 ; Vogt et al., 2017). En accord avec ce résultat, il a été proposé que CASPR2 pourrait réguler, de façon intrinsèque, les propriétés électrophysiologiques des interneurones inhibiteurs corticaux, parvalbumine-positifs, (Vogt et al., 2017).

En corrélation avec un défaut d'inhibition, l'enregistrement de cellules pyramidales de la région CA1 sur des tranches aigües d'hippocampe de souris KO, révèle une altération de la transmission inhibitrice au niveau du compartiment périsomatique (Figure 13C) (Jurgensen et Castillo, 2015). Cette altération ne serait pas liée à une réduction du relargage de neurotransmetteurs mais plus vraisemblablement à un déficit en interneurones parvalbumine-positifs qui contactent majoritairement la région périsomatique des neurones enregistrés (Jurgensen & Castillo, 2015). Des résultats allant dans le même sens, à savoir, une réduction de l'inhibition phasique et tonique, ont été obtenus sur des neurones pyramidaux des couches 2/3 du cortex visuel issus de tranches de cerveau prélevées chez les souris CASPR2 KO adultes (6-8 semaines) (Bridi et al., 2017). Par ailleurs, chez ces souris, ni la transmission excitatrice, ni les propriétés des potentiels d'action (PA) ne se trouvent altérés (Bridi et al., 2017). Dans l'ensemble, ces résultats suggèrent un rôle prépondérant de CASPR2 dans la mise en place du réseau inhibiteur.

A contrario, dans une étude récente, seuls des défauts d'excitation du réseau neuronal ont été observés chez les souris *Cntnap2* KO, sans défauts de migration ou du nombre de neurones inhibiteurs (Scott et al., 2017). Le modèle expérimental étant très proche des études précédentes (souris *Cntnap2* KO, âge et populations de neurones étudiées), de telles différences dans les résultats restent difficilement interprétables.

Enfin, une étude révèle à la fois des défauts d'inhibition et d'excitation dans des cultures de neurones invalidés pour CASPR2 après 4 jours *in vitro* (Anderson et al., 2012). Un point intéressant de cette étude est l'effet opposé de l'invalidation de CASPR2 comparé à TAG-1. En effet, l'invalidation de CASPR2 diminue l'amplitude des courants excitateurs post-synaptiques spontanés, alors que celle de TAG-1 induit un effet opposé résultant d'une augmentation de la durée du signal excitateur (Figure 13D) (Anderson et al., 2012). Il est

pour l'instant difficile d'interpréter de tels résultats mais il est possible que CASPR2 et TAG-1 exercent des fonctions opposées sur l'excitabilité neuronale.

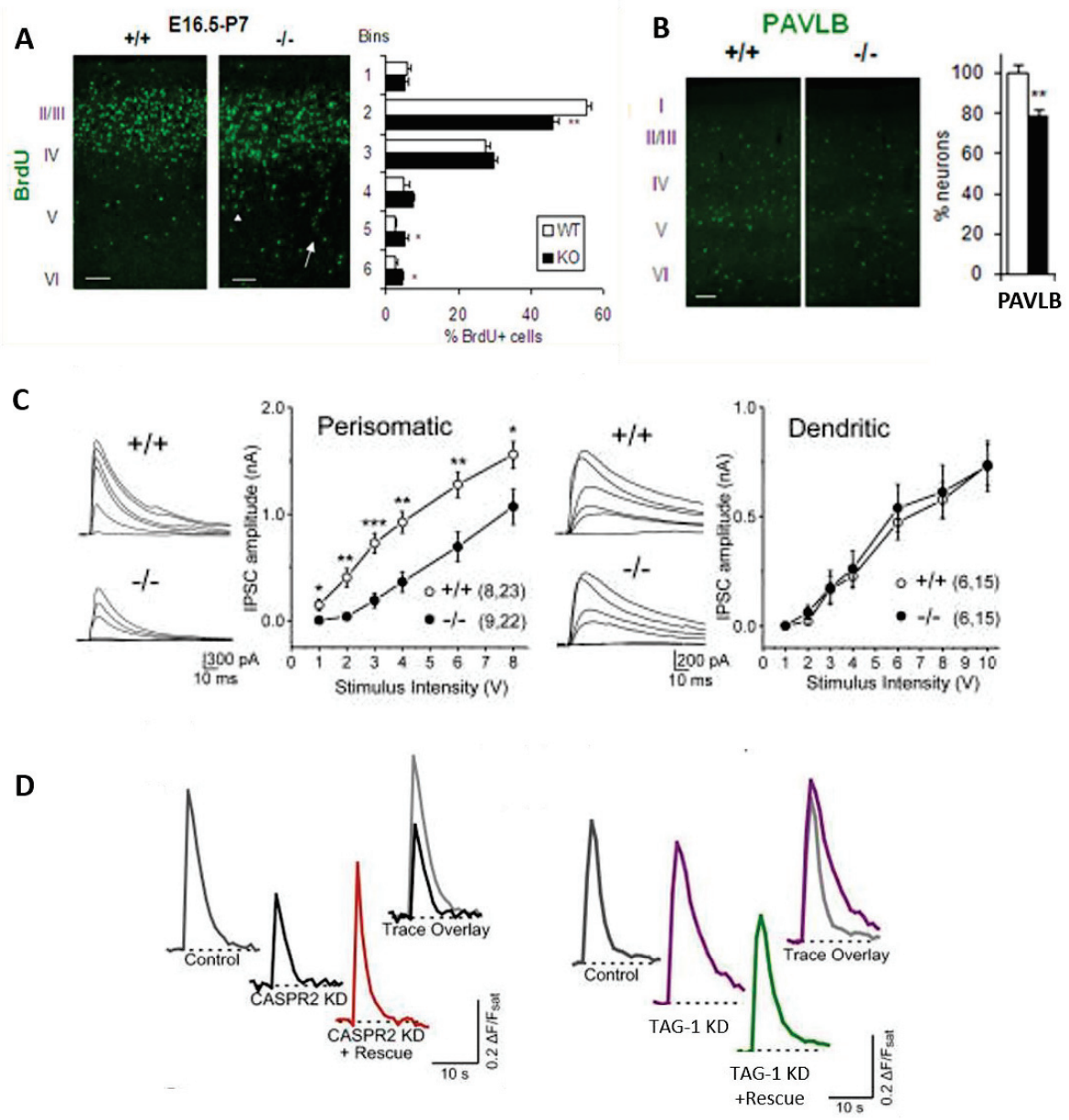

Figure 13 : Fonction de CASPR2 dans le développement du système nerveux. A) Analyse de la migration des neurones. Le BrdU injecté à E16,5 est marqué à P7. Les neurones sont distribués anormalement dans les couches profondes du cortex de souris *Cntnap2* KO (flèches, Peñagarikano et al., 2011). **B)** L'analyse de l'expression du marqueur parvalbumine (PAVLB) à P14 dans le cortex somatosensoriel montre une diminution du signal chez les souris *Cntnap2* KO (Peñagarikano et al., 2011). **C)** Courbes entrée/sortie et traces représentatives des courants post-synaptiques inhibiteurs évoqués périsomatiques et dendritiques dans les cellules pyramidales de la région CA1 de l'hippocampe. L'amplitude des courants post-synaptiques inhibiteurs périsomatiques est diminuée dans les souris KO (Jurgensen et Castillo, 2015). **D)** Mesure du signal Ca2+ somatique, après induction de l'activité neuronale dans des cultures invalidées pour CASPR2 ou TAG-1. L'invalidation de CASPR2 induit une diminution de l'amplitude des signaux Ca2+ durant l'activité neuronale

qui est rétablie par l'expression de CASPR2. L'invalidation de TAG-1 induit une augmentation de la durée du signal qui est restaurée par l'expression de TAG-1 (Anderson et al., 2012).

2. A l'échelle du neurone

Plusieurs études suggèrent que CASPR2 jouerait un rôle dans la pousse des neurites. Ainsi, il a été montré, à partir de cultures de neurones corticaux, que l'absence d'expression de CASPR2 induirait une diminution de la longueur des axones dès DIV3 (Canali et al., 2018). De plus, des défauts d'arborisation dendritique sont également observés à des stades plus tardifs (DIV14-18) sur des neurones corticaux en culture invalidés pour CASPR2 à DIV4 (Figure 14) (Anderson et al., 2012).

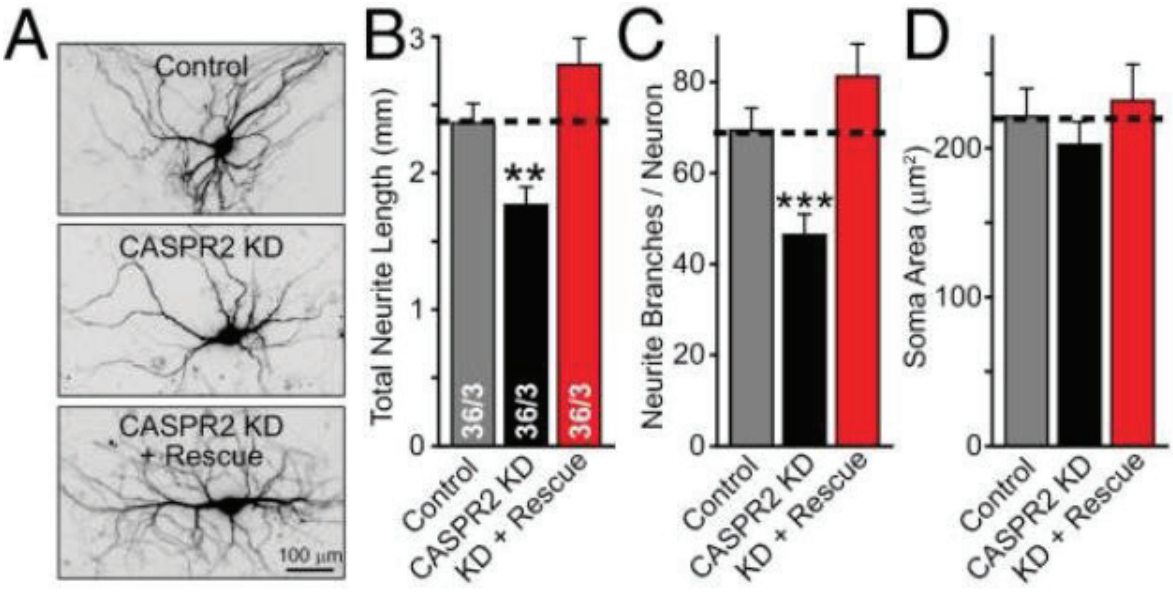

Figure 14 : Fonction de CASPR2 dans l'arborisation dendritique (Anderson et al., 2012). A) Image représentative de l'arborisation dendritique lors de l'invalidation de CASPR2. **B)** L'invalidation de CASPR2 induit une diminution de la longueur totale des neurites. **C)** L'invalidation de CASPR2 induit une diminution du nombre de branchements par neurone. **D)** L'invalidation de CASPR2 n'impacte pas l'aire du soma. Les paramètres analysés chez les souris KD pour CASPR2 reviennent à la normale en restaurant son expression.

3. A l'échelle de la synapse

Si de nombreuses études montrent un impact de CASPR2 sur la formation des synapses, il n'en demeure pas moins qu'elles divergent sur certains points. Des résultats *in vivo* et *in vitro* montrent une diminution du nombre d'épines dendritiques (caractéristique du compartiment post-synaptique excitateur) chez les souris *Cntnap2* KO (Gdalyahu et al., 2015 ; Varea et al., 2015). Ce défaut n'a cependant pas été retrouvé sur des cultures de

neurones invalidés pour CASPR2 à DIV4 (Anderson et al., 2012). Ce résultat pourrait s'expliquer par la présence de CASPR2 dans les neurones en culture en différenciation avant le *knockdown* contrairement aux modèles KO. Néanmoins, dans cette étude, la largeur de la tête des épines dendritiques, qui peut être corrélée avec la maturité de la synapse, se révèle être plus petite à DIV14-18, suggérant un défaut de maturation des synapses (Figure 15A) (Anderson et al., 2012). Au contraire, une autre étude réalisée sur des cultures de neurones corticaux *Cntnap2* KO montre que le ratio largeur/longueur de la tête est augmenté (Figure 15B) (Varea et al., 2015). Dans la mesure où cet effet s'accompagne d'une diminution du nombre d'épines (Figure 15B), il est possible que les synapses restantes se retrouvent renforcées par un effet d'homéostasie, ce qui ne serait pas le cas dans l'étude de Anderson (2012).

Enfin, une étude comparative sur la dynamique de formation des synapses *in vivo* montre que l'absence de CASPR2 n'impacte pas la formation de nouvelles épines dendritiques mais augmente leur élimination (Figure 15C). Ce résultat pointe un défaut de stabilisation des synapses chez les souris déficientes en CASPR2 (Gdalyahu et al., 2015). Ces altérations, qui expliqueraient la diminution du nombre d'épines chez ces souris, pourraient être dues à un défaut de trafic des récepteurs AMPA vers la synapse, observés chez les souris *Cntnap2* KO (Varea et al., 2015).

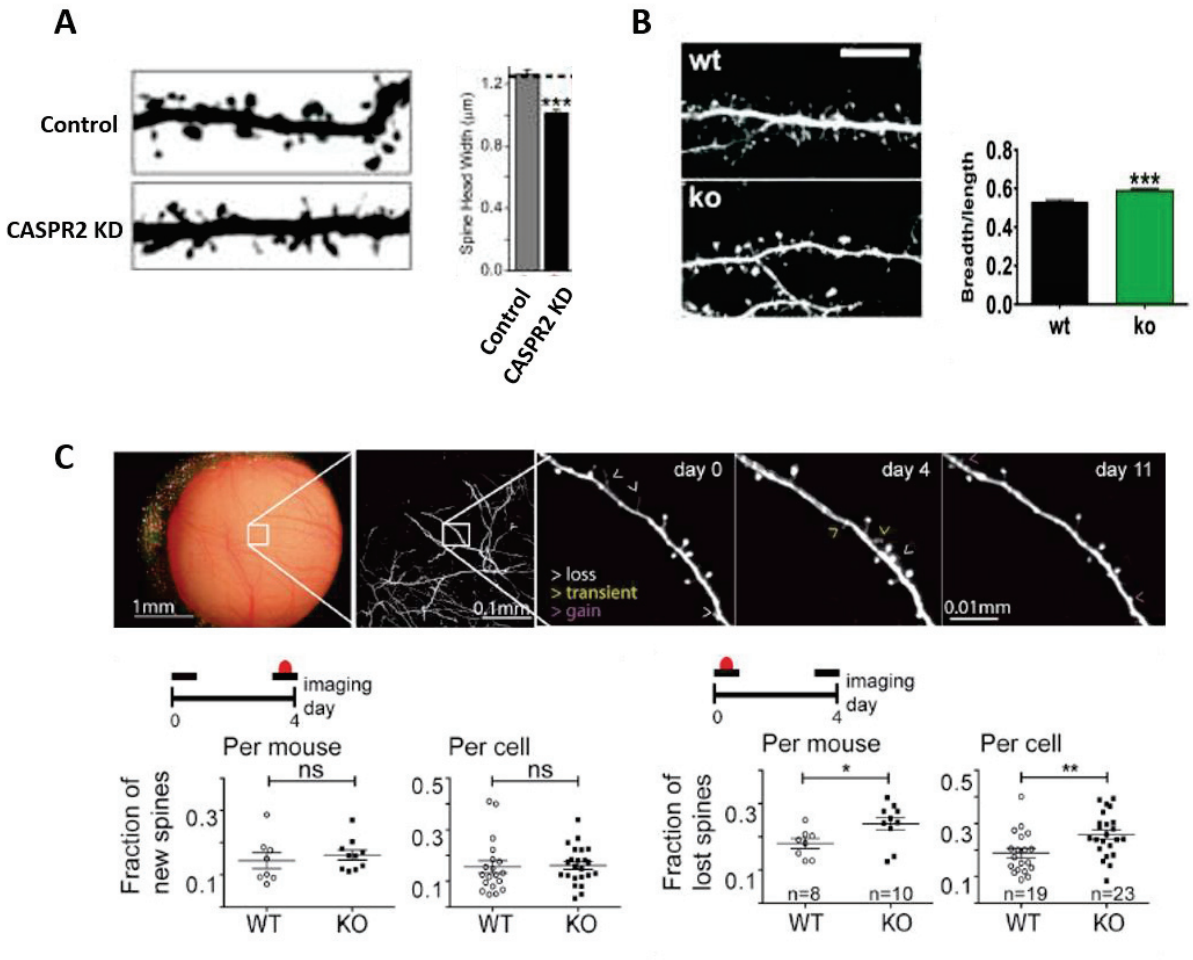

Figure 15 : CASPR2 dans le développement synaptique. A) L'invalidation de CASPR2 dans des neurones corticaux en culture à DIV4 induit une diminution de la largeur de la tête des épines (Anderson et al., 2012). **B)** Dans les neurones corticaux CASPR2 KO en culture, la largeur de la tête des épines est augmentée (Varea et al., 2015). **C)** Etude de la dynamique de formation des synapses *in vivo.* Dans les souris KO, alors qu'aucune différence du nombre d'épines nouvelles n'est observée, on note une augmentation du nombre d'épines éliminées (Gdalyahu et al., 2015).

D. Les protéines du complexe VGKC

Un des points les plus marquants quant à l'enrichissement de CASPR2 au segment initial de l'axone et à la région juxtaparanodale, est sa proximité constante avec TAG-1 et les canaux potassiques voltage-dépendants (VGKC) Kv1.1 et Kv1.2 (Figure 11) (Poliak et al., 1999).

1. Les canaux potassiques Kv1

Les canaux potassiques voltage-dépendants (Kv) permettent la sortie des ions potassium à la suite d'une dépolarisation de la membrane neuronale permettant ainsi sa

repolarisation (Figure 16) (revue, Rasband, 2010). Par ce rôle, les canaux potassiques régulent le potentiel de repos membranaire ainsi que la durée et la fréquence des potentiels d'action (PA), impactant par conséquent le relargage de neurotransmetteurs à la synapse (Ovsepian et al., 2016).

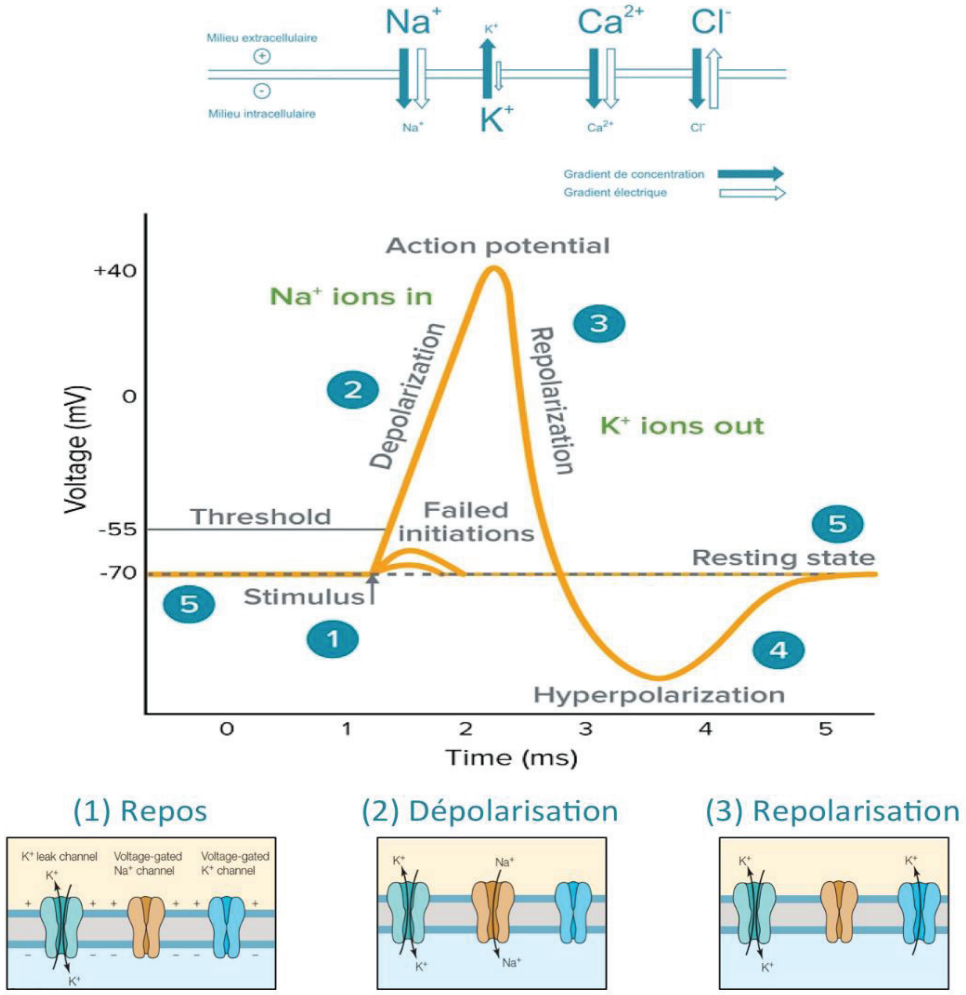

Figure 16 : Le potentiel d'action. A) Répartition des ions de chaque côté de la membrane neuronale, avec une forte concentration d'ions Na+ extracellulaires et K+ intracellulaires. Au repos, la membrane est polarisée à un potentiel de -70mV. **B)** Courbe du potentiel d'action. Au potentiel de repos, les canaux ioniques voltage-dépendants ne laissent pas passer d'ions (1). À la suite d'un stimulus, les canaux sodiques voltage-dépendants s'ouvrent pour permettre le passage des ions Na+ dans la cellule induisant sa dépolarisation (2). Puis, les canaux potassiques voltage dépendants s'ouvrent pour laisser sortir les ions K+ de la cellule permettant sa repolarisation et son retour au potentiel de repos (3).

(a) Structure des canaux potassiques Kv1

Les canaux Kv1 se composent d'une combinaison de quatre sous-unités α (Kv1.1 à Kv1.8 codés par les gènes KCNA 1 à 8) associées en homo- ou hétérotétramères ainsi que de quatre sous-unités β intracellulaires (Kvβ1, β2 et β3) (Figure 17A) (Ovsepian et al., 2016).

Des études suggèrent que les canaux contenant la sous-unité Kv1.2 représentent 85% des canaux liées à la dendrotoxine (toxine ciblant les canaux Kv1.1, Kv1.2 et Kv1.6) contre 47% pour la sous-unité Kv1.1, 16% pour la sous-unité Kv1.6 et 8% pour la sous-unité Kv1.4 (Ovsepian et al., 2016). Ces données suggèrent que la plupart des sous-unités Kv1.1, Kv1.4 et Kv1.6 sont associées en hétérotétramères avec la sous-unité Kv1.2 et que les sous-unités les plus abondantes sont Kv1.2 et Kv1.1 (Ovsepian et al., 2016).

Chaque sous-unité α possède 6 segments transmembranaires (S1-S6) reliés par des boucles hydrophiles intra- et extracellulaires (Figure 17A) (Grizel et al., 2014 ; Ovsepian et al., 2016). Le segment quatre (S4), chargé positivement, est sensible aux changements de potentiel. Lors d'une dépolarisation, celui-ci est déplacé vers l'extérieur induisant un changement de conformation à l'origine de l'ouverture du canal. L'espace entre les segments S5 et S6, lui, forme le pore.

Les sous-unités β, quant à elles, se lient à la région N-terminale intracellulaire des sous-unités α (domaine T1) et régulent l'expression du canal ainsi que son inactivation (Long et al., 2005 ; revue Grizel et al., 2014). En effet, les sous-unités β possèdent une structure appelée « *ball and chain* » constituée d'un domaine en forme de boule, capable de bloquer rapidement le canal et de l'inactiver (Figure 17B) (Rettig et al., 1994 ; Peters et al., 2009). Ainsi, le canal peut se trouver sous trois états : fermé, ouvert ou inactivé par le « ball and chain » (Figure 17C).

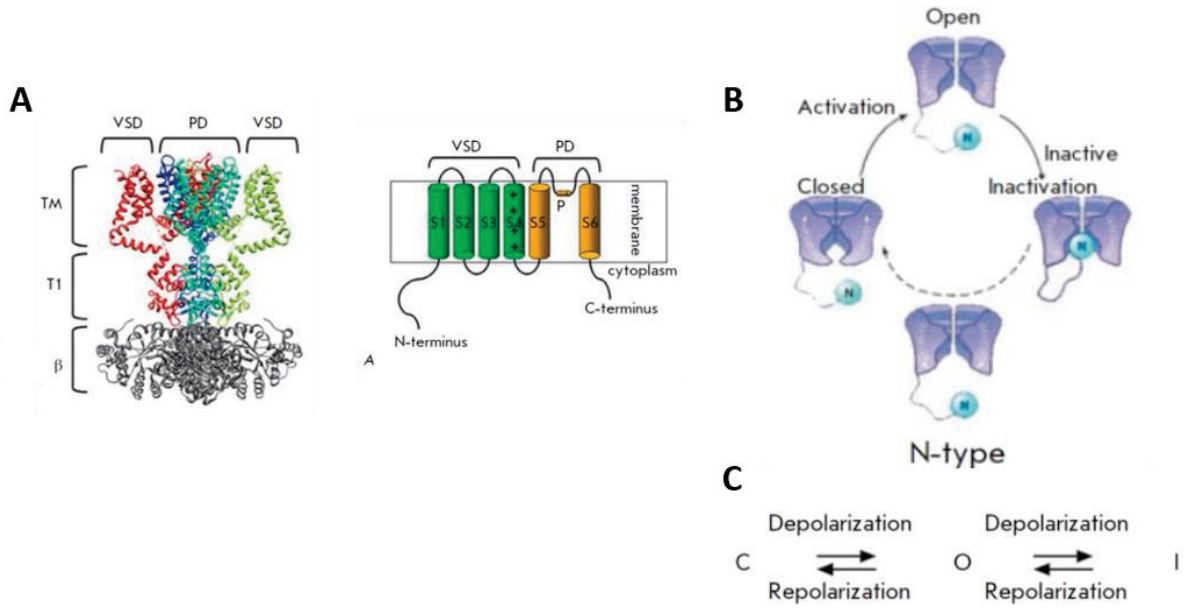

Figure 17 : Structure des canaux potassiques Kv1 (Grizel et al., 2014). A) Schéma d'une sous-unité α des canaux Kv et structure en cristallographie du canal Kv1.2 homo-tétramérique en complexe avec la sous-unité β. La sous-unité α se compose de 6 segments transmembranaires S1-S6 d'une boucle P formant le pore. **B)** Inactivation de type N. La boule d'inactivation pénètre le pore et bloque physiquement le passage des ions après activation du canal. **C)** Schéma des transitions conformationnelles du canal Kv. C : Closed, O : Open, I : Inactivated.

Enfin, si les canaux potassiques présentent de courtes régions extracellulaires limitant leur interaction avec des partenaires extracellulaires, ceux-ci possèdent néanmoins des régions intracellulaires permettant par exemple leur liaison à des protéines d'échafaudage. Entre autres, Kv1.1 et Kv1.2 possèdent un domaine de liaison PDZ dans leur partie cytoplasmique C-terminale qui permet leur liaison avec les protéines PSD95 et 93 (Kim et al., 1995 ; Ogawa et al., 2008).

(b) Expression des canaux potassiques Kv1

La majorité des canaux Kv1 sont des hétérotétramères dont l'expression dépend des sous-unités qui les composent (Manganas et Trimmer, 2000). Par exemple, la sous-unité Kv1.4 et les sous-unités β favorisent l'expression en surface ; au contraire la sous-unité Kv1.1 a tendance à retenir le canal dans le réticulum endoplasmique (RE). La sous-unité Kv1.2, quant à elle, est répartie entre surface et RE (Shi et al., 1996 ; Manganas et Trimmer, 2000).

Dans le système nerveux central, les Kv1 sont exprimés au niveau du soma, de l'axone, des dendrites et des terminaisons synaptiques mais leur composition varie en

fonction de leur localisation (Figure 18). Les sous-unités Kv1.1/Kv1.2 sont particulièrement enrichies dans les terminaisons des cellules en panier inhibitrices du cervelet (Figure 18A1 et A2), aux nœuds de Ranvier (Figure 18B1 et B2), au segment initial (Figure 18C1 et C2) et au soma des cellules dans les couches profondes du cervelet (Figure 18D1 et D2) (Rasband et al., 2010, Ovsepian et al., 2016). Dans l'hippocampe, les sous-unités Kv1.1 et 1.2 sont préférentiellement exprimées au niveau des terminaisons axonales de la voie perforante, ainsi que dans les terminaisons des fibres moussues et des collatérales de Schaffer au niveau des régions CA3 et CA1 (Ovsepian et al., 2016).

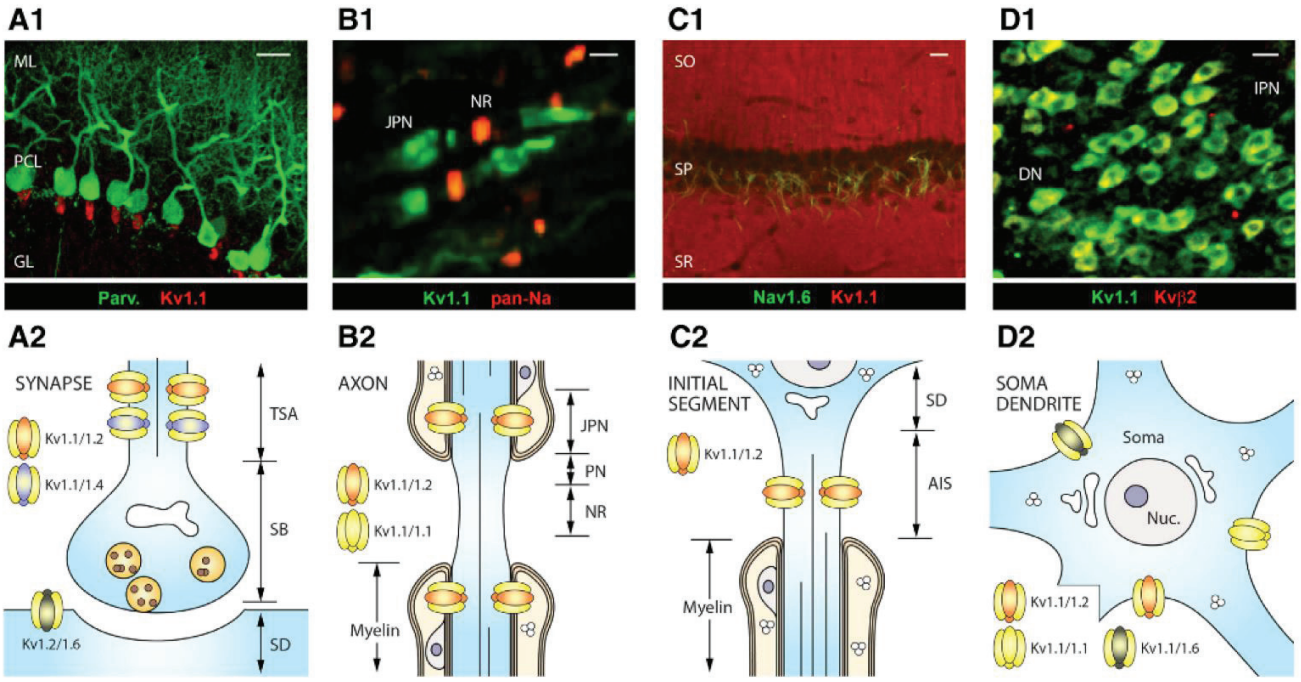

Figure 18 : Distribution sub-cellulaire des canaux Kv1 (Ovsepian et al., 2016). Les sous-unités Kv1.1/Kv1.2 sont particulièrement enrichies dans les terminaisons des cellules en panier du cervelet **(A)** aux nœuds de Ranvier **(B)**, au segment initial **(C)** et au soma des cellules dans les couches profondes du cervelet **(D)**.

(c) Fonction des canaux potassiques Kv1

La fonction des canaux potassiques Kv1 et en particulier Kv1.1 et Kv1.2 a été largement étudiée grâce aux modèles knockout et aux toxines bloquantes telles que la dendrotoxine ou la 4-aminopyridine (4-AP) (revue Lai & Jan, 2006). Les deux modèles montrent que la perturbation des canaux potassiques induit une hyperexcitabilité neuronale accompagnée de crises épileptiques (Velluti et al., 1987 ; Smart et al., 1998). En effet, en présence de 4-AP ou de DTX, l'excitabilité neuronale est augmentée : le seuil de déclenchement des potentiels d'actions est diminué et leur fréquence est doublée (Bekkers

et Delaney, 2001). De plus, le blocage des Kv1 par la dendrotoxine augmente la durée des potentiels d'action (Figure 19) (Weller et al., 1985 ; revue Jan et Jan, 2012). Cette augmentation conduit à une augmentation de la concentration pré-synaptique en calcium associée à une augmentation du relargage des neurotransmetteurs (Geiger et Jonas, 2000 ; Revue Kress et Mennerick, 2009).

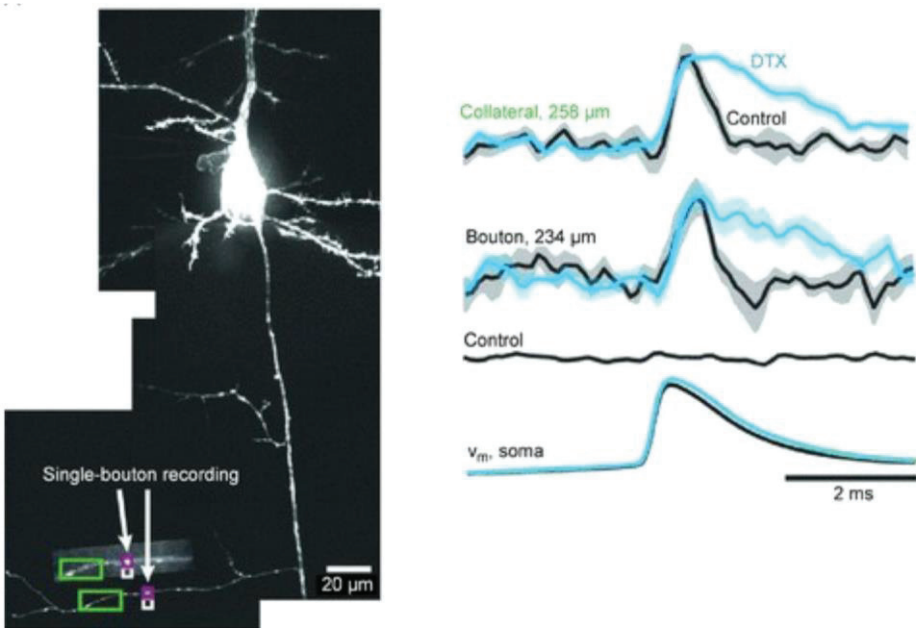

Figure 19 : Fonction des canaux Kv1.1 et Kv1.2 (Jan et Jan, 2012). Enregistrement d'un neurone pyramidal dans la couche 5 du cortex. L'application de DTX ralentit le potentiel d'action mesuré au niveau des collatérales d'axones et des boutons pré-synaptiques mais impacte peu le potentiel d'action au niveau du soma.

Aux nœuds de Ranvier, le rôle des canaux potassiques Kv1.1 et Kv1.2 est moins clair. Il a été montré que ceux-ci jouent un rôle avant et pendant le processus de myélinisation afin de réguler l'excitabilité neuronale lors de ces phases clé du développement (Vabnick et al., 1999 ; Devaux et al., 2002). Une fois les axones myélinisés, les canaux se retrouvent électriquement isolés sous la gaine de myéline et l'ajout de toxines bloquantes n'impacte plus la forme des PA à ce stade (Kocsis et Waxman, 1980 ; Devaux et al., 2002).

(d) Pathologies associées aux Kv1

Les pathologies associées aux canaux potassiques sont de deux types : auto-immunes avec les anticorps anti-VGKC et génétiques avec des mutations dans les gènes codant pour les sous-unités α et β du canal. Le plus souvent, ces mutations sont associées à des troubles

de l'excitabilité neuronale tel que l'épilepsie ou l'ataxie cérébelleuse de type 1 (EA1) (review D'Adamo et al., 2013).

Chez la souris, le KO de *Kcna1* ou *Kcna2* induit deux phénotypes épileptiques distincts. Les souris *Kcna1* KO présentent des épilepsies de type temporal avec des crises chroniques récurrentes dont 50% survivent jusqu'à l'âge adulte (Smart et al., 1998) ; les souris *Kcna2* KO présentent quant à elles, de sévères crises généralisées et ne survivent pas au-delà de 19 jours (Brew et al., 2007 ; review Robbins et Tempel 2012).

2. La protéine d'adhésion cellulaire, TAG-1

TAG-1 (Transient Axonal Glycoprotein-1), aussi connue sous le nom de contactine-2 est une protéine d'adhésion cellulaire de la superfamille des immunoglobulines (IgSF) (Furley et al., 1990).

(a) Structure de TAG-1

La protéine TAG-1, se compose de six domaines immunoglobuline (Ig ; domaines caractéristiques des protéines de la IgSF) et de quatre domaines fibronectine III (Fn) extracellulaires mais ne possède pas de domaine intracellulaire (Figure 20A) (Zuellig et al., 1992). Elle est liée à la membrane par une ancre GPI (Glycosylphosphatidylinositol) favorisant sa localisation au sein des radeaux lipidiques (microdomaines membranaires riches en cholestérol et sphingolipides, insolubles dans les détergents doux). Elle peut également être trouvée sous forme soluble, clivée de son ancre GPI par l'enzyme BACE1 (Harel et Futerman et al., 1996 ; Gautam et al., 2014).

Des études de la protéine entière en microscopie électronique et de certaines régions en cristallographie ont permis de mieux comprendre la structure 3D de TAG-1. Sous forme soluble, TAG-1 est repliée sur elle-même dans une conformation dite « fermée » (Figure 20B) (Rader et al., 1996) ; cette conformation serait rendue possible par des interactions entre les domaines Ig1-4 N-terminaux et Fn3-4 C-terminaux (Figure 20B) (Freigang et al., 2000). De plus, la cristallographie montre que les quatre premiers domaines Ig de TAG-1 sont repliés en forme de fer à cheval grâce à des interactions entre les domaines Ig1/Ig4 et Ig2/Ig3 (Figure 20B) (Mörtl et al., 2007). Par ailleurs, par l'intermédiaire de ces domaines Ig1-4, TAG-1 est capable d'interagir avec elle-même en trans (Figure 20C) (Freigang et al., 2000 ; Mörtl et al., 2007). Cette interaction homophilique en trans serait favorisée par une interaction homophilique en cis à travers les domaines Fn (Figure 20C) (Kunz et al., 2002).

Ainsi, il a été suggéré que la protéine pouvait arborer deux conformations : « fermée », repliée sur elle-même et « ouverte », dépliée (Figure 20C) (Kunz et al., 2002). Si la conformation « ouverte » de TAG-1 n'a jamais été observée en microscopie, elle est cependant supposée médier les contacts homophiliques en trans en permettant une meilleure présentation des domaines Ig1-4. De plus, des études portant sur différents mutants TAG-1 ont montré que les mutants ΔIg5 et ΔIg6 ont tendance à s'accumuler aux contacts cellulaires (Figure 20D) (Rader et al., 1996 ; Kunz et al., 2002). Pour cette raison, il a été proposé que ces mutants, en empêchant le repliement de la protéine, favoriseraient la forme ouverte de TAG-1 et les contacts homophiliques en trans.

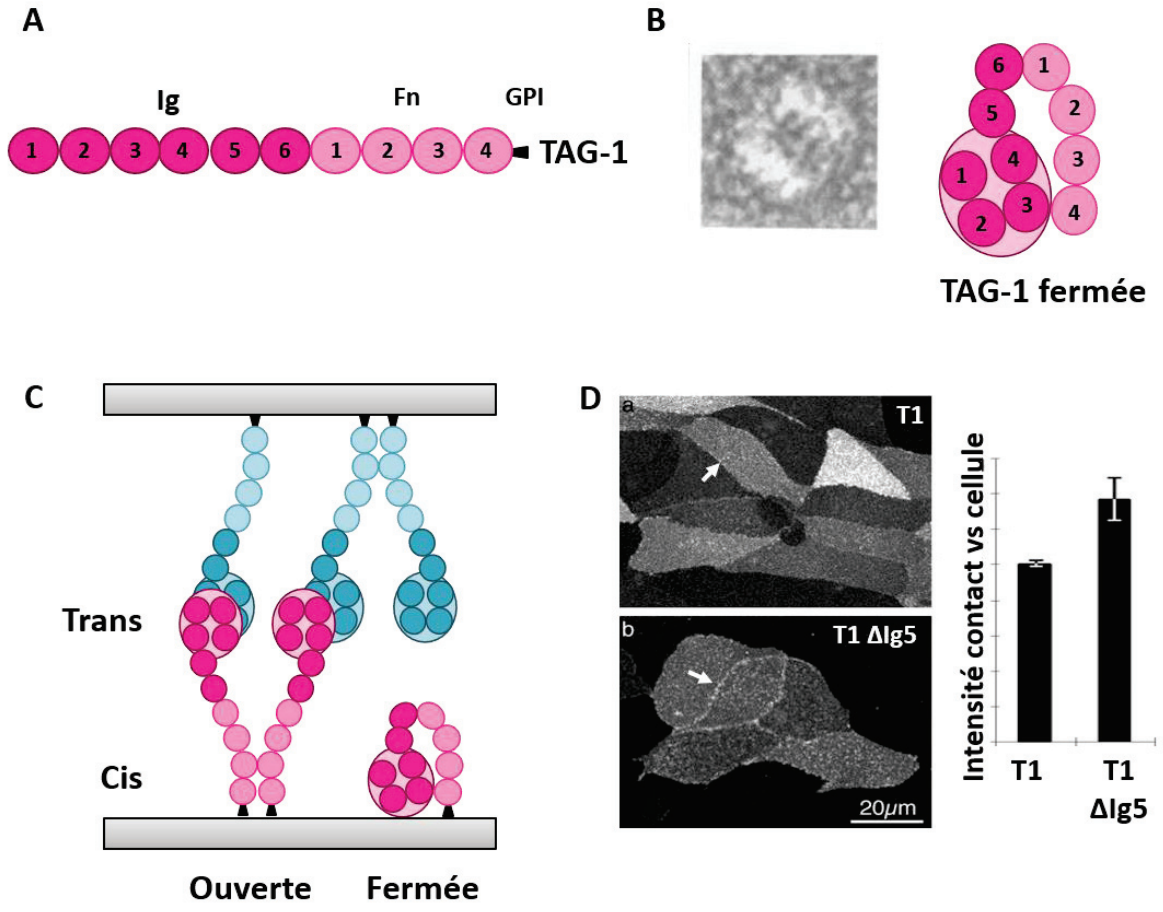

Figure 20 : Structure et fonction de TAG-1. **A)** TAG-1 est composée de six domaines immunoglobuline (Ig) et de quatre domaines fibronectine III (Fn) extracellulaires. Elle est liée à la membrane par une ancre GPI et peut également se trouver sous forme soluble. **B)** Structure de TAG-1 en microscopie électronique (Rader et al., 1996). Sous sa forme soluble TAG-1 est repliée sur elle-même, supposément par des interactions entre ses domaines Ig1-4 et ses domaines Fn3-4. **C)** A la surface des cellules, TAG-1 se trouverait sous deux conformations « ouverte » et « fermée ». En conformation ouverte, TAG-1 est capable de médier des interactions homophiliques en trans et en cis, permettant ainsi l'adhésion

cellulaire. **D)** TAG-1 et son mutant ΔIg5 sont transfectés dans des cellules COS. Les flèches montrent des zones de contact entre deux cellules transfectées. La densité de TAG-1 aux contacts entre les cellules est comparé dans les deux conditions. Le mutant ΔIg5 augmente l'intensité de TAG-1 aux contacts et favoriserait les interactions homophiliques en trans (Kunz et al., 2002).

(b) Expression de TAG-1

TAG-1 est exprimée dans de nombreuses populations de neurones dans le système nerveux central et périphérique dès les stades précoces du développement (E11) (Karagogeos et al., 1991). Elle est notamment exprimée dans les cellules nerveuses du ganglion spinal (DRG), dans la couche moléculaire du cervelet, dans le corps calleux et dans les commissures antérieure et hippocampale (Wolfer et al., 1994). Son patron d'expression varie en fonction du stade de développement et du type cellulaire, suggérant son implication dans une multitude de mécanismes durant la mise en place du réseau neuronal (Wolfer et al., 1994). Notamment, TAG-1 est exprimée de façon transitoire à la surface des prolongements axonaux des interneurones commissuraux et des motoneurones en croissance (Dodd et al., 1988). Initialement, elle est localisée dans les cônes de croissance puis le long de l'axone (Vogt et al., 1996), suggérant un rôle de TAG-1 dans la croissance axonale. Chez l'adulte, TAG-1 est présente au niveau des cellules granulaires du cervelet, des cellules mitrales du bulbe olfactif et des cellules pyramidales des régions CA1 et CA3 de l'hippocampe (Wolfer et al., 1998). En lien avec ce patron d'expression, il a été suggéré que TAG-1 pourrait jouer un rôle dans la plasticité neuronale dans le système nerveux mature (Wolfer et al., 1998).

TAG-1 est également exprimée dans les cellules de Schwann (SNP) et les oligodendrocytes (SNC) à partir de P5 où son expression augmente jusqu'à l'âge adulte (Traka et al., 2002). Ces cellules gliales forment une gaine de myéline sur les axones de certaines populations de neurones et permettent la conduction rapide des message nerveux.

(c) Fonctions de TAG-1 dans le système nerveux

Au cours du développement, TAG-1 joue un rôle dans la migration neuronale, la pousse et le guidage axonal. L'étude de ses fonctions a été réalisée grâce aux modèles de KO mais également grâce à l'utilisation d'anticorps bloquants ou de la forme soluble de TAG-1, tous deux capables d'empêcher les interactions TAG-1/TAG-1 homophiliques en trans

(Tsiotra et al., 1996 ; Kunz et al., 2002). Ainsi, la perturbation de TAG-1 par les anticorps ou la protéine soluble lors du développement *in vivo* ou *in vitro* induit des erreurs de guidage axonal des neurones commissuraux (Stoeckli et al., 1995 ; 1997) et de migration des interneurones GABAergiques corticaux (Denaxa et al., 2001).

Un point clé de la fonction de TAG-1 est sa capacité à médier l'adhésion cellulaire en recrutant de nombreux partenaires (Furley et al., 1990 ; Stoeckli et al., 1991). Par exemple, l'interaction de TAG-1 en trans avec NrCAM permet la pousse et le guidage axonal (Lustig et al., 1999). D'autre part, l'interaction de TAG-1 avec NgCAM (orthologue de L1 chez le poulet) en cis par ses domaines Ig1-4 en conformation fermée, favorise la croissance axonale et le recrutement de protéines d'échafaudage (comme l'ankyrine) dans les zones de contact cellulaire TAG-1/TAG-1 (Figure 21) (Buchstaller et al., 1996 ; Malhotra et al., 1998).

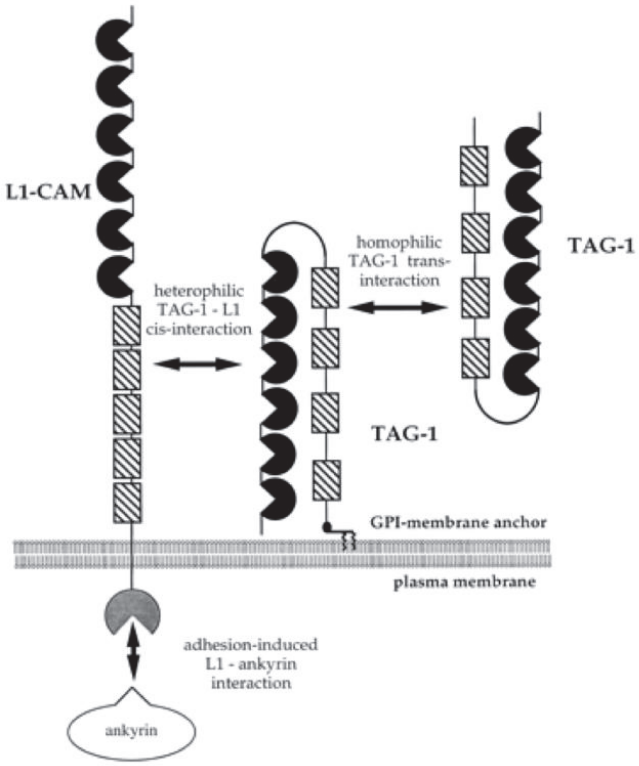

Figure 21 : Modèles d'interaction TAG-1/ L1 (NgCAM) (Malhotra et al., 1998). L'interaction homophilique en trans entre les molécules TAG-1 exprimées dans différentes cellules serait médiée par les domaines Fn de TAG-1 alors que les domaines Ig de TAG-1 (en conformation fermée) interagiraient avec L1 en cis. Les interactions TAG-1 en trans sont nécessaires pour le recrutement de l'ankyrine par la protéine L1.

Dans les axones myélinisés, la protéine TAG-1 exprimée dans les cellules gliales myélinisantes assure le rassemblement des canaux potassiques aux JXP en collaboration avec les protéines TAG-1 et CASPR2 exprimées dans l'axone (Traka et al., 2003) et sera détaillée dans le prochain chapitre.

Dans les axones non myélinisés, il a été montré que TAG-1 est capable de former des clusters avec les canaux Kv1.2. Cette accumulation dépendrait de la phosphorylation d'un résidu tyrosine dans la partie C-terminale de la sous-unité Kv1.2 (Tyr458) (Gu & Gu, 2011). De plus, la perturbation de cette phosphorylation ou la perte des radeaux lipidiques induit une diminution des clusters Kv1.2/TAG-1. Dans la mesure où TAG-1 ne possède pas de domaines intracellulaires et est enrichie dans les radeaux lipidiques, les mécanismes permettant le rassemblement des canaux potassiques avec TAG-1 pourraient être régulés par ces microdomaines.

Enfin, il a été montré que dans des cellules HEK transfectées, TAG-1 était capable de moduler l'activité des Kv1.2 en diminuant leur seuil d'activation et en les rendant moins dépendants du voltage. Ces changements, induiraient ainsi une diminution de l'excitabilité de ces cellules (Gu & Gu, 2011).

(d) Pathologies associées à TAG-1

Des anticorps dirigés contre TAG-1 ont été trouvés chez des patients atteints de sclérose en plaques (Derfuss et al., 2009) ainsi que chez des patients atteints d'encéphalite limbique (Irani et al., 2010). Dans le cas des encéphalites limbiques, les anti-TAG-1 comme pour les anti-CASPR2, étaient initialement supposés cibler les canaux potassiques et connus sous le nom d'anti-VGKC (Irani et al., 2010).

Par ailleurs, comme pour les pathologies liées à des mutations des gènes codant pour les sous-unités Kv1.1 et 1.2, les mutations de TAG-1 sont associées à des troubles de l'excitabilité neuronale. Ainsi, des mutations du gène codant pour TAG-1 ont été identifiées chez des patients avec des tremblements myocloniques corticaux associés à une épilepsie (Stogmann et al., 2013). Les souris KO, quant à elles, présentent une susceptibilité aux crises convulsives (Fukamauchi et al., 2001) ainsi que des troubles de l'apprentissage et de la mémoire (Savvaki et al., 2008).

E. Assemblage du complexe CASPR2/TAG-1/Kv1.2

1. Assemblage du complexe au nœud de Ranvier

Au nœud de Ranvier, les protéines CASPR2, TAG-1, Kv1.1 et Kv1.2 co-localisent dans la région juxtaparanodale (Poliak et al., 2003 ; Traka et al., 2003). Chez la souris, l'invalidation des gènes codant pour les protéines CASPR2 ou TAG-1, induit une perte des canaux Kv1.1 et Kv1.2 aux JXP (Figure 22A). De plus, l'invalidation de CASPR2 ou TAG-1 s'accompagne, respectivement, d'une perte de l'enrichissement des protéines TAG-1 et CASPR2 aux JXP (Figure 22B) (Poliak et al., 2003 ; Traka et al., 2003 ; Scott et al., 2017). L'interdépendance entre ces trois protéines suggère l'importance de l'interaction CASPR2/TAG-1 pour assurer l'enrichissement des canaux Kv1 aux nœuds de Ranvier. Alors que CASPR2 et les canaux Kv1 sont exprimées dans la membrane axonale, TAG-1 est exprimée à la fois dans l'axone et dans la glie (Figure 22B) (Poliak et al., 1999 ; Traka et al., 2002). L'interaction de TAG-1 avec CASPR2 ayant été montrée uniquement en cis (Poliak et al., 2003 ; Traka et al., 2003), il a été proposé que la protéine TAG-1 axonale interagirait en trans avec la protéine TAG-1 gliale et en cis avec CASPR2 permettant ainsi le rassemblement des canaux Kv1 aux JXP (Figure 22C).

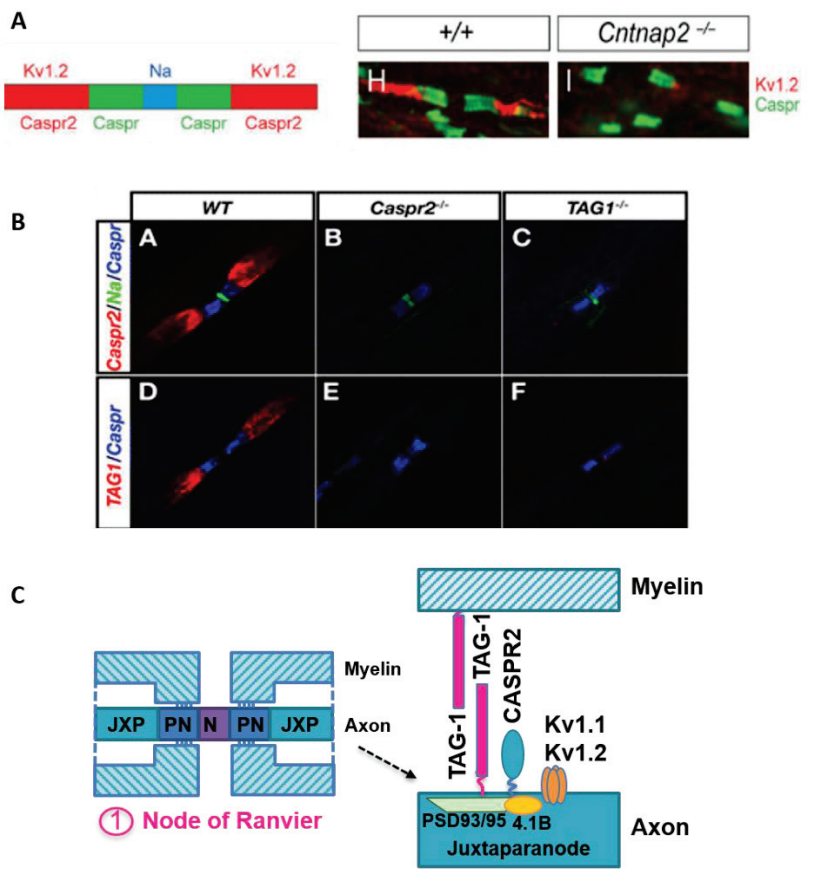

Figure 22 : Le complexe CASPR2/TAG-1/Kv1 aux JXP des nœuds de Ranvier. A) Marquage de CASPR2, CASPR et Kv1.2 aux nœuds de Ranvier (NOR) des axones myélinisés dans le

système nerveux central (Scott et al., 2017). L'enrichissement des Kv1.2 aux JXP est perdu en l'absence de CASPR2. **B)** Perte de l'enrichissement de CASPR2 et TAG-1 aux JXP dans les modèles de souris TAG-1 KO et CASPR2 KO (Horresh et al., 2008). **C)** Représentation de l'organisation des complexes VGKC au JXP (Saint-Martin et al., 2018). TAG-1 interagit en trans avec elle-même et en cis avec CASPR2, liée au cytosquelette par la protéine 4.1B. Leur association pourrait conditionner le rassemblement des canaux Kv1 au JXP.

Cette hypothèse a été ensuite remise en question par un modèle murin transgénique exprimant TAG-1 dans les cellules gliales uniquement (Tag-1-/- ; plp Tg(rTag-1)). D'après ce modèle, la protéine TAG-1 axonale serait dispensable pour la formation du complexe CASPR2/TAG-1/Kv1.2. En effet, même en l'absence de la protéine TAG-1 axonale, les trois protéines sont immunoprécipitées ensemble, prouvant leur association (Savvaki et al., 2010). De plus, les protéines CASPR2, TAG-1, Kv1.1 et Kv1.2 sont correctement localisées aux JXP. Il a ainsi été postulé que la protéine TAG-1 gliale pouvait interagir en trans avec la protéine CASPR2 axonale afin de permettre le rassemblement des canaux Kv1. En effet, en utilisant différentes conditions expérimentales, des interactions CASPR2/TAG-1 en trans ont été montrées (Savvaki et al., 2010 ; Lu et al., 2016). Néanmoins, une autre étude sur des co-cultures de neurones avec des cellules HEK293, montre au contraire que les interactions CASPR2/TAG-1 en trans ne permettent pas la formation de clusters Kv1.2 à la membrane axonale. Ces clusters se formeraient uniquement grâce aux interactions TAG-1/TAG-1 homophiliques en trans (Gu & Gu, 2011). Il reste donc des zones d'incertitudes quant aux mécanismes impliqués dans l'association entre CASPR2, TAG-1 et Kv1. Entre autres, il est possible que ces divergences dépendent de la contribution d'autres facteurs sur les protéines du complexe CASPR2/TAG-1/Kv1. Par exemple, les interactions entre CASPR2 et TAG-1 pourraient être modulées par la forme soluble de TAG-1 relarguée par les neurones et la glie (Stoeckli et al., 1991 ; Savvaki et al., 2010). La forme soluble de TAG-1 étant à priori incapable d'interagir avec la protéine CASPR2 membranaire (Poliak et al., 2003 ; Traka et al., 2003), celle-ci pourrait interagir avec la protéine TAG-1 exprimée par les cellules et empêcher l'interaction CASPR2/TAG-1 cis ou trans comme elle le fait pour l'interaction TAG-1/TAG-1 en trans.

Au sein du complexe CASPR2/TAG-1/Kv1, le meilleur candidat pour réguler la localisation du complexe est la protéine CASPR2, qui est reliée au cytosquelette par la protéine 4.1B. Plusieurs études montrent que CASPR2 est capable de moduler la localisation

de TAG-1 au sein de la cellule. En effet, dans les cellules COS, TAG-1 transfectée seule se trouve en partie dans la fraction membranaire insoluble au Triton, correspondant à la fraction des radeaux lipidiques (Figure 23A). Au contraire, CASPR2 se trouve dans la fraction soluble lourde, pouvant témoigner de son association avec les protéines du cytosquelette (Figure 23B) (Traka et al., 2003). Lorsque TAG-1 et CASPR2 sont co-exprimées dans les cellules COS, TAG-1 n'est plus retrouvée dans la fraction des radeaux lipidiques mais est présente dans la même fraction que CASPR2 (Figure 23A et B). Ainsi, CASPR2 serait capable de modifier la distribution de TAG-1 en changeant son microenvironnement et/ou en permettant le lien aux protéines du cytosquelette (Traka et al., 2003). De la même façon, sur des neurones hippocampiques en culture, TAG-1 transfectée seule forme des clusters au niveau des radeaux lipidiques (Figure 23C) (Gu & Gu, 2011). La co-expression de CASPR2 avec TAG-1 dans ces neurones, induit une perte des clusters TAG-1 qui est alors uniformément répartie le long de l'axone (Figure 23C) (Gu & Gu, 2011). A noter néanmoins que cette dernière étude est la seule à reporter un tel effet.

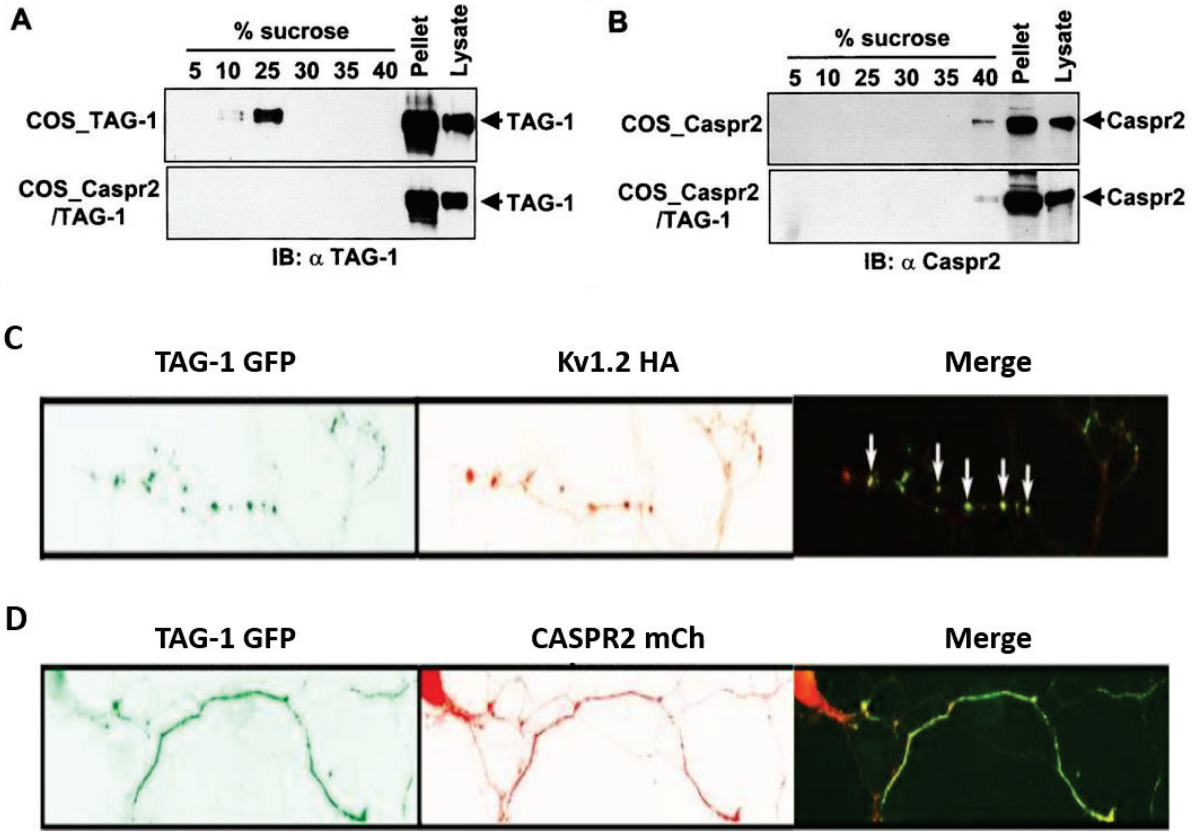

Figure 23 : Localisation de CASPR2 et TAG-1 dans différents compartiments lipidiques. A) Expression de TAG-1 dans différents compartiments lipidiques. Des cellules COS exprimant TAG-1 seul ou avec CASPR2 sont lysées avec un tampon contenant du triton X-100 et les différentes fractions sont séparées sur un gradient de sucrose. TAG-1 transfectée seule est retrouvée dans les fractions 25% de sucrose correspondant aux radeaux lipidiques et dans le

culot. En présence de CASPR2, TAG-1 est uniquement retrouvée dans le culot. **B)** Expression de CASPR2 dans différents compartiments lipidiques. CASPR2 est principalement retrouvée dans la fraction 40% de sucrose et dans le culot avec ou sans TAG-1 (Traka et al., 2003). **C)** Expression de TAG-1 et Kv1.2 dans les axones de neurones en culture. TAG-1 et Kv1.2 co-localisent et forment des clusters (flèches). **D)** Expression de TAG-1 et CASPR2 dans les axones de neurones en culture. La co-expression de CASPR2 induit une perte des clusters TAG-1 qui devient uniformément répartie sur l'axone (Gu & Gu, 2011).

De la même façon, plusieurs données montrent une interaction entre CASPR2 et les canaux potassiques. Ainsi, le domaine cytoplasmique de CASPR2 est capable de co-précipiter Kv1.2 et sa sous-unité β dans des lysats membranaires de cerveaux de rat (Poliak et al., 1999 ; Horresh et al., 2008). De plus, le domaine cytoplasmique de CASPR2 est également nécessaire pour la formation des complexes VGKC aux JXP (Figure 24A) (Horresh et al., 2008). Dans la mesure où CASPR2 et Kv1.2 possèdent tous deux des domaines de liaison au PDZ (Poliak et al., 1999), il a été initialement suggéré que leur association pourrait être médiée par une protéine commune contenant un domaine PDZ telles que les protéines PSD-93 ou PSD-95 (Poliak et al., 1999). Cependant, chez les souris invalidées pour PSD-95 (Rasband et al., 2002), PSD-93, PSD-95/93 (Horresh et al., 2008), ou chez les souris dans lesquelles le domaine de liaison au PDZ de CASPR2 est délété (Horresh et al., 2008), le complexe VGKC se forme normalement. Ces données indiquent que la formation du complexe VGKC ne dépend pas du domaine de liaison au PDZ. Par contre, il a été montré que CASPR2 interagit avec la protéine de lien au cytosquelette 4.1B (Denisenko-Nehrbass et al., 2003) et que cette interaction est nécessaire pour la formation des complexes aux JXP. En effet, chez les souris 4.1B KO ou chez les souris présentant une délétion du domaine de liaison 4.1B de CASPR2, non seulement CASPR2 mais également les protéines TAG-1, Kv1 et PSD-93 ne sont plus retrouvées enrichies aux JXP (Figure 24A et B) (Horresh et al., 2010 ; Buttermore et al., 2011 ; Cifuentes-Diaz et al., 2011 ; Einheber et al., 2013).

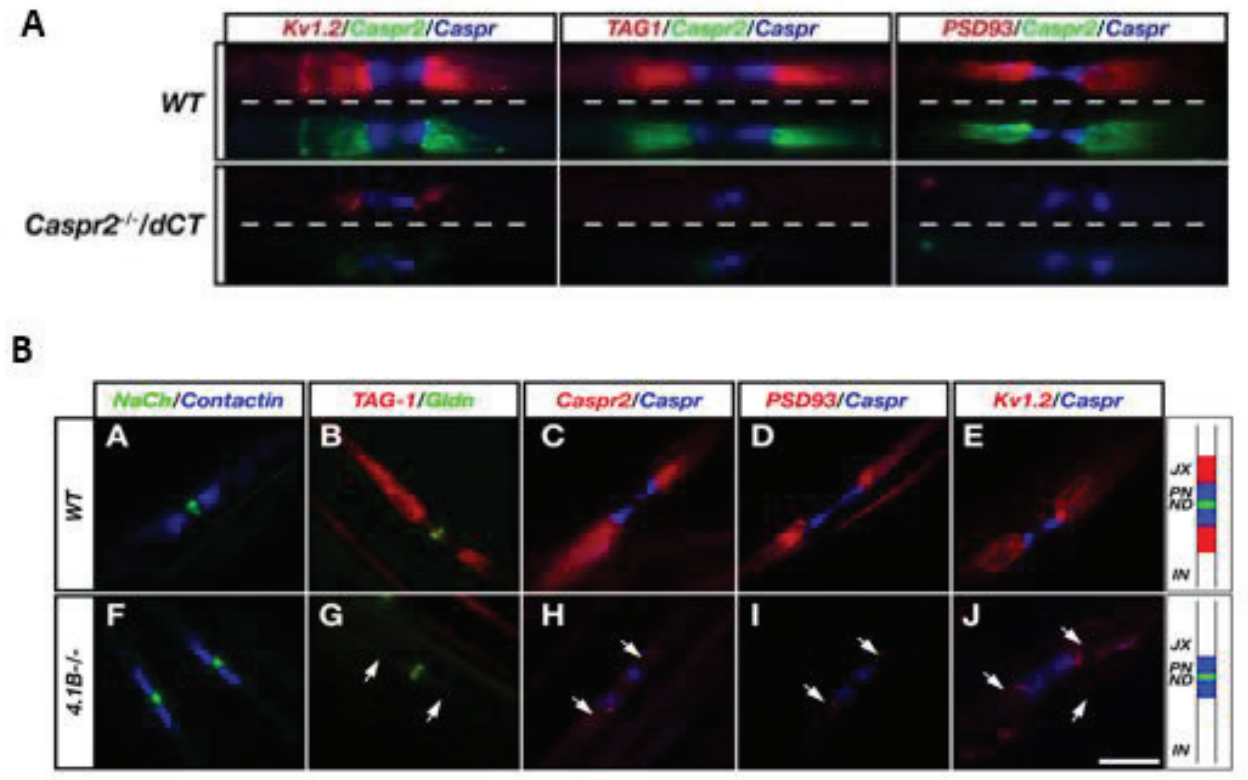

Figure 24 : Rôle de CASPR2 dans la localisation du complexe VGKC aux JXP (Horresh et al., 2008 ; 2010). **A)** La délétion de la partie intracellulaire de CASPR2 induit une perte de l'enrichissement du complexe VGKC au JXP. **B)** L'absence de protéine 4.1B induit une perte de l'enrichissement du complexe VGKC au JXP.

2. Assemblage du complexe au segment initial et à l'héminode

CASPR2 est également enrichie avec TAG-1 et les canaux Kv1 dans deux régions clés de l'axone : l'héminode et le segment inital qui sont soumis à des mécanismes d'assemblage similaires. L'héminode est une région semblable au NOR identifiée dans les motoneurones (Duflocq et al., 2011). Cette région, adjacente au AIS, est le lieu d'initiation de la gaine de myéline et se compose d'un pseudo-paranode (para-AIS) et d'un pseudo-juxtaparanode (JXP-AIS) où est localisé le complexe (Duflocq et al., 2011).

Le segment initial de l'axone, est le site d'initiation du potentiel d'action. Comme le NOR, il se caractérise par une forte concentration en canaux ioniques voltage-dépendants, molécules d'adhésion cellulaire et protéines d'échafaudage telles que l'ankyrine G (Revue, Nelson & Jenkins, 2017). Cette dernière est exprimée tout le long du segment initial et est essentielle pour son organisation. En outre, du fait de sa forte densité en protéines, le segment initial joue un rôle de barrière, limitant la mobilité des protéines entre le compartiment somato-dendritique et le compartiment axonal. Au sein du segment initial,

CASPR2 co-localise avec TAG-1 et Kv1 dans sa partie distale, la plus éloignée du corps cellulaire (Figure 11C et Figure 25A) (Inda et al., 2006 ; Ogawa et al., 2008 et 2010).

Au contraire des JXP, la localisation des canaux potassiques au AIS et aux JXP-AIS ne semble pas dépendre de CASPR2 ou de TAG-1 (Ogawa et al., 2010 ; Duflocq et al., 2011). Néanmoins, une corrélation positive entre la quantité de Kv1 et la quantité de TAG-1 au AIS a été rapportée (Figure 25B) (Pinatel et al., 2017). De plus, le positionnement des Kv1 au AIS, ne semble pas non plus dépendre des protéines PSD-93, PSD-95 et ADAM22 (Ogawa et al., 2010). Ainsi, malgré une composition en protéines proches entre le JXP et le AIS, des mécanismes distincts sont responsables de l'assemblage des complexes VGKC dans ces deux régions et les mécanismes permettant l'assemblage du complexe au AIS devront être clarifiés.

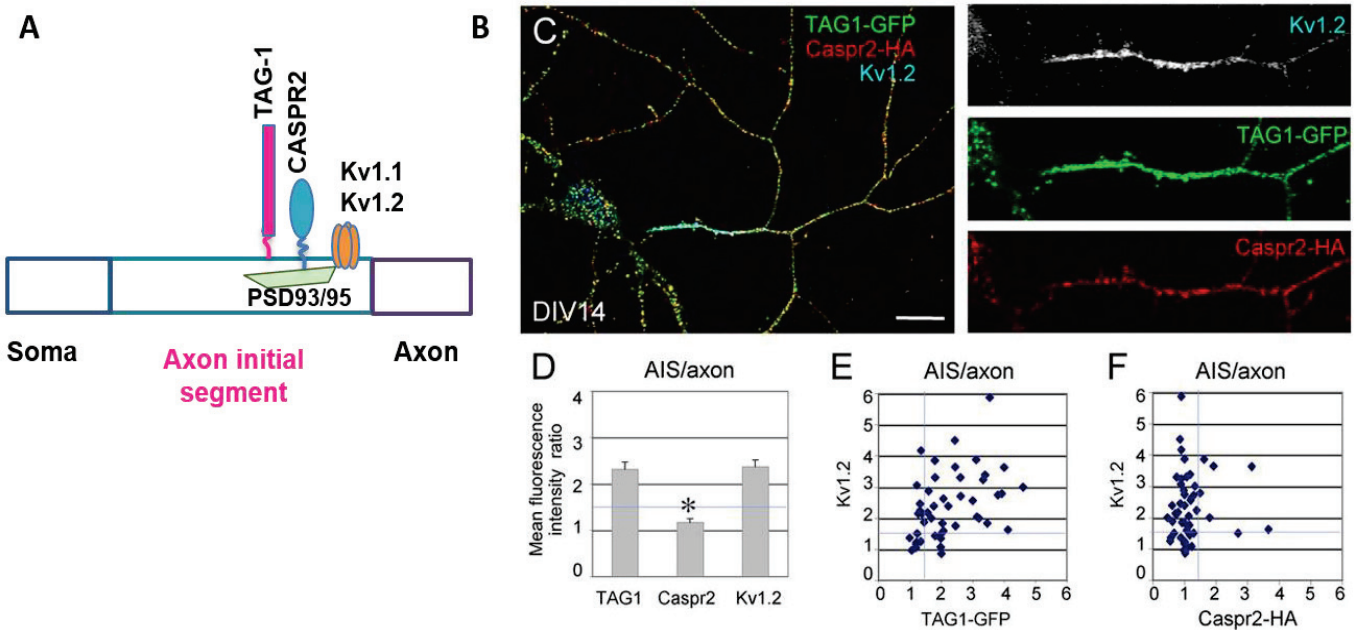

Figure 25 : Le complexe VGKC au segment initial. **A)** CASPR2 se situe dans la partie distale du segment initial avec TAG-1 et Kv1. Leur localisation dépend des protéines PSD93/95. **B)** Distribution de CASPR2, TAG-1 and Kv1.2 le long de l'axone. TAG-1 et Kv1.2 sont particulièrement enrichies au AIS mais pas CASPR2. La quantité de TAG-1 au AIS est positivement corrélée à la quantité de Kv1.2 mais pas CASPR2 (Pinatel et al., 2017).

Enfin, un nombre croissant de résultats montrent que d'autres protéines sont associées au complexe CASPR2/TAG-1/Kv1. Il s'agit de la protéine LGI-1 cytoplasmique et sécrétée, des protéines d'échafaudage ainsi que des protéines ADAM22 et ADAM23. L'association de ces protéines au complexe CASPR2/TAG-1/Kv1 a été mise en évidence au travers des maladies auto-immunes à auto-anticorps anti-VGKC (Irani et al., 2010 ; Lai et al.,

2010). Elles ont également été retrouvées par spectrométrie de masse, co-immunoprécipitées avec CASPR2 (Chen et al., 2015). Par ailleurs, à l'aide de cette technique sur des souris WT et KO, une isoforme de CASPR2 constituée essentiellement de ses domaines intracellulaires a été révélée. Celle-ci est capable de co-immunoprécipiter les protéines LGI-1, Kvβ2 et ADAM22 (Chen et al., 2015), montrant que leur association passe par des interactions intracellulaires. D'autres partenaires intracellulaires de CASPR2 ont été identifiés pouvant réguler la localisation de CASPR2 dans divers compartiments cellulaires (MPP, CASK, SAP97, la carboxypeptidase E) (Horresh et al., 2008 ; Chen et al., 2015 ; Tanabe et al., 2015). Par exemple, la protéine CASK qui est une protéine d'échafaudage localisée à la synapse, pourrait moduler l'expression de CASPR2 dans ce compartiment neuronal ; ou bien encore, l'interaction de CASPR2 avec la carboxypeptidase E pourrait permettre son transport à la membrane dendritique par les voies golgi-dépendantes (Oiso et al., 2009).

F. Rôle de CASPR2 dans la fonction du complexe VGKC

Les données rapportées soulignent un rôle important de CASPR2 dans l'enrichissement des canaux potassiques aux JXP. Cependant, ces canaux étant électriquement isolés sous la gaine de myéline (voir chapitre sur les Kv), l'importance de cette fonction reste à définir.

Ainsi, dans les nerfs sciatique et optique de souris *Cntnap2* KO, malgré la perte de l'enrichissement de TAG-1 et des canaux potassiques aux JXP, les processus de myélinisation ainsi que la vitesse de propagation des PA et leur période réfractaire semblent normaux (Poliak et al., 2003). Néanmoins, l'enregistrement de l'activité électrique axonale globale dans des tranches corticales aigües de souris *Cntnap2* KO de 8 semaines, montre une diminution de l'amplitude de la volée afférente résultant d'un ralentissement de la phase de repolarisation (Scott et al., 2017). Il s'ensuit alors une augmentation du relargage de neurotransmetteurs, suivie par une augmentation de la réponse post-synaptique excitatrice (Scott et al., 2017). Ces évènements, notamment, le ralentissement de la phase de repolarisation, pourraient être attribués à une distribution altérée des Kv1.

Par ailleurs, une diminution de l'expression des Kv1 en surface a été observée chez les souris *Cntnap2* KO au niveau du soma de neurones DRG (Figure 26A). Cette diminution semble rendre les neurones hyperexcitables, se traduisant par une augmentation du nombre

de PA (Figure 26B) (Dawes et al., 2018). Dans l'ensemble, ces données renforcent l'idée que CASPR2 affecte l'excitabilité neuronale en impactant la distribution des Kv1 à la membrane.

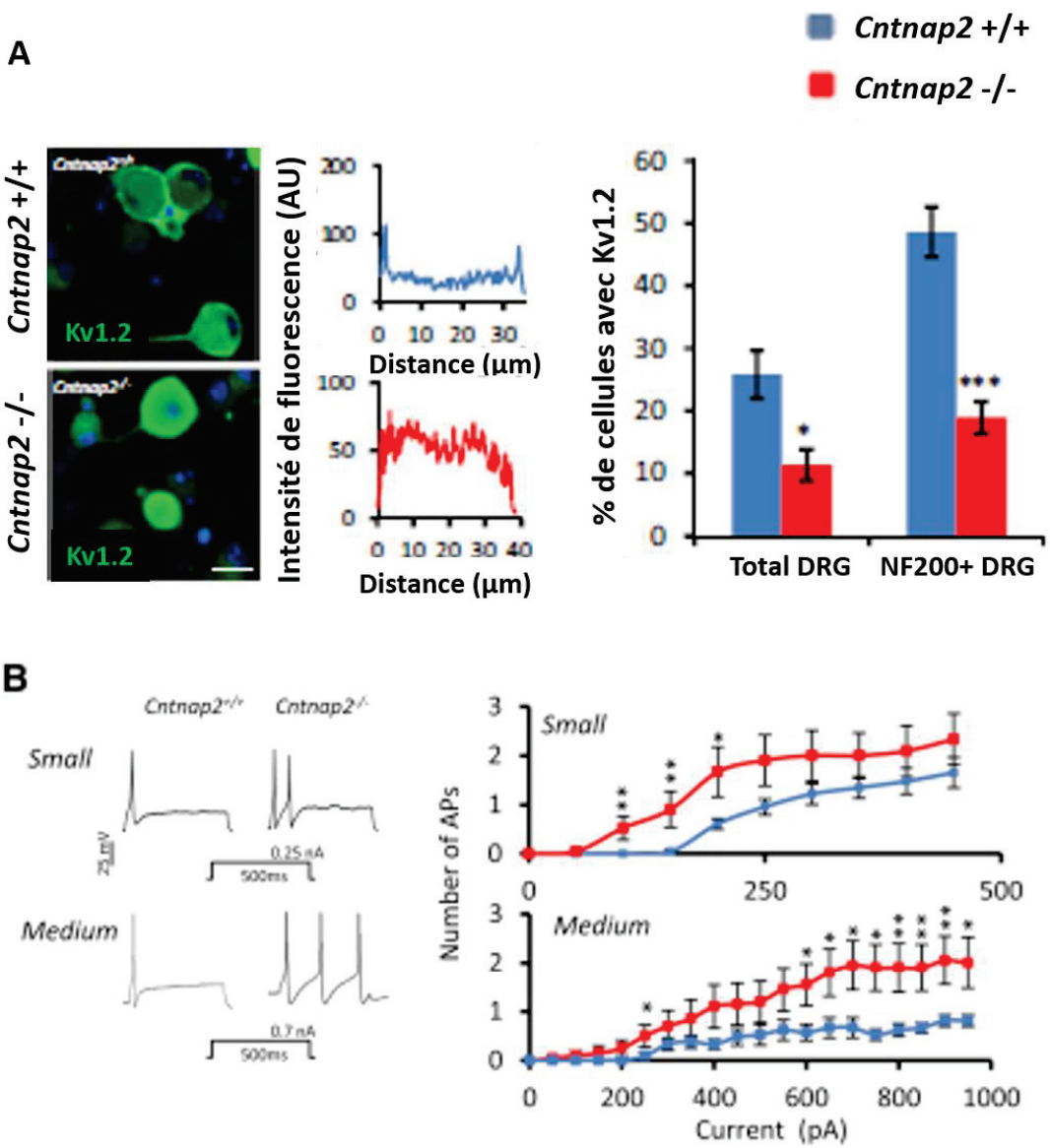

Figure 26 : Rôle de CASPR2 sur la fonction des Kv1 (Dawes et al., 2018). A) Marquage de la sous-unité Kv1.2 dans des neurones DRG en culture. Le profil d'immunofluorescence de la sous-unité Kv1.2 est représenté pour chaque condition. Un ratio entre le marquage membranaire et intracellulaire est calculé permettant de définir des cellules avec un fort marquage membranaire. Dans les souris CASPR2 KO, le nombre de cellules exprimant les Kv1.2 à la surface est diminué, particulièrement dans les neurones NF200 positifs, marqueur des neurones DRG myélinisés. **B)** Enregistrements représentatifs de train de PA. Chez les souris CASPR2 KO, le nombre de PA est augmenté dans les fibres de petit à moyen diamètre.

Si le rôle des complexes VGKC aux JXP reste à clarifier chez l'adulte, leur rôle au cours du processus de myélinisation est davantage établi (voir chapitre sur les Kv) (Vabnick et al., 1999). De façon intéressante, à un âge précoce (3 semaines) correspondant aux phases de

myélinisation, la mise en place de la myéline est retardée chez les souris *Cntnap2* KO. Ce retard coïncide avec un défaut de la conduction des message nerveux se manifestant par une diminution de la vitesse moyenne de propagation des PA (Scott et al., 2017). De tels défauts se produisant durant une phase critique pour le développement des réseaux neuronaux pourraient affecter sa dynamique et ainsi perturber la consolidation des connexions neuronales à longue distance, souvent altérées chez les enfants atteints d'autisme (Scott-Van Zeeland et al., 2010 ; Liska et al., 2018).

III. Maladies associées à CASPR2

En lien avec le rôle de CASPR2 dans le développement, des mutations du gène *CNTNAP2* codant pour CASPR2 ont été identifiées chez des patients atteints de maladies neurodéveloppementales.

A. Maladies génétiques associées à CASPR2

1. Cas cliniques associés à une mutation du gène CNTNAP2

La première description d'une pathologie associée à une mutation de *CNTNAP2* date de 2003, chez un père et ses deux enfants, présentant un trouble obsessionnel compulsif (Verkerk et al., 2003). Ce trouble s'accompagnait, chez les enfants, d'un syndrome de Gilles de la Tourette et reste à ce jour le seul cas de syndrome de Gilles de la Tourette associé à une mutation de *CNTNAP2* (Belloso et al., 2007). Les trois patients présentant une translocation chromosomique hétérozygote et donc des réarrangements chromosomiques complexes, il n'est pas possible d'impliquer directement la mutation *CNTNAP2* dans la pathologie. Suite à ce premier cas, un nombre croissant d'altérations du gène *CNTNAP2* a été rapporté chez des patients avec des troubles neurodéveloppementaux divers impliquant essentiellement le système nerveux central tels que les troubles du spectre autistique, l'épilepsie, la déficience intellectuelle, les troubles du langage, la schizophrénie, la dysplasie corticale focale (CDFE) et des troubles d'hyperactivité avec déficit de l'attention (ADHD) (revue Rodenas-Cuadrado et al., 2014 ; Poot, 2015 et 2017). Seule une neuropathie périphérique, la maladie de Charcot-Marie-Tooth, a été rapportée chez deux sœurs présentant une duplication de l'exon 4 de *CNTNAP2* (Høyer et al., 2015).

Les neuropathies associées à des mutations de *CNTNAP2* touchent majoritairement les enfants et dans 60% des cas, le sexe masculin. Les mutations sont majoritairement

hétérozygotes, suggérant que la perte d'un seul allèle pourrait suffire pour perturber la fonction de la protéine. Néanmoins, certaines mutations ne semblent affecter le développement neuronal que dans un état homozygote. Par exemple, une mutation ponctuelle homozygote de *CNTNAP2* dans l'exon 22 (3709delG ; I1253X) a été rapportée chez 13 enfants d'un vieil ordre Amish présentant comme trouble majeur une dysplasie corticale focale (Strauss et al., 2006). La même mutation se trouvait de façon hétérozygote chez leurs parents et chez quatre individus sains (Strauss et al., 2006). Trois autres cas de délétions homozygotes dans la région proximale de *CNTNAP2* ont été décrits (Rodenas-Cuadrado et al., 2016 ; Watson et al., 2014, Zweier et al., 2009). Ces patients présentaient une déficience intellectuelle sévère, une épilepsie précoce résistante aux traitements accompagnés d'une régression du langage, une altération de la communication et des troubles du spectre autistique.

Il est important de noter que du fait du large éventail de présentations cliniques, des altérations génétiques souvent complexes et de la présence de certains variants *CNTNAP2* chez les individus sains, les pathologies associées à *CNTNAP2* mettent probablement en jeu une combinaison de facteurs, qui restent encore à déterminer (Bakkaloglu et al., 2008 ; Murdoch et al., 2015).

2. Modèle pathologique

L'impact des mutations *CNTNAP2* sur l'expression, le repliement ou la fonction de CASPR2 est encore loin d'être connu mais plusieurs pistes commencent à émerger. En analysant les mutations, on note que certaines d'entre elles pourraient être considérées comme proche d'un KO (pas d'expression de la protéine). Par exemple, la délétion des exons 2-3 (qui introduit un décalage du cadre de lecture) introduirait un codon stop prématuré (L39X), tronquant sévèrement la protéine (Rodenas-Cuadrado et al., 2016). D'autres mutations ont été étudiées dans les cellules HEK ; par exemple, la mutation I1253X induit la production d'une protéine tronquée et secrétée tandis que la mutation D1129H impacte le repliement de CASPR2, induisant sa rétention dans le réticulum endoplasmique (RE) (Falivelli et al., 2012). Néanmoins, ces modèles ne sont pas suffisants pour appréhender l'impact réel d'une mutation, tout particulièrement dans le cas des mutations hétérozygotes, lorsque la protéine WT est également exprimée. En effet, dans ce cas, différents scénarios sont envisageables dont un effet dominant négatif, une augmentation ou réduction du nombre de copies, de l'expression ou de l'activité du gène et de la protéine (revue Veitia et al.,

2018). Une étude récente s'est penchée sur l'impact de ces mutations hétérozygotes sur la forme WT de CASPR2 en lien avec la croissance axonale *in vitro* (Canali et al., 2018). Elle montre que CASPR2 joue un rôle dose-dépendant dans la croissance axonale des neurones corticaux en culture et que les mutants R1119H et N407S ont un effet dominant négatif sur cette fonction. En effet, dans les cellules COS, le mutant R1119H est capable de s'oligomériser avec la protéine CASPR2 WT dans le RE provoquant ainsi sa rétention intracellulaire, expliquant son effet dominant négatif. De plus, deux autres mutants : I869T et G731S, sont incapables de restaurer les défauts de pousse axonale dans les neurones corticaux *Cntnap2* KO. Si ces mutants ne provoquent pas la rétention intracellulaire de CASPR2, ils sont néanmoins incapables d'interagir avec la protéine TAG-1 (Figure 27A) (Canali et al., 2018). Ainsi, les mutations ponctuelles hétérozygotes de *CNTNAP2* pourraient contribuer à la pathogénicité à travers divers mécanismes.

L'utilisation de modèles d'étude animal pour appréhender la fonction de CASPR2 est possible du fait de sa forte homologie entre les espèces : 98,6% d'homologie entre l'humain et le rhésus macaque et 93,8% entre l'humain et la souris (UNIPROT). Par exemple, les souris *Cntnap2* KO homozygotes mais pas hétérozygotes présentent un phénotype de type autistique associé à de l'hyperactivité, des crises d'épilepsie ainsi qu'un retard d'apprentissage très proche du profil clinique des patients (Figure 27B) (Peñagarikano et al., 2011 ; Rendall et al., 2016). De plus, comme mentionné précédemment, l'analyse du cerveau de ces souris avant le début des crises d'épilepsies ne révèle pas de changements morphologiques majeurs. On observe néanmoins chez ces souris, des défauts de migration neuronale avec un nombre réduit d'interneurones GABAergiques et une activité asynchrone du réseau qui pourraient contribuer aux troubles développementaux (ASD, épilepsie et hyperactivité) observés chez ces souris (Figure 27B). En effet, les troubles du spectre autistique observés chez les souris *Cntnap2* KO sont corrélées avec une activité anormale des interneurones inhibiteurs parvalbumine positifs (Selimbeyoglu et al., 2017). Or, un mécanisme potentiel de l'ASD est le déséquilibre de la balance excitation/inhibition (balance E/I) résultant par exemple d'un défaut d'inhibition (Nelson & Valakh, 2015). La réduction de la balance E/I chez les souris *Cntnap2* KO, permet de remédier à leurs troubles comportementaux, argumentant en faveur d'un rôle de l'inhibition dans la pathologie de ces souris (Selimbeyoglu et al., 2017).

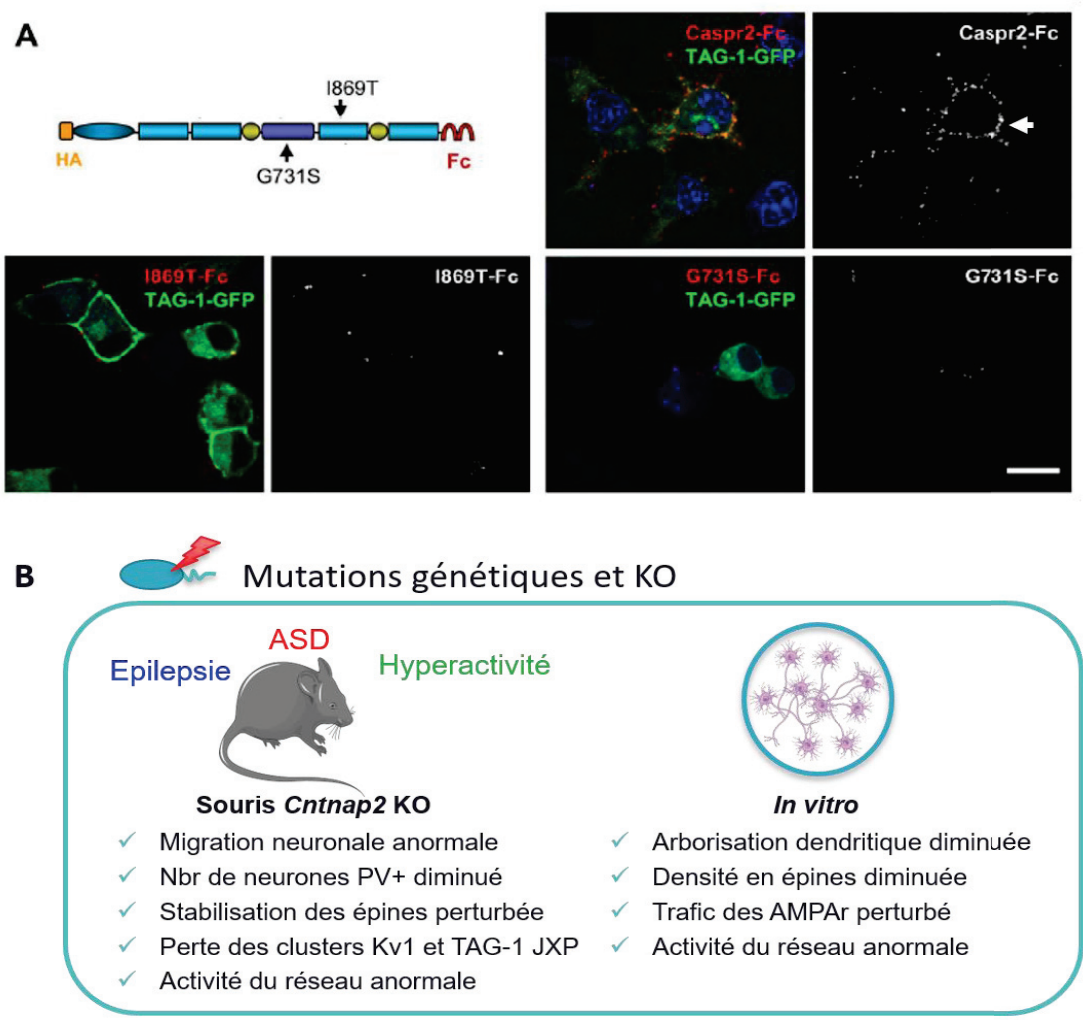

Figure 27 : Modèles pathologiques des mutations CNTNAP2. A) Impact des mutations sur l'interaction entre CASPR2-Fc et TAG-1. CASPR2-Fc est capable d'interagir avec TAG-1 exprimée à la surface des cellules COS. Les mutations I869T et G731S sur la protéine CASPR2 perturbent son interaction avec TAG-1. **B)** Impacts majeurs de la perte de CASPR2 dans les modèles *in vivo* et *in vitro*.

Chez des souris WT transplantées avec des interneurones dérivés de l'éminence ganglionnaire médiane (EGM) de souris *Cntnap2* KO, le nombre d'interneurones parvalbumine positifs est réduit (Vogt et al., 2017). De plus, l'expression du gène *Cntnap2* est capable de rétablir le nombre d'interneurones mais pas ses mutants ponctuels N407S, N418D, G731S et T1278I suggérant que ces mutants pourraient agir comme des allèles nuls ou hypomorphiques (moins exprimés ou moins actifs). De plus, dans une étude récente, des fibroblastes de patients présentant une délétion hétérozygote du gène *CNTNAP2* ont été reprogrammés en cellules souches pluripotentes induites humaines (hiPSCs). Ces cellules, une fois différenciées en neurones présentent une expression accrue de *CNTNAP2* et le

réseau formé par celles-ci présente une augmentation de l'activité spontanée (Flaherty et al., 2017).

Dans l'ensemble, ces résultats fournissent un premier lien entre les mutations et leur impact fonctionnel, renforçant la relation de cause à effet entre mutations et pathologies.

B. Maladies associées aux anti-CASPR2

Si les anticorps anti-CASPR2, comme nous l'avons vu, ont été associés à des pathologies auto-immunes centrales et périphériques (EL, MoS et NMT), ils peuvent également être liés à des pathologies neurodéveloppementales.

1. Les anti-CASPR2 dans les pathologies neurodéveloppementales

Plusieurs études ont montré une fréquence plus élevée de troubles neurodéveloppementaux tels que l'ASD et la déficience intellectuelle chez les enfants de mères présentant des anticorps anti-CASPR2 dans leur sérum. Il est important de noter que la présence d'anticorps anti-CASPR2 dans le sérum de ces mères n'est associé à aucun trouble neurologique (Brimberg et al., 2016 ; Coutinho et al., 2017). Plus généralement, les mères d'enfants présentant des troubles du spectre autistique ont tendance à avoir plus fréquemment des autoanticorps anti-neuronaux dans leur sérum par rapport à la population normale (Singer et al., 2008 ; Brimberg et al., 2013). De plus, il a été montré que les anticorps de mères d'enfants autistes injectés par voie systémique chez des souris gestantes sont capables d'accéder au cerveau du fœtus, affectant son développement (Dalton et al., 2003 ; Singer et al., 2009).

Dans une étude récente, des anticorps monoclonaux anti-CASPR2 clonés d'une mère d'enfant autiste ont été injectés à des souris gestantes (Brimberg et al., 2016). La progéniture, exposée aux anticorps *in-utero*, présente un phénotype de type autistique associé à des défauts morphologiques du cerveau (développement anormal du cortex, baisse de la complexité de l'arborisation dendritique des neurones excitateurs et nombre réduit de neurones inhibiteurs dans l'hippocampe) (Figure 28A) (Brimberg et al., 2016). Des résultats similaires ont été observés chez la progéniture de souris injectées avec des anticorps anti-CASPR2 de patients présentant une EL. Les souris exposées *in-utero* aux anticorps présentaient des comportements de type autistique associés à des défauts cellulaires tels qu'une localisation aberrante des neurones glutamatergiques, une diminution

du nombre de synapses glutamatergiques et une activation microgliale (Coutinho et al., 2017).

Ces résultats, impliquent d'une part CASPR2 dans la mise en place du réseau neuronal au cours du développement et d'autre part, sont en faveur d'un effet pathogénique des auto-anticorps anti-CASPR2.

2. Les anti-CASPR2 dans l'encéphalite limbique

Les anticorps peuvent jouer un rôle pathologique à travers trois principaux mécanismes d'action (Figure 28B). En jouant un rôle agoniste ou antagoniste sur leur cible, en modulant l'expression de leur cible (par exemple, par internalisation) ou en interagissant avec divers acteurs du système immunitaire (complément, cellules T cytotoxiques) (Figure 28B). A l'heure actuelle, peu d'études se sont intéressées à la pathophysiologie des anticorps anti-CASPR2 dans les maladies auto-immunes. En comparaison, la pathogénicité des auto-anticorps dirigés contre le récepteur NMDA (anti-NMDAr) a été largement étudiée. Des études *in vitro* montrent la capacité des anti-NMDAr à internaliser leur cible, perturbant ainsi sa fonction (Dalmau et al., 2008 ; Hughes et al., 2010 ; Manto et al., 2010 ; Mikasova et al., 2012). De plus, des études *in vivo* montrent la capacité de ces anticorps à reproduire de nombreux aspects de la maladie lorsqu'ils sont injectés au niveau de l'hippocampe, chez la souris (Planagumà et al., 2015 et 2016). Enfin, les anti-NMDAr étant essentiellement de la sous-classe IgG1, leur liaison aux récepteurs NMDA pourrait entrainer des processus immunologiques (activation de la microglie et immunité adaptative via la liaison aux récepteurs Fcγ et la réponse cytotoxique) en plus de leur effet sur la fonction des récepteurs. A contrario, les anticorps anti-MUSK et anti-LGI-1 qui sont majoritairement de la sous-classe IgG4, agiraient uniquement en bloquant la fonction de leur cible sans provoquer son internalisation (Huijbers et al., 2013 ; Ohkawa et al., 2013). De la même façon, les anticorps anti-CASPR2 ne semblent pas provoquer l'internalisation de leur cible après 24h d'incubation sur des cultures de neurones hippocampiques de rat ou sur des cellules HEK transfectées (Figure 28A) (Patterson et al., 2018). Par ailleurs, en diminuant le nombre de synapses inhibitrices dans des cultures de neurones hippocampiques après 1h d'incubation seulement, les anti-CASPR2 pourraient perturber la balance E/I, rendant le réseau hyperexcitable (Pinatel et al. 2015). Si les mécanismes à l'origine cet effet sont inconnus, ces résultats sont cohérents avec le phénotype épileptique observé chez les patients (Joubert et al., 2016 ; van Sonderen et al., 2016).

Les mécanismes d'action des anticorps anti-CASPR2 pourraient aussi impliquer les partenaires de CASPR2 dont TAG-1 et les canaux Kv1. Ceux-ci ont fait l'objet d'une partie de mon travail de thèse et seront développés dans la partie résultat. D'autres équipes travaillant sur les encéphalites limbiques ont également proposé des mécanismes d'action passant par une perturbation de l'interaction CASPR2/TAG-1 (Patterson et al., 2018) et une diminution de l'expression des canaux Kv1 à la surface (Dawes et al., 2018).

En conclusion, si les mécanismes par lesquels les anticorps anti-CASPR2 mènent à l'EL, la NMT et au MoS demeurent hypothétiques, leur rôle pathologique est avancé par un nombre croissant de résultats.

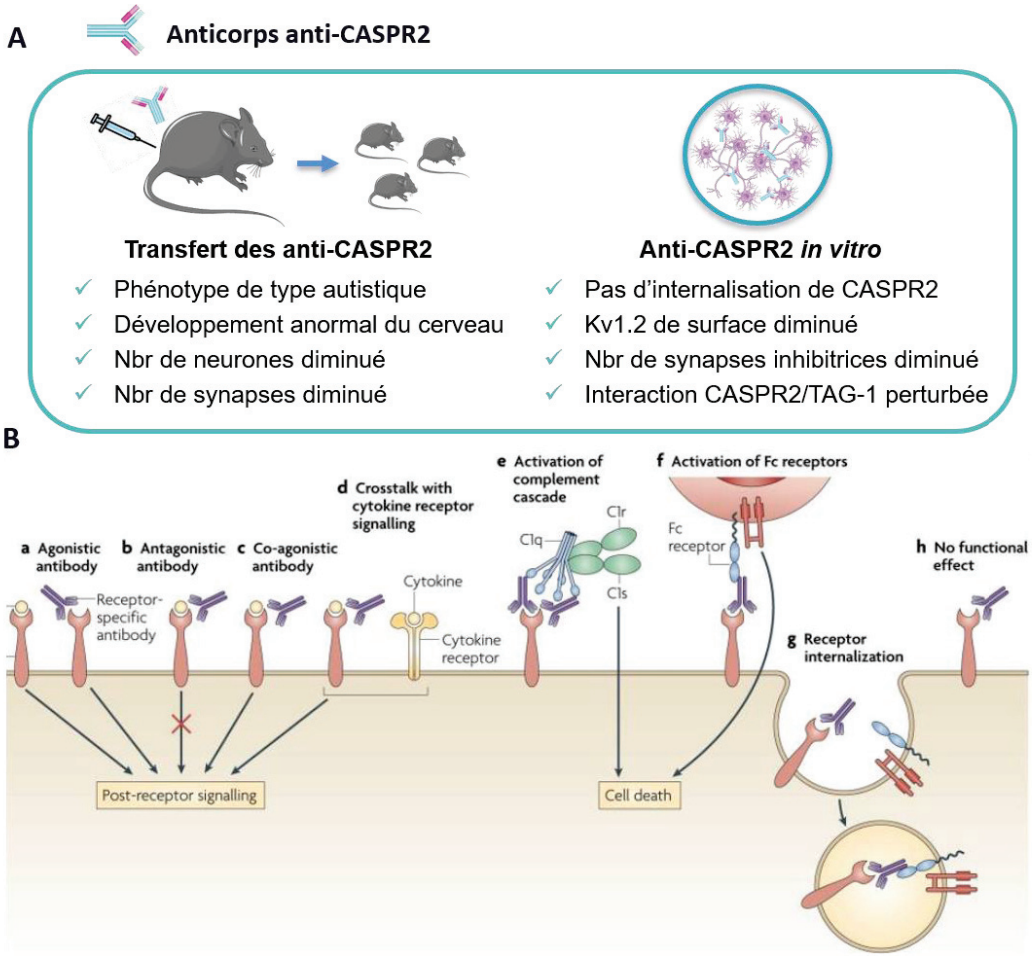

Figure 28 : Modèles pathologiques des anti-CASPR2. A) Effet des anticorps anti-CASPR2 de patients dans des modèles *in vivo* et *in vitro* (Saint-Martin et al., 2018). **B)** Différents modes d'action possibles des auto-anticorps (Diamond et al., 2009).

PRESENTATION DES TRAVAUX

Les patients atteints d'encéphalite limbique à auto-anticorps anti-CASPR2 présentent majoritairement des troubles de la mémoire et des crises d'épilepsie. Si le rôle de ces anticorps dans la pathologie reste loin d'être compris, leur découverte chez des patients sans troubles neurologiques préalables, suggère un rôle de CASPR2 dans le système nerveux mature en lien avec l'excitabilité neuronale et les processus de mémorisation. CASPR2 est une protéine d'adhésion cellulaire initialement connue pour son rôle dans le rassemblement des canaux potassiques aux nœuds de Ranvier. Mais, des études récentes suggèrent l'existence d'autres fonctions de CASPR2 dans le système nerveux central mature. L'intérêt des auto-anticorps est la possibilité de les utiliser comme des outils pour étudier la fonction de CASPR2 dans le système nerveux mature et les mécanismes qui la sous-tendent. De plus, l'étude et la caractérisation des anticorps anti-CASPR2 permettront de mieux comprendre les mécanismes mis en jeu dans la pathologie.

Mon projet de thèse s'est articulé en deux axes :

I) **La caractérisation des anticorps anti-CASPR2 de patients atteints d'encéphalite limbique auto-immune.** Pour ce faire, j'ai obtenu les titres en anticorps et sous-classes d'IgG pour une cohorte de 19 patients présentant une EL et 15 patients présentant une NMT ou un MoS. Les prélèvements de sérum et de liquide céphalorachidien des patients proviennent du centre de référence des syndromes neurologiques paranéoplasiques et encéphalites auto-immunes localisé à Lyon et dirigé par Jérôme HONNORAT. J'ai également réalisé par diverses approches, une étude approfondie de la cible épitopique des anticorps chez les patients atteints d'EL. Ces travaux ont mené à trois publications au sein de l'équipe (Article 1 : Joubert et al., 2016 ; Article 2 : Saint-Martin et al., accepté ; Annexe 3 : Joubert et al., 2017). De plus, dans le cadre de ces travaux, j'ai réalisé un travail de revue bibliographique dans lequel j'ai identifié, en particulier, de potentiels domaines d'intérêt pour la fonction de CASPR2 dans le système nerveux (Annexe 1 : Revue Saint-Martin et al., 2018). Enfin, une partie de ces travaux a mené également à deux publications en collaboration avec l'équipe de Catherine Faivre-Sarrailh du Centre de Recherche en Neurobiologie et Neurophysiologie de Marseille et l'équipe de Laurence Goutebroze de l'institut du Fer à Moulin à Paris (Annexe 5 : Pinatel et al., 2015 ; Annexe 2 : Canali et al., 2018).

II) **L'étude de l'impact des auto-anticorps anti-CASPR2 de patients sur le complexe CASPR2/TAG-1/Kv1.2.** Pour ce faire, j'ai étudié l'impact des anti-CASPR2 sur les interactions de CASPR2 avec son partenaire TAG-1 et analysé leurs domaines d'interaction. Ensuite, toujours en utilisant ces anticorps je me suis intéressée à la relation fonctionnelle entre CASPR2 et ses partenaires TAG-1 et Kv1.2. Les principaux résultats de cette étude font l'objet d'un article en cours de finalisation (Article 3 : Saint-Martin et al., en rédaction) et une partie a déjà été publié en collaboration avec l'équipe de Catherine Faivre-Sarrailh du Centre de Recherche en Neurobiologie et Neurophysiologie de Marseille (Annexe 4 : Pinatel et al., 2017).

I. Caractérisation des anticorps anti-CASPR2 de patients atteints d'encéphalite limbique auto-immune

A. Article 1 :

Characterization of a subtype of autoimmune encephalitis with anti-Contactin-associated protein-like 2 antibodies in the cerebrospinal fluid, prominent limbic symptoms and seizures

Joubert B, **Saint-Martin M**, Noraz N, Picard G, Rogemond V, Ducray F, Desestret V, Psimaras D, Delattre JY, Antoine JC, Honnorat J. JAMA Neurol. **2016** Sep 1;73(9):1115-24.

L'étude de la clinique des patients présentant des anticorps anti-CASPR2 ainsi que la caractérisation de ces anticorps (titre, sous-classe d'IgG et région ciblée) est essentielle à la compréhension de la pathologie et de son origine. Par exemple, une étude montre chez les patients avec des anticorps anti-NMDAr, une corrélation entre le titre des anticorps et l'évolution de la pathologie (Gresa-Arribas et al., 2014). Par ailleurs, la connaissance de la sous-classe d'IgG ainsi que l'identification du ou des domaines cibles des anticorps permet d'émettre des hypothèses quant aux mécanismes d'action de ces derniers.

Nous nous sommes basés sur une cohorte de 18 patients présentant une EL et 15 patients présentant une NMT ou un MoS. Nous avons étudié les caractéristiques des anticorps de patients à l'aide de techniques d'immunomarquages sur des cellules HEK et de nombreux mutants de délétion. Nous avons également analysé chez ces patients s'il existait une relation entre les caractéristiques de leurs anticorps et leur présentation clinique. Nous

avons ainsi trouvé que la présence d'anticorps anti-CASPR2 dans le LCR des patients est systématiquement associée à une EL. Par ailleurs, les EL, NMT et MoS affectent toutes majoritairement les hommes mais leurs caractéristiques cliniques et biologiques sont très différentes. Entre autres, L'EL est rarement associée à un cancer ou d'autres troubles auto-immuns contrairement aux NMT et MoS. Nous avons également pu déterminer que les patients présentant une EL possèdent majoritairement des anticorps de la sous-classe IgG4 dirigés contre les domaines N-terminaux, discoidine et laminine G1 de CASPR2.

En conclusion, les anticorps de patients atteints d'EL pourraient directement perturber la fonction de la protéine en agissant sur les domaines discoidine et laminine G1. Ces résultats suggèrent un rôle clé de ces domaines dans la fonction de la protéine dans le système nerveux adulte.

Original Investigation

Characterization of a Subtype of Autoimmune Encephalitis With Anti–Contactin-Associated Protein-like 2 Antibodies in the Cerebrospinal Fluid, Prominent Limbic Symptoms, and Seizures

Bastien Joubert, MD; Margaux Saint-Martin, MSc; Nelly Noraz, PhD; Géraldine Picard, MSc; Veronique Rogemond, PhD; François Ducray, MD, PhD; Virginie Desestret, MD, PhD; Dimitri Psimaras, MD; Jean-Yves Delattre, MD, PhD; Jean-Christophe Antoine, MD; Jérôme Honnorat, MD, PhD

IMPORTANCE Autoantibodies against contactin-associated protein-like 2 (CASPR2) are observed in several neurological syndromes, including neuromyotonia (NMT), Morvan syndrome (MoS), and limbic encephalitis.

OBJECTIVE To characterize the clinical and biological presentations of patients with anti-CASPR2 antibodies in the cerebrospinal fluid (CSF).

DESIGN, SETTING, AND PARTICIPANTS We conducted a retrospective cohort analysis of 18 patients who had anti-CASPR2 antibodies in their CSF between March 2009 and November 2015 at the Centre National de Référence pour les Syndromes Neurologiques Paranéoplasiques in Lyon, France. Additionally, we analyzed 15 patients who were diagnosed as having NMT or MoS as a comparative group.

MAIN OUTCOMES AND MEASURES Clinical presentations, anti-CASPR2 antibodies specificities, brain magnetic resonance imaging, and CSF analyses, cancer prevalence, and evolution.

RESULTS In this cohort of 18 patients with anti-CASPR2 antibodies in their CSF, 17 (94.4%) were male and had a median (range) age of 64.5 (53-75) years; in the second group, 9 of 15 patients (60.0%) with NMT or MoS were male and had a median (range) age of 51 years (1 month to 75 years). Only 3 patients (16.7%) in this cohort had a previous or concomitant history of cancer (prostate, hematological, or thyroid), whereas 9 patients (60.0%) in the second group had a malignant thymoma. Symptoms of limbic encephalitis were observed in all patients, including temporal lobe seizures in 16 patients (88.9%) and memory disorders in 17 patients (94.4%) from the cohort. Extralimbic signs were also evident in 12 of 18 patients (66.7%), including cerebellar ataxia in 6 patients (33.3%). Only 2 patients (11.1%) from the cohort were diagnosed as having NMT. Brain magnetic resonance imaging displayed T2-weighted temporolimbic abnormalities in 14 of 15 patients (93.3%) in the second group. Cerebrospinal fluid analysis was abnormal in 9 of 12 patients (75.0%). For 16 of 18 patients (88.9%), follow-up was performed for at least a 6-month period (median [range], 34 [11-114] months). Of these, 15 (93.8%) improved and 6 (37.5%) relapsed. In all patients in this cohort, IgG4 autoantibodies were detected in the CSF. Anti-CASPR2 antibodies in the CSF targeted the laminin G1 and discoidin domains of CASPR2 in all patients. Importantly, anti-CASPR2 antibodies were detected in the serum but not in the CSF of all patients with NMT or MoS.

CONCLUSIONS AND RELEVANCE In this cohort study, anti-CASPR2 antibodies in the CSF are associated with a subtype of autoimmune encephalitis with prominent limbic involvement and seizures that is rarely associated with cancer. Conversely, patients with NMT and MoS have anti-CASPR2 antibodies only in the serum but not in the CSF and frequently present with a malignant thymoma. The anti-CASPR2 antibodies found in these patients targeted the discoidin and laminin G1 domains of CASPR2 and always included IgG4 autoantibodies.

JAMA Neurol. doi:10.1001/jamaneurol.2016.1585
Published online July 18, 2016.

Editorial

Author Affiliations: Author affiliations are listed at the end of this article.

Corresponding Author: Jérôme Honnorat, MD, PhD, Centre de Référence National pour les Syndromes Neurologiques Paranéoplasiques, Hôpital Neurologique, 59 Boulevard Pinel, 69677 Bron Cedex, France (jerome.honnorat@chu-lyon.fr).

Antibodies directed against contactin-associated protein-like 2 (CASPR2) have been described in the sera of patients with peripheral and central neurological syndromes, including neuromyotonia (NMT), Morvan syndrome (MoS), and autoimmune limbic encephalitis.[1] Anti-CASPR2 antibodies belong to the anti–voltage-gated potassium channel antibody complex, a biomarker that has been shown to include autoantibodies targeting CASPR2, leucin-rich glioma 1 protein, and other unknown antigens.[2] In addition, CASPR2 antibody-related syndromes have been frequently described in patients with malignant thymoma, a potential source of impaired T-cell maturation that may lead to autoantibody production.[3,4] Although CASPR2 is involved in the organization of the juxtaparanodal regions of myelinated nerves, it is also expressed in the axons of hippocampal cells.[5,6] A recent study[7] has suggested that anti-CASPR2 antibodies from the cerebrospinal fluid (CSF) of patients with limbic encephalitis bind to hippocampal inhibitory interneurons at the presynaptic level and have a disruptive effect on inhibitory synapses. Moreover, anti-CASPR2 antibodies in the serum and CSF have predominantly been shown to be IgG4 and to target multiple extracellular epitopes of CASPR2, including its discoidin and laminin G1 domains.[7,8] Therefore, the diversity of CASPR2 antibody–associated diseases may rely on the implication of various factors, including the site of autoantibody synthesis, the epitope specificities of anti-CASPR2 antibodies, or the IgG subtypes involved. To further characterize patients with anti-CASPR2 antibodies, we analyzed clinical and biological data from patients who were positive for anti-CASPR2 antibodies in the CSF.

Key Points

Question What are the clinical features associated with anti–contactin-associated protein-like 2 (CASPR2) antibodies in the cerebrospinal fluid?

Findings In this cohort study of 18 patients with anti-CASPR2 antibodies in the cerebrospinal fluid, all patients displayed limbic symptoms, including temporal lobe seizures in 16 patients and memory disorders in 17 patients. Extralimbic signs were seen in 12 patients, including cerebellar ataxia in 6 patients.

Meaning The presence of anti-CASPR2 antibodies in the cerebrospinal fluid is associated with a subtype of autoimmune encephalitis with predominant temporal lobe epilepsy and memory disorders.

Methods

In this study, we retrospectively included all patients with CSF samples positive for anti-CASPR2 antibodies at the Centre National de Référence pour les Syndromes Neurologiques Paranéoplasiques in Lyon, France, between March 2009 and November 2015. During this period, we tested 6650 CSF samples from French hospitals sent for routine diagnostic workup in patients with suspected autoimmune encephalitis or paraneoplastic neurological disorders. Cerebrospinal fluid samples from the patients were screened by immunohistofluorescence on rat brain sections, and anti-CASPR2 antibodies were subsequently identified by a cell-based binding assay (CBA). In addition, serum samples from patients with confirmed anti-CASPR2 antibodies in the CSF were screened for anti-CASPR2 antibodies using a CBA. Approval for this study was granted by the institutional review board of the Hospices Civils de Lyon (Comité de Protection des Personnes SUD-EST IV). Written informed consent was obtained from all patients.

Serum and CSF samples were deposited in the NeuroBioTec biobank (Hospices Civils de Lyon). Clinical data were collected from the referring physicians by telephone and email. We focused on the modes of onset, clinical symptoms, ancillary results, therapy regimens, cancer prevalence, and outcomes. In addition, patients diagnosed in our center as having NMT or MoS were tested for anti-CASPR2 antibodies by CBA in both the serum and CSF and were used as a comparative group. Age differences between groups were compared by Mann-Whitney *U* test. Sex ratio, anti-CASPR2 antibody levels in the serum and CSF, and comorbidities between groups were compared using Fisher exact test. Statistical significance was set at $P < .05$.

For immunohistofluorescence assays, sagittal slices obtained from adult rat brains were incubated with patient CSF samples (diluted 1:10) overnight at 4°C. Brain slices were fixed by immersion into 4% paraformaldehyde for 1 hour, followed by immersion in a 30% sucrose solution for 24 hours. Histological slices were produced using the Leica CM1950 cryostat microtome (Leica Biosystems Nussloch GmbH). Tissues were subsequently washed and incubated with 488 Alexa Fluor–conjugated goat antihuman IgG (A-21433; Thermofisher). For the CBA, cultured human embryonic kidney 293 cells were transfected using the Lipofectamine LTX kit (Invitrogen), with plasmids coding for full-length or deleted CASPR2 fused to an influenza virus hemagglutinin tag. Cells were incubated for 48 hours after transfection with CSF (diluted 1:10) or sera (diluted 1:20) and for 2 hours with mouse anti-hemagglutinin antibody (diluted 1:1000; H3663; Sigma-Aldrich) in Dulbecco modified eagle medium, 25 mmol/L 4-(2-hydroxyetyl)-1-piperazineethanesulfonic acid, 3% bovine serum albumin, and 5% normal goat serum. Cells were subsequently washed in Dulbecco modified eagle medium and 4-(2-hydroxyetyl)-1-piperazineethanesulfonic acid for 15 minutes and incubated with Alexa Fluor–conjugated secondary antibodies (diluted 1:1000), including goat antihuman total IgG-555 (A-21433; Thermofisher), -488 (A-11013; Thermofisher), goat anti-mouse IgG-555 (A-21424; Thermofisher), -488 (A-11029; Thermofisher), mouse antihuman IgG1-488 (F9890; Sigma-Aldrich) and mouse antihuman IgG4-488 (F0767; Sigma-Aldrich). Bound antibodies were visualized using the Zeiss Axiophot Imager.Z1. Anti-CASPR2 antibodies titers in patient sera or CSF were assessed by serial 2-fold dilutions in CBA. Titers were determined as the lowest dilution that gave a positive signal, according to 2 blinded investigators (V.R., M.S.M.). The epitopes targeted by patient autoantibodies were examined on CBA using CASPR2 with hemagglutinin-deleted constructs as previously described[7] with the same dilutions (CSF, 1:10; serum, 1:20).

Two blinded investigators (V.R., M.S.M.) assessed epitope and isotype specificities of anti-CASPR2 antibodies. The IgG and albumin concentrations in the CSF and serum were evaluated using nephelometry (IMMAGE Immunochemistry Systems;

Beckman-Coulter). The CSF/serum albumin quotient was used to evaluate the integrity of the CSF-blood barrier. To characterize intrathecal immunoglobulin synthesis, the immunoglobulin quotient (immunoglobulin levels in the CSF divided by immunoglobulin levels in the serum) was calculated and adjusted to the corresponding maximum immunoglobulin quotient that can be expected at a given albumin quotient in the absence of intrathecal immunoglobulin synthesis[9] to quantify the CSF/serum anti-CASPR2 antibodies index. An antibody index greater than 4.0 was considered to reflect intrathecal synthesis.[9]

Results

Clinical Findings

Among the 6650 CSF samples tested by immunohistochemistry, we identified 18 patients with anti-CASPR2 antibodies in the CSF. During the same period, we identified 15 patients with NMT or MoS and anti-CASPR2 antibodies in the serum. Samples of CSF from all patients with NMT or MoS were tested for anti-CASPR2 antibodies and found to be normal. The clinical findings, ancillary results, and outcomes of the patients with anti-CASPR2 antibodies in the CSF are shown in **Table 1**. **Table 2** summarizes the baseline characteristics and immunological findings of patients with anti-CASPR2 antibodies in the CSF compared with patients with NMT or MoS. Compared with the group of patients with NMT or MoS, the cohort had a significantly higher number of males (94.4% vs 66.7%; $P = .03$) and median age (64.5 vs 51 years; $P < .01$). Only 1 patient (5.6%) in our cohort was diagnosed as having another autoimmune disorder (thyroiditis), whereas autoimmune comorbidities were seen in 8 of 15 patients (53.3%) with NMT or MoS ($P < .01$; 7 of these 8 had myasthenia gravis). Only 3 patients (16.7%) in our cohort had a previous or concomitant history of cancer (prostate adenocarcinoma and chronic lymphoid leukemia in 1 patient and papillary thyroid cancer in 2 patients). Although a malignant thymoma had been found prior to or following the neurological disorder in 9 of 15 patients (60.0%) with NMT or MoS, none of the patients with anti-CASPR2 antibodies in the CSF had such a tumor ($P < .01$).

For most patients with anti-CASPR2 antibodies in the CSF (13 of 18 [72.2%]), admission to the referring hospital occurred because of partial temporal seizures. In these patients, other symptoms installed acutely over the course of a few days to 1 week, simultaneously to epilepsy in 9 patients and only a few months after the onset of epilepsy in the 3 remaining patients (median [range] delay, 6 [5-18] months). In the remaining 5 patients (27.8%), admission was requested because of memory disorders, which had developed progressively over several months in 4 patients and acutely in 1. All patients in our cohort had symptoms of limbic structure impairment, including 17 (94.4%) with anterograde and episodic memory disorders, 16 (88.9%) with temporal lobe seizures, 10 (55.6%) with symptoms of frontal lobe dysfunction, and 4 (22.2%) with psychiatric symptoms (eg, depressed mood or persecutory thoughts). None of the patients presented with the acute confusion or behavioral disorders classically reported in autoimmune limbic encephalitis. Extralimbic symptoms were observed in 12 patients (66.7%), including 6 (33.3%) with cerebellar ataxia, 4 (22.2%) with sleep disorders, and 3 (16.7%) with peripheral neuropathy. Signs of NMT were present in only 2 patients (11.1%).

Ancillary

Hyponatremia was observed in only 1 of 18 patients (5.6%). Anti-SOX1 antibodies were detected in 1 patient (5.6%), although no evidence of cancer was demonstrated. None of the other patients had additional antibodies against neuronal antigens. Brain magnetic resonance imaging (MRI) data were available for 15 patients (83.3%). Of these 15 patients, brain MRI results remained normal in only 1 patient (6.7%). Twelve patients (80.0%) had temporolimbic hyperintensities on T2-weighted images (**Figure 1**), which appeared subsequently in 3 patients. Bilateral hippocampal atrophy was observed in 2 of 15 patients (13.3%) on the first imaging analysis. In 1 patient, temporomesial hyperintensities were observed in the first MRI and secondarily evolved into bilateral hippocampal atrophy. Cytochemical data analysis results in the CSF were available for 12 patients and were normal in only 3 patients (25.0%). Increased white blood cell counts were observed in 8 of 12 patients (66.7%; median [range], 4000 [3000-32 000] cells/μL [to convert to 10^9/L, multiply by .001]), and elevated protein levels were observed in 1 patient (8.3%; 0.11 g/dL). Of note, brain MRI and CSF analyses were normal in all 11 patients with NMT and all 9 with MoS for whom data were available. Interictal electroencephalograms displayed focal abnormalities in 4 of 18 patients (22.2%). Brain positron emission tomography scans were performed in 5 patients (27.8%) and were pathological in 4. Positron emission tomography scan findings were not reproducible from one patient to another; 1 patient had diffuse hypometabolism, another had temporomesial hypometabolism, and 2 patients had frontotemporal hypermetabolism. Therefore, we were unable to determine a pattern specifically associated with CASPR2 antibody-related encephalitis. Nonetheless, it has to be noted that in contrast with patients with anti-leucin-rich glioma 1 proteinencephalitis,[10] increased metabolism in the basal ganglia was not observed in any of the 5 patients.

Treatments

Oral steroids were given to a total of 4 patients. One patient was treated only with oral steroids, while 3 patients were treated with oral steroids combined with other treatments. Eleven of 18 patients (61.1%) were treated with intravenous immunoglobulins (0.4 g/kg/d for 3 to 5 days as part of 1 to 9 monthly courses), 8 (44.4%) with high-dose corticosteroid boluses (0.5-1 g/d for 3 to 5 days as part of 1 to 6 monthly courses), 1 (5.6%) with plasmapheresis (6 monthly courses), 3 (16.7%) with intravenous cyclophosphamide (1-g infusion every month for 2 to 8 months), and 2 (11%) with rituximab (375 mg/m^2 administered intravenously once a week for 1 month). Three patients (16.7%) were given mycophenolate mofetil (1 g/24 h administered orally) on a long-term basis. Four patients (22.2%) were given 2 lines of treatment, and 2 patients (11.1%) needed 3 different lines of treatment.

Follow-up and Outcomes

The median (interquartile range) follow-up time was 27.4 (19-51) months. All patients survived. Follow-up was

Table 1. Clinical Findings, Brain MRI, and Evolution of Patients With Anti-CASPR2 Antibodies in the CSF

Patient Age, y/Sex	Symptoms Leading to Admission	Other Symptoms	Brain MRI Hypersignal	Follow-up, mo	Evolution	Relapse	mRS at Onset	mRS at Last Visit	Residual Symptoms
62/M	Partial temporal seizures	Acute anterograde and autobiographic memory impairment simultaneous to epilepsy	Temporomesial (bilateral)	55	Improvement after 3 monthly courses of IVIg, started 5 mo after onset	1 y After onset; seizure and memory disorders	1	1	Defects in autobiographic memory
57/M	Partial temporal seizures	Acute autobiographic memory impairment and insomnia simultaneous to epilepsy	Temporomesial (left)	114	With AEDs only, progressive improvement until stabilization 2 y after onset; 1 steroid bolus 6 y after onset for memory improvement	NMT 8 y after onset, without worsening of encephalitis signs	2	2	NMT
60/M	Anterograde and episodic memory impairment	Partial and tonic-clonic generalized seizures and hypersomnia 2 wk after the onset of memory impairment	Temporomesial (bilateral)	51	Improvement with steroids and plasmaphersis 8 mo after onset after initial course of IVIg, which was inefficient; after relapses, improvement with plasmapheresis and steroid increase	2 Relapses (15 and 28 mo after onset); increased seizures at steroid decrease	2	1	Altered visuospatial memory
71/M	Partial temporal seizures	Acute autobiographic memory impairment, frontal syndrome, cerebellar syndrome, and pseudobulbar syndrome 18 mo after onset of epilepsy	NA	46	Marked improvement after 6 courses of Solu-Medrol that were started 23 mo after disease onset; MMF was given as long-term immunosuppression	No	4	1	Moderate anterograde amnesia and slightly unstable gait
60/M	Partial temporal seizures	Acute anterograde and autobiographic memory impairment and cerebellar ataxia simultaneous to epilepsy	Normal	22	Spontaneous improvement 5 mo after disease onset; 1 course of steroid boluses prescribed 6 mo after onset; after relapse, no improvement despite steroid boluses, 1 course of IVIg, and 8 courses of CPA	Increased seizures 7 mo after onset, followed by worsening of cerebellar ataxia	2	3	Refractory temporal epilepsy and cerebellar ataxia
68/M	Partial temporal seizures	Acute anterograde memory impairment, frontal signs, cerebellar ataxia, and mild NMT simultaneous to epilepsy	Temporomesial (left)	11	Marked improvement on cognitive functions and gait after 6 courses of IVIg with steroid boluses, started 1 mo after onset	No	2	1	Mildly impaired executive functions at NPT
69/M	Partial temporal seizures	Acute anterograde memory impairment, frontal features, and persecuted thoughts 6 mo after onset of epilepsy	Temporomesial (right)	25	Improvement with AEDs; oral steroids started 2 y after onset	No	2	0	None
66/M	Partial temporal and generalized seizures	Acute anterograde and autobiographic memory impairments and frontal features 5 mo after onset of epilepsy	Temporomesial (bilateral)	19	Improvement after 3 courses of IVIg and steroid boluses, started 9 mo after onset; after relapse, improvement with 6 courses of IVIg and CPA	Increased seizures and memory impairment 13 mo after onset	2	2	Slight autobiographic amnesia and impaired executive functions
75/M	Partial temporal and generalized seizures	Acute anterograde memory impairment and frontal syndrome simultaneous to epilepsy	Temporomesial (right)	3	1 Course of Solu-Medrol bolus and IVIg	NA	3	NA	Follow-up <6 mo

(continued)

Table 1. Clinical Findings, Brain MRI, and Evolution of Patients With Anti-CASPR2 Antibodies in the CSF (continued)

Patient Age, y/Sex	Symptoms Leading to Admission	Other Symptoms	Brain MRI Hypersignal	Follow-up, mo	Evolution	Relapse	mRS at Onset	mRS at Last Visit	Residual Symptoms
69/M	Partial temporal seizures	Acute anterograde amnesia and inferior limb sensory neuropathy simultaneous to epilepsy	NA	19	Dramatic improvement after 2 courses of IVIg, started 17 mo after onset	No	2	1	Slight memory and executive function impairment and neurogenic pain
61/M	Partial temporal seizures	Acute anterograde and autobiographic amnesia simultaneous to epilepsy	Hippocampal atrophy	12	Greatly improved after 5 courses of IVIg, started 10 mo after onset; treatment with rituximab owing to the persistence of detectable CSF anti-CASPR2 antibodies	No	1	1	Reported memory troubles and difficulty concentrating
63/M	Partial temporal seizures	Acute anterograde amnesia and anxiety simultaneous to epilepsy	Temporomesial (bilateral)	59	Improvement with steroids 3 mo after onset; after relapses, partial improvement after IVIg and steroid increase and no improvement with MMF; return to baseline after rituximab therapy	2 Relapses (3 and 13 mo from onset); increased seizures at steroid decrease	2	0	None
61/M	Partial temporal and generalized tonic-clonic seizures	Acute slight frontal syndrome simultaneous to epilepsy	Temporomesial (left)	78	Spontaneous improvement in seizure frequency 2 y after onset	No	1	1	Daily partial temporal seizures
62/F	Partial temporal seizures	Acute anterograde and autobiographic amnesia, frontal signs, hemihypesthesia, insomnia, and depressed mood simultaneous to epilepsy	Hippocampal atrophy	29	Improvement with IVIg, started18 mo after onset	No	2	1	Slight anterograde amnesia and executive impairment at NPT and insomnia
53/M	Axonal sensory-motor neuropathy with neuralgic pain and progressive autobiographic amnesia, with installation over several months	Frontal features, cerebellar ataxia, insomnia, and depressed mood	NA	25	Greatly improved after 6 steroid boluses, started 25 mo after onset	No	3	1	Neuropathic pain and depressed mood
66/M	Progressive amnesia, cerebellar ataxia, and sensory neuropathy	Partial temporal seizures and frontal features parallel to progressive amnesia over several months	Temporomesial (bilateral)	5	Partial improvement after 4 courses of IVIg, started 1 mo after onset	NA	3	NA	Follow-up <6 mo
75/M	Progressive amnesia, aphasia, and cerebellar ataxia, with installation over several months	None	Temporomesial (bilateral)	39	Stabilization after 9 courses of IVIg, started 1 y after onset; switch to CPA afterwards with no improvement	No	4	4	Severe anterograde amnesia, ataxia, and aphasia
66/M	Progressive anterograde amnesia	Partial temporal seizures, tetrapyramidal signs, and frontal features parallel to amnesia, over several months	Temporomesial (bilateral) and later hippocampal atrophy	92	9 Steroid boluses, started 50 mo after onset; afterwards, progressive improvement, with MMF as long-term immunosuppressive therapy	No	4	1	Slight anterograde amnesia

Abbreviations: AEDs, antiepileptic drugs; CPA, cyclophosphamide; IVIg, intravenous immunoglobulin; MRI, magnetic resonance imaging; mRS, modified Rankin score; MMF, mycophenolate mofetil; NMT, neuromyotonia; NA, not applicable; NPT, neuropsychological tests.

Table 2. Baseline Characteristics and Immunological Findings of Patients With Anti-CASPR2 Antibodies in the CSF Compared With Patients With NMT or MoS

Characteristic	No./Total No. (%)		
	Patients With Anti-CASPR2 Antibodies in the CSF	Patients With NMT or MoS	*P* Value
No. of patients	18	15	
Male	17/18 (94.4)	9/15 (60.0)	.03
Age, y, median (range)	64.5 (53-75)	51 (1 mo-75 y)	.002
Serum titers, median (range)	1/15 360 (1/10 240-1/81 920)	1/800 (1/20-1/5120)	<.001
CSF titers, median (range)	1/1280 (1/80-1/10 240)	0	<.001
Detected IgG4 anti-CASPR2 antibodies			
Serum	11/12 (91.7)	512 (41.7)	.03
CSF	17/17 (100)	0	<.001
Detected IgG1 anti-CASPR2 antibodies			
Serum	12/12 (100)	10/12 (83.3)	.48
CSF	10/17 (58.8)	0	<.005
Recognition of discoidin and laminin G1	18/18 (100)	11/11 (100)	>.99
Additional epitopes	10/18 (55.6)	8/11 (72.7)	.45
Malignant thymoma	0	9/15 (60.0)	.001
Other cancers	3/18 (16.7)	0	.23
Other autoimmune disturbances	1/18 (5.6)	8/15 (53.3)	.004

Abbreviations: CSF, cerebrospinal fluid; CASPR2, contactin-associated protein-like 2; MoS, Morvan syndrome; NMT, neuromyotonia.

Figure 1. Fluid-Attenuated Inversion Recovery Imaging of a Patient With Epilepsy, Partial Temporal Seizures, and Anterograde Memory Impairments

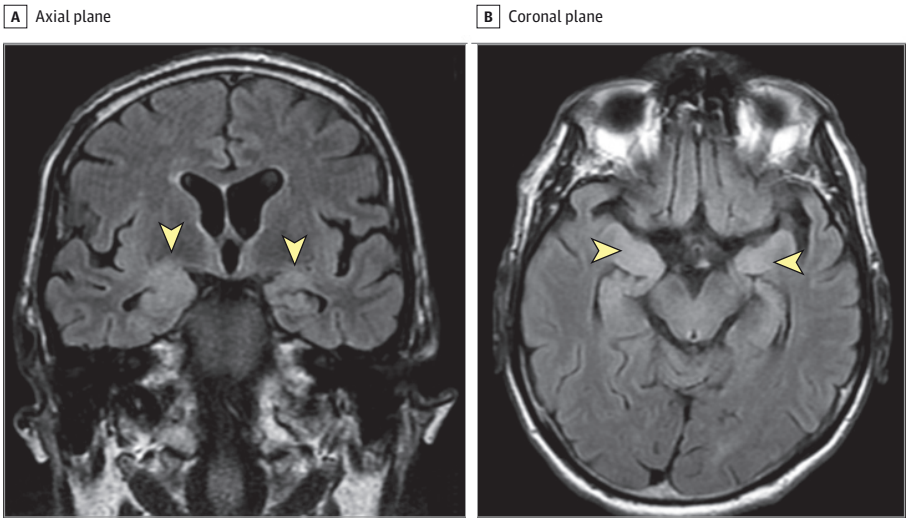

In these T2-weighted magnetic resonance images, note the asymmetrical hyperintensities involving both temporomesial regions (arrowheads).

performed for at least 6 months in 16 of 18 patients (88.9%). Of these, 15 (93.8%) progressively improved, with 11 improving after immunomodulatory treatment and 4 spontaneously (Table 1). One patient remained stable with ataxia and severe cognitive defects. Six of 16 patients (37.5%) had 1 or 2 relapses. Five of these patients had relapses presenting as an increase in seizure frequency. In 2 patients, epileptic relapses occurred when steroid medications were decreased and were easily controlled by increasing steroid dosages. The relapse of 1 patient consisted of the development of NMT 8 years after the onset of encephalitis, without concomitant worsening of the encephalitic symptoms. The median (interquartile range) modified Rankin score for all patients was 2 (2-3) at onset and 1 (1-2) at the end of follow-up. At the end of follow-up, 4 of 16 patients (25.0%) still had symptoms that significantly altered their quality of life (modified Rankin score ≥2), including NMT (1 patient), cerebellar ataxia (3 patients), and amnesia (3 patients). Two of 16 patients (12.5%) recovered completely. Brain MRI follow-up data were available for 9 patients. The MRI results remained stable in 6 of 9 patients (66.7%), while temporomesial hyperintensities decreased partially or com-

Figure 2. Reactivity of Anti–Contactin-Associated Protein-like 2 Antibodies from Patients' Cerebrospinal Fluid (CSF) With Rat Brain

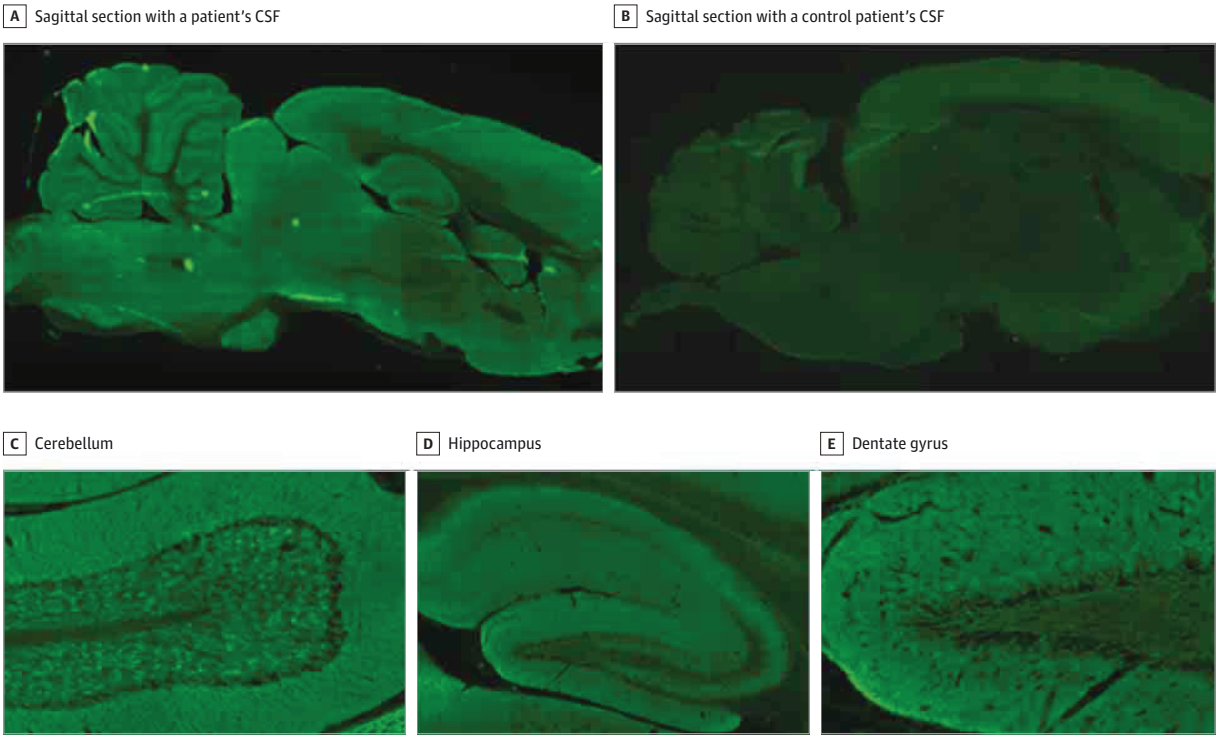

The CSF of 2 patients was used for immunostaining; fluorescent antihuman IgG mouse antibodies were used as secondary antibodies. Sagittal section of rat brain immunostained with a patient's CSF (A, dilution 1:10; original magnification × 7). There was diffuse staining of the neuropil that was not observed when rat brain sections were incubated with a control patient's CSF (B, dilution 1:10; original magnification × 7). Immunoreactivity was particularly strong in the molecular and the granular cell layers of the cerebellum (C; original magnification × 70) and the hippocampus (D; original magnification × 35); in addition, there was diffuse staining of the molecular layer of the dentate gyrus (E; original magnification × 70).

pletely in 2 patients (22.2%) and evolved from unilateral to bilateral in 1 patient (11.1%). One patient (11.1%) secondarily developed bilateral hippocampal atrophy.

Anti-CASPR2 Antibody Characteristics

As previously reported,[11] studies on immunohistochemistry in the CSF revealed a similar staining pattern in all patients with strong fixation of the granular and molecular layers of the cerebellar cortex and hippocampus along with a diffuse staining of the molecular layer of the dentate gyrus (**Figure 2**). The median anti-CASPR2 antibodies end point dilution in the CSF was 1/1280 (range, 1/80-1/10 240). All serum samples from the patients were also positive for anti-CASPR2 antibodies. The median anti-CASPR2 antibodies end point dilution in the serum were significantly higher in patients in our cohort than in patients with NMT or MoS (1/15 360 vs 1/800; $P < .001$). Albumin levels in the CSF and serum were available for 2 patients, allowing for the assessment of intrathecal synthesis. In both of the patients, the immunoglobulin quotient values (0.03 and 0.06) were larger than the maximum immunoglobulin serum/CSF quotient values, calculated using the Reiber hyperbolic function[9] (0.004 and 0.011). The CASPR2 antibody indices were 7.4 and 5.6, suggesting intrathecal synthesis of anti-CASPR2 antibodies in both patients. In all patients, anti-CASPR2 antibodies levels in the serum and CSF were directed against the discoidin and laminin G1 domains of CASPR2, as illustrated in **Figure 3**A. IgG isotypes were determined in 17 patients (Figure 3B). Importantly, IgG4 antibodies were detected in the CSF of all patients along with IgG1 antibodies in 10 of 17 patients (58.8%). Interestingly, IgG4 anti-CASPR2 antibodies were found in the serum of 11 of 12 patients (91.7%) with anti-CASPR2 antibodies in the CSF and in only 5 patients (41.7%) with NMT or MoS ($P = .03$). We observed 3 patients with anti-CASPR2 antibodies in the CSF that were of the IgG4 but not IgG1 isotype, which targeted the discoidin and laminin G1 domains only. All 3 of these patients had anterograde and episodic amnesia and temporal seizures. One patient also reported persecutory thoughts, and another patient exhibited hypersomnia. Notably, all 3 patients with hippocampal atrophy on brain MRI had anti-CASPR2 antibodies in the CSF of both the IgG4 and IgG1 isotypes.

Discussion

Clinical Patterns

It has been previously reported[4,11-13] that patients with anti-CASPR2 antibodies present with symptoms of MNT, MoS, and various patterns of autoimmune encephalitis. However, our study indicates that the presence of anti-CASPR2

Figure 3. CASPR2 Autoantibody Characterization

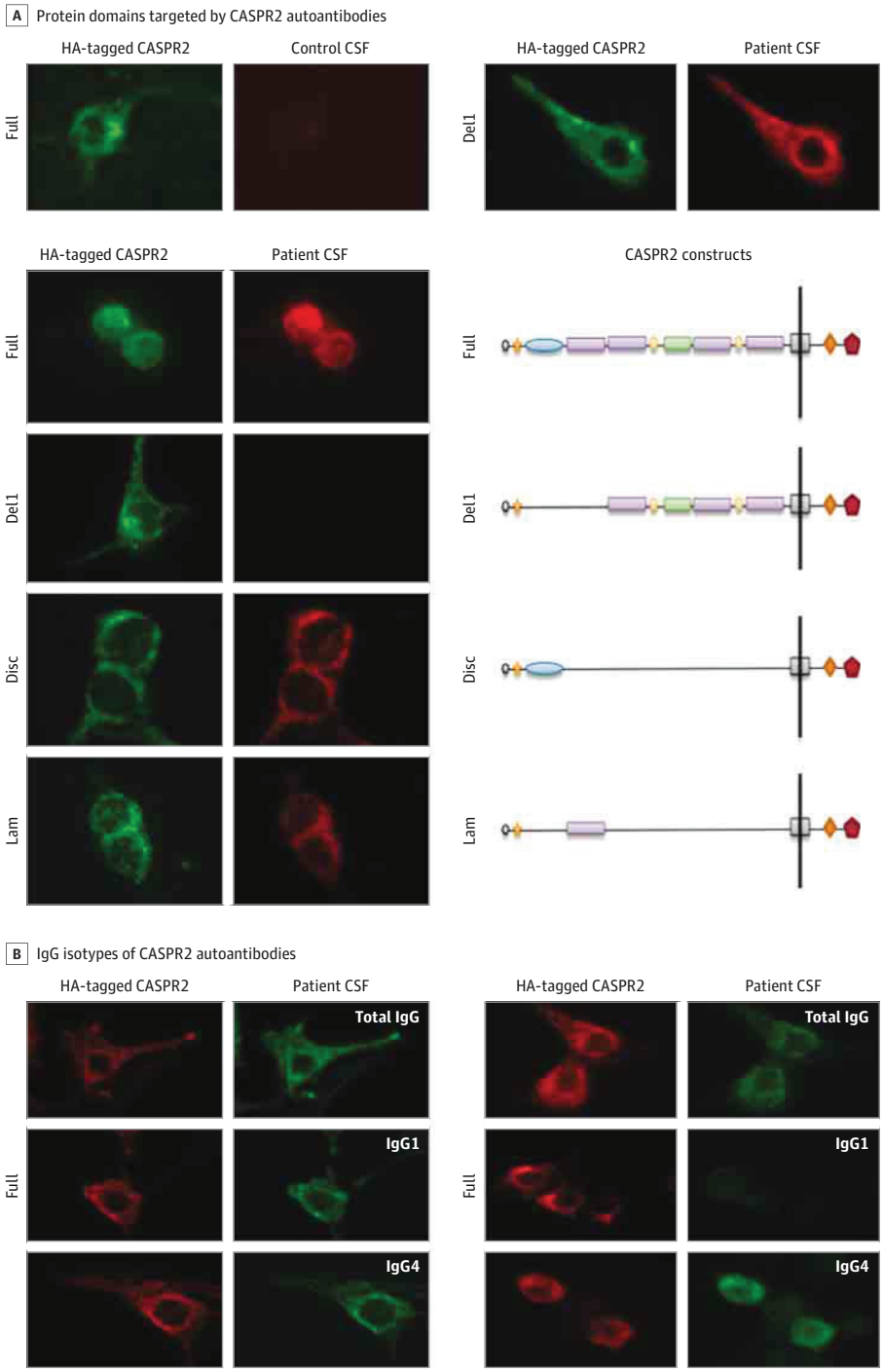

A, Human embryonic kidney 293 cells were transfected to express the full-length contactin-associated protein-like 2 (CASPR2) protein- or domain-deletion constructs tagged with hemagglutinin (HA), visualized in the first column. The transfected cells were incubated with patients' cerebrospinal fluid (CSF; dilution 1:10), visualized in the second column. Top left: CASPR2 cells were not recognized in the CSF of any control patients. Bottom left: Constructs only including the discoidin domain (Disc), laminin G1 domain (Lam), or both domains (not shown) were recognized in all 18 samples for patients with CASPR2 cells in the CSF, but the Del1 construct, lacking Disc and Lam, was not recognized in 8 of 18 patients. Top right: Example of 1 of 10 patients in whom the Del1 construct was recognized. Bottom right: Illustration of the different CASPR2 domains deleted in our constructs. B, Human embryonic kidney 293 cells were transfected with the HA-tagged full-length CASPR2 protein and incubated with patients' CSF (dilution 1:10) to determine the IgG isotypes of CASPR2 autoantibodies. We observed 10 of 17 patients with both IgG4 and IgG1 antibody subtypes (left panel), but only IgG4 antibodies were observed in the remaining 7 patients (right panel).

antibodies in the CSF is associated with a homogeneous clinical pattern of autoimmune encephalitis with prevalent limbic involvement and seizures. As reported before,[1,11] we observed an overrepresentation of male patients in our cohort, which was significantly higher than in patients with NMT or MoS. Epilepsy was the main symptom that led the patients to seek medical attention. Neither confusion nor behavioral disorders were observed in any of the patients. All patients had anterograde or episodic memory disorders and/or temporal seizures, which suggests a constant involvement of the hippocampus. Brain MRIs were in accordance with this result, as most patients displayed temporomesial hyperintensities or hippocampal atrophy on T2-weighted images (Figure 1). Nonetheless, extralimbic symptoms were observed as well, the most frequent being cerebellar ataxia, in accordance with previous results.[12] Neuromyotonia was rare in our cohort. Relapses were observed in 6 patients, most often in the form of an increase in seizure activity. In some cases, this increased seizure activity was steroid-dependent and steroid-responsive, indicating the possible direct responsibility of anti-CASPR2 autoimmunity for the epileptogenic process. In contrast with patients with NMT or MoS, none of the patients in our cohort had a malignant thymoma.

Our data suggest that the presence of anti-CASPR2 antibodies in the CSF is associated with a subtype of autoimmune encephalitis that is mostly nonparaneoplastic. By comparison, patients with NMT or MoS do not have detectable anti-CASPR2 antibodies in the CSF and are frequently affected by a malignant thymoma. The absence of detectable anti-CASPR2 antibodies in the CSF of patients with NMT or MoS could reflect an autoimmune reaction strictly developed outside of the central nervous system. Alternatively, it might be because of extremely low titers of anti-CASPR2 antibodies in the CSF, as serum titers were much lower in patients with NMT or MoS. Therefore, variations of the autoantibodies production within the intrathecal compartment are likely to underline the observed differences in clinical presentation between the 2 groups.

Epitope Specificities

Interestingly, the anti-CASPR2 antibodies in the CSF from all patients targeted the discoidin and laminin G1 domains of CASPR2, suggesting that recognition of these domains is involved in the genesis of symptoms. To our knowledge, the precise roles of the discoidin and laminin G1 domains have not yet been clearly determined.

IgG Subtypes

Importantly, IgG4 anti-CASPR2 antibodies were detected in the CSF of all patients. IgG4 antibodies cannot bind to complement or form immune complexes and have a low affinity for Fc receptors.[14,15] Moreover, IgG4 antibodies have the ability to exchange fragment antigen-binding arms, and a fraction of them are therefore bispecific, suggesting that some of the anti-CASPR2 antibodies of our patients may have bispecificity for the laminin G1 and discoidin domains.[16,17] Interestingly, fragment antigen-binding fragments of anti-Musk IgG4 autoantibodies from patients with myasthenia gravis have been shown to be pathogenic in vitro, suggesting the involvement of mechanisms other than the classical cross-linking and internalization that was observed with other autoantibodies directed against synaptic proteins.[18] It remains to be seen whether IgG4 anti-CASPR2 antibodies are bispecific for the discoidin and laminin G1 domain and whether they are able to cross-link CASPR2 and induce its internalization or alter its function by other mechanisms. Additionally, IgG1 autoantibodies were found in all the patients with hippocampal atrophy, implying the possible involvement of complement or antibody-dependent cell death. This view is supported by 1 biopsied case of CASPR2 antibody encephalitis in which immunoglobulin and complement depositions were reported in neurons along with cell degeneration in the hippocampus.[19] Therefore, distinct pathological processes can occur during the course of CASPR2 antibody encephalitis, ranging from functional alterations involving IgG4 autoantibodies to complement-mediated cell toxicity induced by IgG1 autoantibodies.

This study has several limitations. Because of the rarity of the disease, we only analyzed retrospective data from a small series of patients. We also cannot exclude low titers of anti-CASPR2 antibodies in the CSF of patients with NMT or MoS not detected by our methods. Our results need to be confirmed in futures studies.

Conclusions

In conclusion, anti-CASPR2 antibodies are found in the CSF only in patients with CASPR2 antibody-associated autoimmune encephalitis, whereas anti-CASPR2 antibodies are detected only in the serum in patients with NMT or MoS. Contactin-associated protein-like 2 antibody-associated encephalitis is observed predominantly in males and is characterized by prominent limbic symptoms and temporal lobe epilepsy. Malignant thymoma was found only in patients with NMT or MoS. Recognition of the discoidin and laminin G1 domains by the autoantibodies is constant and may be important in the genesis of limbic symptoms. Additionally, anti-CASPR2 antibodies of the IgG4 isotype may play a fundamental role in the pathogenic processes through a functional effect on CASPR2, although complement-mediated cell death induced by IgG1 autoantibodies may also occur in some patients. These hypotheses must be further supported by future functional studies focused on antibody specificities.

ARTICLE INFORMATION

Accepted for Publication: April 8, 2016.

Published Online: July 18, 2016. doi:10.1001/jamaneurol.2016.1585.

Author Affiliations: Centre National de Référence pour les Syndromes Neurologiques Paranéoplasiques, Hôpital Neurologique, Hospices Civils de Lyon, Lyon, France. (Joubert, Picard, Rogemond, Ducray, Psimaras, Delattre, Antoine, Honnorat); Institut NeuroMyoGene, INSERM 1217/CNRS 5310, Université de Lyon, Lyon, France. (Joubert, Saint-Martin, Noraz, Rogemond, Ducray, Desestret, Honnorat); Université Claude-Bernard Lyon 1, Université de Lyon, Lyon, France. (Joubert,

Saint-Martin, Noraz, Rogemond, Ducray, Honnorat); Département de Neurologie, Groupe Hospitalier Pitié-Salpêtrière, Paris, France (Psimaras, Delattre); Service de Neurologie, Hôpital Bellevue, Centre Hospitalier Universitaire de Saint-Étienne, Saint-Étienne, France (Antoine).

Author Contributions: Drs Honnorat and Joubert had full access to all the data in the study and take responsibility for the integrity of the data and the accuracy of the data analysis.
Study concept and design: Joubert, Honnorat.
Acquisition, analysis, or interpretation of data: All authors.
Drafting of the manuscript: Joubert, Honnorat.
Critical revision of the manuscript for important intellectual content: All authors.
Obtained funding: Honnorat.
Administrative, technical, or material support: Rogemond, Delattre.
Study supervision: Honnorat.

Conflict of Interest Disclosures: None reported.

Funding/Support: This study is supported by research grant ANR-14-CE15-0001-MECANO from the L'Agence Nationale de la Recherche and the 2014 Abnormal Behavior and Immune Dysfunction grant from the Fondation pour la Recherche sur le Cerveau.

Role of the Funder/Sponsor: The funders had no role in the design and conduct of the study; collection, management, analysis, or interpretation of the data; preparation, review, or approval of the manuscript; and decision to submit the manuscript for publication.

Additional Contributions: We thank the referral physicians who kindly transmitted the exhaustive clinical and ancillary information that allowed us to perform this study: Lejla Koric, MD (Assistance Publique–Hôpitaux de Marseille, Marseille, France); Isabelle Lambert, MD (Assistance Publique–Hôpitaux de Marseille, Marseille, France); Cécile Marchal, MD (Centre Hospitalier Universitaire de Bordeaux, Bordeaux, France); Philippe Kassiotis, MD (Centre Hospitalier Bretagne Atlantique, Vannes, France); Fabienne Ory-Magne, MD (Centre Hospitalier Universitaire de Toulouse, Toulouse, France); Jérémie Pariente, MD (Centre Hospitalier Universitaire de Toulouse, Toulouse, France); Jonathan Curot, MD (Centre Hospitalier Universitaire de Toulouse, Toulouse, France); Pierric Giraud, MD (Centre Hospitalier Annecy Genevois, Metz-Tessy, France); Laurent Martinez-Almoyna, MD (Centre Hospitalier d'Aix en Provence, Aix-en-Provence, France); Anne-Céline Zeghoudi, MD (Centre Hospitalier de Versailles, Versailles, France); Sylvain Rheims, MD, PhD (Hospices Civils de Lyon, Lyon, France); Ana Gales, MD (Assistance Publique–Hôpitaux de Paris, Paris, France); Charles Behr, MD (Centre Hospitalier Régional Universitaire de Strasbourg, Strasbourg, France); Eric Thouvenot, MD (Centre Hospitalier Universitaire de Nîmes, Nimes, France); Gil Petitnicolas, MD (Centre Hospitalier Intercommunal de Toulon, Toulon, France); and Claire Boutoleau-Bretonniere, MD (Centre Hospitalier Universitaire de Nantes, Nantes, France). None of these contributors were compensated for their work.

REFERENCES

1. Irani SR, Alexander S, Waters P, et al. Antibodies to Kv1 potassium channel-complex proteins leucine-rich, glioma inactivated 1 protein and contactin-associated protein-2 in limbic encephalitis, Morvan's syndrome and acquired neuromyotonia. *Brain*. 2010;133(9):2734-2748.

2. Malter MP, Frisch C, Schoene-Bake JC, et al. Outcome of limbic encephalitis with VGKC-complex antibodies: relation to antigenic specificity. *J Neurol*. 2014;261(9):1695-1705.

3. Irani SR, Pettingill P, Kleopa KA, et al. Morvan syndrome: clinical and serological observations in 29 cases. *Ann Neurol*. 2012;72(2):241-255.

4. Laurencin C, André-Obadia N, Camdessanché JP, et al. Peripheral small fiber dysfunction and neuropathic pain in patients with Morvan syndrome. *Neurology*. 2015;85(23):2076-2078.

5. Poliak S, Salomon D, Elhanany H, et al. Juxtaparanodal clustering of Shaker-like K+ channels in myelinated axons depends on Caspr2 and TAG-1. *J Cell Biol*. 2003;162(6):1149-1160.

6. Bel C, Oguievetskaia K, Pitaval C, Goutebroze L, Faivre-Sarrailh C. Axonal targeting of Caspr2 in hippocampal neurons via selective somatodendritic endocytosis. *J Cell Sci*. 2009;122(pt 18):3403-3413.

7. Pinatel D, Hivert B, Boucraut J, et al. Inhibitory axons are targeted in hippocampal cell culture by anti-Caspr2 autoantibodies associated with limbic encephalitis. *Front Cell Neurosci*. 2015;9:265.

8. Olsen AL, Lai Y, Dalmau J, Scherer SS, Lancaster E. Caspr2 autoantibodies target multiple epitopes. *Neurol Neuroimmunol Neuroinflamm*. 2015;2(4):e127.

9. Reiber H, Lange P. Quantification of virus-specific antibodies in cerebrospinal fluid and serum: sensitive and specific detection of antibody synthesis in brain. *Clin Chem*. 1991;37(7):1153-1160.

10. Navarro V, Kas A, Apartis E, et al. Motor cortex and hippocampus are the two main cortical targets in LGI1-antibody encephalitis. *Brain*. 2016;139(pt 4):1079-1093.

11. Lancaster E, Huijbers MG, Bar V, et al. Investigations of caspr2, an autoantigen of encephalitis and neuromyotonia. *Ann Neurol*. 2011;69(2):303-311.

12. Becker EBE, Zuliani L, Pettingill R, et al. Contactin-associated protein-2 antibodies in non-paraneoplastic cerebellar ataxia. *J Neurol Neurosurg Psychiatry*. 2012;83(4):437-440.

13. Sunwoo JS, Lee ST, Byun JI, et al. Clinical manifestations of patients with CASPR2 antibodies. *J Neuroimmunol*. 2015;281:17-22.

14. Bindon CI, Hale G, Brüggemann M, Waldmann H. Human monoclonal IgG isotypes differ in complement activating function at the level of C4 as well as C1q. *J Exp Med*. 1988;168(1):127-142.

15. Bruhns P, Iannascoli B, England P, et al. Specificity and affinity of human Fcgamma receptors and their polymorphic variants for human IgG subclasses. *Blood*. 2009;113(16):3716-3725.

16. Schuurman J, Van Ree R, Perdok GJ, Van Doorn HR, Tan KY, Aalberse RC. Normal human immunoglobulin G4 is bispecific: it has two different antigen-combining sites. *Immunology*. 1999;97(4):693-698.

17. van der Neut Kolfschoten M, Schuurman J, Losen M, et al. Anti-inflammatory activity of human IgG4 antibodies by dynamic Fab arm exchange. *Science*. 2007;317(5844):1554-1557.

18. Huijbers MG, Zhang W, Klooster R, et al. MuSK IgG4 autoantibodies cause myasthenia gravis by inhibiting binding between MuSK and Lrp4. *Proc Natl Acad Sci U S A*. 2013;110(51):20783-20788.

19. Körtvelyessy P, Bauer J, Stoppel CM, et al. Complement-associated neuronal loss in a patient with CASPR2 antibody-associated encephalitis. *Neurol Neuroimmunol Neuroinflamm*. 2015;2(2):e75.

B. Article 2 :

Structural mapping of hot spots within human CASPR2 Discoidin domain for autoantibody recognition

Margaux Saint-Martin*, Junying Zhang*, Wenjun Liang*, Fei Xu, Nelly Noraz, Jianmei Liu, Jerome Honnorat, Heli Liu. **2018**. Journal of autoimmunity. Accepted for publication on the 01th of October. * first co-author

Nous avons montré précédemment que les anticorps de patients sont majoritairement dirigés contre les domaines discoidine et laminine G1 de CASPR2. Le domaine discoidine est particulièrement intéressant puisqu'il distingue CASPR2 des neurexines. De plus, celui-ci permet l'interaction de nombreuses protéines (facteur de coagulation V, neuropiline, récepteurs à domaine discoidine) avec leurs partenaires, comme par exemple le collagène, dans le cas des récepteurs à domaine discoidine. L'étude de la structure de CASPR2 et des régions clés pour sa reconnaissance par les anticorps de patients permettra de mieux comprendre sa fonction et l'impact des anticorps sur celle-ci.

En collaboration avec l'équipe de Heli Liu du laboratoire des drogues naturelles et biomimétiques à Pékin, nous avons déterminé la structure du domaine discoidine. Celui-ci est formé de feuillets beta, organisés de façon à présenter quatre boucles particulièrement accessibles formant une surface polarisée propice aux interactions avec d'autres protéines. A l'aide d'un logiciel de prédiction d'épitopes basé sur la structure, nous avons généré huit mutants et testé leur capacité à être reconnus par les anticorps de patients. Nous avons trouvé une diminution de la reconnaissance pour trois mutants en particulier, G69N/A71S, S77N et D78R tous situés dans la boucle L1 du domaine discoidine. Nous avons également observé que le mutant composé d'une combinaison de ces trois mutations présente une diminution de la reconnaissance par les anticorps anti-CASPR2 pour 11 des 12 patients testés.

En conclusion, la boucle L1 s'avère être une région clé pour la reconnaissance du domaine discoidine par les anticorps de patients. Par homologie avec le domaine discoidine d'autres protéines (Carafoli et al., 2009), cette boucle pourrait être impliquée dans les interactions de CASPR2 avec ses partenaires.

Journal of Autoimmunity xxx (xxxx) xxx–xxx

Contents lists available at ScienceDirect

Journal of Autoimmunity

journal homepage: www.elsevier.com/locate/jautimm

Structural mapping of hot spots within human CASPR2 discoidin domain for autoantibody recognition

Wenjun Liang[a,b,1], Junying Zhang[a,b,1], Margaux Saint-Martin[c,d,e,1], Fei Xu[a,b], Nelly Noraz[c,d,e], Jianmei Liu[a,b], Jérôme Honnorat[c,d,e,**], Heli Liu[a,b,*]

[a] State Key Laboratory of Natural and Biomimetic Drugs & School of Pharmaceutical Sciences, Peking University Health Science Center, 38 Xueyuan Road, Haidian District, Beijing 100191, China
[b] Department of Molecular and Cellular Pharmacology, School of Pharmaceutical Sciences, Peking University Health Science Center, 38 Xueyuan Road, Haidian District, Beijing 100191, China
[c] French Reference Center on Paraneoplastic Neurological Syndrome, Hospices Civils de Lyon, Hôpital Neurologique, Bron, France
[d] INSERM U1217–CNRS UMR5310, NeuroMyoGene Institute, Lyon, France
[e] Université Claude Bernard Lyon 1, Université de Lyon, France

ARTICLE INFO

Keywords:
CASPR2
Discoidin domain
Crystal structure
Autoantibody
Limbic encephalitis

ABSTRACT

Accumulating evidence has showed that anti-CASPR2 autoantibodies occur in a long list of neurological immune disorders including limbic encephalitis (LE). Belonging to the well-known neurexin superfamily, CASPR2 has been suggested to be a central node in the molecular networks controlling neurodevelopment. Distinct from other subfamilies in the neurexin superfamily, the CASPR subfamily features a unique discoidin (Disc) domain. As revealed by our and others' recent studies, CASPR2 Disc domain bears a major epitope for autoantibodies. However, structural information on CASPR2 recognition by autoantibodies has been lacking. Here, we report the crystal structure of human CASPR2 Disc domain at a high resolution of 1.31 Å, which is the first atomic-resolution structure of the CASPR subfamily members. The Disc domain adopts a total β structure and folds into a distorted jellyroll-like barrel with a conserved disulfide-bond interlocking its N- and C-termini. Defined by four loops and located in one end of the barrel, the "loop-tip surface" is totally polar and easily available for protein docking. Based on structure-guided epitope prediction, we generated nine mutants and evaluated their binding to autoantibodies of cerebrospinal fluid from twelve patients with limbic encephalitis. The quadruple mutant G69N/A71S/S77N/D78R impaired CASPR2 binding to autoantibodies from eleven LE patients, which indicates that the loop L1 in the Disc domain bears hot spots for autoantibody interaction. Structural mapping of autoepitopes within human CASPR2 Disc domain sheds light on how autoantibodies could sequester CASPR2 ectodomain and antagonize its functionalities in the pathogenic processes.

1. Introduction

As a fascinating advancement in the field of neuroimmunology in the last decade, accumulating evidence has revealed that a wide range of neurological diseases are mediated by autoantibodies against neuronal cell surface proteins involved in synaptic signaling and plasticity [1–3]. Among the neuronal cell-surface antigens, CASPR2 is an attractive one, since anti-CASPR2 autoantibodies have been reported in a long list of neurological immune disorders including Morvan's syndrome and limbic encephalitis [4–17]. Our recent cohort study has showed that anti-CASPR2 antibodies in the cerebrospinal fluid (CSF) are closely associated with a subtype of autoimmune encephalitis with prominent limbic involvement and seizures [18].

Human CASPR2 encoded by the *CNTNAP2* gene, is a 1331-residue long and single-passing transmembrane protein that contains an N-terminal signal peptide followed by an extracellular region, one transmembrane domain and a short C-terminal intracellular region. The extracellular region is composed of a mosaic of domains, including the N-terminal discoidin (Disc), laminin G (Lam1), laminin G (Lam2), epidermal growth factor 1 (Egf1), fibrinogen C (FibC), laminin G

* Corresponding author. State Key Laboratory of Natural and Biomimetic Drugs & School of Pharmaceutical Sciences, Peking University Health Science Center, 38 Xueyuan Road, Haidian District, Beijing 100191, China.
** Corresponding author. French Reference Center on Paraneoplastic Neurological Syndrome, Hospices Civils de Lyon, Hôpital Neurologique, Bron, France.
E-mail addresses: jerome.honnorat@chu-lyon.fr (J. Honnorat), liuheli@hsc.pku.edu.cn (H. Liu).
[1] These authors contributed equally.

https://doi.org/10.1016/j.jaut.2018.09.012
Received 31 May 2018; Received in revised form 23 September 2018; Accepted 30 September 2018

(Lam3), Egf (Egf2), and laminin G (Lam4) domains [19]. As a cell-adhesion molecule, CASPR2 belongs to the neurexin superfamily; however, distinct from other members in the neurexin superfamily, the CASPR subfamily members, including CASPR1 through CASPR5 (also named CNTNAP1-CNTNAP5), contain a Disc domain [19]. Like neurexin which is well-known for functioning in synapse formation and association with neurological disorders such as autism [20], CASPR2 plays an important role for neuronal dendritic arborization, spine morphology and synaptic formation [21–23], while mutations in the *CNTNAP2* gene encoding CASPR2 were mainly identified in patients with focal epilepsy, intellectual disability, or autism [24–26]. Worthy to mention, a high concentration of mutations was found in the exons coding for the discoidin domain [27]. In addition, knockout of the *CNTNAP2* gene led to deficits in the core ASD behavioral domains in a mouse model [28]. Multiple-domain organization in CASPR2 implicates that it may engage in a number of protein-protein interactions to regulate functions [29]. Likely owing to multifaceted functions and involvement in extensive protein interactions, CASPR2 has been suggested to be a central node in the molecular networks controlling neurodevelopment [30].

Mapping anti-CASPR2 antibody epitope(s) at the structural level would facilitate revealing mechanisms for autoantibody pathogenicity and improve diagnosis and treatment for CASPR2-associated autoimmune diseases such as limbic encephalitis [31]. Using the cell-based binding and neuron-based functional assays, we have showed that anti-CASPR2 antibodies from a subtype of limbic encephalitis patients selectively reacted with the N-terminal modules, including Disc and Lam1 domains of CASPR2, and that anti-CASPR2 antibodies mainly target hippocampal inhibitory interneurons and may induce alteration of CASPR2-mediated inhibitory synaptic contacts [32]. Deletion of the Disc domain of CASPR2 showed significantly reduced immunoreactivity against antibody-positive patient sera, even though without a complete abrogation of binding [33]. This report further suggests that the Disc domain of CASPR2 contains a major epitope for autoantibodies.

Although molecular architecture of the full-length ectodomain of CASPR2 was constructed by electron microscopy [34,35], no high-resolution structure has been determined for any domain of CASPR2. Structural information on CASPR2 interacting with autoantibodies has also been lacking. Here, we report the crystal structure of human CASPR2 Disc domain at 1.31 Å resolution, which to our best knowledge is the first atomic-resolution structure for the CASPR subfamily. Using structure-guided mutagenesis and protein-based ELISA, we have revealed hot spots within the Disc domain for recognition by anti-CASPR2 autoantibodies from patients with limbic encephalitis. Hopefully, these findings may shed light on how autoantibodies could antagonize CASPR2's functionalities in the pathogenic processes.

2. Methods

2.1. Molecular cloning and baculovirus generation

cDNA fragments encoding the Disc domain (amino-acid residues 35–181) of human CASPR2 (NCBI Reference Sequence: NM_014141.5) were amplified by PCR using gene-specific primers containing *Bam*HI and *Not*I sites. The PCR fragments were subsequently digested and ligated into a modified BacMam vector [36,37]. A hexahistidine tag was introduced to the C-terminus of the construct to facilitate protein purification. After being verified by DNA sequencing, plasmids were co-transfected with BacVector-3000 baculovirus DNA (EMD, USA) using Cellfectin (Life technologies, USA) into *sf9* insect cells in the serum and antibiotics-free SF900-II media (Life technologies, USA). Primary progeny of recombinant virus was used to infect *sf9* cells for amplification. 6 d later, higher-titer baculovirus was harvested by centrifugation at 1000*g* for 10 min.

2.2. Protein expression and purification

For protein expression, an appropriate volume of recombinant baculovirus was used to transduce HEK293S cells cultured in the DMEM/F12 (Gibco, USA) media supplemented with 10% FBS (Life technologies, USA). 72 h post viral transduction, the conditioned medium was centrifuged at 3000 g at 277 K for 15 min. The supernatant was harvested, buffer-exchanged to HBS (HEPES-buffered saline, containing 10 mM HEPES pH 7.5 and 150 mM NaCl) and applied to Ni^{2+}–NTA affinity chromatography. The unbound proteins were subsequently removed from the affinity column using washing buffer (HBS supplemented with 20 mM imidazole). The affinity column eluate from 300 mM imidazole-containing HBS was further applied to a Superdex-200 10/300 GL size-exclusion column (GE Healthcare) pre-equilibrated with HBS. The fractions eluted at 17–18 ml were verified by SDS-PAGE with Coomassie blue staining, pooled and concentrated to 10 mg/ml for crystallization. The protein concentration was determined through measuring OD_{280} values and calculated with extinction coefficients of 46535 $M^{-1}{\cdot}cm^{-1}$.

2.3. Crystallization

The initial crystallization conditions were screened at 293 K by the sitting-drop vapor-diffusion method using the Hampton kit (HR2-130) and the Emerald Biosystems kit (Wizard I and II). 3 d later, microcrystals were found in the No. 8 condition of the Wizard Classic kit II. After optimization, diffraction-quality brick-like crystals, with a typical dimension of 0.2 × 0.2 × 0.3 mm^3, were obtained from a sitting drop in equilibration with the reservoir solution consisting of 20% (w/v) PEG8000, 100 mM Na_2HPO_4/KH_2PO_4 (pH 6.2) and 200 mM NaCl.

2.4. Data collection and structure determination

Crystals were fast-soaked in the crystallization solution supplemented with 22–24% (v/v) ethylene glycerol prior to being flash-cooled in liquid nitrogen. Diffraction data were collected on the beamline BL19U1 at Shanghai Synchrotron Radiation Facility (SSRF). The data sets were indexed and processed using HKL2000 [38]. Phases were calculated with molecular replacement (MR) method in PHASER [39]. The crystal structure of the membrane-binding C2 domain of human coagulation factor V (PDB code: 1CZV) [40] was used as a template for searching MR solution. The resulting solution, with a TFZ score of 15.3, was subjected to Autobuild in the software PHENIX [41]. The auto-built model was improved by iterative manual building in COOT [42] and refinement in PHENIX. During the final stage of refinement, water molecules were introduced using PHENIX and manually edited in COOT. The stereochemistry of the final model was evaluated using Molprobity [43]. The statistics for data collection and refinement are given in Table 1.

2.5. Epitope prediction and structure analysis

The crystal structure of human CASPR2 Disc domain was applied to DiscoTope 2.0 server [44] for epitope prediction, with the threshold for epitope identification set at −3.7. For structure analysis, DALI [45] was used to search for structural homology. Structure-based sequence alignment was executed using ClusterW [46] and mapped using ESPRIPT [47]. Conservation of residues was based on chemical character: aromatic (F, Y, and W), hydrophobic (L, I, V, and M), acidic (E and D), basic (K, R, and H), polar (S and T), tiny (G and A), and amide (N and Q). Conservation was mapped to protein surface using Consurf [48]. Solvent accessible surface area for each atom was calculated using the program AREAIMOL in the CCP4 suite [49].

Table 1
Data collection and refinement statistics for human CASPR2 Disc domain.

Data collection	
X-ray source	SSRF BL19U1
Detector	Pilatus3 6M
Wavelength (Å)	0.978
Crystal-to-detector distance (mm)	200
Oscillation range (°)	180
Oscillation width per image (°)	1
Space group	$P2_12_12_1$
Unit cell dimensions: a, b, c (Å); α, β, γ (°)	36.250, 59.680, 62.599; 90, 90, 90
Resolution range (Å)[a]	50–1.31 (1.33–1.31)
Unique reflections	33381 (1598)
Completeness (%)	99.6 (97.3)
$I/\sigma(I)$	35.4 (2.75)
Redundancy	8.5 (6.1)
R_{merge} (%)[b]	7.8 (53.8)
R_{meas} (%)[b]	8.3 (58.6)
R_{pim} (%)[b]	2.8 (22.7)
Refinement	
Resolution range (Å)	31.37–1.31 (1.36–1.31)
R_{work}[c]	13.33 (15.99)
R_{free}[c]	16.51 (21.11)
Average *B*-factor for protein and solvent (Å^2)	19.99, 34.17
r.m.s.d. bond length (Å)	0.01
r.m.s.d. bond angle (°)	1.18
Ramachandran (%; favored, allowed, generally allowed, disallowed)	98.7, 1.3, 0, 0

[a] Values in parenthesis are for the highest resolution shell.
[b] $R_{merge} = \Sigma_{hkl}|I - \langle I\rangle|/\Sigma_{hkl}I$, where I is the intensity of unique reflection hkl, and $\langle I\rangle$ is the average over symmetry-related observations of unique reflection hkl. R_{pim}: precision-indicating merging R-factor. R_{meas}: multiplicity-corrected merging R-factor.
[c] $R_{work} = \Sigma|F_o - F_c|/\Sigma|F_o|$, where F_o and F_c are the observed and calculated structure factors, respectively. R_{free} was calculated using 5% of the reflections set aside from refinement.

2.6. Structure-based mutagenesis

cDNAs encoding human CASPR2 Disc domain plus the N-terminal segment (residues 28-181) and its mutants S55N, G69N/A71S, S77N, D78R, Y82A, W134S, D143S, R171E and G69N/A71S/S77N/D78R were amplified by a single-step or two-step overlapping PCR. Subcloning, baculovirus recombination and protein preparation for these mutants were performed using the same protocol as used for the construct produced for crystallization.

2.7. Patients

Approval for this study was granted by the institutional review board of the Hospices Civils de Lyon (Comité de Protection des Personnes SUD-EST IV). Written informed consent was obtained from all patients. Titer, IgG subclass and target domains of the auto-antibodies directed against CASPR2 in the limbic encephalitis (LE) patient's CSF were previously characterized [18]. Twelve CSF samples with titers between 1:320 and 1:10240 were obtained from the NeuroBioTec biobank (Hospices Civils de Lyon, France). In these CSF samples, 6 had antibodies directed against the Disc and Lam1 domains only (Disc-Lam1) and 6 against multiple domains of CASPR2 (Mult). Basic immunological features of the LE patients are listed in Table 2.

2.8. Protein-based ELISA

Recombinant human CASPR2 Disc domain plus the N-terminal segment (residues 28-181), or its mutants, or BSA, was coated onto a 96-well plate (Costar 3590, Corning Incorporated) with 0.4 µg protein in 50 µl of Na_2CO_3/$NaHCO_3$ buffer (pH 9.5) per well for overnight incubation at 4 °C. The wells were each washed thrice with 200 µl of phosphate-buffered saline containing 0.05% Tween-20 (PBS-T), and blocked with 200 µl of PBS supplemented with 10% (v/v) fetal bovine serum (FBS) for 2 h at 37 °C. The blocking solution was then removed and 50 µl of CSF diluted in 2% (v/v) FBS-containing PBS was added. After further incubation at 37 °C for 2 h, the wells were washed three times with PBS-T, and incubated for 30 min at 37 °C with 50 µl of 2% (v/v) FBS-containing PBS in the presence of HRP-conjugated goat anti-human IgG antibodies (Jackson Immuno Research, Ref. 109-036-064) (diluted at 1:8000). After three washes in PBS-T, 50 µl of the TMB solution was added to each well (Abcam, AB171523). After 15 min, the reaction was stopped by the addition of 50 µl of 2M HCl. Optical densities (ODs) were recorded at 450 nm using a microplate reader (Tecan). Unless otherwise stated, experiments were performed in triplicate and the data were represented as a mean value ± standard deviation. The represented OD_{450} value was calculated using the OD value for coated Disc proteins subtracted by that for BSA (as a control). The OD decrease was considered significant when it was two times larger than the highest standard deviation (with a threshold set at 20%).

Table 2
Basic immunological features of LE patients with anti-CASPR2 antibodies.

Patient	Titer[a]	Dilution[b]	Epitope[c]
Pat1	1:1280	1:20	Disc-Lam1
Pat2	1:10240	1:100	Disc-Lam1
Pat3	1:640	1:10	Disc-Lam1
Pat4	1:1280	1:20	Disc-Lam1
Pat5	1:10240	1:100	Disc-Lam1
Pat6	1:5120	1:40	Disc-Lam1
Pat7	1:1280	1:20	Mult
Pat8	1:5120	1:40	Mult
Pat9	1:320	1:10	Mult
Pat10	1:2560	1:20	Mult
Pat11	1:10240	1:100	Mult
Pat12	1:5120	1:40	Mult

[a] CSF titers (last dilution of CSF giving a positive signal) were previously determined by cell based assay [18].
[b] Lowest dilution used in the ELISA.
[c] Disc-Lam1: for antibodies targeting the Disc and Lam1 domains only; Mult: antibodies targeting the Disc and Lam1 domains as well as other domains.

3. Results

3.1. Overall structure of the CASPR2 Disc domain

Using baculovirus-transduced mammalian cells, we obtained high-expression of human CASPR2 Disc domain (residues 35-181) and purified it into high homogeneity and purity (Fig. 1A). The recombinant protein had an elution volume of 17.7 ml, corresponding to an estimated molecular mass of ~14 kDa. The estimated molecular mass is close to the calculated value, 17.4 kDa, based on its primary sequence plus cloning scar and tag, which indicates that human CASPR2 Disc domain mainly exists as a monomer in solution. This is consistent with the previous report that the extracellular region of CASPR2 is likely monomeric [50]. The purified protein crystallized in the $P2_12_12_1$ space group, and diffracted to 1.31 Å (Table 1). Given the presence of one molecule of the Disc domain per asymmetric unit, the Matthews coefficient (V_M) was calculated to be 2.53 Å^3·Da^{-1}, corresponding to a reasonable solvent content of 51.3% [51]. Using the structure of the membrane-binding C2 domain of human coagulation factor V [40] as a template for molecular replacement, we solved the crystal structure of human CASPR2 Disc domain, and the final model has relatively low R_{work}/R_{free} factors and a reasonable stereochemistry (Table 1).

Human CASPR2 Disc domain adopts a total β structure and folds into a distorted jellyroll-like barrel, with a dimension of approximately 35 × 30 × 25 Å^3. This barrel mainly consists of eight antiparallel β-strands arranged in two sheets, with five strands β1, β2, β4, β5 and β7 forming one sheet packed against by the other one that is composed of

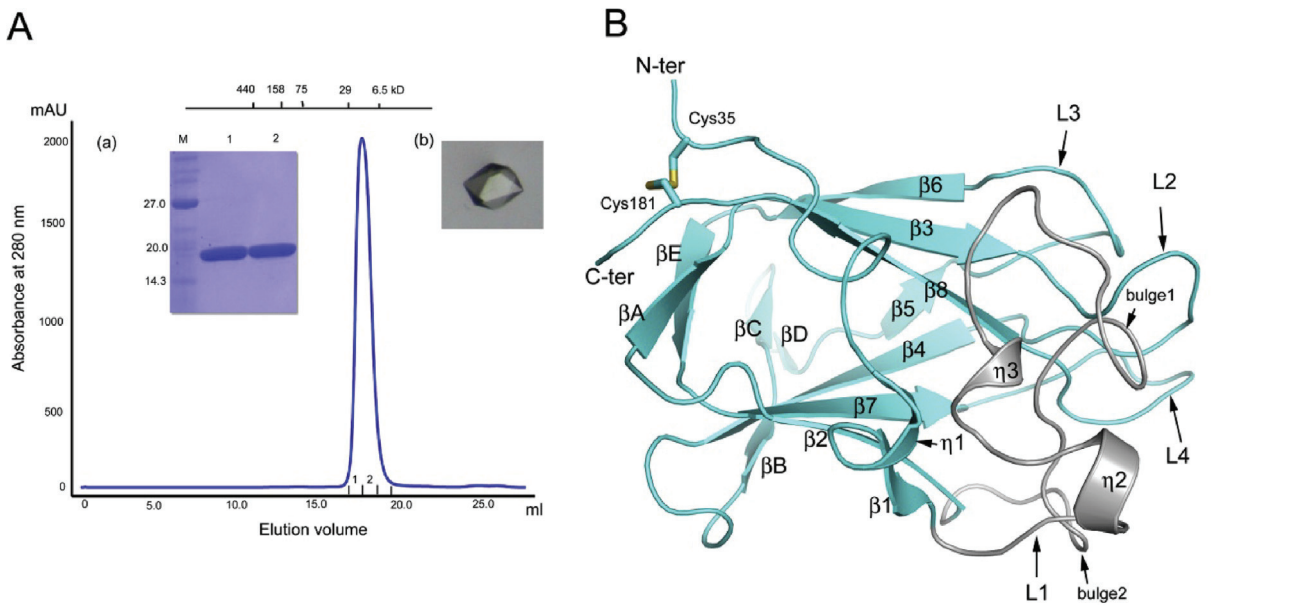

Fig. 1. Biochemical characterization and overall structure of human CASPR2 Disc domain. (A) Gel filtration chromatogram of recombinant human CASPR2 Disc domain. The inset (a) is an image for Coomassie blue-stained SDS-PAGE analysis of two fractions 1 and 2 eluted from a Superdex 200 gel filtration column. M, molecular weight marker in kDa. A crystal of the Disc domain is shown in the inset (b). (B) Ribbon representation of human CASPR2 Disc domain (in cyan) with secondary structure elements labeled and the loop L1 highlighted in grey. The N- and C-termini are respectively labeled as "N-ter" and "C-ter". The disulfide bond Cys35-Cys181 is indicated in sticks. (For interpretation of the references to color in this figure legend, the reader is referred to the Web version of this article.)

three strands β3, β6 and β8 (Fig. 1B). Different from other barrel-wall strands, the strand β5 follows a protruding hairpin that is composed of short strands βC and βD. The strand βC is proceeded by the strand βB which joins the barrel sheet and is antiparallel with the C-terminal half of the strand β4.

On one end of the barrel, the N-terminal residue Cys35 and the C-terminal residue Cys181 forms a disulfide bond that locks the barrel. Preceding the short strand β1, the N-terminal segment (residues 34-47) assumes a loop configuration with residues 45-47 folding into a short 3_{10} helix, η1. Adjacent to the C-terminal segment is an β-sheet of two antiparallel strands βA and βB. The strand βA connects the barrel-wall strands β2 and β3, while the strand βE is located in the middle of the link between the strands β6 and β7. The long axis of the βA/βE sheet is almost perpendicular to that of the barrel.

On the other end of the barrel are distributed four loops (named L1, L2, L3 and L4) each connecting the barrel-wall strands. The L1, linking the strands β1 and β2, is the longest and most twisted loop that contains residues 51–84 and folds into two short 3_{10} helices, η2 at residues 56-58 and η3 at residues 60-62. Noteworthy is that the L1 loop forms two bulges at residues 68-72 (for bulge1) and residues 76-78 (for bulge2), which flank the η2 helix (Fig. 1B). The loops L2 (connecting the strands β3 and β4) and L4 (connecting β6 and β7) are interlocking with each other. Meanwhile, the loop L2 is flanked by the loops L1 and L3 (linking β5 and β6), and the loop L1 adopts a concave configuration and half-wraps the loops L2 and L4 (Fig. S1). The tips of the loops L2, L3 and L4 are almost aligned to the same level with the two bulges and the η2 helix of L1, thus forming a relatively flat surface on one end of the barrel (Fig. S1).

3.2. Structural comparison of CASPR2 Disc domain and its homologues

The overall structure of human CASPR2 Disc domain is similar to that of the membrane-binding C2 domain of human coagulation factor V [40], with an RMSD value of 0.81 Å for 114 aligned C_α atoms. These aligned C_α atoms are mainly located in the barrel-wall strands, indicating that CASPR2 Disc and coagulation factor V C2 domains share the same folding (Fig. 2A). However, unlike the loops (such as L1 and L2) of human CASPR2 Disc domain that constitute a relatively flat

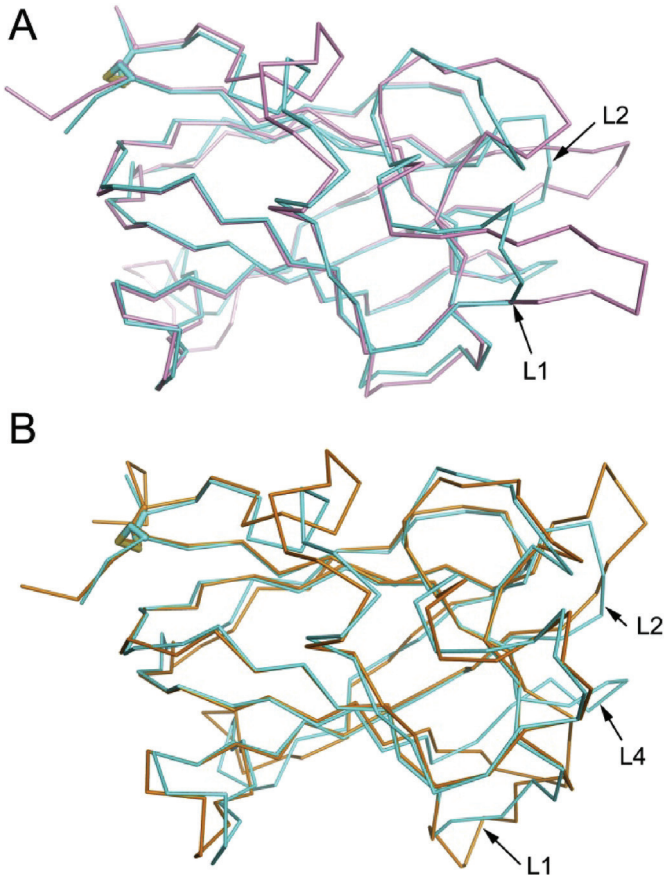

Fig. 2. Structural comparison of human CASPR2 Disc domain (in cyan) with homologues: (A), human coagulation factor V C2 domain (in pink); (B), DDR2 Disc domain (in orange). All structures are shown in cartoons, and the loops with large structural variations are labeled in CASPR2 numbering. (For interpretation of the references to color in this figure legend, the reader is referred to the Web version of this article.)

platform, the homologous counterparts in human coagulation factor V protrude like spikes [40] (Fig. 2A). As revealed by Dali search [45], the structure of the Disc domain of DDR2 (referring to Discoidin Domain Receptor 2; PDB code: 2wuh) [52] can also be superimposed with that of CASPR2 with an RMSD value of 0.75 Å for 127 paired C_α atoms, and their structural variation also mainly occurs to the loops such as L1, L2 and L4 (Fig. 2B). In comparison with human coagulation factor V C2 domain, the Disc domain of both CASPR2 and DDR2 has a compact and flat loop region that might facilitate docking to other proteins. Therefore, similar to the case of DDR2 where the loop region in the Disc domain engages in collagen recognition [52] (Fig. S2), CASPR2 Disc domain might utilize its loop region for protein recognition. Finally, in the human factor VIII C2 domain (PDB code: 1iqd), also able to overlay with CASPR2 Disc domain, the loop region was shown to bind to a patient-derived inhibitory antibody [53] (Fig. S2). This further implicates that the loop region defined by the loops L1-L4 in human CASPR2 Disc domain might constitute an epitope for recognition by other proteins, including autoantibodies.

3.3. Surface properties of human CASPR2 Disc domain

Defined by the loop L1-L4, the loop region is located in one end of the barrel-like human CASPR2 Disc domain, opposite to the other end containing the N- and C-termini. The solvent-accessible surface of this region, hereafter designated "loop-tip surface", is totally polar and hydrophilic, since it is mainly composed of the residues Ile54, Ser55, Ser57, Tyr58, Arg68, Gly69, Ala71, Ser77 and Asp78 from the loop L1, Arg103, Tyr104, Ser105, Ser107 and Asp108 from the loop L2, and Glu169 and Arg171 from the loop L4 (Fig. S1 and Fig. 3). Located in the center of the "loop-tip surface" is Arg103 that forms a salt bridge with Asp108. Around the edge of the "loop-tip surface" are distributed highly solvent-accessible hydrophilic residues such as Ser55, Arg68, Ser77, Asp78, Tyr104, Ser105, Ser107, Glu169 and Arg171. The carbonyl oxygen of Gly69 forms a hydrogen bond with the main chain amide nitrogen of Gly72, thus stabilizing the conformation of the "bulge 1" in the loop L1. The side chains of Arg68 and Tyr104 are in close proximity and form a cation-π interaction. Arg103 and Asp108 are involved in a relay of hydrogen bonds among Try58, Ala71 and Arg171 (Fig. 3). The combination of all these interactions likely maintains the construction of the "loop-tip surface".

Noteworthy, in sharp contrast with Asp78 and Arg171 that respectively have a solvent accessible surface area (SASA) of 92.3 and 128.2 $Å^2$, the surface center residues Asp108 and Arg103 are nearly buried with an SASA of 14.3 and 37.4 $Å^2$, respectively. This implicates that mutation of either Asp108 or Arg103 would likely alter the structure of the "loop-tip surface". Meanwhile, due to residence of the salt-bridged residues Asp108 and Arg103, the surface center is approximately neutralized (Fig. S3). In comparison, the edge of the "loop-tip surface" has considerable electrostatic potential, since its two adjacent sides of the barrel-like domain are distributed with positively or negatively charged patches (Fig. S3).

Also, it is worthy to mention that the residues on the "loop-tip surface" of human CASPR2 Disc domain, except S55, R68 and G69, have relatively low conservation among the five CASPR subfamily members CASPR1-CAPSR5 (Fig. 3B and Fig. S4). Indeed, the residues on the side surface of human CASPR2 Disc domain, such as Arg114 and Arg160 that constitute a positively charged region (Fig. S3B), also have low conservation. This suggests that the Disc domains of the CASPR subfamily have diverse surface properties although the subfamily members might have a conserved topology. The diversity in surface property of the Disc domain in the CASPR subfamily members might confer specificity in their autoantibody recognition.

3.4. Structure-based epitope prediction and mutagenesis

In order to dissect key residues in the epitope(s) within human CASPR2 Disc domain, we first applied its crystal structure to DiscoTope 2.0 server [44] for epitope prediction. Six regions with high DiscoTope scores above the default value of −3.7 are, from the N-terminus of the Disc domain, sequentially named Epitope-1 through Epitope-6 (Fig. 4A). The predicted Epitope-1 (covering residues 52-57), Epitope-2 (residues 68-72) and Epitope-3 (residues 76-84) fall into the loop L1 of the Disc domain, while the Epitope-4 mainly includes residues 103-112 that corresponds to the loop L2. The residues from the protruding hairpin (βC and βD), the barrel wall strand β5, and the loop L3 (residues 140-144) are predicted to constitute the Epitope-5. The Epitope-

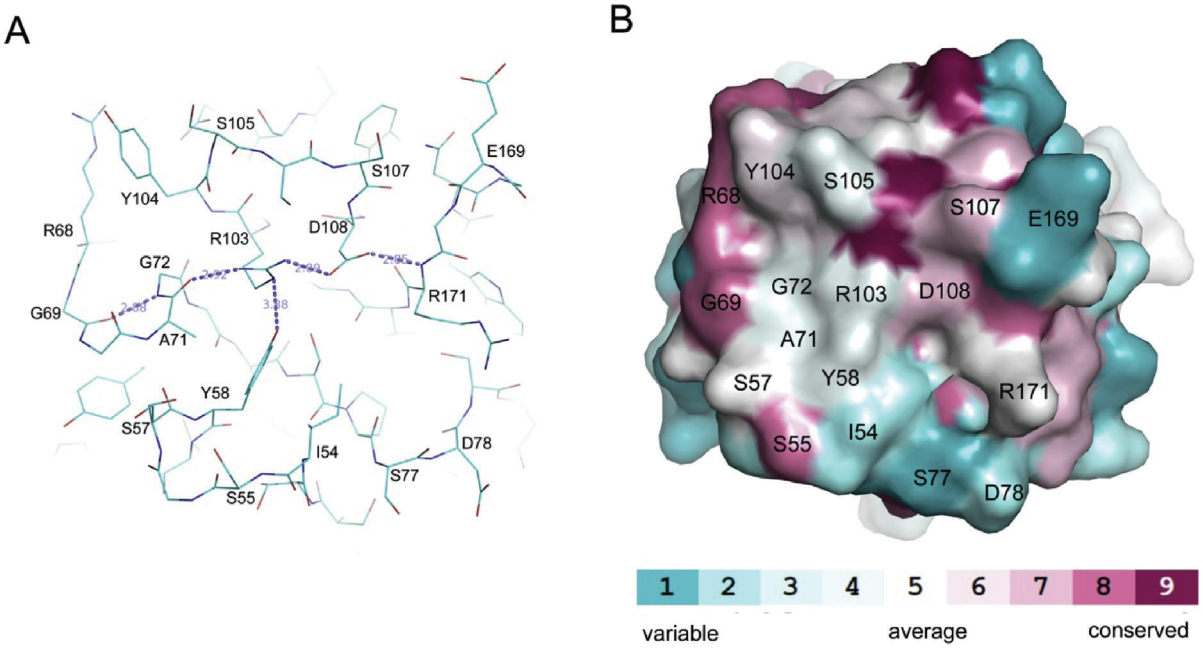

Fig. 3. Residues distributed over the "loop-tip surface" of human CASPR2 Disc domain. (A) Line representation of the residues with hydrogen bonds shown in slate dotted lines. (B) Conservation of each residue among the CASPR subfamily members, CASPR1-5, mapped to the CASPR2 Disc domain surface. Bottom is shown a scale for conservation degree.

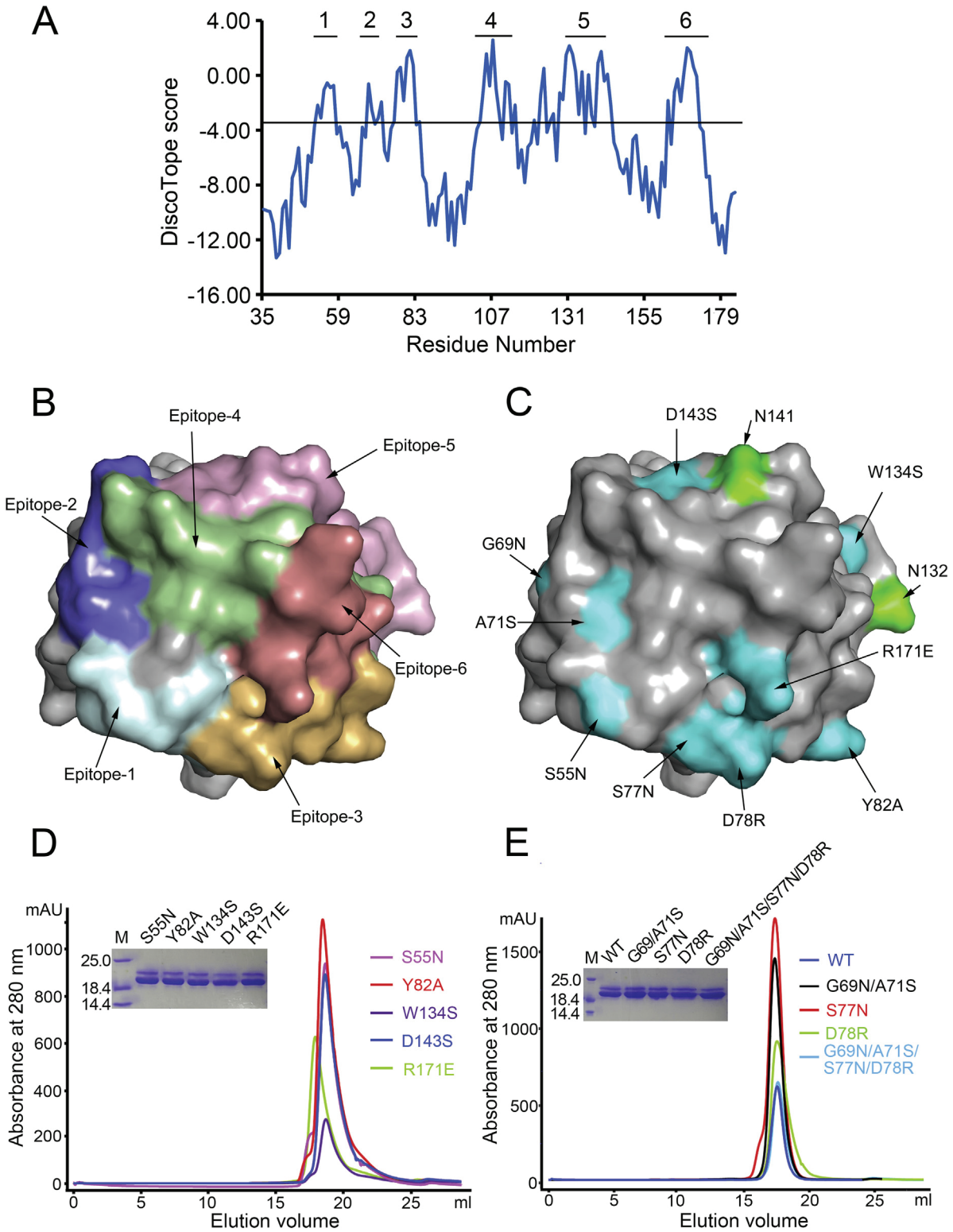

Fig. 4. Structure-based epitope prediction and mutagenesis of human CASPR2 Disc domain. (A) A plot of DiscoTope score (represented by the vertical axis) versus residue number (by the horizontal axis). (B) Predicted epitopes mapped on the Disc domain surface (in grey). Color code: Epitope-1, pale cyan; Epitope-2, slate; Epitope-3, light orange; Epitope-4, pale green; Epitope-5, light pink; Epitope-6, salmon. (C) Mutations mapped on the Disc domain surface and colored in cyan, with S55N located in Epitope-1, G69N/A71S in Epitope-2, S77N, D78R and Y82A in Epitope-3, W134S and D143S in Epitope-5, and R171E in Epitope-6. Two potential N-linked glycosylation sites N132 and N141 are colored in green. The Disc domain in the panels B and C has the same orientation that is related to Fig. 1B by 90° along the vertical axis. (D–E) Gel filtration chromatograms of the wild-type (WT) human CASPR2 Disc domain and its mutants, with S55N, Y82A, W134S, D143S and R171E displayed in the panel D, and G69N/A71S, S77N, D78R, and G69N/A71S/S77N/D78R shown in the panel E. The insets are indicated for SDS-PAGE analysis of the recombinant proteins. The lane M is for molecular weight markers in kDa. (For interpretation of the references to color in this figure legend, the reader is referred to the Web version of this article.)

6 is supposed to cover residues 164-171 that reside in the loop L4. In short, the loop region defined by L1-L4 on one end of the barrel-like Disc domain constitutes the majority of the predicted epitopes.

Correspondingly, we prepared nine mutants of human CASPR2 Disc domain plus the N-terminal segment (residues 28-181). The mutations S55N, G69N/A71S, S77N, D78R and Y82A, were located in the loop L1 and distributed in three predicted epitopes, Epitopes 1-3 (Fig. 4). The mutations W134S and D143S occurred in the Epitope-5, while R171E was located in the Epitope-6. Supposedly, the mutations S55N, G69N/A71S, S77N, W134S and D143S would each introduce N-linked glycans that may act as a wedge to block interaction between human CASPR2 and auto-antibodies. For the mutations W134S and D143S, the N-linked glycans would be attached to N132 and N141, respectively (Fig. 4C). In addition, we created a quadruple mutant that combined the G69N, A71S, S77N and D78R mutations. All of the nine mutants, like the wild-type protein, were expressed well in baculovirus-transduced mammalian cells, and purified into high purity as demonstrated by SDS-PAGE analysis (Fig. 4D and E). Also, all of them exhibited a similar chromatographic peak on a gel-filtration column, indicating that they have similar physical property, such as monodispersity, in solution (Fig. 4D and E). For an unknown reason, these mutants and their wild-type counterpart (including residues 28-181) migrated as two bands on an SDS-PAGE gel, whereas the construct (including residues 35-181) used for crystallization ran as a single band.

3.5. Protein-based ELISA revealed hot spots for autoantibody recognition

Using three rounds of protein-based ELISA assays, we tested if the above mentioned mutations are able to alter interactions between CASPR2 Disc domain and CASPR2 autoantibodies from LE patients. In the ELISA assays, an OD_{450} value is supposed to be proportional to CASPR2 autoantibodies bound to the coated Disc protein. In the first round ELISA assay, CSF from the patient 1 (Pat1, recognizing only Disc-Lam1 domains on CASPR2) was tested at a series of dilutions against eight mutants S55N, G69N/A71S, S77N, D78R, Y82A, W134S, D143S and R171E. Upon either G69N/A71S, S77N or D78R mutations, the binding of Pat1 autoantibodies at a 1:40 dilution to human CASPR2 Disc domain was decreased by ~22% for G69N/A71S, ~28% for S77N and ~31% for D78R in comparison with the wild-type protein (Fig. 5). For the D78R mutant, Pat1 autoantibodies binding to the D78R mutant was decreased by 20–30%, while OD difference was only found at dilutions of 1:40 and 1:80. In contrast, other mutations hardly altered the binding of Pat1 autoantibodies to CASPR2 Disc domain at any dilutions (Fig. 5).

In the second round of ELISA assay, we focused on the mutants of G69N/A71S, S77N and D78R for twelve LE patients including Pat1. Meanwhile, a quadruple mutant of G69N/A71S/S77N/D78R was also included. As indicated in Table 2, CSF antibody titers were variable among patients ranging from 1:320 to 1:10240. All patients' CSF was diluted based on their autoantibody titer at a ratio between 1:10 and 1:100 for ELISA assay (Fig. 6A). For patients Pat2, Pat3, Pat4, Pat8 and Pat9 with CSF diluted at different folds, the four mutations in Disc domain decreased OD_{450} to considerable extents as observed for Pat1 (Fig. 6A). In order to compare the percentage of OD decrease between mutant and wild-type Disc domain protein among these patients with different CSF titers, we chose for each patient the dilution that gave an OD around 0.8 for the wild-type protein. In comparison with the wild-type CASPR2 protein, the quadruple mutant was found to present an OD_{450} decrease of 15%–70% in binding to autoantibodies from eleven patients out of twelve LE patients tested (Fig. 6B and C). Especially, for Pat1 and Pat3, a decrease of 72% and 70% was observed in OD_{450} for the quadruple mutant, implicating that the four residues G69, A71, S77 and D78 have a synergic impact on autoantibody recognition (Fig. 6B and C). The quadruple mutant also significantly impaired autoantibodies binding (from 38% to 51% decrease) to CASPR2 Disc domain for Pat2, Pat4, Pat8 and Pat9. In addition, for the Pat1, Pat2 and Pat3, both S77N and D78R mutations significantly decreased autoantibodies binding to CASPR2 (Fig. 6B and C). Notably, Pat1, Pat2, Pat3 and Pat4 autoantibodies have been previously shown to target Disc-Lam1 domains of CASPR2 only, while Pat8 and Pat9 autoantibodies target multiple domains of CASPR2 (Table 2) [18]. The quadruple mutation consistently impaired Disc domain binding to autoantibodies from these patients (Fig. 6B and C), suggesting that anti-CASPR2 autoantibodies might share the same epitope in Disc domain.

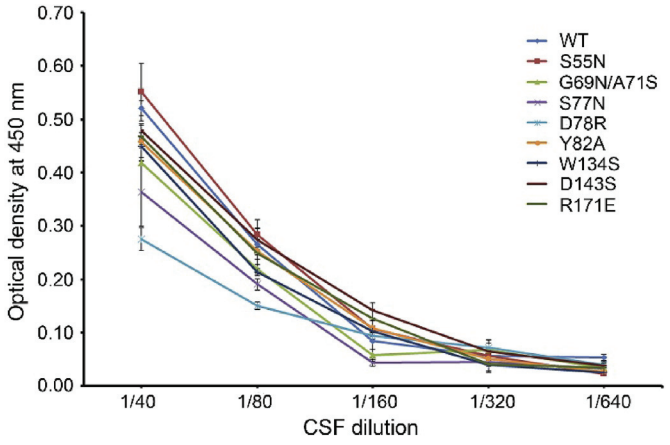

Fig. 5. Protein-based ELISA analysis for Pat1 CSF autoantibodies at the indicated dilutions binding to human CASPR2 Disc domain wild-type and eight mutants.

In the third round of ELISA assay, we compared "relative affinity" of CSF autoantibodies in binding to the wild-type and quadruple mutant Disc domain. Taking into account of that a large amount of CSF sample will be needed to obtain a binding curve with a saturation phase for determining a relative affinity, we selected high-titer Pat5 CSF. Given that the same amount of CSF autoantibodies was added in plates, the maximal OD_{450} should be identical for the wild-type and mutant Disc domain to reach in a saturated phase. In order to characterize the relative affinity, "q50" was used to correspond to the quantity of protein where 50% of maximal OD_{450} is reached. As shown in Fig. 7, a q50 value of 0.07 μg was estimated for the wild-type protein. In contrast, for the quadruple mutant we obtained a q50 value of 0.14 μg. These results indicated that Pat5 CSF presented lower binding affinity with the quadruple mutant than the wild-type Disc domain, and further verified that the spots at the G69, A71, S77 and D78 in Disc domain are determinant for LE autoantibody recognition.

4. Discussion

Autoantibodies directed against CASPR2 have been associated with a long list of neurological immune disorders including limbic encephalitis. Recently we have found that anti-CASPR2 antibodies in the CSF are prone to occur in a subtype of autoimmune encephalitis with limbic involvement and seizures [18]. Although CASPR2 contains different epitopes within the extracellular region [54], we and other have shown that autoantibodies appear to predominantly target the N-terminal region of CASPR2 and that the Disc domain harbors a major epitope [32,33]. Coincidentally, it is the Disc domain that structurally distinguishes the CASPR subfamily from the others in the neurexin superfamily. Structural mapping of autoepitopes within human CASPR2 Disc domain will reveal how autoantibodies affect multifaceted functions and extensive protein interactions of CASPR2.

Using the emerging technology of baculovirus-transduced mammalian cells that we have successfully used for structural biology of glycoproteins [37,55], we fulfilled high expression of human CASPR2 Disc domain as well as its derivates. The crystal structure of human CASPR2 Disc domain was determined to a high resolution of 1.31 Å,

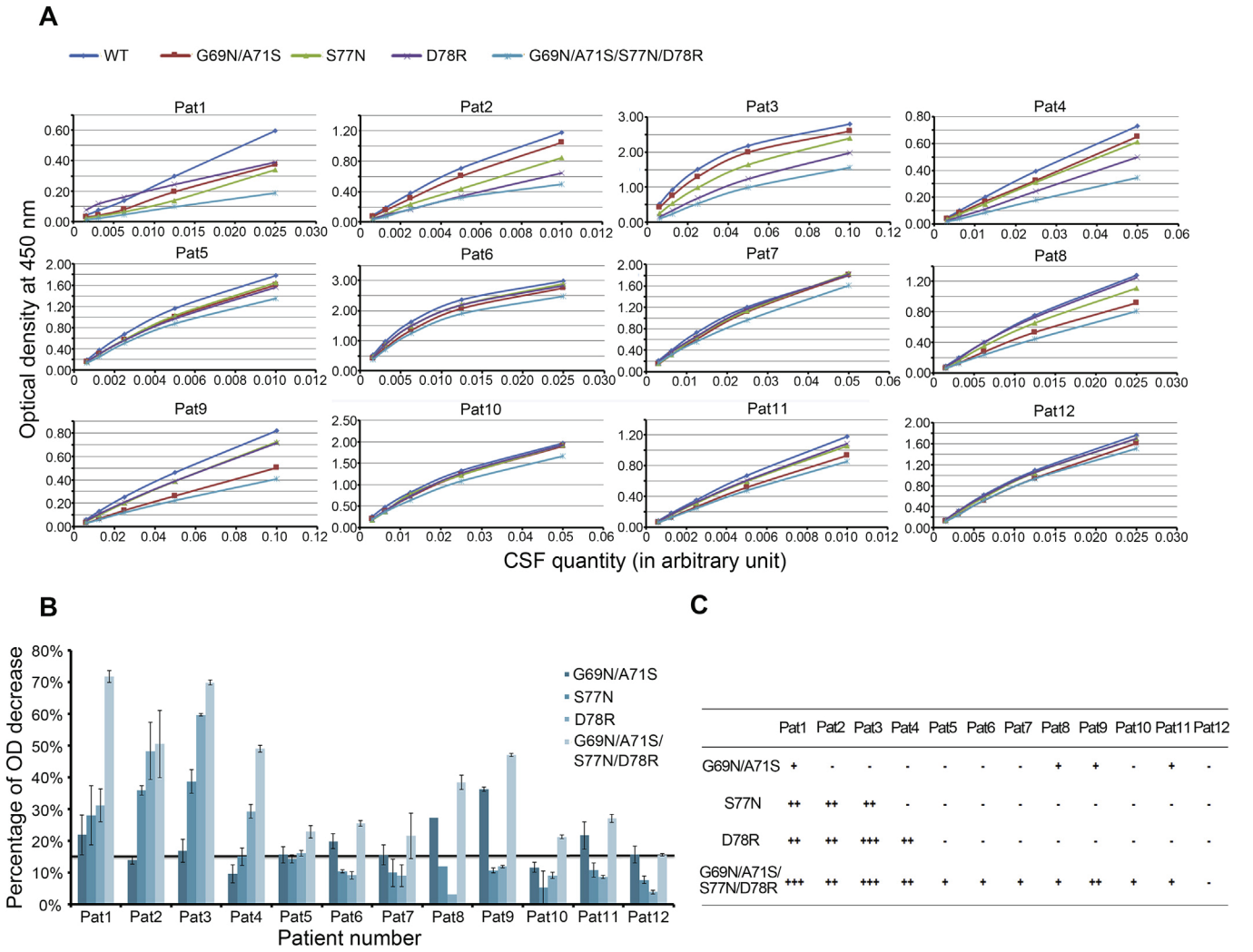

Fig. 6. Protein-based ELISA analysis for 12 LE patients CSF binding to Disc domain and its four variants. (A) Binding of CSF autoantibodies from patients (Pat1 ~ Pat12) at the indicated arbitrary unit of antibody quantity to Disc domain wild-type and mutants. Herein, an arbitrary unit refers to the reciprocal of dilution fold. (B) Percentage of optical density (OD) decrease for the binding of anti-CASPR2 antibodies from twelve LE patients on the indicated mutant versus the wide-type CASPR2 Disc domain. For the patient 9, anti-CASPR2 binding to the mutants G69N/A71S, S77N and D78R was only tested once. (C) Summary of mutations and their impairment on CASPR2 Disc binding to CSF from patients. "+ + +", strong; "+ +", medium; "+", weak; "-", ignorable.

partially due to high purity and monodispersity of the recombinant protein. To our best knowledge, this is the first atomic-resolution structure of the CASPR subfamily members, which reveals that the Disc domain assumes a totally all β structure with a conserved disulfide-bond interlocking its N- and C-termini.

Although human CASPR2 Disc domain and coagulation factor V C2 domain share a barrel-like topology, their loops connecting the barrel-wall β-strands have variable conformations. In human coagulation

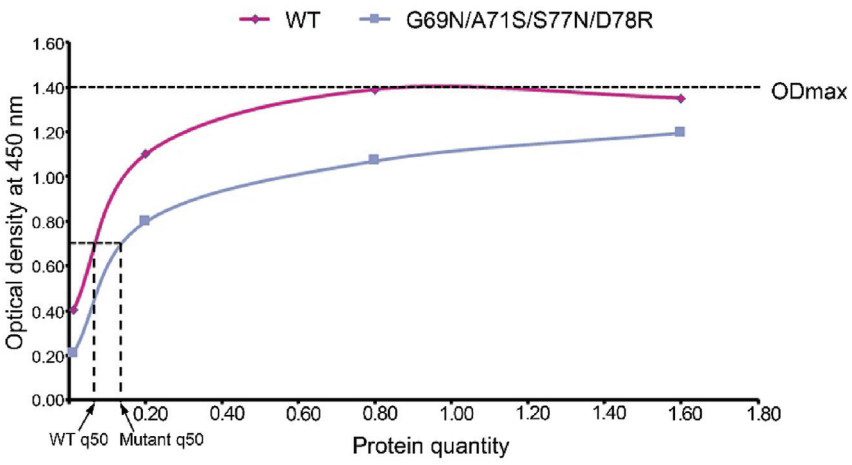

Fig. 7. Binding curves of Pat5 CSF against coated Disc domain wild-type and quadruple mutant G69N/A71S/S77N/D78R. The horizontal coordinate axis represents the protein quantity used to coat the 96-well plates. 0.01, 0.2, 0.8 and 1.6 μg of Disc domain wild-type or quadruple mutant were respectively used to coat the plates, while the same amount of Pat CSF (diluted at 1:100) was added to each well. The relative affinity is represented by "q50" which corresponds to the quantity of protein where 50% of maximal OD_{450} is reached. Given that the same amount of CSF autoantibodies was added, the maximal OD_{450} for the wild-type and mutant Disc domain should be identical and thus labeled as "ODmax". Due to limitation in CSF source, this experiment was performed only once.

factor V C2 domain, loops protrude like spikes out of one end of the barrel and form a predominantly positive-charge region for membrane-binding [40]. In contrast, human CASPR2 Disc domain defines the counterpart end using four loops L1-L4 to constitute a relatively flat surface, named “loop-tip surface”, which is basically neutral in the center and has considerable electrostatic potential on the edge. Such a surface property likely confers human CASPR2 Disc domain binding to other proteins including autoantibodies, similar to the case of DDR2 Disc domain [52]. Consistently, the predicted epitopes by DiscoTope within human CASPR2 Disc domain also point to the “loop-tip surface” and adjacent barrel-wall surfaces (Fig. 4).

Since LE patient CSF samples were truly limited, we adopted three rounds of EILSA assays to investigate which hot spots in CASRP2 Disc domain are critical for CSF autoantibody recognition. In the first round, we used one patient's CSF to screen Disc mutants. Among the eight mutants S55N, G69N/A71S, S77N, D78R, Y82A, W134S, D143S and R171E, three mutants G69N/A71S, S77N and D78R impaired Pat1's CSF autoantibodies binding to the CASPR2 Disc domain (Fig. 5). In the second round, we focused on the three mutants plus their combination. The quadruple mutant of G69N/A71S/S77N/D78R showed a decreased binding for 11 out of 12 LE patients' CSF autoantibodies (Fig. 6). Meanwhile, anti-CASPR2 autoantibodies from two types of LE patients might share the same epitope in Disc domain, since the quadruple mutant impaired Disc binding to autoantibodies not only from patients Pat1, Pat2, Pat3 and Pat4, but also from Pat8 and Pat9 (Fig. 6). Furthermore, the quadruple mutations occur to the “loop-tip-surface” of Disc domain, which implicates that LE patient CSF autoantibodies might bind to Disc domain in a single-epitope fashion. From this point of view, it is reasonable to quantitatively measure a relative affinity of Disc domain binding to CSF although it is a complex mixture of anti-CASPR2 autoantibodies. Therefore, in the third round of ELISA assay, we tried to compare “relative affinity” of CSF autoantibodies in binding to the wild-type and quadruple mutant Disc domain (Fig. 7). Due to limited CSF sample availability, we selected CSF from the patient Pat5 that had highest titer of autoantibodies, coated different amounts of Disc protein in plates, and put forward to the phrase “q50” to present the relative affinity (Fig. 7). The higher q50 value for the quadruple mutant Disc domain means its lower affinity for Pat5 CSF autoantibodies. This result further verified that the spots at the G69, A71, S77 and D78 in Disc domain are determinant for LE autoantibody recognition. Stated differently, the ELISA assay results indicate that the “loop-tip surface” in human CASPR2 Disc domain bears hot spots for LE autoantibodies recognition. Different from either G69N/A71S or S77N mutations that likely introduced N-linked glycans as steric hindrance for antigen-antibody interaction, the charge-reversal mutation of D78R implicated that CASPR2 recognition by autoantibodies in LE patients likely depends on electrostatic complementarity. Interestingly, these hot spots are located on the loop L1. Intrinsic flexibility of this loop might increase the capacity for movement to form strong antigen-antibody interactions by “induced fit” [56]. Indeed, flexibility appears to be a structural feature associated with epitope sites on autoantigenic molecules [57,58].

Recently, some authors showed that anti-CASPR2 antibodies associated with limbic encephalitis mainly target hippocampal inhibitory interneurons and may induce alteration of CASPR2-mediated inhibitory synaptic contacts [32]. It was reported that *in utero* exposure to CASPR2-directed autoantibodies cloned from a mother of an ASD child can lead to an ASD-like phenotype in mice [11], although this observation seemed controversial [59]. Adult CASPR2 KO mice exhibited a significant decrease in the number of inhibitory interneurons and ASD-like behavioral abnormalities [28]. Thus, it seems that anti-CASPR2 autoantibodies could play a fundamental role in the pathogenic processes through a functional effect on CASPR2 [18], which is similar to the effects exerted through gene knockout. Since functions of CASPR2 may operate via interactions with other proteins such as TAG-1 and the VGKC complex subunits [1,21,60,61], we propose that CASPR2 autoantibodies would compete with these proteins for CASPR2 binding. Indeed, it was shown that CASPR2 autoantibodies were able to decrease CASPR2-TAG-1 association in ELISA [62].

As revealed by electron microscopy, the N-terminal domains, including the Disc domain, of CASPR2 form a large lobe that deviates from the main body of molecular architecture [34]. Such a domain arrangement would facilitate exposure of the “loop-tip surface” of the Disc domain for interactions with an endogenous ligand or autoantibodies. From this point, future searching for the endogenous ligand of CASPR2 might be based on the Disc domain. A caveat for this strategy is that autoantibodies against CASPR2 target other regions beyond the Disc domain [18]. The fact that CASPR2 has multiple autoepitopes may explain that Pat12 autoantibodies maintained its binding to the quadruple mutant in the protein-based ELISA assay. This may also underlie the fact that autoantibodies against CASPR2 associate with a wide spectrum of symptoms, including limbic or more extensive encephalitis [63]. Given that autoantibodies from a subset of LE patients may target the Disc domain of CASPR2 and would likely compete with a potential endogenous ligand, some autoantibodies in a wider range of pathogenic conditions might direct against multiple domains of CASPR2 and antagonize interactions with other proteins.

In summary, we have determined the crystal structure of human CASPR2 Disc domain and found that the quadruple mutant G69N/A71S/S77N/D78R impaired CASPR2 binding to autoantibodies from 11 out of 12 LE patients. These findings indicate that the loop L1 in the Disc domain bears hot spots for LE autoantibody interaction. Together with our previous study [32], structural mapping of autoepitopes within human CASPR2 Disc domain sheds light on how autoantibodies might affect CASPR2 functions in the pathological contexts such as limbic encephalitis.

Conflicts of interest

The authors declare that they have no conflicts of interest with the contents of this article.

Author contributions

HL and JH conceived the project, coordinated the study, analyzed the data and wrote the manuscript. WL, JZ, MS, FX, NN and JL performed the experiments, analyzed the data and contributed to manuscript preparation.

Acknowledgements

This work was supported by grants to Heli Liu from “Thousand Talents Program” and National Natural Science Foundation of China (grants No. 81322047 and 81673525), and by grants to Jérôme Honnorat from Agence Nationale de la Recherche (ANR-14-CE15-0001-MECANO), and FRM (Fondation pour la Recherche Médicale) DQ20170336751. Atomic coordinates and structure factor for human CASPR2 Disc domain have been deposited in the Protein Data Bank (PDB) under accession number 5Y4M.

Appendix A. Supplementary data

Supplementary data to this article can be found online at https://doi.org/10.1016/j.jaut.2018.09.012.

References

[1] A. Van Sonderen, M. Petit-Pedrol, J. Dalmau, M.J. Titulaer, The value of LGI1, Caspr2 and voltage-gated potassium channel antibodies in encephalitis, Nat. Rev. Neurol. 13 (2017) 290–301.

[2] A. Chefdeville, J. Honnorat, C.S. Hampe, V. Desestret, Neuronal central nervous system syndromes probably mediated by autoantibodies, Eur. J. Neurosci. 43 (2016) 1535–1552.

[3] J.J. Linnoila, M.R. Rosenfeld, J. Dalmau, Neuronal surface antibody-mediated autoimmune encephalitis, Semin. Neurol. 34 (2014) 458–466.
[4] S.R. Irani, S. Alexander, P. Waters, K.A. Kleopa, P. Pettingill, L. Zuliani, et al., Antibodies to Kv1 potassium channel-complex proteins leucine-rich, glioma inactivated 1 protein and contactin-associated protein-2 in limbic encephalitis, Morvan's syndrome and acquired neuromyotonia, Brain 133 (2010) 2734–2748.
[5] M. Lai, M.G. Huijbers, E. Lancaster, F. Graus, L. Bataller, R. Balicegordon, et al., Investigation of LGI1 as the antigen in limbic encephalitis previously attributed to potassium channels: a case series, Lancet Neurol. 9 (2010) 776–785.
[6] A. Vincent, S.R. Irani, Caspr2 antibodies in patients with thymomas, J. Thorac. Oncol. 5 (2010) S277–S280.
[7] E.B. Becker, L. Zuliani, R. Pettingill, B. Lang, P. Waters, A. Dulneva, et al., Contactin-associated protein-2 antibodies in non-paraneoplastic cerebellar ataxia, J. Neurol. Neurosurg. Psychiatry 83 (2012) 437–440.
[8] B. Joubert, F. Gobert, L. Thomas, M. Saint-Martin, V. Desestret, P. Convers, et al., Autoimmune episodic ataxia in patients with anti-CASPR2 antibody-associated encephalitis, Neurol. Neuroimmunol. Neuroinflamm. 4 (2017) e371.
[9] C.J. Klein, V.A. Lennon, P.A. Aston, A. Mckeon, S.J. Pittock, Chronic pain as a manifestation of potassium channel-complex autoimmunity, Neurology 79 (2012) 1136.
[10] R.E. Rosch, A. Bamford, Y. Hacohen, E. Wraige, A. Vincent, L. Mewasingh, et al., Guillain-Barre syndrome associated with CASPR2 antibodies: two paediatric cases, J. Peripher. Nerv. Syst. 19 (2014) 246–249.
[11] L. Brimberg, S. Mader, V. Jeganathan, R. Berlin, T.R. Coleman, P.K. Gregersen, et al., Caspr2-reactive antibody cloned from a mother of an ASD child mediates an ASD-like phenotype in mice, Mol. Psychiatr. 21 (2016) 1663–1671.
[12] F. Govert, K. Witt, R. Erro, H. Hellriegel, S. Paschen, E. Martinez-Hernandez, et al., Orthostatic myoclonus associated with Caspr2 antibodies, Neurology 86 (2016) 1353–1355.
[13] J. Suleiman, S. Wright, D. Gill, F. Brilot, P. Waters, K. Peacock, et al., Autoantibodies to neuronal antigens in children with new-onset seizures classified according to the revised ILAE organization of seizures and epilepsies, Epilepsia 54 (2013) 2091–2100.
[14] S. Wright, A.T. Geerts, C.M. Jol-van der Zijde, L. Jacobson, B. Lang, P. Waters, et al., Neuronal antibodies in pediatric epilepsy: clinical features and long-term outcomes of a historical cohort not treated with immunotherapy, Epilepsia 57 (2016) 823–831.
[15] G. Unverengil, E.N. Vanli Yavuz, E. Tuzun, E. Erdag, S. Kabadayi, B. Bilgic, et al., Brain infiltration of immune cells in CASPR2-antibody associated mesial temporal lobe epilepsy with hippocampal sclerosis, Noro Psikiyatr Ars 53 (2016) 344–347.
[16] J. Song, S. Jing, C. Quan, J. Lu, X. Qiao, K. Qiao, et al., Isaacs syndrome with CASPR2 antibody: a series of three cases, J. Clin. Neurosci. 41 (2017) 63–66.
[17] Z. Karaaslan, E. Ekizoglu, P. Tekturk, E. Erdag, E. Tuzun, N. Bebek, et al., Investigation of neuronal auto-antibodies in systemic lupus erythematosus patients with epilepsy, Epilepsy Res. 129 (2017) 132–137.
[18] B. Joubert, M. Saint-Martin, N. Noraz, G. Picard, V. Rogemond, F. Ducray, et al., Characterization of a subtype of autoimmune encephalitis with anti-contactin-associated protein-like 2 antibodies in the cerebrospinal fluid, prominent limbic symptoms, and seizures, JAMA Neurol. 73 (2016) 1115–1124.
[19] S. Poliak, L. Gollan, R. Martinez, A. Custer, S. Einheber, J.L. Salzer, et al., Caspr2, a new member of the neurexin superfamily, is localized at the juxtaparanodes of myelinated axons and associates with K+ channels, Neuron 24 (1999) 1037–1047.
[20] T.C. Sudhof, Synaptic neurexin complexes: a molecular code for the logic of neural circuits, Cell 171 (2017) 745–769.
[21] G.R. Anderson, T. Galfin, W. Xu, J. Aoto, R.C. Malenka, T.C. Sudhof, Candidate autism gene screen identifies critical role for cell-adhesion molecule CASPR2 in dendritic arborization and spine development, Proc. Natl. Acad. Sci. U. S. A. 109 (2012) 18120–18125.
[22] O. Varea, M.D. Martin-de-Saavedra, K.J. Kopeikina, B. Schurmann, H.J. Fleming, J.M. Fawcett-Patel, et al., Synaptic abnormalities and cytoplasmic glutamate receptor aggregates in contactin associated protein-like 2/Caspr2 knockout neurons, Proc. Natl. Acad. Sci. U. S. A. 112 (2015) 6176–6181.
[23] A. Gdalyahu, M. Lazaro, O. Penagarikano, P. Golshani, J.T. Trachtenberg, D.H. Geschwind, The Autism Related Protein Contactin-Associated Protein-Like 2 (CNTNAP2) Stabilizes New Spines: an In Vivo Mouse Study, PloS One 10 (2015) e0125633.
[24] K.A. Strauss, E.G. Puffenberger, M.J. Huentelman, S. Gottlieb, S.E. Dobrin, J.M. Parod, et al., Recessive symptomatic focal epilepsy and mutant contactin-associated protein-like 2, N. Engl. J. Med. 354 (2006) 1370–1377.
[25] B. Bakkaloglu, B.J. O'Roak, A. Louvi, A.R. Gupta, J.F. Abelson, T.M. Morgan, et al., Molecular cytogenetic analysis and resequencing of contactin associated protein-like 2 in autism spectrum disorders, Am. J. Hum. Genet. 82 (2008) 165–173.
[26] A.J. Verkerk, C.A. Mathews, M. Joosse, B.H. Eussen, P. Heutink, B.A. Oostra, CNTNAP2 is disrupted in a family with Gilles de la Tourette syndrome and obsessive compulsive disorder, Genomics 82 (2003) 1–9.
[27] M. Saint-Martin, B. Joubert, V. Pellier-Monnin, O. Pascual, N. Noraz, J. Honnorat, Contactin-associated protein-like 2, a protein of the neurexin family involved in several human diseases, Eur. J. Neurosci. 48 (2018) 1906–1923.
[28] O. Penagarikano, B.S. Abrahams, E.I. Herman, K.D. Winden, A. Gdalyahu, H. Dong, et al., Absence of CNTNAP2 leads to epilepsy, neuronal migration abnormalities, and core autism-related deficits, Cell 147 (2011) 235–246.
[29] E. Peles, M. Nativ, M. Lustig, M. Grumet, J. Schilling, R. Martinez, et al., Identification of a novel contactin-associated transmembrane receptor with multiple domains implicated in protein-protein interactions, EMBO J. 16 (1997) 978–988.
[30] M. Poot, Connecting the CNTNAP2 networks with neurodevelopmental disorders, Mol. Syndromol. 6 (2015) 7–22.
[31] N. Sinmaz, T. Nguyen, F. Tea, R.C. Dale, F. Brilot, Mapping autoantigen epitopes: molecular insights into autoantibody-associated disorders of the nervous system, J. Neuroinflammation 13 (2016) 219.
[32] D. Pinatel, B. Hivert, J. Boucraut, M. Saint-Martin, V. Rogemond, L. Zoupi, et al., Inhibitory axons are targeted in hippocampal cell culture by anti-Caspr2 autoantibodies associated with limbic encephalitis, Front. Cell. Neurosci. 9 (2015) 265.
[33] A.L. Olsen, Y. Lai, J. Dalmau, S.S. Scherer, E. Lancaster, Caspr2 autoantibodies target multiple epitopes, Neurol. Neuroimmunol. Neuroinflamm. 2 (2015) e127.
[34] Z. Lu, M.V. Reddy, J. Liu, A. Kalichava, J. Liu, L. Zhang, et al., Molecular architecture of contactin-associated protein-like 2 (CNTNAP2) and its interaction with contactin 2 (CNTN2), J. Biol. Chem. 291 (2016) 24133–24147.
[35] E.N. Rubio-Marrero, G. Vincelli, C.M. Jeffries, T.R. Shaikh, I.S. Pakos, F.M. Ranaivoson, et al., Structural characterization of the extracellular domain of CASPR2 and insights into its association with the novel ligand Contactin1, J. Biol. Chem. 291 (2016) 5788–5802.
[36] A. Dukkipati, H.H. Park, D. Waghray, S. Fischer, K.C. Garcia, BacMam system for high-level expression of recombinant soluble and membrane glycoproteins for structural studies, Protein Expr. Purif. 62 (2008) 160–170.
[37] H. Liu, Z.S. Juo, A.H. Shim, P.J. Focia, X. Chen, K.C. Garcia, et al., Structural basis of semaphorin-plexin recognition and viral mimicry from Sema7A and A39R complexes with PlexinC1, Cell 142 (2010) 749–761.
[38] Z. Otwinowski, W. Minor, Processing of X-ray diffraction data collected in oscillation mode, Methods Enzymol. 276 (1997) 307–326.
[39] A.J. McCoy, Solving structures of protein complexes by molecular replacement with phaser, Acta Crystallogr. D Biol. Crystallogr. 63 (2007) 32–41.
[40] S. Macedo-Ribeiro, W. Bode, R. Huber, M.A. Quinn-Allen, S.W. Kim, T.L. Ortel, et al., Crystal structures of the membrane-binding C2 domain of human coagulation factor V, Nature 402 (1999) 434–439.
[41] P.D. Adams, P.V. Afonine, G. Bunkoczi, V.B. Chen, I.W. Davis, N. Echols, et al., PHENIX: a comprehensive Python-based system for macromolecular structure solution, Acta Crystallogr. D Biol. Crystallogr. 66 (2010) 213–221.
[42] P. Emsley, K. Cowtan, Coot: model-building tools for molecular graphics, Acta Crystallogr. D Biol. Crystallogr. 60 (2004) 2126–2132.
[43] V.B. Chen, W.B. Arendall 3rd, J.J. Headd, D.A. Keedy, R.M. Immormino, G.J. Kapral, et al., MolProbity: all-atom structure validation for macromolecular crystallography, Acta Crystallogr. D Biol. Crystallogr. 66 (2010) 12–21.
[44] J.V. Kringelum, C. Lundegaard, O. Lund, M. Nielsen, Reliable B cell epitope predictions: impacts of method development and improved benchmarking, PLoS Comput. Biol. 8 (2012) e1002829.
[45] L. Holm, P. Rosenstrom, Dali server: conservation mapping in 3D, Nucleic Acids Res. 38 (2010) W545–W549.
[46] M.A. Larkin, G. Blackshields, N.P. Brown, R. Chenna, P.A. McGettigan, H. McWilliam, et al., Clustal W and clustal X version 2.0, Bioinformatics 23 (2007) 2947–2948.
[47] P. Gouet, E. Courcelle, D.I. Stuart, F. Metoz, ESPript: analysis of multiple sequence alignments in PostScript, Bioinformatics 15 (1999) 305–308.
[48] H. Ashkenazy, S. Abadi, E. Martz, O. Chay, I. Mayrose, T. Pupko, et al., ConSurf 2016: an improved methodology to estimate and visualize evolutionary conservation in macromolecules, Nucleic Acids Res. 44 (2016) W344–W350.
[49] M.D. Winn, C.C. Ballard, K.D. Cowtan, E.J. Dodson, P. Emsley, P.R. Evans, et al., Overview of the CCP4 suite and current developments, Acta Crystallogr. D Biol. Crystallogr. 67 (2011) 235–242.
[50] G. Falivelli, A. De Jaco, F.L. Favaloro, H. Kim, J. Wilson, N. Dubi, et al., Inherited genetic variants in autism-related CNTNAP2 show perturbed trafficking and ATF6 activation, Hum. Mol. Genet. 21 (2012) 4761–4773.
[51] B.W. Matthews, Solvent content of protein crystals, J. Mol. Biol. 33 (1968) 491.
[52] F. Carafoli, D. Bihan, S. Stathopoulos, A.D. Konitsiotis, M. Kvansakul, R.W. Farndale, et al., Crystallographic insight into collagen recognition by discoidin domain receptor 2, Structure 17 (2009) 1573–1581.
[53] P.C. Spiegel Jr., M. Jacquemin, J.M. Saint-Remy, B.L. Stoddard, K.P. Pratt, Structure of a factor VIII C2 domain-immunoglobulin G4kappa Fab complex: identification of an inhibitory antibody epitope on the surface of factor VIII, Blood 98 (2001) 13–19.
[54] D.F. Obregon, Y.Y. Zhu, A.R. Bailey, S.M. Portis, H.Y. Hou, J. Zeng, et al., Potential autoepitope within the extracellular region of contactin-associated protein-like 2 in mice, Br. J. Med. Med. Res. 4 (2014) 416.
[55] Z. Lin, J. Liu, H. Ding, F. Xu, H. Liu, Structural basis of SALM5-induced PTPÎ' dimerization for synaptic differentiation, Nat. Commun. 9 (2018) 268.
[56] J.M. Rini, U. Schulze-Gahmen, I.A. Wilson, Structural evidence for induced fit as a mechanism for antibody-antigen recognition, Science 255 (1992) 959–965.
[57] P.H. Plotz, The autoantibody repertoire: searching for order, Nat. Rev. Immunol. 3 (2003) 73–78.
[58] Y. Arafat, G. Fenalti, J.C. Whisstock, I.R. Mackay, M. Garcia de la Banda, M.J. Rowley, et al., Structural determinants of GAD antigenicity, Mol. Immunol. 47 (2009) 493–505.
[59] E.J.L. Coutinho, M.G. Pedersen, M.E. Benros, B. Nørgaard-Pedersen, P.B. Mortensen, P.J. Harrison, A. Vincent, CASPR2 autoantibodies are raised during pregnancy in mothers of children with mental retardation and disorders of psychological development but not autism, J. Neurol. Neurosurg. Psychiatry 88 (2017) 4.
[60] N. Chen, F. Koopmans, A. Gordon, I. Paliukhovich, R.V. Klaassen, R.C. van der Schors, et al., Interaction proteomics of canonical Caspr2 (CNTNAP2) reveals the presence of two Caspr2 isoforms with overlapping interactomes, Biochim. Biophys. Acta 1854 (2015) 827–833.
[61] M. Traka, L. Goutebroze, N. Denisenko, M. Bessa, A. Nifli, S. Havaki, et al., Association of TAG-1 with Caspr2 is essential for the molecular organization of juxtaparanodal regions of myelinated fibers, J. Cell Biol. 162 (2003) 1161–1172.
[62] K.R. Patterson, J. Dalmau, E. Lancaster, Mechanisms of Caspr2 antibodies in autoimmune encephalitis and neuromyotonia, Ann. Neurol. 83 (2018) 40–51.
[63] M.T. Montojo, M. Petit-Pedrol, F. Graus, J. Dalmau, Clinical spectrum and diagnostic value of antibodies against the potassium channel related protein complex, Neurologia 30 (2015) 295–301.

C. Identification des épitopes dans le domaine discoidine et laminine G1, travaux complémentaires non publiés en lien avec l'article 2.

En complément de ces travaux, j'ai cherché à identifier les épitopes reconnus par les anticorps anti-CASPR2 de patients dans les domaines discoidine et laminine G1. L'identification du ou des épitope(s) des anticorps anti-CASPR2 rend possible la création de peptides permettant : (1) la mise en place d'un test diagnostic clinique à moindre coût pour la détection des anticorps anti-CASPR2 ; (2) l'étude de l'impact des anticorps en bloquant leur action ; (3) le développement d'éventuels traitements pour les patients.

Un épitope est une séquence reconnue par les anticorps de 4 à 8 acides aminés (a.a.) qui peut être linéaire ou conformationnel. Dans le cas d'un épitope linéaire, les a.a. se suivent et peuvent être reconnus même lorsque la protéine a perdu sa conformation. Dans le cas d'un épitope conformationnel, les a.a. sont distants les uns des autres et ne sont plus reconnus lorsque la protéine perd sa conformation. Concernant les anticorps anti-CASPR2, l'existence d'épitopes linéaires sur la protéine CASPR2 a été montrée par une étude décrivant la capacité des anticorps de patients à reconnaître la protéine CASPR2 dénaturée en Western Blot (Olsen et al., 2015). Par ailleurs, les épitopes conformationnels étant particulièrement difficiles à identifier, nous nous sommes davantage intéressés aux épitopes linéaires. Pour cela, nous avons utilisé des lames contenant 96 cupules de cellulose recouvertes de peptides (celluspot) en duplicatas. Les peptides recouvrent l'intégralité des domaines discoidine et laminine G1 et sont composés de 15 a.a se chevauchant sur 11 a.a.. De plus, nous avons intégré trois peptides contrôles et des peptides contenant une ou plusieurs des 8 mutations utilisées précédemment (Article 2). Des prélèvements de LCR et de sérum de 10 patients ont été testés. Nous avons considéré la présence d'un épitope lorsque plus de trois peptides à la suite sont reconnus par les auto-anticorps.

La figure 29A présente des exemples de celluspot pour le LCR et sérum d'un patient contrôle et d'un patient avec des anticorps anti-CASPR2. Nous avons pu mettre en évidence des épitopes chez 6/10 patients testés qui peuvent être différents en fonction du patient (Figure 29B). De plus, avec la plupart des LCR, aucun signal n'est observé ; inversement, certains sérums présentent un bruit de fond trop élevé pour discerner un motif de marquage particulier. Le résultat du celluspot dans ces deux cas est noté « négatif » (Figure 29B). Nous

avons ainsi identifié deux épitopes dans le domaine discoidine et deux épitopes dans le domaine laminine G1. Dans le domaine discoidine, un épitope se retrouve majoritaire, puisque retrouvé chez quatre patients ; le second n'étant observé que chez un patient (Figure 29B). Dans le domaine laminine G1, un épitope semble également majoritaire et retrouvé chez trois patients contrairement au second qui n'est observé que chez un patient (Figure 29B). En se basant sur la séquence de chaque peptide nous avons déterminé la séquence maximale en a.a. de chaque épitope (Figure 29C).

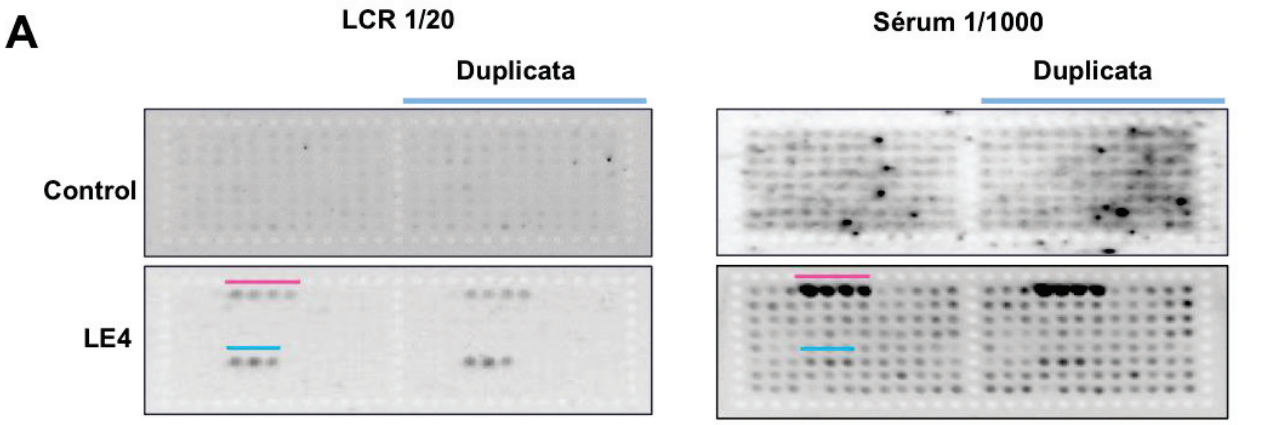

B

	CSF	Sera
LE4	A4-A7 C16-C18	A4-A7 C16-C18
LE6	Negatif	
LE7	Negatif	Negatif
LE8	A4-A7 C21-C23	
LE9		A4-A7
LE10	Negatif	A4-A7
LE11	Negatif	B6-9 C21-C23
LE12	Negatif	Negatif
LE15	Negatif	
LE19	Negatif	C21-C23

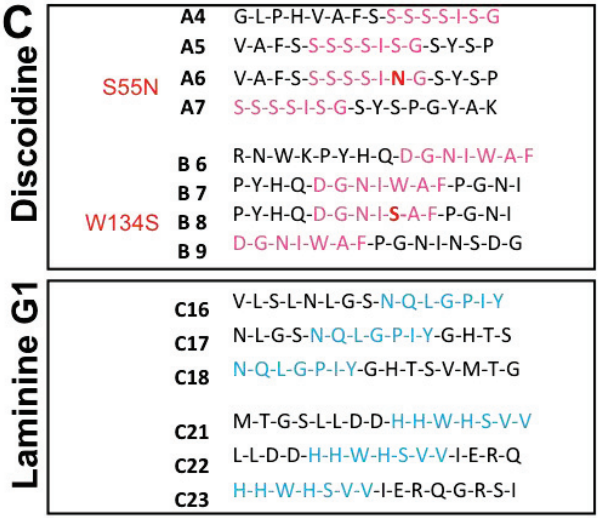

Figure 29 : Détermination des épitopes en celluspot. Les lames sont bloquées 2h à température ambiante en lait 5% puis incubées sur la nuit à 4°C avec les anticorps de patient dilués dans du lait 5%. Elles sont ensuite lavées et incubées 1h à température ambiante avec les anticorps secondaires anti-humain couplés à la peroxydase de raifort (HRP) dilués au 1 :10 000 dans du lait 2,5%. Les lames sont ensuite lavées et révélées en chemiluminescence. **A)** Example d'un test celluspot avec des prélèvements de LCR et de sérum d'individu contrôle (sans anti-CASPR2) et de patient présentant une EL à anti-CASPR2 (LE4). Les barres en rose et bleu montrent les peptides reconnus dans les domaines discoidine et laminine G1 respectivement. **B)** Tableau récapitulatif des résultats celluspot et détermination de la séquence en a.a. reconnue pour les 10 patients testés. Un épitope dans le domaine

discoidine ou laminine G1 a pu être déterminé pour 6/10 patients. Le patient LE8 correspond au patient testé sur toutes les mutations en ELISA. **C)** À partir des séquences en a.a des peptides reconnus, nous avons déterminé la séquence maximale en a.a. de chaque épitope

Pour certains patients, nous n'avons pas réussi à identifier un épitope (négatif). Pour autant, nous savons que tous les patients possèdent des anticorps contre le domaine discoidine. Ainsi, ces résultats peuvent être dus à (1) une sensibilité/résolution du test trop faible ou (2) à la présence d'épitopes conformationnels, indétectables en celluspot.

Par ailleurs les épitopes identifiés dans le domaine discoidine correspondent bien aux régions prédites comme épitopiques grâce à la structure mais ne correspondent pas aux régions identifiées en ELISA (épitope E1 et E2) (Figure 30) (Article 2). Deux explications sont possibles pour de telles différences : (1) il existerait plusieurs épitopes, linéaires et conformationnels. Les épitopes détectés en ELISA (E1 et E2) seraient conformationnels et ne seraient donc pas détectés en celluspot. De plus, les épitopes détectés en celluspot (C1 et C2) n'étant pas impactés par les mutations S55N et W134S, ils ne seraient pas détectés en ELISA. (2) Les épitopes identifiés en celluspot seraient les seuls existants. Les mutations diminuant la reconnaissance par les anticorps de patient en ELISA (épitopes E1 et E2) perturberaient la conformation du domaine discoidine, empêchant l'accès des anticorps à leur épitope : C1 et/ou C2.

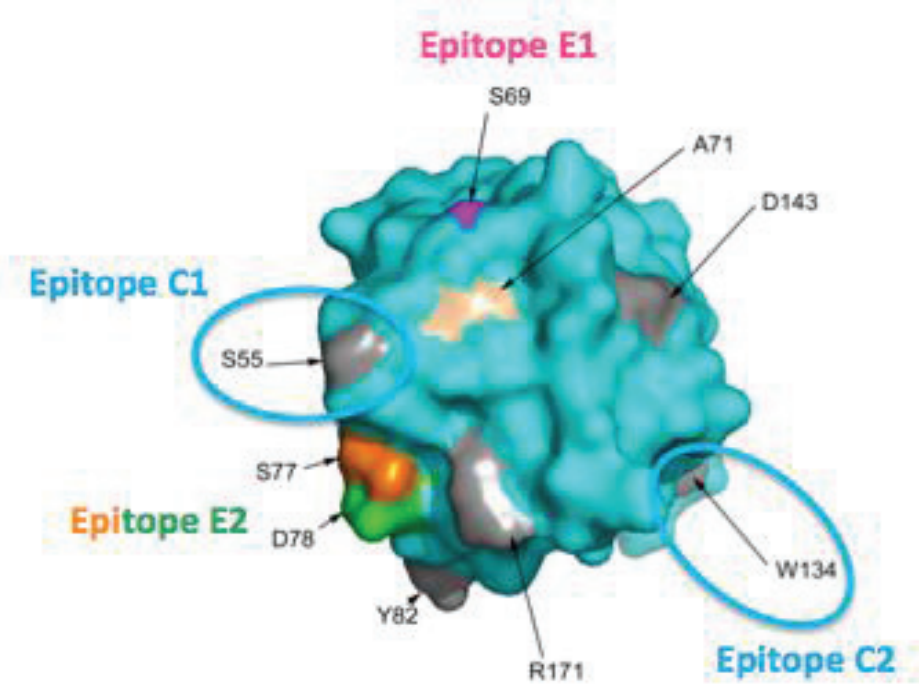

Figure 30 : Epitopes du domaine discoidine déterminés par celluspot et ELISA. La structure 3D du domaine discoidine est représentée ainsi que les 9 acides aminés mutés situés dans les régions épitopiques prédites. En celluspot, nous avons identifié deux épitopes au niveau des a.a. S55 (C1) et W134 (C2). En ELISA les mutations des a.a. S69 (E1) et S77/D78 (E2) induisent une diminution de la reconnaissance du domaine discoidine par les anticorps de patients.

D. Annexe 2 : Importance des domaines discoidine et laminine G1 de CASPR2, étude et cartographie des mutations *CNTNAP2*

Contactin-associated protein-like 2, a protein of the neurexin family involved in several human diseases.

Saint-Martin M, Joubert B, Pellier-Monnin V, Pascual O, Noraz N, Honnorat J. Eur J Neurosci. **2018** Aug;48(3):1906-1923. doi: 10.1111/ejn.14081. Epub 2018 Aug 16. Review.

Nous avons souhaité apporter des éléments pouvant nous renseigner sur l'importance des domaines discoidine et laminine G1 dans la fonction de CASPR2. Un moyen d'évaluer l'importance de ces domaines est d'étudier leur implication dans d'autres pathologies comme les maladies génétiques. Pour ce faire, j'ai répertorié les mutations du gène *CNTNAP2* identifiées chez les patients atteints de maladies neurodéveloppementales. L'analyse de la répartition de ces mutations permet d'identifier des régions du gène particulièrement concernées par les mutations et/ou associées à un type de pathologie et donc potentiellement importantes pour les fonctions de CASPR2.

J'ai donc répertorié et cartographié les mutations du gène *CNTNAP2* touchant uniquement les parties codantes (exons) (Figure 31). Bien que, comme décrit dans le chapitre « maladies associées à CASPR2 », la plupart des patients présentent une combinaison de présentations cliniques, seule la présentation clinique majeure ou initialement diagnostiquée est représentée ici (Figure 31).

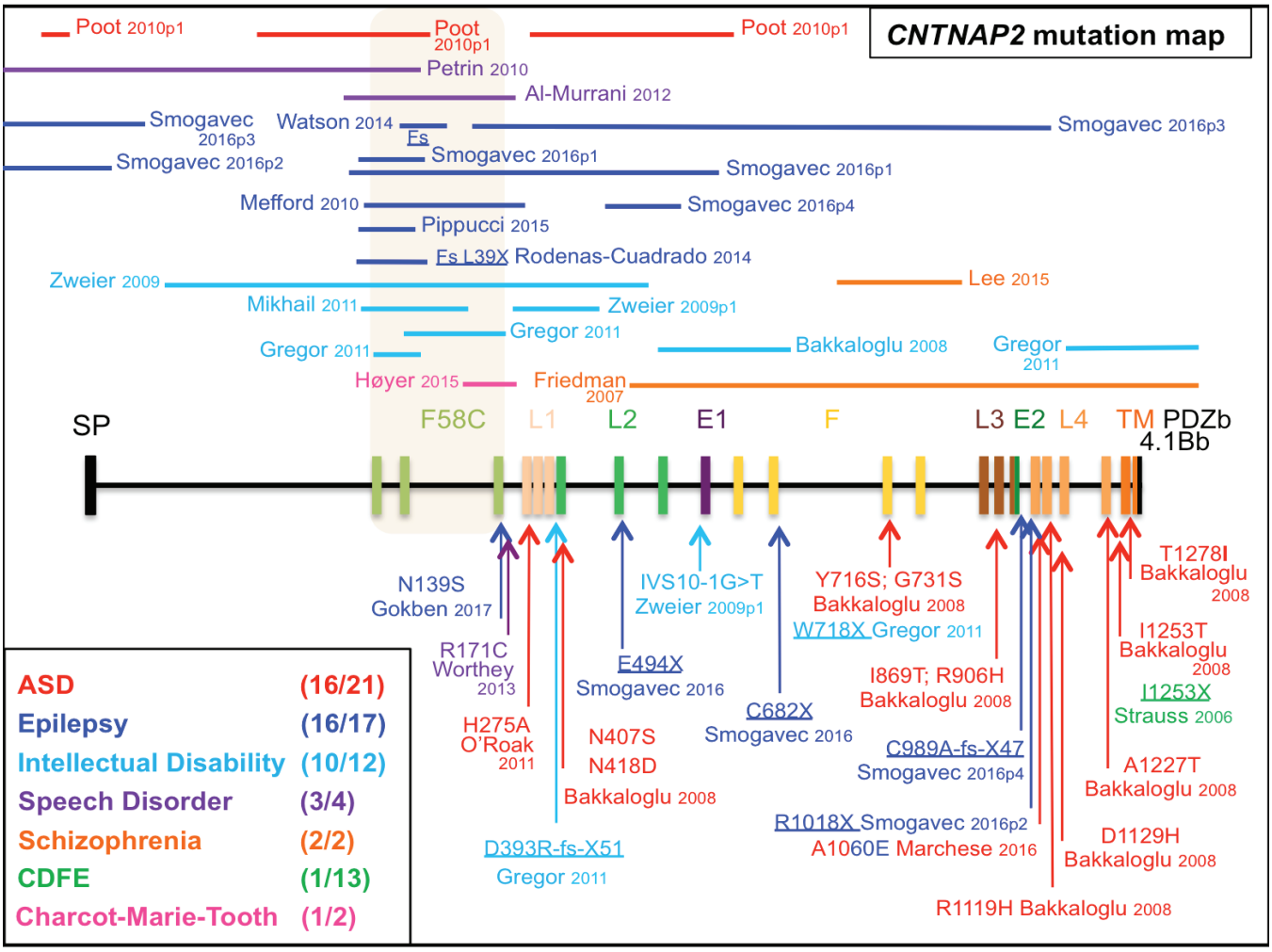

Figure 31 : Cartographie des mutations *CNTNAP2* (Revue Saint-Martin et al., 2018). Le gène CNTNAP2 et ses 24 exons codant pour les différents domaines de CASPR2 sont représentés. Les larges délétions ou duplications de gène (CNVs) sont représentées par des barres au-dessus du gène. Les mutations ponctuelles sont représentées par des flèches sous le gène et les mutations stop sont soulignées. La référence (nom de l'auteur et date de publication) est spécifiée pour chaque mutation. Certains patients possèdent plusieurs mutations du gène CNTNAP2 qui sont indiquées par l'indice p1 (patient 1) à p4 (patient 4). La présentation clinique majeure associée à la mutation est représentée en différentes couleurs (encadré). Pour chaque présentation clinique, le nombre de mutations et de patients répertoriés est indiqué entre parenthèse (encadré).

Une fois les mutations répertoriées j'ai étudié leur distribution sur les 24 exons codant pour CASPR2. Cette distribution est comparée entre les patients rapportés dans cette étude (Figure 31) et les individus sains de la population globale rapportés dans la banque de données ExAC (Exome Aggregation Consortium) (Lek et al., 2016). Cette banque de données a été créée en excluant les individus présentant de sévères maladies pédiatriques. Le nombre de mutations a été répertorié chez les patients (Groupe patient : 49 mutations au total dont 24 mutations ponctuelles (PM) et 25 délétions/duplications (Copy Number Variation, CNVs) ainsi que dans la population ExAC (Groupe ExAC : 539 mutations au total dont 528 PM et 11 CNVs). Ensuite, le pourcentage du nombre total de mutations a été calculé pour chaque exon (nombre de mutations dans l'exon X/nombre total de mutations) et représenté sous forme de courbes (Figure 32). Lorsque tous les types de mutations sont pris en compte, aucune tendance ne ressort pour un exon en particulier (Figure 32A). Par ailleurs, si on étudie séparément les PM et les CNVs, aucune différence n'est observée pour les PM (Figure 32B). Par contre, un nombre élevé de CNVs semblent cibler les exons codant pour le domaine discoidine (F58C) de CASPR2 dans le groupe patient (respectivement 10,8%, 12,8% et 6,9% des mutations totales sur les exons 1-3) comparé au groupe ExAC (respectivement 1,7%, 1,7% et 5,2% des mutations totales sur les exons 1-3) (Figure 32C). Les CNVs identifiées dans ce domaine sont majoritairement associées à l'épilepsie et aux déficiences intellectuelles.

D'autre part, les mutations identifiées chez les patients atteints d'autisme sont en majorité des mutations ponctuelles (Figure 31). En étudiant la répartition de ces mutations ponctuelles, on note un pourcentage légèrement plus élevé de mutations dans le domaine laminine G4 chez ces patients, comparé à la population ExAC (Figure 32D).

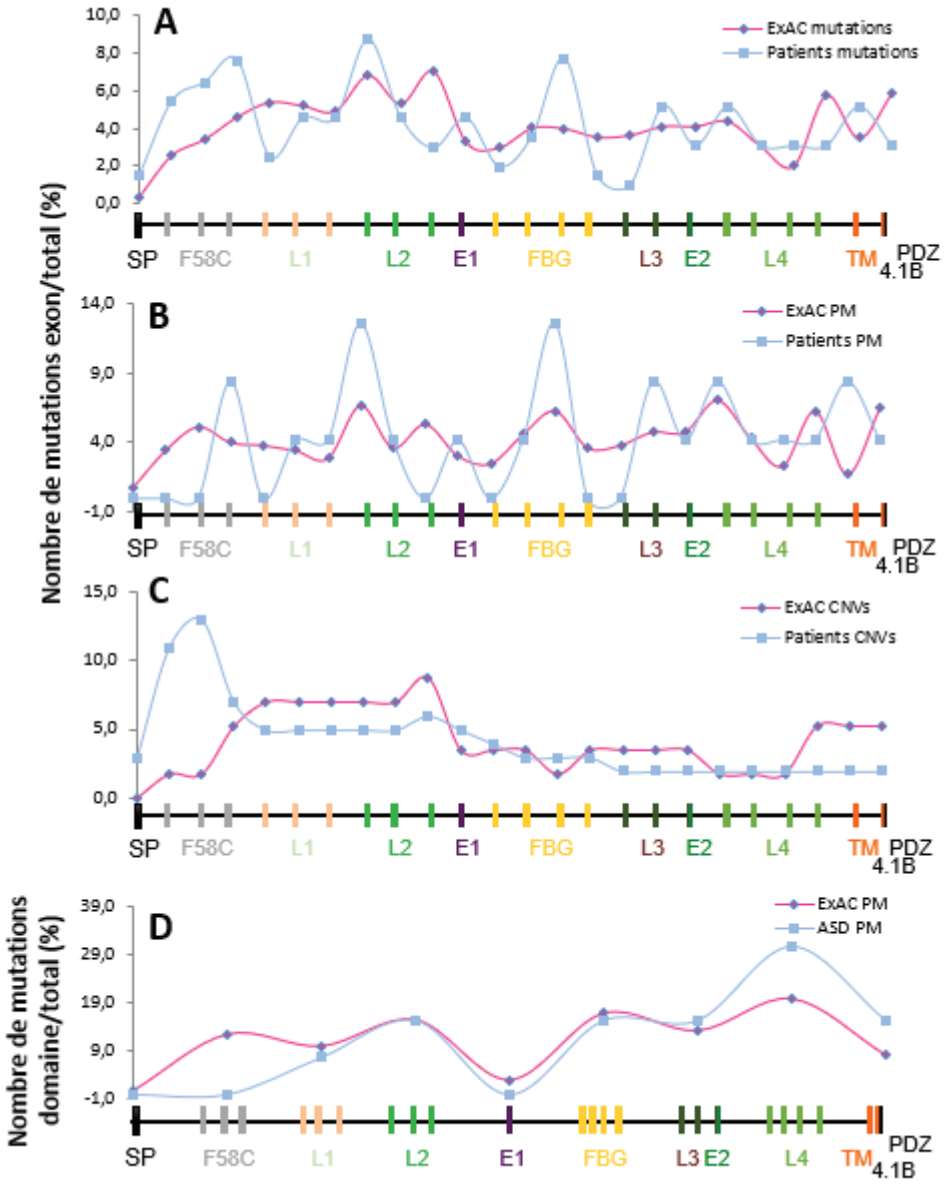

Figure 32 : Etude comparative des mutations de *CNTNAP2* (Revue Saint-Martin et al., 2018). Distribution des mutations sur les 24 exons codant pour CASPR2. Groupe patient : 49 mutations au total dont 24 mutations ponctuelles (PM) et 25 délétions/duplications (Copy Number Variation, CNVs) ; Groupe ExAC : 539 mutations au total dont 528 PM et 11 CNVs. Le pourcentage du nombre total de mutations est calculé pour chaque exon ou domaine (nombre de mutations dans l'exon X/nombre total de mutations) et représenté sous forme de courbes**. A)** Comparaison de toutes les mutations. **B)** Comparaison des mutations pontcuelles. **C)** Comparaison des CNVs. **D)** Comparaison des mutations ponctuelles associées à l'autisme par domaine.

En résumé, il ressort de ce travail deux domaines d'intérêt au regard de la fonction de CASPR2 : le domaine discoidine N-terminal, corroborant son implication potentielle dans l'EL (Article 1) et le domaine laminine G4, proche de la membrane.

II. Etude de l'impact des auto-anticorps anti-CASPR2 de patients sur le complexe CASPR2/TAG-1/Kv1.2

A. Article 3 :

CASPR2/TAG-1/Kv1.2 interactions and impact of anti-CASPR2 auto-antibodies from patients with limbic encephalitis.

Saint-Martin M., Déchelotte B., Honnorat J., Pellier-Monnin V., Noraz N.

La caractérisation des anticorps anti-CASPR2 de patients présentant une EL suggère un rôle direct des anticorps sur la fonction de CASPR2. Or, CASPR2 est essentiellement connue pour son rôle dans le rassemblement des canaux potassiques aux nœuds de Ranvier à l'aide de son partenaire TAG-1. Au sein de ce complexe, CASPR2 pourrait avoir différentes fonctions : (1) réguler la localisation du complexe, de par son association avec les protéines du cytosquelette ; (2) moduler l'adhésion cellulaire, de par son interaction avec TAG-1 ; (3) contrôler l'excitabilité neuronale, de par son interaction avec les Kv1. Notre hypothèse de travail a été de considérer que les anticorps seraient capables de perturber une ou plusieurs de ces fonctions. C'est la raison pour laquelle nous nous sommes intéressés à l'impact des anticorps anti-CASPR2 sur le complexe CASPR2/TAG-1/Kv1.2.

Nous avons montré que les anticorps sont capables de perturber les interactions en cis entre CASPR2 et TAG-1 (de l'ordre de 20% de diminution). Par ailleurs, nos résultats montrent que le domaine discoidine n'interagit pas avec TAG-1 alors que le domaine laminine G1 est suffisant, bien que non nécessaire, pour cette interaction. L'utilisation de mutants de délétion sur toute la protéine nous a permis d'identifier les domaines EGF2-lamininеG4 comme les domaines majeurs d'interaction entre CASPR2 et TAG-1. Nous avons ensuite montré que les domaines Ig et Fn de TAG-1 sont capables d'interagir avec CASPR2 ; cette interaction serait favorisée par le dépliement de TAG-1 en forme ouverte, modulant ainsi les contacts cellulaires. Nous nous sommes ensuite intéressés à la capacité des anticorps anti-CASPR2 à moduler l'adhésion cellulaire par l'intermédiaire de TAG-1. Cependant, nous n'avons observé aucun effet des anticorps anti-CASPR2 dans le modèle cellulaire testé. Pour finir, nous avons étudié la relation possible entre CASPR2 et l'expression des Kv1. Nous avons montré que les anticorps anti-CASPR2 sont capables d'augmenter l'expression en surface des Kv1.2 sans toutefois impacter l'expression de

CASPR2 en surface. De plus, nous avons montré que CASPR2 modulerait l'expression des Kv1.2 en surface de manière dose dépendante.

Ainsi, CASPR2 jouerait un rôle majeur dans l'expression de surface des Kv1.2 et cette expression serait modulée par les anticorps de patient. L'expression de CASPR2 en surface étant inchangée, les mécanismes par lesquels passent cette fonction restent à déterminer. Entre autres, il serait intéressant de connaitre la place de TAG-1 dans cette fonction dont l'interaction avec CASPR2 est perturbée par les auto-anticorps.

Title

Impact of anti-CASPR2 autoantibodies from patients with autoimmune encephalitis on CASPR2/TAG-1 interaction and Kv1 expression.

Author names and affiliations

Margaux Saint-Martin[a,b,c*], Alanah Pieters[a,b,c*], Benoît Déchelotte[a,b,c], Céline Malleval[a,b,c], Delphine Pinatel[a,b,c], Olivier Pascual[a,b,c], Domna Karagogeos[e], Jérôme Honnorat[a,b,c,d], Véronique Pellier-Monnin[a,b,c], Nelly Noraz[a,b,c].

[a] INSERM U1217, Institut NeuroMyoGène, Lyon, F-69000, France.

[b] CNRS UMR5310, Institut NeuroMyoGène, Lyon, F-69000, France.

[c] University Claude Bernard Lyon 1, Lyon, F-69000, France.

[d] Hospices Civils de Lyon, Lyon, F-69000, France.

[e] University of Crete Medical School and IMBB-FORTH, Heraklion, Crete GR-70013, Greece.

* Margaux Saint-Martin and Alanah Pieters have equally contributed to this work

Corresponding author

Nelly Noraz

INSERM U1217, CNRS UMR5310, Institut NeuroMyoGène (INMG), équipe SynatAc, Faculté de Médecine, 8 avenue Rockefeller, F-69008 Lyon, France

Tel. 04 26 68 82 87

Fax. 04 26 68 82 92

nelly.noraz@inserm.fr

Abstract

Autoantibodies against CASPR2 (contactin-associated protein-like 2) have been linked to autoimmune limbic encephalitis that manifests with memory disorders and temporal lobe seizures. According to the growing number of data supporting a role for CASPR2 in neuronal excitability, CASPR2 forms a molecular complex with transient axonal glycoprotein-1 (TAG-1) and shaker-type voltage-gated potassium channels (Kv1.1 and Kv1.2) in compartments critical for neuronal activity and is required for Kv1 proper positioning. Whereas the perturbation of these functions could explain the symptoms observed in patients, the pathogenic role of anti-CASPR2 antibodies has been poorly studied. In the present study, we find that patient autoantibodies alter Caspr2 distribution at the cell membrane promoting cluster formation. We confirm in a HEK cellular model that the anti-CASPR2 antibodies impede CASPR2/TAG-1 interaction and we identify the domains of CASPR2 and TAG-1 taking part in this interaction. Moreover, introduction of CASPR2 into HEK cells induces a marked increase of the level of Kv1.2 surface expression and in cultures of hippocampal neurons Caspr2-positive inhibitory neurons appear to specifically express high levels of Kv1.2. Importantly, in both cellular models, anti-CASPR2 patient autoAb increase Kv1.2 expression. These results provide new insights into the pathogenic role of autoAb in the disease.

Keywords: CASPR2, TAG-1, Kv1, autoimmune encephalitis, autoantibody, domains of interaction

1-Introduction

Contactin-associated protein-like 2 (CASPR2) is a neuronal cell adhesion protein of the neurexin family expressed in the central and peripheral nervous system [1]. Autoantibodies (autoAb) against CASPR2 have been linked to acquired neuromyotonia (NMT) a peripheral nerve hyperexcitability syndrome [2], Morvan's syndrome (MoS), which combines NMT and encephalopathy [3] and autoimmune encephalitis (AE), a CNS-specific syndrome [4,5]. The presence of anti-CASPR2 Ab not only in serum but also in cerebrospinal fluid of AE patients was associated with rather homogeneous clinical features. They are men around 60 years of age with prevalent symptoms of limbic dysfunction, including memory disorders, temporal lobe seizures, and frontal lobe impairment [6,7]. CASPR2 autoAb were initially identified as Ab recognizing voltage-gated potassium channel (VGKC) [2]. However, it has become apparent that they principally target LGI1 or CASPR2. All these proteins belong to a complex referred as VGKC complex [8,9].

CASPR2 is a rather compact transmembrane protein with a C-terminal intracellular region that contains a 4.1B-binding motif and a type II PDZ-binding motif allowing, respectively, its interaction with cytoskeleton-associated proteins and scaffolding proteins. The extracellular part is composed of an N-terminal discoidin-like domain, four laminin G-like domains, two epidermal growth factor-like domains and a fibrinogen-like domain [10]. Anti-CASPR2 autoAb recognize multiple domains of the protein. Interestingly, all patients present autoAb directed against the discoidin and laminin G1 N-terminal domains and some, recognize only those two domains [6,7,11,12], suggesting that autoAb binding to the discoidin and laminin G1 domains is involved in the development of the disease. Besides, anti-CASPR2 autoAb are mainly IgG4 [6,7], a subclass that binds weakly to Fc-γ receptors and do not activate complement. IgG4 could be considered as blocking Ab (i.e. Ab binding to its antigenic target disrupts its function).

CASPR2 forms a molecular complex with shaker-type voltage-gated potassium channels (Kv1.1 and Kv1.2) and transient axonal glycoprotein-1 (TAG-1), a glycosyl-phosphatidylinositol (GPI)-anchored adhesion molecule of the Ig superfamily also referred as Axonin-1 or Contactin-2 [13–16]. Proteins forming this complex were found co-enriched in compartments critical for neuronal activity including the axon initial segment (AIS) [17] and the juxtaparanodal region (JXP) of node of Ranvier (NOR) on myelinated axons [13,15]. Importantly, in CASPR2 KO mice, Kv1 and TAG-1 were no longer enriched at the JXP [13,18] and in the same way, in TAG-1 KO mice, Kv1 and CASPR2 were both mislocalized [15]. These data put into light the co-requirement of CASPR2 and TAG-1 for Kv1 proper positioning. In line with these findings and with the key function of Kv1 in controlling action potential propagation, CASPR2 has been involved in the regulation of intrinsic neuronal

excitability [18,19]. In regards with anti-CASPR2 autoAb, some data support these findings. For instance, anti-CASPR2 autoAb impede CASPR2/TAG-1 interaction in a solid-phase binding assay [20]. Furthermore, CASPR2 autoAb enhance the excitability of DRG (dorsal root ganglion) neurons in a cell-autonomous fashion through regulation of Kv1 channel expression [19]. In the present study, experiments were conducted to bring further evidence of a pathogenic role of anti-CASPR2 autoAb in the disease.

2-Materials and methods.

2.1-Patient sera and IgG purification.

Sera from four patients with AE were obtained from the Centre National de Référence pour les Syndromes Neurologiques Paranéoplasiques in Lyon, France. All patients displayed temporal lobe seizures and memory disorders and were tested positive for anti-CASPR2 autoAb [6,21]. Informed consent was obtained for every patient and the present study was granted by the institutional review board of the Hospices Civils de Lyon (Comité de Protection des Personnes SUD-EST IV). We also used three control sera collected from healthy blood donors at Etablissement Français du Sang. The titer of anti-CASPR2 autoAb in the sera used in this study was previously determined using an HEK cell-based assay [6,21]. Importantly, serum antibody titers (last dilution of serum giving a positive signal) were high around 1:10.000 and equivalent among patients. To purify IgG, sera were incubated with protein-A Sepharose 4 Fast Flow™ beads (SIGMA) 2h at room temperature (RT) on rotation, transferred to columns and washed 3 times with PBS. IgG were eluted in glycine buffer pH2.8, neutralized in Tris buffer pH8.8 and dialyzed overnight at 4°C in PBS (Slide-A-lyser G2 Dialysis Cassettes 0.5-3ml ThermoFisher). IgG concentration was then measured using micro BCA protein assay kit (ThermoFisher). Purified IgG were sterilized on 0.22µm filters and kept at -80°C. Patient (Pat) and control (Ctl) IgG were either used separately or as a pool (pPat: equimolar concentration of Pat 2, Pat 3 and Pat 4 purified IgG; pCtl: equimolar concentration of Ctl 1, Ctl 2 and Ctl 3 purified IgG).

2.2-Constructs.

The CASPR2-GFP plasmid, the CASPR2-HA (Hemagglutinin tag) and derived deleted constructs, CASPR2 Δ1, CASPR2 Δ2, CASPR2 Δ3, and CASPR2 Δ4, kindly provided by C. Faivre-Sarrailh, as well as CASPR2-Discoidin (D) and CASPR2-LaminiG1 (L1) constructs were previously described [12]. The CASPR2-EGF2-LaminineG4 (E2L4) construct was obtained using reverse PCR on full-length CASPR2-HA plasmid and In-Fusion kit (Clontech). PCR amplified products were verified by sequencing (Eurofins). The TAG-1-GFP plasmid, TAG-1-GFP ΔFn and TAG-1-GFP ΔIg constructs, kindly provided by D. Karagogeos, were previously described [22]. The TAG-1-GFP ΔIg5 construct was obtained using reverse PCR on TAG-1-GFP full-length plasmid and In-Fusion kit (Clontech). The surface expression of proteins derived from all the plasmids used in this study has been validated in HEK cells **(Fig. S1)**.

2.3-Antibodies

The primary and secondary antibodies used in this study are described in Table 1.

2.4-Cell lines and transfection.

HEK 293T cells were purchased from ATCC and cells referred in this paper as HEK-Kv were kindly provided by A. Morielli. HEK-Kv are HEK 293 cells stably expressing m1 mAChR, Kv1.2 and its Kvβ2 subunit [23]. Cells were grown in DMEM (ThermoFisher) SVF 10%, P/S 1% and transfected using the lipofectamine LTX kit (Invitrogen).

2.5-Immunoprecipitation and Western Blot.

For immunoprecipitation (IP) and Western Blot analysis, 24 hours after transfection HEK cells were lysed 10min at 4°C in lysis buffer pH7.5 containing NaCl 150mM, HEPES 50mM, Triton 1%, octyl-β-glucoside 60mM (ThermoFisher), protease (Roche) and phosphatase (0.1mM NaF, 0.1mM Na3VO4, 1mM PMSF, 1mM benzamidine) inhibitors. Lysates were centrifuged at 4°C, 10min 12000g, supernatant was collected and protein concentration was evaluated using the micro BCA protein assay kit (ThermoFisher). Immunoprecipitation was performed using 150µg of protein lysate and 1µg of indicated Ab. Tubes were placed at 4°C with rotation overnight and then protein G agarose fast flow beads (Millipore) were added for 2h. Supernatant was discarded and beads were washed three times in 500µl lysis buffer. Immunoprecipitated proteins were then eluted in Laemmli DTT buffer, 5min at 95°C. Proteins were separated onto Criterion XT Bis-Tris precast 10% gels (Bio-Rad) and transferred onto nitrocellulose membrane (GE Healthcare). Membranes were blotted with the indicated Abs and revealed using Substrat HRP Immobilon Western (Millipore). Reactive proteins were visualized using the Chemidoc MP Imaging System (Bio-Rad). Band intensities were quantified using ImageJ and the ratio of protein co-immunoprecipitated/protein immunoprecipitated was calculated. In order to normalize for inter-experiment variations, ratios obtained for each condition were summed and results were expressed as a fraction of the summed ratios.

For surface immunoprecipitation transfected HEK cells were incubated with control or patient purified IgG (5µg/mL) for 24h at 37°C. After one wash in PBS, cells were incubated with an anti-HA Ab or control anti-myc Ab (2µg/mL) for 1h at room temperature, washed twice in PBS and lysed. Protein lysates were then processed as described above.

For the Biotinylation experiments hippocampal neurons (21 DIV) were treated for 24 hours with pooled patient or control IgG and cell surface proteins were biotinylated using the Pierce Cell Surface Protein Isolation Kit (ThermoFisher) following manufacturer's instructions. The obtained total and surface fractions were denaturated for 5min at 95°C in Laemmli DTT and separated onto 4-15% Criterion TGX Stain-Free Precast Gels (Bio-Rad). Loaded proteins were quantified after transfer to nitrocellulose membrane using the Chemidoc MP Imaging System. Membranes were blotted with anti-CASPR2 Ab (ab33994).

Reactive proteins were visualized with SuperSignal West Pico Chemiluminiscent Substrate (ThermoFisher, 34580) using the Chemidoc MP Imaging System. Band intensities were measured using Image Lab (version 5.2.1, Bio-Rad) and for each sample the ratio of Caspr2 to total loaded protein was calculated.

2.6-Flow cytometry.

HEK-Kv cells were used for flow cytometry analysis. Cells were incubated with either patient or healthy control purified IgG at a concentration of 16µg/mL for 24h at 37°C. HEK cells were washed with PBS one time and incubated with 154mM sodium azide for 10 minutes at 37°C, to limit endocytosis as previously described [24]. Cells were then washed with PBS and primary antibody was incubated for 1h at 4°C in PBS 2% BSA. Cells were washed three times in PBS and secondary antibody was incubated for 30 minutes at 4°C in PBS 2% BSA. After three washes in PBS, cells were then processed in the cytometer (three-laser FACS Canto II) and median of fluorescence intensity was measured for each parameter. In these experiments, Kv1.2 was labeled with anti-Kv1.2 Ab (APC 162) and Alexa647-conjugated secondary Ab; CASPR2 was labeled with anti-HA Ab and Alexa405-conjugated secondary Ab; TAG-1-GFP expression was directly measured. In order to normalize for inter-experiment variations, medians of fluorescence intensity obtained for each condition were summed and results were expressed as a fraction of the summed medians.

2.7-Primary hippocampal neuronal culture.

Primary hippocampal neuron cultures were prepared from E18 Wistar rat embryos (Janvier Labs). Pregnant rats were deeply anesthetized by isoflurane (Ceva) inhalation and embryos were taken out by Caesarean section. Hippocampi were isolated in Hank's buffered salt solution (HBSS) (Gibco) and transferred for dissociation in HBSS supplemented with 10% (v/v) trypsin (Gibco) for 10min at 37°C. Hippocampi were then washed with 4% (w/v) bovine serum albumin (BSA) and triturated. Cells were plated onto poly-L-lysine (0.5mg/mL) coated coverslips in Neurobasal medium (Gibco) supplemented with 2% (v/v) B27 (Gibco), 0.3% (v/v) L-glutamine (Invitrogen) and 1% (v/v) penicillin-streptomycin (invitrogen). Cells were cultured for 14 or 21 days at 37°C in a humidified atmosphere containing 5% CO_2. Animal care and procedures were conducted according to the European Community Council Directive 2010/63/UE and the French Ethical Committee.

2.8-Immunocytofluorescence.

For surface Caspr2 and total Kv1.2/GAD65 staining hippocampal neurons were treated at 20 DIV (days *in vitro*) with patient or control purified IgG at 16µg/mL, for 24h at 37°C. At 21 DIV neurons were washed in Neurobasal and surface Caspr2 was stained using

the pool of patient IgG (pPat) as primary Ab at 5µg/mL, for 30min at 37°C. Neurons were then washed in Neurobasal, fixed in 4% (v/v) PFA for 10min, blocked with 3% (w/v) BSA in PBS for 30min and incubated for 30min at RT with secondary Ab. After washing in PBS neurons were permeabilized for 30min at RT with 3% (w/v) BSA in PBS 0.3% (v/v) Triton X-100 (PBS-T) and incubated for 1h at RT with anti-Kv1.2 (K14/16) and anti-GAD65 primary Ab. Neurons were then washed in PBS-T and incubated for 1h at RT with secondary Ab. After washing in PBS, nuclei were stained using 0.1µg/mL Hoechst (ThermoFisher) for 5min at RT.

For surface and total CASPR2-GFP staining, neurons were transfected at 11 DIV with CASPR2-GFP plasmid using the Lipofectamine LTX kit (Invitrogen) and treated at 13 DIV with patient 1 or control 1 IgG at 16µg/mL for 24h at 37°C. Neurons were washed in Neurobasal and surface CASPR2-GFP was stained with anti-GFP primary Ab for 30 min at 37°C. Neurons were then washed in Neurobasal, fixed in 4% (v/v) PFA for 10min, blocked with 3% (w/v) BSA in PBS for 30min and incubated for 30min at RT with alexa555 secondary Ab. After washing in PBS neurons were permeabilized for 30min at RT with 3% (w/v) BSA in PBS-T and incubated for 1h at RT with anti-GFP primary Ab. Neurons were then washed in PBS-T and incubated for 1h with alexa488 secondary Ab. After washing in PBS, nuclei were stained using 0.1µg/mL Hoechst (ThermoFisher) for 5min at RT.

For all experiments coverslips were mounted in FluorPreserve Reagent (Calbiochem) and stored at 4°C until image acquisition.

2.9-Image acquisition and analysis

Images were acquired using Zeiss Axio Imager Z.I ApoTome microscope and for the quantitative analysis a fixed exposition time was applied to the different experimental conditions. To quantify surface Caspr2 signal intensities, images were analyzed using ICY Spotdetector Plugin (version 1.9.10.0, BioImage Analysis Unit Institut Pasteur). The mean intensity of the clusters/spots detected was multiplied by cluster area to get total signal intensity per cluster. Values were summed and divided by total surface occupied by clusters. Results were expressed as mean Caspr2 signal intensity.

To analyze surface CASPR2-GFP expression, a ROI corresponding to transfected neuron was defined based on the surface occupied by green signal (total CASPR2-GFP). Red signals (surface CASPR2-GFP) included in the ROI were then quantified using ICY Spotdetector and results depicted as cluster size, cluster intensity and cluster number per μm^2 of neuron.

To analyze Kv1.2 expression, ROIs with the same surface across different experimental conditions were defined along neurites based on the red signal (surface

Caspr2). Green signal intensities (total Kv1.2) included in the ROI were then quantified using ICY and results depicted as intensity arbitrary units.

2.10-Statistical analysis

GraphPad Prism software was used for all statistical tests. Depending on the experimental setting, data were compared using a Mann-Whitney, a Kruskal-Wallis or a Wilcoxon signed-rank test. Data were represented as mean±SD and significance was set for a p value ≤ 0.05.

3-Results.

3.1-Patient anti-CASPR2 autoAb impede CASPR2/TAG-1 interaction.

Using an acellular solid phase binding assay, it has been shown that CASPR2 and TAG-1 directly interact through their extracellular domains and that anti-CASPR2 patient sera inhibited this interaction [20]. Here, in a first set of experiments, we asked whether anti-CASPR2 autoAb from AE patients were able to perturb CASPR2/TAG-1 interaction in a cellular model. HEK cells co-transfected with CASPR2-HA and TAG-1-GFP were incubated for 24 hours with healthy donor (Ctl) or patient (Pat) IgG purified from serum to avoid any side effects due to other serum proteins. Cells were then further incubated with an anti-HA Ab before lysis to specifically immunoprecipitate the fraction of CASPR2 present at the cell surface. The ratio of TAG-1 co-immunoprecipitated (co-IP) over CASPR2 immunoprecipitated (IP) was assessed. As shown in **Figure 1A**, co-IP TAG-1 was observed in surface CASPR2 immunoprecipitates obtained from cells treated with Ctl or Pat IgG, but not in the control immunoprecipitates (Ctl IP) for which co-transfected HEK cells were incubated 24 hours with PBS and incubated with an irrelevant control Ab before lysis. Compared with Ctl IgG the level of co-IP TAG-1 was diminished in Pat IgG treated cells (Ctl: 0.55±0.09; Pat: 0.44±0.09 $p<0.01$). Notably, a 20% and 19% decrease of TAG1-binding was observed using patient 2 and patient 3 IgG respectively whereas decreased binding was rather low on cells incubated with patient 1 IgG (7% decrease) and not observed with patient 4 IgG **(Fig. 1B)**.

3.2-The EGF2 and laminin G4 domains of CASPR2 are critical for TAG-1 interaction.

To get a better understanding of the decreased CASPR2/TAG-1 binding observed in the presence of patient autoAb, we conducted experiments to determine which domain(s) of either protein was responsible for their interaction. Notably, both CASPR2/TAG-1 cis- and trans-interactions have been reported [13,15,25] and in CASPR2 and TAG-1 co-transfected HEK cells, both types of interactions are possible. We therefore first evaluated the contribution of CASPR2/TAG-1 trans-interactions in our model. To this end, HEK cells were either, co-transfected with plasmids coding for CASPR2-HA and TAG-1-GFP proteins (C2T1) allowing cis and trans associations or, cells were separately transfected with either one plasmids and subsequently put together (C2+T1) allowing CASPR2/TAG-1 trans-associations only **(Fig. 2A** left panel). Cells were lysed and CASPR2 was immunoprecipitated using a commercial antibody directed against its intracellular domain (ab33994). As shown in **Figure 2A** right panel, the level of TAG-1 co-IP was much higher in co-transfected cells (C2T1) than in cells separately transfected (C2+T1) for which TAG-1 was barely detectable even at long exposure times. These data indicate that the majority of

the TAG-1 co-IP with CASPR2 in co-transfected cells comes from cis-interaction between the two proteins.

Anti-CASPR2 autoAb from AE patients all recognize the N-terminal discoidin (D) and laminin G1 (L1) domains of CASPR2 and more importantly, 45% of patient autoAb recognize only these two domains [6], suggesting that they could be critical for CASPR2/TAG-1 interaction. To test this hypothesis, TAG-1 co-IP were repeated as described above in cells expressing the full-length (C2) or only the discoidin (D) or laminin G1 (L1) domains of CASPR2. No TAG-1 co-IP was detected in cells expressing the discoidin domain of CASPR2 **(Fig. 2B)**. In contrast, the laminin G1 domain of CASPR2 was sufficient to co-IP TAG-1 **(Fig. 2B)**. To further characterize the domains of CASPR2 involved in TAG-1 interaction, the same experiment was performed using deletion constructs covering the entire CASPR2 protein. CASPR2 was IP and co-IP TAG-1 was quantified **(Fig. 2C)**. As previously shown [26], compared with CASPR2 full-length (C2), deletion of the laminin G2 and EGF1 domains of CASPR2 (Δ2) increased the quantity of TAG-1 co-IP (C2: 0.19±0.06; Δ2: 0.38±0.04 $p<0.01$) **(Fig. 2C)**. Although this result did not tell much about the TAG-1-binding propensity of the laminin G2 and EGF1 domains of CASPR2, it suggested that CASPR2/TAG-1 interaction is constrained by conformational hindrances. Equal levels of TAG-1 were co-IP in cells transfected with the CASPR2 construct lacking the discoidin and laminin G1 domains (Δ1) or the fibrinogen and laminin G3 domains (Δ3) (C2: 0.19±0.06; Δ1: 0.24±0.06; Δ3: 0.15±0.06, $p>0.05$) indicating that these domains are dispensable for CASPR2/TAG-1 interaction **(Fig. 2C)**. In contrast, the Δ4 construct lacking the EGF2 and laminin G4 domains of CASPR2 led to a drastic decrease of CASPR2/TAG1 interaction (C2 : 0.19±0.06; Δ4: 0.05±0.07 $p<0.05$) **(Fig. 2C)** indicating that they are major domains of interaction. According to this, the construct expressing only the EGF2 and laminin G4 domains of CASPR2 (E2L4) was sufficient to co-IP TAG-1 **(Fig. 2D)**.

To recapitulate, of the two discoidin and laminin G1 domains, only the laminin G1 domain is involved in CASPR2/TAG-1 interaction and the removal of these domains does not significantly hamper CASPR2/TAG-1 binding. On the contrary, the EGF2 and laminin G4 domains are critical for CASPR2/TAG-1 interaction.

3.3- Both the Ig and Fn domains of TAG-1 are involved in CASPR2/TAG-1 interaction.

TAG-1 consists of 6 immunoglobulin (Ig) domains followed by 4 fibronectin domains (Fn) tethered to the cell surface by a GPI anchor **(Fig 3A)**. The fact that the EGF2-laminin G4 domains of CASPR2, the main interaction domains involved in CASPR2/TAG-1 interaction, are located near the membrane was difficult to conciliate with previous findings showing that CASPR2 interacts in cis with the Ig but not the Fn domains of TAG-1 [22]. Therefore, the ability of CASPR2 to interact with the Ig and Fn domains of TAG-1 was re-considered.

Deletion of neither TAG-1 Fn1-4 domains (ΔFn) nor Ig1-6 domains (ΔIg) prevented CASPR2 binding to TAG-1 indicating that both are involved in CASPR2/TAG-1 interaction. Moreover, the removal of TAG-1 Ig domains increased CASPR2 binding suggesting that Ig domains placed constraints on CASPR2 accessibility to TAG-1 Fn domains **(Fig. 3B)**. It has been proposed that TAG-1 could adopt various shapes ranging from a horseshoe-shape or closed conformation to an extended shape or opened conformation **(Fig. 3A)** [27]. One can therefore postulate that in the closed conformation the Fn domains could be masked by the Ig domains thus limiting their binding to CASPR2. Inversely, in the opened conformation accessibility of Fn domains to CASPR2 could be promoted. To test this hypothesis, we used the TAG-1 ΔIg5 mutant previously described to shift the conformation of the protein toward an extended shape favoring Fn domains exposure [28]. As shown in **Fig. 3C**, the level of TAG-1 co-IP was higher in cells transfected with TAG-1 ΔIg5 than the full-length construct.

Together, these results indicate that although both the Fn and Ig domains of TAG-1 are involved in CASPR2/TAG-1 interaction, in the TAG-1 back-folded conformation Ig domains could limit TAG-1 binding to CASPR2.

3.4-Patient autoAb do not alter CASPR2 surface expression but increase Kv1.2 surface expression.

Based on findings suggesting that CASPR2 and TAG-1 affect intrinsic neuronal excitability by impacting Kv1 expression/distribution at the membrane [18,19,29], we wanted to test the hypothesis that patient anti-CASPR2 autoAb could alter Kv1.2 surface expression. As a preliminary experiment, we wished to determine whether CASPR2 or TAG-1 expression could impact Kv1.2 surface expression. To this end, we used HEK cells stably expressing Kv1.2 and its Kvβ2 subunit (HEK-Kv) [23]. HEK-Kv cells were transfected with CASPR2-HA or TAG-1-GFP and the level of Kv1.2 surface expression was quantified by flow cytometry **(Fig. 4A)**. As depicted in **Fig. 4B**, the level of Kv1.2 in TAG-1-positive gated cells was not different from the control non-transfected cells (NT) (0.23±0.03 versus 0.20±0.05, $p>0.05$). In contrast, Kv1.2 expression was markedly increased following CASPR2 transfection (CASPR2: 0.57±0.07 versus NT: 0.20±0.05, $p<0.0001$).

Next, HEK-Kv co-transfected with CASPR2-HA and TAG-1-GFP were incubated for 24 hours in the presence of Ctl IgG or Pat IgG and the level of CASPR2 and Kv1.2 surface expression was assessed **(Fig. 4C)**. Whereas CASPR2 surface expression was not affected, (Ctl: 0.52±0.02; Pat: 0.48±0.02, $p>0.05$), the level of Kv1.2 surface expression was significantly increased by patient IgG (Ctl: 0.44±0.03; Pat: 0.56±0.03, $p<0.0001$). Patient 2, 3 and 4 increased Kv1.2 surface expression to a similar extent, 15.22%, 16.71%, and 16.52% respectively while Patient 1 only induced a 3.15% increase **(Fig 4D)**.

3.5-Patient autoAb alter CASPR2 surface distribution in hippocampal neurons.

To study the impact of anti-CASPR2 autoAb in a more relevant cellular model, cultures of primary hippocampal neurons were treated at 20 DIV with patient IgG (Pat 2, Pat 3, Pat 4) or control IgG (Ctl 1, Ctl 2). Since no commercial Ab targeting the extracellular part of Caspr2 was available at that time, surface Caspr2 labeling was performed using a pool of patient IgG (pPat). In agreement with previous data [12], Caspr2 staining appeared as clusters of various sizes and intensities. Only a subpopulation representing approximately 20% of neurons expressed Caspr2. Moreover, Caspr2 was essentially localized along axons **(Fig. 5A** and data not shown**)**.

All tested patient IgG did not induce Caspr2 internalization. In contrast, compared with Ctl IgG, a two-fold increase of Caspr2 surface intensity was observed upon incubation with patient IgG. To gain confidence in these results, the experiment was repeated using pooled patient (pPat) or control (pCtl) IgG and surface Caspr2 was assessed by a cell surface biotinylation assay **(Fig. 5B)**. Notably, the level of Caspr2 in the biotinylated fraction of the proteins as well as the level of total Caspr2 was not different between the two conditions. Finally, to get a better idea of the impact of patient IgG on Caspr2 level of expression and distribution at the cell surface, hippocampal neurons were transfected with a plasmid coding for CASPR2-GFP and then treated (14 DIV) with patient IgG (Pat 1) or control IgG (Ctl 1). To analyze the fraction of CASPR2 present at the cell surface, live cells were labeled with an anti-GFP primary Ab and an anti-rabbit Alexa555-conjugated secondary Ab, therefore avoiding any interference between patient Ab used during the 24h incubation and Ab used for Caspr2 surface labeling**.** Caspr2 overall surface intensity in cells incubated with Pat IgG was not different than Ctl IgG (Pat: 50.72±33.89; Ctrl: 40.78±34.46 $p<0.05$) (data not shown). The size, intensity and number of Caspr2 clusters were then quantified for each condition and compared **(Fig. 5C)**. Whereas no change in the size of clusters was observed (Ctl1: 0.208±0.006; Pat1: 0.203±0.011 $p>0.05$), Pat IgG induced a decrease of cluster intensity (Ctl1: 248.8±28.8; Pat1: 161.3±10.8 $p<0.05$) and a marked increase of Caspr2 cluster number at the cell surface (Ctl1: 0.144±0.015; Pat1: 0.295±0.033 $p<0.0001$).

Taken together, these results demonstrated that patient IgG did not significantly change the surface level of Caspr2 but altered its distribution at the cell membrane promoting Caspr2 cluster formation.

3.6-Patient autoAb increase Kv1.2 expression in hippocampal neurons.

In line with the results we obtained on HEK cells, the impact of anti-CASPR2 patient autoAb on Kv1.2 expression was assessed in hippocampal neurons (21 DIV). Firstly, cells were stained for Kv1.2 surface expression but we were not able to observe any signal. Therefore, Caspr2 expression was assessed on live cells (surface) using the pool of patient

IgG and Kv1.2 expression was assessed on permeabilized cells (total). As illustrated in **Fig. 6A**, fibers expressing high level of Kv1.2 could be clearly distinguished and strikingly an obvious co-labeling was observed with axons highly positive for Caspr2. Since in cultured hippocampal neurons Caspr2 is essentially expressed in inhibitory neurons [12], cells were stained for GAD65, a typical marker of inhibitory neurons **(Fig. 6A)**. As expected the population of axons highly positive for Caspr2 was essentially GAD65-positive (98%) moreover, 90% of the Caspr2/GAD65-double positive axons also expressed high level of Kv1.2. Therefore, it appeared that Caspr2-positive inhibitory neurons also express high level of Kv1.2. Secondly, to determine whether anti-CASPR2 patient Ab modulate Kv1.2 expression, primary hippocampal neurons were treated at 20 DIV with the pool of patient or control IgG and stained for surface Caspr2 and total Kv1.2 **(Fig. 6B)**. Compared with control IgG, treatment with patient IgG significantly increased Kv1.2 signal intensity (Ctl: 409.8±83.2 versus Pat: 568.9±193.6, $p<0.01$).

4-Discussion

Anti-CASPR2 patient autoAb alter CASPR2 surface distribution.

We show in this study that patient autoAb do not induce CASPR2 internalization using two cellular models, HEK cells and more importantly cultured primary hippocampal neurons. Upon patient autoAb addition the level of CASPR2 at the cell surface remained essentially unchanged. However, CASPR2 membrane distribution was altered with the formation of an elevated number of CASPR2 clusters. In view of these observations, it appears that the pathogenic effect of autoAb rely on CASPR2 redistribution at the cell membrane rather than internalization. These results are consistent with the fact that anti-CASPR2 patient autoAb are often IgG4 [6,7,12], a subclass presenting several unique biophysical properties. In particular, IgG4 can undergo half-molecule exchange rendering them bispecific and thereby functionally monovalent. This implies that IgG4 are unable to crosslink their targets which is often a prerequisite for the process of internalization [30].

Anti-CASPR2 patient autoAb impede CASPR2/TAG-1 interaction.

It was suggested that patient autoAb could directly perturb CASPR2 function by preventing CASPR2/TAG-1 interaction. For instance, using an acellular solid phase binding assay, Patterson et al. [20] showed that patient Ab decrease CASPR2/TAG-1 binding by 30% to 90% depending on the patient serum tested. In this paper, using purified serum IgG, we find that the decrease of CASPR2/TAG-1 binding upon anti-CASPR2 autoAb addition still occurs in a cellular environment, although to a lower extent (under 20% of decrease). Moreover, we identified regions taking part in CASPR2/TAG-1 cis-interactions, the Ig1-6 and Fn1-4 domains on TAG-1 side as well as the laminin G1 and the EGF2-laminin G4 domains on CASPR2 side. However, the removal of the laminin G1 domain of CASPR2 did not significantly hamper CASPR2/TAG-1 interaction, whereas removal of the EGF2-laminin G4 domains drastically impeded CASPR2/TAG-1 interaction, pointing the EGF2-laminin G4 domains as key domains of interaction. EGF-like domains consist of molecular hinges (small linear solenoid domain) permitting the lobes of the protein to flex with respect to each other [31,32]. In contrast, laminin G-like domains are large globular domains involved in interactions with other proteins (neuroligin, cerebellin, GABAa receptor) [33,34]. It is therefore likely that the laminin G4 domain of CASPR2, rather than the EGF2 domain, mediates CASPR2/TAG-1 interactions. Considering the molecular shape and dimension of these two molecules a model can be proposed for which the laminin G4 domain of CASPR2 interacts with the fibronectin domains of TAG-1 and the laminin G1 domain of CASPR2 interacts with the immunoglobulin domains of TAG-1 **(Fig. 7A)**. Essentially obtained with deletion mutants, this model has nevertheless to be taken with caution since we find here

that as depicted by others [32], CASPR2/TAG-1 interactions are constrained by conformational hindrances.

Regarding the impact of anti-CASPR2 autoAb on this model of interaction, we know that patient Ab are polyclonal and mostly target the N-terminal half of CASPR2 ectodomain (D-L1-L2-E1), all recognizing at least the discoidin and laminin G1 domains [6,11,12]. Moreover, patient Ab rarely target the C-terminal half of the protein (F-L3-E2-L4), where the main interaction domain of CASPR2, the laminin G4 domain, is located [11]. Thus, anti-CASPR2 autoAb would mainly perturb CASPR2/TAG-1 interaction trough the laminin G1 domain, which may explain their low propensity to impede CASPR2/TAG-1 interaction **(Fig 7B)**. In addition, in our cellular model, CASPR2/TAG-1 interactions are mainly occurring in cis with high constraints due to a complex environment, whereas in the solid phase binding assay, CASPR2 and TAG-1 can freely adopt several orientations. Such differences may explain the higher blocking propensity of patient Ab in the solid phase binding assay [20].

Besides, as for the solid phase binding assay, the extent of inhibition varied between patients although the 4 sera tested in this study presented similar anti-CASPR2 Ab titers. Differences in the localization of targeted epitopes or the Ab affinity/avidity for their targets as well as the Ab titer for each subclass of IgG (IgG1 or IgG4) may account for the variations in the degree of inhibition. Additional studies with higher number of patients are needed to determine factors responsible for the difference observed between patients.

CASPR2 and Kv1 expression are linked.

We showed herein that the introduction of CASPR2 into HEK cells induces a marked increase of the level of Kv1.2 surface expression. Moreover, it appears that Caspr2-positive inhibitory neurons also express high level of Kv1.2. These results are in line with previous findings showing a decreased membrane expression of Kv1.2 in *Cntnap2* KO DRG neurons in culture. Notably, in these cells the KO of Caspr2 resulted in enhanced excitability with a large reduction in the DTX-sensitive outward current, indicating a reduction in the function of Kv1 channels [19]. Moreover, in wild-type DRG neurons cultured *in vitro* for 5 days, a spontaneous reduction in Kv1 (membrane) and Caspr2 (mRNA) expression coincided with hyperexcitabilty. Importantly, enhanced excitability was reversed by Caspr2-forced expression in a Kv1 channel-dependent manner [19]. Therefore, one can speculate that CASPR2, by interfering with surface expression of Kv1 channels is an important modulator of neuronal excitability.

Anti-CASPR2 patient autoAb increase Kv1.2 expression.

In HEK cells, patient autoAb increase Kv1.2 surface expression. Importantly, such an increase is also observed in hippocampal neurons although we could not determine if this

occurs at the cells surface. These results are in contrast with a previous study showing that in cultured DRG neurons treated with anti-CASPR2 patient Ab the number of cells expressing Kv1.2 at the surface was decreased [19]. Since Kv1 expression may vary with CASPR2 expression levels, it would be interesting to assess the impact of anti-CASPR2 autoAb on the level of CASPR2 surface expression in these neurons. Nevertheless, diverse mechanisms might regulate Kv1 surface expression depending on the cell type, in the same way as different mechanisms are responsible for Kv1 enrichment at the AIS and JXP. Of particular interest, a decrease of CASPR2 and Kv1.1 expression was observed at JXP following systemic injection of anti-CASPR2 patient Ab despite the fact that no patient Ab binding was detected in this region. On the other hand, a clear patient Ab binding was observed on DRG cell soma [19]. It is therefore tempting to speculate that decreased JXP expression of CASPR2 and Kv1.1 might be due to patient Ab-induced retention of these molecules at the soma, thereby impairing their axonal membrane lateral diffusion.

Since CASPR2 interacts with Kv1 channels indirectly through their intracellular cytoplasmic domains [1], the mechanism by which CASPR2 promotes Kv1.2 surface expression likely relies on intracellular motifs. Both proteins present a cytoskeleton-binding motif as well as a PDZ-binding motif, which could lead to restricted diffusion and co-clustering of CASPR2 and Kv1.2 at the membrane. For instance, the 4.1B-cytoskeleton-binding motif of CASPR2 was depicted as required for the enrichment of Kv1 channels at the NOR [35]. Kv1.2 surface expression relies on tyrosine residues present in its intracellular domain. Their phosphorylation leads to Kv1.2 reduced binding to the cytoskeleton and endocytosis [36,37]. Of particular interest, TAG-1-induced clustering of Kv1.2 along axons was shown to depend on Kv1.2 phosphorylation [29]. Whether CASPR2 could modulate Kv1 surface expression by impinging Kv1 phosphorylation directly or indirectly, by altering TAG-1 membrane distribution, [15,29] remains to be established. Regarding the possible mechanism(s) by which anti-CASPR2 autoAb may lead to increased Kv1.2 expression, patient Ab binding may restrict CASPR2 diffusion thereby promoting cluster formation. This may in turn retain Kv1.2 at the membrane possibly by stabilizing CASPR2/Kv1.2 interactions, thus limiting Kv1 endocytosis.

Kv1 channels play a major role in membrane repolarization following action potential. A decrease in Kv1 expression leads to higher neuronal excitability characterized by an increase of action potential frequency and repolarization latency [38]. This results in increased neurotransmitter release at the synapse [39]. On the contrary, an increase of Kv1 expression could lead to a decrease of action potential frequency and neurotransmitter release [40]. Since CASPR2 is mainly expressed in inhibitory neurons, anti-CASPR2 autoAb, by increasing Kv1 expression, could specifically result in decreased inhibition, a defect consistent with the seizure disorders observed in patients.

In conclusion, we bring further evidences of two potential pathogenic mechanisms of anti-CASPR2 autoAb in patients with AE namely disturbing CASPR2/TAG-1 interaction and Kv1.2 expression. By impacting on neuronal excitability, these pathogenic mechanisms could contribute to the clinical features of patients with AE. Furthermore, our data provide new insights into the interaction constraints between CASPR2 and TAG-1, which might prove useful to study the relevance of this interaction in the formation and localization of the CASPR2/TAG-1/Kv1 complex.

Acknowledgements

We are grateful to C. Faivre-Sarrailh (Institut de Neurobiologie de la Méditerranée, Aix Marseille Université, INSERM UMR1249, Marseille) for providing the CASPR2 full-length and derived plasmids as well as scientific and technical advice and, A. Vandermoeten, LM. Illartein, O. Martin and A. Meunier (Scar, Faculté Rockefeller, Lyon) for taking care of the animals.

Funding

This work was supported by INSERM, CNRS, University Lyon 1, the Agence Nationale de la Recherche (ANR-14-CE15-0001-MECANO), the Fondation pour la Recherche Médicale (FRM DQ20170336751) and the fonds de dotation CSL Behring pour la recherche.

References

[1] S. Poliak, L. Gollan, R. Martinez, A. Custer, S. Einheber, J.L. Salzer, J.S. Trimmer, P. Shrager, E. Peles, Caspr2, a new member of the neurexin superfamily, is localized at the juxtaparanodes of myelinated axons and associates with K+ channels, Neuron. 24 (1999) 1037–1047.

[2] P. Shillito, P.C. Molenaar, A. Vincent, K. Leys, W. Zheng, R.J. van den Berg, J.J. Plomp, G.T. van Kempen, G. Chauplannaz, A.R. Wintzen, Acquired neuromyotonia: evidence for autoantibodies directed against K+ channels of peripheral nerves, Ann. Neurol. 38 (1995) 714–722. doi:10.1002/ana.410380505.

[3] R. Liguori, A. Vincent, L. Clover, P. Avoni, G. Plazzi, P. Cortelli, A. Baruzzi, T. Carey, P. Gambetti, E. Lugaresi, P. Montagna, Morvan's syndrome: peripheral and central nervous system and cardiac involvement with antibodies to voltage-gated potassium channels, Brain J. Neurol. 124 (2001) 2417–2426.

[4] C. Buckley, J. Oger, L. Clover, E. Tüzün, K. Carpenter, M. Jackson, A. Vincent, Potassium channel antibodies in two patients with reversible limbic encephalitis, Ann. Neurol. 50 (2001) 73–78.

[5] J. Newsom-Davis, C. Buckley, L. Clover, I. Hart, P. Maddison, E. Tüzüm, A. Vincent, Autoimmune disorders of neuronal potassium channels, Ann. N. Y. Acad. Sci. 998 (2003) 202–210.

[6] B. Joubert, M. Saint-Martin, N. Noraz, G. Picard, V. Rogemond, F. Ducray, V. Desestret, D. Psimaras, J.-Y. Delattre, J.-C. Antoine, J. Honnorat, Characterization of a Subtype of Autoimmune Encephalitis With Anti-Contactin-Associated Protein-like 2 Antibodies in the Cerebrospinal Fluid, Prominent Limbic Symptoms, and Seizures, JAMA Neurol. 73 (2016) 1115–1124. doi:10.1001/jamaneurol.2016.1585.

[7] A. van Sonderen, H. Ariño, M. Petit-Pedrol, F. Leypoldt, P. Körtvélyessy, K.-P. Wandinger, E. Lancaster, P.W. Wirtz, M.W.J. Schreurs, P.A.E. Sillevis Smitt, F. Graus, J. Dalmau, M.J. Titulaer, The clinical spectrum of Caspr2 antibody-associated disease, Neurology. 87 (2016) 521–528. doi:10.1212/WNL.0000000000002917.

[8] S.R. Irani, S. Alexander, P. Waters, K.A. Kleopa, P. Pettingill, L. Zuliani, E. Peles, C. Buckley, B. Lang, A. Vincent, Antibodies to Kv1 potassium channel-complex proteins leucine-rich, glioma inactivated 1 protein and contactin-associated protein-2 in limbic encephalitis, Morvan's syndrome and acquired neuromyotonia, Brain. 133 (2010) 2734–2748. doi:10.1093/brain/awq213.

[9] M. Lai, M.G.M. Huijbers, E. Lancaster, F. Graus, L. Bataller, R. Balice-Gordon, J.K. Cowell, J. Dalmau, Investigation of LGI1 as the antigen in limbic encephalitis previously attributed to potassium channels: a case series, Lancet Neurol. 9 (2010) 776–785. doi:10.1016/S1474-4422(10)70137-X.

[10] M. Saint-Martin, B. Joubert, V. Pellier-Monnin, O. Pascual, N. Noraz, J. Honnorat, Contactin-associated protein-like 2, a protein of the neurexin family involved in several human diseases, Eur. J. Neurosci. 48 (2018) 1906–1923. doi:10.1111/ejn.14081.

[11] A.L. Olsen, Y. Lai, J. Dalmau, S.S. Scherer, E. Lancaster, Caspr2 autoantibodies target multiple epitopes, Neurol. Neuroimmunol. Neuroinflammation. 2 (2015) e127. doi:10.1212/NXI.0000000000000127.

[12] D. Pinatel, B. Hivert, J. Boucraut, M. Saint-Martin, V. Rogemond, L. Zoupi, D. Karagogeos, J. Honnorat, C. Faivre-Sarrailh, Inhibitory axons are targeted in hippocampal cell culture by anti-Caspr2 autoantibodies associated with limbic encephalitis, Front. Cell. Neurosci. 9 (2015) 265. doi:10.3389/fncel.2015.00265.

[13] S. Poliak, D. Salomon, H. Elhanany, H. Sabanay, B. Kiernan, L. Pevny, C.L. Stewart, X. Xu, S.-Y. Chiu, P. Shrager, A.J.W. Furley, E. Peles, Juxtaparanodal clustering of Shaker-

like K+ channels in myelinated axons depends on Caspr2 and TAG-1, J. Cell Biol. 162 (2003) 1149–1160. doi:10.1083/jcb.200305018.

[14] M.N. Rasband, E.W. Park, D. Zhen, M.I. Arbuckle, S. Poliak, E. Peles, S.G.N. Grant, J.S. Trimmer, Clustering of neuronal potassium channels is independent of their interaction with PSD-95, J. Cell Biol. 159 (2002) 663–672. doi:10.1083/jcb.200206024.

[15] M. Traka, L. Goutebroze, N. Denisenko, M. Bessa, A. Nifli, S. Havaki, Y. Iwakura, F. Fukamauchi, K. Watanabe, B. Soliven, J.-A. Girault, D. Karagogeos, Association of TAG-1 with Caspr2 is essential for the molecular organization of juxtaparanodal regions of myelinated fibers, J. Cell Biol. 162 (2003) 1161–1172. doi:10.1083/jcb.200305078.

[16] N. Chen, F. Koopmans, A. Gordon, I. Paliukhovich, R.V. Klaassen, R.C. van der Schors, E. Peles, M. Verhage, A.B. Smit, K.W. Li, Interaction proteomics of canonical Caspr2 (CNTNAP2) reveals the presence of two Caspr2 isoforms with overlapping interactomes, Biochim. Biophys. Acta. 1854 (2015) 827–833. doi:10.1016/j.bbapap.2015.02.008.

[17] M.C. Inda, J. DeFelipe, A. Muñoz, Voltage-gated ion channels in the axon initial segment of human cortical pyramidal cells and their relationship with chandelier cells, Proc. Natl. Acad. Sci. U. S. A. 103 (2006) 2920–2925. doi:10.1073/pnas.0511197103.

[18] R. Scott, A. Sánchez-Aguilera, K. van Elst, L. Lim, N. Dehorter, S.E. Bae, G. Bartolini, E. Peles, M.J.H. Kas, H. Bruining, O. Marín, Loss of Cntnap2 Causes Axonal Excitability Deficits, Developmental Delay in Cortical Myelination, and Abnormal Stereotyped Motor Behavior, Cereb. Cortex N. Y. N 1991. 29 (2019) 586–597. doi:10.1093/cercor/bhx341.

[19] J.M. Dawes, G.A. Weir, S.J. Middleton, R. Patel, K.I. Chisholm, P. Pettingill, L.J. Peck, J. Sheridan, A. Shakir, L. Jacobson, M. Gutierrez-Mecinas, J. Galino, J. Walcher, J. Kühnemund, H. Kuehn, M.D. Sanna, B. Lang, A.J. Clark, A.C. Themistocleous, N. Iwagaki, S.J. West, K. Werynska, L. Carroll, T. Trendafilova, D.A. Menassa, M.P. Giannoccaro, E. Coutinho, I. Cervellini, D. Tewari, C. Buckley, M.I. Leite, H. Wildner, H.U. Zeilhofer, E. Peles, A.J. Todd, S.B. McMahon, A.H. Dickenson, G.R. Lewin, A. Vincent, D.L. Bennett, Immune or Genetic-Mediated Disruption of CASPR2 Causes Pain Hypersensitivity Due to Enhanced Primary Afferent Excitability, Neuron. 97 (2018) 806-822.e10. doi:10.1016/j.neuron.2018.01.033.

[20] K.R. Patterson, J. Dalmau, E. Lancaster, Mechanisms of Caspr2 antibodies in autoimmune encephalitis and neuromyotonia, Ann. Neurol. 83 (2018) 40–51. doi:10.1002/ana.25120.

[21] B. Joubert, F. Gobert, L. Thomas, M. Saint-Martin, V. Desestret, P. Convers, V. Rogemond, G. Picard, F. Ducray, D. Psimaras, J.-C. Antoine, J.-Y. Delattre, J. Honnorat, Autoimmune episodic ataxia in patients with anti-CASPR2 antibody-associated encephalitis, Neurol. Neuroimmunol. Neuroinflammation. 4 (2017) e371. doi:10.1212/NXI.0000000000000371.

[22] A. Tzimourakas, S. Giasemi, M. Mouratidou, D. Karagogeos, Structure-function analysis of protein complexes involved in the molecular architecture of juxtaparanodal regions of myelinated fibers, Biotechnol. J. 2 (2007) 577–583. doi:10.1002/biot.200700023.

[23] T.G. Cachero, A.D. Morielli, E.G. Peralta, The small GTP-binding protein RhoA regulates a delayed rectifier potassium channel, Cell. 93 (1998) 1077–1085.

[24] E. Nesti, B. Everill, A.D. Morielli, Endocytosis as a mechanism for tyrosine kinase-dependent suppression of a voltage-gated potassium channel, Mol. Biol. Cell. 15 (2004) 4073–4088. doi:10.1091/mbc.e03-11-0788.

[25] M. Savvaki, K. Theodorakis, L. Zoupi, A. Stamatakis, S. Tivodar, K. Kyriacou, F. Stylianopoulou, D. Karagogeos, The Expression of TAG-1 in Glial Cells Is Sufficient for the Formation of the Juxtaparanodal Complex and the Phenotypic Rescue of Tag-1

Homozygous Mutants in the CNS, J. Neurosci. 30 (2010) 13943–13954. doi:10.1523/JNEUROSCI.2574-10.2010.

[26] D. Pinatel, B. Hivert, M. Saint-Martin, N. Noraz, M. Savvaki, D. Karagogeos, C. Faivre-Sarrailh, The Kv1-associated molecules TAG-1 and Caspr2 are selectively targeted to the axon initial segment in hippocampal neurons, J. Cell Sci. 130 (2017) 2209–2220. doi:10.1242/jcs.202267.

[27] C. Rader, B. Kunz, R. Lierheimer, R.J. Giger, P. Berger, P. Tittmann, H. Gross, P. Sonderegger, Implications for the domain arrangement of axonin-1 derived from the mapping of its NgCAM binding site, EMBO J. 15 (1996) 2056–2068.

[28] B. Kunz, R. Lierheimer, C. Rader, M. Spirig, U. Ziegler, P. Sonderegger, Axonin-1/TAG-1 mediates cell-cell adhesion by a cis-assisted trans-interaction, J. Biol. Chem. 277 (2002) 4551–4557. doi:10.1074/jbc.M109779200.

[29] C. Gu, Y. Gu, Clustering and activity tuning of Kv1 channels in myelinated hippocampal axons, J. Biol. Chem. 286 (2011) 25835–25847. doi:10.1074/jbc.M111.219113.

[30] M.G. Huijbers, L.A. Querol, E.H. Niks, J.J. Plomp, S.M. van der Maarel, F. Graus, J. Dalmau, I. Illa, J.J. Verschuuren, The expanding field of IgG4-mediated neurological autoimmune disorders, Eur. J. Neurol. 22 (2015) 1151–1161. doi:10.1111/ene.12758.

[31] E.N. Rubio-Marrero, G. Vincelli, C.M. Jeffries, T.R. Shaikh, I.S. Pakos, F.M. Ranaivoson, S. von Daake, B. Demeler, A. De Jaco, G. Perkins, M.H. Ellisman, J. Trewhella, D. Comoletti, Structural Characterization of the Extracellular Domain of CASPR2 and Insights into Its Association with the Novel Ligand Contactin1, J. Biol. Chem. 291 (2016) 5788–5802. doi:10.1074/jbc.M115.705681.

[32] Z. Lu, M.V.V.V.S. Reddy, J. Liu, A. Kalichava, J. Liu, L. Zhang, F. Chen, Y. Wang, L.M.F. Holthauzen, M.A. White, S. Seshadrinathan, X. Zhong, G. Ren, G. Rudenko, Molecular Architecture of Contactin-associated Protein-like 2 (CNTNAP2) and its Interaction with Contactin 2 (CNTN2), J. Biol. Chem. (2016) jbc.M116.748236. doi:10.1074/jbc.M116.748236.

[33] F. Chen, V. Venugopal, B. Murray, G. Rudenko, The structure of neurexin 1α reveals features promoting a role as synaptic organizer, Struct. Lond. Engl. 1993. 19 (2011) 779–789. doi:10.1016/j.str.2011.03.012.

[34] C. Reissner, F. Runkel, M. Missler, Neurexins, Genome Biol. 14 (2013) 213. doi:10.1186/gb-2013-14-9-213.

[35] I. Horresh, V. Bar, J.L. Kissil, E. Peles, Organization of myelinated axons by Caspr and Caspr2 requires the cytoskeletal adapter protein 4.1B, J. Neurosci. Off. J. Soc. Neurosci. 30 (2010) 2480–2489. doi:10.1523/JNEUROSCI.5225-09.2010.

[36] D. Hattan, E. Nesti, T.G. Cachero, A.D. Morielli, Tyrosine phosphorylation of Kv1.2 modulates its interaction with the actin-binding protein cortactin, J. Biol. Chem. 277 (2002) 38596–38606. doi:10.1074/jbc.M205005200.

[37] H.C. Lai, L.Y. Jan, The distribution and targeting of neuronal voltage-gated ion channels, Nat. Rev. Neurosci. 7 (2006) 548–562. doi:10.1038/nrn1938.

[38] S.L. Smart, V. Lopantsev, C.L. Zhang, C.A. Robbins, H. Wang, S.Y. Chiu, P.A. Schwartzkroin, A. Messing, B.L. Tempel, Deletion of the K(V)1.1 potassium channel causes epilepsy in mice, Neuron. 20 (1998) 809–819.

[39] J.R. Geiger, P. Jonas, Dynamic control of presynaptic Ca(2+) inflow by fast-inactivating K(+) channels in hippocampal mossy fiber boutons, Neuron. 28 (2000) 927–939.

[40] S. He, L.-R. Shao, W.B. Rittase, S.B. Bausch, Increased Kv1 Channel Expression May Contribute to Decreased sIPSC Frequency Following Chronic Inhibition of NR2B-

Containing NMDAR, Neuropsychopharmacology. 37 (2012) 1338–1356. doi:10.1038/npp.2011.320.

Antibodies	Species	Reference	Dilution
Anti-TAG-1 intra	rabbit	Millipore ABN1379	1/5000 (WB)
Anti-CASPR2 intra	rabbit	Abcam ab33994	1/5000 (WB)
Anti-CASPR2 intra	rabbit	Genscript A01426	1µg (IP)
Anti-GFP	rabbit	ThermoFisher A-11122	1/5000 (WB), 1/1000 (IF)
Anti-HA	mouse	Sigma-Aldrich H3663	1/5000 (WB) 1/1000 (IF)
Anti-myc	mouse	Abcam ab9106	1µg (IP)
Anti-Kv1.2 intra	mouse	NeuroMab K14/16	1/5000 (WB), 1/100 (IF)
Anti-Kv1.2 extra	rabbit	Alomone APC 162	1/100 (IF)
Anti-GAD65	mouse	Milipore MAB351	1/400 (IF)
Alexa 647 anti-rabbit	goat	Molecular Probes A21244	1/2000 (IF)
Alexa 405 anti-mouse	goat	Abcam ab175660	1/2000 (IF)
Alexa 555 anti-mouse IgG2b	goat	Molecular Probes A21147	1/1000 (IF)
Alexa 647 anti-mouse IgG2a	goat	Molecular Probes A21241	1/1000 (IF)
Alexa 488 anti-human	goat	Molecular Probes A11013	1/1000 (IF)
Alexa 488 anti-rabbit	goat	Molecular Probes A11034	1/1000 (IF)

Table 1: Primary and secondary antibodies. IF: Immunofluorescence; WB: Western blot ; IP: Immunoprecipitation.

Figure legends

Figure 1: Patient autoAb impede CASPR2/TAG-1 interaction A) HEK cells co-transfected with CASPR2-HA and TAG-1-GFP were incubated for 24 hours with serum-purified control IgG (Ctl) or patient IgG (Pat). CASPR2 present at the cell surface was IP (surface IP) and the level of CASPR2 IP or TAG-1 co-IP, was analyzed by Western Blot. As control, co-transfected HEK cells were incubated with PBS and IP with a control Ab. The ratios of TAG-1 co-IP over CASPR2 IP signal intensities are depicted. Each color represents a different patient. n=12, **p<0.01 Mann-Whitney test. **B)** Ratios of TAG-1 Co-IP over CASPR2 IP are represented separately for each patient.

Figure 2: The EGF2 and laminin G4 domains of CASPR2 are critical for TAG-1 interaction. A) HEK cells were co-transfected with CASPR2-HA and TAG-1-GFP (C2T1) or separately transfected with either one and subsequently put together (C2+T1). CASPR2 was IP and the level of CASPR2 IP or TAG-1 co-IP was analyzed by Western Blot. n=3. **B-D)** HEK cells were co-transfected with TAG-1-GFP and CASPR2-HA full-length (C2) or the indicated mutants. CASPR2 was IP and the level of CASPR2 IP and TAG-1 co-IP was analyzed by Western Blot. **(B)** CASPR2 discoidin (D) and laminin G1 (L1) mutants. n=3. **(C)** CASPR2 Δ1 to Δ4 deletion mutants. The ratios of TAG-1 co-IP over CASPR2 IP signal intensities are depicted in a dot plot. n=6, *p<0.05, **p<0.01 Mann-Whitney test. **(D)** CASPR2 EGF2-laminin G4 mutant (E2L4). n=3. D: discoidin-like domain, L: laminin G-like domain, E: EGF-like domain, F: fibrinogen-like domain, 4.1B: 4.1B-binding motif, PDZ: PDZ-binding motifs.

Figure 3: Both the Ig and Fn domains of TAG-1 are involved in CASPR2/TAG-1 interaction. A) Models of CASPR2 and TAG-1 domain assignment in three dimensions. **B-C)** HEK cells were co-transfected with CASPR2-HA and TAG-1-GFP full-length (T1) or deletion mutants. (**B)** TAG-1 ΔFn and TAG-1 ΔIg. (**C)** TAG-1 ΔIg5. CASPR2 was IP and the level of CASPR2 IP and TAG-1 co-IP was analyzed by Western Blot. The ratios of TAG-1 co-IP over CASPR2 IP signal intensities are depicted in a dot plot. n=3.

Figure 4: Patient autoAb do not alter CASPR2 surface expression but increase Kv1.2 surface expression. HEK cells stably expressing Kv1.2 (HEK-Kv) were either non-transfected (NT) or transfected with CASPR2-HA or TAG-1-GFP. The level of Kv1.2 surface expression was quantified by flow cytometry. **A)** Dot plot representation of TAG-1 and CASPR2 fluorescence intensity in the whole population of cells. Non-transfected, TAG-1-positive and CASPR2-positive gated populations are shown in color boxes. **B)** Histogram

representation of surface Kv1.2 fluorescence intensity measured in the gated populations shown in A). Results are depicted in a dot plot as mean Kv1.2 fluorescence intensity ratio. n=5, p<0.0001 Mann-Whitney test. **C)** HEK-Kv cells co-transfected with CASPR2-HA and TAG-1-GFP were incubated for 24 hours with pooled control (pCtl) or Patient (Pats) IgG. CASPR2 and Kv1.2 surface fluorescence intensity was measured. Results are depicted as a fraction of the summed median fluorescence intensities. Each color represents a different patient. n=11, ****p<0.0001 Mann-Whitney test. **D)** Surface Kv1.2 fluorescence intensity for each patient.

Figure 5: Patient autoAb changed CASPR2 surface distribution in hippocampal neurons. A) hippocampal neurons (21 DIV) treated for 24h with control (Ctl) or patient (Pat) IgG were stained for surface Caspr2 and signal intensities were quantified. n=17-24 image fields per condition, **** p<0.0001 Kruskal-Wallis test. **B)** Hippocampal neurons (21 DIV) treated with pooled patient (pPat) or control (pCtl) IgG were subjected to cell surface biotinylation or left non-biotinylated as control (NB). Caspr2 surface and Caspr2 total proteins were quantified by Western-Blot and results expressed as ratios over total protein loaded. Each color represents a different experiment. n=3 , Wilcoxon signed-rank test. **C)** Hippocampal neurons transfected with CASPR2-GFP were treated (14 DIV) with patient IgG (Pat 1) or control IgG (Ctl 1). The size, intensity and number of surface CASPR2-GFP clusters was analyzed on live cells using anti-GFP primary Ab/Alexa555 secondary Ab. Results are depicted as a dot plot. n=16-17 neurons per condition, * p<0.05, ****p<0.0001 Mann-Whitney test. Scale bar 10µm.

Figure 6: Patient autoAb increase Kv1.2 expression in hippocampal neurons. A) hippocampal neurons (21 DIV) stained on live cells for surface Caspr2 and on permeabilized cells for Kv1.2 and GAD65. **B)** hippocampal neurons (21 DIV) treated for 24h with pooled patient (pPat) or control (pCtl) IgG were stained as in A) and Kv1.2 fluorescence signal intensities were quantified. n=26 neurons per condition, **p<0.01 Mann-Whitney test. Scale bar 10µm.

Figure 7: Model of CASPR2/TAG-1 interaction and impact of anti-CASPR2 autoAb. A) Based on the molecular shape and dimension of these two molecules we propose a model for which laminin G4 (L4), the main interaction domain of CASPR2, interacts with the fibronectin (Fn) domains of TAG-1 and the laminin G1 (L1) domain of CASPR2 interacts with the immunoglobulin (Ig) domains of TAG-1. **B)** Since patient Ab rarely target the laminin G4 domain of the protein, anti-CASPR2 autoAb would mainly perturb CASPR2/TAG-1 interaction trough the laminin G1 domain.

Fig 1

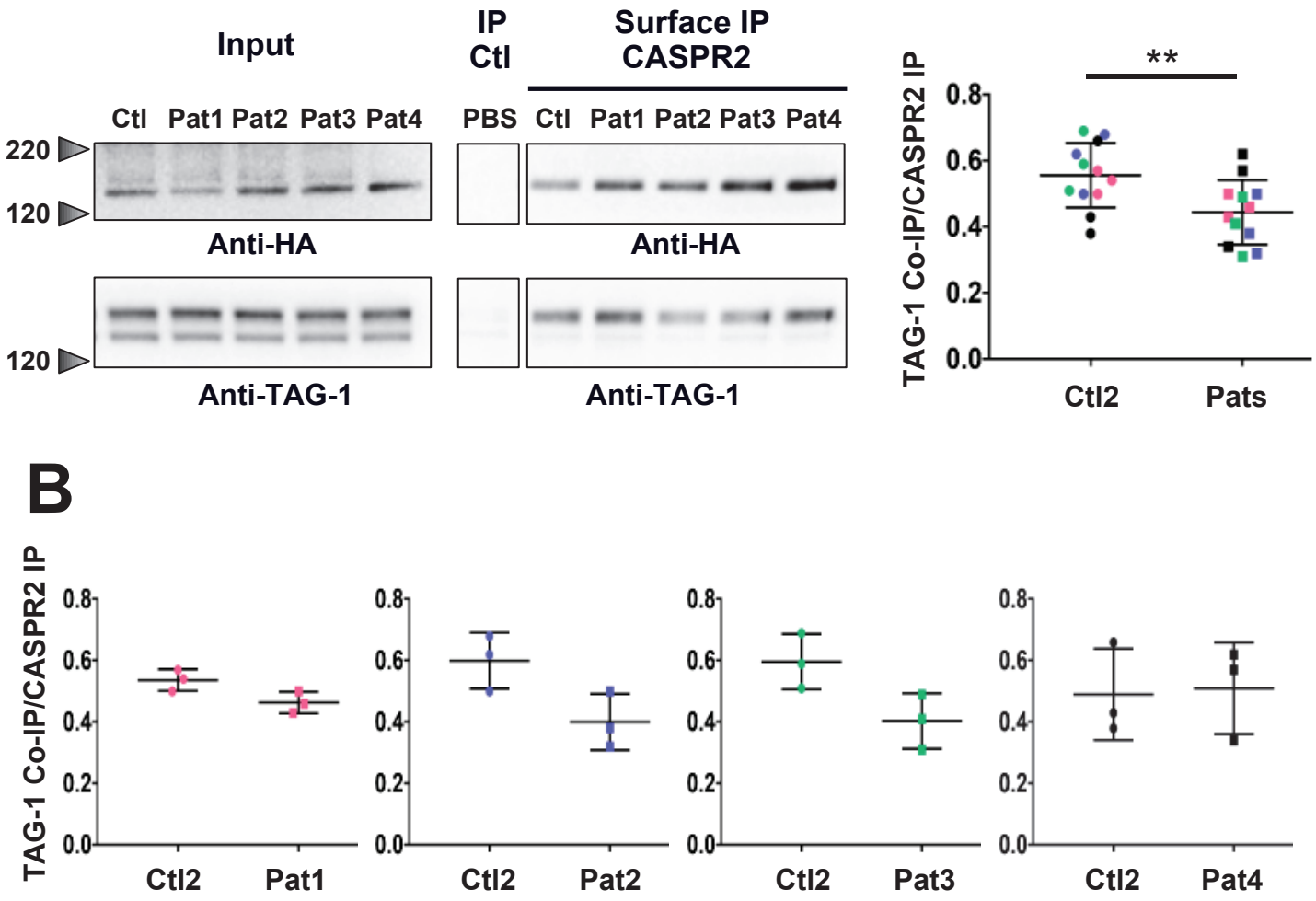
A
Input
IP Ctl
Surface IP CASPR2
Ctl Pat1 Pat2 Pat3 Pat4
PBS Ctl Pat1 Pat2 Pat3 Pat4
220
120
Anti-HA
Anti-HA
120
Anti-TAG-1
Anti-TAG-1
**
TAG-1 Co-IP/CASPR2 IP
0.8
0.6
0.4
0.2
0.0
Ctl2
Pats
B
TAG-1 Co-IP/CASPR2 IP
Ctl2 Pat1
Ctl2 Pat2
Ctl2 Pat3
Ctl2 Pat4

Fig 2

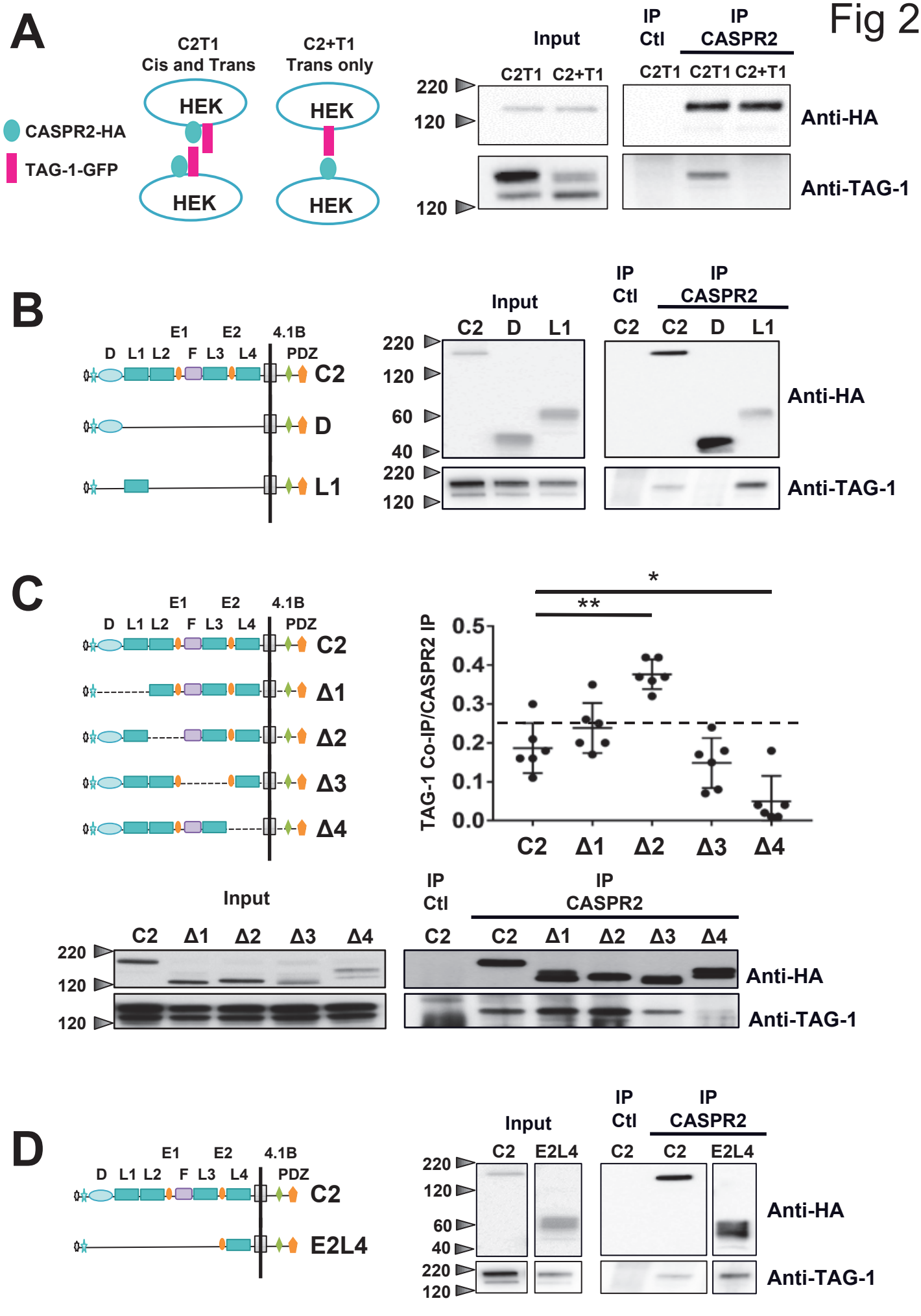
A
C2T1
Cis and Trans
C2+T1
Trans only
HEK
HEK
HEK
HEK
CASPR2-HA
TAG-1-GFP
Input
IP Ctl
IP CASPR2
C2T1 C2+T1
C2T1 C2T1 C2+T1
220
120
120
Anti-HA
Anti-TAG-1
B
E1 E2 4.1B
D L1 L2 F L3 L4 PDZ
C2
D
L1
Input
IP Ctl
IP CASPR2
C2 D L1
C2 C2 D L1
220
120
60
40
220
120
Anti-HA
Anti-TAG-1
C
E1 E2 4.1B
D L1 L2 F L3 L4 PDZ
C2
Δ1
Δ2
Δ3
Δ4
*
**
TAG-1 Co-IP/CASPR2 IP
0.5
0.4
0.3
0.2
0.1
0.0
C2 Δ1 Δ2 Δ3 Δ4
Input
IP Ctl
IP CASPR2
C2 Δ1 Δ2 Δ3 Δ4
C2 C2 Δ1 Δ2 Δ3 Δ4
220
120
120
Anti-HA
Anti-TAG-1
D
E1 E2 4.1B
D L1 L2 F L3 L4 PDZ
C2
E2L4
Input
IP Ctl
IP CASPR2
C2 E2L4
C2 C2 E2L4
220
120
60
40
220
120
Anti-HA
Anti-TAG-1

Fig 3

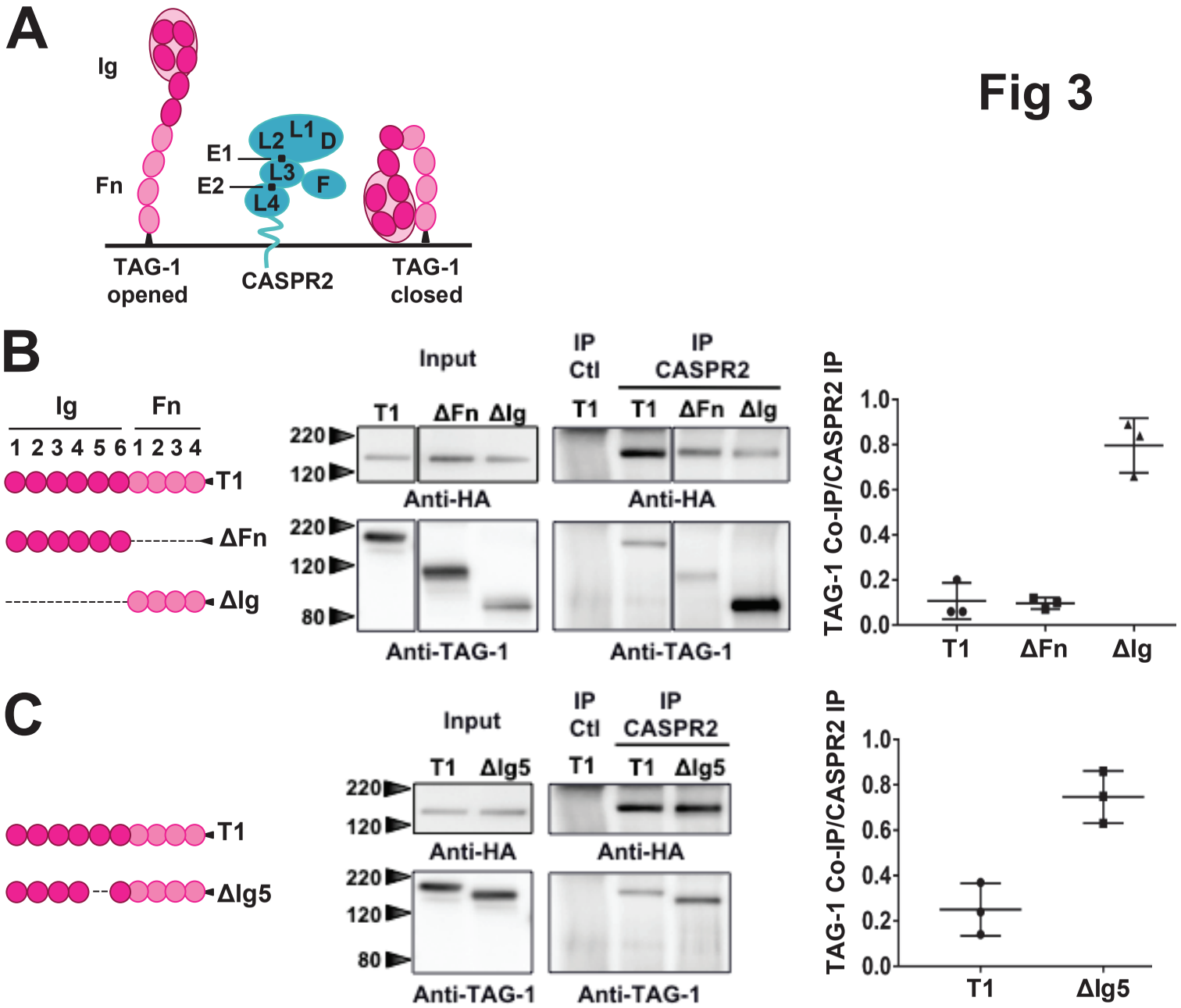
A
Ig
Fn
E1
E2
L1
L2
L3
L4
D
F
TAG-1
opened
CASPR2
TAG-1
closed
B
Ig
Fn
1 2 3 4 5 6 1 2 3 4
T1
ΔFn
Δlg
Input
IP
Ctl
IP
CASPR2
T1
ΔFn
Δlg
220
120
80
Anti-HA
Anti-TAG-1
TAG-1 Co-IP/CASPR2 IP
1.0
0.8
0.6
0.4
0.2
0.0
C
T1
Δlg5
Input
IP
Ctl
IP
CASPR2
T1
Δlg5
220
120
80
Anti-HA
Anti-TAG-1
TAG-1 Co-IP/CASPR2 IP
1.0
0.8
0.6
0.4
0.2
0.0

Fig 4

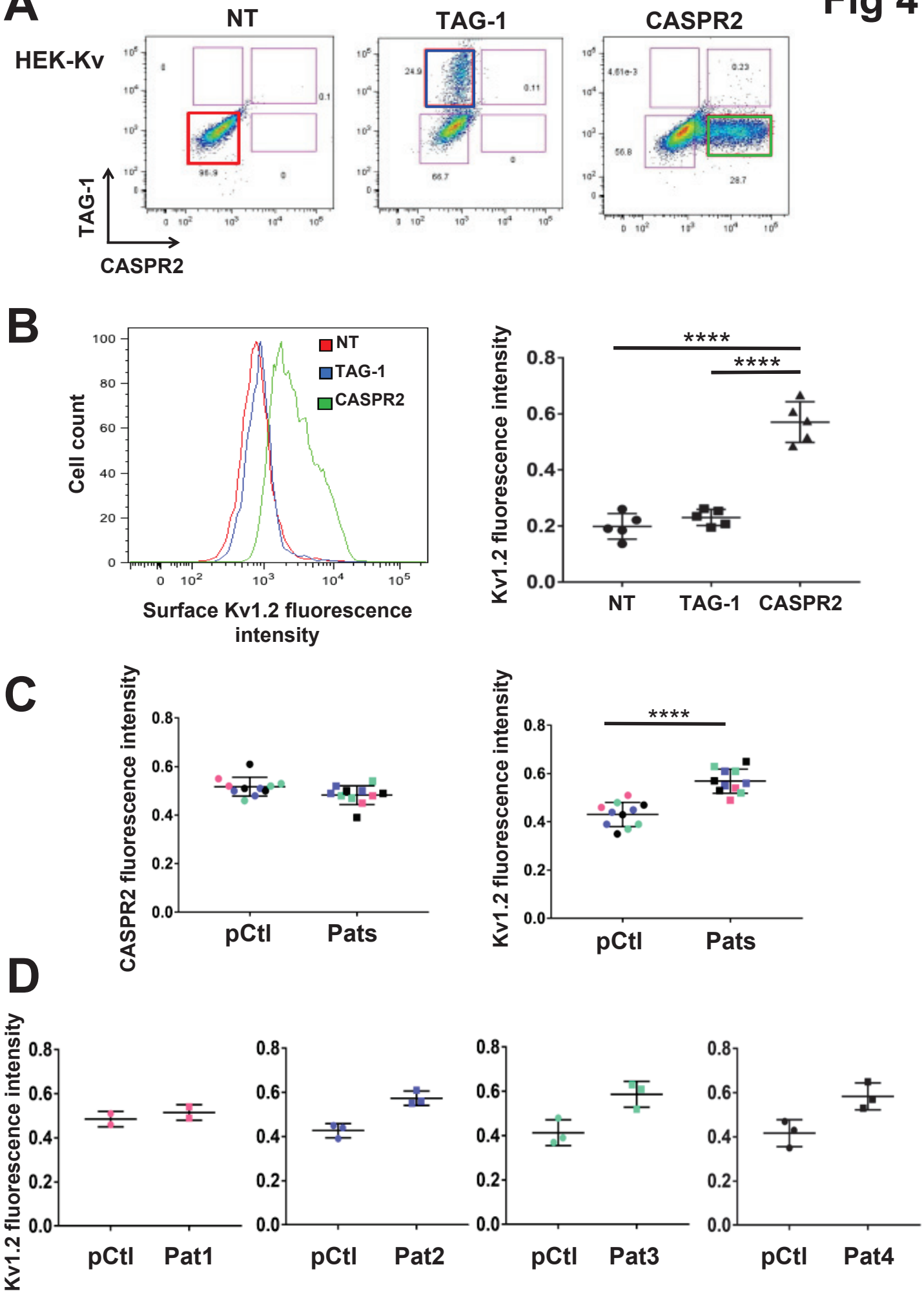
A
NT
TAG-1
CASPR2
HEK-Kv
TAG-1
CASPR2
B
Cell count
Surface Kv1.2 fluorescence intensity
NT
TAG-1
CASPR2
Kv1.2 fluorescence intensity
****
****
NT
TAG-1
CASPR2
C
CASPR2 fluorescence intensity
pCtl
Pats
Kv1.2 fluorescence intensity
****
pCtl
Pats
D
Kv1.2 fluorescence intensity
pCtl
Pat1
pCtl
Pat2
pCtl
Pat3
pCtl
Pat4

Fig 5

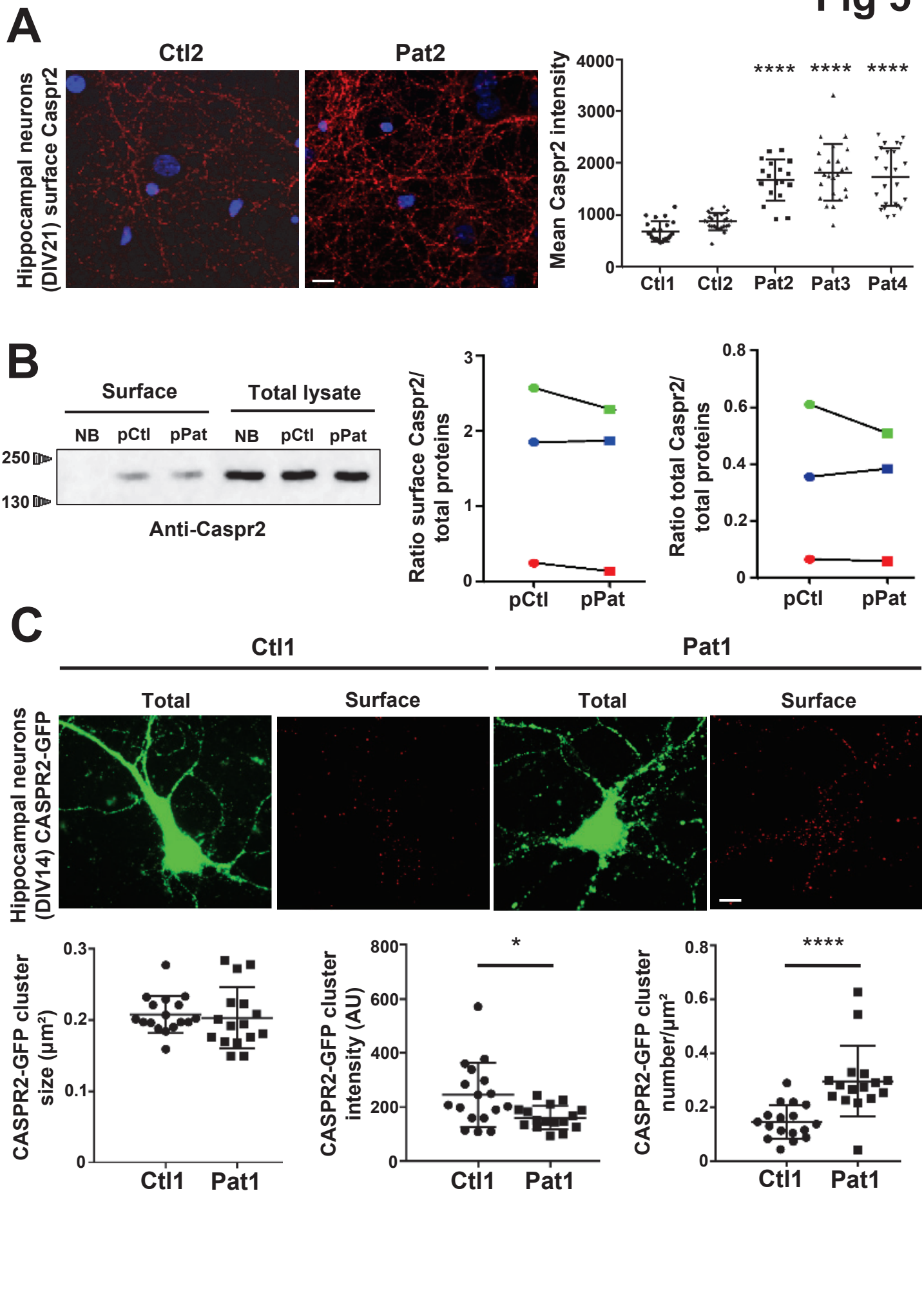
A
Ctl2
Pat2
Hippocampal neurons (DIV21) surface Caspr2
Mean Caspr2 intensity
4000
3000
2000
1000
0
****
****
****
Ctl1
Ctl2
Pat2
Pat3
Pat4
B
Surface
Total lysate
NB
pCtl
pPat
NB
pCtl
pPat
250
130
Anti-Caspr2
Ratio surface Caspr2/ total proteins
3
2
1
0
pCtl
pPat
Ratio total Caspr2/ total proteins
0.8
0.6
0.4
0.2
0
pCtl
pPat
C
Ctl1
Pat1
Total
Surface
Total
Surface
Hippocampal neurons (DIV14) CASPR2-GFP
CASPR2-GFP cluster size (µm²)
0.3
0.2
0.1
0
Ctl1
Pat1
CASPR2-GFP cluster intensity (AU)
800
600
400
200
0
*
Ctl1
Pat1
CASPR2-GFP cluster number/µm²
0.8
0.6
0.4
0.2
0
****
Ctl1
Pat1

Fig 6

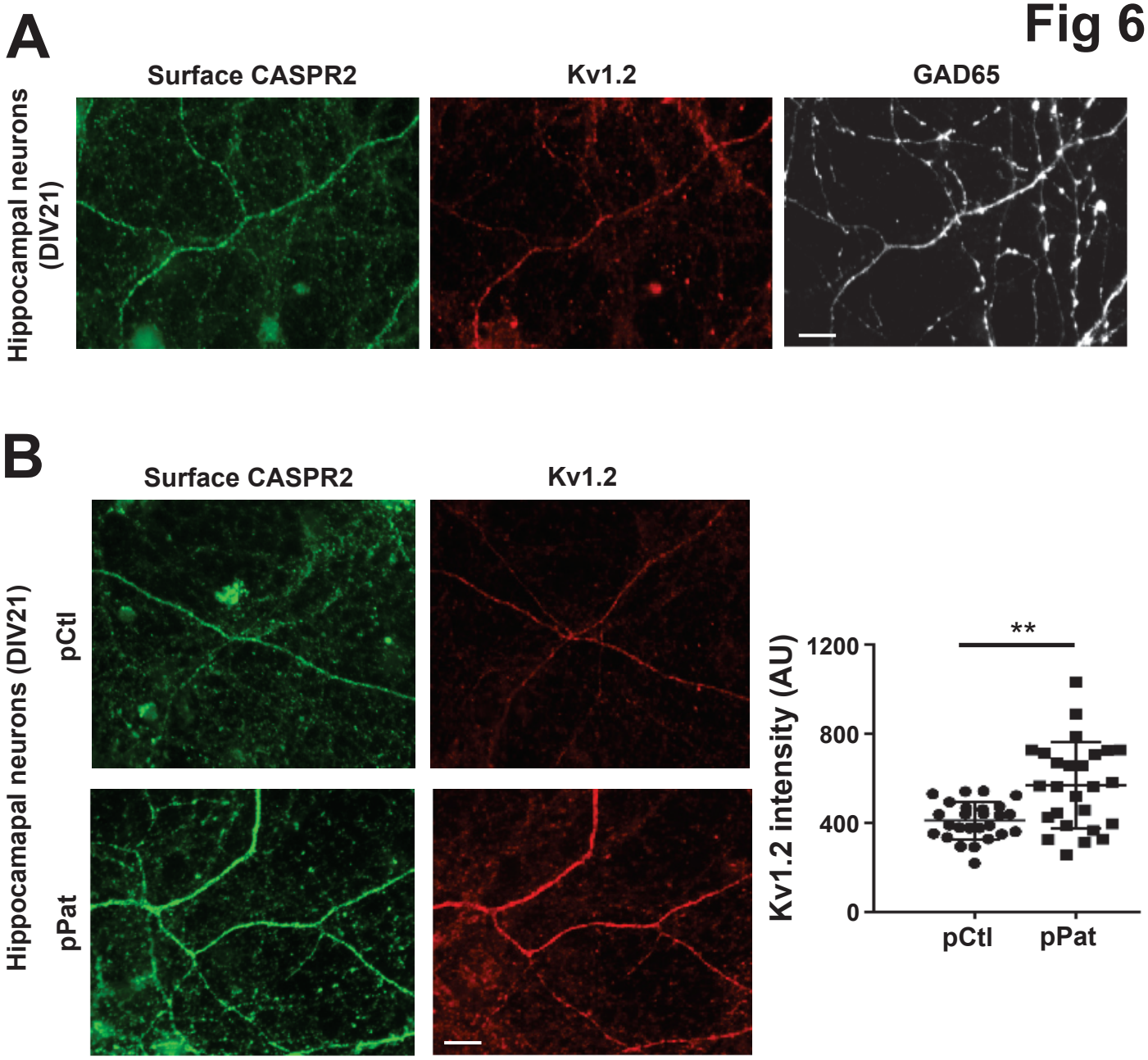
A
Surface CASPR2
Kv1.2
GAD65
Hippocampal neurons (DIV21)
B
Surface CASPR2
Kv1.2
Hippocamapal neurons (DIV21)
pCtl
pPat
Kv1.2 intensity (AU)
1200
800
400
0
**
pCtl
pPat

Fig 7

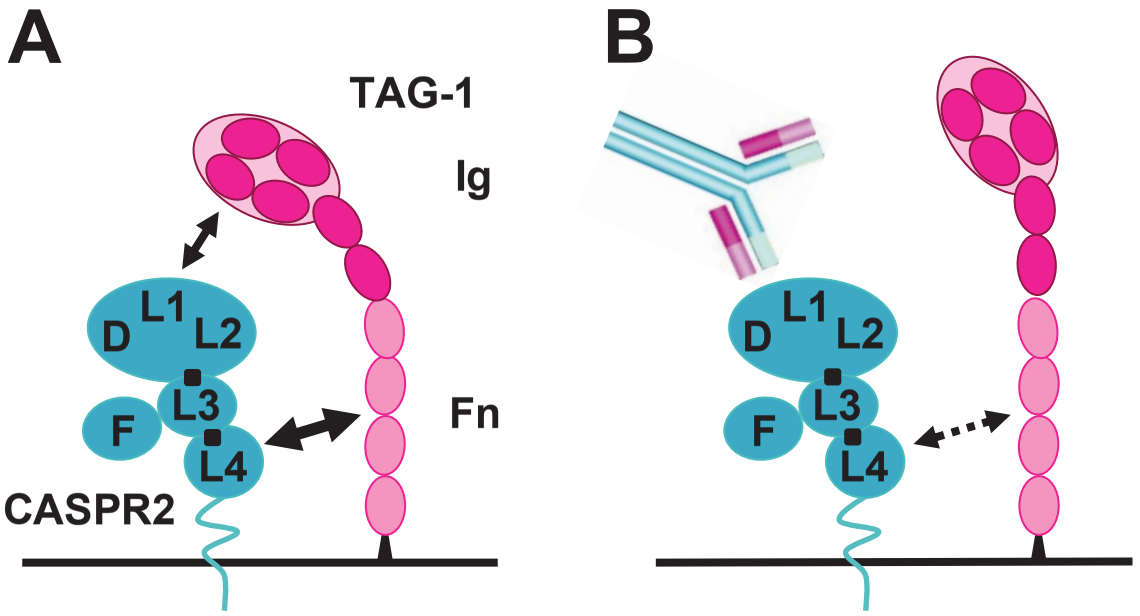

Fig S1

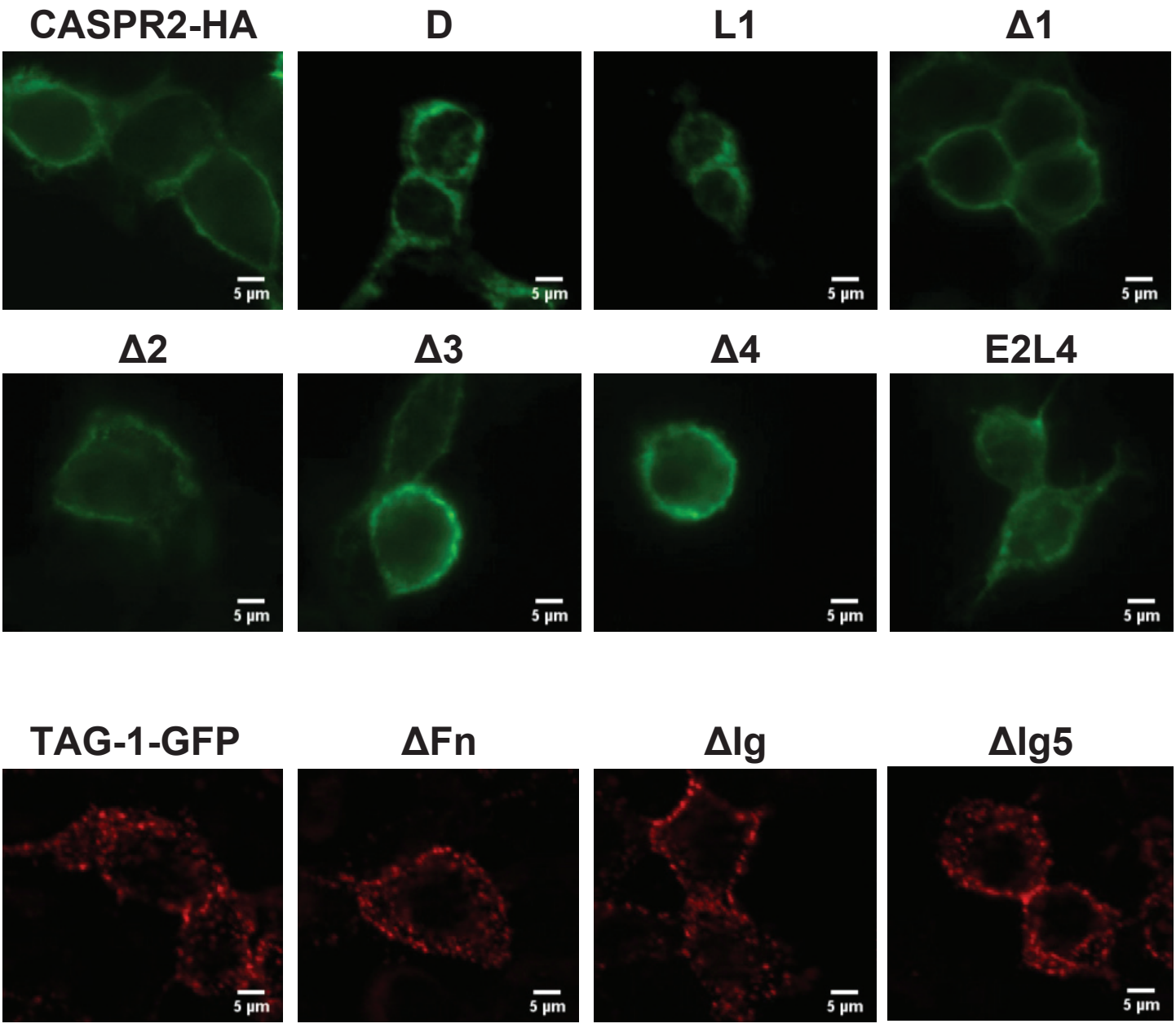

Figure S1: Surface expression of proteins derived from the plasmids used in this study. To control for proper protein surface expression, HEK cells were transfected and stained on live cells for CASPR2, using anti-HA primary Ab/Alexa488 secondary Ab or for TAG-1, using anti-GFP primary Ab/Alexa555 secondary Ab.

B. Etude de l'impact de TAG-1 sur les interactions CASPR2/Kv1.2, travaux complémentaires non publiés en lien avec l'article 3

Aux JXP, CASPR2 et TAG-1 sont toutes deux essentielles pour la localisation des canaux potassiques Kv1, suggérant une interdépendance entre CASPR2, TAG-1 et Kv1. Il a donc été proposé que TAG-1 interagirait en trans avec elle-même et en cis avec CASPR2, qui interagirait avec Kv1.

Afin de connaitre le rôle joué par TAG-1 au sein de ce complexe, nous avons utilisé des cellules HEK co-transfectées avec les canaux Kv1.2 et CASPR2 avec ou sans TAG-1. CASPR2 et les Kv1.2 associés sont ensuite immunoprécipités et révélés par Western Blot (Figure 33A). Les résultats sont présentés sous forme de ratio de la quantité de Kv1.2 co-immunoprécipitée par rapport à la quantité de CASPR2 immunoprécipitée. De façon surprenante, nous avons observé que la co-expression de TAG-1 diminue fortement l'interaction CASPR2/Kv1.2 (Figure 33A). Cette diminution pourrait être due à : (1) une diminution du ratio de Kv1.2/CASPR2 total ; (2) une diminution du pourcentage de cellules co-exprimant CASPR2 et Kv1.2 ; ou (3) une perturbation des interactions CASPR2/Kv1.2 par la transfection du plasmide TAG-1.

Afin de tester la première hypothèse nous avons quantifié la quantité de protéines CASPR2 et Kv1.2 dans les lysats totaux de cellules HEK. Nous avons observé que la co-transfection de TAG-1 diminue l'expression totale de CASPR2 et Kv1.2 sans toutefois modifier le ratio Kv1.2/CASPR2 (Figure 33B). Nous avons testé la seconde hypothèse en utilisant les même cellules transfectées. Nous avons mesuré au FACS le pourcentage de cellules Kv1.2 positives dans la population de cellules CASPR2 positives, et trouvé des pourcentages similaires avec ou sans TAG-1. Enfin, pour tester la troisième hypothèse, nous avons comparé l'impact de la transfection de TAG-1 avec celui de la transfection du plasmide GFP sur l'interaction CASPR2/Kv1.2. Nous avons observé que la co-expression de la GFP induisait également une diminution de l'expression totale de CASPR2 et Kv1.2. Toutefois, contrairement à TAG-1, la co-transfection de la GFP ne perturbe pas les interactions CASPR2/Kv1.2.

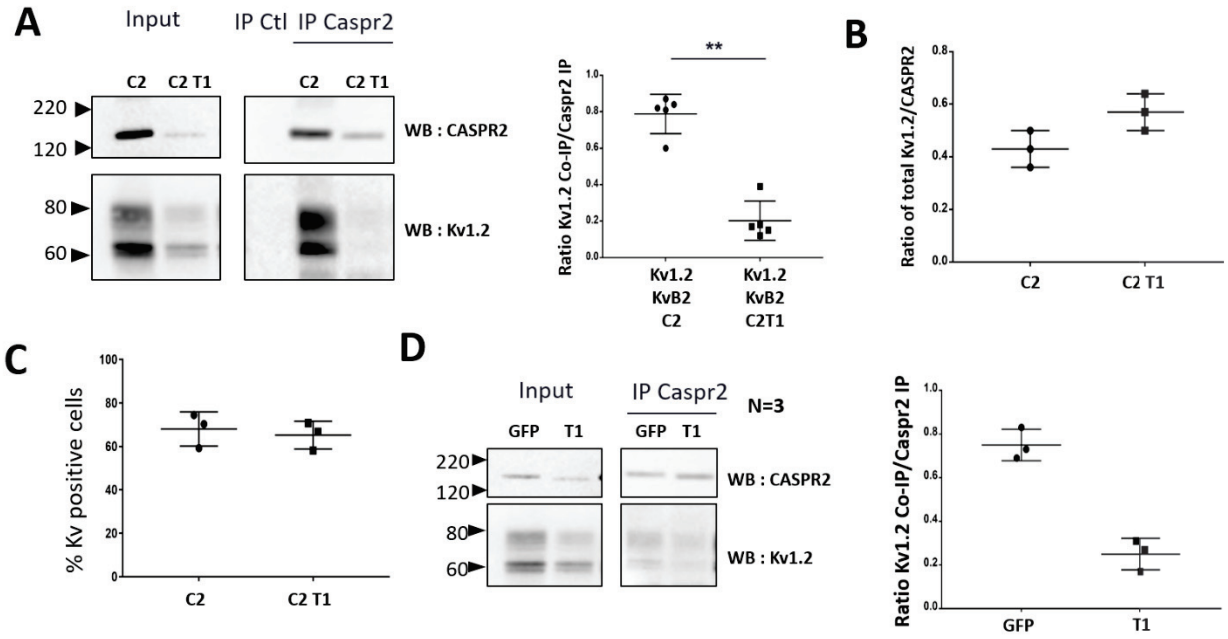

Figure 33 : Impact de TAG-1 sur l'interaction CASPR2/Kv1.2. A) Kv1.2 est transfecté dans les cellules HEK avec CASPR2 (Kv1.2 KvB2 C2) ou CASPR2 et TAG-1 (Kv1.2 KvB2 C2T1). CASPR2 est immunoprécipitée et la quantité de Kv1.2 co-IP est révélée en Western Blot. Le ratio de la quantité de Kv1.2 co-immunoprécipitée sur la quantité de CASPR2 immunoprécipitée est calculé. On observe une diminution significative ($p<0.01$) de la quantité de Kv1.2 co-immunoprécipitée en présence de TAG-1. **B)** La mesure du ratio Kv1.2/CASPR2 dans les lysats totaux ne montre aucune différence en présence de TAG-1. **C)** La mesure en FACS du pourcentage de cellules Kv1.2 positives dans la population de cellules CASPR2 positives ne montre aucune différence en présence de TAG-1. **D)** Afin de tester un impact potentiel de la transfection, Kv1.2 est co-immunoprécipitée avec CASPR2 à partir de cellules co-transfectées avec un plasmide GFP ou un plasmide TAG-1 GFP. Seul le plasmide TAG-1 GFP induit une diminution de la quantité de Kv1.2 co-immunoprécipitée.

Afin de connaitre les mécanismes associés à cette diminution, nous avons utilisé le mutant Δ4 de CASPR2 qui n'interagit que faiblement avec TAG-1. Nous montrons que le mutant Δ4 interagit avec les Kv1.2 et ce, aussi bien que la forme WT de CASPR2. De plus, que ce soit dans les cellules transfectées CASPR2 WT ou CASPR2 Δ4, la co-expression de TAG-1 perturbe l'interaction CASPR2/Kv1.2 (Figure 34). Ainsi, ce n'est vraisemblablement pas en interagissant avec CASPR2 que TAG-1 perturbe l'interaction CASPR2/Kv1.2.

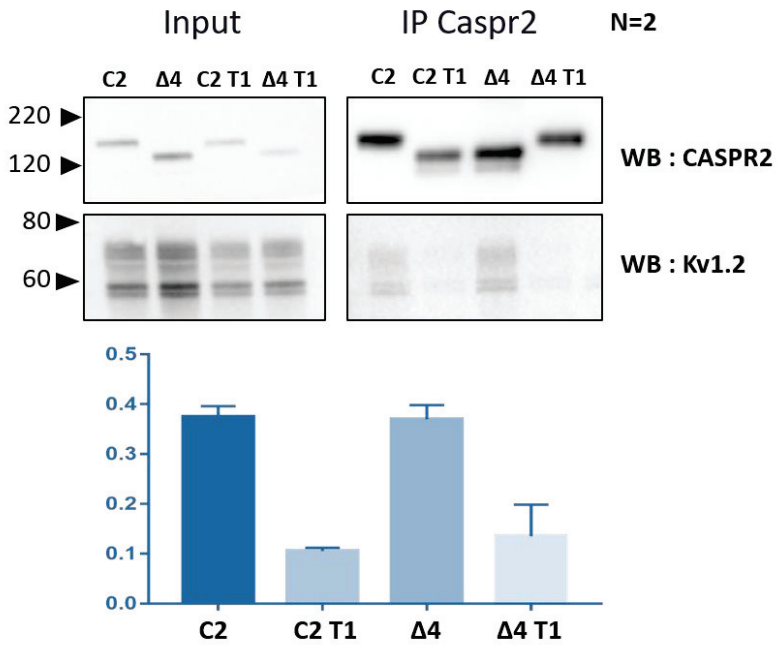

Figure 34 : Capacité du mutant CASPR2 Δ4 à interagir avec Kv1.2. Kv1.2 est transfecté dans les cellules HEK avec CASPR2 (C2) ou CASPR2 Δ4 (Δ4) avec ou sans TAG-1 (C2T1 et Δ4T1). CASPR2 est immunoprécipitée et la quantité de Kv1.2 co-IP est révélée en Western Blot. Le ratio de la quantité de Kv1.2 co-immunoprécipitée sur la quantité de CASPR2 immunoprécipitée est calculé.

Nos résultats sont étonnants puisque les données de la littérature suggèrent que les trois protéines CASPR2/TAG-1/Kv1 forment un complexe (Figure 35A) (Poliak et al., 2003 ; Traka et al., 2003). Nous savons que Kv1.2 exprimé seul dans les neurones en culture est réparti uniformément le long de l'axone (Gu & Gu, 2011) et que la co-expression de TAG-1 induit la formation de clusters Kv1.2 (Gu & Gu, 2011). Ces clusters seraient retenus dans les radeaux lipidiques avec TAG-1 (Gu & Gu, 2011). La perte de l'interaction CASPR2/TAG-1 ne rétablissant pas l'interaction CASPR2/Kv1.2, TAG-1 agirait par d'autres mécanismes, par exemple, en piégeant les canaux Kv1.2 dans les radeaux lipidiques (Figure 35B). D'autres études seront nécessaires afin de mieux comprendre les interactions au sein du complexe CASPR2/TAG-1/Kv1.2.

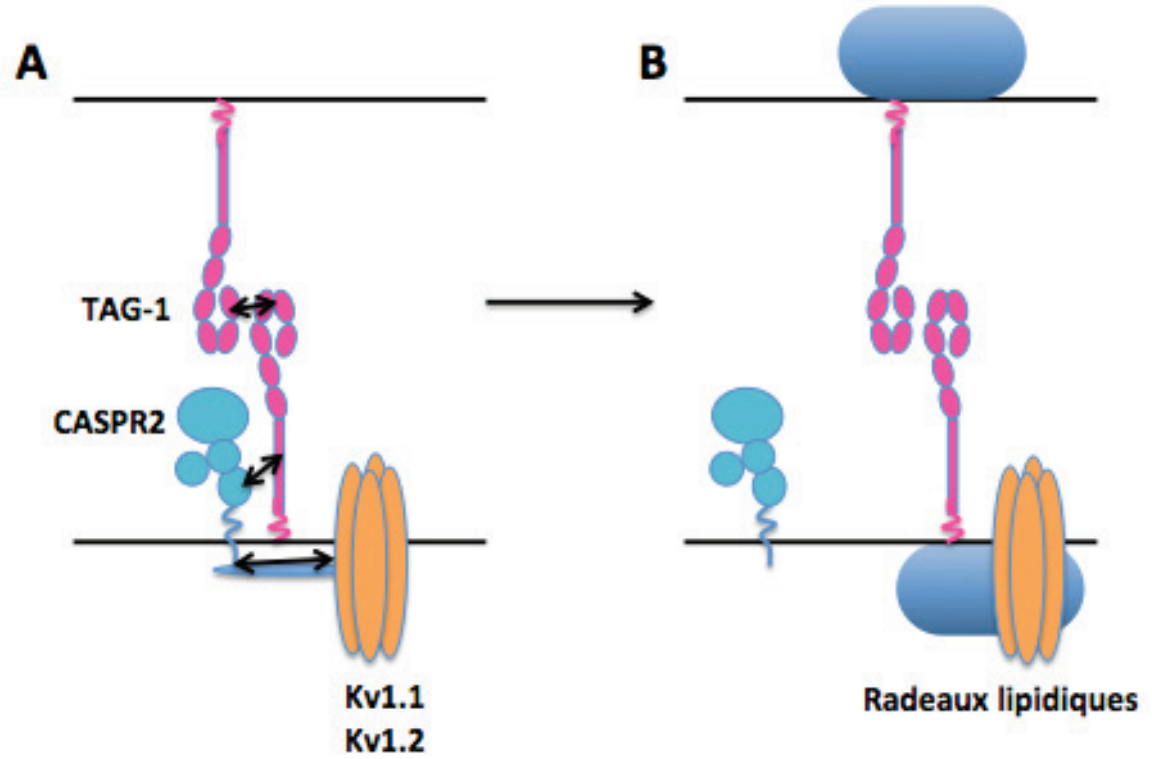

Figure 35 : Modèles d'interactions entre CASPR2, TAG-1, Kv1.1 et Kv1.2. A) Il a été suggéré que TAG-1 interagirait en trans avec elle-même et en cis avec CASPR2. De plus, CASPR2 interagit avec ses domaines intracellulaires avec les Kv1.1 et 1.2. **B)** Nos résultats suggèrent un autre modèle dans lequel TAG-1 empêcherait l'interaction de CASPR2 avec les Kv1.2 en les piégeant dans les radeaux lipidiques.

DISCUSSION

Dans cette partie, j'ai souhaité traiter certains points qui n'apparaissent pas dans les articles mais qui me semblent importants de discuter en prenant en considération l'intégralité des données recueillies pendant ma thèse.

1) Les maladies auto-immunes associées aux anti-CASPR2, des pathologies à part entière ?

Les anticorps anti-CASPR2 ont été identifiés chez des patients présentant une diversité de symptômes : NMT, MoS et EL (Van Sonderen et al., 2016 ; Article 1). Jusqu'à présent, toutes ces pathologies ont été étudiées sous l'intitulé général de maladies auto-immunes à auto-anticorps anti-CASPR2 (Van Sonderen et al., 2016). Notre étude montre que la présence d'anticorps anti-CASPR2 dans le LCR des patients est associée à des atteintes du système limbique mais rarement liée à un cancer. Par opposition, en l'absence d'anticorps dans le LCR, les patients présentent majoritairement des atteintes périphériques souvent associées à un cancer (Article 1). De plus, nous observons que malgré la présence constante d'anticorps anti-CASPR2 dans le sérum, tous les patients ne développent pas de symptômes périphériques. Trois hypothèses sont possibles pour expliquer cette divergence : (1) Un mécanisme lié aux processus d'immunisation. Il a été montré que les tumeurs peuvent être à l'origine de la rupture de tolérance (production d'un anticorps contre un antigène du soi) dans le cas des encéphalites anti-Yo (Small et al., 2018). De la même façon, il serait possible d'envisager que la présence d'une tumeur chez les patients présentant une NMT ou MoS soit à l'origine de la production d'anticorps anti-CASPR2 dans le sérum, contrairement aux EL. (2) La présence ou pas d'un processus inflammatoire. En effet, il a été décrit qu'une inflammation des nerfs périphériques serait nécessaire pour permettre l'accès et l'action des anticorps aux NOR dans le cas des anticorps anti-TAG-1 (Derfuss et al., 2009 ; Howell et al., 2015). Chez les patients ne présentant pas de troubles périphérique, cette dernière ne serait pas présente. (3) Les caractéristiques biologiques des anticorps de patients (titre, sous-classe d'IgG, épitope). Par exemple, il a été montré que seuls les anticorps anti-contactine 1 de la sous-classe IgG4, et non ceux de la sous-classe IgG1, sont capables de pénétrer les paranodes, perturbant ainsi la fonction de leur cible (Manso et al., 2016). Dans le cas des pathologies associées aux anticorps anti-CASPR2, nous avons observé un fort pourcentage de patients présentant des IgG4 chez ceux atteints d'EL comparé à ceux atteints de NMT/MoS. De plus, les titres en anticorps sont bien plus élevés chez les patients présentant

une EL (1/1280 dans le LCR et 1/15360 dans le sérum) que chez les patients NMT/MoS (1/800 dans le sérum). Par ailleurs, les patients présentant un MoS se différencient des patients NMT par la présence de troubles du système nerveux central tels que l'insomnie et des troubles du comportement dont l'origine reste inconnue, compte tenu de l'absence d'anticorps dans le LCR. Il est cependant possible que ces anticorps soient présents mais en faible quantité dans le LCR les rendant indétectables par les méthodes actuelles.

Ces résultats montrent donc l'importance de catégoriser les patients présentant des anti-CASPR2 pour l'étude de leur pathologie.

2) Fonctions des domaines discoidine et laminine G1 ciblés par les anticorps anti-CASPR2 de patient ?

Le fait que les anticorps anti-CASPR2 de patients ciblent systématiquement les domaines discoidine et laminine G1 de CASPR2 (Article 1) suggère que ces domaines sont importants pour la fonction de CASPR2. Par ailleurs, ayant montré que les anticorps anti-CASPR2 de patients perturbent l'interaction CASPR2/TAG-1 (Article 3), les domaines disc-lamG1 pourraient jouer un rôle prépondérant dans ces interactions. Pour ces raisons, nous avons décidé d'étudier l'implication des domaines discoidine et laminine dans les interactions CASPR2/TAG-1.

Le domaine discoidine

Le domaine discoidine est un domaine particulièrement intéressant puisqu'il est la cible de nombreuses mutations identifiées chez des patients présentant des déficiences intellectuelles ou souffrant d'épilepsie (Saint-Martin et al., 2018). De plus, l'étude de sa structure nous a permis d'identifier quatre boucles accessibles ciblées par les anticorps de patient (Article 2). Ces boucles forment une surface relativement plane et particulièrement polarisée sur sa périphérie. De telles caractéristiques pourraient conférer à ce domaine discoidine la capacité d'interagir avec d'autres protéines (Carafoli et al., 2009). Le domaine discoidine n'étant pas impliqué dans les interactions CASPR2/TAG-1 (Article 3), il pourrait interagir avec d'autres protéines extracellulaires. En particulier, les protéines ADAM22 et ADAM23 seraient de bons candidats. Ces dernières font également partie des complexe VGKC et sont connues pour leur rôle dans le rassemblement des récepteurs AMPA à la synapse à l'aide de LGI1. De plus, leur interaction avec CASPR2 par les domaines

extracellulaires a été récemment montrée (Hivert et al., 2018). Il serait donc intéressant d'analyser plus en détail le rôle du domaine discoidine dans cette interaction ainsi que l'impact des anticorps anti-CASPR2.

Les domaines laminine

Nous avons montré que le domaine laminine G1, est capable d'interagir avec TAG-1 contrairement au domaine discoidine. Néanmoins, la délétion des domaines disc-lamG1 n'impacte pas l'interaction de CASPR2 avec TAG-1, suggérant qu'ils ne sont pas nécessaires pour assurer cette fonction (Article 3). En utilisant divers mutants de délétion pour les domaines extracellulaires de CASPR2, nous avons observé que la délétion des domaines EGF2 et laminine G4 induit une forte diminution de l'interaction CASPR2/TAG-1. Inversement, les domaines EGF2 et laminine G4 sont suffisants pour co-immunoprécipiter TAG-1, confirmant ainsi leur rôle majeur dans cette interaction (Article 3). Si on considère les caractéristiques de ces deux domaines chez les neurexines, les domaines EGF sont des domaines de petite taille impactant l'arrangement structural de la protéine (Figure 36A) tandis que les domaines laminine G, volumineux, jouent un rôle dans les interactions des neurexines avec divers partenaires (Figure 36A) (Chen et al., 2011). Il est, par conséquent, plus probable que les interactions de CASPR2 avec TAG-1 soient médiées par le domaine laminine G4. Ainsi, CASPR2 interagirait avec TAG-1 principalement par le domaine laminine G4 tandis que le domaine laminine G1 permettrait de stabiliser cette interaction. Un point intéressant, est que ces deux domaines d'interaction, laminines G1 et G4 de CASPR2, correspondent aux positions des domaines d'interactions, laminines G2 et G6, de la neurexine 1α (Figure 36B) (Revue Reissner et al., 2013). Ces derniers, sont connus pour médier les interactions de la neurexine 1α avec différents partenaires en fonction de son orientation (neuroligine, neurexophiline, cérébelline) (Figure 36A) (Revue Reissner et al., 2013). De la même façon, les domaines laminines G1 et G4 de CASPR2 pourraient interagir avec différents partenaires en fonction de l'orientation de CASPR2.

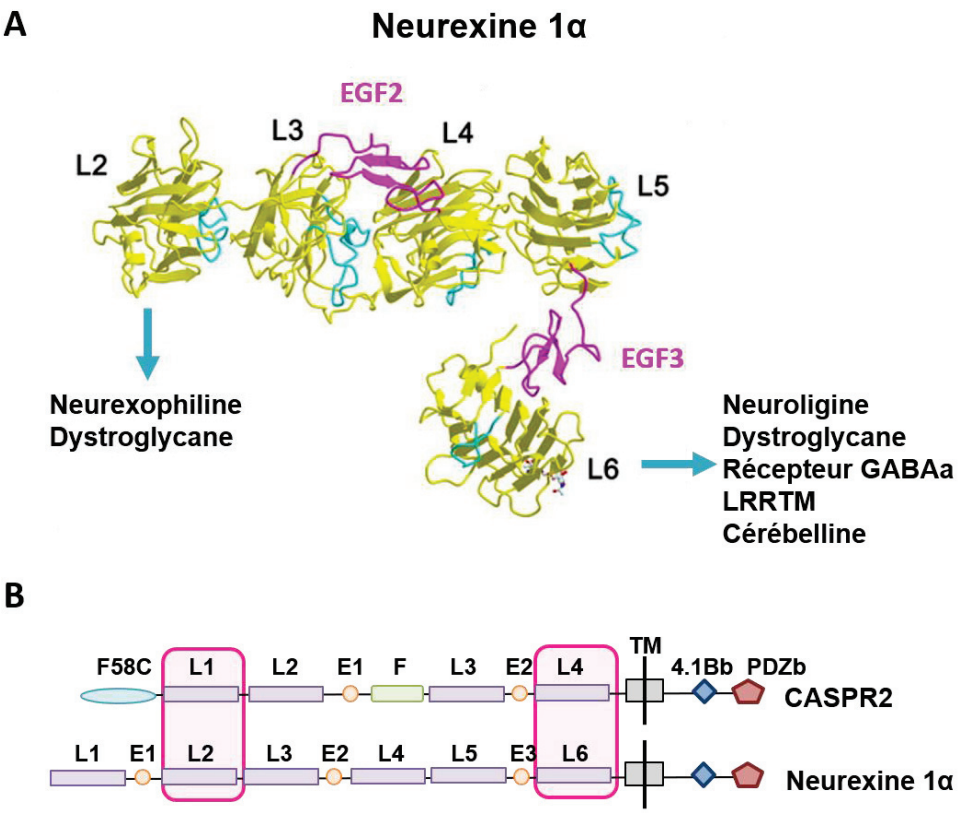

Figure 36 : Structure de la neurexine 1α et domaines d'interaction. A) La neurexine 1α se compose de domaines laminine G (L1-L6) permettant son interaction avec d'autres protéines. Celle-ci est également composée de domaines EGF permettant le maintien de la protéine dans une certaine conformation. **B)** Les domaines d'interaction de CASPR2 avec TAG-1 (L1 et L4) correspondent aux positions des domaines d'interaction de la neurexine 1α (L2 et L6).

Modèles d'interaction CASPR2/TAG-1

Nos résultats montrent que le domaine laminine G4 de CASPR2, est le principal domaine d'interaction avec TAG-1 (Article 3). Par ailleurs, une étude précédente a montré la capacité de TAG-1 à interagir avec CASPR2 par ses domaines Ig mais pas ses domaines Fn (Tzimourakas et al., 2007). Le domaine laminine G4 étant proche de la membrane, l'interaction CASPR2/TAG-1 n'est possible en cis que si les domaines Ig de TAG-1 sont à proximité de la membrane, autrement dit que TAG-1 soit en conformation fermée (Figure 20B). N'ayant pas accès au mutant mimant une conformation fermée, nous avons créé le mutant ΔIg5, qui à l'inverse, est présumé favoriser la conformation ouverte de TAG-1 (Kunz et al., 2002). Dans une telle conformation, nous avons supposé que les domaines Ig de TAG-1 seraient trop éloignés du domaine laminine G4 de CASPR2 pour permettre l'interaction CASPR2/TAG-1 en cis. De façon surprenante, nous avons observé une forte interaction entre CASPR2 et TAG-1 ΔIg5 (Article 3). En testant le mutant TAG-1 ne contenant que les domaines

Ig, nous avons bien retrouvé une interaction avec CASPR2. Cependant, en analysant le mutant TAG-1 ne possédant que les domaines Fn, nous avons également trouvé une forte interaction avec CASPR2 (Article 3). L'augmentation de cette interaction en l'absence des domaines Ig de TAG-1 suggère l'existence de contraintes conformationnelles sur la protéine TAG-1 limitant l'interaction CASPR2/TAG-1. L'augmentation de l'interaction entre CASPR2 et la forme ouverte de TAG-1 permet de supposer que le dépliement de TAG-1 lève cette contrainte conformationnelle, en rendant les domaines Fn potentiellement plus accessibles. Par conséquent, nous proposons un modèle où le domaine laminine G4 de CASPR2 interagirait en cis avec les domaines Fn de TAG-1. Cette interaction serait renforcée par des interactions entre le domaine laminine G1 de CASPR2 et les domaines Ig de TAG-1 (Figure 37A).

En ce qui concerne les interactions CASPR2/TAG-1 en trans, si on considère le positionnement des domaines d'interactions identifiés, les contraintes d'orientation à la membrane et les contraintes conformationnelles, une interaction en trans entre les domaines laminine G4 de CASPR2 et les domaines Fn de TAG-1 semble peu probable. Au contraire, les interactions des domaines Ig de TAG-1 avec les domaines laminine G4 (Figure 37B) ou laminine G1 (Figure 37C) de CASPR2 seraient possibles.

Impact des anti-CASPR2 dans les modèles d'interaction CASPR2/TAG-1

En nous basant sur l'ensemble de ces données, nous pouvons concevoir l'impact des anticorps anti-CASPR2 de patients sur ces modèles d'interactions. Sur les interactions en cis, les anticorps, en ciblant les domaines disc-lamG1, perturberaient l'interaction CASPR2/TAG-1 sans pour autant l'empêcher totalement (Figure 37D). Comme nous avons montré que les anticorps anti-CASPR2 sont capables de diminuer faiblement les interactions CASPR2/TAG-1, cela reste cohérent avec le modèle proposé. Sur les interactions en trans, les anticorps anti-CASPR2 ne perturberaient que faiblement l'interaction CASPR2/TAG-1 par le domaine laminine G4 (Figure 37E) alors que l'interaction par le domaine laminine G1 serait fortement diminuée (Figure 37F).

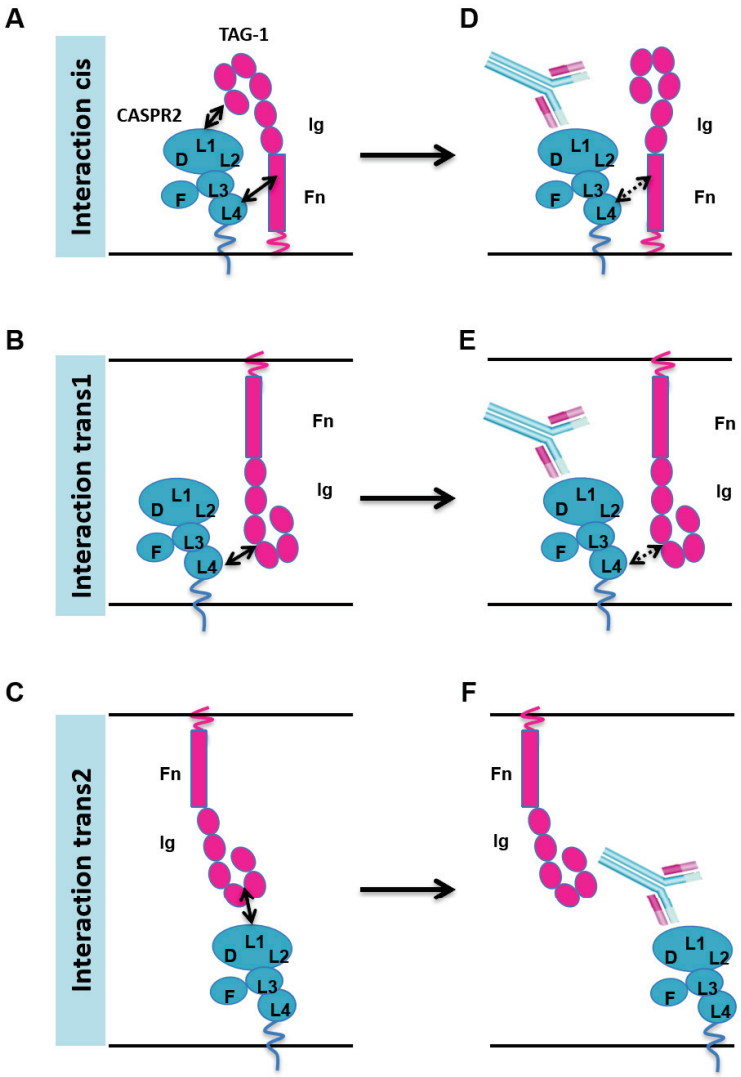

Figure 37 : Modèles d'interaction CASPR2/TAG-1 et impact des anticorps. A) En cis, le domaine laminine G4 de CASPR2 (L4) interagirait avec les domaines fibronectine de TAG-1 (Fn). Cette interaction serait renforcée par une interaction entre le domaine laminine G1 de CASPR2 (L1) et les domaines immunoglobuline de TAG-1 (Ig). En trans, les interactions CASPR2/TAG-1 impliqueraient les domaines Ig de TAG-1 et le domaine L4 **(B)** ou L1 **(C)** de CASPR2. **D)** En cis, les anticorps anti-CASPR2 ciblant les domaines D-L1 de CASPR2 perturberaient faiblement les interactions CASPR2/TAG-1 (les flêches en pointillé indiquent une liaison faible). **E)** En trans, les anticorps anti-CASPR2 pertuberaient faiblement l'interaction de TAG-1 avec le domaine L4 de CASPR2 (les flêches en pointillé indiquent une liaison faible). **F)** En trans, les anticorps anti-CASPR2 perturberaient fortement l'interaction de TAG-1 avec le domaine L1 de CASPR2.

3) CASPR2 régule l'expression de surface des Kv1.2 ?

Nous avons montré que CASPR2 régule de manière dose-dépendante l'expression de surface des canaux Kv1.2 (Article 3). L'interaction entre CASPR2 et Kv1.2 dépendant de leurs domaines cytosoliques (Poliak et al., 1999), il est probable que l'action de CASPR2 sur

l'expression des Kv1.2 passe par des mécanismes de signalisation intracellulaire. Par exemple, il a été montré que la phosphorylation de la tyrosine 458 dans la partie intracellulaire de Kv1.2 perturbe son interaction avec la cortactine et induit son internalisation. Il est donc possible que CASPR2, en empêchant cette phosphorylation, prévienne son endocytose (Figure 38A). De plus, nous avons observé qu'en présence des anticorps anti-CASPR2 de patients, l'expression de surface des Kv1.2 est augmentée dans les cellules HEK et que cette expression ne semble pas dépendre de TAG-1 (Article 3). L'expression de CASPR2 en surface n'étant pas impactée par les anti-CASPR2, il est possible que les anticorps limitent la diffusion de CASPR2 à la surface augmentant les probabilités d'interaction avec les Kv1.2 et favorisant ainsi sa rétention à la surface des cellules (Figure 38B).

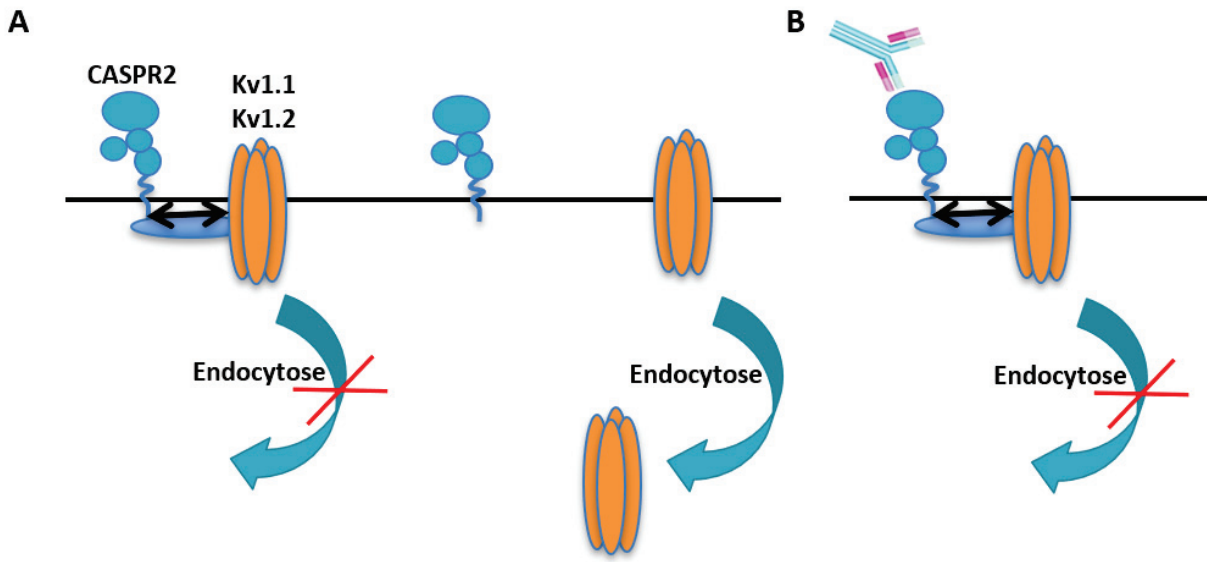

Figure 38 : Modèles de l'effet de CASPR2 et des anti-CASPR2 sur l'expression de surface des Kv1. A) l'interaction de CASPR2 avec les Kv1 pourrait limiter leur endocytose et favoriser leur expression à la surface. **B)** Les anticorps anti-CASPR2 pourraient augmenter les probabilités d'interaction entre CASPR2 et Kv1 et favoriser ainsi leur expression de surface.

CONCLUSION ET PERSPECTIVES

En conclusion, ces travaux ont permis de montrer l'importance d'étudier séparément les patients atteints d'EL ou de NMT et MoS pour comprendre la physiopathologie de ces maladies. La poursuite de ce travail de caractérisation des patients présentant des anticorps anti-CASPR2 permettra d'évaluer les différences cliniques et biologiques entre les patients atteints de NMT et de MoS.

Chez les patients atteints d'EL, nous avons mis en évidence deux mécanismes pathogéniques potentiels des anticorps anti-CASPR2 : (1) la perturbation des interactions CASPR2/TAG-1 et (2) la modulation de l'expression des Kv1.2 en surface. Les anticorps anti-CASPR2 pourront ainsi servir d'outils pour étudier l'impact fonctionnel de ces perturbations sur des cultures de neurones hippocampiques.

En ce qui concerne TAG-1, nos travaux ont permis l'identification de mutants capables d'augmenter (CASPR2 Δ2) ou de diminuer (CASPR2 Δ4) l'interaction CASPR2/TAG-1. Ces mutants constituent également d'excellents outils afin de déterminer l'importance de l'interaction CASPR2/TAG-1 dans la formation et la localisation du complexe CASPR2/TAG-1/Kv1.2. Par ailleurs, nos travaux suggèrent un rôle du domaine laminine G1 ou laminine G4 de CASPR2 dans les interactions CASPR2/TAG-1 en trans. Il serait intéressant de vérifier cette hypothèse en étudiant l'impact du mutant Δ1 (délété des domaines discoidine et laminine G1) ou Δ4 (délété des domaines EGF2 et laminine G4) sur les interactions en trans. Pour ce faire, nous pourrions utiliser un modèle de cellules HEK transfectées séparément avec TAG-1 ou CASPR2 puis mises en contact. L'immunoprécipitation de CASPR2 permettra ensuite d'évaluer la quantité de TAG-1 lui étant associée en trans. En utilisant ce modèle, l'impact des anticorps anti-CASPR2 sur les interactions en trans pourrait également être confirmé.

En ce qui concerne les Kv1.2, nos résultats suggèrent que CASPR2 pourrait limiter l'internalisation des Kv1 par des mécanismes intracellulaires. Il serait intéressant de confirmer cette fonction en utilisant des conditions induisant l'endocytose des Kv1.2 dans les cellules HEK. Dans notre modèle, l'internalisation des Kv1.2 pourrait être induite par l'application de carbachol puis mesurée en FACS. De plus, nous avons montré un impact de TAG-1 sur l'interaction entre CASPR2 et Kv1.2 qui pourrait reposer sur sa capacité à clustériser les Kv1.2 dans les radeaux lipidiques. Il serait donc intéressant de regarder l'impact de la perte des radeaux lipidiques sur l'interaction CASPR2/Kv1.2 en présence de TAG-1.

Nos travaux sur les interactions CASPR2/TAG-1/Kv1.2 et sur les mécanismes d'action des anticorps anti-CASPR2 sont actuellement complétés au sein de l'équipe par des travaux sur des cultures de neurones hippocampiques. Nous étudions la localisation de CASPR2 dans les compartiments neuronaux en microscopie haute résolution ainsi que l'impact des anticorps anti-CASPR2 sur la localisation et l'expression de CASPR2 et Kv1.2. Par ailleurs, nous analysons l'impact des anticorps anti-CASPR2 sur la maturation des synapses excitatrices et inhibitrices ainsi que sur l'excitabilité du réseau en lien avec la fonction des canaux Kv1. Ces travaux permettront à terme, de clarifier le(s) rôle(s) pathogénique(s) des anticorps anti-CASPR2 chez les patients atteints d'EL.

REFERENCES

Abrahams, B.S., Tentler, D., Perederiy, J.V., Oldham, M.C., Coppola, G., & Geschwind, D.H. (2007) Genome-wide analyses of human perisylvian cerebral cortical patterning. *Proc. Natl. Acad. Sci. U.S.A.*, **104**, 17849–17854.

Albert, M.L., Darnell, J.C., Bender, A., Francisco, L.M., Bhardwaj, N., & Darnell, R.B. (1998) Tumor-specific killer cells in paraneoplastic cerebellar degeneration. *Nat. Med.*, **4**, 1321–1324.

Anderson, G.R., Galfin, T., Xu, W., Aoto, J., Malenka, R.C., & Südhof, T.C. (2012) Candidate autism gene screen identifies critical role for cell-adhesion molecule CASPR2 in dendritic arborization and spine development. *Proc. Natl. Acad. Sci. U.S.A.*, **109**, 18120–18125.

Armangue, T., Leypoldt, F., & Dalmau, J. (2014) Autoimmune encephalitis as differential diagnosis of infectious encephalitis. *Curr. Opin. Neurol.*, **27**, 361–368.

Bakkaloglu, B., O'Roak, B.J., Louvi, A., Gupta, A.R., Abelson, J.F., Morgan, T.M., Chawarska, K., Klin, A., Ercan-Sencicek, A.G., Stillman, A.A., Tanriover, G., Abrahams, B.S., Duvall, J.A., Robbins, E.M., Geschwind, D.H., Biederer, T., Gunel, M., Lifton, R.P., & State, M.W. (2008) Molecular cytogenetic analysis and resequencing of contactin associated protein-like 2 in autism spectrum disorders. *Am. J. Hum. Genet.*, **82**, 165–173.

Bataller, L., Wade, D.F., Graus, F., Stacey, H.D., Rosenfeld, M.R., & Dalmau, J. (2004) Antibodies to Zic4 in paraneoplastic neurologic disorders and small-cell lung cancer. *Neurology*, **62**, 778–782.

Bekkers, J.M. & Delaney, A.J. (2001) Modulation of excitability by alpha-dendrotoxin-sensitive potassium channels in neocortical pyramidal neurons. *J. Neurosci.*, **21**, 6553–6560.

Bel, C., Oguievetskaia, K., Pitaval, C., Goutebroze, L., & Faivre-Sarrailh, C. (2009) Axonal targeting of CASPR2 in hippocampal neurons via selective somatodendritic endocytosis. *J. Cell. Sci.*, **122**, 3403–3413.

Belloso, J.M., Bache, I., Guitart, M., Caballin, M.R., Halgren, C., Kirchhoff, M., Ropers, H.-H., Tommerup, N., & Tümer, Z. (2007) Disruption of the CNTNAP2 gene in a t(7;15) translocation family without symptoms of Gilles de la Tourette syndrome. *Eur. J. Hum. Genet.*, **15**, 711–713.

Bien, C.G., Mirzadjanova, Z., Baumgartner, C., Onugoren, M.D., Grunwald, T., Holtkamp, M., Isenmann, S., Kermer, P., Melzer, N., Naumann, M., Riepe, M., Schäbitz, W.R., von Oertzen, T.J., von Podewils, F., Rauschka, H., & May, T.W. (2017) Anti-contactin-associated protein-2 encephalitis: relevance of antibody titres, presentation and outcome. *Eur. J. Neurol.*, **24**, 175–186.

Bien, C.G., Vincent, A., Barnett, M.H., Becker, A.J., Blümcke, I., Graus, F., Jellinger, K.A., Reuss, D.E., Ribalta, T., Schlegel, J., Sutton, I., Lassmann, H., & Bauer, J. (2012) Immunopathology of autoantibody-associated encephalitides: clues for pathogenesis. *Brain*, **135**, 1622–1638.

Blumenthal, D.T., Salzman, K.L., Digre, K.B., Jensen, R.L., Dunson, W.A., & Dalmau, J. (2006) Early pathologic findings and long-term improvement in anti-Ma2-associated encephalitis. *Neurology*, **67**, 146–149.

Boronat, A., Gelfand, J.M., Gresa-Arribas, N., Jeong, H.-Y., Walsh, M., Roberts, K., Martinez-Hernandez, E., Rosenfeld, M.R., Balice-Gordon, R., Graus, F., Rudy, B., & Dalmau, J. (2013) Encephalitis and antibodies to dipeptidyl-peptidase-like protein-6, a subunit of Kv4.2 potassium channels. *Ann. Neurol.*, **73**, 120–128.

Brew, H.M., Gittelman, J.X., Silverstein, R.S., Hanks, T.D., Demas, V.P., Robinson, L.C., Robbins, C.A., McKee-Johnson, J., Chiu, S.Y., Messing, A., & Tempel, B.L. (2007) Seizures and reduced life span in mice lacking the potassium channel subunit Kv1.2, but hypoexcitability and enlarged Kv1 currents in auditory neurons. *J. Neurophysiol.*, **98**, 1501–1525.

Bridi, M.S., Park, S.M., & Huang, S. (2017) Developmental Disruption of GABAAR-Meditated Inhibition in Cntnap2 KO Mice. *eNeuro*, **4**.

Brimberg, L., Mader, S., Jeganathan, V., Berlin, R., Coleman, T.R., Gregersen, P.K., Huerta, P.T., Volpe, B.T., & Diamond, B. (2016) CASPR2-reactive antibody cloned from a mother of an ASD child mediates an ASD-like phenotype in mice. *Mol. Psychiatry*, **21**, 1663–1671.

Brimberg, L., Sadiq, A., Gregersen, P.K., & Diamond, B. (2013) Brain-reactive IgG correlates with autoimmunity in mothers of a child with an autism spectrum disorder. *Mol. Psychiatry*, **18**, 1171–1177.

Buchstaller, A., Kunz, S., Berger, P., Kunz, B., Ziegler, U., Rader, C., & Sonderegger, P. (1996) Cell adhesion molecules NgCAM and axonin-1 form heterodimers in the neuronal membrane and cooperate in neurite outgrowth promotion. *J. Cell Biol.*, **135**, 1593–1607.

Buckley, C., Oger, J., Clover, L., Tüzün, E., Carpenter, K., Jackson, M., & Vincent, A. (2001) Potassium channel antibodies in two patients with reversible limbic encephalitis. *Ann. Neurol.*, **50**, 73–78.

Buttermore, E.D., Dupree, J.L., Cheng, J., An, X., Tessarollo, L., & Bhat, M.A. (2011) The cytoskeletal adaptor protein band 4.1B is required for the maintenance of paranodal axoglial septate junctions in myelinated axons. *J. Neurosci.*, **31**, 8013–8024.

Canali, G., Garcia, M., Hivert, B., Pinatel, D., Goullancourt, A., Oguievetskaia, K., Saint-Martin, M., Girault, J.-A., Faivre-Sarrailh, C., & Goutebroze, L. (2018) Genetic variants in autism-related CNTNAP2 impair axonal growth of cortical neurons. *Hum Mol Genet*, **27**, 1941–1954.

Carafoli, F., Bihan, D., Stathopoulos, S., Konitsiotis, A.D., Kvansakul, M., Farndale, R.W., Leitinger, B., & Hohenester, E. (2009) Crystallographic insight into collagen recognition by discoidin domain receptor 2. *Structure*, **17**, 1573–1581.

Chen, F., Venugopal, V., Murray, B., & Rudenko, G. (2011) The structure of neurexin 1α reveals features promoting a role as synaptic organizer. *Structure*, **19**, 779–789.

Chen, N., Koopmans, F., Gordon, A., Paliukhovich, I., Klaassen, R.V., van der Schors, R.C., Peles, E., Verhage, M., Smit, A.B., & Li, K.W. (2015) Interaction proteomics of canonical CASPR2 (CNTNAP2) reveals the presence of two CASPR2 isoforms with overlapping interactomes. *Biochim. Biophys. Acta*, **1854**, 827–833.

Cifuentes-Diaz, C., Chareyre, F., Garcia, M., Devaux, J., Carnaud, M., Levasseur, G., Niwa-Kawakita, M., Harroch, S., Girault, J.-A., Giovannini, M., & Goutebroze, L. (2011) Protein 4.1B contributes to the organization of peripheral myelinated axons. *PLoS ONE*, **6**, e25043.

Coutinho, E., Menassa, D.A., Jacobson, L., West, S.J., Domingos, J., Moloney, T.C., Lang, B., Harrison, P.J., Bennett, D.L.H., Bannerman, D., & Vincent, A. (2017) Persistent microglial activation and synaptic loss with behavioral abnormalities in mouse offspring exposed to CASPR2-antibodies in utero. *Acta Neuropathol.*, **134**, 567–583.

D'Adamo, M.C., Catacuzzeno, L., Di Giovanni, G., Franciolini, F., & Pessia, M. (2013) K(+) channelepsy: progress in the neurobiology of potassium channels and epilepsy. *Front Cell Neurosci*, **7**, 134.

Dale, R.C., Merheb, V., Pillai, S., Wang, D., Cantrill, L., Murphy, T.K., Ben-Pazi, H., Varadkar, S., Aumann, T.D., Horne, M.K., Church, A.J., Fath, T., & Brilot, F. (2012) Antibodies to surface dopamine-2 receptor in autoimmune movement and psychiatric disorders. *Brain*, **135**, 3453–3468.

Dalmau, J., Geis, C., & Graus, F. (2017) Autoantibodies to Synaptic Receptors and Neuronal Cell Surface Proteins in Autoimmune Diseases of the Central Nervous System. *Physiol. Rev.*, **97**, 839–887.

Dalmau, J., Gleichman, A.J., Hughes, E.G., Rossi, J.E., Peng, X., Lai, M., Dessain, S.K., Rosenfeld, M.R., Balice-Gordon, R., & Lynch, D.R. (2008) Anti-NMDA-receptor encephalitis: case series and analysis of the effects of antibodies. *Lancet Neurol*, **7**, 1091–1098.

Dalmau, J. & Graus, F. (2018) Antibody-Mediated Encephalitis. *N. Engl. J. Med.*, **378**, 840–851.

Dalmau, J., Graus, F., Villarejo, A., Posner, J.B., Blumenthal, D., Thiessen, B., Saiz, A., Meneses, P., & Rosenfeld, M.R. (2004) Clinical analysis of anti-Ma2-associated encephalitis. *Brain*, **127**, 1831–1844.

Dalmau, J. & Rosenfeld, M.R. (2008) Paraneoplastic syndromes of the CNS. *Lancet Neurol*, **7**, 327–340.

Dalmau, J., Tüzün, E., Wu, H., Masjuan, J., Rossi, J.E., Voloschin, A., Baehring, J.M., Shimazaki, H., Koide, R., King, D., Mason, W., Sansing, L.H., Dichter, M.A., Rosenfeld, M.R., & Lynch, D.R. (2007) Paraneoplastic anti-N-methyl-D-aspartate receptor encephalitis associated with ovarian teratoma. *Ann. Neurol.*, **61**, 25–36.

Dalton, P., Deacon, R., Blamire, A., Pike, M., McKinlay, I., Stein, J., Styles, P., & Vincent, A. (2003) Maternal neuronal antibodies associated with autism and a language disorder. *Ann. Neurol.*, **53**, 533–537.

Dawes, J.M., Weir, G.A., Middleton, S.J., Patel, R., Chisholm, K.I., Pettingill, P., Peck, L.J., Sheridan, J., Shakir, A., Jacobson, L., Gutierrez-Mecinas, M., Galino, J., Walcher, J., Kühnemund, J., Kuehn, H., Sanna, M.D., Lang, B., Clark, A.J., Themistocleous, A.C., Iwagaki, N., West, S.J., Werynska, K., Carroll, L., Trendafilova, T., Menassa, D.A., Giannoccaro, M.P., Coutinho, E., Cervellini, I., Tewari, D., Buckley, C., Leite, M.I., Wildner, H., Zeilhofer, H.U., Peles, E., Todd, A.J., McMahon, S.B., Dickenson, A.H., Lewin, G.R., Vincent, A., & Bennett, D.L. (2018) Immune or Genetic-Mediated Disruption of CASPR2 Causes Pain Hypersensitivity Due to Enhanced Primary Afferent Excitability. *Neuron*, **97**, 806-822.e10.

De Camilli, P., Thomas, A., Cofiell, R., Folli, F., Lichte, B., Piccolo, G., Meinck, H.M., Austoni, M., Fassetta, G., Bottazzo, G., Bates, D., Cartlidge, N., Solimena, M., & Kilimann, M.W. (1993) The synaptic vesicle-associated protein amphiphysin is the 128-kD autoantigen of Stiff-Man syndrome with breast cancer. *J. Exp. Med.*, **178**, 2219–2223.

de Graaff, E., Maat, P., Hulsenboom, E., van den Berg, R., van den Bent, M., Demmers, J., Lugtenburg, P.J., Hoogenraad, C.C., & Sillevis Smitt, P. (2012) Identification of delta/notch-like epidermal growth factor-related receptor as the Tr antigen in paraneoplastic cerebellar degeneration. *Ann. Neurol.*, **71**, 815–824.

DeLuca, I., Blachère, N.E., Santomasso, B., & Darnell, R.B. (2009) Tolerance to the neuron-specific paraneoplastic HuD antigen. *PLoS ONE*, **4**, e5739.

Denaxa, M., Chan, C.-H., Schachner, M., Parnavelas, J.G., & Karagogeos, D. (2001) The adhesion molecule TAG-1 mediates the migration of cortical interneurons from the ganglionic eminence along the corticofugal fiber system. *Development*, **128**, 4635–4644.

Denisenko-Nehrbass, N., Oguievetskaia, K., Goutebroze, L., Galvez, T., Yamakawa, H., Ohara, O., Carnaud, M., & Girault, J.-A. (2003) Protein 4.1B associates with both Caspr/paranodin and CASPR2 at paranodes and juxtaparanodes of myelinated fibres. *Eur. J. Neurosci.*, **17**, 411–416.

Derfuss, T., Parikh, K., Velhin, S., Braun, M., Mathey, E., Krumbholz, M., Kümpfel, T., Moldenhauer, A., Rader, C., Sonderegger, P., Pöllmann, W., Tiefenthaller, C., Bauer, J., Lassmann, H., Wekerle, H., Karagogeos, D., Hohlfeld, R., Linington, C., & Meinl, E. (2009a) Contactin-2/TAG-1-directed autoimmunity is identified in multiple sclerosis patients and mediates gray matter pathology in animals. *Proc. Natl. Acad. Sci. U.S.A.*, **106**, 8302–8307.

Derfuss, T., Parikh, K., Velhin, S., Braun, M., Mathey, E., Krumbholz, M., Kümpfel, T., Moldenhauer, A., Rader, C., Sonderegger, P., Pöllmann, W., Tiefenthaller, C., Bauer, J., Lassmann, H., Wekerle, H., Karagogeos, D., Hohlfeld, R., Linington, C., & Meinl, E. (2009b) Contactin-2/TAG-1-directed autoimmunity is identified in multiple sclerosis patients and mediates gray matter pathology in animals. *Proc. Natl. Acad. Sci. U.S.A.*, **106**, 8302–8307.

Devaux, J., Gola, M., Jacquet, G., & Crest, M. (2002) Effects of K+ channel blockers on developing rat myelinated CNS axons: identification of four types of K+ channels. *J. Neurophysiol.*, **87**, 1376–1385.

Diamond, B., Huerta, P.T., Mina-Osorio, P., Kowal, C., & Volpe, B.T. (2009) Losing your nerves? Maybe it's the antibodies. *Nat. Rev. Immunol.*, **9**, 449–456.

Didelot, A. & Honnorat, J. (2009) Update on paraneoplastic neurological syndromes. *Curr Opin Oncol*, **21**, 566–572.

Dodd, J., Morton, S.B., Karagogeos, D., Yamamoto, M., & Jessell, T.M. (1988) Spatial regulation of axonal glycoprotein expression on subsets of embryonic spinal neurons. *Neuron*, **1**, 105–116.

Duflocq, A., Chareyre, F., Giovannini, M., Couraud, F., & Davenne, M. (2011) Characterization of the axon initial segment (AIS) of motor neurons and identification of a para-AIS and a juxtapara-AIS, organized by protein 4.1B. *BMC Biol.*, **9**, 66.

Einheber, S., Meng, X., Rubin, M., Lam, I., Mohandas, N., An, X., Shrager, P., Kissil, J., Maurel, P., & Salzer, J.L. (2013) The 4.1B cytoskeletal protein regulates the domain organization and sheath thickness of myelinated axons. *Glia*, **61**, 240–253.

Falivelli, G., De Jaco, A., Favaloro, F.L., Kim, H., Wilson, J., Dubi, N., Ellisman, M.H., Abrahams, B.S., Taylor, P., & Comoletti, D. (2012) Inherited genetic variants in autism-related CNTNAP2 show perturbed trafficking and ATF6 activation. *Hum. Mol. Genet.*, **21**, 4761–4773.

Flaherty, E., Deranieh, R.M., Artimovich, E., Lee, I.S., Siegel, A.J., Levy, D.L., Nestor, M.W., & Brennand, K.J. (2017) Patient-derived hiPSC neurons with heterozygous CNTNAP2 deletions display altered neuronal gene expression and network activity. *NPJ Schizophr*, **3**, 35.

Freigang, J., Proba, K., Leder, L., Diederichs, K., Sonderegger, P., & Welte, W. (2000) The Crystal Structure of the Ligand Binding Module of Axonin-1/TAG-1 Suggests a Zipper Mechanism for Neural Cell Adhesion. *Cell*, **101**, 425–433.

Fukamauchi, F., Aihara, O., Wang, Y.J., Akasaka, K., Takeda, Y., Horie, M., Kawano, H., Sudo, K., Asano, M., Watanabe, K., & Iwakura, Y. (2001) TAG-1-deficient mice have marked elevation of adenosine A1 receptors in the hippocampus. *Biochem. Biophys. Res. Commun.*, **281**, 220–226.

Furley, A.J., Morton, S.B., Manalo, D., Karagogeos, D., Dodd, J., & Jessell, T.M. (1990) The axonal glycoprotein TAG-1 is an immunoglobulin superfamily member with neurite outgrowth-promoting activity. *Cell*, **61**, 157–170.

Gautam, V., D'Avanzo, C., Hebisch, M., Kovacs, D.M., & Kim, D.Y. (2014) BACE1 activity regulates cell surface contactin-2 levels. *Mol Neurodegener*, **9**, 4.

Gdalyahu, A., Lazaro, M., Penagarikano, O., Golshani, P., Trachtenberg, J.T., Geschwind, D.H., & Gescwind, D.H. (2015) The Autism Related Protein Contactin-Associated Protein-Like 2 (CNTNAP2) Stabilizes New Spines: An In Vivo Mouse Study. *PLoS ONE*, **10**, e0125633.

Geiger, J.R. & Jonas, P. (2000) Dynamic control of presynaptic Ca(2+) inflow by fast-inactivating K(+) channels in hippocampal mossy fiber boutons. *Neuron*, **28**, 927–939.

Gelpi, E., Höftberger, R., Graus, F., Ling, H., Holton, J.L., Dawson, T., Popovic, M., Pretnar-Oblak, J., Högl, B., Schmutzhard, E., Poewe, W., Ricken, G., Santamaria, J., Dalmau, J., Budka, H., Revesz, T., & Kovacs, G.G. (2016) Neuropathological criteria of anti-IgLON5-related tauopathy. *Acta Neuropathol.*, **132**, 531–543.

Gokce, O. & Südhof, T.C. (2013) Membrane-tethered monomeric neurexin LNS-domain triggers synapse formation. *J. Neurosci.*, **33**, 14617–14628.

Gordon, A., Salomon, D., Barak, N., Pen, Y., Tsoory, M., Kimchi, T., & Peles, E. (2016) Expression of Cntnap2 (CASPR2) in multiple levels of sensory systems. *Mol. Cell. Neurosci.*, **70**, 42–53.

Gövert, F., Witt, K., Erro, R., Hellriegel, H., Paschen, S., Martinez-Hernandez, E., Wandinger, K.-P., Deuschl, G., Dalmau, J., & Leypoldt, F. (2016) Orthostatic myoclonus associated with CASPR2 antibodies. *Neurology*, **86**, 1353–1355.

Graf, E.R., Zhang, X., Jin, S.-X., Linhoff, M.W., & Craig, A.M. (2004) Neurexins induce differentiation of GABA and glutamate postsynaptic specializations via neuroligins. *Cell*, **119**, 1013–1026.

Graus, F., Elkon, K.B., Lloberes, P., Ribalta, T., Torres, A., Ussetti, P., Valls, J., Obach, J., & Agusti-Vidal, A. (1987) Neuronal antinuclear antibody (anti-Hu) in paraneoplastic encephalomyelitis simulating acute polyneuritis. *Acta Neurol. Scand.*, **75**, 249–252.

Gresa-Arribas, N., Planagumà, J., Petit-Pedrol, M., Kawachi, I., Katada, S., Glaser, C.A., Simabukuro, M.M., Armangué, T., Martínez-Hernández, E., Graus, F., & Dalmau, J. (2016) Human neurexin-3α antibodies associate with encephalitis and alter synapse development. *Neurology*, **86**, 2235–2242.

Gresa-Arribas, N., Titulaer, M.J., Torrents, A., Aguilar, E., McCracken, L., Leypoldt, F., Gleichman, A.J., Balice-Gordon, R., Rosenfeld, M.R., Lynch, D., Graus, F., & Dalmau, J. (2014) Antibody titres at diagnosis and during follow-up of anti-NMDA receptor encephalitis: a retrospective study. *Lancet Neurol*, **13**, 167–177.

Grizel, A.V., Glukhov, G.S., & Sokolova, O.S. (2014) Mechanisms of activation of voltage-gated potassium channels. *Acta Naturae*, **6**, 10–26.

Gu, C. & Gu, Y. (2011) Clustering and activity tuning of Kv1 channels in myelinated hippocampal axons. *J. Biol. Chem.*, **286**, 25835–25847.

Harel, R. & Futerman, A.H. (1996) A newly-synthesized GPI-anchored protein, TAG-1/axonin-1, is inserted into axonal membranes along the entire length of the axon and not exclusively at the growth cone. *Brain Res.*, **712**, 345–348.

High, B., Cole, A.A., Chen, X., & Reese, T.S. (2015) Electron microscopic tomography reveals discrete transcleft elements at excitatory and inhibitory synapses. *Front Synaptic Neurosci*, **7**, 9.

Hivert, B., Marien, L., Agbam, K.N., & Faivre-Sarrailh, C. (2018) ADAM22 and ADAM23 modulate the targeting of the Kv1 channel-associated protein LGI1 to the axon initial segment. *bioRxiv*, 311365.

Honnorat, J., Cartalat-Carel, S., Ricard, D., Camdessanche, J.P., Carpentier, A.F., Rogemond, V., Chapuis, F., Aguera, M., Decullier, E., Duchemin, A.M., Graus, F., & Antoine, J.C. (2009) Onco-neural antibodies and tumour type determine survival and neurological symptoms in paraneoplastic neurological syndromes with Hu or CV2/CRMP5 antibodies. *J. Neurol. Neurosurg. Psychiatry*, **80**, 412–416.

Honnorat, J., Saiz, A., Giometto, B., Vincent, A., Brieva, L., de Andres, C., Maestre, J., Fabien, N., Vighetto, A., Casamitjana, R., Thivolet, C., Tavolato, B., Antoine, J., Trouillas, P., & Graus, F. (2001) Cerebellar ataxia with anti-glutamic acid decarboxylase antibodies: study of 14 patients. *Arch. Neurol.*, **58**, 225–230.

Horresh, I., Bar, V., Kissil, J.L., & Peles, E. (2010) Organization of myelinated axons by Caspr and CASPR2 requires the cytoskeletal adapter protein 4.1B. *J. Neurosci.*, **30**, 2480–2489.

Horresh, I., Poliak, S., Grant, S., Bredt, D., Rasband, M.N., & Peles, E. (2008) Multiple molecular interactions determine the clustering of CASPR2 and Kv1 channels in myelinated axons. *J. Neurosci.*, **28**, 14213–14222.

Howell, O.W., Schulz-Trieglaff, E.K., Carassiti, D., Gentleman, S.M., Nicholas, R., Roncaroli, F., & Reynolds, R. (2015) Extensive grey matter pathology in the cerebellum in multiple sclerosis is linked to inflammation in the subarachnoid space. *Neuropathol. Appl. Neurobiol.*, **41**, 798–813.

Høyer, H., Braathen, G.J., Eek, A.K., Nordang, G.B.N., Skjelbred, C.F., & Russell, M.B. (2015) Copy number variations in a population-based study of Charcot-Marie-Tooth disease. *Biomed Res Int*, **2015**, 960404.

Huang, A.Y., Yu, D., Davis, L.K., Sul, J.H., Tsetsos, F., Ramensky, V., Zelaya, I., Ramos, E.M., Osiecki, L., Chen, J.A., McGrath, L.M., Illmann, C., Sandor, P., Barr, C.L., Grados, M., Singer, H.S., Nöthen, M.M., Hebebrand, J., King, R.A., Dion, Y., Rouleau, G., Budman, C.L., Depienne, C., Worbe, Y., Hartmann, A., Müller-Vahl, K.R., Stuhrmann, M., Aschauer, H., Stamenkovic, M., Schloegelhofer, M., Konstantinidis, A., Lyon, G.J., McMahon, W.M., Barta, C., Tarnok, Z., Nagy, P., Batterson, J.R., Rizzo, R., Cath, D.C., Wolanczyk, T., Berlin, C., Malaty, I.A., Okun, M.S., Woods, D.W., Rees, E., Pato, C.N., Pato, M.T., Knowles, J.A., Posthuma, D., Pauls, D.L., Cox, N.J., Neale, B.M., Freimer, N.B., Paschou, P., Mathews, C.A., Scharf, J.M., Coppola, G., Tourette Syndrome Association International Consortium for Genetics (TSAICG), & Gilles de la Tourette Syndrome GWAS Replication Initiative (GGRI) (2017) Rare Copy Number Variants in NRXN1 and CNTN6 Increase Risk for Tourette Syndrome. *Neuron*, **94**, 1101-1111.e7.

Hughes, E.G., Peng, X., Gleichman, A.J., Lai, M., Zhou, L., Tsou, R., Parsons, T.D., Lynch, D.R., Dalmau, J., & Balice-Gordon, R.J. (2010) Cellular and synaptic mechanisms of anti-NMDA receptor encephalitis. *J. Neurosci.*, **30**, 5866–5875.

Huijbers, M.G., Lipka, A.F., Plomp, J.J., Niks, E.H., van der Maarel, S.M., & Verschuuren, J.J. (2014) Pathogenic immune mechanisms at the neuromuscular synapse: the role of specific antibody-binding epitopes in myasthenia gravis. *J. Intern. Med.*, **275**, 12–26.

Huijbers, M.G., Querol, L.A., Niks, E.H., Plomp, J.J., van der Maarel, S.M., Graus, F., Dalmau, J., Illa, I., & Verschuuren, J.J. (2015) The expanding field of IgG4-mediated neurological autoimmune disorders. *Eur. J. Neurol.*, **22**, 1151–1161.

Hutchinson, M., Waters, P., McHugh, J., Gorman, G., O'Riordan, S., Connolly, S., Hager, H., Yu, P., Becker, C.-M., & Vincent, A. (2008) Progressive encephalomyelitis, rigidity, and myoclonus: a novel glycine receptor antibody. *Neurology*, **71**, 1291–1292.

Inda, M.C., DeFelipe, J., & Muñoz, A. (2006) Voltage-gated ion channels in the axon initial segment of human cortical pyramidal cells and their relationship with chandelier cells. *Proc. Natl. Acad. Sci. U.S.A.*, **103**, 2920–2925.

Irani, S.R., Alexander, S., Waters, P., Kleopa, K.A., Pettingill, P., Zuliani, L., Peles, E., Buckley, C., Lang, B., & Vincent, A. (2010) Antibodies to Kv1 potassium channel-complex proteins leucine-rich, glioma inactivated 1 protein and contactin-associated protein-2 in limbic encephalitis, Morvan's syndrome and acquired neuromyotonia. *Brain*, **133**, 2734–2748.

Jan, L.Y. & Jan, Y.N. (2012) Voltage-gated potassium channels and the diversity of electrical signalling. *J. Physiol. (Lond.)*, **590**, 2591–2599.

Joubert, B., Gobert, F., Thomas, L., Saint-Martin, M., Desestret, V., Convers, P., Rogemond, V., Picard, G., Ducray, F., Psimaras, D., Antoine, J.-C., Delattre, J.-Y., & Honnorat, J. (2017) Autoimmune episodic ataxia in patients with anti-CASPR2 antibody-associated encephalitis. *Neurol Neuroimmunol Neuroinflamm*, **4**, e371.

Joubert, B., Saint-Martin, M., Noraz, N., Picard, G., Rogemond, V., Ducray, F., Desestret, V., Psimaras, D., Delattre, J.-Y., Antoine, J.-C., & Honnorat, J. (2016) Characterization of a Subtype of Autoimmune Encephalitis With Anti-Contactin-Associated Protein-like 2 Antibodies in the Cerebrospinal Fluid, Prominent Limbic Symptoms, and Seizures. *JAMA Neurol*, **73**, 1115–1124.

Jurgensen, S. & Castillo, P.E. (2015) Selective Dysregulation of Hippocampal Inhibition in the Mouse Lacking Autism Candidate Gene CNTNAP2. *J. Neurosci.*, **35**, 14681–14687.

Karagogeos, D., Morton, S.B., Casano, F., Dodd, J., & Jessell, T.M. (1991) Developmental expression of the axonal glycoprotein TAG-1: differential regulation by central and peripheral neurons in vitro. *Development*, **112**, 51–67.

Kirov, G., Rujescu, D., Ingason, A., Collier, D.A., O'Donovan, M.C., & Owen, M.J. (2009) Neurexin 1 (NRXN1) deletions in schizophrenia. *Schizophr Bull*, **35**, 851–854.

Kocsis, J.D. & Waxman, S.G. (1980) Absence of potassium conductance in central myelinated axons. *Nature*, **287**, 348–349.

Kress, G.J. & Mennerick, S. (2009) Action potential initiation and propagation: upstream influences on neurotransmission. *Neuroscience*, **158**, 211–222.

Kunz, B., Lierheimer, R., Rader, C., Spirig, M., Ziegler, U., & Sonderegger, P. (2002) Axonin-1/TAG-1 mediates cell-cell adhesion by a cis-assisted trans-interaction. *J. Biol. Chem.*, **277**, 4551–4557.

Lai, H.C. & Jan, L.Y. (2006) The distribution and targeting of neuronal voltage-gated ion channels. *Nat. Rev. Neurosci.*, **7**, 548–562.

Lai, M., Hughes, E.G., Peng, X., Zhou, L., Gleichman, A.J., Shu, H., Matà, S., Kremens, D., Vitaliani, R., Geschwind, M.D., Bataller, L., Kalb, R.G., Davis, R., Graus, F., Lynch, D.R., Balice-Gordon, R., & Dalmau, J. (2009) AMPA receptor antibodies in limbic encephalitis alter synaptic receptor location. *Ann Neurol*, **65**, 424–434.

Lai, M., Huijbers, M.G.M., Lancaster, E., Graus, F., Bataller, L., Balice-Gordon, R., Cowell, J.K., & Dalmau, J. (2010) Investigation of LGI1 as the antigen in limbic encephalitis previously attributed to potassium channels: a case series. *Lancet Neurol*, **9**, 776–785.

Lancaster, E., Lai, M., Peng, X., Hughes, E., Constantinescu, R., Raizer, J., Friedman, D., Skeen, M.B., Grisold, W., Kimura, A., Ohta, K., Iizuka, T., Guzman, M., Graus, F., Moss, S.J., Balice-Gordon, R., & Dalmau, J. (2010) Antibodies to the GABAB receptor in limbic encephalitis with seizures: case series and characterisation of the antigen. *Lancet Neurol*, **9**, 67–76.

Lancaster, E., Martinez-Hernandez, E., Titulaer, M.J., Boulos, M., Weaver, S., Antoine, J.-C., Liebers, E., Kornblum, C., Bien, C.G., Honnorat, J., Wong, S., Xu, J., Contractor, A., Balice-Gordon, R., & Dalmau, J. (2011) Antibodies to metabotropic glutamate receptor 5 in the Ophelia syndrome. *Neurology*, **77**, 1698–1701.

Lawn, N.D., Westmoreland, B.F., Kiely, M.J., Lennon, V.A., & Vernino, S. (2003) Clinical, magnetic resonance imaging, and electroencephalographic findings in paraneoplastic limbic encephalitis. *Mayo Clin. Proc.*, **78**, 1363–1368.

Lek, M., Karczewski, K.J., Minikel, E.V., Samocha, K.E., Banks, E., Fennell, T., O'Donnell-Luria, A.H., Ware, J.S., Hill, A.J., Cummings, B.B., Tukiainen, T., Birnbaum, D.P., Kosmicki, J.A., Duncan, L.E., Estrada, K., Zhao, F., Zou, J., Pierce-Hoffman, E., Berghout, J., Cooper, D.N., Deflaux, N., DePristo, M., Do, R.,

Flannick, J., Fromer, M., Gauthier, L., Goldstein, J., Gupta, N., Howrigan, D., Kiezun, A., Kurki, M.I., Moonshine, A.L., Natarajan, P., Orozco, L., Peloso, G.M., Poplin, R., Rivas, M.A., Ruano-Rubio, V., Rose, S.A., Ruderfer, D.M., Shakir, K., Stenson, P.D., Stevens, C., Thomas, B.P., Tiao, G., Tusie-Luna, M.T., Weisburd, B., Won, H.-H., Yu, D., Altshuler, D.M., Ardissino, D., Boehnke, M., Danesh, J., Donnelly, S., Elosua, R., Florez, J.C., Gabriel, S.B., Getz, G., Glatt, S.J., Hultman, C.M., Kathiresan, S., Laakso, M., McCarroll, S., McCarthy, M.I., McGovern, D., McPherson, R., Neale, B.M., Palotie, A., Purcell, S.M., Saleheen, D., Scharf, J.M., Sklar, P., Sullivan, P.F., Tuomilehto, J., Tsuang, M.T., Watkins, H.C., Wilson, J.G., Daly, M.J., MacArthur, D.G., & Exome Aggregation Consortium (2016) Analysis of protein-coding genetic variation in 60,706 humans. *Nature*, **536**, 285–291.

Leterrier, C. (2018) The Axon Initial Segment: An Updated Viewpoint. *J. Neurosci.*, **38**, 2135–2145.

Liguori, R., Vincent, A., Clover, L., Avoni, P., Plazzi, G., Cortelli, P., Baruzzi, A., Carey, T., Gambetti, P., Lugaresi, E., & Montagna, P. (2001) Morvan's syndrome: peripheral and central nervous system and cardiac involvement with antibodies to voltage-gated potassium channels. *Brain*, **124**, 2417–2426.

Liska, A., Bertero, A., Gomolka, R., Sabbioni, M., Galbusera, A., Barsotti, N., Panzeri, S., Scattoni, M.L., Pasqualetti, M., & Gozzi, A. (2018) Homozygous Loss of Autism-Risk Gene CNTNAP2 Results in Reduced Local and Long-Range Prefrontal Functional Connectivity. *Cereb. Cortex*, **28**, 1141–1153.

Long, S.B., Campbell, E.B., & Mackinnon, R. (2005) Crystal structure of a mammalian voltage-dependent Shaker family K+ channel. *Science*, **309**, 897–903.

Lu, Z., Reddy, M.V.V.V.S., Liu, J., Kalichava, A., Liu, J., Zhang, L., Chen, F., Wang, Y., Holthauzen, L.M.F., White, M.A., Seshadrinathan, S., Zhong, X., Ren, G., & Rudenko, G. (2016) Molecular Architecture of Contactin-associated Protein-like 2 (CNTNAP2) and Its Interaction with Contactin 2 (CNTN2). *J. Biol. Chem.*, **291**, 24133–24147.

Lustig, M., Sakurai, T., & Grumet, M. (1999) Nr-CAM promotes neurite outgrowth from peripheral ganglia by a mechanism involving axonin-1 as a neuronal receptor. *Dev. Biol.*, **209**, 340–351.

Malhotra, J.D., Tsiotra, P., Karagogeos, D., & Hortsch, M. (1998) Cis-activation of L1-mediated ankyrin recruitment by TAG-1 homophilic cell adhesion. *J. Biol. Chem.*, **273**, 33354–33359.

Manganas, L.N. & Trimmer, J.S. (2000) Subunit composition determines Kv1 potassium channel surface expression. *J. Biol. Chem.*, **275**, 29685–29693.

Manto, M., Dalmau, J., Didelot, A., Rogemond, V., & Honnorat, J. (2010) In vivo effects of antibodies from patients with anti-NMDA receptor encephalitis: further evidence of synaptic glutamatergic dysfunction. *Orphanet J Rare Dis*, **5**, 31.

Martinez-Hernandez, E., Horvath, J., Shiloh-Malawsky, Y., Sangha, N., Martinez-Lage, M., & Dalmau, J. (2011) Analysis of complement and plasma cells in the brain of patients with anti-NMDAR encephalitis. *Neurology*, **77**, 589–593.

Mason, W.P., Graus, F., Lang, B., Honnorat, J., Delattre, J.Y., Valldeoriola, F., Antoine, J.C., Rosenblum, M.K., Rosenfeld, M.R., Newsom-Davis, J., Posner, J.B., & Dalmau, J. (1997) Small-cell lung cancer, paraneoplastic cerebellar degeneration and the Lambert-Eaton myasthenic syndrome. *Brain*, **120 (Pt 8)**, 1279–1300.

Mikasova, L., De Rossi, P., Bouchet, D., Georges, F., Rogemond, V., Didelot, A., Meissirel, C., Honnorat, J., & Groc, L. (2012) Disrupted surface cross-talk between NMDA and Ephrin-B2 receptors in anti-NMDA encephalitis. *Brain*, **135**, 1606–1621.

Missler, M., Zhang, W., Rohlmann, A., Kattenstroth, G., Hammer, R.E., Gottmann, K., & Südhof, T.C. (2003) Alpha-neurexins couple Ca2+ channels to synaptic vesicle exocytosis. *Nature*, **423**, 939–948.

Møller, R.S., Weber, Y.G., Klitten, L.L., Trucks, H., Muhle, H., Kunz, W.S., Mefford, H.C., Franke, A., Kautza, M., Wolf, P., Dennig, D., Schreiber, S., Rückert, I.-M., Wichmann, H.-E., Ernst, J.P., Schurmann, C., Grabe, H.J., Tommerup, N., Stephani, U., Lerche, H., Hjalgrim, H., Helbig, I., Sander, T., & EPICURE Consortium (2013) Exon-disrupting deletions of NRXN1 in idiopathic generalized epilepsy. *Epilepsia*, **54**, 256–264.

Mörtl, M., Sonderegger, P., Diederichs, K., & Welte, W. (2007) The crystal structure of the ligand-binding module of human TAG-1 suggests a new mode of homophilic interaction. *Protein Sci.*, **16**, 2174–2183.

Murdoch, J.D., Gupta, A.R., Sanders, S.J., Walker, M.F., Keaney, J., Fernandez, T.V., Murtha, M.T., Anyanwu, S., Ober, G.T., Raubeson, M.J., DiLullo, N.M., Villa, N., Waqar, Z., Sullivan, C., Gonzalez, L., Willsey, A.J., Choe, S.-Y., Neale, B.M., Daly, M.J., & State, M.W. (2015) No evidence for association of autism with

rare heterozygous point mutations in Contactin-Associated Protein-Like 2 (CNTNAP2), or in Other Contactin-Associated Proteins or Contactins. *PLoS Genet.*, **11**, e1004852.

Nelson, A.D. & Jenkins, P.M. (2017) Axonal Membranes and Their Domains: Assembly and Function of the Axon Initial Segment and Node of Ranvier. *Front Cell Neurosci*, **11**, 136.

Nelson, S.B. & Valakh, V. (2015) Excitatory/Inhibitory Balance and Circuit Homeostasis in Autism Spectrum Disorders. *Neuron*, **87**, 684–698.

Newsom-Davis, J., Buckley, C., Clover, L., Hart, I., Maddison, P., Tüzüm, E., & Vincent, A. (2003) Autoimmune disorders of neuronal potassium channels. *Ann. N. Y. Acad. Sci.*, **998**, 202–210.

Ogawa, Y., Horresh, I., Trimmer, J.S., Bredt, D.S., Peles, E., & Rasband, M.N. (2008) Postsynaptic density-93 clusters Kv1 channels at axon initial segments independently of CASPR2. *J. Neurosci.*, **28**, 5731–5739.

Ogawa, Y., Oses-Prieto, J., Kim, M.Y., Horresh, I., Peles, E., Burlingame, A.L., Trimmer, J.S., Meijer, D., & Rasband, M.N. (2010) ADAM22, a Kv1 channel-interacting protein, recruits membrane-associated guanylate kinases to juxtaparanodes of myelinated axons. *J. Neurosci.*, **30**, 1038–1048.

Ohkawa, T., Fukata, Y., Yamasaki, M., Miyazaki, T., Yokoi, N., Takashima, H., Watanabe, M., Watanabe, O., & Fukata, M. (2013) Autoantibodies to epilepsy-related LGI1 in limbic encephalitis neutralize LGI1-ADAM22 interaction and reduce synaptic AMPA receptors. *J. Neurosci.*, **33**, 18161–18174.

Oiso, S., Takeda, Y., Futagawa, T., Miura, T., Kuchiiwa, S., Nishida, K., Ikeda, R., Kariyazono, H., Watanabe, K., & Yamada, K. (2009) Contactin-associated protein (Caspr) 2 interacts with carboxypeptidase E in the CNS. *J. Neurochem.*, **109**, 158–167.

Olsen, A.L., Lai, Y., Dalmau, J., Scherer, S.S., & Lancaster, E. (2015) CASPR2 autoantibodies target multiple epitopes. *Neurol Neuroimmunol Neuroinflamm*, **2**, e127.

Ovsepian, S.V., LeBerre, M., Steuber, V., O'Leary, V.B., Leibold, C., & Oliver Dolly, J. (2016) Distinctive role of KV1.1 subunit in the biology and functions of low threshold K(+) channels with implications for neurological disease. *Pharmacol. Ther.*, **159**, 93–101.

Patterson, K.R., Dalmau, J., & Lancaster, E. (2018) Mechanisms of CASPR2 antibodies in autoimmune encephalitis and neuromyotonia. *Ann. Neurol.*, **83**, 40–51.

Peñagarikano, O., Abrahams, B.S., Herman, E.I., Winden, K.D., Gdalyahu, A., Dong, H., Sonnenblick, L.I., Gruver, R., Almajano, J., Bragin, A., Golshani, P., Trachtenberg, J.T., Peles, E., & Geschwind, D.H. (2011) Absence of CNTNAP2 leads to epilepsy, neuronal migration abnormalities, and core autism-related deficits. *Cell*, **147**, 235–246.

Peters, C.J., Vaid, M., Horne, A.J., Fedida, D., & Accili, E.A. (2009) The molecular basis for the actions of KVbeta1.2 on the opening and closing of the KV1.2 delayed rectifier channel. *Channels (Austin)*, **3**, 314–322.

Petit-Pedrol, M., Armangue, T., Peng, X., Bataller, L., Cellucci, T., Davis, R., McCracken, L., Martinez-Hernandez, E., Mason, W.P., Kruer, M.C., Ritacco, D.G., Grisold, W., Meaney, B.F., Alcalá, C., Sillevis-Smitt, P., Titulaer, M.J., Balice-Gordon, R., Graus, F., & Dalmau, J. (2014) Encephalitis with refractory seizures, status epilepticus, and antibodies to the GABAA receptor: a case series, characterisation of the antigen, and analysis of the effects of antibodies. *Lancet Neurol*, **13**, 276–286.

Pinatel, D., Hivert, B., Boucraut, J., Saint-Martin, M., Rogemond, V., Zoupi, L., Karagogeos, D., Honnorat, J., & Faivre-Sarrailh, C. (2015) Inhibitory axons are targeted in hippocampal cell culture by anti-CASPR2 autoantibodies associated with limbic encephalitis. *Front Cell Neurosci*, **9**, 265.

Pinatel, D., Hivert, B., Saint-Martin, M., Noraz, N., Savvaki, M., Karagogeos, D., & Faivre-Sarrailh, C. (2017) The Kv1-associated molecules TAG-1 and CASPR2 are selectively targeted to the axon initial segment in hippocampal neurons. *J. Cell. Sci.*, **130**, 2209–2220.

Planagumà, J., Haselmann, H., Mannara, F., Petit-Pedrol, M., Grünewald, B., Aguilar, E., Röpke, L., Martín-García, E., Titulaer, M.J., Jercog, P., Graus, F., Maldonado, R., Geis, C., & Dalmau, J. (2016) Ephrin-B2 prevents N-methyl-D-aspartate receptor antibody effects on memory and neuroplasticity. *Ann. Neurol.*, **80**, 388–400.

Planagumà, J., Leypoldt, F., Mannara, F., Gutiérrez-Cuesta, J., Martín-García, E., Aguilar, E., Titulaer, M.J., Petit-Pedrol, M., Jain, A., Balice-Gordon, R., Lakadamyali, M., Graus, F., Maldonado, R., & Dalmau, J. (2015) Human N-methyl D-aspartate receptor antibodies alter memory and behaviour in mice. *Brain*, **138**, 94–109.

Platt, M.P., Agalliu, D., & Cutforth, T. (2017) Hello from the Other Side: How Autoantibodies Circumvent the Blood-Brain Barrier in Autoimmune Encephalitis. *Front Immunol*, **8**, 442.

Poliak, S., Gollan, L., Martinez, R., Custer, A., Einheber, S., Salzer, J.L., Trimmer, J.S., Shrager, P., & Peles, E. (1999) CASPR2, a new member of the neurexin superfamily, is localized at the juxtaparanodes of myelinated axons and associates with K+ channels. *Neuron*, **24**, 1037–1047.

Poliak, S., Salomon, D., Elhanany, H., Sabanay, H., Kiernan, B., Pevny, L., Stewart, C.L., Xu, X., Chiu, S.-Y., Shrager, P., Furley, A.J.W., & Peles, E. (2003) Juxtaparanodal clustering of Shaker-like K+ channels in myelinated axons depends on CASPR2 and TAG-1. *J. Cell Biol.*, **162**, 1149–1160.

Poot, M. (2015) Connecting the CNTNAP2 Networks with Neurodevelopmental Disorders. *Mol Syndromol*, **6**, 7–22.

Poot, M. (2017) Intragenic CNTNAP2 Deletions: A Bridge Too Far? *Mol Syndromol*, **8**, 118–130.

Rader, C., Kunz, B., Lierheimer, R., Giger, R.J., Berger, P., Tittmann, P., Gross, H., & Sonderegger, P. (1996) Implications for the domain arrangement of axonin-1 derived from the mapping of its NgCAM binding site. *EMBO J.*, **15**, 2056–2068.

Rasband, M.N. (2010) Clustered K+ channel complexes in axons. *Neurosci. Lett.*, **486**, 101–106.

Rasband, M.N., Park, E.W., Zhen, D., Arbuckle, M.I., Poliak, S., Peles, E., Grant, S.G.N., & Trimmer, J.S. (2002) Clustering of neuronal potassium channels is independent of their interaction with PSD-95. *J. Cell Biol.*, **159**, 663–672.

Rasband, M.N. & Peles, E. (2015) The Nodes of Ranvier: Molecular Assembly and Maintenance. *Cold Spring Harb Perspect Biol*, **8**, a020495.

Reichelt, A.C., Rodgers, R.J., & Clapcote, S.J. (2012) The role of neurexins in schizophrenia and autistic spectrum disorder. *Neuropharmacology*, **62**, 1519–1526.

Reissner, C., Runkel, F., & Missler, M. (2013) Neurexins. *Genome Biol.*, **14**, 213.

Rendall, A.R., Truong, D.T., & Fitch, R.H. (2016) Learning delays in a mouse model of Autism Spectrum Disorder. *Behav. Brain Res.*, **303**, 201–207.

Rettig, J., Heinemann, S.H., Wunder, F., Lorra, C., Parcej, D.N., Dolly, J.O., & Pongs, O. (1994) Inactivation properties of voltage-gated K+ channels altered by presence of beta-subunit. *Nature*, **369**, 289–294.

Rispens, T., Ooijevaar-de Heer, P., Bende, O., & Aalberse, R.C. (2011) Mechanism of immunoglobulin G4 Fab-arm exchange. *J. Am. Chem. Soc.*, **133**, 10302–10311.

Robbins, C.A. & Tempel, B.L. (2012) Kv1.1 and Kv1.2: similar channels, different seizure models. *Epilepsia*, **53 Suppl 1**, 134–141.

Rodenas-Cuadrado, P., Ho, J., & Vernes, S.C. (2014) Shining a light on CNTNAP2: complex functions to complex disorders. *Eur. J. Hum. Genet.*, **22**, 171–178.

Rodenas-Cuadrado, P., Pietrafusa, N., Francavilla, T., La Neve, A., Striano, P., & Vernes, S.C. (2016) Characterisation of CASPR2 deficiency disorder--a syndrome involving autism, epilepsy and language impairment. *BMC Med. Genet.*, **17**, 8.

Rojas, I., Graus, F., Keime-Guibert, F., Reñé, R., Delattre, J.Y., Ramón, J.M., Dalmau, J., & Posner, J.B. (2000) Long-term clinical outcome of paraneoplastic cerebellar degeneration and anti-Yo antibodies. *Neurology*, **55**, 713–715.

Rubio-Marrero, E.N., Vincelli, G., Jeffries, C.M., Shaikh, T.R., Pakos, I.S., Ranaivoson, F.M., von Daake, S., Demeler, B., De Jaco, A., Perkins, G., Ellisman, M.H., Trewhella, J., & Comoletti, D. (2016) Structural Characterization of the Extracellular Domain of CASPR2 and Insights into Its Association with the Novel Ligand Contactin1. *J. Biol. Chem.*, **291**, 5788–5802.

Saint-Martin, M., Joubert, B., Pellier-Monnin, V., Pascual, O., Noraz, N., & Honnorat, J. (2018) Contactin-associated protein-like 2, a protein of the neurexin family involved in several human diseases. *Eur. J. Neurosci.*, **48**, 1906–1923.

Savvaki, M., Panagiotaropoulos, T., Stamatakis, A., Sargiannidou, I., Karatzioula, P., Watanabe, K., Stylianopoulou, F., Karagogeos, D., & Kleopa, K.A. (2008) Impairment of learning and memory in TAG-1 deficient mice associated with shorter CNS internodes and disrupted juxtaparanodes. *Mol. Cell. Neurosci.*, **39**, 478–490.

Savvaki, M., Theodorakis, K., Zoupi, L., Stamatakis, A., Tivodar, S., Kyriacou, K., Stylianopoulou, F., & Karagogeos, D. (2010) The expression of TAG-1 in glial cells is sufficient for the formation of the

juxtaparanodal complex and the phenotypic rescue of tag-1 homozygous mutants in the CNS. *J. Neurosci.*, **30**, 13943–13954.

Schaaf, C.P., Boone, P.M., Sampath, S., Williams, C., Bader, P.I., Mueller, J.M., Shchelochkov, O.A., Brown, C.W., Crawford, H.P., Phalen, J.A., Tartaglia, N.R., Evans, P., Campbell, W.M., Tsai, A.C.-H., Parsley, L., Grayson, S.W., Scheuerle, A., Luzzi, C.D., Thomas, S.K., Eng, P.A., Kang, S.-H.L., Patel, A., Stankiewicz, P., & Cheung, S.W. (2012) Phenotypic spectrum and genotype-phenotype correlations of NRXN1 exon deletions. *Eur. J. Hum. Genet.*, **20**, 1240–1247.

Scott, R., Sánchez-Aguilera, A., van Elst, K., Lim, L., Dehorter, N., Bae, S.E., Bartolini, G., Peles, E., Kas, M.J.H., Bruining, H., & Marín, O. (2017) Loss of Cntnap2 Causes Axonal Excitability Deficits, Developmental Delay in Cortical Myelination, and Abnormal Stereotyped Motor Behavior. *Cereb. Cortex*,.

Scott-Van Zeeland, A.A., Abrahams, B.S., Alvarez-Retuerto, A.I., Sonnenblick, L.I., Rudie, J.D., Ghahremani, D., Mumford, J.A., Poldrack, R.A., Dapretto, M., Geschwind, D.H., & Bookheimer, S.Y. (2010) Altered functional connectivity in frontal lobe circuits is associated with variation in the autism risk gene CNTNAP2. *Sci Transl Med*, **2**, 56ra80.

Selimbeyoglu, A., Kim, C.K., Inoue, M., Lee, S.Y., Hong, A.S.O., Kauvar, I., Ramakrishnan, C., Fenno, L.E., Davidson, T.J., Wright, M., & Deisseroth, K. (2017) Modulation of prefrontal cortex excitation/inhibition balance rescues social behavior in CNTNAP2-deficient mice. *Sci Transl Med*, **9**.

Shams'ili, S., Grefkens, J., de Leeuw, B., van den Bent, M., Hooijkaas, H., van der Holt, B., Vecht, C., & Sillevis Smitt, P. (2003) Paraneoplastic cerebellar degeneration associated with antineuronal antibodies: analysis of 50 patients. *Brain*, **126**, 1409–1418.

Shi, G., Nakahira, K., Hammond, S., Rhodes, K.J., Schechter, L.E., & Trimmer, J.S. (1996) Beta subunits promote K+ channel surface expression through effects early in biosynthesis. *Neuron*, **16**, 843–852.

Shillito, P., Molenaar, P.C., Vincent, A., Leys, K., Zheng, W., van den Berg, R.J., Plomp, J.J., van Kempen, G.T., Chauplannaz, G., & Wintzen, A.R. (1995) Acquired neuromyotonia: evidence for autoantibodies directed against K+ channels of peripheral nerves. *Ann. Neurol.*, **38**, 714–722.

Sillevis Smitt, P., Kinoshita, A., De Leeuw, B., Moll, W., Coesmans, M., Jaarsma, D., Henzen-Logmans, S., Vecht, C., De Zeeuw, C., Sekiyama, N., Nakanishi, S., & Shigemoto, R. (2000) Paraneoplastic cerebellar ataxia due to autoantibodies against a glutamate receptor. *N. Engl. J. Med.*, **342**, 21–27.

Singer, H.S., Morris, C., Gause, C., Pollard, M., Zimmerman, A.W., & Pletnikov, M. (2009) Prenatal exposure to antibodies from mothers of children with autism produces neurobehavioral alterations: A pregnant dam mouse model. *J. Neuroimmunol.*, **211**, 39–48.

Singer, H.S., Morris, C.M., Gause, C.D., Gillin, P.K., Crawford, S., & Zimmerman, A.W. (2008) Antibodies against fetal brain in sera of mothers with autistic children. *J. Neuroimmunol.*, **194**, 165–172.

Small, M., Treilleux, I., Couillault, C., Pissaloux, D., Picard, G., Paindavoine, S., Attignon, V., Wang, Q., Rogemond, V., Lay, S., Ray-Coquard, I., Pfisterer, J., Joly, F., Du Bois, A., Psimaras, D., Bendriss-Vermare, N., Caux, C., Dubois, B., Honnorat, J., & Desestret, V. (2018) Genetic alterations and tumor immune attack in Yo paraneoplastic cerebellar degeneration. *Acta Neuropathol.*, **135**, 569–579.

Smart, S.L., Lopantsev, V., Zhang, C.L., Robbins, C.A., Wang, H., Chiu, S.Y., Schwartzkroin, P.A., Messing, A., & Tempel, B.L. (1998) Deletion of the K(V)1.1 potassium channel causes epilepsy in mice. *Neuron*, **20**, 809–819.

Song, J., Jing, S., Quan, C., Lu, J., Qiao, X., Qiao, K., Lu, J., Xi, J., & Zhao, C. (2017) Isaacs syndrome with CASPR2 antibody: A series of three cases. *J Clin Neurosci*, **41**, 63–66.

Stoeckli, E.T., Kuhn, T.B., Duc, C.O., Ruegg, M.A., & Sonderegger, P. (1991) The axonally secreted protein axonin-1 is a potent substratum for neurite growth. *J. Cell Biol.*, **112**, 449–455.

Stoeckli, E.T. & Landmesser, L.T. (1995) Axonin-1, Nr-CAM, and Ng-CAM play different roles in the in vivo guidance of chick commissural neurons. *Neuron*, **14**, 1165–1179.

Stoeckli, E.T., Sonderegger, P., Pollerberg, G.E., & Landmesser, L.T. (1997) Interference with axonin-1 and NrCAM interactions unmasks a floor-plate activity inhibitory for commissural axons. *Neuron*, **18**, 209–221.

Stogmann, E., Reinthaler, E., Eltawil, S., El Etribi, M.A., Hemeda, M., El Nahhas, N., Gaber, A.M., Fouad, A., Edris, S., Benet-Pages, A., Eck, S.H., Pataraia, E., Mei, D., Brice, A., Lesage, S., Guerrini, R., Zimprich, F.,

Strom, T.M., & Zimprich, A. (2013) Autosomal recessive cortical myoclonic tremor and epilepsy: association with a mutation in the potassium channel associated gene CNTN2. *Brain*, **136**, 1155–1160.
Strauss, K.A., Puffenberger, E.G., Huentelman, M.J., Gottlieb, S., Dobrin, S.E., Parod, J.M., Stephan, D.A., & Morton, D.H. (2006) Recessive symptomatic focal epilepsy and mutant contactin-associated protein-like 2. *N. Engl. J. Med.*, **354**, 1370–1377.
Südhof, T.C. (2017) Synaptic Neurexin Complexes: A Molecular Code for the Logic of Neural Circuits. *Cell*, **171**, 745–769.
Tanabe, Y., Fujita-Jimbo, E., Momoi, M.Y., & Momoi, T. (2015) CASPR2 forms a complex with GPR37 via MUPP1 but not with GPR37(R558Q), an autism spectrum disorder-related mutation. *J. Neurochem.*, **134**, 783–793.
Titulaer, M.J., Klooster, R., Potman, M., Sabater, L., Graus, F., Hegeman, I.M., Thijssen, P.E., Wirtz, P.W., Twijnstra, A., Smitt, P.A.E.S., van der Maarel, S.M., & Verschuuren, J.J.G.M. (2009) SOX antibodies in small-cell lung cancer and Lambert-Eaton myasthenic syndrome: frequency and relation with survival. *J. Clin. Oncol.*, **27**, 4260–4267.
Traka, M., Dupree, J.L., Popko, B., & Karagogeos, D. (2002) The neuronal adhesion protein TAG-1 is expressed by Schwann cells and oligodendrocytes and is localized to the juxtaparanodal region of myelinated fibers. *J. Neurosci.*, **22**, 3016–3024.
Traka, M., Goutebroze, L., Denisenko, N., Bessa, M., Nifli, A., Havaki, S., Iwakura, Y., Fukamauchi, F., Watanabe, K., Soliven, B., Girault, J.-A., & Karagogeos, D. (2003) Association of TAG-1 with CASPR2 is essential for the molecular organization of juxtaparanodal regions of myelinated fibers. *J. Cell Biol.*, **162**, 1161–1172.
Tsiotra, P.C., Theodorakis, K., Papamatheakis, J., & Karagogeos, D. (1996) The fibronectin domains of the neural adhesion molecule TAX-1 are necessary and sufficient for homophilic binding. *J. Biol. Chem.*, **271**, 29216–29222.
Tüzün, E. & Dalmau, J. (2007) Limbic encephalitis and variants: classification, diagnosis and treatment. *Neurologist*, **13**, 261–271.
Tüzün, E., Rossi, J.E., Karner, S.F., Centurion, A.F., & Dalmau, J. (2007) Adenylate kinase 5 autoimmunity in treatment refractory limbic encephalitis. *J. Neuroimmunol.*, **186**, 177–180.
Tüzün, E., Zhou, L., Baehring, J.M., Bannykh, S., Rosenfeld, M.R., & Dalmau, J. (2009) Evidence for antibody-mediated pathogenesis in anti-NMDAR encephalitis associated with ovarian teratoma. *Acta Neuropathol.*, **118**, 737–743.
Tzimourakas, A., Giasemi, S., Mouratidou, M., & Karagogeos, D. (2007) Structure-function analysis of protein complexes involved in the molecular architecture of juxtaparanodal regions of myelinated fibers. *Biotechnol J*, **2**, 577–583.
Vabnick, I., Trimmer, J.S., Schwarz, T.L., Levinson, S.R., Risal, D., & Shrager, P. (1999a) Dynamic potassium channel distributions during axonal development prevent aberrant firing patterns. *J. Neurosci.*, **19**, 747–758.
Vabnick, I., Trimmer, J.S., Schwarz, T.L., Levinson, S.R., Risal, D., & Shrager, P. (1999b) Dynamic potassium channel distributions during axonal development prevent aberrant firing patterns. *J. Neurosci.*, **19**, 747–758.
van Gerpen, J.A., Ahlskog, J.E., Chen, R., Fung, V.S.C., Hallett, M., Gövert, F., Deuschl, G., & Leypoldt, F. (2016) Orthostatic myoclonus associated with CASPR2 antibodies. *Neurology*, **87**, 1187–1188.
van Sonderen, A., Ariño, H., Petit-Pedrol, M., Leypoldt, F., Körtvélyessy, P., Wandinger, K.-P., Lancaster, E., Wirtz, P.W., Schreurs, M.W.J., Sillevis Smitt, P.A.E., Graus, F., Dalmau, J., & Titulaer, M.J. (2016) The clinical spectrum of CASPR2 antibody-associated disease. *Neurology*, **87**, 521–528.
van Sonderen, A., Roelen, D.L., Stoop, J.A., Verdijk, R.M., Haasnoot, G.W., Thijs, R.D., Wirtz, P.W., Schreurs, M.W.J., Claas, F.H.J., Sillevis Smitt, P.A.E., & Titulaer, M.J. (2017) Anti-LGI1 encephalitis is strongly associated with HLA-DR7 and HLA-DRB4. *Ann. Neurol.*, **81**, 193–198.
Varea, O., Martin-de-Saavedra, M.D., Kopeikina, K.J., Schürmann, B., Fleming, H.J., Fawcett-Patel, J.M., Bach, A., Jang, S., Peles, E., Kim, E., & Penzes, P. (2015) Synaptic abnormalities and cytoplasmic glutamate receptor aggregates in contactin associated protein-like 2/CASPR2 knockout neurons. *Proc. Natl. Acad. Sci. U.S.A.*, **112**, 6176–6181.

Veitia, R.A., Caburet, S., & Birchler, J.A. (2018) Mechanisms of Mendelian dominance. *Clin. Genet.*, **93**, 419–428.

Velluti, J.C., Caputi, A., & Macadar, O. (1987) Limbic epilepsy induced in the rat by dendrotoxin, a polypeptide isolated from the green mamba (Dendroaspis angusticeps) venom. *Toxicon*, **25**, 649–657.

Venkatesan, A., Tunkel, A.R., Bloch, K.C., Lauring, A.S., Sejvar, J., Bitnun, A., Stahl, J.-P., Mailles, A., Drebot, M., Rupprecht, C.E., Yoder, J., Cope, J.R., Wilson, M.R., Whitley, R.J., Sullivan, J., Granerod, J., Jones, C., Eastwood, K., Ward, K.N., Durrheim, D.N., Solbrig, M.V., Guo-Dong, L., Glaser, C.A., Sheriff, H., Brown, D., Farnon, E., Messenger, S., Paterson, B., Soldatos, A., Roy, S., Visvesvara, G., Beach, M., Nasci, R., Pertowski, C., Schmid, S., Rascoe, L., Montgomery, J., Tong, S., Breiman, R., Franka, R., Keuhnert, M., Angulo, F., & Cherry, J. (2013) Case Definitions, Diagnostic Algorithms, and Priorities in Encephalitis: Consensus Statement of the International Encephalitis Consortium. *Clin Infect Dis*, **57**, 1114–1128.

Verkerk, A.J.M.H., Mathews, C.A., Joosse, M., Eussen, B.H.J., Heutink, P., Oostra, B.A., & Tourette Syndrome Association International Consortium for Genetics (2003) CNTNAP2 is disrupted in a family with Gilles de la Tourette syndrome and obsessive compulsive disorder. *Genomics*, **82**, 1–9.

Vidarsson, G., Dekkers, G., & Rispens, T. (2014) IgG subclasses and allotypes: from structure to effector functions. *Front Immunol*, **5**, 520.

Vogt, D., Cho, K.K.A., Shelton, S.M., Paul, A., Huang, Z.J., Sohal, V.S., & Rubenstein, J.L.R. (2017) Mouse Cntnap2 and Human CNTNAP2 ASD Alleles Cell Autonomously Regulate PV+ Cortical Interneurons. *Cereb. Cortex*, 1–12.

Vogt, L., Giger, R.J., Ziegler, U., Kunz, B., Buchstaller, A., Hermens WTJMC, null, Kaplitt, M.G., Rosenfeld, M.R., Pfaff, D.W., Verhaagen, J., & Sonderegger, P. (1996) Continuous renewal of the axonal pathway sensor apparatus by insertion of new sensor molecules into the growth cone membrane. *Curr. Biol.*, **6**, 1153–1158.

Watson, C.M., Crinnion, L.A., Tzika, A., Mills, A., Coates, A., Pendlebury, M., Hewitt, S., Harrison, S.M., Daly, C., Roberts, P., Carr, I.M., Sheridan, E.G., & Bonthron, D.T. (2014) Diagnostic whole genome sequencing and split-read mapping for nucleotide resolution breakpoint identification in CNTNAP2 deficiency syndrome. *Am. J. Med. Genet. A*, **164A**, 2649–2655.

Weller, U., Bernhardt, U., Siemen, D., Dreyer, F., Vogel, W., & Habermann, E. (1985) Electrophysiological and neurobiochemical evidence for the blockade of a potassium channel by dendrotoxin. *Naunyn Schmiedebergs Arch. Pharmacol.*, **330**, 77–83.

Whitley, R.J., Soong, S.J., Linneman, C., Liu, C., Pazin, G., & Alford, C.A. (1982) Herpes simplex encephalitis. Clinical Assessment. *JAMA*, **247**, 317–320.

Wolfer, D.P., Giger, R.J., Stagliar, M., Sonderegger, P., & Lipp, H.P. (1998) Expression of the axon growth-related neural adhesion molecule TAG-1/axonin-1 in the adult mouse brain. *Anat. Embryol.*, **197**, 177–185.

Wolfer, D.P., Henehan-Beatty, A., Stoeckli, E.T., Sonderegger, P., & Lipp, H.P. (1994) Distribution of TAG-1/axonin-1 in fibre tracts and migratory streams of the developing mouse nervous system. *J. Comp. Neurol.*, **345**, 1–32.

Zuellig, R.A., Rader, C., Schroeder, A., Kalousek, M.B., Von Bohlen und Halbach, F., Osterwalder, T., Inan, C., Stoeckli, E.T., Affolter, H.U., & Fritz, A. (1992) The axonally secreted cell adhesion molecule, axonin-1. Primary structure, immunoglobulin-like and fibronectin-type-III-like domains and glycosyl-phosphatidylinositol anchorage. *Eur. J. Biochem.*, **204**, 453–463.

Zweier, C., de Jong, E.K., Zweier, M., Orrico, A., Ousager, L.B., Collins, A.L., Bijlsma, E.K., Oortveld, M.A.W., Ekici, A.B., Reis, A., Schenck, A., & Rauch, A. (2009) CNTNAP2 and NRXN1 are mutated in autosomal-recessive Pitt-Hopkins-like mental retardation and determine the level of a common synaptic protein in Drosophila. *Am. J. Hum. Genet.*, **85**, 655–666.

ANNEXES

Liste des publications :

Under revision. CASPR2/TAG-1/Kv1 interactions and impact of anti-CASPR2 autoantibodies from patients with limbic encephalitis. **Saint-Martin M.,** Déchelotte B., Honnorat J., Pellier-Monnin V., Noraz N. (Article 3)

1. Structural mapping hot spots within human CASPR2 Discoidin domain for autoantibody recognition. **Margaux Saint-Martin*,** Junying Zhang*, Wenjun Liang*, Fei Xu, Nelly Noraz, Jianmei Liu, Jerome Honnorat, Heli Liu. **2018**. Journal of autoimmunity. Accepted for publication on the 01th of october. * first co-author (Article 2)

2. Contactin-associated protein-like 2, a protein of the neurexin family involved in several human diseases. **Saint-Martin M**, Joubert B, Pellier-Monnin V, Pascual O, Noraz N, Honnorat J. Eur J Neurosci. **2018** Aug;48(3):1906-1923. doi: 10.1111/ejn.14081. Epub 2018 Aug 16. Review. (Annexe 1)
PMID: 30028556

3. Genetic variants in autism-related CNTNAP2 impair axonal growth of cortical neurons. Canali G, Garcia M, Hivert B, Pinatel D, Goullancourt A, Oguievetskaia K, **Saint-Martin M**, Girault JA, Faivre-Sarrailh C, Goutebroze L. Hum Mol Genet. **2018** Jun 1;27(11):1941-1954. doi: 10.1093/hmg/ddy102. (Annexe 2)
PMID: 29788201

4. Autoimmune episodic ataxia in patients with anti-CASPR2 antibody-associated encephalitis. Joubert B, Gobert F, Thomas L, **Saint-Martin M**, Desestret V, Convers P, Rogemond V, Picard G, Ducray F, Psimaras D, Antoine JC, Delattre JY, Honnorat J. Neurol Neuroimmunol Neuroinflamm. **2017** Jun 14;4(4):e371. (Annexe 3)
PMID: 28638854

5. The Kv1-associated molecules TAG-1 and Caspr2 are selectively targeted to the axon initial segment in hippocampal neurons. Pinatel D, Hivert B, **Saint-Martin M**, Noraz N, Savvaki M, Karagogeos D, Faivre-Sarrailh C. J Cell Sci. **2017** Jul 1;130(13):2209-2220. (Annexe 4)
PMID: 28533267

6. Characterization of a Subtype of Autoimmune Encephalitis With Anti-Contactin-Associated Protein-like 2 Antibodies in the Cerebrospinal Fluid, Prominent Limbic Symptoms, and Seizures. Joubert B, **Saint-Martin M**, Noraz N, Picard G, Rogemond V, Ducray F, Desestret V, Psimaras D, Delattre JY, Antoine JC, Honnorat J. JAMA Neurol. **2016** Sep 1;73(9):1115-24. (Article 1)
PMID: 27428927

7. Inhibitory axons are targeted in hippocampal cell culture by anti-Caspr2 autoantibodies associated with limbic encephalitis. Pinatel D, Hivert B, Boucraut J, **Saint-Martin M**, Rogemond V, Zoupi L, Karagogeos D, Honnorat J, Faivre-Sarrailh C. Front Cell Neurosci. **2015** Jul 9;9:265. (Annexe 5)
PMID: 26217189

Received: 28 March 2018 | Revised: 8 June 2018 | Accepted: 2 July 2018

DOI: 10.1111/ejn.14081

REVIEW ARTICLE

WILEY EJN European Journal of Neuroscience FENS

Contactin-associated protein-like 2, a protein of the neurexin family involved in several human diseases

Margaux Saint-Martin[1] | **Bastien Joubert**[1,2] | **Véronique Pellier-Monnin**[1] | **Olivier Pascual**[1] | **Nelly Noraz**[1] | **Jérôme Honnorat**[1,2]

[1]Institut NeuroMyoGene INSERM U1217/CNRS UMR 5310, Université de Lyon, Université Claude Bernard Lyon 1, Lyon, France

[2]French Reference Center on Paraneoplastic Neurological Syndrome, Hospices Civils de Lyon, Hôpital Neurologique, Bron, France

Correspondence
Jérôme Honnorat, Neuro-Oncologie, Hôpital Neurologique Pierre Wertheimer, 59 Boulevard Pinel, 69677 Bron Cedex, France.
Email: jerome.honnorat@chu-lyon.fr

Abstract

Contactin-associated protein-like 2 (CASPR2) is a cell adhesion protein of the neurexin family. Proteins of this family have been shown to play a role in the development of the nervous system, in synaptic functions, and in neurological diseases. Over recent years, CASPR2 function has gained an increasing interest as demonstrated by the growing number of publications. Here, we gather published data to comprehensively review CASPR2 functions within the nervous system in relation to CASPR2-related diseases in humans. On the one hand, studies on *Cntnap2* (coding for CASPR2) knockout mice revealed its role during development, especially, in setting-up the inhibitory network. Consistent with this result, mutations in the *CNTNAP2* gene coding for CASPR2 in human have been identified in neurodevelopmental disorders such as autism, intellectual disability, and epilepsy. On the other hand, CASPR2 was shown to play a role beyond development, in the localization of voltage-gated potassium channel (VGKC) complex that is composed of TAG-1, Kv1.1, and Kv1.2. This complex was found in several subcellular compartments essential for action potential propagation: the node of Ranvier, the axon initial segment, and the synapse. In line with a role of CASPR2 in the mature nervous system, neurological autoimmune diseases have been described in patients without neurodevelopmental disorders but with antibodies directed against CASPR2. These autoimmune diseases were of two types: central with memory disorders and temporal lobe seizures, or peripheral with muscular hyperactivity. Overall, we review the up-to-date knowledge on CASPR2 function and pinpoint confused or lacking information that will need further investigation.

KEYWORDS

autoimmunity, *CNTNAP2*, Kv1, neurodevelopment, TAG-1

Abbreviations: ADAM-22, Disintegrin and metalloproteinase domain-containing protein 22; ADAM-23, Disintegrin and metalloproteinase domain-containing protein 23; ADHD, Attention deficit hyperactivity disorder; AE, Autoimmune encephalitis; AIS, Axon initial segment; AMPAr, Amino-3-hydroxy-5-méthylisoazol-4-propionate receptor; AP, Action potential; ASD, Autism spectrum disorder; CA1, Cornu Ammonis 1; CA3, Cornu Ammonis 3; CASK, Calcium/calmodulin-dependant serine protein kinase 3; CASPR2-Abs, Anti-CASPR2 antibodies; CASPR2, Contactin-associated protein-like 2; CDFE, Cortical dysplasia-focal epilepsy; CNV, Copy Number Variation; CSF, Cerebrospinal fluid; DG, Dentate gyrus; DIV, Days in vitro; E15, Embryonic day 15; EGF (E), Epidermal growth factor-like domain; F58C, Discoidin-like domain; F, Fibrinogen-like domain; GABA, γ-aminobutyric acid; GAD-65, Glutamic acid decarboxylase 65; GluA1, Glutamate receptor subunit A1; GPI, Glycosylphosphatidylinositol; HEK cell, Human embryonic kidney cell; ID, Intellectual disability; JXP, Juxtaparanode; KO, Knockout; LGI1, Leucine-rich glioma inactivated 1; L, Laminin G-like domain; MGE, Medial ganglionic eminence; MoS, Morvan syndrome; MPP, Membrane palmitoylated protein; NMDAr, N-methyl-D-aspartate receptor; NMT, Neuromyotonia; P7, Postnatal day 7; PN, Paranode; PSD-93, Postsynaptic density-93; PSD-95, Postsynaptic density-95; PV+, Parvalbumin positive; TAG-1, Transient axonal glycoprotein-1; TM, Transmembrane domain; VGAT, Vesicular GABA transporter; VGKC, Voltage-gated potassium channel; VLGUT, Vesicular glutamate transporter.

Edited by Patricia Gaspar. Reviwed by Eric Lancaster, Martin Poot and Laurence Goutebroze.
All peer review communications can be found with the online version of the article.

1 | INTRODUCTION

Contactin-associated protein-like 2 belongs to a distinct subgroup of the neurexin superfamily along with four different proteins in human CASPR1 and CASPR3–CASPR5 (for review see Zou et al., 2017). Neurexins are cell adhesion proteins known for their role in synapse formation and in the regulation of synapse properties (Gokce & Südhof, 2013; Graf, Zhang, Jin, Linhoff, & Craig, 2004; Missler et al., 2003). Located at the presynaptic compartment, neurexins are able to induce the formation of excitatory or inhibitory synapses through interaction with a diversity of neuroligin postsynaptic partners (Graf et al., 2004). In mice, triple or single knockouts (KO) of neurexin (neurexin-1α, 2α, and 3α) impaired survival or induced severe synapse dysfunction (Chen, Jiang, Zhang, Gokce, & Südhof, 2017; for review see Südhof, 2017). In humans, mutation of genes coding for neurexins or their partners have been associated with autism (Reichelt, Rodgers, & Clapcote, 2012; Schaaf et al., 2012), epilepsy (Møller et al., 2013), intellectual disability (ID) (Schaaf et al., 2012), schizophrenia (Kirov et al., 2009; Reichelt et al., 2012), and Gilles de la Tourette syndrome (Huang et al., 2017). Furthermore, autoantibodies directed against neurexin-3α have been described in patients with encephalitis and were shown to alter synapse development in vitro (Gresa-Arribas et al., 2016). Like other members of the neurexin superfamily, CASPR2 is involved in genetic and autoimmune neurological diseases, although its role in the nervous system remains less understood.

Herein, we aim to comprehensively review all available data on CASPR2 functions within the nervous system in relation with the developing field of CASPR2-related diseases in humans.

2 | STRUCTURE, EXPRESSION, AND FUNCTION OF CASPR2

2.1 | CASPR2 structure

Contactin-associated protein-like 2 is a transmembrane protein with a C-terminal intracellular region that contains a 4.1B-binding motif (4.1Bb), also called Glycophorin-NeurexinIV-Paranodin (GNP) motif and a type II PDZ-binding motif (PDZb) (Figure 1a) allowing, respectively, its interaction with cytoskeleton-associated proteins containing a Four-point-one, Ezrin, Radixin, Moesin (FERM) domain, and scaffolding proteins (Denisenko-Nehrbass et al., 2003;

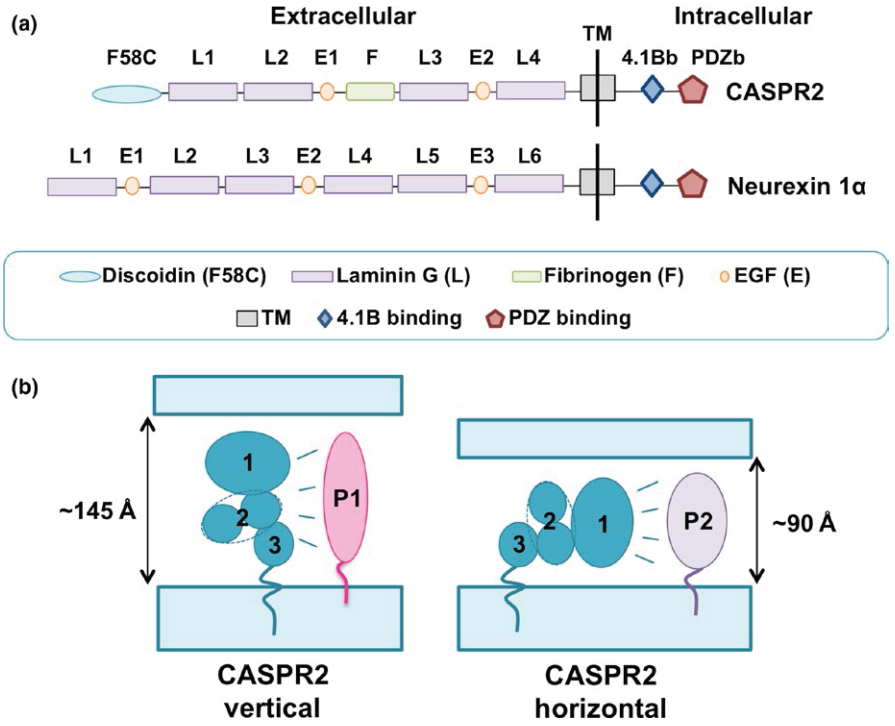

FIGURE 1 Domain organization and 3D structure of CASPR2 and neurexin-1α. (a) CASPR2 and neurexin-1α both contain extracellular laminin G-like domains (L) and EGF-like domains (E), a transmembrane domain (TM) and intracellular 4.1B- and PDZ-binding motifs. In contrast, CASPR2 contains two supplemental extracellular domains: a discoidin-like domain (F58C) and a fibrinogen-like domain (F). (b) Structure of CASPR2 proposed by Lu et al. (2016). CASPR2 is a ~145 Å-long, ~90 Å-wide, and ~50 Å-thick protein composed of three lobes (1, 2, and 3) flexible between each other allowing vertical or horizontal presentations. Such flexibility could reveal different domains of the protein and thus modulate its binding capability with multiple partners (P1 and P2). Furthermore, the localization of the protein at multiple neuronal subcellular regions could vary depending on its orientation. For example only horizontal CASPR2 could fit in the narrow inhibitory synaptic cleft (Lu et al., 2016)

Horresh, Bar, Kissil, & Peles, 2010; and Horresh et al., 2008). The extracellular part of CASPR2 is composed of an N-terminal discoidin-like domain (F58C), four laminin G-like domains (L1–L4), two epidermal growth factor-like (EGF) domains (E1-E2), and a fibrinogen-like domain (F; Figure 1a) (Poliak et al., 1999).

The amino acid sequence of CASPR2 is close to that of neurexin-1α; these two proteins present homologous intracellular 4.1B- and PDZ-binding motifs as well as laminin G-like or EGF-like extracellular domains. On the other hand, the N-terminal discoidin-like domain and the fibrinogen-like domain are specific to CASPR2 (Figure 1a) (Poliak et al., 1999). Differences between the two proteins were also evidenced by recent electron microscopy studies; CASPR2 appeared as a compact protein while neurexin-1α presents an elongated structure (Lu et al., 2016; Rubio-Marrero et al., 2016). Notably, CASPR2 is organized into three lobes flexible between each other, which could harbor two main orientations, vertical, or horizontal (Figure 1b) (Lu et al., 2016). Such flexibility could eventually modulate its binding capability with multiple partners and its localization at multiple neuronal subcellular regions (Figure 1b) (Lu et al., 2016).

2.2 | CASPR2 expression

In the adult mouse brain, CASPR2 is strongly expressed in the cortex, in areas related to motor activities, such as the basal ganglia, the substantia nigra, and the pontine nucleus as well as in areas of the limbic circuitry including the hippocampus, the amygdala, the interpeduncle nucleus, and the mammillary bodies (Gordon et al., 2016). CASPR2 expression is also found in nervous structures involved in sensory pathways including the visual, olfactory, auditory, gustatory, and somatosensory systems. For all these sensory modalities, CASPR2 was first detected in primary sensory organs then in specific brainstem and thalamic nuclei and finally in the corresponding cortical areas (Gordon et al., 2016). In the developing rodent nervous system CASPR2 is detected prenatally from embryonic day 14 (E14) and gradually increases through to adulthood following a posterior to anterior progression pattern (Gordon et al., 2016; Peñagarikano et al., 2011; Poliak et al., 1999). In the hippocampus, CASPR2 is detected initially in the dentate gyrus (DG) at E18. From postnatal day 7 (P7) to adult, CASPR2 expression decreases in the DG and increases gradually in the CA1 and CA2 regions (Gordon et al., 2016). In the developing cortex, CASPR2 is first detected in the marginal zone at E14 (Peñagarikano et al., 2011). At later postnatal stages, its expression gradually migrates into deeper layers in such a way that in adults CASPR2 is found in all layers of the cortex (Bakkaloglu et al., 2008; Gordon et al., 2016).

In humans, *CNTNAP2* mRNA is found at low levels in the ovary and prostate, and predominantly in the adult nervous system including the spinal cord and the brain (Poliak et al., 1999). In the latter, it is found in nervous structures similar to those described in rodents (Poliak et al., 1999). However, the pattern of *CNTNAP2* mRNA expression in cortical regions markedly differs between these two species during the early stages of development (Abrahams et al., 2007). Thus, CASPR2 appears specifically enriched in the developing human anterior temporal and prefrontal cortex in contrast to rodents (Abrahams et al., 2007). This may reflect a role of CASPR2 in higher cognitive functions such as language learning (Abrahams et al., 2007).

In conclusion, the spatiotemporal pattern of CASPR2 expression in different structures of the developing and adult brain points to a role of this protein in the establishment of the neuronal network and its involvement in sensory and higher cognitive functions in the mature nervous system.

At the cellular level, CASPR2 is detected in a large variety of neurons in adult rat brain (Poliak et al., 1999). In the pyramidal neurons of the CA3 region of the hippocampus and of the cortex, it is expressed at both soma and dendrites (Poliak et al., 1999). CASPR2 is also enriched at the distal part of the axon initial segment (AIS) and in the juxtaparanodal (JPX) region of nodes of Ranvier (NOR) present on myelinated axons of the peripheral and central nervous system (Figure 2a, b, and c) (Inda, DeFelipe, & Muñoz, 2006; Ogawa et al., 2008; Poliak et al., 1999; Scott et al., 2017).

In cultured hippocampal neurons at DIV4, 58% of the GAD65-positive inhibitory neurons expressed CASPR2 versus only 4% of the GAD65-negative excitatory neurons (Pinatel et al., 2015). This suggests that in vitro, CASPR2 expression is found in a subpopulation of neurons and preferentially in inhibitory neurons. At this stage of culture, CASPR2 was expressed at the surface of neurons both in the somato-dendritic and axonal compartments. At later stages (DIV7–DIV8) a decrease in CASPR2 surface expression was observed in the somato-dendritic compartment through endocytic retrieval (Bel, Oguievetskaia, Pitaval, Goutebroze, & Faivre-Sarrailh, 2009; Pinatel et al., 2015). Thus, the maturation of cultured hippocampal neurons is associated with a redistribution of surface CASPR2 with a preferential localization along axons. CASPR2 is also found in the synaptic membrane fraction (Bakkaloglu et al., 2008) and in synaptosomes (Chen et al., 2015). CASPR2 partially colocalized with presynaptic markers such as VGLUT1 and VGAT, which identify excitatory and inhibitory synapses, respectively, (Pinatel et al., 2015) and with excitatory postsynaptic AMPA receptor GluA1 subunit (Figure 2d) (Varea et al., 2015). In agreement with the preferential expression of CASPR2 in GAD65-positive inhibitory neurons, a strong colocalization was observed with presynaptic terminals positive for GAD65 apposed to Gephyrin clusters, characterizing the inhibitory postsynaptic compartment (Pinatel et al., 2015). Together, these data suggest that in cultured hippocampal neurons, CASPR2 is preferentially associated with inhibitory axonal presynaptic sites (Figure 2d).

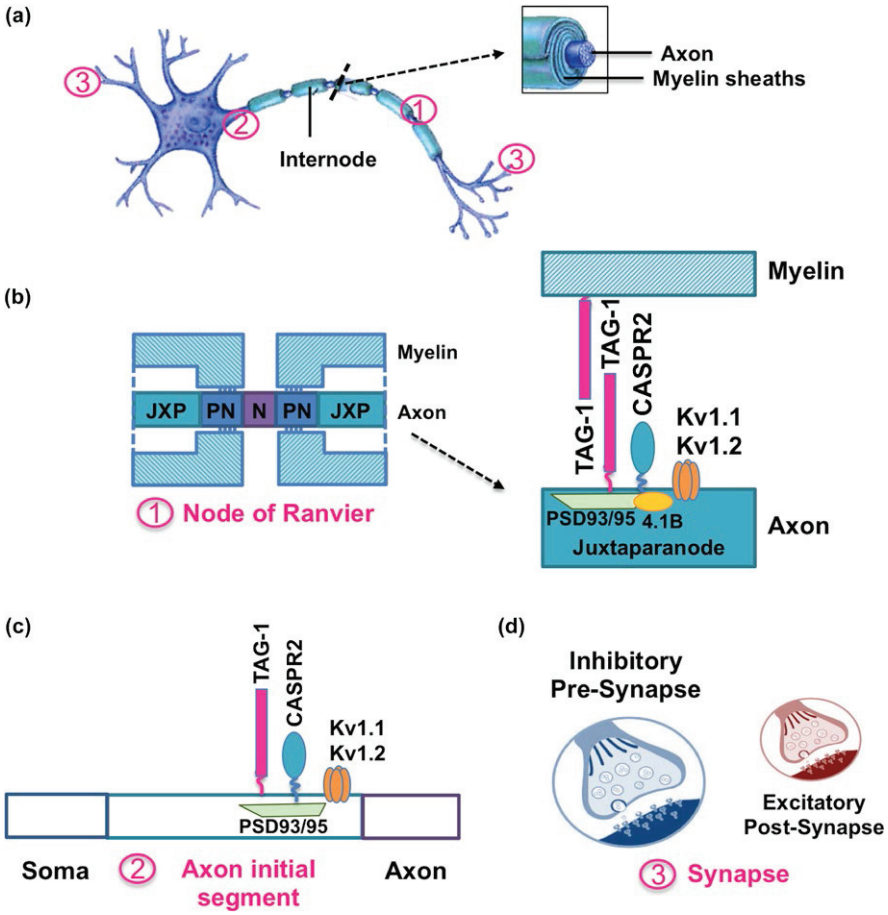

FIGURE 2 CASPR2 localization and partners. (a) CASPR2 can be found in a diversity of subcellular compartments: the node of Ranvier (1), the axon initial segment (2), and the synapse (3). (b) At the node of Ranvier (1), CASPR2 is located in the juxtaparanodal region, under the myelin sheaths. In this region, CASPR2 is essential for the clustering and localization of Kv1, TAG-1, PSD-93, and PSD-95. CASPR2 interacts with the Kv1.1 and Kv1.2 channels through its binding to the 4.1B protein. CASPR2 also interacts with axonal TAG-1 in cis which interacts with glial TAG-1 in trans. N: Node, PN: Paranode, JXP: Juxtaparanode. (c) At the axon initial segment (2), CASPR2 is mainly found in the distal region. It is also found in complex with Kv1.1, Kv1.2, and TAG-1 but does not seem essential for their correct localization. (d) At the synapse (3), CASPR2 seems mainly found in inhibitory presynaptic compartment and to a lower extent in excitatory postsynaptic compartment

In summary, it appears difficult to restrain CASPR2 to a single type of synapse although its localization in inhibitory synapse seems more obvious. Even though CASPR2 appears preferentially expressed in the presynaptic axonal terminals, further studies are needed to determine without ambiguity its synaptic distribution.

2.3 | CASPR2 function

2.3.1 | CASPR2, organizer of axonal microdomains

A striking feature of CASPR2 enrichment at the AIS and NOR is its close vicinity with the voltage-gated potassium channels (VGKC) of the Kv1 subfamily, Kv1.1 and Kv1.2 (Figure 2b and c) (Poliak et al., 1999), that are essential for the repolarization of the neuronal membrane following an action potential (Lai & Jan, 2006).

Nodes of Ranvier are small axonal sections devoid of myelin, separating two myelinated segments also known as internodes (Figure 2a). The node is characterized by a high density of voltage-dependent sodium channels and flanked by two distinct regions of the axolemma, the paranodal (PN) junction, and the juxtaparanodal (JXP) region, both characterized by the organization of macromolecular complexes (Figure 2b) (Rasband & Peles, 2015). The JXP are characterized by a molecular complex consisting of Kv1, CASPR2, and TAG-1 (Transient Axonal Glycoprotein-1), a glycosylphosphatidylinositol (GPI)-anchored adhesion molecule of the Ig superfamily also referred to as Axonin-1 or Contactin-2 (Figure 2b) (Poliak et al., 2003; Rasband et al., 2002; Traka et al., 2003).

In CASPR2 KO mice, Kv1 and TAG-1 were no longer enriched at the JXP (Poliak et al., 2003; Scott et al., 2017). In the same way, in TAG-1 KO mice, Kv1 and CASPR2 were both mislocalized (Traka et al., 2003). The interdependent

relationship between these three proteins put into light the requirement of a CASPR2/TAG-1 cell adhesion complex for Kv1 positioning at the JXP. While CASPR2 and Kv1 were shown to be expressed at the axonal membrane, TAG-1 was present on both the axonal and the glial membrane (Poliak et al., 1999; Traka, Dupree, Popko, & Karagogeos, 2002) (Figure 2b). Based on the well-described TAG-1/TAG-1 trans-homophilic-binding propensity (Kunz et al., 2002) and the well-documented direct interaction between CASPR2 and TAG-1 through their extracellular domains (Lu et al., 2016; Pinatel et al., 2015; Poliak et al., 2003; Savvaki et al., 2010; Traka et al., 2003; Tzimourakas, Giasemi, Mouratidou, & Karagogeos, 2007), it was postulated that axonal TAG-1 interacts in trans with glial TAG-1 and in cis with CASPR2 allowing Kv1 clustering (Figure 2b).

These results were later on questioned by a transgenic mice model expressing TAG-1 exclusively in glial cells (*Tag*-1-/-; plp Tg(r*Tag*-1)) in which, at least in the CNS, the JXP complex formed normally. In this model, TAG-1, CASPR2, and Kv1.2 were also found in the same immunoprecipitated complex (Savvaki et al., 2010). It was, therefore, postulated that glial TAG-1 was sufficient to form a trans-complex with axonal CASPR2. Indeed, using different experimental settings, both cis- and trans-TAG-1/CASPR2 interactions have been reported (Poliak et al., 2003; Savvaki et al., 2010; Traka et al., 2003). However, using a neuron/HEK293 coculture assay, other authors showed that TAG-1/TAG-1 but not TAG-1/ CASPR2 transinteractions allowed Kv1.2 cluster formation on axonal membranes (Gu & Gu, 2011). Therefore, there is an apparent confusion regarding the mechanisms involved in CASPR2/TAG-1/Kv1 association. This may arise from the contribution of a soluble form of TAG-1 released by neuronal and glial cells which could modulate the binding of glial TAG-1 with axonal CASPR2 (Savvaki et al., 2010; Stoeckli, Kuhn, Duc, Ruegg, & Sonderegger, 1991).

In addition, the cytoplasmic domain of CASPR2 has been shown to be sufficient to coprecipitate Kv1.2 and its Kvbeta subunit from rat brain membrane lysate (Horresh et al., 2010; Poliak et al., 1999) and to be required for the JXP complex formation (Horresh et al., 2010). As both CASPR2 and Kv1.2 contain a PDZ-binding domain (Poliak et al., 1999) it was initially proposed that their association was mediated through a common PDZ domain-containing protein such as PSD-93 or PSD-95, and that these scaffold proteins could participate in the assembly of the JXP complex (Poliak et al., 1999). However, in mice knocked out for PSD-95 (Rasband et al., 2002), PSD-93 or both PSD-95 and PSD-93 (Horresh et al., 2008), or in mice in which the PDZ-binding motif of CASPR2 was deleted (Horresh et al., 2008), the JXP complex assembled normally indicating that this process does not rely on PDZ-binding motif. Conversely, CASPR2 and TAG-1 were necessary for PSD-93 and PSD-95 accumulation at JXP (Horresh et al., 2008). In contrast, CASPR2 was shown to interact with the 4.1B cytoskeletal protein (Denisenko-Nehrbass et al., 2003) and this interaction appeared necessary for JXP complex formation. Indeed, in 4.1B-/- mice or in mice in which the 4.1B-binding motif of CASPR2 was deleted not only CASPR2 but also Kv1, TAG-1, and PSD-93 were no longer accumulated at the JXP (Buttermore et al., 2011; Cifuentes-Diaz et al., 2011; Einheber et al., 2013; Horresh et al., 2010).

Although the NOR is critical for AP propagation, it has been commonly assumed that the AIS is the site at which the AP is generated (Nelson & Jenkins, 2017). Another organization that likely contributes to the control of AP generation was referred to as heminode. Identified in motor neurons, this region is adjacent to the AIS, where the myelin sheath begins, and composed of a paranode-type (para-AIS) as well as a juxtaparanode-type (JXP-AIS) compartment (Duflocq, Chareyre, Giovannini, Couraud, & Davenne, 2011). CASPR2 colocalize with TAG-1 and Kv1 in the distal region of the AIS (Figure 2c), and at the JXP-AIS (Duflocq et al., 2011; Inda et al., 2006; Ogawa et al., 2008, 2010). For unknown reasons, CASPR2 enrichment at this site was not always observed in neurons cultured in vitro (Pinatel et al., 2017). Distinctly from the JXP, Kv1 proper positioning at the AIS and JXP-AIS does not rely on CASPR2 or TAG-1 expression (Duflocq et al., 2011; Ogawa et al., 2010). Nevertheless, a positive correlation between the amount of Kv found at the AIS and CASPR2 or TAG-1 expression has been reported (Pinatel et al., 2017). With respect to the involvement of PSD-93 in Kv1 positioning at the AIS, a decrease in Kv expression was observed in cultured hippocampal neurons treated with PSD-93 shRNA (Ogawa et al., 2008), whereas no alterations were detected in PSD-93 or PSD-93/PSD-95 KO mice (Ogawa et al., 2010). Therefore, despite similar protein components, distinct mechanisms are responsible for the molecular assembly of the JXP and the AIS.

In addition, there is increasing evidence that Kv1 associate into large complex with proteins other than CASPR2 and TAG-1, controlling their localization and activity. These include Kvbeta2, cytoplasmic LGI1, scaffold and adaptor proteins as well as adhesion molecules such as ADAM-22, ADAM-23, and secreted LGI1 (Fukata et al., 2010). This complex was further put into light through neuropathy-associated autoantibodies (see below) and referred to as the VGKC complex (Irani et al., 2010; Lai et al., 2010). Moreover, the existence of this complex was recently confirmed by CASPR2 immunoprecipitation from a hippocampal synaptosomal fraction followed by quantitative mass spectrometry (Chen et al., 2015). Interestingly, by performing the same experiments in CASPR2 KO mice the authors found that LGI1, Kvbeta2, and ADAM22 coprecipitated with a small isoform of CASPR2 present in both WT and KO mice at a level 10 times lower than full-length CASPR2 (Chen et al., 2015). As

this isoform is truncated for almost all the extracellular parts, interactions with these partners are likely to rely on CASPR2 intracellular domains.

Other proteins interacting with CASPR2 cytoplasmic domains have been reported, for which function may lie outside of the JXP or AIS complex assembly. Among these, are several scaffolding proteins interacting directly (i.e., MPPs and CASK), or indirectly (i.e., SAP97), with CASPR2 (Chen et al., 2015; Horresh et al., 2008; Tanabe, Fujita-Jimbo, Momoi, & Momoi, 2015). CASPR2 was also shown to interact intracellularly with carboxypeptidase E that may allow CASPR2 trafficking to the dendritic membrane through a Golgi-dependent pathway (Oiso et al., 2009).

2.3.2 | CASPR2-associated microdomains in action potential propagation

Although the role of CASPR2 in Kv1 and TAG-1 clustering at the juxtaparanodal region of the NOR is well documented, the function of this complex in neuronal activity remains unclear. Given that in adulthood, once the myelination process is completed, JXP Kv1 channels are electrically isolated from the node of Ranvier by compact myelin, their functional implication in AP propagation is still a matter of debate (for review see Rosenbluth, Mierzwa, & Shroff, 2013). Notably, they were shown to play a role in small but not large myelinated axon (Devaux & Gow, 2008). In line with this issue, despite JXP complex mislocalization in *Cntnap2* KO mice, the myelination process as well as the AP conduction velocity and refractory period appeared normal in sciatic and optic nerves (Poliak et al., 2003). In contrast, by recording the global axonal electrical activity in acute cortical slice of 8-week-old *Cntnap2* KO animals, a decrease in fiber volleys amplitudes was observed with a slowdown of the AP repolarization phase that could be attributed to improper Kv1 distribution. This led to an increase in neurotransmitter release and a consecutive increase in postsynaptic excitatory responses (Scott et al., 2017). According to these findings, Kv1 surface expression was decreased at the soma of a subpopulation of DRG neurons in *Cntnap2* KO mice, rendering them hyperexcitable (Dawes et al., 2018). These results strengthened the idea that CASPR2 affects intrinsic neuronal excitability by impacting Kv1 distribution at the neuronal membrane. Of note, such neuronal electrophysiological properties changes could account for the alterations of the neuromuscular junction found in *Cntnap2* KO mice at P180 (Saifetiarova, Liu, Taylor, Li, & Bhat, 2017).

Although the role of VGKC complexes at the JXP remains unclear in fully myelinated axons, they were found to play a role in axonal excitability before or during axonal myelination (Vabnick et al., 1999). Interestingly, at the age of 3 weeks, a time at which the myelination process is ongoing, myelination was delayed in *Cntnap2* KO mice and this defect coincided with impaired conduction that was manifested by a lower average speed of AP propagation (Scott et al., 2017). Importantly, those defects in a phase critical for neuronal network development may affect its dynamics and perturb the consolidation of long-range functional connectivity (Liska et al., 2018; Scott-Van Zeeland et al., 2010).

2.3.3 | CASPR2 in network formation

The function of CASPR2 has thus been extended beyond its role as an organizer of axonal microdomains and was proposed to play a role in the formation of the neuronal network during development. Indeed, *Cntnap2* KO mice displayed cortical neuronal migration abnormalities manifested by ectopic neurons in the corpus callosum and abnormal distribution of cortical projections in the somato-sensory cortex (Peñagarikano et al., 2011). Accordingly, asynchronous neuronal firing was found in these mice, likely due to network dysfunction rather than abnormal neuronal activity *per se* (Peñagarikano et al., 2011).

Another important feature of *Cntnap2* KO mice at postnatal day 14 or 30 is the deficit of some subpopulations of inhibitory GABAergic interneurons (i.e., no defect in the production/migration or survival but defect in their differentiation/activity), in the striatum, the hippocampus, and the somato-sensory cortex (Peñagarikano et al., 2011; Vogt et al., 2017). Accordingly, CASPR2 was proposed to cell autonomously regulate the electrophysiological properties of the cortical parvalbumin-positive (PV+) interneurons (Vogt et al., 2017). Consistent with the notion of a disrupted inhibition, CA1 pyramidal cells recordings in acute hippocampal slices from *Cntnap2* KO mice showed an alteration of inhibitory but not excitatory transmission (Jurgensen & Castillo, 2015). More precisely, the alteration of inhibition was only found on the perisomatic but not dendritic compartment. This alteration was not due to a reduction in neurotransmitter release but most likely to the loss of PV+ interneurons, that normally highly innervate the perisomatic regions of the recorded neurons (Jurgensen & Castillo, 2015). Similar results were found in pyramidal cells of the visual cortex 2/3 layers in cortical slices from 6 to 8-week-old (but not 3 to 4 week old) *Cntnap2* KO mice, with reduced phasic and tonic inhibitions (Bridi, Park, & Huang, 2017). The fact that in the visual cortex neither intrinsic excitability nor the spike features were altered in these mice supports a developmental role for CASPR2 in the maturation and stability of GABAergic synapses (Bridi et al., 2017). In contrast to these findings, Scott et al. (2017) did not find any deficit of inhibitory GABAergic interneurons in the somatosensory cortex or any deficits in inhibitory postsynaptic currents in adult *Cntnap2* KO mice (Scott et al., 2017). Further investigations are needed to explain these discrepancies.

In addition, CASPR2 was shown to play a role in neurite outgrowth. A decrease in neurite outgrowth was observed at DIV 3 in culture of cortical neurons established from *Cntnap2* KO

mice embryos (E14) (Canali et al., 2018) but not from newborn mice (P0) (Varea et al., 2015). In addition, *Cntnap2* knockdown at DIV4 (using shRNA) in cortical neuronal cultures from newborn mice (P0) induced a decrease in neurite outgrowth and dendritic arborization at DIV14-18 (Anderson et al., 2012).

Contactin-associated protein-like 2 was also involved in synapse formation, as a lower number of spines was found in *Cntnap2* KO cortical neurons in vitro and in vivo (Gdalyahu et al., 2015; Varea et al., 2015). Furthermore, smaller spine heads were found in DIV14-18 cortical cultures knocked down for *Cntnap2* (Anderson et al., 2012). In line with these findings, a comparative study of synapse formation dynamics in vivo on *Cntnap2* KO and WT live animals found that CASPR2 is involved in synapse stabilization (Gdalyahu et al., 2015). Of particular interest, the CASPR2-associated synapse stabilization defect could be explained by impaired AMPA receptor trafficking to the synapse (Varea et al., 2015). Overall, these data support a role of CASPR2 in the establishment of neuronal connectivity.

3 | CASPR2 AND NEURODEVELOPMENTAL DISEASES

3.1 | CNTNAP2 mutations

Contactin-associated protein-like 2 is encoded by the *CNTNAP2* gene located in the chromosomal region 7q35 and is one of the genome's largest genes (2.3Mb and 24 exons; NCBI Genebank). The first report of a disorder associated with a *CNTNAP2* mutation dates from 2003; it was found in a father and his two children who all presented with obsessive-compulsive disorder (Verkerk et al., 2003). This disorder was accompanied, for the children, with Gilles de la Tourette syndrome (GTS), which remains to date the only reported case of *CNTNAP2* mutation associated with GTS (Belloso et al., 2007). All three of them harbored a heterozygous chromosomal translocation implying a complex genomic rearrangements thus questioning the clinical significance of this variant. After this first case, an increasing number of *CNTNAP2* alterations have been reported in patients with various neurodevelopmental disorders involving essentially the central nervous system such as autism spectrum disorder (ASD), epilepsy, intellectual disability, speech disorders, schizophrenia, CDFE, and ADHD (reviewed by Rodenas-Cuadrado, Ho, & Vernes, 2014; Poot et al., 2015; and Poot, 2017). Solely one peripheral neuropathy, Charcot–Marie–Tooth disease, has been reported in two sisters with a duplication of the exon 4 of *CNTNAP2* (Høyer et al., 2015).

In this review, we published up-to-date exonic (protein coding) *CNTNAP2* mutations (reported in Figure 3a). Although most of the cases displayed a combination of several of the disorders described above, only the primary clinical feature was depicted (Figure 3a). Neuropathies associated with *CNTNAP2* mutations reported here were often with a childhood onset and in male patients in around 60.9% of the cases. Although *CNTNAP2* mutations were mostly heterozygous, implying that the loss of a single allele might be sufficient to disrupt the function of the protein, some mutations seemed to affect neurodevelopment only in a homozygous state. For example, a homozygous *CNTNAP2* point mutation (3709delG) in exon 22 was reported in 13 Old Ordrer Amish children with cortical dysplasia-focal epilepsy (CDFE) as primary clinical feature. The same mutation was found heterozygous in their parents and four healthy individuals (Strauss et al., 2006). Three other cases with homozygous *CNTNAP2* deletions in the proximal region of the gene were reported (Rodenas-Cuadrado et al., 2016; Watson et al., 2014; Zweier et al., 2009). Patients presented severe ID, early onset drug-resistant epilepsy with concomitant regression of language, communicative impairments, and autistic features.

Importantly, the large spectrum of clinical presentations, the highly complex genetic alterations, and the presence of some *CNTNAP2* variants in healthy individuals indicate the involvement of a combination of factors in *CNTNAP2*-associated diseases (Bakkaloglu et al., 2008; Murdoch et al., 2015). However, in order to determine if specific exons of CNTNAP2 are affected by disease-associated mutations, we compared the distribution of mutations over the 24 exons between the patients reported here and individuals of the global population reported in the Exome Aggregation Consortium (ExAC) database (Lek et al., 2016). Of note, individuals in this database should not present any severe pediatric disease. We counted the number of mutations identified in patients (patient group: a total of 49 mutations including 24 point mutations and 25 deletions/duplications (Copy Number Variation, CNVs)) and in individuals of the ExAC database (ExAC group: a total of 539 natural mutations, including 528 point mutations and 11 CNVs). When taking all types of mutations into account we did not see any tendency towards a particular exon. However, when looking at point mutations and CNVs separately, although no marked difference was observed between the patients and ExAC groups for the point mutations, we found a high number of CNVs impacting the F58C coding exons in the patient group (10.8%, 12.8%, and 6.9% of total mutations on exons 1–3, respectively) but a very low number in the ExAC group (1.7%, 1.7%, and 5.2% of total mutations are on exons 1–3, respectively) (Figure 3a and Figure S1). We find this finding rather striking with regard to the fact that this same domain (F58C) is targeted by autoantibodies in CASPR2-associated autoimmune diseases.

3.2 | Pathological models

Regarding the impact of *CNTNAP2* mutations on CASPR2 expression, folding, or function, some mutations could

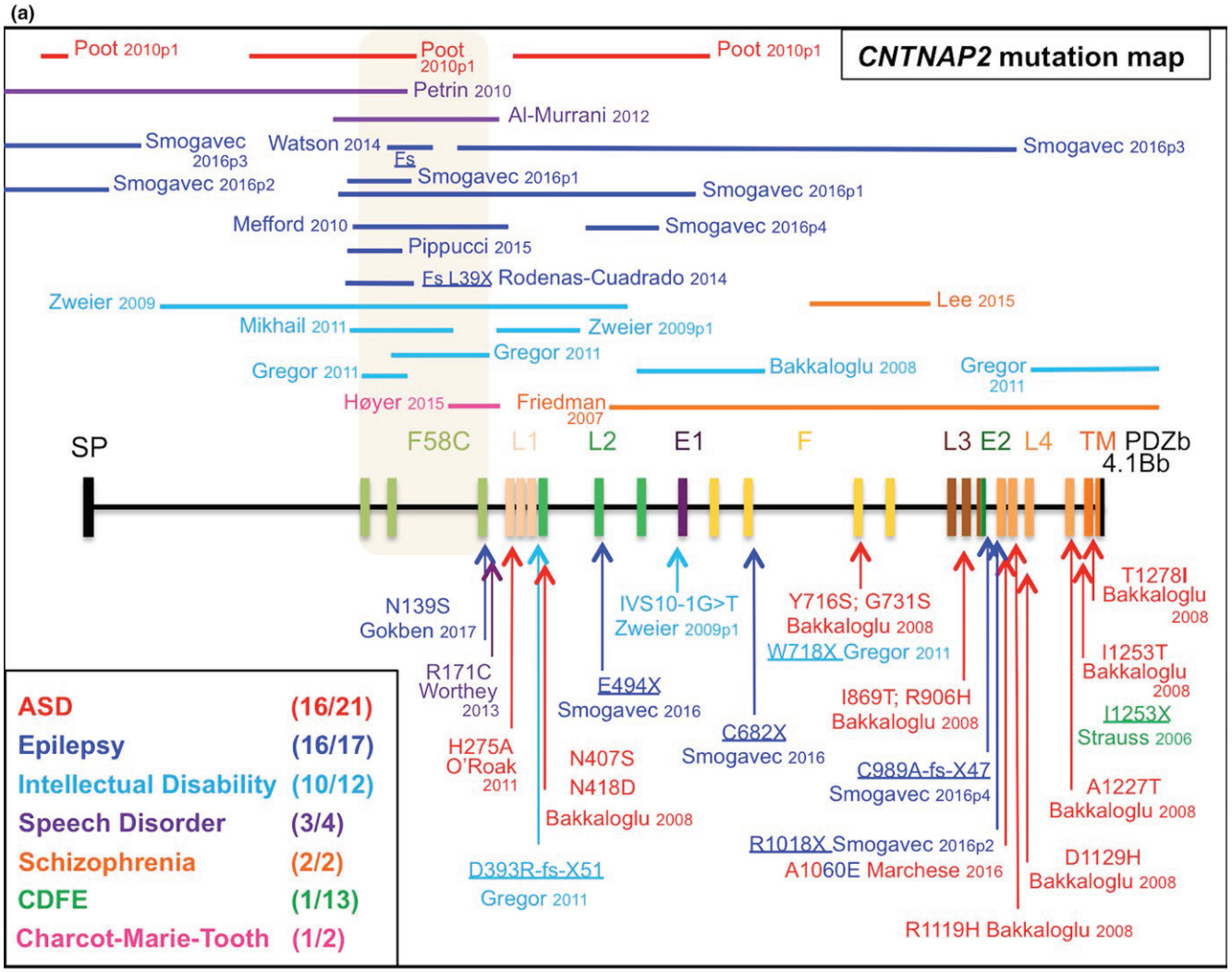

be considered as close to KO mutations (i.e., no protein expressed) like the deletion of exons 2–3 introducing a frameshift that is predicted to cause an early stop codon L39X severely truncating the CASPR2 protein (Rodenas-Cuadrado et al., 2016). Other mutations were studied in HEK cells, for example, the I1253X mutation was shown to produce a truncated and secreted protein (Falivelli et al., 2012), while the D1129H was shown to impact the folding of CASPR2, which is then largely retained in the endoplasmic reticulum (Falivelli et al., 2012). However, this is not enough to fully

FIGURE 3 CASPR2 and genetic diseases. (a) *CNTNAP2* mutation map. The *CNTNAP2* gene and its 24 exons coding for different domains of CASPR2 is presented. Large DNA deletions or duplications (Copy Number Variations, CNVs) are shown by lines above the *CNTNAP2* gene. Point mutations are shown with arrows under the *CNTNAP2* gene and stop mutations are underlined. References (authors' name) are specified for each mutation. The beige quadrant highlights CNVs identified in the F58C coding exons. Some patients present a combination of CNTNAP2 gene mutations indicated with p1 (patient 1) to p4 (patient 4). Primary or main clinical presentations associated with the mutation(s) are presented in different colors (legend box). For each category, the number of distinct mutations and the number of patients are indicated in brackets. Fs: Frameshift. (b) Pathological models of *CNTNAP2* mutations. A *Cntnap2* KO mouse model was developed presenting clinical and biological disorders sometimes close to those found in patients with *CNTNAP2* mutations. The function of *Cntnap2* was also assessed in vitro, using *Cntnap2* knockout and knockdown cultured neurons or reprogrammed fibroblasts from patients with *CNTNAP2* mutations. SP: Signal peptide; F58C: Discoidin-like domain; L: Laminin G-like domain; E: Epidermal growth factor-like domain; TM: Transmembrane domain; 4.1Bb: 4.1B-binding domain; PDZb: PDZ-binding domain

apprehend the impact of a mutation, especially in the case of heterozygous mutations, when the wild-type protein is also expressed. Indeed, in this case, several scenarios are possible including dominant negative mutations and reduced or increased gene dosage, expression or activity (Veitia, Caburet, & Birchler, 2018). A recent study focused on the impact of these heterozygous *CNTNAP2* mutations on axonal growth in vitro (Canali et al., 2018). They found that CASPR2 plays a dose-dependent role in cortical neuron axonal growth and that the R1119H and the N407S mutations had a dominant negative effect on this function. Of particular interest, in COS cells, the R1119H mutant protein oligomerized with wild-type CASPR2 in the endoplasmic reticulum inducing its intracellular retention. Authors also found two mutations, I869T and G731S, which impaired CASPR2/TAG-1 interaction and were unable to rescue axonal growth defects in *Cntnap2* KO cortical neurons (Canali et al., 2018). Thus, heterozygous *CNTNAP2* missense variants may contribute through selective mechanisms to pathogenicity.

Notably, CASPR2 amino acid composition is highly conserved between species; 98.6% homology between human and rhesus macaque and 93.8% between human and mouse (UNIPROT), making animal models very useful for studying its function and related diseases. Indeed, *Cntnap2* homozygous but not heterozygous KO mice presented an ASD-like phenotype associated with hyperactivity and epileptic seizures as well as delayed learning resembling clinical descriptions of patients (Figure 3b) (Peñagarikano et al., 2011; Rendall, Truong, & Fitch, 2016). Furthermore, as documented previously, brain analysis before the onset of epileptic seizures in these mice found no gross morphological changes but neuronal migration abnormalities, reduced number of GABAergic interneurons, and abnormal network activity (Figure 3b) which may contribute to the developmental disorders (ASD, epilepsy, and hyperactivity) found in those mice. Indeed, the ASD-like behavior observed in *Cntnap2* KO mice correlated with an abnormal PV+ interneuron activity (Selimbeyoglu et al., 2017). Of note, alterations in inhibitory network activity can lead to an imbalance between excitatory and inhibitory currents (E/I balance), a mechanism that likely underlies ASD (Nelson & Valakh, 2015). In this regard, the reduction of the E/I balance in *Cntnap2* KO mice was able to acutely rescue their hyperactivity and deficits in social behavior (Selimbeyoglu et al., 2017).

Notably, as reported previously, WT mice transplanted with medial ganglionic eminence (MGE)-derived interneurons isolated from *Cntnap2* KO mice, presented a reduced number of PV+ interneurons (Vogt et al., 2017). This phenotype was rescued by *Cntnap2* gene transduction into KO MGE interneurons but not by 4 *Cntnap2* missense mutants (N407S, N418D, G731S, and T1278I), which could act as null/hypomorphic alleles. Furthermore, a recent study using fibroblasts from patients with heterozygous intragenic deletion of the *CNTNAP2* gene (Lee et al., 2015) reprogrammed them into human-induced pluripotent stem cells (hiPSCs). These cells once differentiated in neurons presented increased *CNTNAP2* expression and increased spontaneous network activity (Flaherty et al., 2017). Together, these findings provide a first link between mutations and their functional implications reinforcing the relationship between mutations and diseases.

4 | CASPR2 AND AUTOIMMUNE DISEASES

The description of anti-CASPR2 antibodies (CASPR2-Abs) derives from the characterization of autoantibodies that initially were thought to target voltage-gated potassium channels (VGKC) (Shillito et al., 1995). First identified in patients with a peripheral nerve hyperexcitability syndrome known as acquired neuromyotonia (NMT) (Shillito et al., 1995), anti-VGKC antibodies (VGKC-Abs) were later reported in patients with Morvan's syndrome (MoS), which mixes NMT and encephalopathy (Liguori et al., 2001), and in patients with autoimmune encephalitis (AE), a pure CNS syndrome characterized by memory disorders and temporal lobe seizures (Buckley et al., 2001; review Newsom-Davis et al., 2003). VGKC-Abs were detected using immunoprecipitation assays, in which VGKC subtypes Kv1.1, 1.2, and 1.6 precipitated from brain lysates with patients' sera immunoglobulins are labeled with ^{25}I-labeled dendrotoxin (Shillito et al., 1995). Recently, it was shown that most of VGKC-Abs do not actually target

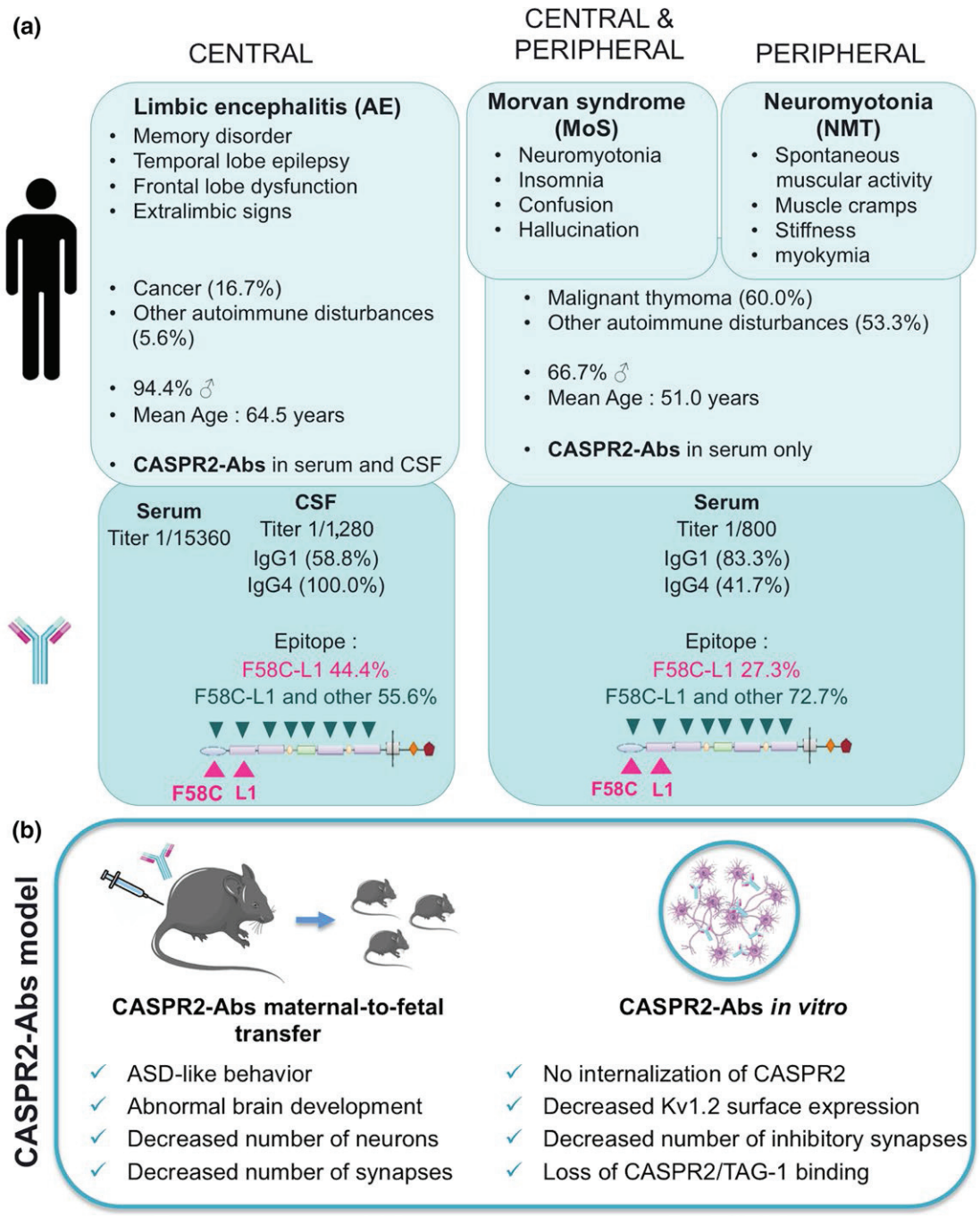

FIGURE 4 CASPR2 and autoimmune diseases. (a) CASPR2 is associated with central and peripheral autoimmune diseases. Patients with central disorders present autoimmune encephalitis (AE) with memory disorders, temporal lobe epilepsy, frontal lobe dysfunction, and extralimbic signs. Association with other autoimmune disturbances or cancer is rare. The disease is mainly found in men around 64.5 years with CASPR2-Abs in the serum and CSF. Patients all present IgG4 subtype CASPR2-Abs in their CSF and the main epitopes are within the discoidin and laminin G1 domains. Patients with peripheral disorders present neuromyotonia with spontaneous muscular activity, muscle cramps, stiffness, and myokimia. Patients with Morvan syndrome present a combination of peripheral and central disorders with neuromyotonia, insomnia, confusion, and hallucinations. Association with other autoimmune disturbances or malignant thymoma is common. The disease is mainly found in men around 51.0 years with CASPR2-Abs in the serum only. Patients mainly have IgG1 subtype CASPR2-Abs and the main epitopes are within the discoidin and laminin G1 domains. F58C: Discoidin-like domain; L1: Laminin G-like domain 1. (b) Effect of CASPR2-Abs. An effect of CASPR2-Abs was found in vivo in a maternal-to-fetal transfer model and in vitro in neuronal cell cultures or ELISA

potassium channels, but CASPR2 and LGI1, that coprecipitate with VGKC subunits in dendrotoxin immunoassays (Irani et al., 2010; Lai et al., 2010; Vincent & Irani, 2010). Clinically, CASPR2-Abs and LGI1-Abs delineate two different groups of syndromes: LGI1-Abs determine a subtype of autoimmune encephalitis with frequent paroxystic facio-brachial dystonia

(Navarro et al., 2016), while CASPR2-Abs associate indifferently with AE, MoS, and NMT (van Sonderen et al., 2016) (Figure 4a). Notably, the late occurrence of these pathologies in patients without any neurological antecedents puts forward a role of CASPR2 in the mature nervous system while neuronal connectivity developed normally.

4.1 | Clinical features

Despite an increasing number of patients reported with CASPR2-Abs over recent years, such cases remain rare (Bien et al., 2017; Joubert et al., 2016; van Sonderen et al., 2016). This rarity, and the clinical overlap that exists between NMT, MoS, and AE, has made systematic clinical analysis difficult. Illustrative of this complexity, most studies failed to clearly delineate clinical subgroups within cohorts of CASPR2-Abs patients (Lancaster et al., 2011; van Sonderen et al., 2016; Vincent & Irani, 2010). However, even if these three syndromes can overlap, NMT, MoS, and AE each have their clinical and immunological specificities (Figure 4a).

Neuromyotonia, or Isaacs' syndrome, is a strictly peripheral syndrome and manifests with stiffness, muscle cramps, fasciculations, myokimia, and mild dysautonomia (Song et al., 2017). Most patients are elderly and male. Electromyography displays spontaneous motor unit activities including fasciculations as well as neuromyotonic and myokimic discharges. These electrophysiological features are not blocked by general anesthesia but disappear after neuromuscular junction blockade, as expected with a peripheral nerve hyperexcitability syndrome (Isaacs, 1961).

Morvan syndrome, however, combines the features of NMT with signs of encephalopathy, such as insomnia, confusion, and hallucinations. There is still a controversy in the current literature as to whether MoS should be considered as a distinct entity or merely as the combination of AE and NMT (van Sonderen et al., 2016). Nonetheless, MoS seems to have distinct features: patients lack the limbic signs characteristic of AE, namely, temporal lobe seizures and anterograde amnesia (Irani et al., 2012). Signs of dysautonomia are particularly severe in MoS patients, who usually present with profuse sweating and tachycardia. Additionally, an underlying malignant thymoma is frequent, as are other autoimmune disorders such as connective tissue disorders and myasthenia gravis (Joubert et al., 2016; van Sonderen et al., 2016).

Autoimmune encephalitis, in contrast, is a pure CNS syndrome that manifests with symptoms of limbic dysfunction, including memory disorders, temporal lobe seizures, and frontal lobe impairment. In addition, one-third of patients have cerebellar ataxia, and 18.0% report neuropathic pain (Joubert et al., 2016; van Sonderen et al., 2016). In the series that we have reported, in which we differentiate MoS encephalopathy from AE, NMT associated with AE in only 10% of the cases (Joubert et al., 2016). Interestingly, various paroxysmal symptoms have been reported, such as orthostatic myoclonus (van Gerpen et al., 2016; Gövert et al., 2016), hyperkinetic movement disorders (Bien et al., 2017), and paroxysmal cerebellar ataxia (Joubert et al., 2017). Most AE patients are elderly and male. The disease is rarely associated with a cancer (16.7%) or with other autoimmune disorders (5.6%) (Joubert et al., 2016; van Sonderen et al., 2016).

4.2 | Immunological features

In the cohort that we have previously reported, patients with NMT or MoS had mainly IgG1 subtype in their sera (83.3%) in association with IgG4 in 41.7% of the cases. Patients with NMT or MoS had detectable CASPR2-Abs only in the serum, but not in the CSF, whereas AE patients had detectable CASPR2-Abs in both serum and CSF, and had higher serum titers (mean titer 1/15360 vs. 1/800) (Figure 4a) (Joubert et al., 2016). This finding is discrepant with previous case reports, possibly due to technical differences between labs, or because of the nonconsensual definition of MoS (Joubert et al., 2016; van Sonderen et al., 2016). The absence of CASPR2-Abs in the CSF of MoS patients is intriguing considering the encephalopathy they present with. As serum titers are much lower in MoS patients compared to LE patients, it is possible that a small number of antibodies are present in their CSF but are not detectable with our current methods. The implication of other, yet unknown, antibodies targeting alternative antigens is another hypothesis (Torres-Vega et al., 2017). In the cases of AE that we have reported, CASPR2-Abs titers were much higher in the serum than in the CSF (mean titer 1/15,360 in serum vs. 1/1,280 in CSF) (Joubert et al., 2016). When present in the CSF, that is, in patients with AE, CASPR2-Abs are always of the IgG4 subtype, sometimes with IgG1 subtype antibodies in 58.8% of the cases (Joubert et al., 2016). In all patients, CASPR2-Abs are polyclonal and target multiple epitopes, which are distributed along the whole protein in around a half of the cases. However, the discoidin-like and the laminin G1-like N-terminal domains seem to be obligatory epitopes (Figure 4a) (Joubert et al., 2016; Olsen, Lai, Dalmau, Scherer, & Lancaster, 2015; Pinatel et al., 2015).

4.3 | Pathological model

The pathophysiology of CASPR2-Abs-related autoimmune disorders remains unclear. In comparison, NMDAR-Abs encephalitis, another AE with autoantibodies targeting NMDA receptors associated with manifestations of subacute limbic symptoms such as amnesia and seizures (Dalmau et al., 2008) has been well documented. NMDAR-Abs have been shown to impair NMDAR functions in vitro (Dalmau et al., 2008; Hughes et al., 2010; Manto, Dalmau, Didelot, Rogemond, & Honnorat, 2010;

Mikasova et al., 2012), likely through cross-linking and internalization of the NMDAR, and to replicate several features of the disease when injected in mice (Planagumà et al., 2015, 2016). Furthermore, since NMDAR-Abs are mainly of the IgG1 subtype, their binding to the NMDAR is likely to have immunological consequences (activation of microglia and adaptative immunity through Fc-γ receptors binding, antibody-mediated cytotoxicity) in addition to these functional effects. In contrast, IgG4 antibodies, which represent the main subtype of CASPR2-Abs, do not activate complement, and bind weakly to Fc-γ receptors (for review see Huijbers et al., 2015). Furthermore, IgG4 antibodies can exchange Fab arms due to the lack of covalent bonds between their heavy chains, leading to bispecificity of a fraction of IgG4 in healthy humans (van der Neut Kolfschoten et al., 2007; Schuurman et al., 1999). IgG4 antibodies induced by immunization with an alloantigen are therefore functionally monovalent and are unable to cross-link antigens and to form immune complexes (van der Zee, van Swieten, & Aalberse, 1986). This unique feature might play a role in IgG4-related autoimmune disorders. In other IgG4-related autoimmune neurological disorders, such as myasthenia gravis with anti-MUSK antibodies, and AE with anti-LGI1 antibodies, experimental data suggest a functional effect of IgG4 autoantibodies without internalization of the targeted antigen (Huijbers et al., 2013; Ohkawa et al., 2013). In agreement, CASPR2-Abs did not induce internalization of their target after a 24-hr incubation period on rat hippocampal neuronal cultures or transfected HEK cells (Patterson, Dalmau, & Lancaster, 2018). Interestingly, in a similar experimental model, CASPR2-Abs from AE patients decreased the number of inhibitory synapses after 1 hr of incubation (Pinatel et al., 2015) which could lead to neuronal hyperexcitability, consistent with the seizures observed in patients (Joubert et al., 2016; van Sonderen et al., 2016). Furthermore, CASPR2-Abs were shown to prevent CASPR2/TAG-1 binding in ELISA assays (Figure 4b) (Patterson et al., 2018). Consequently, a working hypothesis could be that CASPR2-Abs impair CASPR2/TAG-1-dependent Kv1 clustering at the NOR thus altering action potential propagation. However, in two recent studies in which mice were given systemic injections of patient CASPR2-Abs, antibodies did not reach the JXP (Dawes et al., 2018; Manso, Querol, Mekaouche, Illa, & Devaux, 2016). Nevertheless, CASPR2-Abs deposition was observed on the soma of DRG neurons associated with a decrease in Kv1 expression. This decrease was also found at the JXP indicating that CASPR2-Abs could impinge Kv1 longitudinal movement towards this region. This was associated with an increased neuronal excitability, which could account for the pain hypersensitivity found in the CASPR2-Abs-injected mice (Dawes et al., 2018).

Overall, although the mechanism by which CASPR2-Abs lead to AE, NMT, and MoS remains far from clear, a growing body of evidence supports their pathological implication.

4.4 | Antibodies and neurodevelopmental disorders

Several studies suggested that neurodevelopmental disorders such as ASD and ID could be more frequent in children from CASPR2-Abs-positive mothers. Notably, the presence of CASPR2-Abs in the sera of these mothers was not associated with any neurological disorders (Brimberg et al., 2016; Coutinho et al., 2017). More generally, mothers of ASD children tend to more frequently have brain reactive autoantibodies in their sera than controls (Brimberg, Sadiq, Gregersen, & Diamond, 2013; Singer et al., 2008). Furthermore, antibodies injected into pregnant mice were able to access the fetal brain and to affect its development (Dalton et al., 2003; Singer et al., 2009). In a recent study, a maternal-to-fetal transfer experiment in mice was performed using monoclonal CASPR2-Abs cloned from a mother of an ASD child (Brimberg et al., 2016). This resulted in ASD-like behavior and brain morphology defects (abnormal cortical development, decreased dendritic complexity of excitatory neurons, and reduced number of inhibitory neurons in the hippocampus) in the offspring (Brimberg et al., 2016). Similar results were obtained in another study in which pregnant mice were injected with CASPR2-Abs from patients with AE. Offspring presented ASD-like behavior and cellular defects such as glutamatergic neurons mislocalization, microglial cell activation, decreased glutamatergic synapses (Figure 4b) (Coutinho et al., 2017).

These results further implicate CASPR2 in brain development while arguing for a pathogenic effect of CASPR2-Abs.

5 | GENDER

Interestingly, CASPR2-associated diseases seem to target more specifically men; patients with CASPR2 mutation or CASPR2-Abs are mainly male, respectively, 60.9% and 89.5%. Notably, a sex-dependent effect was found on the activity of visual cortex areas in the CASPR2 KO mice (Townsend & Smith, 2017). Furthermore, in the maternal-to-fetal transfer model, CASPR2-Abs from the mother of a child with ASD had an impact on male offspring only (Brimberg et al., 2016). Of note, a similar experiment with CASPR2-Abs from patients with AE did not show any gender effect (Coutinho et al., 2017). Finally, Hoffman et al. (2016) screened pharmacological molecules to find a suppressor for the autism-like behavior in a *Cntnap2* KO zebrafish model. They found that phytoestrogen biochanin A,

an agonist of estrogen receptors, reverses the autism-like behavior (Hoffman et al., 2016) raising the question of gender involvement in CASPR2-associated disease.

6 | CONCLUSION

To conclude, knockout models of CASPR2 revealed its role during development in setting the inhibitory network while studies on CASPR2 mutants provided a first link between mutations and their functional implications in CASPR2-associated genetic diseases. The growing body of evidence supporting a pathological role of CASPR2-Abs in CASPR2-associated autoimmune diseases pinpointed a role of the protein in the mature nervous system. Interestingly, CASPR2-Abs could be used as a tool to study the role of CASPR2 beyond development and to determine the mechanisms underlying CASPR2 function in the nervous system.

ACKNOWLEDGEMENTS

This study is supported by research grants from ANR (ANR-14-CE15-0001-MECANO), CSL Behring France and Fondation pour la recherche médicale FRM DQ20170336751.

CONFLICT OF INTEREST STATEMENT

The authors confirm that they have no potential conflicts of interest with respect to this review article.

DATA ACCESSIBILITY

This publication is supported by multiple datasets, which are openly available at locations cited in the reference section.

AUTHOR CONTRIBUTION

All authors contributed to the writing or critical revision of this manuscript. Furthermore, all authors reviewed the final version of the manuscript.

REFERENCES

Abrahams, B. S., Tentler, D., Perederiy, J. V., Oldham, M. C., Coppola, G., & Geschwind, D. H. (2007). Genome-wide analyses of human perisylvian cerebral cortical patterning. *Proceedings of the National Academy of Sciences of the United States of America*, *104*, 17849–17854. https://doi.org/10.1073/pnas.0706128104

Al-Murrani, A., Ashton, F., Aftimos, S., George, A. M., & Love, D. R. (2012). Amino-terminal microdeletion within the CNTNAP2 gene associated with variable expressivity of speech delay. *Case Reports in Genetics*, *2012*, 172408.

Anderson, G. R., Galfin, T., Xu, W., Aoto, J., Malenka, R. C., & Südhof, T. C. (2012). Candidate autism gene screen identifies critical role for cell-adhesion molecule CASPR2 in dendritic arborization and spine development. *Proceedings of the National Academy of Sciences of the United States of America*, *109*, 18120–18125. https://doi.org/10.1073/pnas.1216398109

Bakkaloglu, B., O'Roak, B. J., Louvi, A., Gupta, A. R., Abelson, J. F., Morgan, T. M., … State, M. W. (2008). Molecular cytogenetic analysis and resequencing of contactin associated protein-like 2 in autism spectrum disorders. *American Journal of Human Genetics*, *82*, 165. https://doi.org/10.1016/j.ajhg.2007.09.017

Bel, C., Oguievetskaia, K., Pitaval, C., Goutebroze, L., & Faivre-Sarrailh, C. (2009). Axonal targeting of Caspr2 in hippocampal neurons via selective somatodendritic endocytosis. *Journal of Cell Science*, *122*, 3403–3413. https://doi.org/10.1242/jcs.050526

Belloso, J. M., Bache, I., Guitart, M., Caballin, M. R., Halgren, C., Kirchhoff, M., … Tümer, Z. (2007). Disruption of the CNTNAP2 gene in a t(7;15) translocation family without symptoms of Gilles de la Tourette syndrome. *European Journal of Human Genetics*, *15*, 711–713. https://doi.org/10.1038/sj.ejhg.5201824

Bien, C. G., Mirzadjanova, Z., Baumgartner, C., Onugoren, M. D., Grunwald, T., Holtkamp, M., … May, T. W. (2017). Anti-contactin-associated protein-2 encephalitis: Relevance of antibody titres, presentation and outcome. *European Journal of Neurology*, *24*, 175–186. https://doi.org/10.1111/ene.13180

Bridi, M. S., Park, S. M., & Huang, S. (2017). Developmental disruption of GABAAR-meditated inhibition in Cntnap2 KO mice. *eNeuro*, *4*, ENEURO.0162-17.2017.https://doi.org/10.1523/ENEURO.0162-17.2017

Brimberg, L., Mader, S., Jeganathan, V., Berlin, R., Coleman, T. R., Gregersen, P. K., … Diamond, B. (2016). Caspr2-reactive antibody cloned from a mother of an ASD child mediates an ASD-like phenotype in mice. *Molecular Psychiatry*, *21*, 1663–1671. https://doi.org/10.1038/mp.2016.165

Brimberg, L., Sadiq, A., Gregersen, P. K., & Diamond, B. (2013). Brain-reactive IgG correlates with autoimmunity in mothers of a child with an autism spectrum disorder. *Molecular Psychiatry*, *18*, 1171–1177. https://doi.org/10.1038/mp.2013.101

Buckley, C., Oger, J., Clover, L., Tüzün, E., Carpenter, K., Jackson, M., & Vincent, A. (2001). Potassium channel antibodies in two patients with reversible limbic encephalitis. *Annals of Neurology*, *50*, 73–78. https://doi.org/10.1002/ana.1097

Buttermore, E. D., Dupree, J. L., Cheng, J., An, X., Tessarollo, L., & Bhat, M. A. (2011). The cytoskeletal adaptor protein band 4.1B is required for the maintenance of paranodal axoglial septate junctions in myelinated axons. *Journal of Neuroscience*, *31*, 8013–8024. https://doi.org/10.1523/JNEUROSCI.1015-11.2011

Canali, G., Garcia, M., Hivert, B., Pinatel, D., Goullancourt, A., Oguievetskaia, K., … Goutebroze, L. (2018). Genetic variants in autism-related CNTNAP2 impair axonal growth of cortical neurons. *Human Molecular Genetics*, *27*, 1941–1954. https://doi.org/10.1093/hmg/ddy102

Chen, L. Y., Jiang, M., Zhang, B., Gokce, O., & Südhof, T. C. (2017). Conditional deletion of all neurexins defines diversity of essential synaptic organizer functions for neurexins. *Neuron*, *94*, 611–625.e4. https://doi.org/10.1016/j.neuron.2017.04.011

Chen, N., Koopmans, F., Gordon, A., Paliukhovich, I., Klaassen, R. V., van der Schors, R. C., … Li, K. W. (2015). Interaction proteomics of canonical Caspr2 (CNTNAP2) reveals the presence of two Caspr2 isoforms with overlapping interactomes. *Biochimica et Biophysica Acta*, *1854*, 827–833. https://doi.org/10.1016/j.bbapap.2015.02.008

Cifuentes-Diaz, C., Chareyre, F., Garcia, M., Devaux, J., Carnaud, M., Levasseur, G., … Goutebroze, L. (2011). Protein 4.1B contributes to the organization of peripheral myelinated axons. *PLoS ONE*, *6*, e25043. https://doi.org/10.1371/journal.pone.0025043

Coutinho, E., Menassa, D. A., Jacobson, L., West, S. J., Domingos, J., Moloney, T. C., … Vincent, A. (2017). Persistent microglial activation and synaptic loss with behavioral abnormalities in mouse offspring exposed to CASPR2-antibodies in utero. *Acta Neuropathologica*, *134*, 567–583. https://doi.org/10.1007/s00401-017-1751-5

Dalmau, J., Gleichman, A. J., Hughes, E. G., Rossi, J. E., Peng, X., Lai, M., … Lynch, D. R. (2008). Anti-NMDA-receptor encephalitis: Case series and analysis of the effects of antibodies. *Lancet Neurology*, *7*, 1091–1098. https://doi.org/10.1016/S1474-4422(08)70224-2

Dalton, P., Deacon, R., Blamire, A., Pike, M., McKinlay, I., Stein, J., … Vincent, A. (2003). Maternal neuronal antibodies associated with autism and a language disorder. *Annals of Neurology*, *53*, 533–537. https://doi.org/10.1002/(ISSN)1531-8249

Dawes, J. M., Weir, G. A., Middleton, S. J., Patel, R., Chisholm, K. I., Pettingill, P., … Bennett, D. L. (2018). Immune or genetic-mediated disruption of CASPR2 causes pain hypersensitivity due to enhanced primary afferent excitability. *Neuron*, *97*, 806–822.e10. https://doi.org/10.1016/j.neuron.2018.01.033

Denisenko-Nehrbass, N., Oguievetskaia, K., Goutebroze, L., Galvez, T., Yamakawa, H., Ohara, O., … Girault, J.-A. (2003). Protein 4.1B associates with both Caspr/paranodin and Caspr2 at paranodes and juxtaparanodes of myelinated fibres. *European Journal of Neuroscience*, *17*, 411–416. https://doi.org/10.1046/j.1460-9568.2003.02441.x

Devaux, J., & Gow, A. (2008). Tight junctions potentiate the insulative properties of small CNS myelinated axons. *Journal of Cell Biology*, *183*, 909. https://doi.org/10.1083/jcb.200808034

Duflocq, A., Chareyre, F., Giovannini, M., Couraud, F., & Davenne, M. (2011). Characterization of the axon initial segment (AIS) of motor neurons and identification of a para-AIS and a juxtapara-AIS, organized by protein 4.1B. *BMC Biology*, *9*, 66. https://doi.org/10.1186/1741-7007-9-66

Einheber, S., Meng, X., Rubin, M., Lam, I., Mohandas, N., An, X., … Salzer, J. L. (2013). The 4.1B cytoskeletal protein regulates the domain organization and sheath thickness of myelinated axons. *Glia*, *61*, 240–253. https://doi.org/10.1002/glia.22430

Falivelli, G., Jaco, A. D., Favaloro, F. L., Kim, H., Wilson, J., Dubi, N., … Comoletti, D. (2012). Inherited genetic variants in autism-related CNTNAP2 show perturbed trafficking and ATF6 activation. *Human Molecular Genetics*, *21*, 4761. https://doi.org/10.1093/hmg/dds320

Flaherty, E., Deranieh, R. M., Artimovich, E., Lee, I. S., Siegel, A. J., Levy, D. L., … Brennand, K. J. (2017). Patient-derived hiPSC neurons with heterozygous CNTNAP2 deletions display altered neuronal gene expression and network activity. *NPJ Schizophr*, *3*, 35. https://doi.org/10.1038/s41537-017-0033-5

Friedman, J. I., Vrijenhoek, T., Markx, S., Janssen, I. M., van der Vliet, W. A., Faas, B. H. W., … Veltman, J. A. (2007). CNTNAP2 gene dosage variation is associated with schizophrenia and epilepsy. *Molecular Psychiatry*, *13*, 261–266.

Fukata, Y., Lovero, K. L., Iwanaga, T., Watanabe, A., Yokoi, N., Tabuchi, K., … Fukata, M. (2010). Disruption of LGI1-linked synaptic complex causes abnormal synaptic transmission and epilepsy. *Proceedings of the National Academy of Sciences of the United States of America*, *107*, 3799. https://doi.org/10.1073/pnas.0914537107

Gdalyahu, A., Lazaro, M., Penagarikano, O., Golshani, P., Trachtenberg, J. T., Geschwind, D. H., & Gescwind, D. H. (2015). The autism related protein contactin-associated protein-like 2 (CNTNAP2) stabilizes new spines: An in vivo mouse study. *PLoS ONE*, *10*, e0125633. https://doi.org/10.1371/journal.pone.0125633

van Gerpen, J. A., Ahlskog, J. E., Chen, R., Fung, V. S. C., Hallett, M., Gövert, F., … Leypoldt, F. (2016). Orthostatic myoclonus associated with Caspr2 antibodies. *Neurology*, *87*, 1187–1188. https://doi.org/10.1212/WNL.0000000000003140

Gokben, S., Onay, H., Yilmaz, S., Atik, T., Serdaroglu, G., Tekin, H., & Ozkinay, F. (2017). Targeted next generation sequencing: The diagnostic value in early-onset epileptic encephalopathy. *Acta Neurologica Belgica*, *117*, 131–138. https://doi.org/10.1007/s13760-016-0709-z

Gokce, O., & Südhof, T. C. (2013). Membrane-tethered monomeric neurexin LNS-domain triggers synapse formation. *Journal of Neuroscience*, *33*, 14617. https://doi.org/10.1523/JNEUROSCI.1232-13.2013

Gordon, A., Salomon, D., Barak, N., Pen, Y., Tsoory, M., Kimchi, T., & Peles, E. (2016). Expression of Cntnap2 (Caspr2) in multiple levels of sensory systems. *Molecular and Cellular Neurosciences*, *70*, 42–53. https://doi.org/10.1016/j.mcn.2015.11.012

Gövert, F., Witt, K., Erro, R., Hellriegel, H., Paschen, S., Martinez-Hernandez, E., … Leypoldt, F. (2016). Orthostatic myoclonus associated with Caspr2 antibodies. *Neurology*, *86*, 1353–1355. https://doi.org/10.1212/WNL.0000000000002547

Graf, E. R., Zhang, X., Jin, S.-X., Linhoff, M. W., & Craig, A. M. (2004). Neurexins induce differentiation of GABA and glutamate postsynaptic specializations via neuroligins. *Cell*, *119*, 1013–1026. https://doi.org/10.1016/j.cell.2004.11.035

Gregor, A., Albrecht, B., Bader, I., Bijlsma, E. K., Ekici, A. B., Engels, H., … Zweier, C. (2011). Expanding the clinical spectrum associated with defects in CNTNAP2 and NRXN1. *BMC Medical Genetics*, *12*, 106. https://doi.org/10.1186/1471-2350-12-106

Gresa-Arribas, N., Planagumà, J., Petit-Pedrol, M., Kawachi, I., Katada, S., Glaser, C. A., … Dalmau, J. (2016). Human neurexin-3α antibodies associate with encephalitis and alter synapse development. *Neurology*, *86*, 2235–2242. https://doi.org/10.1212/WNL.0000000000002775

Gu, C., & Gu, Y. (2011). Clustering and activity tuning of Kv1 channels in myelinated hippocampal axons. *Journal of Biological Chemistry*, *286*, 25835–25847. https://doi.org/10.1074/jbc.M111.219113

Hoffman, E. J., Turner, K. J., Fernandez, J. M., Cifuentes, D., Ghosh, M., Ijaz, S., … Giraldez, A. J. (2016). Estrogens suppress a behavioral phenotype in zebrafish mutants of the autism risk gene, CNTNAP2. *Neuron*, *89*, 725–733. https://doi.org/10.1016/j.neuron.2015.12.039

Horresh, I., Bar, V., Kissil, J. L., & Peles, E. (2010). Organization of myelinated axons by Caspr and Caspr2 requires the cytoskeletal adapter protein 4.1B. *Journal of Neuroscience*, *30*, 2480–2489. https://doi.org/10.1523/JNEUROSCI.5225-09.2010

Horresh, I., Poliak, S., Grant, S., Bredt, D., Rasband, M. N., & Peles, E. (2008). Multiple molecular interactions determine the clustering of Caspr2 and Kv1 channels in myelinated axons. *Journal of Neuroscience*, *28*, 14213–14222. https://doi.org/10.1523/JNEUROSCI.3398-08.2008

Høyer, H., Braathen, G. J., Eek, A. K., Nordang, G. B. N., Skjelbred, C. F., & Russell, M. B. (2015). Copy number variations in a population-based study of Charcot-Marie-Tooth disease. *BioMed Research International*, *2015*, 960404.

Huang, A. Y., Yu, D., Davis, L. K., Sul, J. H., Tsetsos, F., Ramensky, V., … Coppola, G. (2017). Rare copy number variants in NRXN1 and CNTN6 increase risk for tourette syndrome. *Neuron*, *94*, 1101–1111.e7. https://doi.org/10.1016/j.neuron.2017.06.010

Hughes, E. G., Peng, X., Gleichman, A. J., Lai, M., Zhou, L., Tsou, R., … Balice-Gordon, R. J. (2010). Cellular and synaptic mechanisms of anti-NMDA receptor encephalitis. *Journal of Neuroscience*, *30*, 5866–5875. https://doi.org/10.1523/JNEUROSCI.0167-10.2010

Huijbers, M. G., Querol, L. A., Niks, E. H., Plomp, J. J., van der Maarel, S. M., Graus, F., … Verschuuren, J. J. (2015). The expanding field of IgG4-mediated neurological autoimmune disorders. *European Journal of Neurology*, *22*, 1151–1161. https://doi.org/10.1111/ene.12758

Huijbers, M. G., Zhang, W., Klooster, R., Niks, E. H., Friese, M. B., Straasheijm, K. R., … Verschuuren, J. J. (2013). MuSK IgG4 autoantibodies cause myasthenia gravis by inhibiting binding between MuSK and Lrp4. *Proceedings of the National Academy of Sciences of the United States of America*, *110*, 20783–20788. https://doi.org/10.1073/pnas.1313944110

Inda, M. C., DeFelipe, J., & Muñoz, A. (2006). Voltage-gated ion channels in the axon initial segment of human cortical pyramidal cells and their relationship with chandelier cells. *Proceedings of the National Academy of Sciences of the United States of America*, *103*, 2920. https://doi.org/10.1073/pnas.0511197103

Irani, S. R., Alexander, S., Waters, P., Kleopa, K. A., Pettingill, P., Zuliani, L., … Vincent, A. (2010). Antibodies to Kv1 potassium channel-complex proteins leucine-rich, glioma inactivated 1 protein and contactin-associated protein-2 in limbic encephalitis, Morvan's syndrome and acquired neuromyotonia. *Brain*, *133*, 2734–2748. https://doi.org/10.1093/brain/awq213

Irani, S. R., Pettingill, P., Kleopa, K. A., Schiza, N., Waters, P., Mazia, C., … Vincent, A. (2012). Morvan syndrome: Clinical and serological observations in 29 cases. *Annals of Neurology*, *72*, 241–255. https://doi.org/10.1002/ana.23577

Isaacs, H. (1961). A syndrome of continuous muscle-fibre activity. *Journal of Neurology, Neurosurgery and Psychiatry*, *24*, 319–325. https://doi.org/10.1136/jnnp.24.4.319

Joubert, B., Gobert, F., Thomas, L., Saint-Martin, M., Desestret, V., Convers, P., … Honnorat, J. (2017). Autoimmune episodic ataxia in patients with anti-CASPR2 antibody-associated encephalitis. *Neurology: Neuroimmunology & Neuroinflammation*, *4*, e371.

Joubert, B., Saint-Martin, M., Noraz, N., Picard, G., Rogemond, V., Ducray, F., … Honnorat, J. (2016). Characterization of a subtype of autoimmune encephalitis with anti-contactin-associated protein-like 2 antibodies in the cerebrospinal fluid, prominent limbic symptoms, and seizures. *JAMA Neurology*, *73*, 1115–1124. https://doi.org/10.1001/jamaneurol.2016.1585

Jurgensen, S., & Castillo, P. E. (2015). Selective dysregulation of hippocampal inhibition in the mouse lacking autism candidate gene CNTNAP2. *Journal of Neuroscience*, *35*, 14681–14687. https://doi.org/10.1523/JNEUROSCI.1666-15.2015

Kirov, G., Rujescu, D., Ingason, A., Collier, D. A., O'Donovan, M. C., & Owen, M. J. (2009). Neurexin 1 (NRXN1) deletions in schizophrenia. *Schizophrenia Bulletin*, *35*, 851. https://doi.org/10.1093/schbul/sbp079

Kunz, B., Lierheimer, R., Rader, C., Spirig, M., Ziegler, U., & Sonderegger, P. (2002). Axonin-1/TAG-1 mediates cell-cell adhesion by a cis-assisted trans-interaction. *Journal of Biological Chemistry*, *277*, 4551–4557. https://doi.org/10.1074/jbc.M109779200

Lai, M., Huijbers, M. G. M., Lancaster, E., Graus, F., Bataller, L., Balice-Gordon, R., … Dalmau, J. (2010). Investigation of LGI1 as the antigen in limbic encephalitis previously attributed to potassium channels: A case series. *Lancet Neurology*, *9*, 776–785. https://doi.org/10.1016/S1474-4422(10)70137-X

Lai, H. C., & Jan, L. Y. (2006). The distribution and targeting of neuronal voltage-gated ion channels. *Nature Reviews Neuroscience*, *7*, 548–562. https://doi.org/10.1038/nrn1938

Lancaster, E., Huijbers, M. G. M., Bar, V., Boronat, A., Wong, A., Martinez-Hernandez, E., … Dalmau, J. (2011). Investigations of caspr2, an autoantigen of encephalitis and neuromyotonia. *Annals of Neurology*, *69*, 303–311. https://doi.org/10.1002/ana.22297

Lee, I. S., Carvalho, C. M. B., Douvaras, P., Ho, S.-M., Hartley, B. J., Zuccherato, L. W., … Brennand, K. J. (2015). Characterization of molecular and cellular phenotypes associated with a heterozygousCNTNAP2deletion using patient-derived hiPSC neural cells. *NPJ Schizophr*, *1*, 15019.

Lek, M., Karczewski, K. J., Minikel, E. V., Samocha, K. E., Banks, E., Fennell, T., … MacArthur, D. G. (2016). Analysis of protein-coding genetic variation in 60,706 humans. *Nature*, *536*, 285. https://doi.org/10.1038/nature19057

Liguori, R., Vincent, A., Clover, L., Avoni, P., Plazzi, G., Cortelli, P., … Montagna, P. (2001). Morvan's syndrome: Peripheral and central nervous system and cardiac involvement with antibodies to voltage-gated potassium channels. *Brain*, *124*, 2417–2426. https://doi.org/10.1093/brain/124.12.2417

Liska, A., Bertero, A., Gomolka, R., Sabbioni, M., Galbusera, A., Barsotti, N., … Gozzi, A. (2018). Homozygous loss of autism-risk gene CNTNAP2 results in reduced local and long-range prefrontal functional connectivity. *Cerebral Cortex*, *28*, 1141–1153. https://doi.org/10.1093/cercor/bhx022

Lu, Z., Reddy, M. V. V. V. S., Liu, J., Kalichava, A., Liu, J., Zhang, L., … Rudenko, G. (2016). Molecular architecture of contactin-associated protein-like 2 (CNTNAP2) and its interaction with contactin 2 (CNTN2). *Journal of Biological Chemistry*, *291*, 24133–24147. https://doi.org/10.1074/jbc.M116.748236

Manso, C., Querol, L., Mekaouche, M., Illa, I., & Devaux, J. J. (2016). Contactin-1 IgG4 antibodies cause paranode dismantling and conduction defects. *Brain*, *139*, 1700–1712. https://doi.org/10.1093/brain/aww062

Manto, M., Dalmau, J., Didelot, A., Rogemond, V., & Honnorat, J. (2010). In vivo effects of antibodies from patients with anti-NMDA receptor encephalitis: Further evidence of synaptic glutamatergic dysfunction. *Orphanet Journal of Rare Diseases*, *5*, 31. https://doi.org/10.1186/1750-1172-5-31

Marchese, M., Valvo, G., Moro, F., Sicca, F., & Santorelli, F. M. (2016). Targeted gene resequencing (Astrochip) to explore the tripartite synapse in autism-epilepsy phenotype with macrocephaly. *NeuroMolecular Medicine*, *18*, 69–80. https://doi.org/10.1007/s12017-015-8378-2

Mefford, H. C., Muhle, H., Ostertag, P., von Spiczak, S., Buysse, K., Baker, C., … Eichler, E. E. (2010). Genome-wide copy number variation in epilepsy: Novel susceptibility loci in idiopathic generalized and focal epilepsies. *PLoS Genetics*, *6*, e1000962.

Mikasova, L., De Rossi, P., Bouchet, D., Georges, F., Rogemond, V., Didelot, A., … Groc, L. (2012). Disrupted surface cross-talk between NMDA and Ephrin-B2 receptors in anti-NMDA encephalitis. *Brain*, *135*, 1606–1621. https://doi.org/10.1093/brain/aws092

Mikhail, F. M., Lose, E. J., Robin, N. H., Descartes, M. D., Rutledge, K. D., Rutledge, S. L., … Carroll, A. J. (2011). Clinically relevant single gene or intragenic deletions encompassing critical neurodevelopmental genes in patients with developmental delay, mental retardation, and/or autism spectrum disorders. *American Journal of Medical Genetics*, *155*, 2386–2396. https://doi.org/10.1002/ajmg.a.34177

Missler, M., Zhang, W., Rohlmann, A., Kattenstroth, G., Hammer, R. E., Gottmann, K., & Südhof, T. C. (2003). Alpha-neurexins couple Ca^{2+} channels to synaptic vesicle exocytosis. *Nature*, *423*, 939–948. https://doi.org/10.1038/nature01755

Møller, R. S., Weber, Y. G., Klitten, L. L., Trucks, H., Muhle, H., Kunz, W. S., … EPICURE Consortium (2013). Exon-disrupting deletions of NRXN1 in idiopathic generalized epilepsy. *Epilepsia*, *54*, 256–264. https://doi.org/10.1111/epi.12078

Murdoch, J. D., Gupta, A. R., Sanders, S. J., Walker, M. F., Keaney, J., Fernandez, T. V., … State, M. W. (2015). No evidence for association of autism with rare heterozygous point mutations in Contactin-Associated Protein-Like 2 (CNTNAP2), or in other contactin-associated proteins or contactins. *PLoS Genetics*, *11*, e1004852. https://doi.org/10.1371/journal.pgen.1004852

Navarro, V., Kas, A., Apartis, E., Chami, L., Rogemond, V., Levy, P., … Collaborators (2016). Motor cortex and hippocampus are the two main cortical targets in LGI1-antibody encephalitis. *Brain*, *139*, 1079–1093. https://doi.org/10.1093/brain/aww012

Nelson, A. D., & Jenkins, P. M. (2017). Axonal membranes and their domains: Assembly and function of the axon initial segment and node of Ranvier. *Frontiers in Cellular Neuroscience*, *11*, 136. https://doi.org/10.3389/fncel.2017.00136

Nelson, S. B., & Valakh, V. (2015). Excitatory/inhibitory balance and circuit homeostasis in autism spectrum disorders. *Neuron*, *87*, 684–698. https://doi.org/10.1016/j.neuron.2015.07.033

van der Neut Kolfschoten, M., Schuurman, J., Losen, M., Bleeker, W. K., Martínez-Martínez, P., Vermeulen, E., … Parren, P. W. H. I. (2007). Anti-inflammatory activity of human IgG4 antibodies by dynamic Fab arm exchange. *Science*, *317*, 1554–1557. https://doi.org/10.1126/science.1144603

Newsom-Davis, J., Buckley, C., Clover, L., Hart, I., Maddison, P., Tüzüm, E., & Vincent, A. (2003). Autoimmune disorders of neuronal potassium channels. *Annals of the New York Academy of Sciences*, *998*, 202–210. https://doi.org/10.1196/annals.1254.022

Ogawa, Y., Horresh, I., Trimmer, J. S., Bredt, D. S., Peles, E., & Rasband, M. N. (2008). PSD-93 clusters Kv1 channels at axon initial segments independent of Caspr2. *Journal of Neuroscience*, *28*, 5731–5739. https://doi.org/10.1523/JNEUROSCI.4431-07.2008

Ogawa, Y., Oses-Prieto, J., Kim, M. Y., Horresh, I., Peles, E., Burlingame, A. L., … Rasband, M. N. (2010). ADAM22, a Kv1 channel interacting protein, recruits maguks to juxtaparanodes of myelinated axons. *Journal of Neuroscience*, *30*, 1038. https://doi.org/10.1523/JNEUROSCI.4661-09.2010

Ohkawa, T., Fukata, Y., Yamasaki, M., Miyazaki, T., Yokoi, N., Takashima, H., … Fukata, M. (2013). Autoantibodies to epilepsy-related LGI1 in limbic encephalitis neutralize LGI1-ADAM22 interaction and reduce synaptic AMPA receptors. *Journal of Neuroscience*, *33*, 18161–18174. https://doi.org/10.1523/JNEUROSCI.3506-13.2013

Oiso, S., Takeda, Y., Futagawa, T., Miura, T., Kuchiiwa, S., Nishida, K., … Yamada, K. (2009). Contactin-associated protein (Caspr) 2 interacts with carboxypeptidase E in the CNS. *Journal of Neurochemistry*, *109*, 158–167. https://doi.org/10.1111/j.1471-4159.2009.05928.x

Olsen, A. L., Lai, Y., Dalmau, J., Scherer, S. S., & Lancaster, E. (2015). Caspr2 autoantibodies target multiple epitopes. *Neurology: Neuroimmunology & Neuroinflammation*, *2*, e127.

O'Roak, B. J., Deriziotis, P., Lee, C., Vives, L., Schwartz, J. J., Girirajan, S., … Eichler, E. E. (2011). Exome sequencing in sporadic autism spectrum disorders identifies severe de novo mutations. *Nature Genetics*, *43*, 585–589. https://doi.org/10.1038/ng.835

Patterson, K. R., Dalmau, J., & Lancaster, E. (2018). Mechanisms of Caspr2 antibodies in autoimmune encephalitis and neuromyotonia. *Annals of Neurology*, *83*, 40–51. https://doi.org/10.1002/ana.25120

Peñagarikano, O., Abrahams, B. S., Herman, E. I., Winden, K. D., Gdalyahu, A., Dong, H., … Geschwind, D. H. (2011). Absence of CNTNAP2 leads to epilepsy, neuronal migration abnormalities, and core autism-related deficits. *Cell*, *147*, 235–246. https://doi.org/10.1016/j.cell.2011.08.040

Petrin, A. L., Giacheti, C. M., Maximino, L. P., Abramides, D. V. M., Zanchetta, S., Rossi, N. F., … Murray, J. C. (2010). Identification of a microdeletion at the 7q33-q35 disrupting the CNTNAP2 gene in a Brazilian stuttering case. *American Journal of Medical Genetics. Part A*, *152A*, 3164–3172. https://doi.org/10.1002/ajmg.a.33749

Pinatel, D., Hivert, B., Boucraut, J., Saint-Martin, M., Rogemond, V., Zoupi, L., … Faivre-Sarrailh, C. (2015). Inhibitory axons are targeted in hippocampal cell culture by anti-Caspr2 autoantibodies associated with limbic encephalitis. *Frontiers in Cellular Neuroscience*, *9*, 265.

Pinatel, D., Hivert, B., Saint-Martin, M., Noraz, N., Savvaki, M., Karagogeos, D., & Faivre-Sarrailh, C. (2017). The Kv1-associated molecules TAG-1 and Caspr2 are selectively targeted to the axon initial segment in hippocampal neurons. *Journal of Cell Science*, *130*, 2209–2220. https://doi.org/10.1242/jcs.202267

Pippucci, T., Licchetta, L., Baldassari, S., Palombo, F., Menghi, V., D'Aurizio, R., … Bisulli, F. (2015). Epilepsy with auditory features: A heterogeneous clinico-molecular disease. *Neurology: Genetics*, *1*, e5.

Planagumà, J., Haselmann, H., Mannara, F., Petit-Pedrol, M., Grünewald, B., Aguilar, E., … Dalmau, J. (2016). Ephrin-B2 prevents N-methyl-D-aspartate receptor antibody effects on memory and neuroplasticity. *Annals of Neurology*, *80*, 388–400. https://doi.org/10.1002/ana.24721

Planagumà, J., Leypoldt, F., Mannara, F., Gutiérrez-Cuesta, J., Martín-García, E., Aguilar, E., … Dalmau, J. (2015). Human N-methyl D-aspartate receptor antibodies alter memory and behaviour in mice. *Brain*, *138*, 94–109. https://doi.org/10.1093/brain/awu310

Poliak, S., Gollan, L., Martinez, R., Custer, A., Einheber, S., Salzer, J. L., … Peles, E. (1999). Caspr2, a new member of the neurexin superfamily, is localized at the juxtaparanodes of myelinated axons and associates with K+ channels. *Neuron*, *24*, 1037–1047. https://doi.org/10.1016/S0896-6273(00)81049-1

Poliak, S., Salomon, D., Elhanany, H., Sabanay, H., Kiernan, B., Pevny, L., … Peles, E. (2003). Juxtaparanodal clustering of Shaker-like K+ channels in myelinated axons depends on Caspr2 and TAG-1. *Journal of Cell Biology*, *162*, 1149–1160. https://doi.org/10.1083/jcb.200305018

Poot, M. (2015). Connecting the CNTNAP2 networks with neurodevelopmental disorders *Molecular Syndromology*, *6*, 7–22.

Poot, M. (2017). Intragenic CNTNAP2 deletions: A bridge too far? *Molecular Syndromology*, *8*, 118–130. https://doi.org/10.1159/000456021

Poot, M., Beyer, V., Schwaab, I., Damatova, N., van't Slot, R., Prothero, J., … Haaf, T. (2010). Disruption of CNTNAP2 and

additional structural genome changes in a boy with speech delay and autism spectrum disorder. *Neurogenetics*, *11*, 81–89. https://doi.org/10.1007/s10048-009-0205-1

Rasband, M. N., Park, E. W., Zhen, D., Arbuckle, M. I., Poliak, S., Peles, E., … Trimmer, J. S. (2002). Clustering of neuronal potassium channels is independent of their interaction with PSD-95. *Journal of Cell Biology*, *159*, 663–672. https://doi.org/10.1083/jcb.200206024

Rasband, M. N., & Peles, E. (2015). The nodes of Ranvier: Molecular assembly and maintenance. *Cold Spring Harbor Perspectives in Biology*, *8*, a020495.

Reichelt, A. C., Rodgers, R. J., & Clapcote, S. J. (2012). The role of neurexins in schizophrenia and autistic spectrum disorder. *Neuropharmacology*, *62*, 1519–1526. https://doi.org/10.1016/j.neuropharm.2011.01.024

Rendall, A. R., Truong, D. T., & Fitch, R. H. (2016). Learning delays in a mouse model of Autism Spectrum Disorder. *Behavioral Brain Research*, *303*, 201–207. https://doi.org/10.1016/j.bbr.2016.02.006

Rodenas-Cuadrado, P., Ho, J., & Vernes, S. C. (2014). Shining a light on CNTNAP2: Complex functions to complex disorders. *European Journal of Human Genetics*, *22*, 171–178. https://doi.org/10.1038/ejhg.2013.100

Rodenas-Cuadrado, P., Pietrafusa, N., Francavilla, T., Neve, A. L., Striano, P., & Vernes, S. C. (2016). Characterisation of CASPR2 deficiency disorder – a syndrome involving autism, epilepsy and language impairment. *BMC Medical Genetics*, *17*, 8. https://doi.org/10.1186/s12881-016-0272-8

Rosenbluth, J., Mierzwa, A., & Shroff, S. (2013). Molecular architecture of myelinated nerve fibers: Leaky paranodal junctions and paranodal dysmyelination. *Neuroscientist*, *19*, 629–641. https://doi.org/10.1177/1073858413504627

Rubio-Marrero, E. N., Vincelli, G., Jeffries, C. M., Shaikh, T. R., Pakos, I. S., Ranaivoson, F. M., … Comoletti, D. (2016). Structural characterization of the extracellular domain of CASPR2 and insights into its association with the novel ligand contactin1. *Journal of Biological Chemistry*, *291*, 5788–5802. https://doi.org/10.1074/jbc.M115.705681

Saifetiarova, J., Liu, X., Taylor, A. M., Li, J., & Bhat, M. A. (2017). Axonal domain disorganization in Caspr1 and Caspr2 mutant myelinated axons affects neuromuscular junction integrity, leading to muscle atrophy. *Journal of Neuroscience Research*, *95*, 1373–1390. https://doi.org/10.1002/jnr.24052

Savvaki, M., Theodorakis, K., Zoupi, L., Stamatakis, A., Tivodar, S., Kyriacou, K., … Karagogeos, D. (2010). The expression of TAG-1 in glial cells is sufficient for the formation of the juxtaparanodal complex and the phenotypic rescue of tag-1 homozygous mutants in the CNS. *Journal of Neuroscience*, *30*, 13943–13954. https://doi.org/10.1523/JNEUROSCI.2574-10.2010

Schaaf, C. P., Boone, P. M., Sampath, S., Williams, C., Bader, P. I., Mueller, J. M., … Cheung, S. W. (2012). Phenotypic spectrum and genotype–phenotype correlations of *NRXN1* exon deletions. *European Journal of Human Genetics*, *20*, 1240. https://doi.org/10.1038/ejhg.2012.95

Schuurman, J., Van Ree, R., Perdok, G. J., Van Doorn, H. R., Tan, K. Y., & Aalberse, R. C. (1999). Normal human immunoglobulin G4 is bispecific: It has two different antigen-combining sites. *Immunology*, *97*, 693–698. https://doi.org/10.1046/j.1365-2567.1999.00845.x

Scott, R., Sánchez-Aguilera, A., van Elst, K., Lim, L., Dehorter, N., Bae, S. E., … Marín, O. (2017). Loss of Cntnap2 causes axonal excitability deficits, developmental delay in cortical myelination, and abnormal stereotyped motor behavior. *Cerebral Cortex*. https://doi.org/10.1093/cercor/bhx341

Scott-Van Zeeland, A. A., Abrahams, B. S., Alvarez-Retuerto, A. I., Sonnenblick, L. I., Rudie, J. D., Ghahremani, D., … Bookheimer, S. Y. (2010). Altered functional connectivity in frontal lobe circuits is associated with variation in the autism risk gene CNTNAP2. *Science Translational Medicine*, *2*, 56ra80.

Selimbeyoglu, A., Kim, C. K., Inoue, M., Lee, S. Y., Hong, A. S. O., Kauvar, I., … Deisseroth, K. (2017). Modulation of prefrontal cortex excitation/inhibition balance rescues social behavior inCNTNAP2-deficient mice. *Science Translational Medicine*, *9*, eaah6733. https://doi.org/10.1126/scitranslmed.aah6733

Shillito, P., Molenaar, P. C., Vincent, A., Leys, K., Zheng, W., van den Berg, R. J., … Wintzen, A. R. (1995). Acquired neuromyotonia: Evidence for autoantibodies directed against K+ channels of peripheral nerves. *Annals of Neurology*, *38*, 714–722. https://doi.org/10.1002/(ISSN)1531-8249

Singer, H. S., Morris, C. M., Gause, C. D., Gillin, P. K., Crawford, S., & Zimmerman, A. W. (2008). Antibodies against fetal brain in sera of mothers with autistic children. *Journal of Neuroimmunology*, *194*, 165–172. https://doi.org/10.1016/j.jneuroim.2007.11.004

Singer, H. S., Morris, C., Gause, C., Pollard, M., Zimmerman, A. W., & Pletnikov, M. (2009). Prenatal exposure to antibodies from mothers of children with autism produces neurobehavioral alterations: A pregnant dam mouse model. *Journal of Neuroimmunology*, *211*, 39–48. https://doi.org/10.1016/j.jneuroim.2009.03.011

Smogavec, M., Cleall, A., Hoyer, J., Lederer, D., Nassogne, M.-C., Palmer, E. E., … Zweier, C. (2016). Eight further individuals with intellectual disability and epilepsy carrying bi-allelic CNTNAP2 aberrations allow delineation of the mutational and phenotypic spectrum. *Journal of Medical Genetics*, *53*, 820–827. https://doi.org/10.1136/jmedgenet-2016-103880

van Sonderen, A., Ariño, H., Petit-Pedrol, M., Leypoldt, F., Körtvélyessy, P., Wandinger, K.-P., … Titulaer, M. J. (2016). The clinical spectrum of Caspr2 antibody-associated disease. *Neurology*, *87*, 521–528. https://doi.org/10.1212/WNL.0000000000002917

Song, J., Jing, S., Quan, C., Lu, J., Qiao, X., Qiao, K., … Zhao, C. (2017). Isaacs syndrome with CASPR2 antibody: A series of three cases. *Journal of Clinical Neuroscience*, *41*, 63–66. https://doi.org/10.1016/j.jocn.2017.02.063

Stoeckli, E. T., Kuhn, T. B., Duc, C. O., Ruegg, M. A., & Sonderegger, P. (1991). The axonally secreted protein axonin-1 is a potent substratum for neurite growth. *Journal of Cell Biology*, *112*, 449–455. https://doi.org/10.1083/jcb.112.3.449

Strauss, K. A., Puffenberger, E. G., Huentelman, M. J., Gottlieb, S., Dobrin, S. E., Parod, J. M., … Morton, D. H. (2006). Recessive symptomatic focal epilepsy and mutant contactin-associated protein-like 2. *New England Journal of Medicine*, *354*, 1370–1377. https://doi.org/10.1056/NEJMoa052773

Südhof, T. C. (2017). Synaptic neurexin complexes: A molecular code for the logic of neural circuits. *Cell*, *171*, 745–769. https://doi.org/10.1016/j.cell.2017.10.024

Tanabe, Y., Fujita-Jimbo, E., Momoi, M. Y., & Momoi, T. (2015). CASPR2 forms a complex with GPR37 via MUPP1 but not with GPR37(R558Q), an autism spectrum disorder-related mutation. *Journal of Neurochemistry*, *134*, 783–793. https://doi.org/10.1111/jnc.13168

Torres-Vega, E., Mancheño, N., Cebrián-Silla, A., Herranz-Pérez, V., Chumillas, M. J., Moris, G., … Bataller, L. (2017). Netrin-1 receptor antibodies in thymoma-associated neuromyotonia

with myasthenia gravis. *Neurology*, *88*, 1235–1242. https://doi.org/10.1212/WNL.0000000000003778

Townsend, L. B., & Smith, S. L. (2017). Genotype- and sex-dependent effects of altered Cntnap2 expression on the function of visual cortical areas. *Journal of Neurodevelopmental Disorders*, *9*, 2. https://doi.org/10.1186/s11689-016-9182-5

Traka, M., Dupree, J. L., Popko, B., & Karagogeos, D. (2002). The neuronal adhesion protein TAG-1 is expressed by schwann cells and oligodendrocytes and is localized to the juxtaparanodal region of myelinated fibers. *Journal of Neuroscience*, *22*, 3016–3024. https://doi.org/10.1523/JNEUROSCI.22-08-03016.2002

Traka, M., Goutebroze, L., Denisenko, N., Bessa, M., Nifli, A., Havaki, S., … Karagogeos, D. (2003). Association of TAG-1 with Caspr2 is essential for the molecular organization of juxtaparanodal regions of myelinated fibers. *Journal of Cell Biology*, *162*, 1161–1172. https://doi.org/10.1083/jcb.200305078

Tzimourakas, A., Giasemi, S., Mouratidou, M., & Karagogeos, D. (2007). Structure-function analysis of protein complexes involved in the molecular architecture of juxtaparanodal regions of myelinated fibers. *Biotechnology Journal*, *2*, 577–583. https://doi.org/10.1002/(ISSN)1860-7314

Vabnick, I., Trimmer, J. S., Schwarz, T. L., Levinson, S. R., Risal, D., & Shrager, P. (1999). Dynamic potassium channel distributions during axonal development prevent aberrant firing patterns. *Journal of Neuroscience*, *19*, 747–758. https://doi.org/10.1523/JNEUROSCI.19-02-00747.1999

Varea, O., Martin-de-Saavedra, M. D., Kopeikina, K. J., Schürmann, B., Fleming, H. J., Fawcett-Patel, J. M., … Penzes, P. (2015). Synaptic abnormalities and cytoplasmic glutamate receptor aggregates in contactin associated protein-like 2/Caspr2 knockout neurons. *Proceedings of the National Academy of Sciences of the United States of America*, *112*, 6176–6181. https://doi.org/10.1073/pnas.1423205112

Veitia, R. A., Caburet, S., & Birchler, J. A. (2018). Mechanisms of Mendelian dominance. *Clinical Genetics*, *93*, 419–428. https://doi.org/10.1111/cge.13107

Verkerk, A. J. M. H., Mathews, C. A., Joosse, M., Eussen, B. H. J., Heutink, P., & Oostra, B. A. (2003). Cntnap2 is disrupted in a family with gilles de la tourette syndrome and obsessive compulsive disorder. *Genomics*, *82*, 1–9. https://doi.org/10.1016/S0888-7543(03)00097-1

Vincent, A., & Irani, S. R. (2010). Caspr2 antibodies in patients with thymomas. *Journal of Thoracic Oncology*, *5*, S277–S280. https://doi.org/10.1097/JTO.0b013e3181f23f04

Vogt, D., Cho, K. K. A., Shelton, S. M., Paul, A., Huang, Z. J., Sohal, V. S., & Rubenstein, J. L. R. (2017). Mouse Cntnap2 and human CNTNAP2 ASD alleles cell autonomously regulate PV+ cortical interneurons. *Cerebral Cortex*, 1–12. https://doi.org/10.1093/cercor/bhx248

Watson, C. M., Crinnion, L. A., Tzika, A., Mills, A., Coates, A., Pendlebury, M., … Bonthron, D. T. (2014). Diagnostic whole genome sequencing and split-read mapping for nucleotide resolution breakpoint identification in CNTNAP2 deficiency syndrome. *American Journal of Medical Genetics. Part A*, *164A*, 2649–2655. https://doi.org/10.1002/ajmg.a.36679

Worthey, E. A., Raca, G., Laffin, J. J., Wilk, B. M., Harris, J. M., Jakielski, K. J., … Shriberg, L. D. (2013). Whole-exome sequencing supports genetic heterogeneity in childhood apraxia of speech. *Journal of Neurodevelopmental Disorders*, *5*, 29. https://doi.org/10.1186/1866-1955-5-29

van der Zee, J. S., van Swieten, P., & Aalberse, R. C. (1986). Serologic aspects of IgG4 antibodies. II. IgG4 antibodies form small, non-precipitating immune complexes due to functional monovalency. *Journal of Immunology*, *137*, 3566–3571.

Zou, Y., Zhang, W., Liu, H., Li, X., Zhang, X., Ma, X., … Xu, D. (2017). Structure and function of the contactin-associated protein family in myelinated axons and their relationship with nerve diseases. *Neural Regeneration Research*, *12*, 1551.

Zweier, C., de Jong, E. K., Zweier, M., Orrico, A., Ousager, L. B., Collins, A. L., … Rauch, A. (2009). CNTNAP2 and NRXN1 are mutated in autosomal-recessive Pitt-Hopkins-like mental retardation and determine the level of a common synaptic protein in Drosophila. *American Journal of Human Genetics*, *85*, 655–666. https://doi.org/10.1016/j.ajhg.2009.10.004

SUPPORTING INFORMATION

Additional supporting information may be found online in the Supporting Information section at the end of the article.

How to cite this article: Saint-Martin M, Joubert B, Pellier-Monnin V, Pascual O, Noraz N, Honnorat J. Contactin-associated protein-like 2, a protein of the neurexin family involved in several human diseases. *Eur J Neurosci*. 2018;00:1–18. https://doi.org/10.1111/ejn.14081

Human Molecular Genetics, 2018, Vol. 27, No. 11 1941–1954

doi: 10.1093/hmg/ddy102
Advance Access Publication Date: 21 March 2018
Original Article

ORIGINAL ARTICLE

Genetic variants in autism-related *CNTNAP2* impair axonal growth of cortical neurons

Giorgia Canali[1,2,3], Marta Garcia[1,2,3], Bruno Hivert[4,†], Delphine Pinatel[4,‡], Aline Goullancourt[1,2,3], Ksenia Oguievetskaia[1,2,3], Margaux Saint-Martin[5], Jean-Antoine Girault[1,2,3], Catherine Faivre-Sarrailh[4,¶] and Laurence Goutebroze[1,2,3,*]

[1]Inserm, UMR-S 839, F-75005 Paris, France, [2]*Faculté des Sciences et Ingénierie*, Sorbonne Université, F-75005 Paris, France, [3]Institut du Fer à Moulin, F-75005 Paris, France, [4]Aix Marseille Université – CNRS, UMR 7286 CRN2M, F-13344 Marseille, France and [5]CNRS UMR-5310, INSERM U-1217, Institut NeuroMyoGène, Université Claude Bernard Lyon 1, F-69003 Lyon, France

*To whom correspondence should be addressed. Tel: + 33 145876144; Fax: + 33 145876132; Email: laurence.goutebroze@inserm.fr

Abstract

The *CNTNAP2* gene, coding for the cell adhesion glycoprotein Caspr2, is thought to be one of the major susceptibility genes for autism spectrum disorder (ASD). A large number of rare heterozygous missense *CNTNAP2* variants have been identified in ASD patients. However, most of them are inherited from an unaffected parent, questioning their clinical significance. In the present study, we evaluate their impact on neurodevelopmental functions of Caspr2 in a heterozygous genetic background. Performing cortical neuron cultures from mouse embryos, we demonstrate that Caspr2 plays a dose-dependent role in axon growth *in vitro*. Loss of one *Cntnap2* allele is sufficient to elicit axonal growth alteration, revealing a situation that may be relevant for *CNTNAP2* heterozygosity in ASD patients. Then, we show that the two ASD variants I869T and G731S, which present impaired binding to Contactin2/TAG-1, do not rescue axonal growth deficits. We find that the variant R1119H leading to protein trafficking defects and retention in the endoplasmic reticulum has a dominant-negative effect on heterozygous *Cntnap2* cortical neuron axon growth, through oligomerization with wild-type Caspr2. Finally, we identify an additional variant (N407S) with a dominant-negative effect on axon growth although it is well-localized at the membrane and properly binds to Contactin2. Thus, our data identify a new neurodevelopmental function for Caspr2, the dysregulation of which may contribute to clinical manifestations of ASD, and provide evidence that *CNTNAP2* heterozygous missense variants may contribute to pathogenicity in ASD, through selective mechanisms.

Introduction

Autism spectrum disorder (ASD) represents a heterogeneous group of early neurodevelopmental diseases, which are characterized by the presence of repetitive/restricted behaviours and deficits in social interaction and communication (DMS-V). It affects ∼1% of the population, and presents an extremely complex genetic architecture, probably shaped by a

[†]Present address: Institut de Neurosciences de la Timone, UMR 7289, Aix Marseille Université – CNRS, F-13385 Marseille, France.
[‡]Present address: Institut NeuroMyoGène, CNRS UMR-5310, INSERM U-1217, Université Claude Bernard Lyon 1, F-69003 Lyon, France.
[¶]Present address: Aix Marseille Université – INSERM UMR1249, INMED, F-13273 Marseille, France.
Received: January 27, 2018. **Revised:** March 14, 2018. **Accepted:** March 15, 2018

combination of rare deleterious variants and a myriad of low-risk alleles (1). Rather than implicating dysfunction in a particular brain structure, ASD is considered to result from abnormal development and functioning of brain connectivity between cortical areas (2–4). Current genetic and neurobiological data indicate that affected stages of development could include prenatal events such as neuronal migration and axon pathfinding, which establish proper positioning and patterning of basal connectivity, and postnatally events of dendritic development and synaptogenesis (5–7).

The *CNTNAP2* gene is described as one of the major susceptibility genes for neurodevelopmental disorders, including ASD as well as Gilles de la Tourette syndrome, intellectual disability, obsessive compulsive disorder, cortical dysplasia-focal epilepsy syndrome, schizophrenia, Pitt-Hopkins syndrome and attention deficit hyperactivity disorder (8–10). It encodes the neuronal neurexin-like cell adhesion transmembrane glycoprotein Contactin-associated protein-2 (Caspr2), which is well-known for its role in axo-glial contacts of matured myelinated axons, forming a complex *in cis* and *in trans* with the glycosylphosphatidylinositol (GPI)-anchored immunoglobulin cell-adhesion molecule CNTN2/Contactin2/TAG-1 at the juxtaparanodal regions of the nodes of Ranvier (11–13). Caspr2 is required for the clustering of *Shaker*-type voltage-gated potassium channels (Kv1.1 and Kv1.2) in these regions (11,14). Mislocalization of Kv1 channels in *Cntnap2*$^{-/-}$ mice is associated with modifications of axonal action potential wave form and increases in postsynaptic excitatory responses (14), suggesting that Caspr2 is important for proper conductivity of central myelinated fibers. Recent data provided evidence that Caspr2 may play several other roles during early post-natal neurodevelopment and contribute to normal neuronal network assembly and activity. Caspr2 was found to be important for the maturation of the parvalbumin-positive (PV^{+}) GABAergic cortical interneurons and the physiology of fast-spiking PV^{+} neurons (15,16). Knockout and knockdown studies showed that it is required for the normal development of cortical neuron dendritic arborization and spines, synaptic strength and AMPA receptors trafficking (17–19). In addition, a delay in myelination was recently described in juvenile *Cntnap2*$^{-/-}$ mice (14), the mechanisms of which are not clear, but suggesting that Caspr2 may influence network dynamics of cortical neurons.

CNTNAP2 genetic alterations identified in ASD patients include complex genomic rearrangements, heterozygous intragenic deletions and especially a large number of rare heterozygous missense variants distributed over the entire extracellular domain of Caspr2 (8,10,20,21). It has been proposed that *CNTNAP2* intragenic deletions may exert a dominant-negative effect, leading to expression of Caspr2 proteins deleted of part of their extracellular domains, which may perturb the normal functions of Caspr2 (22). Most of the heterozygous missense variants are inherited from an unaffected parent of the ASD patients (21). Also, heterozygous missense *CNTNAP2* variants have been found in control individuals (20), thus questioning the clinical significance of the variants identified in ASD patients, and therefore their contribution to the development of the pathology. So far, the impact of the variants on the functions of Caspr2 has been poorly evaluated because of lack of reliable assay. The extracellular domain of Caspr2 is composed of different structural subdomains and is likely to present an overall compact architecture, suggesting complex structure-function relationships (23,24). Studies in HEK-293 transfected cells showed that some variants are misfolded and present severe trafficking abnormalities, being largely retained in the endoplasmic reticulum (ER), while others are well localized at the plasma membrane (25). However, the functional consequences of the misfolded variants have not been further evaluated. In addition, four variants localized at the plasma membrane were shown to act like null/hypomorphic alleles based on their inability to rescue the maturation of *Cntnap2*$^{-/-}$ PV^{+} cortical interneurons in a transplantation assay (15), but the causes of the phenotype are not clear.

Here, we aimed at developing biochemical approaches and a sensitive developmental *in vitro* cell assay to clarify the potential functional impact of various *CNTNAP2* missense variants in a heterozygous *Cntnap2* background relevant for *CNTNAP2* heterozygosity in ASD patients. The expression pattern of *Cntnap2* in mouse suggested a role for Caspr2 in cortical neurons as early as embryonic day 14 (E14) (16). We performed neuronal cultures from wild-type, *Cntnap2*$^{+/-}$ and *Cntnap2*$^{-/-}$ embryos at E14.5, and showed that Caspr2 regulates axonal outgrowth in a dose-dependent manner. Testing variants in *Cntnap2*$^{+/-}$ neurons, we found that they have different effects on axon elongation, likely through different mechanisms, thus providing a proof of principle that certain *CNTNAP2* heterozygous missense variants may contribute to ASD pathogenicity.

Results

Caspr2 modulates axonal outgrowth of primary E14.5 cortical neurons in a dose-dependent manner

Dissociated E14.5 cortical neurons were first cultured from wild-type (WT) embryos. RT-PCR and immunoblotting experiments showed that these neurons expressed *Cntnap2*/Caspr2 at 3 and 7 days in culture (DIV3 and DIV7) (Fig. 1A and B). Cell surface immunolabelling with purified anti-Caspr2 antibodies from a patient affected by an autoimmune limbic encephalitis (26) demonstrated a faint staining on the soma and along the neurites, including the axon, and at the level of the growth cones (Fig. 1C, left panels). This staining, which was not detectable in neuronal cultures from *Cntnap2*$^{-/-}$ mutant (KO) neurons (Fig. 1C, right panels), suggested that Caspr2 could contribute to neuronal neuritogenesis. We thus analyzed neuronal morphology in cultures generated from WT, *Cntnap2*$^{+/-}$ (HET), and KO embryos. Cultures were fixed at DIV2 and DIV3, and measurements were performed on neurons that exhibited one longer Tuj-1 immunopositive process (axon) and several shorter neurites (not shown). A significantly decreased axon length was observed in mutant neurons both at DIV2 and DIV3 (Fig. 1D). Interestingly, HET neurons displayed an intermediate axon length as compared to those of WT and KO neurons. Axonal defects were rescued by electroporating the neurons before plating with a pCAGGS-IRES construct encoding HA-tagged Caspr2 and the fluorescent protein Tomato to detect transfected cells (Fig. 1E). Axon length of HA-Caspr2-expressing neurons was not significantly different between the three genotypes and also remarkably similar to that from WT neurons electroporated with the control vector. These data indicate a role for Caspr2 in axon elongation, which is tightly regulated and dependent on the expression level of the protein.

Caspr2 oligomerizes during its maturation

The dose-dependent role of Caspr2 in axon growth offered a reliable and sensitive assay to test the impact of ASD-related missense *CNTNAP2* variations, and further suggested diverse scenarios by which they could interfere with the normal cellular

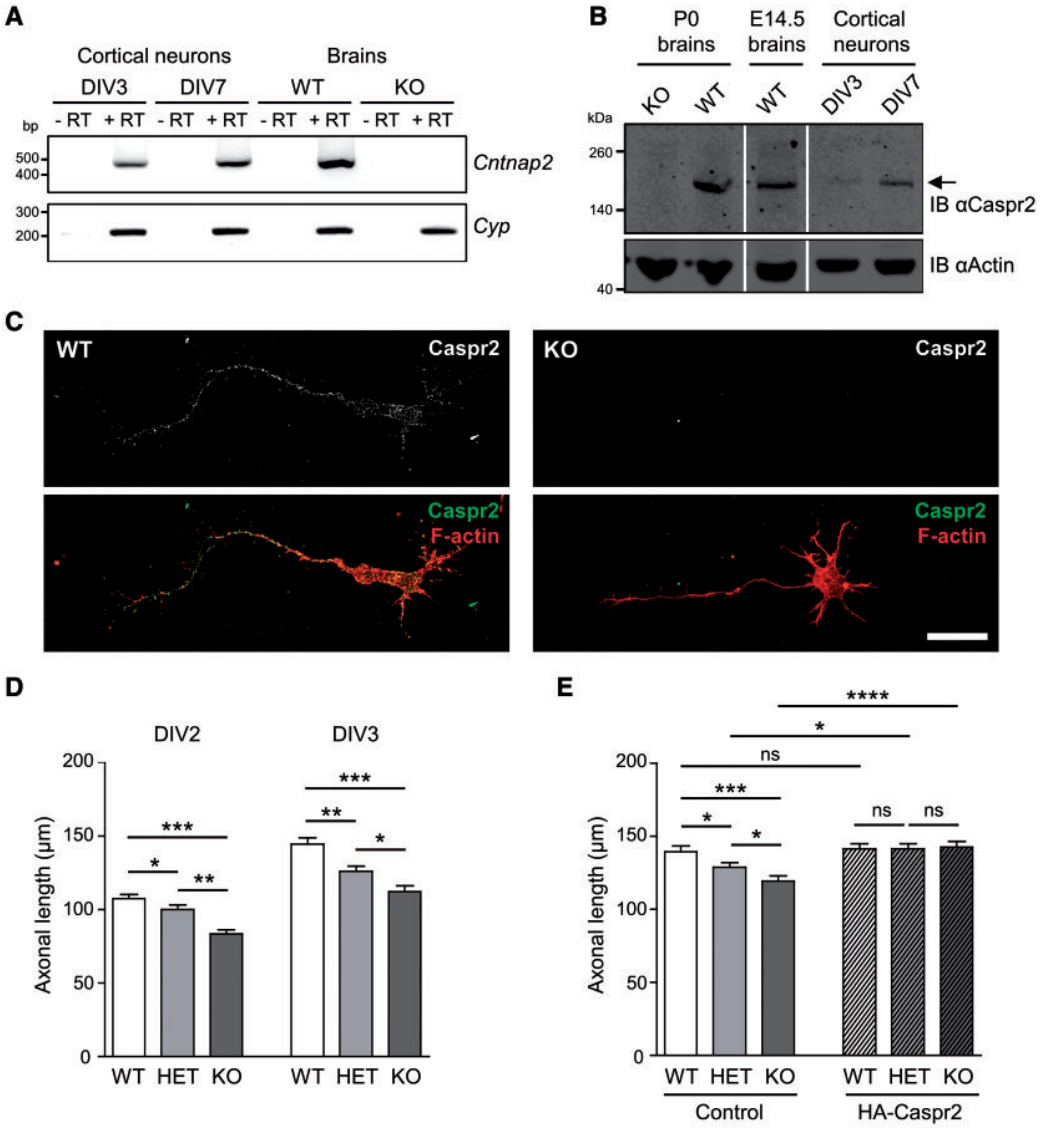

Figure 1. Caspr2 modulates axonal outgrowth of primary E14.5 cortical neuron in a dose-dependent manner. **(A)** *Cntnap2* mRNA levels analysis by RT/PCR on total mRNAs from E14.5 cortical neurons at DIV3 and DIV7, and WT and KO adult mouse brains. *Cyp*, Cyclophilin B as control. Molecular markers are shown in base pairs (bp) on the left of the panels. Expected size of DNA fragments: *Cntnap2*, 476 bp; *Cyp*, 215 bp. **(B)** Caspr2 protein levels analysis by immunoblotting (IB) on lysates from E14.5 cortical neurons at DIV3 and DIV7, WT and KO newborn (P0) mouse brains, and WT E14.5 brains. Actin was used to normalize protein expression. Molecular mass markers positions are shown in kDa on the left of the panels. The arrow indicates the band for Caspr2. **(C)** Representative images of Caspr2 cell surface immunostaining on WT and KO cortical neurons at DIV3 (green). Co-staining of actin with phalloidin (red). **(D)** Quantification of axon length in WT, HET and KO cortical neurons at DIV2 and DIV3. **(E)** Rescue of axon growth by expression of HA-Caspr2 in cortical neurons. Quantification of axon lengths at DIV3 in WT, HET and KO neurons electroporated with the control vector or the HA-Caspr2-expressing vector. (D, E) Data are means + SEM. (D) $n = 7$–9 embryos/genotype, $n = 33$–36 neurons/embryo. (E) $n = 8$–10 embryos/genotype, $n = 40$–43 neurons/embryo. Statistical analyses: Kruskal–Wallis one-way ANOVA test, (D, E) $P < 0.0001$; Dunn's Multiple Comparison post-test, $^{*}P < 0.05$, $^{**}P < 0.01$, $^{***}P < 0.001$; ns, not significant. (C) Scale bar, 25 μm.

functions of Caspr2 on a heterozygous *CNTNAP2* background. One scenario was that Caspr2 variants could interact with WT Caspr2, impair its trafficking, subcellular localization and/or function at the membrane, leading to a homozygous cellular phenotype. This was suggested by the fact that oligomerization in ER is a quite general mechanism used by biosynthetic quality-control checkpoints to make sure that only properly folded membrane glycoproteins reach their site of action. Thus, in preliminary variant studies, we evaluated this possibility and asked whether WT Caspr2 could oligomerize by performing co-immunoprecipitation from lysates of heterologous cells co-expressing HA-Caspr2 and Myc-tagged Caspr2 (Myc-Caspr2) (Fig. 2A). When expressed in COS7 cells, Caspr2 appeared in immunoblotting as a doublet of two protein bands (Fig. 2B, left panel). Surface biotinylation (Fig. 2B) and digestions with endoglycosidases H and F (Fig. 2C) indicated that the upper band corresponds to a mature, glycosylated, transport-competent form that is present at the plasma membrane, while the lower band is an immature glycosylated intracellular form. The mature form of Caspr2 at the cell surface contains complex N-glycans, which are resistant to endoglycosidase H, whereas the immature form of Caspr2 in the ER bears high-mannose N-glycans,

which are sensitive to endoglycosidase H. In cells co-expressing HA-Caspr2 and Myc-Caspr2, HA antibodies pulled down the immature form of Myc-Caspr2 (Fig. 2D, arrows). When cells were treated for 18 h before co-immunoprecipitation with tunicamycin, which blocks the first enzyme of the glycosylation pathway and thus inhibits the synthesis of all N-linked oligosaccharides in cells, HA antibodies also pulled down the non-glycosylated form of Myc-Caspr2 (Fig. 2E, arrowheads). These observations demonstrate the ability of Caspr2 to self-associate during its processing in the ER but likely not at the plasma membrane. Further experiments with HA-Caspr2 proteins encompassing sequential deletions of the extracellular domain (Fig. 2A) showed that co-immunoprecipitation of Myc-Caspr2 was dramatically altered by the deletion of the fibrinogen domain and the third laminin G domain (HA-Caspr2Δ3, Fig. 2F), indicating that Caspr2 oligomerization requires at least one of these two domains.

The variants I869T, R1119H and D1129H oligomerize with WT Caspr2 and have a dominant-negative effect on its subcellular localization in transfected COS7 cells

Since some Caspr2 variants were previously shown to be misfolded and retained in the ER (25), we next asked whether they could form heteromers with WT Caspr2, and therefore impact its trafficking and subcellular localization. We first screened for variants that present trafficking abnormalities among variants previously reported by Bakkaloglu *et al.* (21) (Supplementary Material, Fig. S1A). For this, HA-tagged Caspr2 variants were expressed in COS-7 cells and immunoblotting was performed to evaluate the proportion of the immature glycosylated form for each of them (Supplementary Material, Fig. S1B and C). Two variants, HA-R1119H and HA-D1129H, appeared to be mainly expressed as the immature form when compared to WT Caspr2 (Supplementary Material, Fig. S1B and C). ER retention of these variants was further monitored by quantifying the proportion of protein co-localizing with an ER marker (KDEL) in transfected cells (Supplementary Material, Fig. S2A–C). Consistent with previous observations (25), a large proportion of HA-R1119H and HA-D1129H was significantly retained in the ER as compared to WT Caspr2 (Fig. 3B), the retention being higher for HA-D1129H. A third variant, HA-I869T, also appeared largely as an immature form on immunoblotting (Supplementary Material, Fig. S1B and C). Immunostaining showed that its retention in the ER was higher but not significantly different from that of WT Caspr2 (Fig. 3B; Supplementary Material, Fig. S2A and D). We nevertheless considered pursuing its characterization because it had been found in four different ASD families (20,21).

Co-immunoprecipitation experiments on lysates of COS-7 cells co-expressing Myc-Caspr2 demonstrated that the three variants I869T, R1129H and D1129H, were able to form heteromers with WT Caspr2 (Fig. 3C). The proportion of immature form of Myc-Caspr2 co-immunoprecipitated with the variants was remarkably higher than that pulled down by HA-Caspr2, suggesting a stronger association of WT Caspr2 with the variants than with the WT molecules. Immunostaining confirmed that the three variants were retained in the ER in co-transfected cells similarly as when they were expressed alone, although in this case ER retention of I869T appeared significantly different from that of WT Caspr2 (Fig. 3D). The ability of the variants to induce ER retention of WT Caspr2 was monitored by quantifying the proportion of Myc-Caspr2 co-localizing with the ER marker (Supplementary Material, Fig. S3A–D). The retention of Myc-Caspr2 in the ER was increased in cells co-expressing any of the three variants as compared to cells expressing HA-Caspr2 (Fig. 3E), indicating that these variants have a dominant effect on the subcellular localization of WT Caspr2 in heterologous cells.

The variant R1119H has a dominant-negative effect on axon growth while the variant I869T does not fully rescue axon growth defects of HET neurons

To evaluate the impact of the variants on axonal growth, cortical neurons were electroporated before plating with pCAGGS-IRES-Tomato constructs encoding the HA-tagged proteins and fixed at DIV3. Consistent with observations in COS-7 cells, cell surface immunostaining showed that HA-R1119H and HA-D1129H were poorly expressed at the surface of HET neurons as compared to WT Caspr2 (Fig. 4A–C). Axon length was measured for R1119H, assumed to be representative of these two variants with similar properties, in neurons of the three genotypes (WT, HET and KO) to make sure to detect any minor effect. A significant decrease in axon growth was observed in both WT and HET neurons expressing HA-R1119H as compared to WT and HET neurons electroporated with the control pCAGGS-IRES-Tomato vector or expressing HA-Caspr2 (Fig. 4E). In addition, axon growth of HA-R1119H-expressing WT and HET neurons were comparable and not significantly different from that of KO neurons electroporated with the control vector, demonstrating that HA-R1119H has a dominant-negative effect on the role of WT Caspr2 in axonal outgrowth, likely through oligomerization and retention in the ER. In contrast, HA-I869T was detectable at the surface of the neurons as well as WT Caspr2 (Fig. 4A and D). In addition, axon growth of HA-I869T-expressing HET neurons was not decreased but showed an intermediate phenotype between neurons electroporated with the control vector and neurons expressing exogenous WT Caspr2 (Fig. 4F). This indicates that this variant does not play a dominant effect on WT Caspr2 but does not either fully rescue axon growth defects of HET neurons as compared to wild-type Caspr2, and therefore suggests that its structural changes can be overcome in cortical neurons to allow its trafficking, but nevertheless impair its functions at the plasma membrane.

The cell adhesion-defective variant HA-G731S displays loss of function in axonal outgrowth

One of the most likely causes for the loss of function of the variant I869T could be that its structural changes affect the cell adhesion properties of the protein. To test this hypothesis, as well as to evaluate whether other *CNTNAP2* variations could lead to similar functional impairments, we took advantage that Caspr2 was previously shown to interact *in trans* with the cell-adhesion molecule CNTN2/Contactin2/TAG-1 (26) and asked whether *CNTNAP2* variants could impair this interaction by testing the ability of Caspr2-Fc chimera to bind to N2a cells expressing GFP-tagged TAG-1. Besides I869T, we focused on the five variants N407S, N418D, Y716C, G731S and R906H, which did not appear to present major trafficking defects evaluated by immunoblotting (Supplementary Material, Fig. S1A–C). WT or variant Caspr2-Fc plasmids were transfected in HEK cells and the recombinant proteins were purified from the culture supernatant using Protein A-affinity chromatography. Same amounts of WT or variant chimera were pre-clustered with fluorescent anti-Fc IgGs and incubated on transfected N2a cells. As previously observed (26),

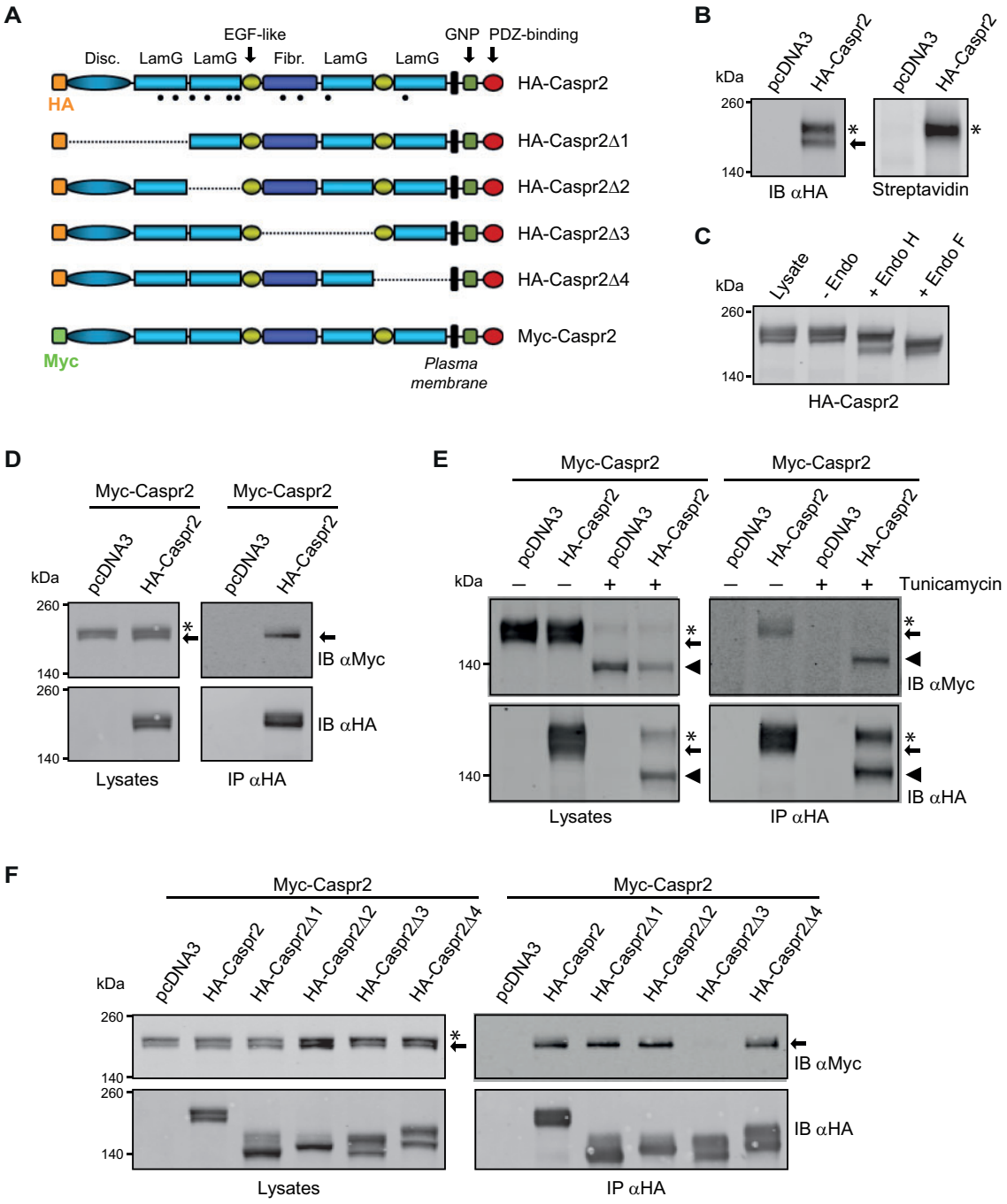

Figure 2. Caspr2 oligomerizes during its maturation. **(A)** Schematic domain organization of HA-Caspr2, HA-tagged deleted Caspr2 and Myc-Caspr2. Disc., discoidin; LamG, laminin G; Fibr., fibrinogen; EGF-like, EGF-like; GNP, Glycophorin C-Neurexin IV-Paranodin; PDZ-binding, PDZ binding domain. Dashed lines substitute for deleted domains. Black dots indicate the positions of the N-glycosylation sites. **(B)** Cell surface biotinylation experiment in COS-7 expressing HA-Caspr2 revealed by blotting with HA antibodies (IB αHA) and streptavidin. The asterisk indicates the mature biotinylated form of HA-Caspr2 and the arrow the immature intracellular form. **(C)** Deglycosylation profiles of HA-Caspr2 digested by endoglycosidase H (Endo H) and endoglycosidase F (Endo F). **(D, E)** Immunoprecipitations (IP) with HA antibodies on lysates from transfected COS-7 cells co-expressing Myc-Caspr2 and HA-Caspr2, non-treated (D) or treated for 18 h with tunicamycin or DMSO as control (E), and revealed by immunoblotting (IB) with Myc or HA antibodies. Crude protein extracts (Lysates) were immunoblotted to verify protein expression. HA antibodies immunoprecipitate the immature form of Myc-Caspr2 in non-treated cells (D), and the non-glycosylated form of Myc-Caspr2 in lysates from tunicamycin-treated cells (E). (D, E) The asterisks indicate the mature forms of Caspr2, the arrows the immature forms, and the arrowheads the non-glycosylated forms Caspr2. **(F)** IP with HA antibodies from lysates of transfected COS-7 cells co-expressing Myc-Caspr2 and HA-Caspr2 or HA-tagged Caspr2 deleted of different subdomains of the extracellular domain (HA-Caspr2Δ1-Δ4) revealed with Myc or HA antibodies. Deletion of the fibrinogen domain and the third laminin G domain (HA-Caspr2Δ3) dramatically altered co-immunoprecipitation of the immature form of Myc-Caspr2. The asterisks indicate the mature forms of Caspr2 and the arrows the immature forms. Molecular mass markers positions are shown in kDa on the left of the panels.

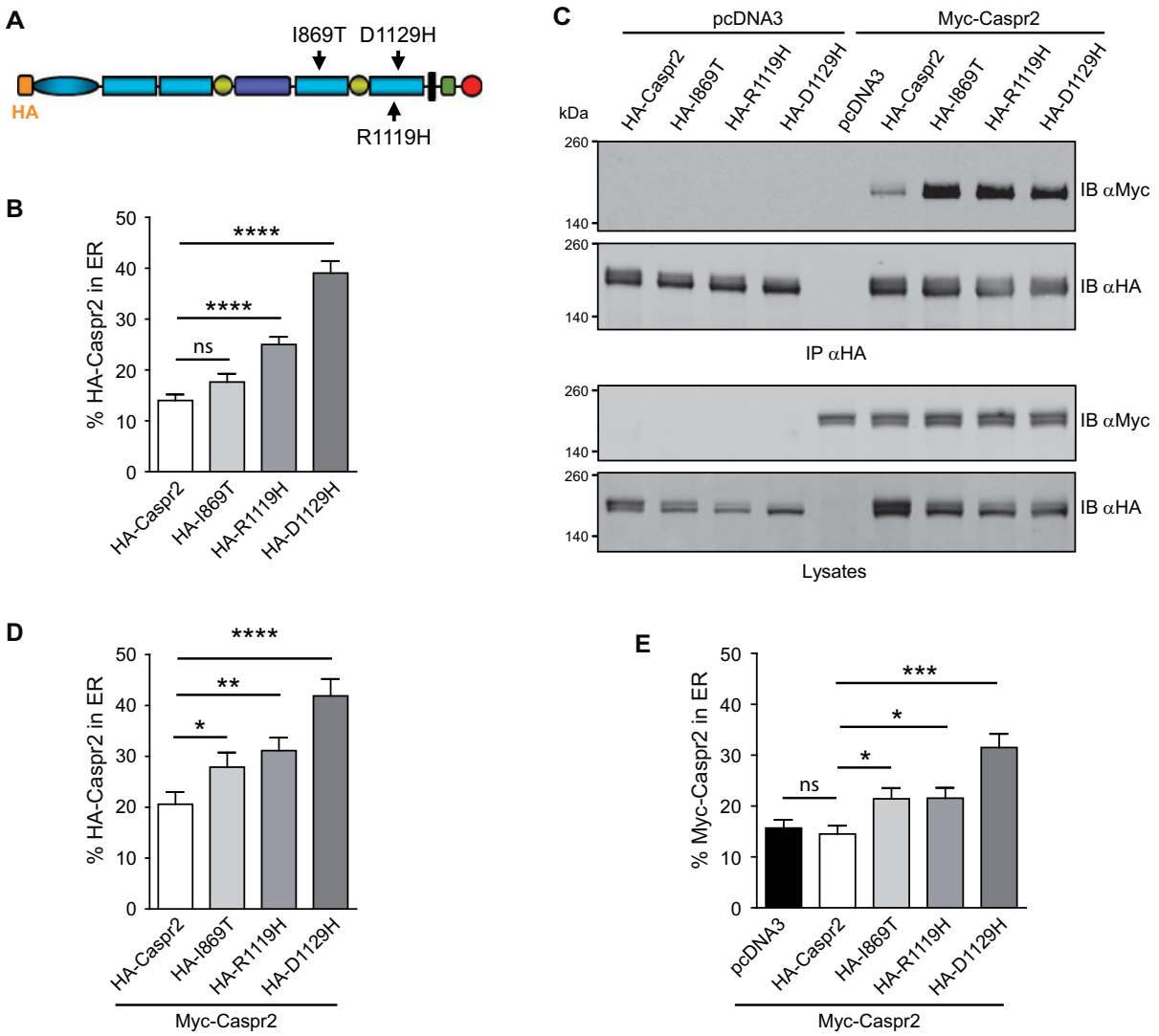

Figure 3. The variants I869T, R1119H and D1129H oligomerize with WT Caspr2 and have a dominant-negative effect on its subcellular localization in transfected COS-7 cells. **(A)** Schematic domain organization of HA-Caspr2 and positions of the variants. **(B)** Percentage of co-localization with the ER marker of WT or variant HA-Caspr2 expressed in transfected COS-7 cells. **(C)** Immunoprecipitation (IP) from lysates of transfected COS-7 cells co-expressing Myc-Caspr2 and WT or variant HA-Caspr2 with HA antibodies and revealed by immunoblotting (IB) with Myc or HA antibodies. Crude protein extracts (Lysates) were immunoblotted to verify protein expression. The proportion of Myc-Caspr2 co-immunoprecipitated with the variants is higher than that pulled down with HA-Caspr2. Molecular mass markers positions are shown in kDa on the left of the panels. **(D, E)** Percentage of co-localization with the ER marker of WT or variant HA-Caspr2 co-expressed with Myc-Caspr2 (D), and of Myc-Caspr2 expressed alone (pcDNA3) or co-expressed with WT or variant HA-Caspr2 (E). (B, D, E) Data are means + SEM of two experiments, 10 cells/condition/experiment. Statistical analyses: (B, D) Mann–Whitney test to compare each variant to HA-Caspr2; (E) Kruskal–Wallis one-way ANOVA test to compare pcDNA3, HA-Caspr2 and each variant condition, Dunn's Multiple Comparison post-test, $^{*}P < 0.05$, $^{**}P < 0.01$, $^{***}P < 0.0001$, $^{****}P < 0.0001$; ns, not significant.

Caspr2-Fc chimera bound specifically the surface of TAG-1-expressing cells after incubation at 37°C for 30 min (Fig. 5B), without any detectable endocytosis at this time point (Supplementary Material, Fig. S4). Similar binding was observed for the variants N407S, N418D, Y716C and R906H (Fig. 5C–F). In contrast, binding was dramatically decreased for the variant I869T (Fig. 5G), thus supporting the fact that its phenotype in axon growth may be caused by cell adhesion defects. Interestingly, binding was also strongly impaired for the variant G731S (Fig. 5H). Since this variant is localized in the fibrinogen domain, we further tested its ability to form oligomers with WT Caspr2 in COS-7 cells. In contrast to HA-I869T (Fig. 3C), the proportion of the immature form of Myc-Caspr2 co-immunoprecipitated with HA-G731S was similar to that pulled down with HA-Caspr2 (Fig. 6A). In addition, immunostaining confirmed that HA-G731S was not significantly retained in the ER and did not induce ER retention of Myc-Caspr2 (Fig. 6B and C; Supplementary Material, Figs S2E and S3E). We thus evaluated its impact on axonal growth of WT, HET and KO cortical neurons. Consistent with the observations in COS-7 cells, HA-G731S was expressed at the surface of the neurons similarly to WT Caspr2 (Fig. 7A and B). Measurements showed that HA-G731S did not rescue axon growth defects of HET and KO neurons (Fig. 7D). In addition, whatever the genotype of the neurons, axon growth was not significantly different from that of neurons

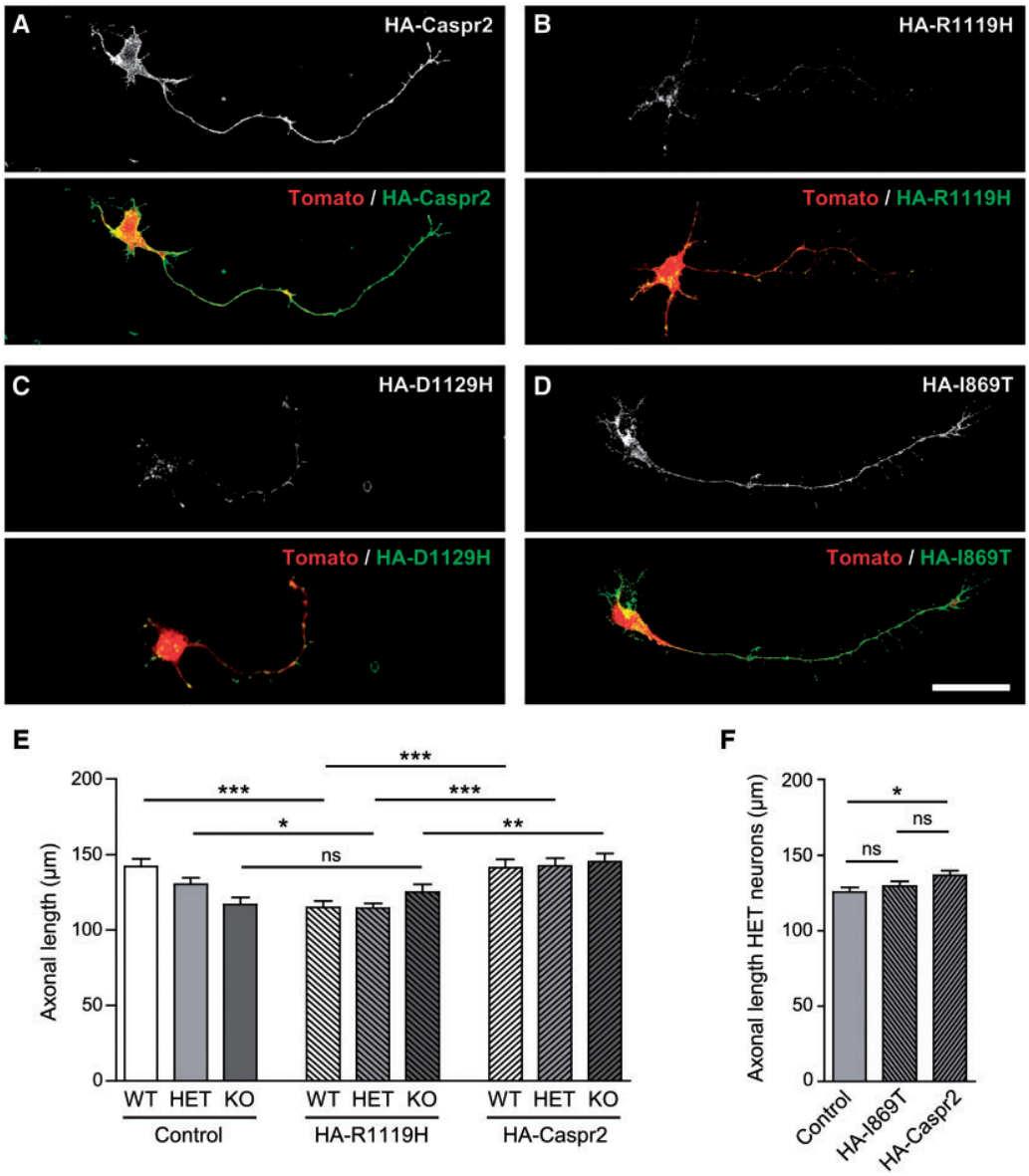

Figure 4. The variant R1119H has a dominant negative effect on axon growth while the variant I869T does not fully rescue axon growth defects of HET neurons. **(A–D)** Representative images of cell surface immunostaining of electroporated HET neurons co-expressing Tomato and HA-Caspr2 (A) or the variants HA-R1119H (B), HA-D1129H (C) and HA-I869T (D). HA-I869T is expressed at the plasma membrane as well as HA-Caspr2 whereas HA-R1119H and HA-D1129H are poorly detectable at the plasma membrane. **E.** Quantification of axon length at DIV3 of WT, HET and KO neurons electroporated with the control vector or vectors expressing HA-Caspr2 or the variant HA-R1119H. **F.** Quantification of axon length at DIV3 of HET neurons electroporated with the control vector or vectors expressing HA-Caspr2 or the variant HA-I869T. (E, F) Data are means + SEM. (E) $n = 4$–6 embryos/genotype, $n = 42$–46 neurons/embryo. (F) $n = 6$ embryos/genotype, $n = 31$–36 neurons/embryo. Statistical analyses: Kruskal–Wallis one-way ANOVA test, (E) $P < 0.001$, (F) $P < 0.05$; Dunn's Multiple Comparison post-test, $^{*}P < 0.05$, $^{**}P < 0.01$, $^{***}P < 0.001$; ns, not significant. (A–D) Scale bar, 25 µm.

electroporated with the control vector. This indicates that, similarly to I869T, the variant G731S presents a loss-of-function in axonal outgrowth, likely because of cell adhesion defects although with probably minor structural changes as compared to I869T.

The cell-membrane variant HA-N407S has a dominant-negative effect in axonal outgrowth

Our approach using Caspr2-Fc chimera was designed to screen for protein structural changes in variants expressed at the plasma membrane but faced limits to reveal subtle physiologically relevant cell-adhesion defects or any other impairments. Thus, in a last step, we decided to evaluate directly whether one of the four variants which interacted *in trans* with TAG-1 (N407S, N418D, Y716C and R906H) may affect cortical neuron axon growth. We arbitrarily choose the variant N407S, which appeared to present minor trafficking defects (Supplementary Material, Fig. S1A–C). COS-7 cell studies confirmed that HA-N407S was not significantly retained in the ER and did not induce ER retention of Myc-Caspr2 (Fig. 6D and E; Supplementary Material, Figs S2F and S3F). In addition, the

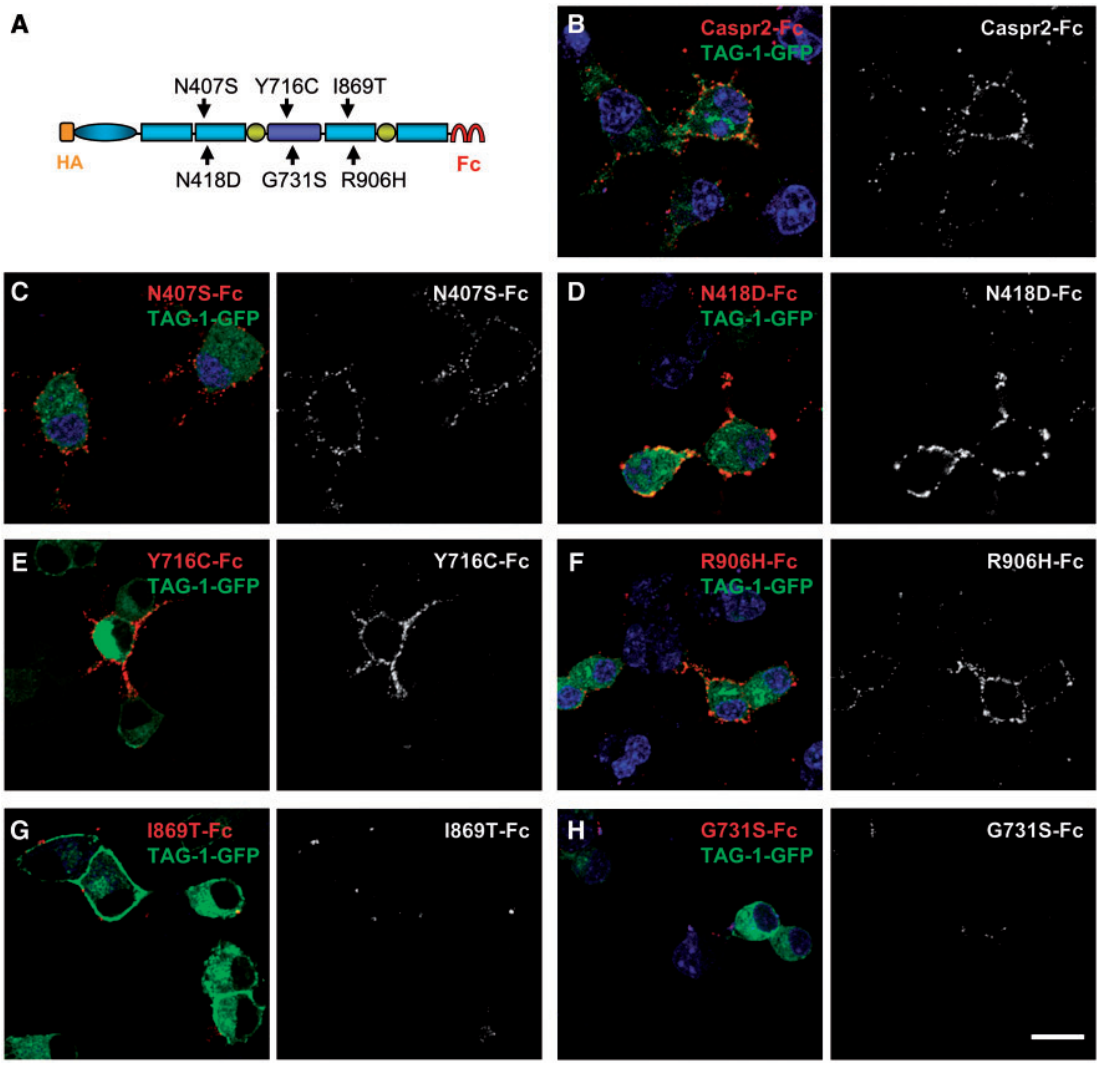

Figure 5. The variant fusion proteins G731S-Fc and I869T-Fc do not bind *in trans* GFP-tagged TAG-1 expressed in N2a cells. **(A)** Schematic domain organization of Caspr2-Fc and position of the variant missense mutations. **(B–H)** Binding of Caspr2-Fc (B) or the variants N407S-Fc (C), N418D-Fc (D), Y716C-FC (E), R906H-Fc (F), I869T-Fc (G) and G731S-Fc (H) (red) on N2a cells expressing GFP-TAG-1 (green). Single optical sections of confocal images. Blue, Hoechst staining, nuclei. (B, H) Scale bar, 20 μm.

proportion of the immature form of Myc-Caspr2 co-immunoprecipitated with this variant was similar to that pulled down with HA-Caspr2 (Fig. 6A). Cell surface immunostaining showed that HA-N407S was expressed at the surface of HET neurons similarly to WT Caspr2 (Fig. 7A and C). However and unexpectedly, axon growth of HA-N407S-expressing HET neurons was significantly decreased as compared to neurons electroporated with the control vector or expressing exogenous WT Caspr2 (Fig. 7E), suggesting that this variant has a dominant-negative effect in axonal outgrowth, in spite of its normal surface expression and probably mild or no structural changes.

Discussion

Previous studies indicated that Caspr2 may play several roles during post-natal development of cortical neurons and contribute to normal neuronal network assembly and activity (14–19). In this study, we demonstrate a new role for Caspr2, earlier during embryonic cortical neuron differentiation, showing that Caspr2 regulates axon growth. Importantly, we find that a haplo-insufficiency reducing the expression of Caspr2 to about half is sufficient to elicit axon growth defects. This offered a reliable assay to identify the effects of ASD-related heterozygous *CNTNAP2* missense variants. These mutants displayed either a dominant-negative effect or a loss-of-function during axon growth in a *Cntnap2* heterozygous genetic background. Thus, our results provide evidence that *CNTNAP2* variants could be clinically relevant in the pathogenicity in ASD.

During embryonic development, axon growth and guidance are early events essential for establishing the basal brain connectivity. They control the development of projections between the cortex and other brain regions, as well as cortico-cortical projections forming the corpus callosum, which is a major myelinated interhemispheric tract allowing bilateral integration of lateralized sensory inputs and regulation of higher-order cognitive, social and emotional processing (27). The cell-autonomous function of Caspr2 in axon growth that we describe was observed in cortical neurons from embryos at E14.5, a stage of active axon

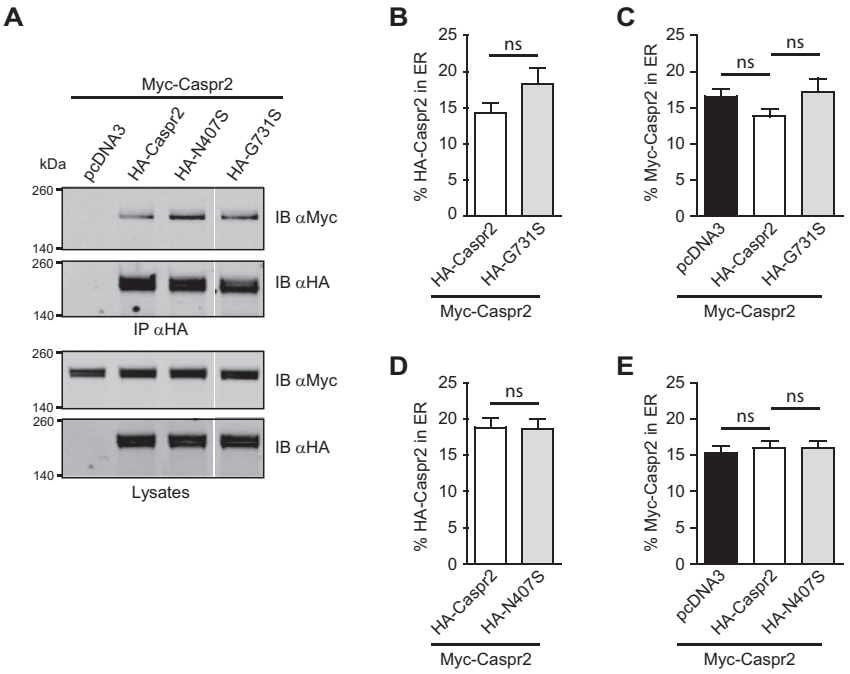

Figure 6. The variants G731S and N407S oligomerize with WT Caspr2 but do not induce ER retention of Myc-Caspr2 in transfected COS7 cells. **(A)** Immunoprecipitation (IP) from lysates of transfected COS-7 cells co-expressing Myc-Caspr2 and WT or the variants HA-N407S and HA-G731S with HA antibodies and revealed by immunoblotting (IB) with Myc or HA antibodies. Crude protein extracts (Lysates) were immunoblotted to verify protein expression. The proportion of the immature form of Myc-Caspr2 co-immunoprecipitated with the variants is similar to that pulled down with HA-Caspr2. Molecular mass markers positions are shown in kDa on the left of the panels. **(B, C)** Percentage of co-localization with the ER marker of HA-Caspr2 or HA-G731S co-expressed with Myc-Caspr2 (B), and of Myc-Caspr2 expressed alone (pcDNA3) or co-expressed with HA-Caspr2 or HA-G731S (C). **(D, E)** Percentage of co-localization with the ER marker of HA-Caspr2 or HA-N407S co-expressed with Myc-Caspr2 (D), and of Myc-Caspr2 expressed alone (pcDNA3) or co-expressed with HA-Caspr2 or HA-N407S (E). (B–E) Data are means + SEM of two experiments, 10 cells/condition/experiment. Statistical analyses: (B, D) Mann–Whitney test to compare each variant to HA-Caspr2; (C, E) Kruskal–Wallis one-way ANOVA test to compare pcDNA3, HA-Caspr2 and variant conditions, Dunn's Multiple Comparison post-test, ns, not significant.

growth in the mouse, strongly supporting the hypothesis that Caspr2 could contribute to the normal development and patterning of cortical projections *in vivo*. Consistent with this hypothesis, Scott *et al.* recently showed that 3-week old *Cntnap2*$^{-/-}$ mice do not present obvious morphological abnormalities of the corpus callosum, but a decrease in the density of myelinated axons in the superficial layers of the cortex, which is compensated at adulthood (14). This phenotype, reflecting a delay in myelination, may be a direct consequence of a delay in the development of the axons, which not only support myelination but also stimulate the proliferation of oligodendrocyte precursor cells through their electrical activity (28). During development, axon growth delay may influence networks dynamics of cortical neurons and perturb long-distance functional connectivity, as previously described in adult ASD patients in whom long-range cortico-cortical functional and structural connectivity appears to be weaker than in controls (3,4). It might also contribute to transient defects in the corpus callosum observed in young toddlers later diagnosed with ASD (29,30). These observations argue that *CNTNAP2*-associated axon growth anomalies may contribute to the manifestations of ASD.

Axon elongation is mainly triggered by the navigation of growth cones, which sense a variety of surrounding environmental signals. It is controlled by a combination of complex mechanisms working in concert, including integration of extracellular signals into intracellular second messenger networks and downstream remodelling of cytoskeletal components driving growth cone mobility (31). Our data showing that *Cntnap2*$^{+/-}$ cortical neurons exhibit an intermediate axon growth phenotype between WT and *Cntnap2*$^{-/-}$ neurons indicate that Caspr2 may act as a modulator in these processes. Adhesive contacts during axon growth are mainly triggered by cadherins, integrins and members of the immunoglobulin superfamily (IgSF-CAMs) (32–35). Caspr2 is known to interact in mature myelinated axons with the IgSF-CAM CNTN2/Contactin2/TAG-1 through its ectodomain and with protein 4.1B that associates with the spectrin/actin cytoskeleton through its cytoplasmic tail (11,12,36). It is therefore possible that Caspr2 modulates axon growth by interacting with IgSF-CAMs and regulating cell adhesion and cytoskeleton remodelling at growth cones and along the axon. Remarkably, TAG-1 promotes neurite outgrowth but only when presented as substrates or as soluble molecules (37), suggesting that it might not cooperate *in cis* with Caspr2 in axon growth. Beside IgSF-CAMs, we showed that β1-integrin is able to interact with another member of the Caspr family, Caspr1/paranodin (38), raising the intriguing possibility that Caspr2 could also regulate integrin-based adhesions, cytoskeleton dynamics and signalling upon binding to molecules of the extracellular matrix (32). Other studies indicate that axon growth and guidance could be modulated by voltage-gated potassium channel activity (39,40). Since Caspr2 is required for Kv1 clustering in myelinated axons (11,14), it could be possible that, in addition or alternatively, it regulates Kv1 surface expression, localization and/or activity during axon elongation.

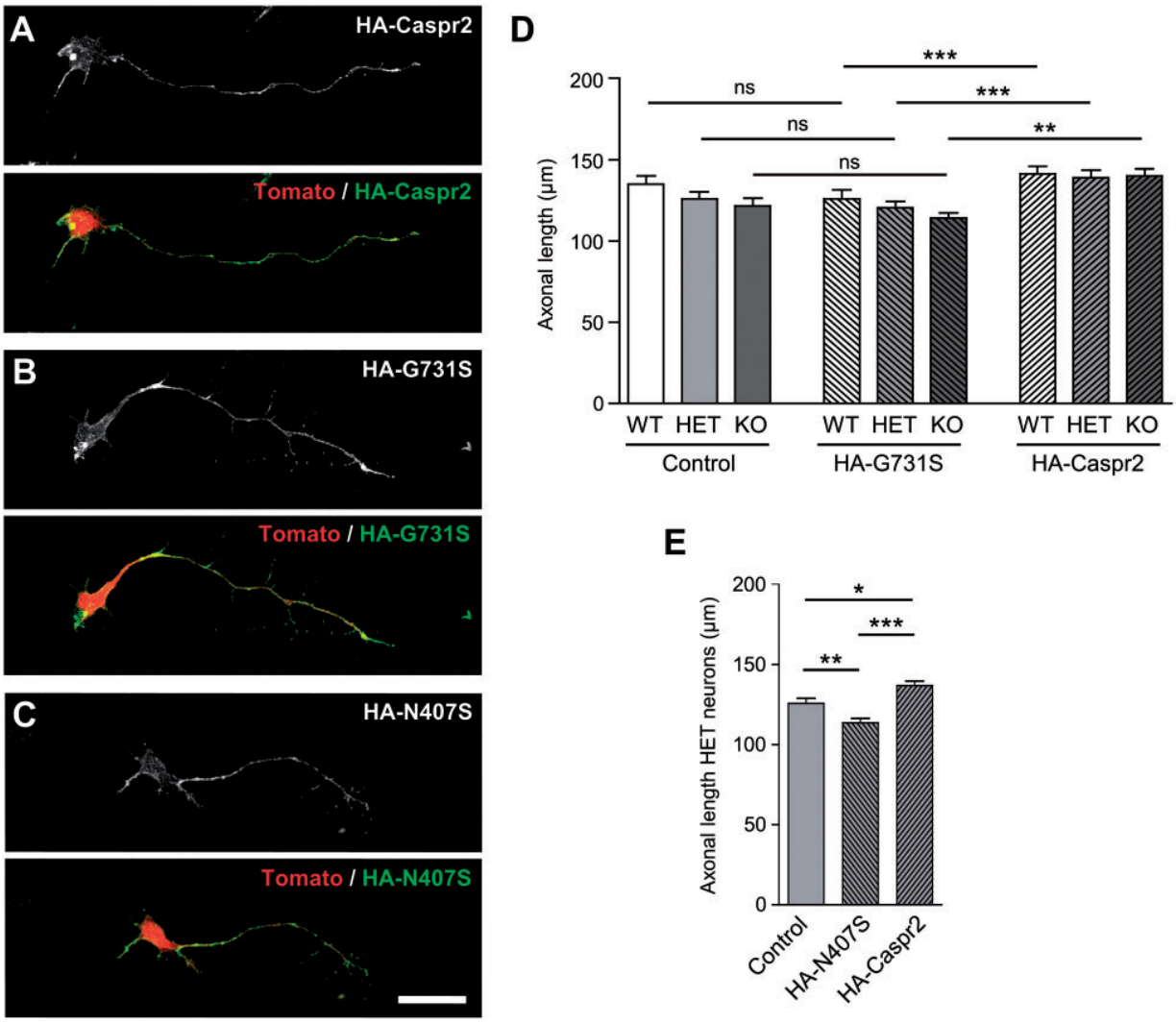

Figure 7. The variant G731S is defective in axon growth while the variant N407S has a dominant-negative effect on axon growth. **(A–C)** Representative images of cell surface immunostaining of HET electroporated neurons co-expressing Tomato and HA-Caspr2 (A) or the variants HA-G731S (B) and HA-N407S (C). HA-G731S and HA-N407S are expressed at the plasma membrane as well as HA-Caspr2. **(D)** Quantification of axon lengths at DIV3 of WT, HET and KO neurons electroporated with the control vector or vectors expressing HA-Caspr2 or the variant HA-G731S. **(E)** Quantification of axon length at DIV3 of HET neurons electroporated with the control vector or vectors expressing HA-Caspr2 or the variant HA-N407S. (D, E) Data are means + SEM. (D) $n = 3$–5 embryos/genotype, $n = 35$–40 neurons/embryo. (E) $n = 6$ embryos/genotype, $n = 31$–36 neurons/embryo. Statistical analyses: Kruskal–Wallis one-way ANOVA test, (D) $P < 0.001$, (E) $P < 0.001$; Dunn's Multiple Comparison post-test, $^{*}P < 0.05$, $^{**}P < 0.01$, $^{***}P < 0.001$; ns, not significant. (A–C) Scale bar, 25 µm.

While genetic data question the clinical significance of *CNTNAP2* variants in ASD, our study using axon growth as readout demonstrates for the first time that some mutations have functional consequences in a genetic background relevant for *CNTNAP2* heterozygosity in ASD. The variants G731S and I869T, which likely present structural changes preventing their interactions with cell adhesion partners, do not rescue the heterozygous axon growth phenotype, indicating that phenotypes related to *CNTNAP2* heterozygosity may exist in human. The misfolded ER-retained variant R1119H plays a dominant-negative effect in axon growth, arguing that phenotypes mimicking homozygous *CNTNAP2* null mutation may also exist in human. Falliveli *et al.* previously demonstrated that variants of this category could associate with chaperones in the ER, leading to stimulation of the unfolded protein response and subsequent proteasomal degradation (25). We found that they are able to oligomerize with WT Caspr2 and induce its ER retention, thus leading to a lack or decrease of functional protein at the plasma membrane. We identified a third type of variants, N407S, which is well-localized at the membrane but also appears to play a dominant-negative effect on axon growth. This variant is not expected to exert a direct effect on WT Caspr2 since it does not interact with the plasma membrane form (Fig. 6A), indicating that it impairs WT Caspr2 functions through a mechanism that remains to be identified. Altogether these data show that *CNTNAP2* variants can impact axon growth in a heterozygous background through at least three different mechanisms, and may therefore be responsible for a variety of phenotypes in human. Of note, experiments in COS-7 cells further suggest that the variants likely display a gradient of intracellular retention rather than being either strictly retained in the ER or strictly addressed at the plasma membrane, raising the possibility that

all *CNTNAP2* variants identified so far could induce a continuum of phenotypes rather than discrete phenotypes strictly mimicking *CNTNAP2* heterozygous or homozygous null mutation.

Our observations further predict that *CNTNAP2* variants may lead to a high heterogeneity of phenotypes at the scale of the whole brain. In line with the dose-dependent function of Caspr2 in axon growth, *Cntnap2*$^{+/-}$ fast-spiking PV^{+} cortical interneurons exhibit an intermediate electrophysiological phenotype between WT and *Cntnap2*$^{-/-}$ interneurons (15), suggesting that several functions of Caspr2 may be dose-sensitive. In contrast, the maturation of PV^{+} GABAergic cortical interneurons is only altered in *Cntnap2*$^{-/-}$ mice, indicating that other functions may not be affected by a partial deficit in Caspr2 (15). This implies that Caspr2 functions may be differentially affected in each individual variant, depending both on their sensitivity to Caspr2 level and the direct impact of the variants on the structure, trafficking and/or interactions of the protein. Consistently, the variants N407S and G731S do not impair interneuron maturation in a *Cntnap2*$^{+/-}$ genetic background although they demonstrate a decrease/loss-of-function in a *Cntnap2*$^{-/-}$ genetic background (15).

The potential impact of *CNTNAP2* variants was until now evaluated by bioinformatics analyses using SIFT and Polyphen-2 software, which predict whether an amino acid substitution may affect protein structure. Consistent with our experimental results, these programs predicted that the variants R1119H and G731S may be 'damaging' and/or 'probably damaging', respectively (20). In contrast, the variants N407S and I869T were predicted to be 'tolerated' and 'benign' (20) and therefore not expected to induce major functional impairments such as we observed. This discrepancy may find an explanation in the fact that the extracellular domain of Caspr2 presents a very compact subdomain organization, probably flexible upon protein partner binding, and therefore complex structure-function relationships (23,24). The variant I869T, which is localized in a laminin G domain, may not induce a predictable structural disorganization of this domain but a disorganization of the overall structure of the protein by disrupting inter-domain interactions. The variant N407S, which seems to have a mild effect on the structure, may be in an exposed region essential for partner interactions other than CNTN2/Contactin2/TAG-1. Without available high resolution structural information for Caspr2, these observations raise the important question of the limits of bioinformatics predictions, especially for the variants which have been predicted to be non-deleterious and which represent a large proportion of all *CNTNAP2* variants identified so far. Furthermore, they strongly support the hypothesis that more variants than originally predicted may be functionally deleterious, and thus highlight the possibility that *CNTNAP2* variants may define an overall endophenotype shaping a risk for ASD.

Recent genetic studies did not find evidence for statistical differences for *CNTNAP2* variants between ASD and control subjects (20). Similarly to the variants identified in ASD patients, the variants found in controls are distributed over the entire extracellular domain of Caspr2, and some of them are predicted to be 'deleterious' and/or 'probably damaging' by SIFT and Polyphen-2 software, respectively. However, none of the variants we examined here, including the variant I869T identified in several ASD families (20,21), were found in controls. It is therefore possible that only some point mutations in *CNTNAP2* have biological consequences and clinical relevance. Alternatively, it is also possible that the variants found in controls have biological consequences similar to that of ASD variants but in genetic backgrounds which do not favour to the manifestations the pathology, as it is likely the case for unaffected parents of ASD patients. Systematic investigation of many *CNTNAP2* variants in *in vitro* assays such as those we have used will help clarifying this issue.

In conclusion, our data provide a proof of principle that *CNTNAP2* heterozygous variants may contribute to the pathophysiology of ASD. They further underline the importance to pursue the characterization of the functional and behavioural consequences of missense variants in a heterozygote background *in vivo* as well as to evaluate their interaction with additional genetic and/or environmental risk factors for the development of ASD-related phenotypes. Moreover, considering the large number of variants identified in ASD patients and in the control population, they point at the necessity to resolve the structure of Caspr2 to improve the predictions of the potential impact of all variants.

Materials and Methods

Antibodies

The rabbit antibody directed against the intracellular domain of Caspr2 (residues 1284–1331) and purified anti-Caspr2 IgGs from a patient affected by an autoimmune limbic encephalitis were previously described (26,36). Commercial primary antibodies were from the following sources: Myc, rabbit #2272 or mouse clone 9B11 #2276, Cell Signalling; HA, rat clone 3F10 #11 867 423 001, Roche; KDEL, mouse #SPA-827, Stressgen; Class III β3 tubulin, mouse clone TUJ1 #MMS-435P, Covance; Actin, mouse clone C4 #MAB1501, Merck-Millipore. Secondary antibodies for immunohistochemistry and phalloidin (Alexa Fluor 488, 546, 568 or 633 conjugated) were from Thermo Fisher scientific. IRDye^{TM}800CW- and IRDye^{TM}700CW-conjugated secondary antibodies for immunoblotting and IRDye^{TM}800CW-conjugated streptavidin were from Rockland Immunochemicals.

Plasmid constructs

The pCDNA-HA-Caspr2 and pCDNA-Myc-Caspr2 constructs encode human Caspr2 (Accession number NM_014141, KIAA0868) with the HA epitope and the Myc epitope, respectively, inserted downstream of the signal peptide between the residues Trp26 and Thr27, in pCDNA3 and pCDNA5/FRT vectors, respectively. The Caspr2-Fc construct encodes the human Caspr2 extracellular domain (amino acids 1–1242) inserted upstream the human Fc sequence in the pIg-plus vector (26). The pCDNA-HA-Caspr2 deleted constructs Caspr2Δ1 (Δ32–361), Caspr2Δ2 (Δ362–600), Caspr2Δ3 (Δ600–950) and Caspr2Δ4 (Δ955–1169) were previously described (26). Mutated pCDNA-HA-Caspr2 and Caspr2-Fc constructs expressing Caspr2 variant proteins were generated by site-directed mutagenesis using specific oligonucleotides (Supplementary Material, Table S1). Constructs for expression of WT and variant Caspr2 in cortical neurons were generated by subcloning the cDNAs coding for the HA-tagged proteins in the vector pCAGGS-IRES-Tomato (generous gift from Sophie Lebrand) upstream the IRES sequence. The TAG-1-GFP vector encodes human TAG-1 (Accession number X67734) with the GFP tag inserted downstream the signal peptide (26).

Animals

Cntnap2 mutant mice, previously described (11), were obtained from the Jackson Laboratory and maintained in a C57BL/6J

background. They were group housed with *ad libitum* access to food and water and a 12 h–12 h light–dark cycle (light phase onset at 7 a.m.). For staging of embryos, the day of vaginal plug was considered E0.5. All the experiments were approved by the French Agriculture and Forestry Ministry (C75-05-22).

Primary cultures of dissociated cortical neurons

For cortical neuron cultures, the cortex from mouse E14.5 embryos was dissected in ice-cold 0.02 M HEPES in Ca^{2+}/Mg^{2+}-free HBSS (Sigma), and mechanically dissociated after trypsin (2.5 mg/ml) incubation. For axonal growth analysis, dissociated cells were plated on 14 mm-diameter coverslips (0.3×10^5 cells/coverslip) coated with poly-L-lysine (0.05 mg/ml, Sigma) and natural mouse laminin (0.01 mg/ml, Invitrogen), and cultured in Neurobasal medium supplemented with B27 serum-free supplement (20 µl/ml, Gibco®), Glutamax (10 µl/ml, Invitrogen), penicillin (100 units/ml) and streptomycin (100 µg/ml) at 37°C in presence of 5% CO_2. To express WT Caspr2 and variants, pCAGGS-HACaspr2-IRES-Tomato constructs were electroporated in neurons (1.25×10^5 cells/coverslip) before plating using the Neon Transfection System (Invitrogen) according to the manufacturer's protocol (two 20-ms pulses, 1350 V). For *Cntnap2* and Caspr2 expression analyses, dissociated neurons were plated in in 6-well plates coated with poly-L-lysine and laminin (5×10^5 cells/well).

Cell line cultures, transfections, tunicamycin treatment and Caspr2-fc binding

For co-immunoprecipitation experiments and sub-cellular localization analyses, COS-7 grown in DMEM containing 10% foetal calf serum were transiently transfected using Polyethylenimine (PEI), using 10 µg of plasmid/30 µg PEI/2×10^6 cells/100 mm-diameter dish and 1 µg of plasmid/3 µg PEI/5×10^4 cells/20 mm-diameter coverslip, respectively. After transfection, cells were grown for 24 h before processing or before treatment with 2 µg/ml tunicamycin (or DMSO as control) during an additional period of 18 h. Caspr2-Fc fusion protein binding experiments were performed as previously described (26). Briefly, WT and variant Caspr2-Fc fusion proteins were produced in the supernatant of transfected HEK-293 cells, affinity purified using Protein-A Sepharose, pre-clustered with Alexa Fluor conjugated anti-human Fc IgGs and incubated with N2a cells expressing GFP-tagged TAG-1 for 30 min at 37°C, before cell fixation with paraformaldehyde. Using these conditions, Caspr2-Fc was only detected at the surface of TAG-1-expressing cells without any detectable endocytosis.

Biochemical experiments

To analyze endogenous expression of Caspr2 or expression of WT and variant HA-Caspr2 in transfected COS-7, brains, cortical neurons and cells were lysed in RIPA buffer (50 mM Tris, pH 8.0, 150 mM NaCl, 10 µl/ml NP-40, 5 µg/ml sodium deoxycholate, 1 µg/ml SDS) containing Complete protease inhibitors (Roche). Equal amounts of proteins were load on NuPAGE 8–12% Bis-Tris gels (Thermo Fisher scientific) and transferred to 0.45 µm Nitrocellulose membrane in 25 mM Tris–HCl, pH 7.4, 192 mM glycine and 200 ml/l ethanol. Membranes were blocked with 50 g/l non-fat dry milk in Tris-buffered saline (TBS; 0.25 M Tris/0.5 M NaCl, pH 7.5)-Tween 1 ml/l (TBST) for 1 h at room temperature, incubated with primary antibodies in the same buffer for 2 h and then 1 h with appropriate IRDye-conjugated secondary antibodies, and imaged and quantified using Odyssey Imaging System (LI-COR Biosciences). For endoglycosidase digestions, transfected cells were lysed in a buffer containing 50 mm Tris, pH 7.4, 30 mM NaCl, 1 mM EDTA, 10 µl/ml Triton X-100, Complete protease inhibitors (Roche) and 1 mM phenylmethanesulfonyl fluoride (PMSF). After centrifugation, protein extracts were supplemented with SDS (final concentration 1 µg/ml), β-mercaptoethanol (final concentration 10 µl/ml) and PMSF (final concentration 1 mM), and equal amounts (50 µl) were digested at 37°C for 3 h with endoglycosidase H (Roche; 1 mU) and endoglycosidase F (Roche; 43 mU), respectively, before loading on gels. Co-immunoprecipitations were performed essentially as previously described (12). The extraction buffer contained 85 mM Tris, pH 7.5, 30 mM NaCl, 1 mM EDTA, 120 mM glucose, 10 µl/ml Triton X-100 and Complete protease inhibitors (Roche). The washing buffer contained 50 mM Tris, pH 7.5, 150 mM NaCl, 5 µl/ml Triton X-100 and Complete protease inhibitors. For cell surface biotinylation experiments, transfected cells were washed three times for 10 min with PBS at 4°C and then biotinylated with 0.5 mg/ml sulfo-NHS-LC biotin (Pierce) in 10 mM triethanolamine, pH 9, 140 mM NaCl for 20 min at 4°C. After two washes in PBS at 4°C, cells were lysed and immunoprecipitation was carried out as described above. After migration and transfert, membranes were blotted with IRDye™800CW conjugated streptavidin to detect biotinylated Caspr2.

Cntnap2 mRNA expression analysis

For mRNA expression analysis, total mRNA was extracted from brains and cortical neurons in culture using the TRIzol® Reagent (Life Technologies) following the manufacturer's recommendations. Reverse transcription (RT) was performed with the SuperScript II reverse transcriptase (Invitrogen, #18064-022) and random primers. Primers for Caspr2 cDNA amplification (PCR) were designed to amplify a 476-bp DNA fragment overlapping the 5′ non-coding region: primer sens (5′-CAGCGAGCTTTTGGA GTACCACTG), nucleotides 191 to 214 of mouse cDNA (accession number NM_001004357); primer anti-sens (5′-GACCACGCTGT CAGAATTGACGTT), nucleotides 644 to 667. For expression analysis of the housekeeping gene peptidylpropyl isomerase B (Cyclophilin B, Cyp), RT/PCR was performed using the primers (5′-CCATCGTGTCATCAAGGACTT) and (5′-TTGCCATCCAGCCAGGAG GTC). The expected size of the amplified DNA was 215 bp.

Immunofluorescence staining

For transfected COS-7 cell staining, cells were fixed with paraformaldehyde (PFA, 40 mg/ml) in PBS for 30 min at room temperature (RT) and permeabilized in PBS-Triton X-100 2 µl/ml for 5 min at RT. Coverslips were incubated in a saturation solution (50 mg/ml bovine serum albumin in PBS), and with primary antibodies and Alexa Fluor conjugated-secondary antibodies (diluted in the saturation solution) at RT for 2 and 1 h, respectively.

To quantify axonal growth in non-electroporated neurons, cells were fixed by adding in the medium 1/3 volume of pre-heated PFA (80 mg/ml)/sucrose (200 mg/ml) in PBS for 20 min and immunostaining was performed as previously described (41). Briefly, coverslips were incubated in a permeabilization/saturation solution (PS; 2.5 µl/ml Triton X-100, 50 mg/ml bovine serum albumin, PBS) for 2 h at RT, with TUJ1 primary antibodies diluted in PS overnight at 4°C, with Alexa Fluor conjugated-

secondary antibodies diluted in PS for 2 h at RT, and finally with Alexa Fluor 488/546/633 conjugated-phalloidin diluted in PBS for 30 min at RT. To quantify axonal growth in neurons expressing WT or variant HA-Caspr2, coverslips were incubated with Alexa Fluor conjugated-phalloidin only.

To reveal the endogenous expression of Caspr2 and the subcellular localization of WT and variant HA-Caspr2 in cortical neurons, live neurons were incubated in the culture medium with the purified IgGs from the patient affected by an autoimmune limbic encephalitis (20 μg/ml) and HA antibodies, respectively, for 20 min at RT and fixed with 40 mg/ml PFA in PBS for 15 min at RT. Coverslips were incubated in a saturation solution (50 mg/ml bovine serum albumin in PBS) at RT for 30 min and with Alexa Fluor conjugated-secondary antibodies at RT for 60 min (endogenous expression) or 30 min (WT or variant HA-Caspr2). After three washes with PBS, neurons were fixed, permeabilized and incubated with Alexa Fluor conjugated-phalloidin as above.

Image acquisition and analysis

To monitor the subcellular localization of Myc-Caspr2 and WT or variant HA-Caspr2 in transfected COS-7 cells, images were acquired using a Leica SP5 confocal laser-scanning microscope (Leica microsystems, Z stack 1 μm) with constant parameters and colocalization analyses were performed using the software Imaris (Bitplane). The volume of the cell (Surface tool) was defined using Myc-Caspr2 or cortical actin staining to delimit the plasma membrane. The volume of the cytoplasm was isolated by subtracting the volume of the nucleus. The Mask tool was applied to the cytoplasm volume to define ER staining as Region Of Interest (ROI), which then served to determine the percentage of co-localization of Myc-Caspr2 and WT or variant HA-Caspr2 with ER using the Colocalization Tool.

For cortical neuronal morphological analyses, images were randomly acquired using an epifluorescence microscope (DM6000 or DM6002, Leica) equipped with a CCD camera and axon lengths were measured manually using Image J.

Statistical analysis

Statistical analyses were performed with GraphPad Prism 5 software. For variables that did not follow a normal distribution, statistical analyses were carried out using the Mann–Whitney rank sum test to compare 2 quantitative variables, or the Kruskal–Wallis one-way ANOVA test to compare 3 or more variables. Significant main effects were further analyzed by post hoc comparisons of means using *t*-tests. The significance was established at a P-value < 0.05.

Supplementary Material

Supplementary Material is available at *HMG* online.

Acknowledgements

We are grateful to R. Boukhari, N. Roblot, Y. Bertelle, A. Rousseau, M. Savariradjane and T. Eirinopoulou (*Institut du Fer à Moulin Cell and Tissue Imaging facility*) for animal care and assistance with microscopes. This work was supported by Inserm, Université Pierre et Marie Curie, and grants from the Fondation Orange and the Bio-Psy laboratory of excellence. G.C., K.O. and D.P. were recipients of a doctoral fellowship from the *Ministère de la Recherche et de l'Enseignement Supérieur*, and a post-doctoral fellowship from the *Association pour la Recherche sur la Sclérose en Plaques* (ARSEP). Equipment at the IFM was also supported by DIM NeRF from *Région Ile-de-France* (NERF, 10016908) and by the FRC/Rotary 'Espoir en tête'. The teams of J.A.G. and L.G. are affiliated with the Paris School of Neuroscience (ENP) and the Bio-Psy laboratory of excellence.

Conflict of Interest statement. None declared.

References

1. De Rubeis, S. and Buxbaum, J.D. (2015) Recent advances in the genetics of autism spectrum disorder. *Curr. Neurol. Neurosci. Rep.*, **15**, 36.
2. Geschwind, D.H. and Levitt, P. (2007) Autism spectrum disorders: developmental disconnection syndromes. *Curr. Opin. Neurobiol.*, **17**, 103–111.
3. Vissers, M.E., Cohen, M.X. and Geurts, H.M. (2012) Brain connectivity and high functioning autism: a promising path of research that needs refined models, methodological convergence, and stronger behavioral links. *Neurosci. Biobehav. Rev.*, **36**, 604–625.
4. Rane, P., Cochran, D., Hodge, S.M., Haselgrove, C., Kennedy, D.N. and Frazier, J.A. (2015) Connectivity in autism: a review of MRI connectivity studies. *Harv. Rev. Psychiatry*, **23**, 223–244.
5. Gilbert, J. and Man, H.Y. (2017) Fundamental elements in autism: from neurogenesis and neurite growth to synaptic plasticity. *Front. Cell. Neurosci.*, **11**, 359.
6. Van Battum, E.Y., Brignani, S. and Pasterkamp, R.J. (2015) Axon guidance proteins in neurological disorders. *Lancet Neurol.*, **14**, 532–546.
7. McFadden, K. and Minshew, N.J. (2013) Evidence for dysregulation of axonal growth and guidance in the etiology of ASD. *Front. Hum. Neurosci.*, **7**, 671.
8. Rodenas-Cuadrado, P., Ho, J. and Vernes, S.C. (2014) Shining a light on CNTNAP2: complex functions to complex disorders. *Eur. J. Hum. Genet*, **22**, 171–178.
9. Penagarikano, O. and Geschwind, D.H. (2012) What does CNTNAP2 reveal about autism spectrum disorder?. *Trends Mol. Med.*, **18**, 156–163.
10. Poot, M. (2015) Connecting the CNTNAP2 Networks with Neurodevelopmental Disorders. *Mol. Syndromol.*, **6**, 7–22.
11. Poliak, S., Salomon, D., Elhanany, H., Sabanay, H., Kiernan, B., Pevny, L., Stewart, C.L., Xu, X., Chiu, S.Y. and Shrager, P. (2003) Juxtaparanodal clustering of Shaker-like K+ channels in myelinated axons depends on Caspr2 and TAG-1. *J. Cell. Biol.*, **162**, 1149–1160.
12. Traka, M., Goutebroze, L., Denisenko, N., Bessa, M., Nifli, A., Havaki, S., Iwakura, Y., Fukamauchi, F., Watanabe, K., Soliven, B. *et al.* (2003) Association of TAG-1 with Caspr2 is essential for the molecular organization of juxtaparanodal regions of myelinated fibers. *J. Cell. Biol.*, **162**, 1161–1172.
13. Poliak, S., Gollan, L., Martinez, R., Custer, A., Einheber, S., Salzer, J.L., Trimmer, J.S., Shrager, P. and Peles, E. (1999) Caspr2, a new member of the neurexin superfamily, is localized at the juxtaparanodes of myelinated axons and associates with K+ channels. *Neuron*, **24**, 1037–1047.
14. Scott, R., Sanchez-Aguilera, A., van Elst, K., Lim, L., Dehorter, N., Bae, S.E., Bartolini, G., Peles, E., Kas, M.J.H., Bruining, H. *et al.* (2017) Loss of Cntnap2 causes axonal excitability deficits, developmental delay in cortical myelination, and

abnormal stereotyped motor behavior. *Cereb. Cortex*. doi: 10.1093/cercor/bhx341.
15. Vogt, D., Cho, K.K.A., Shelton, S.M., Paul, A., Huang, Z.J., Sohal, V.S. and Rubenstein, J.L.R. (2017) Mouse Cntnap2 and human CNTNAP2 ASD alleles cell autonomously regulate PV+ cortical interneurons. *Cereb. Cortex*, **28**, 1–12.
16. Penagarikano, O., Abrahams, B.S., Herman, E.I., Winden, K.D., Gdalyahu, A., Dong, H., Sonnenblick, L.I., Gruver, R., Almajano, J., Bragin, A. *et al.* (2011) Absence of CNTNAP2 leads to epilepsy, neuronal migration abnormalities, and core autism-related deficits. *Cell*, **147**, 235–246.
17. Anderson, G.R., Galfin, T., Xu, W., Aoto, J., Malenka, R.C. and Sudhof, T.C. (2012) Candidate autism gene screen identifies critical role for cell-adhesion molecule CASPR2 in dendritic arborization and spine development. *Proc. Natl. Acad. Sci. U.S.A.*, **109**, 18120–18125.
18. Varea, O., Martin-de-Saavedra, M.D., Kopeikina, K.J., Schurmann, B., Fleming, H.J., Fawcett-Patel, J.M., Bach, A., Jang, S., Peles, E., Kim, E. *et al.* (2015) Synaptic abnormalities and cytoplasmic glutamate receptor aggregates in contactin associated protein-like 2/Caspr2 knockout neurons. *Proc. Natl. Acad. Sci. U.S.A.*, **112**, 6176–6181.
19. Gdalyahu, A., Lazaro, M., Penagarikano, O., Golshani, P., Trachtenberg, J.T. and Gescwind, D.H. (2015) The autism related protein contactin-associated protein-like 2 (CNTNAP2) stabilizes new spines: an in vivo mouse study. *PLoS One*, **10**, e0125633.
20. Murdoch, J.D., Gupta, A.R., Sanders, S.J., Walker, M.F., Keaney, J., Fernandez, T.V., Murtha, M.T., Anyanwu, S., Ober, G.T., Raubeson, M.J. *et al.* (2015) No evidence for association of autism with rare heterozygous point mutations in Contactin-Associated Protein-Like 2 (CNTNAP2), or in other contactin-associated proteins or contactins. *PLoS Genet.*, **11**, e1004852.
21. Bakkaloglu, B., O'Roak, B.J., Louvi, A., Gupta, A.R., Abelson, J.F., Morgan, T.M., Chawarska, K., Klin, A., Ercan-Sencicek, A.G., Stillman, A.A. *et al.* (2008) Molecular cytogenetic analysis and resequencing of contactin associated protein-like 2 in autism spectrum disorders. *Am. J. Hum. Genet.*, **82**, 165–173.
22. Poot, M. (2017) Intragenic CNTNAP2 deletions: a bridge too far?. *Mol. Syndromol.*, **8**, 118–130.
23. Rubio-Marrero, E.N., Vincelli, G., Jeffries, C.M., Shaikh, T.R., Pakos, I.S., Ranaivoson, F.M., von Daake, S., Demeler, B., De Jaco, A., Perkins, G. *et al.* (2016) Structural characterization of the extracellular domain of CASPR2 and insights into its association with the novel ligand contactin1. *J. Biol. Chem.*, **291**, 5788–5802.
24. Lu, Z., Reddy, M.V., Liu, J., Kalichava, A., Zhang, L., Chen, F., Wang, Y., Holthauzen, L.M., White, M.A., Seshadrinathan, S. *et al.* (2016) Molecular architecture of contactin-associated protein-like 2 (CNTNAP2) and its interaction with contactin 2 (CNTN2). *J. Biol. Chem.*, **291**, 24133–24147.
25. Falivelli, G., De Jaco, A., Favaloro, F.L., Kim, H., Wilson, J., Dubi, N., Ellisman, M.H., Abrahams, B.S., Taylor, P. and Comoletti, D. (2012) Inherited genetic variants in autism-related CNTNAP2 show perturbed trafficking and ATF6 activation. *Hum. Mol. Genet.*, **21**, 4761–4773.
26. Pinatel, D., Hivert, B., Boucraut, J., Saint-Martin, M., Rogemond, V., Zoupi, L., Karagogeos, D., Honnorat, J. and Faivre-Sarrailh, C. (2015) Inhibitory axons are targeted in hippocampal cell culture by anti-Caspr2 autoantibodies associated with limbic encephalitis. *Front. Cell. Neurosci.*, **9**, 265.
27. Leyva-Diaz, E. and Lopez-Bendito, G. (2013) In and out from the cortex: development of major forebrain connections. *Neuroscience*, **254**, 26–44.
28. Barres, B.A. and Raff, M.C. (1993) Proliferation of oligodendrocyte precursor cells depends on electrical activity in axons. *Nature*, **361**, 258–260.
29. Wolff, J.J., Gerig, G., Lewis, J.D., Soda, T., Styner, M.A., Vachet, C., Botteron, K.N., Elison, J.T., Dager, S.R., Estes, A.M. *et al.* (2015) Altered corpus callosum morphology associated with autism over the first 2 years of life. *Brain*, **138**, 2046–2058.
30. Fingher, N., Dinstein, I., Ben-Shachar, M., Haar, S., Dale, A.M., Eyler, L., Pierce, K. and Courchesne, E. (2017) Toddlers later diagnosed with autism exhibit multiple structural abnormalities in temporal corpus callosum fibers. *Cortex*, **97**, 291–305.
31. Vitriol, E.A. and Zheng, J.Q. (2012) Growth cone travel in space and time: the cellular ensemble of cytoskeleton, adhesion, and membrane. *Neuron*, **73**, 1068–1081.
32. Myers, J.P., Santiago-Medina, M. and Gomez, T.M. (2011) Regulation of axonal outgrowth and pathfinding by integrin-ECM interactions. *Dev. Neurobiol.*, **71**, 901–923.
33. Hansen, S.M., Berezin, V. and Bock, E. (2008) Signaling mechanisms of neurite outgrowth induced by the cell adhesion molecules NCAM and N-cadherin. *Cell. Mol. Life Sci.*, **65**, 3809–3821.
34. Maness, P.F. and Schachner, M. (2007) Neural recognition molecules of the immunoglobulin superfamily: signaling transducers of axon guidance and neuronal migration. *Nat. Neurosci.*, **10**, 19–26.
35. Sakurai, T. (2012) The role of NrCAM in neural development and disorders–beyond a simple glue in the brain. *Mol. Cell. Neurosci.*, **49**, 351–363.
36. Denisenko-Nehrbass, N., Oguievetskaia, K., Goutebroze, L., Galvez, T., Yamakawa, H., Ohara, O., Carnaud, M. and Girault, J.A. (2003) Protein 4.1B associates with both Caspr/paranodin and Caspr2 at paranodes and juxtaparanodes of myelinated fibres. *Eur. J. Neurosci.*, **17**, 411–416.
37. Gennarini, G., Bizzoca, A., Picocci, S., Puzzo, D., Corsi, P. and Furley, A.J.W. (2017) The role of Gpi-anchored axonal glycoproteins in neural development and neurological disorders. *Mol. Cell. Neurosci.*, **81**, 49–63.
38. Denisenko-Nehrbass, N., Goutebroze, L., Galvez, T., Bonnon, C., Stankoff, B., Ezan, P., Giovannini, M., Faivre-Sarrailh, C. and Girault, J.A. (2003) Association of Caspr/paranodin with tumour suppressor schwannomin/merlin and beta1 integrin in the central nervous system. *J. Neurochem.*, **84**, 209–221.
39. Pollock, N.S., Atkinson-Leadbeater, K., Johnston, J., Larouche, M., Wildering, W.C. and McFarlane, S. (2005) Voltage-gated potassium channels regulate the response of retinal growth cones to axon extension and guidance cues. *Eur. J. Neurosci.*, **22**, 569–578.
40. McFarlane, S. and Pollock, N.S. (2000) A role for voltage-gated potassium channels in the outgrowth of retinal axons in the developing visual system. *J. Neurosci.*, **20**, 1020–1029.
41. Klingler, E., Martin, P.M., Garcia, M., Moreau-Fauvarque, C., Falk, J., Chareyre, F., Giovannini, M., Chedotal, A., Girault, J.A. and Goutebroze, L. (2015) The cytoskeleton-associated protein SCHIP1 is involved in axon guidance, and is required for piriform cortex and anterior commissure development. *Development*, **142**, 2026–2036.

Autoimmune episodic ataxia in patients with anti-CASPR2 antibody-associated encephalitis

OPEN

Bastien Joubert, MD
Florent Gobert, MD
Laure Thomas, MD
Margaux Saint-Martin, MSc
Virginie Desestret, MD, PhD
Philippe Convers, MD
Véronique Rogemond, PhD
Géraldine Picard, MSc
François Ducray, MD, PhD*
Dimitri Psimaras, MD
Jean-Christophe Antoine, MD, PhD*
Jean-Yves Delattre, MD, PhD*
Jérôme Honnorat, MD, PhD

Correspondence to Dr. Honnorat: jerome.honnorat@chu-lyon.fr

ABSTRACT

Objective: To report paroxysmal episodes of cerebellar ataxia in a patient with anti–contactin-associated protein-like 2 (CASPR2) antibody-related autoimmune encephalitis and to search for similar paroxysmal ataxia in a cohort of patients with anti–CASPR2 antibody-associated autoimmune encephalitis.

Methods: We report a patient with paroxysmal episodes of cerebellar ataxia observed during autoimmune encephalitis with anti-CASPR2 antibodies. In addition, clinical analysis was performed in a retrospective cohort of 37 patients with anti-CASPR2 antibodies to search for transient episodes of ataxia. Paroxysmal symptoms were further specified from the referral physicians, the patients, or their relatives.

Results: A 61-year-old man with limbic encephalitis and anti-CASPR2 antibodies developed stereotyped paroxysmal episodes of cerebellar ataxia, including gait imbalance, dysarthria, and dysmetria, 1 month after the onset of the encephalitis. The ataxic episodes were specifically triggered by orthostatism and emotions. Both limbic symptoms and transient ataxic episodes resolved after treatment with steroids and IV cyclophosphamide. Among 37 other patients with anti-CASPR2 antibodies, we identified 5 additional cases with similar paroxysmal ataxic episodes that included gait imbalance (5 cases), slurred speech (3 cases), limb dysmetria (3 cases), and nystagmus (1 case). All had concomitant limbic encephalitis. Paroxysmal ataxia was not observed in patients with neuromyotonia or Morvan syndrome. Triggering factors (orthostatism or anger) were reported in 4 patients. Episodes resolved with immunomodulatory treatments in 4 patients and spontaneously in 1 case.

Conclusions: Paroxysmal cerebellar ataxia must be added to the spectrum of the anti-CASPR2 antibody syndrome. ***Neurol Neuroimmunol Neuroinflamm* 2017;4:e371; doi: 10.1212/NXI.0000000000000371**

GLOSSARY

EA = episodic ataxia.

Episodic ataxias (EAs) are a group of hereditary channelopathies whose common feature is the occurrence of paroxysmal episodes of cerebellar ataxia.[1] Ataxic episodes usually last a few minutes to a few days and can be triggered by emotions, abrupt movements, exercise, or fever. Depending on which ion channel gene is mutated, additional symptoms, such as neuromyotonia or epilepsy, can occur.[2] Conversely, paroxysmal symptoms are rare in patients with antineuronal antibody-associated neurologic disorders, and EAs have not yet been reported in such cases. In this study, we report a patient with paroxysmal episodes of ataxia developed during autoimmune encephalitis with anti-CASPR2 antibodies. To assess the relevance of our case, we retrospectively

Supplemental data at Neurology.org/nn

*These authors contributed equally to this work.

From the Centre National de Référence pour les Syndromes Neurologiques Paranéoplasiques (B.J., L.T., V.D., V.R., G.P., F.D., D.P., J.-C.A., J.-Y.D., J.H.), Service de Neuro-Réanimation (F.G.), Hôpital Neurologique, Hospices Civils de Lyon, Bron; Institut NeuroMyoGene INSERM U1217/CNRS UMR 5310 (B.J., F.G., L.T., M.S.-M., V.D., V.R., G.P., F.D., J.H.), University of Lyon–Université Claude Bernard Lyon 1; Service de Neurologie (P.C., J.-C.A.), Hôpital Bellevue, Centre Hospitalier Universitaire de Saint-Étienne; and Département de Neurologie (D.P., J.-Y.D.), Groupe Hospitalier Pitié-Salpêtrière, Assistance Publique–Hôpitaux de Paris, France.

Funding information and disclosures are provided at the end of the article. Go to Neurology.org/nn for full disclosure forms. The Article Processing Charge was funded by INSERM ADR05.

searched for similar episodes of transient ataxia in a cohort of patients with anti-CASPR2 antibodies. Anti–CASPR2 antibody-related disorders encompass a wide range of neurologic autoimmune syndromes, including autoimmune encephalitis, neuromyotonia, and Morvan syndrome. A recent publication by Van Sonderen et al.[3] showed that up to 77% of the patients with such antibodies had at least 3 cumulated core neurologic symptoms, including encephalic signs, cerebellar symptoms, peripheral nerve hyperexcitability, dysautonomia, neuropathic pain, insomnia, and weight loss. Our study may contribute to further delineate anti–CASPR2 antibody-related clinical presentation.

METHODS We report a patient with autoimmune encephalitis, anti-CASPR2 antibodies, and paroxysmal cerebellar ataxia. Anti-CASPR2 antibodies were screened in serum and CSF as previously described.[4] Positivity of both an immunohistofluorescent assay on rat brain slices and a cell-based binding assay with HEK-293–transfected cells were needed to confirm the presence of anti-CASPR2 antibodies. A signed patient consent-to-disclose form has been obtained from the patient for a video recording of one of the episodes.

We also studied the clinical files of 37 patients with anti-CASPR2 antibodies, detected in their CSF or sera at the *Centre de Référence National pour les Syndromes Neurologiques Paranéoplasiques* (Lyon, France) between March 2009 and August 2016, to search for similar transient cerebellar symptoms. Thirty-three of those patients have been previously reported.[4] Written informed consent was obtained from all patients with approval of the Institutional Review Board of the Hospices Civils de Lyon. We selected all patients who had been reported by their referral physicians to have symptoms that were both transient and suggestive of cerebellar impairment, i.e., gait imbalance, slurred speech, or limb dysmetria. Further information was collected by telephone from the referral physicians, and, when possible, from the patients themselves or their relatives.

RESULTS **Index case.** A 61-year-old man was hospitalized for evaluation after a tonic-clonic generalized seizure. He was still active as a corporate executive, and his medical history included high blood pressure, diabetes, myocardial infarction, and a smoking habit. No prodromal or postictal symptom was reported, but the patient reported slight memory impairment, difficulties to concentrate at work, unusual emotiveness, and anxiety over a few days before the seizure. The patient was treated with levetiracetam and clobazam. However, the cognitive symptoms persisted and several partial temporal lobe seizures occurred. One month after the first seizure, the patient began to experience repeated episodes of slurred speech, gait ataxia, and slight dysmetria of the limbs (see video at Neurology.org/nn). These events occurred 3–4 times a day, were often triggered by emotions and orthostatism, and lasted less than 1 minute. No cerebellar symptom was observed between the episodes. Levetiracetam was switched to lacosamide without any improvement of the symptoms.

Brain MRI was normal. EEG found an asymmetric temporal lobe slowing. CSF analysis found 16 white blood cells/mm^3, a protein level of 65 mg/dL, and no oligoclonal band. Anti-CASPR2 antibodies were detected (end-point dilution using cell-binding–based assay, 1/40,960, in serum and 1/5,120 in CSF). Brain single-photon emission CT found bilateral frontotemporal hypoperfusion with normal perfusion of basal ganglia and cerebellum. Full-body CT was normal. Sequencing of the genes involved in EA types 1 and 2, *KCNA1* and *CACNA1A*, found that the patient carried a rare polymorphism in intron 39 of *CACNA1A* (c5843-14G>A).[5,6] *KCNA1* was normal. The patient was treated with 3 daily injections of 1 g methylprednisolone followed by 6 monthly pulses of 1 g cyclophosphamide. The frequency of the ataxia episodes decreased immediately; they had totally stopped 5 days after the end of the methylprednisolone pulses. The patient recovered all his cognitive abilities 2 weeks after the initiation of the treatment and had his last seizure 3 months after the first visit. At month 7 of follow-up, the patient remained asymptomatic and seizure free. At the peak of his disease, the patient had presented with only 2 core symptoms as defined by Van Sonderen et al.[3] (encephalic signs and cerebellar ataxia).

Cohort study. Among the cohort of 37 other patients with anti-CASPR2 antibodies (20 with encephalitis and 17 with neuromyotonia or Morvan syndrome), we retrospectively identified 5 patients with transient symptoms suggestive of cerebellar impairment. All the patients were men, with a median age of 60 years (range 57–69). Median follow-up (range) was 45.6 months (19.3–113.6). One patient had a history of surgically treated thyroid carcinoma. All these 5 patients had anti-CASPR2 antibodies in both serum and CSF and had a presentation of autoimmune encephalitis with prominent seizures and amnesia, as we previously reported.[4] Three patients also developed mild permanent cerebellar symptoms, concomitantly to (2 cases) or after (1 case) the onset of paroxysmal ataxia.

None of them exhibited neuromyotonia or Morvan syndrome. Two of the 5 patients had ≥3 core symptoms as defined in the study by Van Sonderen et al.[3] The transient episodes are described in the table. They were stereotyped and included, according to the cases, gait imbalance (5/5, 100%), slurred speech (3/5, 60%), limb dysmetria (3/5, 60%), and nystagmus (1/5, 20%).

Table Characteristics of the ataxia episodes in patients with autoimmune encephalitis and anti-CASPR2 antibodies

Age, y, sex	Follow-up, mo	Symptoms during the episodes	Triggering factors	Impact on daily activities	Duration of the episodes	Frequency at peak	Permanent cerebellar symptoms also present	Onset in relation to the onset of the limbic symptoms	Period during which paroxysmal ataxia occurred	Anti-CASPR2 ab titers		Treatments before resolution of the episodes
										Serum	CSF	
61, M	7	Gait imbalance, slurred speech, and limb dysmetria	Anxiety and orthostatism	No	<1 min	3–4/d	No	1 mo later	3 wk	1/40,960	1/1,520	Methylprednisolone, cyclophosphamide
62, M	114	Gait imbalance and slurred speech	None	No	A few minutes	2 episodes with an interval of 2 wk	No	10 mo later	2 wk	NA	1/320	None
57, M	51	Gait imbalance	Orthostatism	No	A few minutes to 2 h	3–5/wk	No	4 mo later	4 mo	1/10,240	1/640	Methylprednisolone, plasmapheresis
60, M	46	Gait imbalance, slurred speech, limb dysmetria, and neck stiffness	Orthostatism	Yes	A few minutes	2–3/d	Yes (gait imbalance and inferior limb dysmetria)	7 mo before	33 mo	1/10,240	1/10,240	Methylprednisolone
60, M	22	Gait imbalance, slurred speech, limb dysmetria, nystagmus, and neck stiffness	Orthostatism, anger	Yes	A few minutes	6–7/d	Yes (slight imbalance)	Concomitant	13 mo	1/10,240	1/10,240	Rituximab
69, M	19	Gait imbalance and limb dysmetria	Orthostatism	No	<1 min	<5/wk	Yes (slight imbalance)	17 mo later	2 mo	1/10,240	1/10,240	Prednisolone and IV immunoglobulin

Abbreviations: ab = antibodies; NA = not available.
The first line refers to the index case.

Two patients (40%) reported concomitant sensations of neck stiffness. Myoclonic jerks were not observed in any of the patients. Of interest, the ataxia episodes preceded by 7 months the full development of the encephalitis in 1 patient. The apparition of the ataxia was not subsequent to a change of antiepileptic medication in any of the patients. The attacks were reported to last from a few minutes to 2 hours, according to the cases, with triggering factors identified in 4 patients (80%; orthostatism in 4 patients and anger in 1 patient). Ataxia episodes occurred during a mean period of 4 months (range, 0.5–32.5) and stopped after the initiation of an immunomodulatory treatment in 4 patients (steroids alone, steroids and plasmapheresis, steroids and IV immunoglobulin, or rituximab) and spontaneously in 1 case. Interictal, milder cerebellar symptoms were observed in 3/5 cases (60%). Interictal brain MRI was unremarkable in all patients; magnetic resonance spectroscopy was not performed during the episodes. We did not perform genetic studies in these 5 patients.

DISCUSSION In this study, we report stereotyped episodes of paroxysmal cerebellar ataxia in a patient with anti–CASPR2 antibody-related autoimmune encephalitis. We also retrospectively identified similar paroxysmal symptoms in 5 of 20 other patients with autoimmune encephalitis and anti-CASPR2 antibodies, suggesting that episodic cerebellar ataxia could be observed in up to 25% of such patients.

As they developed during the course of encephalitis and resolved after immunomodulating therapy in most of the patients, we can speculate an immune origin of these paroxysmal ataxias. Moreover, the association of gait imbalance, slurred speech, and limb dysmetria during these episodes was highly suggestive of cerebellar impairment; although because of the retrospective collection of the data, we cannot completely exclude that the alleged cerebellar symptoms were actually of another nature (e.g., orthostatic hypotension, seizures, or peri-ictal autonomic manifestations).

Paroxysmal neurologic symptoms have already been reported in autoimmune encephalitis. For instance, faciobrachial dystonic seizures are caused by the activation of the motor cortex in patients with anti–leucine-rich glioma1 (Lgi1) antibody-associated encephalitis.[7] Of interest, Lgi1 is a secreted protein that complexes with CASPR2 and the potassium channel $K_V1.1$.[5,8] More recently, orthostatic myoclonus has been observed in a patient with anti-CASPR2 antibodies.[9] Although permanent ataxia without remissions is a well-described feature of anti–CASPR2 antibody-associated encephalitis, to our knowledge, EA has never been reported before in patients with

autoimmune encephalitis, including for instance patients with anti-Lgi1 encephalitis.[4,3,10,11]

Anti-CASPR2 antibodies associate with various neurologic disorders, including limbic encephalitis, neuromyotonia, and Morvan syndrome.[3,4,12–14] In a recent published cohort of 38 anti–CASPR2 antibody-positive patients, 77% of the cases had ≥3 core symptoms (encephalic signs, cerebellar symptoms, peripheral nerve hyperexcitability, dysautonomia, neuropathic pain, insomnia, and weight loss).[3] In our previously published cohort of 33 patients with anti-CASPR2 antibodies, only 16/33 (48%) of the patients presented with ≥3 of those core symptoms.[4] However, patients with limbic encephalitis were overrepresented and we found a greater number of patients with ≥3 core symptoms in the group of patients diagnosed with neuromyotonia or Morvan syndrome (13/15, 87%) than in the group of patients diagnosed with limbic encephalitis (3/18, 17%). Only 2/6 (33%) of our patients with paroxysmal ataxia had ≥3 core symptoms, which reflects that this paroxysmal syndrome is mostly associated with limbic encephalitis rather than neuromyotonia or Morvan syndrome.

The resemblance of the patients' paroxysmal ataxia with manifestations observed in hereditary channelopathies such as EA is striking. Of interest, neuromyotonia can be observed in patients with EA type 1 and anti-CASPR2 antibodies, suggesting similar ion channel dysfunctions in both diseases. EA type 1 is due to mutations of *KCNA1*, a gene coding for the voltage-gated potassium channel $K_V1.1$.[5,13] The clustering of $K_V1.1$ at the nodes of Ranvier depends on CASPR2, and electrophysiologic experiments have suggested an impairment of voltage-gated potassium channels in autoimmune neuromyotonia, implying that anti-CASPR2 antibodies might indirectly alter the functions of $K_V1.1$ at the nodes of Ranvier.[15,16] However, previous studies have failed to demonstrate a role of CASPR2 in $K_V1.1$ clustering at the synaptic level, and the exact role of anti-CASPR2 antibodies in the CNS is unknown.[16,17] Nevertheless, our observation supports the hypothesis of immune-mediated ion channel dysfunction in anti-CASPR2 antibody syndromes. The polymorphism of *CACNA1A* in the index patient is interesting because this gene codes for the $Ca_V2.1$ subunit of the P/Q type voltage-gated calcium channel that is mutated in patients with EA type 2.[6] We have no data about the significance of this polymorphism, whose overall frequency in the general population is estimated at less than 1/1,000. However, we can hypothesize that it may provoke a partial impairment of $Ca_V2.1$.[6] We can thus speculate that in the case, this polymorphism of *CACNA1A* may have led to the failure of compensatory mechanisms dependent on $Ca_V2.1$ and necessary to counterbalance the effects of anti-CASPR2 antibodies. Therefore, this polymorphism may have favored the development of episodic cerebellar symptoms in the patient.

Overall, our findings suggest that transient cerebellar ataxia should be added to the spectrum of anti–CASPR2 antibody-related symptoms. Such paroxysmal symptoms are similar to the symptoms of hereditary channelopathies, suggesting that ion channel dysfunction is involved in the pathogenesis of anti-CASPR2 antibody syndromes.

AUTHOR CONTRIBUTIONS

Dr. Joubert: study concept and design; acquisition of data; and analysis and interpretation. Dr. Gobert: acquisition of data and critical revision of the manuscript for important intellectual content. Dr. Thomas and Ms. Saint-Martin: acquisition of data. Dr. Desestret: critical revision of the manuscript for important intellectual content. Dr. Convers, Dr. Rogemond, and Ms. Picard: acquisition of data. Prof. Ducray, Dr. Psimaras, Prof. Antoine, and Prof. Delattre: critical revision of the manuscript for important intellectual content. Dr. Honnorat: study supervision; acquisition of data; study concept and design; and critical revision of the manuscript for important intellectual content.

ACKNOWLEDGMENT

The authors thank Dr. Cécile Marchal, Dr. Philippe Kassiotis, Dr. Jacques Testaud, Dr. Lejla Koric, and Dr. Isabelle Lambert, who provided CSF, serum samples, and clinical data for the study.

STUDY FUNDING

This study is supported by institutional grants from Agence Nationale de la Recherche (ANR-14-CE15-0001-MECANO), Fondation pour la Recherche Médicale (Neurodon2014), and CSL Behring France.

DISCLOSURE

B. Joubert, F. Gobert, L. Thomas, M. Saint-Martin, V. Desestret, P. Convers, V. Rogemond, G. Picard, F. Ducray, and D. Psimaras report no disclosures. J.-C. Antoine served on the scientific advisory board for Pfizer; received travel funding and/or speaker honoraria from Pfizer and Laboratoire Français des Biotechnologies et du Fractionnement; served as an associate editor for *Revue Neurologique*; and holds a patent for diagnostic test for anti-CV2/CRMP5 andibody detection. J.-Y. Delattre served on the editorial board for *The Oncologist*; received research support from Institut National du Cancer; reference center for anaplastic oligodendrogliomas. J. Honnorat reports no disclosures. Go to Neurology.org/nn for full disclosure forms.

Received March 3, 2017. Accepted in final form April 24, 2017.

REFERENCES

1. Tomlinson SE, Hanna MG, Kullmann DM, Tan SV, Burke D. Clinical neurophysiology of the episodic ataxias: insights into ion channel dysfunction in vivo. Clin Neurophysiol 2009;120:1768–1776.
2. D'Adamo MC, Hasan S, Guglielmi L, et al. New insights into the pathogenesis and therapeutics of episodic ataxia type 1. Front Cell Neurosci 2015;9:317.
3. Van Sonderen A, Ariño H, Petit-Pedrol M, et al. The clinical spectrum of Caspr2 antibody-associated disease. Neurology 2016;87:521–528.
4. Joubert B, Saint-Martin M, Noraz N, et al. Characterization of a subtype of autoimmune encephalitis with anti-contactin-associated protein-like 2 antibodies in the cerebrospinal fluid, prominent limbic symptoms, and seizures. JAMA Neurol 2016;73:1115–1124.

5. Browne DL, Gancher ST, Nutt JG, et al. Episodic ataxia/myokymia syndrome is associated with point mutations in the human potassium channel gene, KCNA1. Nat Genet 1994;8:136–140.
6. Terwindt GM, Ophoff RA, Haan J, et al. Variable clinical expression of mutations in the P/Q-type calcium channel gene in familial hemiplegic migraine. Dutch Migraine Genetics Research Group. Neurology 1998; 50:1105–1110.
7. Navarro V, Kas A, Apartis E, et al. Motor cortex and hippocampus are the two main cortical targets in LGI1-antibody encephalitis. Brain J Neurol 2016; 139:1079–1093.
8. Lai M, Huijbers MGM, Lancaster E, et al. Investigation of LGI1 as the antigen in limbic encephalitis previously attributed to potassium channels: a case series. Lancet Neurol 2010;9:776–785.
9. Gövert F, Witt K, Erro R, et al. Orthostatic myoclonus associated with Caspr2 antibodies. Neurology 2016;86: 1353–1355.
10. Becker EBE, Zuliani L, Pettingill R, et al. Contactin-associated protein-2 antibodies in non-paraneoplastic cerebellar ataxia. J Neurol Neurosurg Psychiatry 2012;83:437–440.
11. Balint B, Regula JU, Jarius S, Wildemann B. Caspr2 antibodies in limbic encephalitis with cerebellar ataxia, dyskinesias and myoclonus. J Neurol Sci 2013;327:73–74.
12. Irani SR, Pettingill P, Kleopa KA, et al. Morvan syndrome: clinical and serological observations in 29 cases. Ann Neurol 2012;72:241–255.
13. Lancaster E, Huijbers MG, Bar V, et al. Investigations of Caspr2, an autoantigen of encephalitis and neuromyotonia. Ann Neurol 2011;69:303–311.
14. Bien CG, Mirzadjanova Z, Baumgartner C, et al. Anti-contactin-associated protein-2 encephalitis: relevance of antibody titres, presentation and outcome. Eur J Neurol 2017;24:175–186.
15. Horresh I, Poliak S, Grant S, Bredt D, Rasband MN, Peles E. Multiple molecular interactions determine the clustering of Caspr2 and Kv1 channels in myelinated axons. J Neurosci 2008;28:14213–14222.
16. Sinha S, Newsom-Davis J, Mills K, Byrne N, Lang B, Vincent A. Autoimmune aetiology for acquired neuromyotonia (Isaacs' syndrome). Lancet 1991;338:75–77.
17. Ogawa Y, Horresh I, Trimmer JS, Bredt DS, Peles E, Rasband MN. Postsynaptic density-93 clusters Kv1 channels at axon initial segments independently of Caspr2. J Neurosci 2008;28:5731–5739.

© 2017. Published by The Company of Biologists Ltd | Journal of Cell Science (2017) 130, 2209-2220 doi:10.1242/jcs.202267

RESEARCH ARTICLE

The Kv1-associated molecules TAG-1 and Caspr2 are selectively targeted to the axon initial segment in hippocampal neurons

Delphine Pinatel[1], Bruno Hivert[1], Margaux Saint-Martin[2], Nelly Noraz[2], Maria Savvaki[3], Domna Karagogeos[3] and Catherine Faivre-Sarrailh[1,*]

ABSTRACT

Caspr2 and TAG-1 (also known as CNTNAP2 and CNTN2, respectively) are cell adhesion molecules (CAMs) associated with the voltage-gated potassium channels Kv1.1 and Kv1.2 (also known as KCNA1 and KCNA2, respectively) at regions controlling axonal excitability, namely, the axon initial segment (AIS) and juxtaparanodes of myelinated axons. The distribution of Kv1 at juxtaparanodes requires axo-glial contacts mediated by Caspr2 and TAG-1. In the present study, we found that TAG-1 strongly colocalizes with Kv1.2 at the AIS of cultured hippocampal neurons, whereas Caspr2 is uniformly expressed along the axolemma. Live-cell imaging revealed that Caspr2 and TAG-1 are sorted together in axonal transport vesicles. Therefore, their differential distribution may result from diffusion and trapping mechanisms induced by selective partnerships. By using deletion constructs, we identified two molecular determinants of Caspr2 that regulate its axonal positioning. First, the LNG2-EGF1 modules in the ectodomain of Caspr2, which are involved in its axonal distribution. Deletion of these modules promotes AIS localization and association with TAG-1. Second, the cytoplasmic PDZ-binding site of Caspr2, which could elicit AIS enrichment and recruitment of the membrane-associated guanylate kinase (MAGuK) protein MPP2. Hence, the selective distribution of Caspr2 and TAG-1 may be regulated, allowing them to modulate the strategic function of the Kv1 complex along axons.

KEY WORDS: Polarity, Axonal transport, Cell adhesion molecule, Axon initial segment, Juxtaparanode

INTRODUCTION

The axon initial segment (AIS) is a specialized region of neurons where action potentials are initiated. The high density of specific voltage-gated Na^+ and K^+ channels gives the AIS unique electrical properties. The voltage-gated Na^+ channels Nav1.2 and Nav1.6 (also known as SCN2A and SCN8A, respectively) are anchored at the AIS via the ankyrinG scaffold, which is the major organizer of this axonal subdomain (Yoshimura and Rasband, 2014; Zhou et al., 1998). A variety of voltage-gated K^+ channels are localized at AIS, including Kv7.2 and Kv7.3 (also known as KCNQ2 and KCNQ3, respectively), Kv1.1 and Kv1.2 (KCNA1 and KCNA2, respectively) and Kv2.1 (KCNB1), which function as modulators of action potential initiation and frequency (Devaux et al., 2004; King et al., 2014; Trimmer, 2015; Van Wart et al., 2007). The Kv7.2 and Kv7.3 channels are tethered at the AIS through ankyrinG binding (Pan et al., 2006), while the mechanisms responsible for Kv2.1 and Kv1.1/Kv1.2 enrichment are poorly understood. The distribution of Kv channels at the AIS and along axon may influence intrinsic excitability and transmitter release (Kole and Stuart, 2012; Rama et al., 2015).

The Kv1 channels co-purify with several cell adhesion molecules (CAMs) including Caspr2 (also known as CNTNAP2), TAG-1 (also known as CNTN2), LGI1 and ADAM22 proteins. These CAMs are autoimmune targets in limbic encephalitis that is associated with voltage-gated K^+ channels (Irani et al., 2010; Lancaster et al., 2011). The role of Caspr2 and TAG-1 has been well established at the juxtaparanodes of myelinated axons where they mediate axo-glial contacts and induce the clustering of Kv1.1 and Kv1.2 to control the internodal resting potential (Poliak et al., 2003; Traka et al., 2003). The intracellular protein 4.1B (also known as EPB41L3), which binds Caspr2 is required for assembling the juxtaparanodal scaffold (Buttermore et al., 2011; Cifuentes-Diaz et al., 2011; Einheber et al., 2013; Horresh et al., 2010). In contrast to juxtaparanodes, Caspr2, and TAG-1, although present at the AIS are dispensable for the recruitment of Kv1 channels there (Duflocq et al., 2011; Inda et al., 2006; Ogawa et al., 2008). In addition, protein 4.1B is not enriched at the AIS while the membrane-associated guanylate kinase (MAGuK) PSD-93 (also known as DLG2) is present at that site (Duflocq et al., 2011; Ogawa et al., 2008). Other membrane proteins interacting with Kv1 channels could be localized at the AIS. In particular, ADAM22 is recruited at the AIS of cultured hippocampal neurons with PSD-93, but is not required for the clustering of Kv1 channels (Ogawa et al., 2010).

Whether CAMs can modulate Kv1 channel surface expression and activity tuning at the AIS is still unclear. In this regard, it would be important to analyze the molecular mechanisms that are implicated in the recruitment of Caspr2 and TAG-1 at the AIS. We have previously shown that Caspr2 is delivered both to the somatodendritic and axonal compartments in hippocampal neurons, and its polarized expression is achieved through selective endocytosis from the somatodendritic plasma membrane. The cell surface expression of Caspr2 is regulated through an endocytosis motif that overlaps with the 4.1B-binding sequence (Bel et al., 2009). Caspr2 does not interact with type I PDZ proteins, like PSD-93, but may associate with MAGuK proteins of the MPP2 family and MUPP1 (also known as MPDZ) (Horresh et al., 2008; Tanabe et al., 2015). In the present study, we used deletion or chimeric constructs to identify cytoplasmic and extracellular determinants implicated in the AIS versus axonal distribution of Caspr2.

[1]Aix-Marseille Université, CNRS, Centre de Recherche en Neurobiologie et Neurophysiologie de Marseille, Marseille UMR7286, France. [2]Institut Neuromyogène, CNRS UMR 5310, INSERM U1217, Université Claude Bernard Lyon 1, 69 372 Lyon, France. [3]Department of Basic Sciences, University of Crete Medical School and Institute of Molecular Biology and Biotechnology, Foundation for Research and Technology, University of Crete, Heraklion, Crete 711 10, Greece.

*Author for correspondence (catherine.sarrailh@univ-amu.fr)

D.P., 0000-0001-5514-0551; B.H., 0000-0002-3371-6123; M.S., 0000-0003-2240-4543; N.N., 0000-0003-4076-9773; M.S., 0000-0001-9094-1055; D.K., 0000-0002-8129-9731; C.F., 0000-0002-1718-0533; C.F., 0000-0002-1718-0533

Received 6 February 2017; Accepted 18 May 2017

Journal of Cell Science

Journal of Cell Science (2017) 130, 2209-2220 doi:10.1242/jcs.202267

In addition, we examined the interdependence of the two CAMs, Caspr2 and TAG-1 for their axonal transport and targeting.

RESULTS

TAG-1 is enriched at the AIS whereas Caspr2 is expressed along the axon in cultured hippocampal neurons

Caspr2 and TAG-1 have been reported to colocalize with Kv1 channels at the AIS in several neuronal subtypes, such as motor and cortical neurons (Duflocq et al., 2011; Inda et al., 2006). We analyzed the surface expression of endogenous Caspr2 and TAG-1 in hippocampal neurons in culture using live double-immunostaining at 14 days *in vitro* (DIV14). We observed that Caspr2 and TAG-1 were differentially distributed. As previously reported (Pinatel et al., 2015), we used anti-Caspr2 auto-antibodies from patients with limbic encephalitis to show that Caspr2 surface labeling was polarized to axons (Fig. 1A, red), but not enriched at the AIS, which can be labeled for ankyrinG (Fig. 1A, blue). In contrast, TAG-1 was enriched at the AIS, as shown using mouse anti-TAG-1 monoclonal antibody (mAb) 1C12 (Fig. 1A, green). As observed for endogenous molecules, transfected Caspr2–HA was distributed all along the axonal membrane (Fig. 1B, red), whereas TAG-1–GFP was enriched at the AIS (Fig. 1B, green).

We asked whether the AIS versus axonal distribution of TAG-1–GFP and Caspr2–HA might be correlated with the concentration of Kv1 channels at the AIS. Hippocampal neurons were double-transfected with both CAMs at DIV14, and their surface expression was measured at the AIS and along the axon (Fig. 1C–F). TAG-1–GFP, but not Caspr2–HA, was enriched at the AIS, as also observed for Kv1.2 (Fig. 1C). Quantitative analysis was performed by measuring the ratio of the mean fluorescence intensity at the AIS versus at the axon. The mean AIS:axon ratios were 2.31±0.16 for

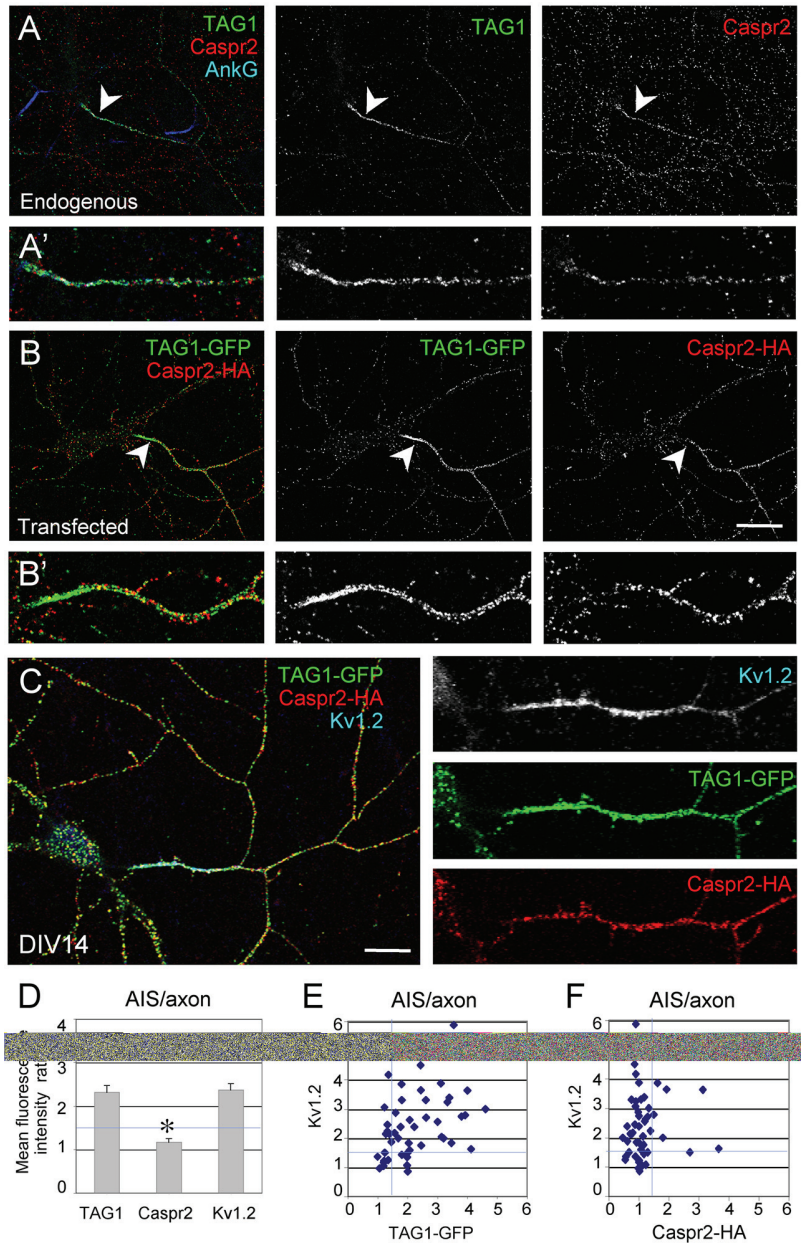

Fig. 1. TAG-1 is enriched at the AIS and Caspr2 is uniformly targeted along the axon in cultured hippocampal neurons. (A,A′) Hippocampal neurons at DIV14 were surface labeled using human anti-Caspr2 autoantibodies (red) and mouse anti-TAG-1 1C12 mAb (green), and were then fixed and permeabilized before staining for the AIS marker ankyrinG (blue). Endogenous TAG-1 was enriched at the AIS whereas Caspr2 was uniformly detected along the axon. (B,B′) Hippocampal neurons at DIV14 were co-transfected with TAG-1–GFP and Caspr2–HA and surface labeled for GFP (green) and HA (red). The AIS is indicated with arrowheads. (C–F) DIV14 hippocampal neurons were co-transfected with TAG-1–GFP and Caspr2–HA and surface labeled for GFP (green) and HA (red). Neurons were fixed, permeabilized and immunostained for Kv1.2 (blue). The AIS:axon ratio (denoted AIS/axon) of fluorescence intensity was calculated and expressed as the mean±s.e.m. (n=46) (D), or plotted for individual neurons (E,F). *P<0.01 by comparison with TAG-1 (ANOVA). Note that TAG-1–GFP enrichment at the AIS correlates with the level of AIS enrichment of endogenous Kv1.2, whereas that for Caspr2–HA does not. Scale bars: 20 µm (B); 10 µm (C).

Journal of Cell Science

Journal of Cell Science (2017) 130, 2209-2220 doi:10.1242/jcs.202267

TAG-1–GFP, 1.16±0.09 for Caspr2-HA and 2.37±0.15 for Kv1.2 (mean±s.e.m.; Fig. 1D). The individual values (n=46) were plotted, showing that the AIS:axon ratio for TAG-1 was correlated with the AIS:axon ratio value for the Kv1.2 channel (Fig. 1E). In contrast, Caspr2–HA was not enriched at the AIS of neurons, even in axons where the Kv1.2 channels were highly enriched in the AIS (Fig. 1F). This result indicates that TAG-1 and Kv1 may be anchored to the AIS in a complex within the same scaffold.

Since TAG-1 is a glycophosphatidylinositol (GPI)-anchored CAM, it does not directly interact with intracellular AIS components. The Ig domains of TAG-1 interact with multiple binding partners including NrCAM and the neurofascin isoform 186 (neurofascin-186) (Fig. S1). These two related CAMs are trapped at the AIS via their ankyrin-binding motif (Davis et al., 1996). Therefore, we analyzed the role of the Ig and fibronectin type III (FnIII) domains of TAG-1 in its enrichment at the AIS (Fig. 2). GFP-tagged full-length TAG-1, and GFP-tagged deletion mutants TAG-1-Ig (containing only the Ig domain) and TAG-1-Fn (containing only the FnIII domains) (schematized in Fig. 2D) were transfected in hippocampal neurons at DIV14 (Fig. 2A–C). The AIS:axon ratio was significantly reduced for the TAG-1-Ig and TAG-1-Fn deletion mutants (1.38±0.08 and 1.14±0.09, respectively) compared to that seen for full-length TAG-1 (2.53±0.14) (Fig. 2E). Next, we analyzed the Kv1.2 expression in neurons transfected with TAG-1-Ig and TAG-1-Fn. Kv1.2 (red) was enriched at the AIS labeled for ankyrinG (blue), whereas both TAG-1 deletion mutants (green) were evenly distributed along the axon (Fig. 2G,H). The AIS:axon ratio for Kv1.2 was 2.23±0.15 (n=26) and 2.81±0.24 (n=15) in neurons transfected with TAG-1-Ig and TAG-1-Fn, respectively. Plotting of individual values did not indicate any correlation between the AIS:axon ratios of Kv1.2 and TAG1 deletion mutants (Fig. 2I,J). Thus, the conformation of the full-length TAG-1 molecule seems to be required for its proper targeting at the AIS. These data also suggest that TAG-1 might be

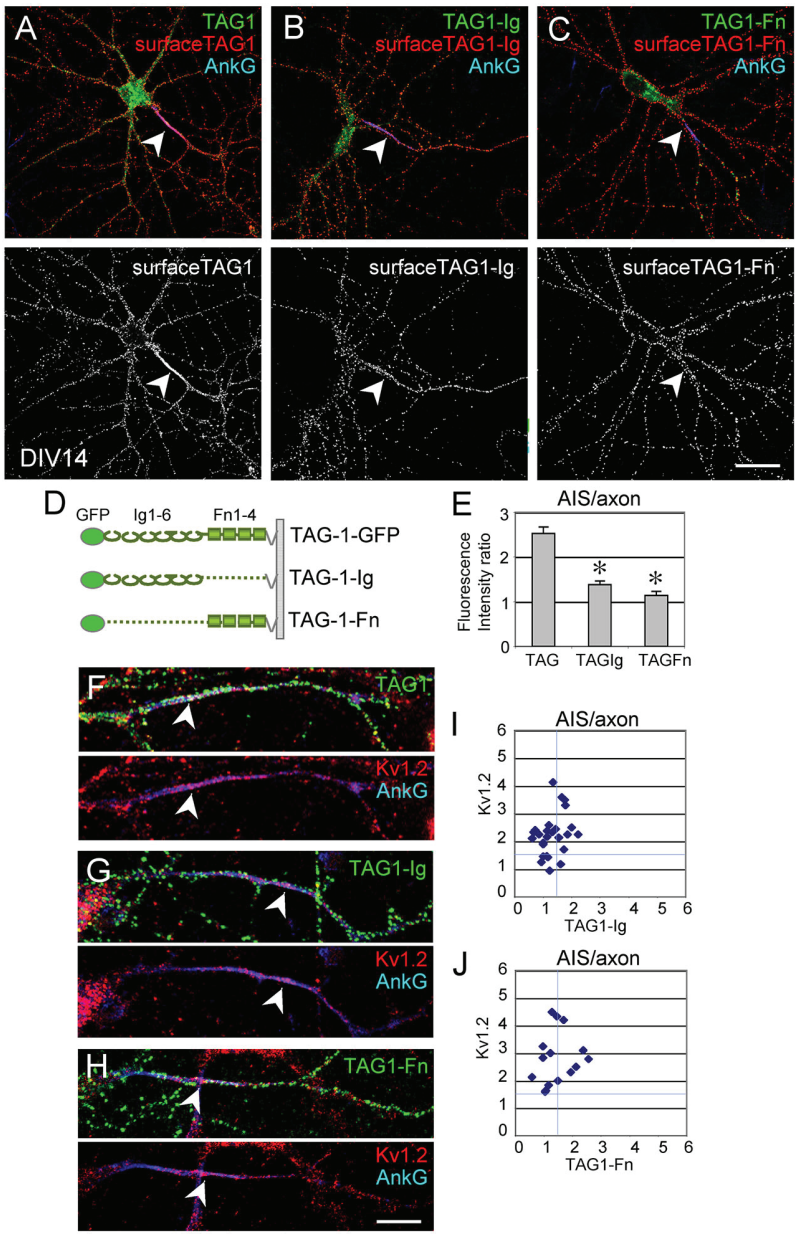

Fig. 2. Deletion of the Ig or FnIII domains of TAG-1 prevents its enrichment at the AIS in cultured hippocampal neurons. Neurons at DIV14 were transfected with TAG-1–GFP (A,F), TAG-1-Ig (B,G) or TAG-1-Fn (C,H). (A–C) Neurons were surface labeled for GFP (red), then permeabilized and immunostained for ankyrinG (blue). Note that only full-length TAG-1–GFP is highly recruited to the AIS. (D) Schematic drawing of the TAG-1 deletion mutants. (E) AIS:axon ratios of fluorescence intensity (mean±s.e.m., n=18). *P<0.01 by comparison with full-length TAG-1–GFP (ANOVA). (F–H) Neurons were surface labeled for GFP (green), then permeabilized and immunostained for ankyrinG (blue) and Kv1.2 (red). Arrowheads in A–C and F–H indicate the AIS. (I,J) The AIS:axon ratio (AIS/axon) of fluorescence intensity for TAG-1-Ig or TAG-1-Fn versus Kv1.2 was plotted for individual neurons. Scale bars: 20 µm (C); 5 µm (H).

Journal of Cell Science (2017) 130, 2209-2220 doi:10.1242/jcs.202267

recruited to the Kv1 complex independently of the neurofascin–NrCAM–ankyrinG complex.

The LNG2 and EGF1 modules in the ectodomain of Caspr2 determine its axonal distribution

Next, we addressed the role of the Caspr2 ectodomain in its polarized expression to the axonal surface. We analyzed the distribution of a series of HA-tagged Caspr2 constructs with sequential deletions of modules in the ectodomain (Fig. 3A; Pinatel et al., 2015). After transfection at DIV7, hippocampal neurons were surface labeled for HA (green), and then fixed and permeabilized before staining for ankyrinG as an AIS marker (blue). Strikingly, Caspr2Δ2, which has a deletion of the laminin-G2 (LNG2) and EGF-like1 (EGF1) modules, was strongly enriched at the AIS (Fig. 3C,F) by contrast with full-length Caspr2 (Fig. 3B,D). All the other deletion mutants (Caspr2Δ1, Caspr2Δ3 and Caspr2Δ4) were distributed along the axon (Fig. 3E,G,H). Quantitative analysis indicated that the mean AIS:axon ratio of Caspr2Δ2 (2.4±0.4) was significantly increased in comparison with that for full-length Caspr2 (0.95±0.1) (Fig. 3I). We observed that Caspr2Δ2 enrichment at the AIS of transfected neurons correlated with the level of endogenous Kv1.2 enrichment by plotting individual values for the AIS:axon ratios (n=27) (Fig. S2A–C). Therefore, the LNG2 and EGF1 modules in the ectodomain may exert a dominant effect, promoting the distribution of Caspr2 all along the axon. Alternatively, deletion of these modules may induce a conformational change and influence the association between Caspr2 and TAG-1.

To analyze the interaction between Caspr2 and TAG-1, co-immunoprecipitation experiments were performed using extracts

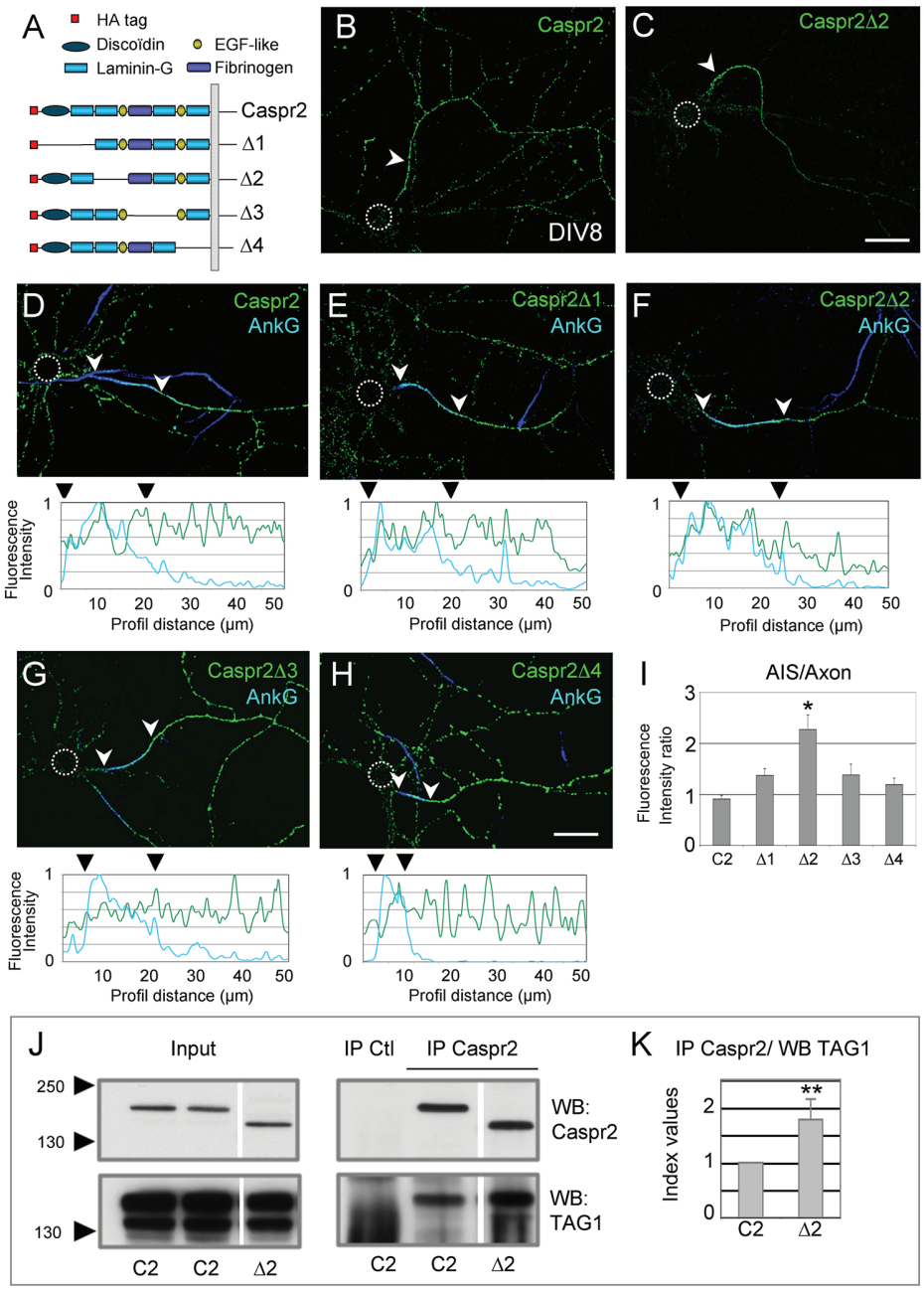

Fig. 3. The expression of the Caspr2Δ2 deletion mutant is restricted to the AIS. (A) Caspr2–HA constructs encompassing sequential deletions: Δ1 has a deletion of the N-terminal discoïdin and LNG1 domains, Δ2 has a deletion of the LNG2 and EGF1 domains, Δ3 has a deletion of the central fibrinogen and LNG3 domains, and Δ4 has a deletion of the EGF2 and LNG4 domains. (B–H) Rat hippocampal neurons were transfected with the Caspr2 constructs and surface labeled at DIV7 with anti-HA mAb (green). The Caspr2Δ2 mutant (C) is highly enriched at the AIS by comparison with full-length Caspr2 (B). Cells were fixed with 4% paraformaldehyde, permeabilized and double-stained for ankyrinG (blue). The soma is indicated with circles and AIS highlighted with arrowheads. (D–H) Axonal profiles of fluorescence intensity of Caspr2 constructs (green) and ankyrinG (blue). Arrowheads mark each end of the AIS. Scale bars: 20 µm (C); 10 µm (H). (I) Ratio of fluorescence intensity for Caspr2 constructs measured at the AIS and along the axon (mean±s.e.m., n=10). *P<0.01 by comparison with full-length Caspr2 (C2) (ANOVA). (J) Co-immunoprecipitation experiments from HEK cells transfected with TAG-1–GFP and HA-tagged Caspr2, either full-length (C2) or Caspr2Δ2 (Δ2). Immunoprecipitation was performed using a rabbit antiserum directed against the cytoplasmic tail of Caspr2 (IP Caspr2) or with control rabbit IgGs (IP Ctl). Western blotting (WB) was performed using rabbit anti-Caspr2 or anti-TAG-1 antibody in the lysates (input) and immunoprecipitates. (K) Quantitative (mean±s.e.m.) analysis of the level of co-immunoprecipitated proteins was performed from five independent experiments with the ImageJ software. The ratio of co-immunoprecipitated TAG1 over immunoprecipitated Caspr2 signal intensities was calculated. Results were presented as index values relative to the full-length Caspr2 condition. **P<0.01 (Mann–Whitney's test).

Journal of Cell Science (2017) 130, 2209-2220 doi:10.1242/jcs.202267

from HEK cells co-transfected with TAG-1–GFP and Caspr2–HA constructs. As shown in Fig. 3J, both Caspr2 and Caspr2Δ2 constructs interacted with TAG-1. Quantitative analysis indicated that the Δ2 deletion significantly increased co-immunoprecipitation of TAG-1 (+78%, n=5) by comparison with full-length Caspr2 (Fig. 3K). Thus, Caspr2Δ2 might be enriched at the AIS because of its tight binding with endogenous TAG-1. Deletion of the LNG2 and EGF1 domains in the Caspr2Δ2 mutant may induce a conformational change favoring TAG-1 binding or association of the Caspr2Δ2 cytoplasmic tail to scaffolding molecules.

Caspr2 and TAG-1 are colocalized in axonal transport vesicles

Caspr2 and TAG-1 are known to interact in cis (Fig. 3J; Traka et al., 2003). However, they are differentially distributed along the axon, as TAG-1 is enriched at the AIS whereas Caspr2 evenly detected all along the axon. We performed time-lapse recording of neurons transfected at DIV7 with Caspr2–mCherry and TAG-1–GFP to get some insight into their axonal-targeting mechanisms (Fig. 4). The axon was clearly identified on the basis of its length, and was strongly enriched in transport vesicles by comparison with dendrites. In addition, live immunolabeling of neurofascin-186 was used to precisely localize the AIS after time-lapse recording (Fig. 5, blue). We found that most of the axonal transport vesicles were colabeled for Caspr2 and TAG-1 (Fig. 4E; Movie 1). Kymograph analysis of transport events indicated that double-labeled vesicles moved bi-directionally as illustrated in Fig. 4B–D. In neurons that were transfected with TAG-1–GFP alone, we observed that labeled vesicles were mostly axonally transported in the retrograde direction with a maximal velocity (V_m) of 0.34–0.64 µm/s (Table S1; Fig. 5A). In neurons that were transfected with Caspr2–mCherry alone, labeled vesicles were transported in the anterograde and retrograde directions with a V_m of 0.66–1.46 and 0.75–0.95 µm/s, respectively (Table S1; Fig. 5B,C). The vesicular transport of Caspr2–mCherry was similar to that described previously for Caspr2–GFP (Bel et al., 2009). Of note, mCherry was fused at the C-terminal of Caspr2 and did not perturb its transport by comparison with GFP, which was inserted downstream the signal peptide. Finally, when double-transfected for Caspr2 and TAG-1, some neurons exhibited bidirectional transport of colabeled vesicles (Fig. 5D; Table S1), whereas in most neurons, the vesicular transport was mainly observed in the retrograde direction with a velocity of 0.35–0.62 µm/s (Fig. 5E,F; Movie 2, Table S1). Some vesicles were observed moving retrogradely starting from the axonal growth cone (Movie 3) and may result from endocytosis as previously described (Bel et al., 2009). The retrograde axonal transport may indicate a very dynamic renewal of Caspr2 and TAG-1 at the axonal membrane.

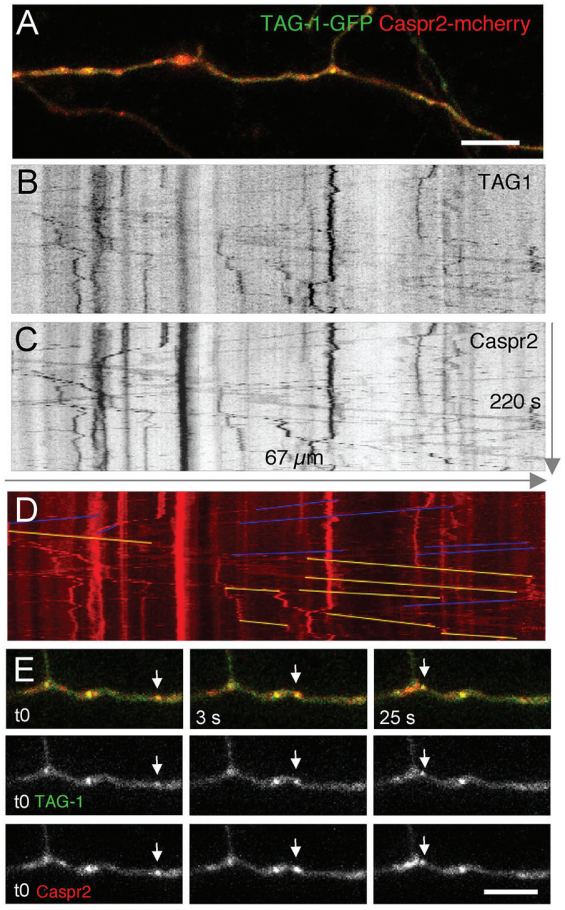

Fig. 4. Caspr2 and TAG-1 are colocalized within axonal transport vesicles. (A) Axon of hippocampal neuron co-transfected at DIV7 with TAG-1–GFP and Caspr2–mCherry. Time-lapse images of axonal transport vesicles were acquired at 1 frame every 1.5 s for 220 s. (B–D) Corresponding kymographs showing overlapping trajectories of vesicles labeled for TAG-1–GFP (B) and Caspr2–mCherry (C). (D) Anterograde and retrograde events are underlined with yellow and blue lines, respectively, and the velocity measured for each transport event. (E) Time-lapse sequence showing a moving vesicle that contains both TAG-1–GFP and Caspr2—mCherry indicated with arrows. Scale bars: 10 µm (A); 6 µm (E). See also the corresponding Movie 1.

In conclusion, Caspr2 and TAG-1 are sorted within the same axonal vesicles even if they are distributed to distinct locations along the axon. Thus, we hypothesize that these proteins may be differentially distributed to AIS or axon according to diffusion and/or trapping mechanisms.

The cytoplasmic tail of Caspr2 promotes the recruitment of the MAGuK protein MPP2 at the AIS

Next, we addressed the role of the cytoplasmic tail of Caspr2 and whether it may contain a motif for its recruitment to the axon. We generated a Nr–Caspr2cyt construct (Fig. 6A) with the cytoplasmic tail of Caspr2 fused to the reporter NrCAM-Ig previously described in Falk et al., (2004). Strikingly, we observed that this chimera (green) was strongly enriched at the AIS surface of DIV8 hippocampal neurons double-stained for ankyrinG (blue) (Fig. 6B,C), with an AIS:axon ratio of 4±0.6 (Fig. 6G). Deletion of the C-terminal region or the PDZ-binding motif induced re-localization all along the axon with an AIS:axon ratio of 1.5±0.3 and 1.6±0.2, respectively (Fig. 6E–G). We also observed that deletion of the 4.1B-binding site induced a significant decrease in the AIS enrichment. The Δ4.1B mutant displayed an AIS:axon ratio of 2.1±0.3 (Fig. 6D,G). These results indicate that the cytoplasmic region of Caspr2 contains determinants for its AIS enrichment, namely, the 4.1B- and PDZ-binding domains. However, in the context of full-length Caspr2, its ectodomain exerts a dominant effect promoting axonal distribution.

The PDZ-binding domain of Caspr2 is a type II binding sequence and does not interacting with type I PSD-93 or PSD-95 as reported for Kv1 channels (Ogawa et al., 2008). It was reported to associate with MAGuK proteins of the CASK and MPP2 family in GST pulldown assays (Horresh et al., 2008). Hence, we generated CASK–mCherry and MPP2–mCherry constructs and observed that these MAGuK proteins were strongly recruited to the plasma

Journal of Cell Science

Journal of Cell Science (2017) 130, 2209-2220 doi:10.1242/jcs.202267

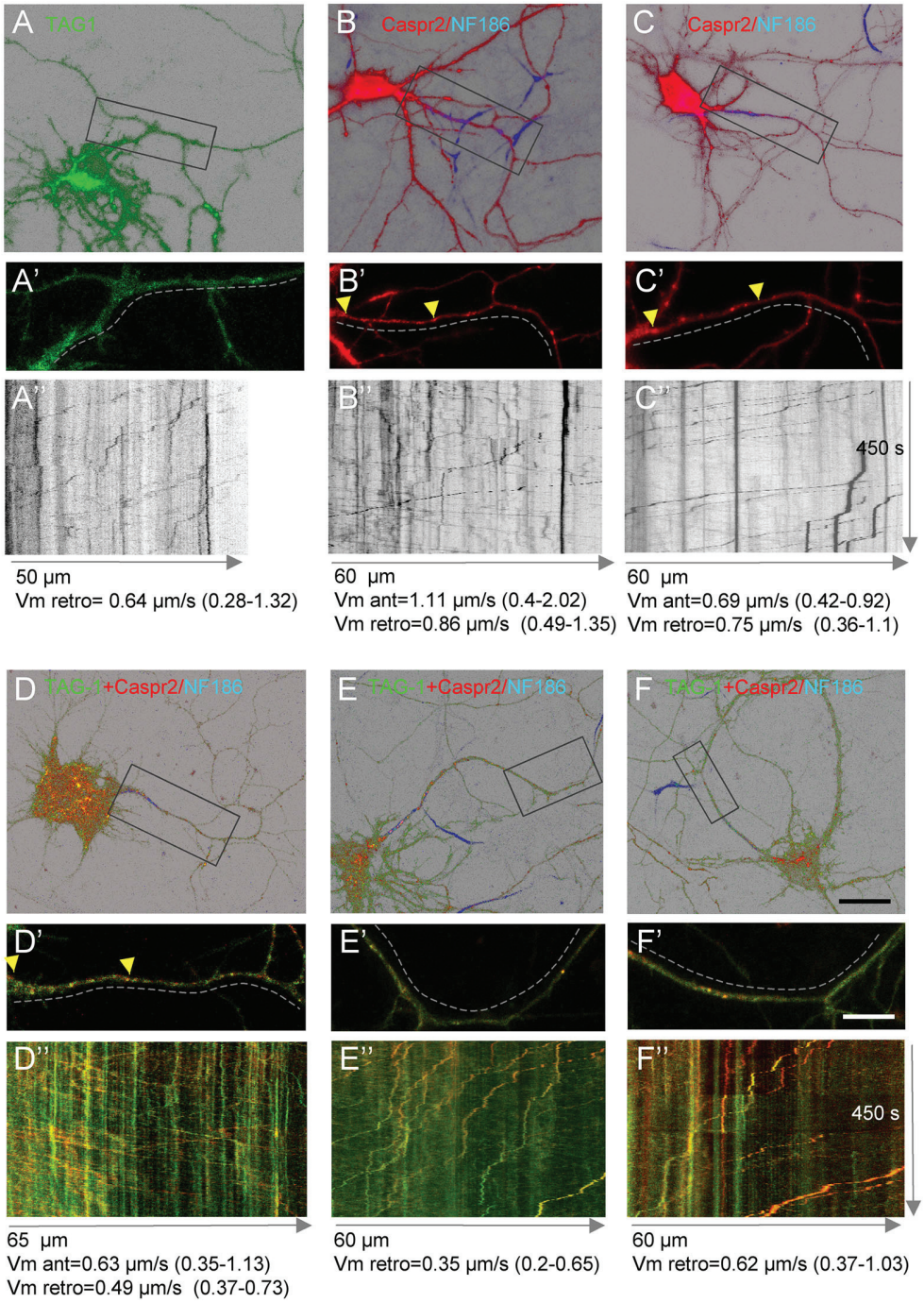

Fig. 5. Hippocampal neurons showing different types of axonal transport events for TAG-1–GFP and Caspr2–mCherry vesicles. Hippocampal neurons were transfected at DIV7 with TAG-1–GFP (A), Caspr2–mCherry (B,C) or double-transfected with both CAMs (D–F). Time-lapse images of axonal transport vesicles were acquired at 1 frame every 1.5 s for 450 s. (B–F) Live immunostaining with Alexa-Fluor-647-coupled anti-neurofascin-186 was performed to determine the AIS location (blue), as indicated with arrowheads in B′–D′. The insets in A′–F′ show the scanned axonal regions. Underlined axonal segments were used for kymograph analysis (axonal length in *x*-axis, time in *y*-axis) (A″–F″) and the maximal velocity (V_m) was determined for anterograde (ant) and retrograde (retro) events. Note that in A″,E″ and F″, transport events were mostly in the retrograde direction for TAG-1–GFP (A″), Caspr2–mCherry (C″) and double-labeled vesicles (E″,F″). In some neurons, bidirectional events were detected for Caspr2–mCherry and double-labeled vesicles (B″,D″). See also Movie 2 showing retrograde transport of double-labeled vesicles. Scale bar: 20 µm (F); 10 µm (F′).

membrane when co-transfected with Nr–Caspr2cyt in HEK cells, as shown for MPP2 (Fig. 7A). MPP2 was not recruited to the plasma membrane by Nr–Caspr2cyt with a deletion of its PDZ-binding domain (Fig. 7B). Next, we performed co-immunoprecipitation experiments after transfection in HEK cells. Caspr2 was precipitated with MPP2 (Fig. 7D–G, last lane) and with CASK (data not shown). Nr–Caspr2cyt was even more strongly precipitated by MPP2 (Fig. 7D–G, first lane). As expected, co-immunoprecipitation of Nr–Caspr2cyt with MPP2 was prevented by deletion of its C-terminal region or PDZ-binding domain (Fig. 7D–G, ΔC and ΔZ). Deletion of the 4.1B-binding site also significantly inhibited co-immunoprecipitation with MPP2 (Fig. 7D–G, Δ4.1), indicating that it may participate in stabilizing the interaction with the MAGuK protein.

To examine whether MAGuK proteins could be recruited to the AIS, hippocampal neurons were co-transfected with Caspr2, Caspr2Δ2, or Nr–Caspr2cyt and MPP2–mCherry (Fig. 8). When co-transfected with full-length Caspr2, MPP2–mCherry was homogenously distributed in the cytoplasm of hippocampal neurons and did not colocalize with Caspr2 along the axon (Fig. 8A). Strikingly, MPP2–mCherry became recruited to the AIS when co-transfected with Caspr2Δ2 (Fig. 8B,B′) or Nr–Caspr2cyt (Fig. 8C,D,D′). In addition, MPP2–mCherry colocalized with Nr–Caspr2cyt in intracellular vesicles (Fig. 8D″) in accordance

Journal of Cell Science (2017) 130, 2209-2220 doi:10.1242/jcs.202267

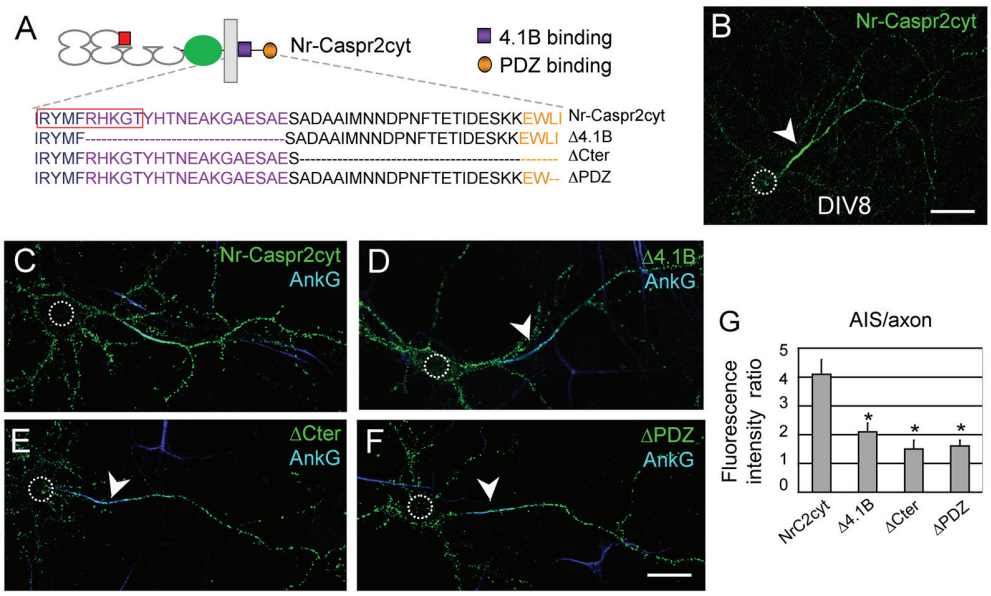

Fig. 6. The Caspr2 cytoplasmic region promotes enrichment at the AIS. (A) The Nr–Caspr2cyt reporter construct contains the Caspr2 transmembrane and cytoplasmic regions fused to the NrCAM signal peptide and Ig domains, tagged with HA and GFP. The sequence of the cytoplasmic tail of Caspr2 contains a 4.1B-binding region (purple), an endocytosis motif (red box) and a PDZ-binding motif (orange). Deletions in Δ4.1B, ΔCter and ΔPDZ mutants are indicated. (B–F) Hippocampal neurons transfected at DIV7 with the reporter Nr–Caspr2cyt constructs and surface labeled with anti-HA mAb (green). Double-staining was performed for the AIS marker ankyrinG (blue). The soma is indicated with circles and AIS highlighted with arrowheads. Note that only Nr–Caspr2cyt is highly enriched at the AIS (B,C). Scale bars: 20 µm (B); 10 µm (F). (G) AIS:axon (AIS/axon) ratios of fluorescence intensity measured for Nr–Caspr2cyt (NrC2cyt) and the deleted constructs Δ4.1B, ΔCter and ΔPDZ (means±s.e.m.; n=10). *P<0.05 by comparison with Nr–Caspr2cyt (ANOVA).

with endocytosis mediated by the Caspr2 cytoplasmic tail (Bel et al., 2009).

The fact that, upon transfection of Caspr2, MPP2 was not recruited to the AIS or along the axon, indicated that an outside-in mechanism might regulate this association. The C-terminal region of Caspr2 contains several consensus sites for phosphorylation by the casein kinase 2 (CK2) (Thr1319, Thr1321 and Ser1325; NetPhos 3.1 prediction server) that might regulate the PDZ-binding site of Caspr2. We generated several constructs of Nr–Caspr2cyt as shown in Fig. 7C including mutating Thr1319 and Thr1321 into alanine (TTAA) or glutamate (TTEE) residues and mutation of Ser1325 to a glutamate residue (SE). When transfected into hippocampal neurons, all these mutated constructs were recruited to the AIS (not shown). In addition, co-immunoprecipitation experiments did not show any effect of these mutations on MPP2 binding (Fig. 7D–G). Thus, we could not identify a phosphorylation mechanism possibly regulating the recruitment of Caspr2 at the AIS through its interaction with a MAGuK protein. Alternatively, we showed that the 4.1B-binding domain plays a modulating role on this interaction.

We examined whether the recruitment of Nr–Caspr2cyt and MPP2 at the AIS may be correlated with the concentration of Kv1 channels at that site. Hippocampal neurons were co-transfected with Nr–Caspr2cyt and MPP2. The mean AIS:axon ratio of fluorescence intensity was 3.10±0.17 for Nr–Caspr2cyt, 3.09±0.56 for MPP2, and 2.94±0.32 for Kv1.2 (Fig. S2). The individual values (n=18) were plotted showing that the AIS:axon ratios for both Nr–Caspr2cyt and MMP2 were correlated with that of the Kv1.2 channels. This result indicated that MPP2 can be recruited by the scaffold associated with the Kv1.2 complex.

Taken together, these data indicate that MPP2 could be trapped at the AIS through its association with the Caspr2 PDZ-binding domain. This MPP2 interaction appears to be downregulated in full-length Caspr2. An important point will be to determine which endogenous MAGuK protein of the MPP2 family could be present at the AIS.

DISCUSSION

The precise sub-compartmental profile of Kv1 channels at AIS and along axons is critical for the shaping of neuronal signaling. In the present study, we showed that two CAMs associated with Kv1, TAG-1 and Caspr2, are distinctly targeted along the axon in hippocampal neurons. TAG-1 strongly colocalizes with Kv1.2 channels at the AIS whereas Caspr2 is evenly distributed along the axon, in contrast to their colocalization at juxtaparanodes. Live imaging of Caspr2 and TAG-1 vesicular transport revealed that they are sorted together in the same axonal transport vesicles. Thus, we hypothesize that their differential distribution may result from diffusion and/or trapping mechanisms induced by selective partnerships. We identified two molecular determinants of Caspr2 that regulate its axonal positioning. First, we showed that deletion of the LNG2-EGF1 extracellular modules in Caspr2Δ2 induces its restricted localization at the AIS and strengthened its association with TAG-1. Second, we demonstrated that the cytoplasmic tail of Caspr2 contains a PDZ-binding site that elicits AIS enrichment and recruitment of the MAGuK protein MPP2. Hence, the distribution of Caspr2 and TAG-1 at the AIS versus all along the axon may be regulated and participate in the strategic function of the Kv1 complex along axons.

We previously showed that Caspr2 is both inserted at the axonal and somatodendritic membranes (Bel et al., 2009). The selective endocytosis of Caspr2 in the somatodendritic compartment further promotes its polarized expression at the axonal surface (Bel et al., 2009). The distinct distribution of TAG-1 and Caspr2 at the AIS and along the axon could have been due to their sorting in dedicated vesicles that would then fuse to specific domains. However, in live-cell imaging experiments, we observed that TAG-1 and Caspr2

Journal of Cell Science (2017) 130, 2209-2220 doi:10.1242/jcs.202267

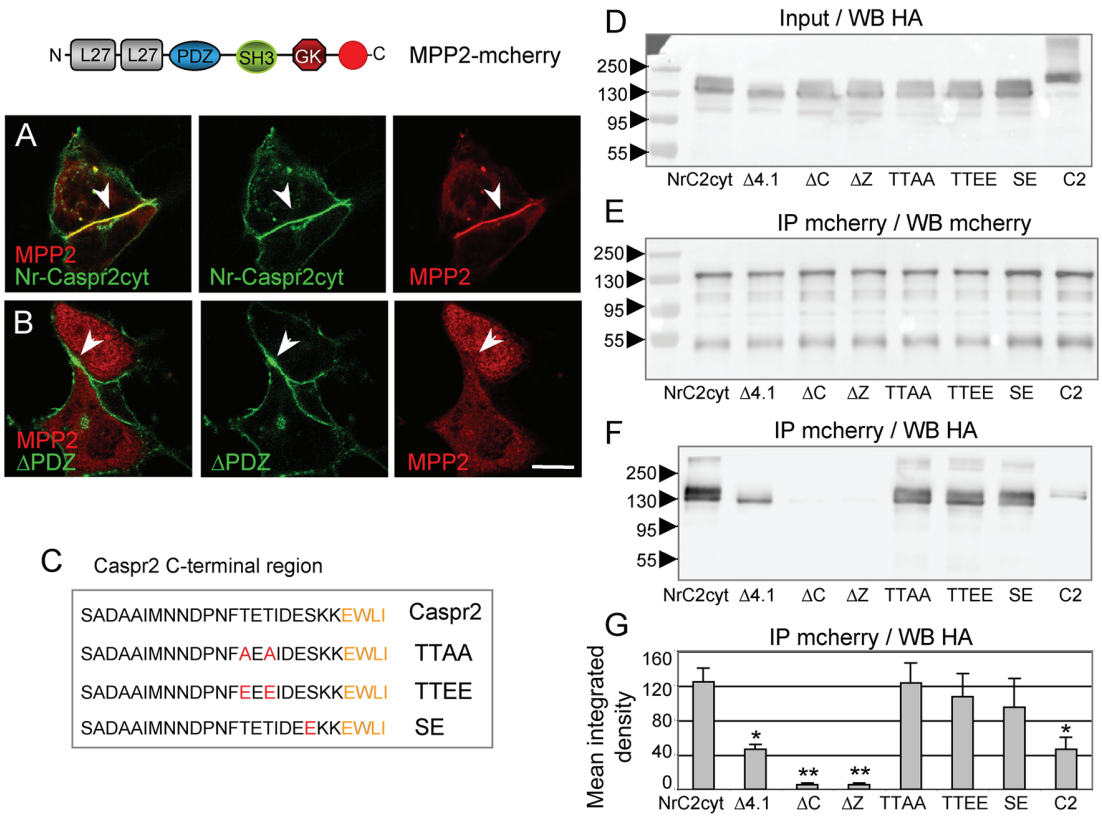

Fig. 7. The PDZ-protein MPP2 interacts with Caspr2 in transfected HEK cells. (A,B) HEK cells were co-transfected with MPP2–mCherry and Nr–Caspr2cyt (A) or ΔPDZ (B) constructs. Cells were fixed with methanol and the fluorescence was directly imaged in confocal sections. The cytoplasmic tail of Caspr2 induced the recruitment of MPP2 at the cell membrane (arrowheads in A) and deletion of the PDZ-binding regions prevented its recruitment (arrowheads in B). Scale bar: 5 µm. (C) Nr–Caspr2cyt constructs were generated with mutations (indicated in red) of the Thr and Ser-phosphorylation sites in the C-terminal region upstream the PDZ-binding sequence (orange). Thr1319 and Thr1321 were mutated to alanine residues (TTAA) or glutamate residues (TTEE), or the Ser1325 was mutated into a glutamate residue (SE). (D–F) HEK cells were co-transfected with MPP2–mCherry and HA-tagged full-length Caspr2 or Nr–Caspr2cyt mutants. Cells were lysed and the supernatants analyzed for expression of Caspr2 and Nr–Caspr2cyt mutants by western blotting (WB) for HA (D, input). Immunoprecipitation (IP) was performed using rabbit anti-mCherry antibody and the immunoprecipitates (IP) analyzed by western blotting for MPP2–mCherry (E) and HA-tagged constructs (F). Caspr2 (C2) and Nr–Caspr2cyt (NrC2cyt) constructs were co-immunoprecipitated with MPP2. Mutants with deletion of the C-terminal (ΔC) or PDZ-binding (ΔZ) domain were not co-precipitated, and mutations of the Ser- or Thr-phosphorylation sites in the C-terminal region had no effect. Deletion of the 4.1B-binding (Δ4.1) region strongly reduced the interaction with MPP2. The experiments were performed in triplicate. Quantitative analysis of co-immunoprecipitated proteins was performed using the ImageJ software and expressed as a mean±s.e.m. percentage of the Nr–Caspr2cyt value. *P<0.05; ** P<0.01 by comparison with Nr-Caspr2cyt (ANOVA).

are colocalized in axonal transport vesicles. We noticed that both TAG-1 and Caspr2 are mostly transported in the retrograde direction. Hence, these proteins are not packaged into separate vesicles and their proper cell surface accumulation at different axonal sites may depend on diffusion-trapping mechanisms. The AIS is a zone of restricted diffusion for the lateral mobility of transmembrane proteins that are anchored to the ankyrin–spectrin–actin cytoskeleton, like neurofascin-186 and voltage-gated Na^+ channels (Jenkins and Bennett, 2001; Leterrier, 2016). This zone contains a high density of proteins that are anchored to cortical actin and act as a picket fence that restrains the diffusion of unanchored constituents (Winckler et al., 1999), such as GPI-anchored proteins like TAG-1. The limited diffusion of GPI-anchored proteins at the AIS may be also related to the periodic organization of the actin cytoskeleton recently revealed by super-resolution microscopy (Albrecht et al., 2016). In addition, the AIS is the site of a selective barrier for vesicles carrying dendritic cargoes that only enter into the base of the axon, before stopping and returning to the soma. In contrast, axonal cargo vesicles pass through the AIS and proceed to the distal axon (Al-Bassam et al., 2012; Petersen et al., 2014). Here, we observed that both Caspr2 and TAG-1 vesicles are axonally transported through the AIS without impediment both in the anterograde and retrograde directions and we did not observe any fusion of vesicles within the AIS. Retrogradely moving vesicles were also observed starting from the axonal growth cone and likely result from endocytosis. In a previous paper (Bel et al., 2009), we reported that Caspr2 is strongly internalized in the somato-dendritic compartment by comparison with the axon. Since axons are highly ramified at DIV8, even if endocytosis occurred at a low rate, the multiple axonal tips might produce a number of retrogradely moving vesicles. The retrograde axonal transport suggests a very dynamic renewal of Caspr2 and TAG-1 at the axonal membrane.

TAG-1 is a GPI-anchored molecule, indicating that its ectodomain may drive its distribution at the AIS. As an Ig-CAM, TAG-1 displays a broad activity of binding and may associate with NrCAM or neurofascin-186 (Lustig et al., 1999), which are trapped at the AIS via an ankyrin-binding motif (Davis et al., 1996). However, we showed that the TAG-1-Ig construct is poorly enriched at the AIS when compared with full-length TAG-1, indicating

Journal of Cell Science (2017) 130, 2209-2220 doi:10.1242/jcs.202267

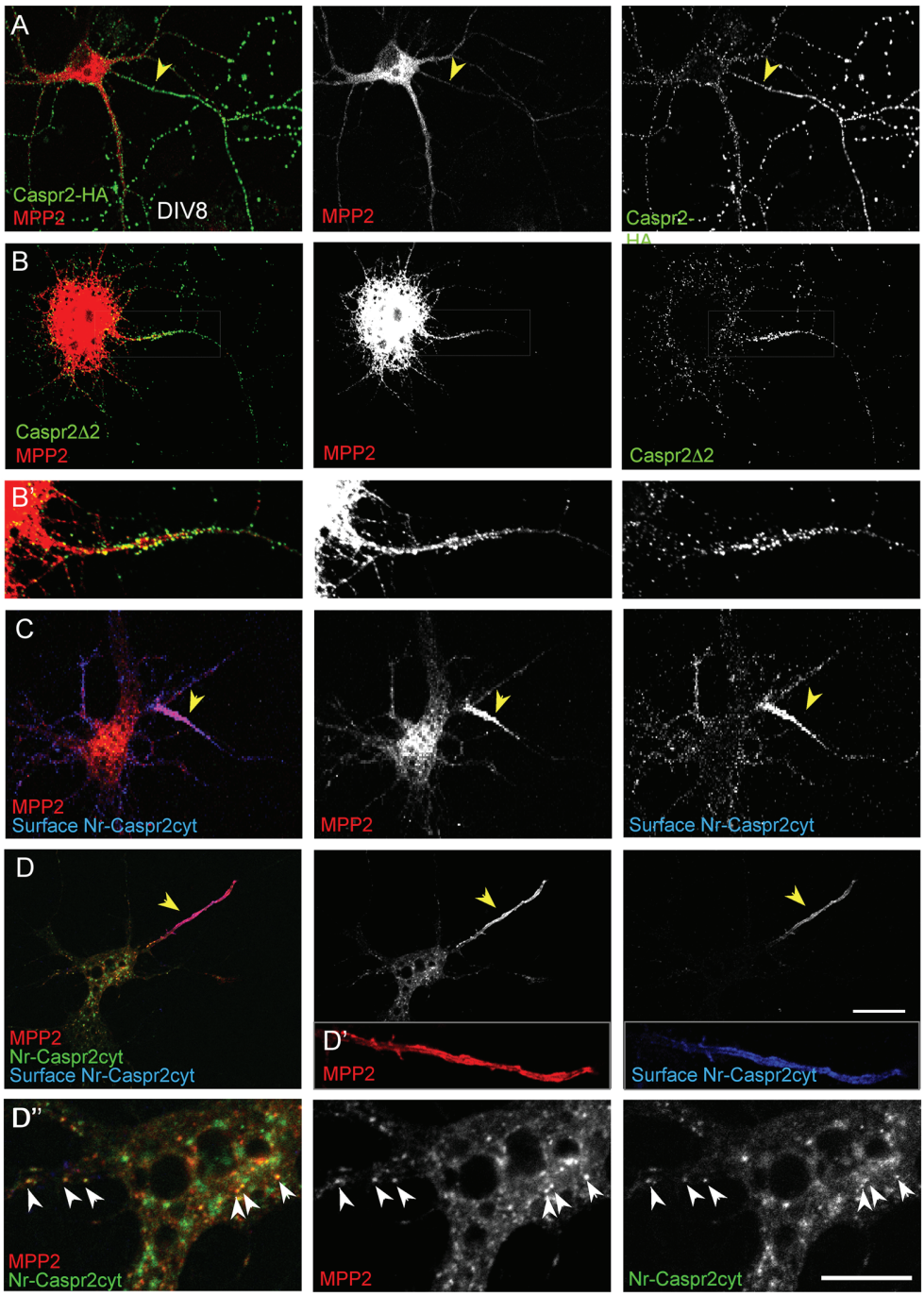

Fig. 8. The PDZ-protein MPP2 is recruited by the Caspr2 cytoplasmic tail at the AIS of hippocampal neurons. (A,B) Hippocampal neurons were co-transfected at DIV7 with MPP2–mCherry and full-length Caspr2 (A) or Caspr2Δ2 (B,B′). Neurons were surface labeled at DIV8 with anti-HA mAb (green) and fixed. The fluorescence for MPP2–mCherry was directly imaged (red). Note that MPP2 colocalized in clusters with Caspr2Δ2 at the AIS (arrowheads). (C,D) Hippocampal neurons were transfected with MPP2–mCherry and GFP-tagged Nr–Caspr2cyt. Cells were surface labeled for GFP (blue) and fixed. The fluorescence for MPP2–mCherry (red) and Nr–Caspr2cyt (green) was directly imaged. Note, that MPP2 strongly colocalized with Nr-Caspr2cyt at the AIS (yellow arrowheads in C,D) and in intracellular vesicles (white arrowheads in D″). Scale bar: 20 µm (D), 10 µm (D″).

that the conformation of the intact molecule is essential for its enrichment at the AIS, which may occur independently of NrCAM/neurofascin-186 binding. The extracellular domain of Caspr2 is implicated in its axonal versus AIS distribution. Deletion of the LNG2-EGF1 region induces the concentration of Caspr2Δ2 at the AIS. One hypothesis could be that these modules interact with a cis-partner that drives the distribution of Caspr2 all along the axon. Alternatively, given the overall organization of Caspr2, the LNG2-EGF1 deletion may induce a structural change favoring TAG-1 binding. The architecture of Caspr2 is composed of three lobes with the discoidin, LNG1 and LNG2 domains forming a large lobe, the fibrinogen and LNG3 a middle lobe, and LNG4 a small lobe (Lu et al., 2016; Rubio-Marrero et al., 2016). In support of this second hypothesis, we showed that deletion of the LNG2-EGF1 modules of Caspr2 increases its cis-association with TAG-1 as analyzed using co-immunoprecipitation experiments from double-transfected HEK cells.

The cytoplasmic tail of Caspr2 contains a juxtamembrane 4.1B-binding sequence and a C-terminal PDZ type II-binding motif. We showed that deletion of each of these motifs decreases the AIS enrichment of the Caspr2 cytoplasmic tail reporter construct. Proteomic analysis had revealed that Caspr2 may interact with a set of scaffolding proteins including the MAGuKs MPP2 and CASK, and the multiple PDZ domain protein MUPP1 (Horresh

Journal of Cell Science

Journal of Cell Science (2017) 130, 2209-2220 doi:10.1242/jcs.202267

et al., 2008; Tanabe et al., 2015). Horresh et al. also reported that the association of Caspr2 with MPP2 requires its 4.1B- and PDZ-binding regions (Horresh et al., 2008). We showed here that Caspr2 could be co-immunoprecipitated with MPP2 or CASK from the lysate of co-transfected HEK cells. Deletion of the 4.1B-binding domain significantly decreases co-immunoprecipitation and also prevents the recruitment of MPP2 to the plasma membrane of HEK cells. In contrast, we did not see any effect of mutating the consensus sites for CK2 phosphorylation located in the C-terminal region. Interestingly, the Caspr2 cytoplasmic tail in the reporter construct and in the Caspr2Δ2 mutant strongly recruits MPP2–mCherry at the AIS of transfected hippocampal neurons. We noticed that in the context of Caspr2 full-length molecule, MPP2 was not recruited by the Caspr2 cytoplasmic tail at the AIS or along the axon. The ectodomain of Caspr2 contains the LNG2-EGF1 modules implicated in its axonal targeting, likely by regulating cis-interaction with CAMs. Hence, an outside-in mechanism might regulate the recruitment of a MAGuK protein and 4.1B to stabilize Caspr2 at the AIS depending on the neuronal cell type or cellular context. It would be interesting to elucidate whether any endogenous proteins of the MPP2 family may be present at the AIS. MPP2 is a MAGuK protein that contains two L27 domains belonging to a subfamily which also contains Varicose, a component of *Drosophila* septate junctions that binds neurexin IV, the homolog of Caspr and Caspr2 (Laval et al., 2008; Wu et al., 2007). CASK, which contains a calmodulin kinase domain and binds neurexin, is implicated in synaptic protein targeting (Hsueh, 2006). Caspr2 has been also reported to interact with MUPP1, which may play a role at the post-synapse (Krapivinsky et al., 2004; Tanabe et al., 2015). To our knowledge, none of these scaffolding proteins have been identified at the AIS and we were not able to detect MPP2 or CASK at this axonal sub-region using available commercial antibodies (data not shown).

The AIS diversity may reflect the physiological properties of the different neuronal cell types. In addition, the AIS may be a dynamic unit regulating intrinsic excitability of neurons during homeostatic plasticity or in pathological conditions (Kuba et al., 2010). Indeed, the position of AIS moves distally in hippocampal neurons after depolarization, and this movement correlates with change in current threshold for spike firing (Grubb and Burrone, 2010). We hypothesize that the AIS distribution of the Kv1 complex may be regulated depending on the neuronal cell type, differentiation stage or activity to fine-tune neuronal excitability. During the maturation of cultured hippocampal neurons, the Nav1.2 channels are recruited to the AIS shortly after ankyrinG at around DIV3, while the Kv1 channels begin to concentrate at DIV10 at that site (Sanchez-Ponce et al., 2012). TAG-1 is enriched at the AIS at DIV14, as observed for Kv1 channels. Since several CAMs associated with the Kv1 channels, including Caspr2 and LGI1, are implicated in genetic or autoimmune psychiatric diseases (Lai et al., 2010), it will be important to study whether their distribution at the AIS may provide clues on neuronal excitability in physiological and pathological conditions.

MATERIALS AND METHODS

Constructs

The pCDNA3-Caspr2-HA construct encodes human Caspr2 with the HA epitope inserted downstream of the signal peptide between the residues Trp26 and Thr27 (Bel et al., 2009). The Caspr2–HA deletion constructs, Caspr2Δ1 (Δ32-361), Caspr2Δ2 (Δ362-600), Caspr2Δ3 (Δ600-950), Caspr2Δ4 (Δ955-1169) were as described previously (Pinatel et al., 2015). The NrCAM–Caspr2cyt construct was generated by insertion of the Caspr2 transmembrane and cytoplasmic regions downstream the signal peptide and Ig domains of NrCAM, and is tagged with HA and GFP (Falk et al., 2004). NrCAM–GFP, TAG-1-Fc, TAG-1-Ig-Fc and neurofascin-186–HA were as described previously (Falk et al., 2004; Labasque et al., 2011). Nr-Caspr2cyt constructs with deletions of the binding site for 4.1B (Δ1288-1305), the PDZ-binding domain (stop at residue 1330) or the C-terminal region (stop codon at residue 1306) were generated. The human TAG-1–GFP and Caspr2–GFP constructs with GFP downstream of the signal peptide were as described previously (Bel et al., 2009; Pinatel et al., 2015). The human TAG-1–GFP deletion constructs were generated by PCR amplification from the previously described TAG-1-Ig and TAG-1-Fn constructs (Tzimourakas et al., 2007), and were inserted in the XhoI/ HindIII sites of a pEGFP-C1 plasmid vector modified to contain the signal peptide of TAG-1 upstream of GFP. Caspr2–mCherry, with mCherry at the C-terminus, was generated by insertion into the EcoRI-BamHI sites of pmCherry-N1. The coding sequence of human CASK and MPP2 were obtained from OriGene (Rockville, USA) and inserted into the EcoR1-BamH1 sites of pmCherry-N1 vector. PCR amplified products were verified by sequencing (Genewiz, Takeley, GB).

Antibodies and immunofluorescence staining

The rat anti-HA mAb (clone 3F10, ref. 11867423001) was purchased from Roche (Meylan, France), the goat anti-GFP antibody (ab5450) from abcam (Paris, France), the rabbit anti-GFP antibody (A11122) from Molecular Probes (ThermoFisher, Courtaboeuf, France), the rabbit anti-RFP (anti-mCherry) antibody from Rockland (Limerick, USA), the rabbit anti-TAG-1 antibody (ABN1379) from Millipore (MerckMillipore, Fontenay sous Bois, France). The mouse anti-ankyrinG (N106/36), anti-CASK (clone K56A/50), and anti-neurofascin186 (clone A12/18) mAbs were obtained from the UC Davis/NIH NeuroMab facility. The mouse anti-TAG-1 1C12 mAb and the rabbit anti-Caspr2 antiserum were as previously described (Bel et al., 2009; Traka et al., 2003). Anti-Caspr2 antibodies from limbic encephalitis patients were characterized previously (Pinatel et al., 2015). Alexa Fluor 488-, 568- and 647-conjugated secondary antibodies were obtained from Molecular Probes (ThermoFisher). Immunostaining for Caspr2–HA, Caspr2–GFP and TAG-1–GFP was performed on live cells with antibodies against HA or GFP, diluted 1:1000 in culture medium, for 30–60 min. Cells were fixed with 4% paraformaldehyde in PBS for 10 min and permeabilized with 0.1% Triton X-100 for 10 min. Immunofluorescence staining was performed using mouse anti-ankyrinG (1:100) antibodies, and with secondary antibodies diluted in PBS containing 3% bovine serum albumin. After washing in PBS, cells were mounted in Mowiol (Calbiochem, MerckMillipore). The dilution of primary antibodies used for immunofluorescence staining is indicated in Table S2.

Cell culture

Cell culture media and reagents were from Gibco (ThermoFisher). HEK-293 cells (ATCC, Teddington, UK) were grown in Dulbecco's modified Eagle's medium (DMEM) containing 10% fetal calf serum, and were transiently transfected using jet PEI (Polyplus transfection, Ozyme, St Quentin en Yvelines, France). Primary hippocampal cell cultures were from embryonic day 18 Wistar rats. Hippocampi were collected in Hanks' balanced salt solution, dissociated with trypsin and plated at a density of 1.2 10^5 cells/cm^2 on poly-L-lysine-coated coverslips. The hippocampal neurons were cultured in Neurobasal supplemented with 2% B-27, 1% penicillin-streptomycin and 0.3% glutamine in a humidified atmosphere containing 5% CO_2 at 37° C. Hippocampal neurons were transfected with Lipofectamine 2000 (Invitrogen, ThermoFisher) at DIV7 or DIV14. All animal experiments were carried out according to the animal care and experimentation committee rules approved by CNRS.

Confocal microscopy and image analysis

Image acquisition was performed on a Zeiss (Carl Zeiss France, Marly le Roi) laser-scanning microscope equipped with 63×1.32 NA oil-immersion objective. Images of GFP or mCherry or Alexa-Fluor-stained cells were obtained using the 488 nm band of an Argon laser and the 568 nm and 647 nm bands of a solid-state laser for excitation. Fluorescence images were collected automatically with an average of two-frame scans. Quantitative image analysis was performed by using ImageJ on confocal sections (20

Journal of Cell Science

neurons in each condition). The fluorescence intensity was measured in two regions of interest (the ankyrinG-positive AIS and the axon) using identical confocal parameters. The fluorescence intensity profiles were obtained by using Zen software (Zeiss). Statistical analysis was performed with ANOVA.

Imaging vesicle transport

Coverslips with neurons were loaded into a sealed heated chamber in imaging medium (Hank's balanced salt solution pH 7.2 with 10 mM HEPES and 0.6% glucose). Recordings were made 18 h after transfection. The axons were selected on the basis of their much greater length by comparison with dendrites. Live immunostaining using Alexa-Fluor-647-coupled anti-neurofascin-186 was performed after recordings to detect the AIS. Vesicle transport was imaged using Zeiss laser-scanning microscope equipped with 63×1.32 NA oil-immersion objective and 37°C heating chamber. Dual-color recordings were acquired by using simultaneous excitation with 488 (2–4%) and 561 lasers (1–2%), and a GaSP PMT1 detector for 499–551 nm and PMT2 detector for 569-735 nm (562×240 pixels, average 2, open pinhole, 1.5 s scanning time, streamed time-lapse recording during 4–8 min). Kymographs were generated by using ImageJ software and were contrast inverted so that the fluorescent vesicles corresponded to dark lines. Overlapping transport events were analyzed and the velocity measured for each transport event.

Western blot and immunoprecipitation

HEK cells were co-transfected with Caspr2–HA or NrCAM–Caspr2cyt constructs and CASK–mCherry or MPP2–mCherry, or with Caspr2–HA deletion constructs and TAG-1-GFP. Cells were lyzed for 30 min on ice with 50 mM Tris, pH 7.5, 1% NP-40, 10 mM MgCl2 and protease inhibitors, centrifuged at 4°C for 15 min at 15,000 rpm. After preclearing for 1 h at 4°C with protein A-Sepharose, supernatants were immunoprecipitated overnight at 4°C with protein A–Sepharose coated with rabbit anti-mCherry antibody (2 µg), or rabbit anti-Caspr2 antiserum (2 µl). The beads were washed twice with 50 mM Tris-HCl pH 7.4, 150 mM NaCl and 1% NP-40, twice in 50 mM Tris-HCl, 150 mM NaCl and twice in 50 mM Tris-HCl. Immune precipitates were analyzed by immunoblotting with rat anti-HA and rabbit anti-mCherry, or rabbit anti-Caspr2 and rabbit anti-TAG-1 antibodies. Blots were developed using the ECL chemiluminescent detection system (Roche). Quantitative analysis of co-immunopecipitated proteins was performed by using the ImageJ software.

Acknowledgements

We wish to thank Marie-Pierre Blanchard of the CRN2M imaging core facility for help with time-lapse recording and image analysis. We are grateful to Laurence Goutebroze and Christophe Leterrier for helpful discussions. We thank the UC Davis/NIH NeuroMab facility.

Competing interests

The authors declare no competing or financial interests.

Author contributions

Conceptualization: D.P., B.H., C.F.; Methodology: B.H., C.F.; Validation: D.P., M. Saint-Martin, N.N., C.F.; Formal analysis: C.F.; Investigation: D.P., B.H., M. Saint-Martin, C.F.; Resources: M. Savvaki, D.K., C.F.; Writing - original draft: C.F.; Writing - review & editing: D.P., N.N., M. Savvaki, D.K., C.F.; Supervision: C.F.; Project administration: C.F.; Funding acquisition: C.F.

Funding

This work was supported by the Fondation pour l'Aide à la Recherche sur la Sclérose en Plaques (ARSEP) to C.F.-S. and D.K.

Supplementary information

Supplementary information available online at
http://jcs.biologists.org/lookup/doi/10.1242/jcs.202267.supplemental

References

Al-Bassam, S., Xu, M., Wandless, T. J. and Arnold, D. B. (2012). Differential trafficking of transport vesicles contributes to the localization of dendritic proteins. *Cell Rep.* **2**, 89-100.

Albrecht, D., Winterflood, C. M., Sadeghi, M., Tschager, T., Noé, F. and Ewers, H. (2016). Nanoscopic compartmentalization of membrane protein motion at the axon initial segment. *J. Cell Biol.* **215**, 37-46.

Bel, C., Oguievetskaia, K., Pitaval, C., Goutebroze, L. and Faivre-Sarrailh, C. (2009). Axonal targeting of Caspr2 in hippocampal neurons via selective somatodendritic endocytosis. *J. Cell Sci.* **122**, 3403-3413.

Buttermore, E. D., Dupree, J. L., Cheng, J., An, X., Tessarollo, L. and Bhat, M. A. (2011). The cytoskeletal adaptor protein band 4.1B is required for the maintenance of paranodal axoglial septate junctions in myelinated axons. *J. Neurosci.* **31**, 8013-8024.

Cifuentes-Diaz, C., Chareyre, F., Garcia, M., Devaux, J., Carnaud, M., Levasseur, G., Niwa-Kawakita, M., Harroch, S., Girault, J.-A., Giovannini, M. et al. (2011). Protein 4.1B contributes to the organization of peripheral myelinated axons. *PLoS ONE* **6**, e25043.

Davis, J. Q., Lambert, S. and Bennett, V. (1996). Molecular composition of the node of Ranvier: identification of ankyrin-binding cell adhesion molecules neurofascin (mucin+/third FNIII domain-) and NrCAM at nodal axon segments. *J. Cell Biol.* **135**, 1355-1367.

Devaux, J. J., Kleopa, K. A., Cooper, E. C. and Scherer, S. S. (2004). KCNQ2 is a nodal K+ channel. *J. Neurosci.* **24**, 1236-1244.

Duflocq, A., Chareyre, F., Giovannini, M., Couraud, F. and Davenne, M. (2011). Characterization of the axon initial segment (AIS) of motor neurons and identification of a para-AIS and a juxtapara-AIS, organized by protein 4.1B. *BMC Biol.* **9**, 66.

Einheber, S., Meng, X., Rubin, M., Lam, I., Mohandas, N., An, X., Shrager, P., Kissil, J., Maurel, P. and Salzer, J. L. (2013). The 4.1B cytoskeletal protein regulates the domain organization and sheath thickness of myelinated axons. *Glia* **61**, 240-253.

Falk, J., Thoumine, O., Dequidt, C., Choquet, D. and Faivre-Sarrailh, C. (2004). NrCAM coupling to the cytoskeleton depends on multiple protein domains and partitioning into lipid rafts. *Mol. Biol. Cell* **15**, 4695-4709.

Grubb, M. S. and Burrone, J. (2010). Activity-dependent relocation of the axon initial segment fine-tunes neuronal excitability. *Nature* **465**, 1070-1074.

Horresh, I., Poliak, S., Grant, S., Bredt, D., Rasband, M. N. and Peles, E. (2008). Multiple molecular interactions determine the clustering of Caspr2 and Kv1 channels in myelinated axons. *J. Neurosci.* **28**, 14213-14222.

Horresh, I., Bar, V., Kissil, J. L. and Peles, E. (2010). Organization of myelinated axons by Caspr and Caspr2 requires the cytoskeletal adapter protein 4.1B. *J. Neurosci.* **30**, 2480-2489.

Hsueh, Y.-P. (2006). The role of the MAGUK protein CASK in neural development and synaptic function. *Curr. Med. Chem.* **13**, 1915-1927.

Inda, M. C., DeFelipe, J. and Munoz, A. (2006). Voltage-gated ion channels in the axon initial segment of human cortical pyramidal cells and their relationship with chandelier cells. *Proc. Natl. Acad. Sci. USA* **103**, 2920-2925.

Irani, S. R., Bien, C. G. and Lang, B. (2010). Autoimmune epilepsies. *Curr. Opin. Neurol.* **24**, 146-153.

Jenkins, S. M. and Bennett, V. (2001). Ankyrin-G coordinates assembly of the spectrin-based membrane skeleton, voltage-gated sodium channels, and L1 CAMs at Purkinje neuron initial segments. *J. Cell Biol.* **155**, 739-746.

King, A. N., Manning, C. F. and Trimmer, J. S. (2014). A unique ion channel clustering domain on the axon initial segment of mammalian neurons. *J. Comp. Neurol.* **522**, 2594-2608.

Kole, M. H. P. and Stuart, G. J. (2012). Signal processing in the axon initial segment. *Neuron* **73**, 235-247.

Krapivinsky, G., Medina, I., Krapivinsky, L., Gapon, S. and Clapham, D. E. (2004). SynGAP-MUPP1-CaMKII synaptic complexes regulate p38 MAP kinase activity and NMDA receptor-dependent synaptic AMPA receptor potentiation. *Neuron* **43**, 563-574.

Kuba, H., Oichi, Y. and Ohmori, H. (2010). Presynaptic activity regulates Na(+) channel distribution at the axon initial segment. *Nature* **465**, 1075-1078.

Labasque, M., Devaux, J. J., Lévêque, C. and Faivre-Sarrailh, C. (2011). Fibronectin type III-like domains of neurofascin-186 protein mediate gliomedin binding and its clustering at the developing nodes of Ranvier. *J. Biol. Chem.* **286**, 42426-42434.

Lai, M., Huijbers, M. G. M., Lancaster, E., Graus, F., Bataller, L., Balice-Gordon, R., Cowell, J. K. and Dalmau, J. (2010). Investigation of LGI1 as the antigen in limbic encephalitis previously attributed to potassium channels: a case series. *Lancet Neurol.* **9**, 776-785.

Lancaster, E., Huijbers, M. G. M., Bar, V., Boronat, A., Wong, A., Martinez-Hernandez, E., Wilson, C., Jacobs, D., Lai, M., Walker, R. W. et al. (2011). Investigations of caspr2, an autoantigen of encephalitis and neuromyotonia. *Ann. Neurol.* **69**, 303-311.

Laval, M., Bel, C. and Faivre-Sarrailh, C. (2008). The lateral mobility of cell adhesion molecules is highly restricted at septate junctions in Drosophila. *BMC Cell Biol.* **9**, 38.

Leterrier, C. (2016). The axon initial segment, 50 years later: a nexus for neuronal organization and function. *Curr. Top. Membr.* **77**, 185-233.

Lu, Z., Reddy, M. V., Liu, J., Kalichava, A., Liu, J., Zhang, L., Chen, F., Wang, Y., Holthauzen, L. M., White, M. A. et al. (2016). Molecular Architecture of

Contactin-associated Protein-like 2 (CNTNAP2) and Its Interaction with Contactin 2 (CNTN2). *J. Biol. Chem.* **291**, 24133-24147.

Lustig, M., Sakurai, T. and Grumet, M. (1999). Nr-CAM promotes neurite outgrowth from peripheral ganglia by a mechanism involving axonin-1 as a neuronal receptor. *Dev. Biol.* **209**, 340-351.

Ogawa, Y., Horresh, I., Trimmer, J. S., Bredt, D. S., Peles, E. and Rasband, M. N. (2008). Postsynaptic density-93 clusters Kv1 channels at axon initial segments independently of Caspr2. *J. Neurosci.* **28**, 5731-5739.

Ogawa, Y., Oses-Prieto, J., Kim, M. Y., Horresh, I., Peles, E., Burlingame, A. L., Trimmer, J. S., Meijer, D. and Rasband, M. N. (2010). ADAM22, a Kv1 channel-interacting protein, recruits membrane-associated guanylate kinases to juxtaparanodes of myelinated axons. *J. Neurosci.* **30**, 1038-1048.

Pan, Z., Kao, T., Horvath, Z., Lemos, J., Sul, J. Y., Cranstoun, S. D., Bennett, V., Scherer, S. S. and Cooper, E. C. (2006). A common ankyrin-G-based mechanism retains KCNQ and NaV channels at electrically active domains of the axon. *J. Neurosci.* **26**, 2599-2613.

Petersen, J. D., Kaech, S. and Banker, G. (2014). Selective microtubule-based transport of dendritic membrane proteins arises in concert with axon specification. *J. Neurosci.* **34**, 4135-4147.

Pinatel, D., Hivert, B., Boucraut, J., Saint-Martin, M., Rogemond, V., Zoupi, L., Karagogeos, D., Honnorat, J. and Faivre-Sarrailh, C. (2015). Inhibitory axons are targeted in hippocampal cell culture by anti-Caspr2 autoantibodies associated with limbic encephalitis. *Front. Cell Neurosci.* **9**, 265.

Poliak, S., Salomon, D., Elhanany, H., Sabanay, H., Kiernan, B., Pevny, L., Stewart, C. L., Xu, X., Chiu, S.-Y., Shrager, P. et al. (2003). Juxtaparanodal clustering of Shaker-like K+ channels in myelinated axons depends on Caspr2 and TAG-1. *J. Cell Biol.* **162**, 1149-1160.

Rama, S., Zbili, M. and Debanne, D. (2015). Modulation of spike-evoked synaptic transmission: the role of presynaptic calcium and potassium channels. *Biochim. Biophys. Acta* **1853**, 1933-1939.

Rubio-Marrero, E. N., Vincelli, G., Jeffries, C. M., Shaikh, T. R., Pakos, I. S., Ranaivoson, F. M., von Daake, S., Demeler, B., De Jaco, A., Perkins, G. et al. (2016). Structural characterization of the extracellular domain of CASPR2 and insights into its association with the novel ligand contactin1. *J. Biol. Chem.* **291**, 5788-5802.

Sanchez-Ponce, D., DeFelipe, J., Garrido, J. J. and Muñoz, A. (2012). Developmental expression of Kv potassium channels at the axon initial segment of cultured hippocampal neurons. *PLoS ONE* **7**, e48557.

Tanabe, Y., Fujita-Jimbo, E., Momoi, M. Y. and Momoi, T. (2015). CASPR2 forms a complex with GPR37 via MUPP1 but not with GPR37(R558Q), an autism spectrum disorder-related mutation. *J. Neurochem.* **134**, 783-793.

Traka, M., Goutebroze, L., Denisenko, N., Bessa, M., Nifli, A., Havaki, S., Iwakura, Y., Fukamauchi, F., Watanabe, K., Soliven, B. et al. (2003). Association of TAG-1 with Caspr2 is essential for the molecular organization of juxtaparanodal regions of myelinated fibers. *J. Cell Biol.* **162**, 1161-1172.

Trimmer, J. S. (2015). Subcellular localization of K+ channels in mammalian brain neurons: remarkable precision in the midst of extraordinary complexity. *Neuron* **85**, 238-256.

Tzimourakas, A., Giasemi, S., Mouratidou, M. and Karagogeos, D. (2007). Structure-function analysis of protein complexes involved in the molecular architecture of juxtaparanodal regions of myelinated fibers. *Biotechnol. J.* **2**, 577-583.

Van Wart, A., Trimmer, J. S. and Matthews, G. (2007). Polarized distribution of ion channels within microdomains of the axon initial segment. *J. Comp. Neurol.* **500**, 339-352.

Winckler, B., Forscher, P. and Mellman, I. (1999). A diffusion barrier maintains distribution of membrane proteins in polarized neurons. *Nature* **397**, 698-701.

Wu, V. M., Yu, M. H., Paik, R., Banerjee, S., Liang, Z., Paul, S. M., Bhat, M. A. and Beitel, G. J. (2007). Drosophila Varicose, a member of a new subgroup of basolateral MAGUKs, is required for septate junctions and tracheal morphogenesis. *Development* **134**, 999-1009.

Yoshimura, T. and Rasband, M. N. (2014). Axon initial segments: diverse and dynamic neuronal compartments. *Curr. Opin. Neurobiol.* **27**, 96-102.

Zhou, D., Lambert, S., Malen, P. L., Carpenter, S., Boland, L. M. and Bennett, V. (1998). AnkyrinG is required for clustering of voltage-gated Na channels at axon initial segments and for normal action potential firing. *J. Cell Biol.* **143**, 1295-1304.

Journal of Cell Science

Table S1:
Kymograph analysis of anterograde and retrograde axonal transport of Caspr2-mcherry and TAG-1-GFP in DIV8 hippocampal neurons

	Anterograde			Retrograde			Behaviour*
	Events (n)	Total Δx (µm) (%)	Vm (µm/s)	Events (n)	Total Δx (µm)	Vm (µm/s)	
TAG-1-GFP							
Neuron 1	0	-	-	10	167	0.64	retro
Neuron 2	4	69 (30)	1.2	12	160	0.48	bidir
Neuron 3	0	-	-	8	92	0.36	retro
Neuron 4	1	8 (7)	0.33	9	102	0.34	retro
Caspr2-mcherry							
Neuron 1	4	72 (34)	0.83	7	137	0.87	bidir
Neuron 2	2	37 (8)	0.69	19	441	0.75	retro
Neuron 3	4	70 (32)	0.66	10	248	0.95	bidir
Neuron 4	13	399 (77)	1.11	4	122	0.86	antero
Neuron 5	5	112 (37)	1.46	7	187	0.87	bidir
Neuron 6	2	19 (10)	0.78	11	166	0.71	retro
Neuron 7	4	80 (40)	1.96	7	121	0.66	bidir
Neuron 8	0	-	-	8	169	0.58	retro
Neuron 9	4	144 (50)	0.98	5	141	0.67	bidir
TAG-1-GFP + Caspr2-mcherry							
Neuron 1	0	-	-	20	277	0.35	retro
Neuron 2	6	126 (63)	0.66	6	74	0.35	bidir
Neuron 3	5	81 (22)	1.17	26	282	0.42	retro
Neuron 4	11	155 (69)	0.63	4	76	0.49	bidir
Neuron 5	0	-	-	16	227	0.35	retro
Neuron 6	2	24 (13)	0.7	10	162	0.62	retro

*The vesicular transport was considered as predominantly oriented when the sum of displacements (Total Δx) in one direction was more than 70 % of the total displacements during the 7-10 min period of recording. The behaviour was classified as retrograde (retro), anterograde (antero), or bidirectional (bidir).

Table S2: Dilutions of primary antibodies used for immunofluorescence staining.

Primary antibodies	Dilution for immunofluorescence staining
Mouse anti-ankyrinG, clone N106/36, NeuroMab	1:100 (0.2 µg/ml)
Human anti-Caspr2 IgG	1:500
Rabbit anti-GFP, A1122, Molecular Probes	1:1000 (2 µg/ml)
Goat anti-GFP, ab5450, abcam	1:2000 (0.2 µg/ml)
Rat anti-HA, clone 3F10, Roche	1:1000 (0.1 µg/ml)
Mouse anti-Kv1.2, clone K14/13, NeuroMab	1:500 (2 µg/ml)
Mouse anti-neurofascin186, clone A12/18, NeuroMab	1:1000 (1 µg/ml)
Mouse anti-TAG-1, clone 1C12	1:2000

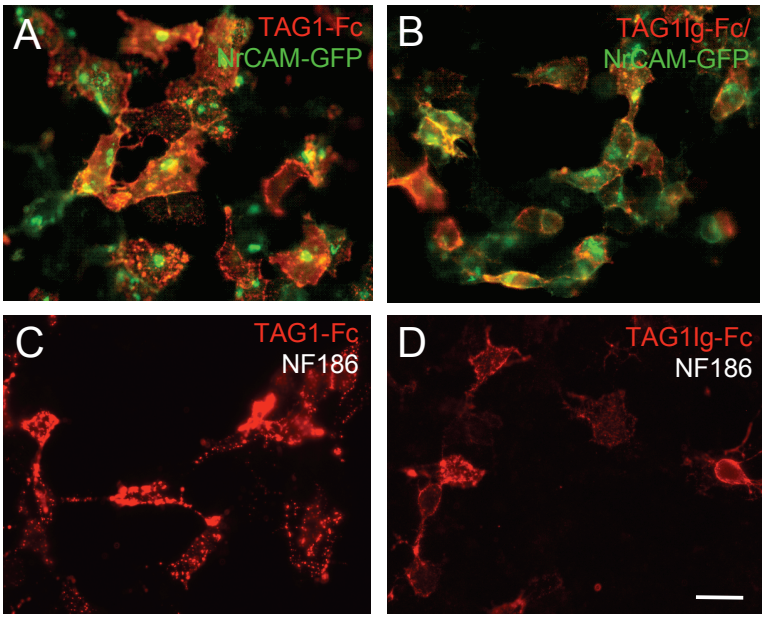

Figure S1: The Ig domains of TAG-1 are only required for binding to NrCAM and Neurofascin-186.
HEK cells transfected with NrCAM-GFP (A, B) or Neurofascin-186 (C, D). Cells were incubated for 30 min with 10 µg/ml of TAG-1-Fc (A, C) or TAG-1Ig-Fc (B, D) preclustered with Alexa568 anti-Fc IgGs. Note that both TAG-1-Fc and TAG1Ig-Fc strongly bound to NrCAM or Neurofascin-186 transfected cells. Bar: 15 µm.

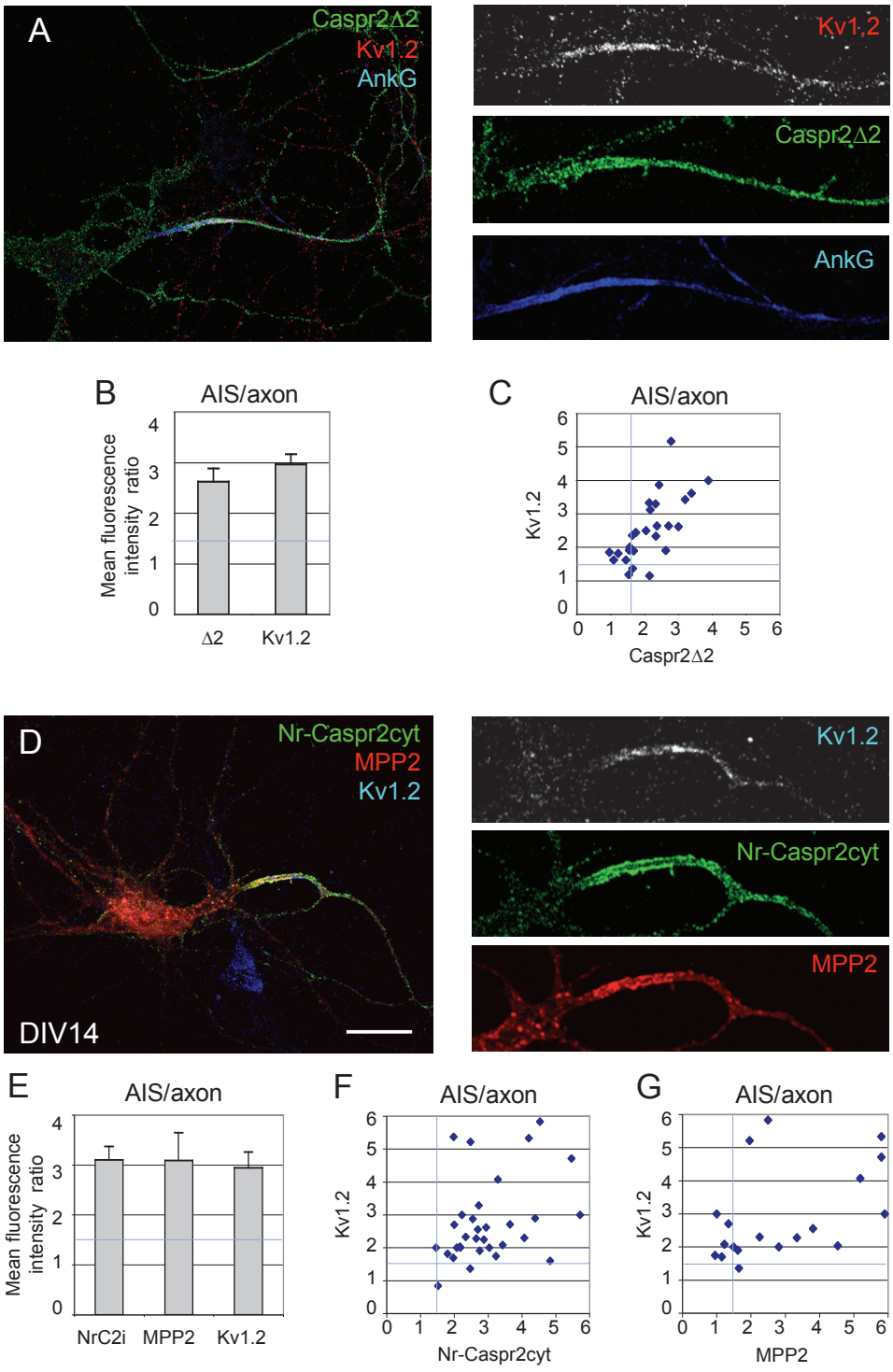

Figure S2: The AIS enrichment in Caspr2Δ2, Nr-Caspr2cyt and MPP2-mcherry correlated with endogenous Kv1.2 expression.
(A) DIV14 hippocampal neurons were transfected with Caspr2Δ2 and surface labeled for HA (green). Neurons were fixed, permeabilized and immunostained for Kv1.2 (red) and ankyrinG (blue). (D) DIV14 hippocampal neurons were co-transfected with Nr-Caspr2cyt and MPP2-mcherry (red), surface labeled for HA (green), fixed, permeabilized and immunostained for Kv1.2 (blue). The AIS/axon ratios of fluorescence intensity were expressed as means ± SEM (B, E), or plotted for individual neurons (C, F, G). Note that the enrichment of Caspr2Δ2, Nr-Caspr2cyt and MPP2 at the AIS was correlated with the level of endogenous Kv1.2 enrichment. Bar: 20 µm in A, D.

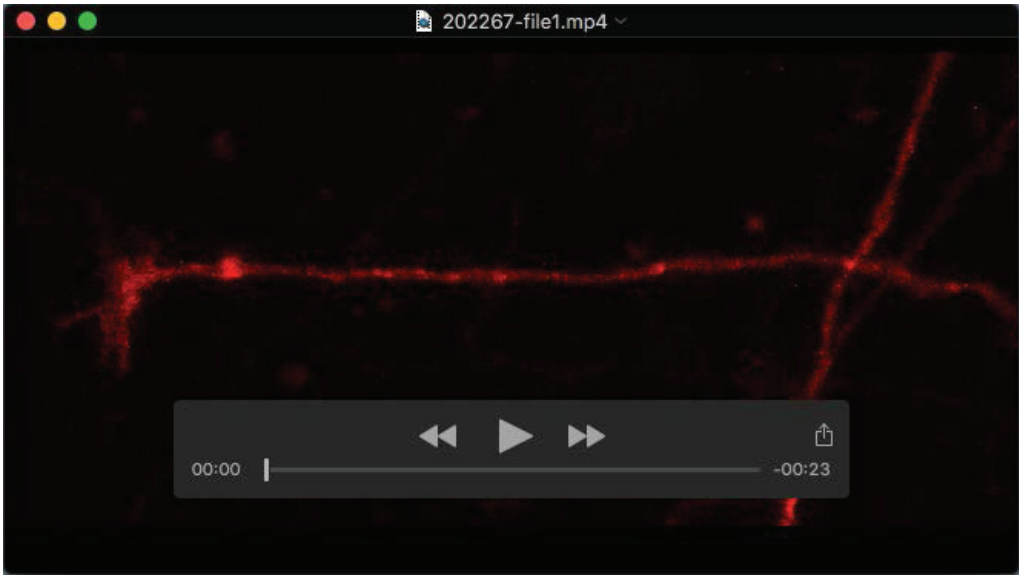

Movie 1: Bidirectional axonal transport vesicles containing TAG-1-GFP and Caspr2-mcherry.
A neuron co-transfected at DIV7 with TAG-1-GFP and Caspr2-mcherry. Axonal transport visualized 16 h after transfection using two-channel overlay recording. Streamed time-lapse images were acquired with 40 frames per 60 s for 220 s. Movie is played at 5.3 frames per second.

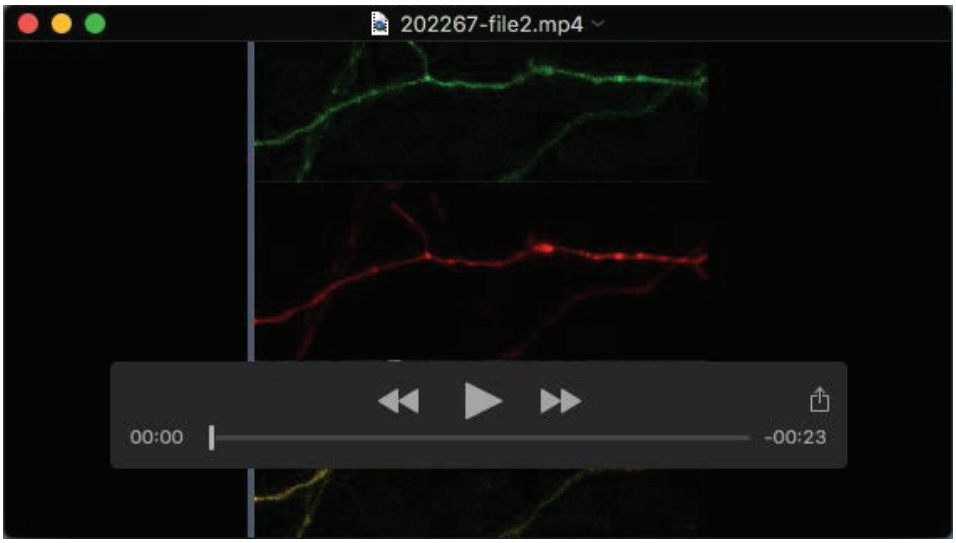

Movie 2: Retrograde axonal transport vesicles containing TAG-1-GFP and Caspr2-mcherry at the AIS region.
A neuron co-transfected at DIV7 with TAG-1-GFP and Caspr2-mcherry. Axonal transport visualized 16 h after transfection using two-channel overlay recording. Streamed time-lapse images were acquired with 40 frames per 60 s for 450 s. Movie is played at 5.3 frames per second.

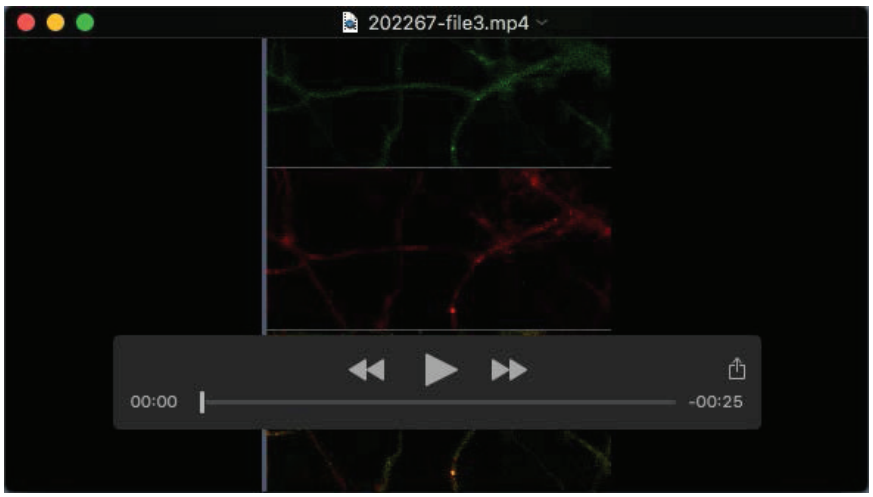

Movie 3: Retrograde axonal transport of Caspr2-mcherry vesicles at the growth cone.
Axonal transport visualized 16 h after Caspr2-mcherry transfection at DIV7. Streamed time-lapse images were acquired with 40 frames per 60 s for 300 s. Movie is played at 5.3 frames per second.

frontiers in Cellular Neuroscience

ORIGINAL RESEARCH
published: 09 July 2015
doi: 10.3389/fncel.2015.00265

Inhibitory axons are targeted in hippocampal cell culture by anti-Caspr2 autoantibodies associated with limbic encephalitis

*Delphine Pinatel[1], Bruno Hivert[1], José Boucraut[1,2], Margaux Saint-Martin[3,4,5], Véronique Rogemond[3,4,5], Lida Zoupi[6], Domna Karagogeos[6], Jérôme Honnorat[3,4,5] and Catherine Faivre-Sarrailh[1]**

[1] Aix Marseille Université, CNRS, Centre de Recherche en Neurobiologie et Neurophysiologie de Marseille, CRN2M-UMR7286, Faculté de Médecine Nord, Marseille, France, [2] Laboratoire d'Immunologie et d'Immunopathologie, AP-HM, Hôpital de la Conception, Marseille, France, [3] French Reference Center on Paraneoplastic Neurological Syndrome, Hospices Civils de Lyon, Hôpital Neurologique, Bron, France, [4] INSERM U1028 – CNRS UMR 5292, Lyon Neuroscience Research Center, Lyon, France, [5] Université de Lyon – Université Claude Bernard Lyon 1, Lyon, France, [6] Institute of Molecular Biology and Biotechnology – Foundation for Research and Technology, University of Crete, Heraklion, Greece

OPEN ACCESS

Edited by:
Tommaso Pizzorusso, University of Florence and Institute of Neuroscience, National Research Council, Italy

Reviewed by:
Xiang Yu, Institute of Neuroscience, Shanghai Institutes for Biological Sciences – Chinese Academy of Sciences, China
Enrica Strettoi, Institute of Neuroscience, National Research Council, Italy

***Correspondence:**
Catherine Faivre-Sarrailh, Aix Marseille Université, CNRS, Centre de Recherche en Neurobiologie et Neurophysiologie de Marseille, CRN2M-UMR7286, Faculté de Médecine Nord, Boulevard Pierre Dramard, Marseille 13344, France catherine.sarrailh@univ-amu.fr

Received: *10 March 2015*
Accepted: *25 June 2015*
Published: *09 July 2015*

Citation:
Pinatel D, Hivert B, Boucraut J, Saint-Martin M, Rogemond V, Zoupi L, Karagogeos D, Honnorat J and Faivre-Sarrailh C (2015) Inhibitory axons are targeted in hippocampal cell culture by anti-Caspr2 autoantibodies associated with limbic encephalitis. Front. Cell. Neurosci. 9:265. doi: 10.3389/fncel.2015.00265

Contactin-associated protein-like 2 (Caspr2), also known as CNTNAP2, is a cell adhesion molecule that clusters voltage-gated potassium channels (Kv1.1/1.2) at the juxtaparanodes of myelinated axons and may regulate axonal excitability. As a component of the Kv1 complex, Caspr2 has been identified as a target in neuromyotonia and Morvan syndrome, but also in some cases of autoimmune limbic encephalitis (LE). How anti-Caspr2 autoimmunity is linked with the central neurological symptoms is still elusive. In the present study, using anti-Caspr2 antibodies from seven patients affected by pure LE, we determined that IgGs in the cerebrospinal fluid of four out seven patients were selectively directed against the N-terminal Discoïdin and LaminG1 modules of Caspr2. Using live immunolabeling of cultured hippocampal neurons, we determined that serum IgGs in all patients strongly targeted inhibitory interneurons. Caspr2 was highly detected on GAD65-positive axons that are surrounding the cell bodies and at the VGAT-positive inhibitory presynaptic contacts. Functional assays indicated that LE autoantibodies may induce alteration of Gephyrin clusters at inhibitory synaptic contacts. Next, we generated a Caspr2-Fc chimera to reveal Caspr2 receptors on hippocampal neurons localized at the somato-dendritic compartment and post-synapse. Caspr2-Fc binding was strongly increased on TAG-1-transfected neurons and conversely, Caspr2-Fc did not bind hippocampal neurons from TAG-1-deficient mice. Our data indicate that Caspr2 may participate as a cell recognition molecule in the dynamics of inhibitory networks. This study provides new insight into the potential pathogenic effect of anti-Caspr2 autoantibodies in central hyperexcitability that may be related with perturbation of inhibitory interneuron activity.

Keywords: CNTNAP2, TAG-1, contactin 2, voltage-gated potassium channels, autoimmunity, interneurons, cell adhesion

Abbreviations: CAM, cell adhesion molecule; CIDP, chronic inflammatory demyelinating polyneuropathy; DIV, day *in vitro*; DRG, dorsal root ganglia; EGF, epidermal growth factor-like; GPI, glycan phosphatidyl inositol; Ig, immunoglobulin; LE, limbic encephalitis; PDZ, PSD95/Dlg1/Zo-1; VGKC, voltage-gated potassium channels.

Introduction

Contactin-associated protein-like 2 Caspr2 (also known as CNTNAP2) is a CAM that belongs to the Neurexin family and is associated with both neuropsychiatric disorders and autoimmune diseases. One function of Caspr2 has been well characterized as a component of the juxtaparanodes of myelinated fibers in the CNS and PNS (Poliak et al., 2003). Caspr2 extracellular domain interacts with contactin 2/TAG-1, a glycosyl-phosphatidyl-inositol anchored Ig-CAM expressed by both axonal and facing glial membranes (Traka et al., 2003). Caspr2 cytoplasmic tail contains a binding site for the cytoskeleton adaptor protein 4.1B and a C-terminal PDZ binding sequence (Horresh et al., 2008). The Caspr2 complex mediates the clustering of VGKCs, mainly Kv1.1 and Kv1.2 at juxtaparanodes (Poliak et al., 2003; Traka et al., 2003). The role attributed to these channels is to stabilize conduction at the nodes of Ranvier, avoid repetitive firing and help to maintain the internodal resting potential (Rasband, 1998; Devaux and Gow, 2008). Knock-out mice for either Caspr2, TAG-1, or protein 4.1B display diffused of Kv1.1/1.2 along the internode, albeit, the mis-localization of Kv1 channels does not affect nerve conduction (Poliak et al., 2003; Traka et al., 2003; Cifuentes-Diaz et al., 2011). Caspr2 also co-localizes with the Kv1.1/Kv1.2 channels at the axon initial segment and may regulate axonal excitability at this site (Inda et al., 2006; Ogawa et al., 2008).

Apart from its well-known function in Kv1 channel clustering at juxtaparanodes, Caspr2 may also act as a cell recognition molecule during development and synaptic network formation. Caspr2-deficient mice show a defect in the migration of cortical neurons and a reduction in the number of GABAergic interneurons which are associated with an epileptic phenotype and autism-related behaviors (Penagarikano et al., 2011). RNAi-mediated knockdown of Caspr2 affects synaptic organization and function in culture (Anderson et al., 2012). Mutations of the Caspr2 gene (*cntnap2*) have been unambiguously associated with neuropsychiatric disorders, such as developmental language impairment and autistic spectrum disorders (Strauss et al., 2006; Bakkaloglu et al., 2008; Penagarikano and Geschwind, 2012; Rodenas-Cuadrado et al., 2013). However, the altered neuronal functions underlying these disorders remain elusive.

Numerous studies have implicated the VGKC-complex as an autoimmune target in generalized neuromyotonia, persistent facial myokymia, Morvan's syndrome, and in LE (Vincent et al., 2004). Recent studies revealed that in most patients with anti-VGKC-complex antibodies, the immune targets are in fact Leucine-rich glioma inactivated 1 (LGI1), a secreted protein associated with presynaptic Kv1 channels (Lai et al., 2010) or the juxtaparanodal CAMs, Caspr2 and TAG-1 (Irani et al., 2010; Lancaster et al., 2011). In the present study, we used anti-Caspr2 IgGs of patients with pure LE to label cultured hippocampal neurons and characterize targeted cell types and subcellular compartments. In addition, we generated a Caspr2-Fc chimera to analyze the distribution of Caspr2 binding sites on hippocampal neurons. We showed that Caspr2 is mainly expressed by inhibitory axons and may participate to trans-synaptic adhesion complexes. This study provides new insight into the potential pathogenic effect of anti-Caspr2 autoantibodies in central hyperexcitability that may be related with perturbation of inhibitory synaptic transmission.

Materials and Methods

Constructs

The pCDNA3-Caspr2-HA construct encodes human Caspr2 with the HA epitope inserted downstream the signal peptide between the residues Trp26 and Thr27 (Bel et al., 2009). Caspr2-mcherry was generated by PCR amplification and insertion into the EcoR1-BamH1 sites of pmCherry-N1 vector. The Caspr2-HA deleted constructs, Caspr2Δ1 (Δ32-361), Caspr2Δ2 (Δ362-600), Caspr2Δ3 (Δ600-950), Caspr2Δ4 (Δ955–1169) were generated by QuickChange mutagenesis (Agilent Technologies). The Caspr2-Discoïdin-LamininG1, Caspr2-Discoïdin, Caspr2-LamininG1 (**Figure 2A**) were obtained using reverse PCR on HA-tagged full length Caspr2 plasmid and the fragment fusion was performed using the In-Fusion kit (Clontech). The Caspr2-Fc construct was generated by PCR amplification of Caspr2 extracellular domain (amino acids 1–1242) and insertion into the Kpn1-Not1 cloning sites of pIg-plus vector. The human TAG-1-GFP construct was generated by inserting GFP downstream the signal peptide. PCR amplified products were verified by sequencing (Beckman Coulter Genomics). Plasmids encoding human LGI1, ADAM22, ADAM23 were purchased from Origene. Gephyrin-GFP is a kind gift of Dr. F. Ango.

Patient's Serum and CSF

The presence of anti-Caspr2 autoantibodies was assessed using the patient's cerebrospinal fluid (CSF) as previously described (Viaccoz et al., 2014). Patients were considered positive when positive staining of a cell-based assay with human embryonic kidney cells (HEK-293) cells overexpressing the Caspr2 protein was observed. After the identification of anti-Caspr2 antibodies by the French PNS Reference Center, serum and CSF samples were frozen and conserved at −80°C. A written consent was obtained from all patients, and the use of samples for this study was approved by the institutional review board of the University Claude Bernard Lyon 1/Hospices Civils de Lyon. The patient's clinical data were prospectively collected at least twice a year by phone or mail.

Antibodies and Immunofluorescence Staining

The IgGs from patients' sera were purified using the Melon gel kit (Pierce). Rabbit anti-Caspr and rat anti-Gliomedin were described previously (Labasque et al., 2011), rabbit anti-MAP2 was a gift from Dr. J. F. Leterrier, rabbit anti-AnkyrinG from Dr. G. Alcaraz, and rabbit anti-vGLUT1 from Dr. S. El Mestikawy. The mouse anti-GAD65 mAb was obtained from Developmental Studies Hybridoma Bank, University of Iowa and anti-Kv1.2 (clone K14/16) mAb from UC Davis/NIH NeuroMab Facility, UCDavis, mouse anti-tau mAb was purchased from Sigma, mouse anti-Synaptophysin mAb from Chemicon, guinea-pig anti-VGAT from Synaptic Systems and rat anti-HA mAb

was purchased from Roche. AlexaFluor488-, 568-, and 647-conjugated secondary antibodies were obtained from Molecular Probes. Immunostaining with IgGs from LE patients was performed on live cells diluted 1:500 in culture medium for 30–60 min. Cells were fixed with 4% paraformaldehyde in PBS for 10 min and permeabilized with 0.1% Triton-X100 for 10 min. Immunofluorescence staining was performed using rabbit anti-MAP2 (1:2000), rabbit anti-vGLUT1 (1:100), rabbit anti-AnkyrinG (1:500), or guinea-pig anti-VGAT (1:400) antibodies, or mouse anti-tau (1:500), anti-Kv1.2 (1:500), anti-GAD65 (1:200), or anti-Synaptophysin (1:200) mAbs, and with secondary antibodies diluted in PBS containing 3% bovine serum albumin. After washing in PBS, cells were mounted in Mowiol (Calbiochem).

Flow Cytometry and Isotyping

HEK-293 cells were transfected with Caspr2-HA, harvested and double-labeled using anti-HA mAb and IgGs from LE patients and secondary antibodies conjugated with FITC or Phycoerythrin (Beckman Coulter). FITC-conjugated anti-human IgG1, IgG2, IgG3, and IgG4 were purchased from Bindingsite. Cells were washed and fixed with 2% paraformaldehyde and analyzed on FACSCanto with the CellQuest software (Becton Dickinson).

Cell Culture

Cell culture media and reagents were from Invitrogen. Neuroblastoma N2a cells and HEK-293 cells were grown in DMEM containing 10% fetal calf serum and were transiently transfected using jet PEI (Polyplus transfection, Ozyme). Caspr2-Fc, control and deletion mutants were produced in the supernatant of transfected HEK-293 cells and affinity purified using Protein-A Sepharose. Transfected N2a cells and hippocampal neurons were incubated with Caspr2-Fc (10 μg/ml) pre-clustered with Alexa488 or 568 conjugated anti-human Fc (50 μg/ml) for 30 min at 37°C. Primary hippocampal cell cultures were performed from embryonic day 18-Wistar rats. Hippocampi were collected in Hanks' balanced salt solution, dissociated with trypsin and plated at a density of $1.2.10^5$ cells/cm^2 on poly L-lysine coated coverslips. The hippocampal neurons were cultured in Neurobasal supplemented with 2% B-27, 1% penicillin-streptomycin, and 0.3% glutamine in a humidified atmosphere containing 5% CO_2 at 37°C. Hippocampal neurons were transfected using Lipofectamine 2000 with Gephyrin-GFP or GFP at DIV 14, or with TAG-1-GFP, LGI1-GFP, ADAM22, and ADAM23 at DIV8. Hippocampal cell cultures were prepared from embryonic day 16 C57BL6 wild-type and *Tag-1*$^{-/-}$ mice (Traka et al., 2003) with the same protocol. For functional perturbing assays, DIV17 neurons transfected with Gephyrin-GFP were incubated for 1 h at 37°c with culture medium, control, LE5 or LE6 IgGs using 1/100 dilution in 100 μl volume before fixation and immunostaining for GAD65. Experiments were performed in duplicate and four coverslips analyzed under each condition. All animal experiments were carried out according to the animal care and experimentation committee rules approved by CNRS.

Confocal Microscopy and Image Analysis

Image acquisition was performed on a Zeiss laser-scanning microscope equipped with 63 × 1.32 NA oil-immersion objective. Images of GFP or AlexaFluor-stained cells were obtained using the 488 nm band of an Argon laser and the 568 and 647 nm bands of a solid state laser for excitation. Fluorescence images were collected automatically with an average of two-frame scans and collected as frame-by-frame sequential series for tiles. To quantify the number of inhibitory pre-synaptic contacts immunostained for Caspr2, we estimated the number of GAD65 clusters that were positive or negative for Caspr2 along 25 μm-dendrite lengths ($n = 14$ neurons). To quantify the number of post-synaptic contacts labeled for Caspr2-Fc, we estimated the number of Synaptophysin clusters contacting the shaft and spines that were positive or negative for Caspr2-Fc along 50 μm-dendrite lengths ($n = 21$ dendrites, 7 neurons) using the image-J software. To quantify the number of synaptic and total Gephyrin-GFP clusters per neuron, we used Imaris as software (BitplaneAG, Switzerland) with automatic detection of objects in 3-dimensional space using six *z*-stack projections. The *"spot"* tool of surpass function was used to detect the GAD65 pre-synaptic clusters and post-synaptic Gephyrin-GFP clusters and the same segmentation threshold was used for all the images in each channel. The intracellular aggregates of Gephyrin-GFP (spot diameter >0.6 μm) were removed. We selected the post-synaptic spots opposed to pre-synaptic spots within a 0.6 μm distance with the "*co-localize spots*" option. The ratio of synaptic relative to total Gephyrin clusters and the number of synaptic Gephyrin clusters per neuron were determined under each condition. The total number GAD65 clusters contacting the somato-dendritic compartment was determined using the *"find spots close to surface"* tool. To analyze the effect of incubation with control and LE IgGs, data were pooled from two independent cultures (four coverslips, $n = 23$–36 neurons analyzed under each condition) and significant differences were determined using ANOVA followed by Fisher's test.

Results

Autoantibodies to Caspr2 in LE Bind Hippocampal Neurons in Culture

We identified Caspr2 as a target antigen in a series of seven patients with LE. The clinical features in **Table 1** indicate that these patients showed pure LE characterized by confusion, amnesia, and seizures, without neuromyotonia. All the sera (named LE1-LE7) were reactive for dendrotoxin-precipitated VGKC as analyzed using radio-immunoassays, negative for LGI1 and reacted against Caspr2 at high titer as assayed using cell binding assays and flow cytometry (**Table 1**).

As shown for patients LE1-4, these autoantibodies strongly labeled Caspr2-transfected N2a cells (**Figure 1A**). Since Caspr2 is a component of the juxtaparanodal VGKC complex, the serum IgGs of patients with LE were tested on teased mouse sciatic nerves. We determined that the serum IgGs of patients bound juxtaparanodes after methanol fixation as shown for LE1, LE6, and LE7 (**Figure 1B**). Next, we showed that the serum IgGs

TABLE 1 | Basic epidemiological, immunological, and clinical features of LE patients with antibodies against Caspr2.

Patient	Age (gender)	Titers	Clinical features	Treatment with improvement
LEI	73 (M)	1/51,200	limbic encephalitis, confusion, seizures, prostate cancer	IVIg
LE2	62 (M)	1/12,800	limbic encephalitis, confusion, temporal seizures, prostate cancer	IVIg
LE3	60 (M)	1/6,400	memory disturbances, thyroid cancer with metastasis	plasmapheresis
LE4	71 (M)	1/51,200	memory disturbances, temporal seizures	corticosteroids, mycophenolate, mofetil
LE5	64 (M)	1/51,200	limbic encephalitis, confusion, ataxia, seizures	corticosteroids
LE6	60 (M)	1/51,200	limbic encephalitis, confusion, amnesia, sub-clinical seizures	corticosteroids
LE7	72 (M)	1/12,800	limbic encephalitis, confusion, amnesia, seizures	corticosteroids, anti-convulsant

These patients did not present neuromyotonia. The titer of serum IgGs was determined using flow cytometry.

of all patients bound rat hippocampal neurons in culture using live immunostaining (**Figure 1**; **Supplementary Figure S1**). We showed that immunostaining with LE1–LE5 serum IgGs was abolished by pre-adsorption on HEK cells transfected with Caspr2 (**Figure 1G** and **Supplementary Figures S1B,D,F,H**). These data indicate that the IgGs from these patients recognized only Caspr2 in cultured hippocampal neurons.

Previous studies using rabbit anti-Caspr2 antibodies directed against the cytoplasmic region of the molecule, showed that Caspr2 is expressed at low level in axons of cultured hippocampal neurons (Ogawa et al., 2008; Bel et al., 2009) when compared with juxtaparanodes of myelinated axons (Traka et al., 2003). Using anti-Caspr2 LE1 IgGs, we observed surface labeling of the somato-dendritic and axonal compartments of DIV4 neurons double-stained for MAP2 and tau, respectively, (**Figures 1C,D,D'**). At DIV7, a punctate staining of neurites was detected. Double-staining for MAP2 indicated that Caspr2 was faintly expressed at the surface of the somato-dendritic compartment at that stage (**Figures 1E,F,F'**). In contrast, Caspr2 strongly colocalized with the axonal marker tau. Only a subpopulation of axons was immunostained (**Figure 1F**, arrows) whereas some axons were unlabeled (**Figures 1F,F'**, arrowheads). This preferential distribution of Caspr2 at the axonal surface of hippocampal neurons was also observed using live immunostaining with LE2–LE5 serum IgGs at DIV7 (**Supplementary Figures S1A,C,E,G**).

As Caspr2 is known to be associated with Kv1.1/1.2 channels at juxtaparanodes of myelinated fibers and at axon initial segments in various neuronal cell types such as motoneurons or cortical pyramidal cells (Inda et al., 2006; Duflocq et al., 2011), we tested for a possible co-localization in cultured hippocampal neurons. As shown using LE1 serum IgGs in **Figures 1H,H'** surface staining for Caspr2 was observed along the axon but was not enriched at the axon initial segment, which was strongly stained for Kv1.2 and AnkyrinG at DIV14.

The N-Terminal Modules of Caspr2 Can be Selectively Targeted by Autoantibodies in LE Patients

Recent studies pointed to the importance of the IgG4 subtype in autoimmune neurological diseases such as myasthenia gravis and CIDP (Huijbers et al., 2013; Labasque et al., 2014; Querol et al., 2014). Using flow cytometry, we studied the IgG specificities of our samples and determined that anti-Caspr2 IgG4 were present in all the LE patients. In addition, IgG4 was the predominant isotype in four out of seven patient's sera (**Table 2**). The IgG4 do not mediate complement activation, nor bind Fc receptors on effector cells. This could be an indication that the IgG4 in the CSF of LE patients may be pathogenic via functional blocking activity.

Next, to determine if IgGs of LE patients with anti-Caspr2 autoimmunity may recognize specific modules of Caspr2, we generated Caspr2 constructs encompassing sequential deletions Δ1, Δ2, Δ3, and Δ4 of the protein (**Figure 2A**). Flow cytometry and cell based assays were performed on HEK cells expressing Caspr2 constructs (**Figure 2B**). All patients' sera recognized the Caspr2-Δ2, Δ3, and Δ4 constructs. On the opposite, three sera and four CSF out of seven did not recognize Caspr2-Δ1 (**Figure 2C**; **Table 2**). Thus, the N-terminal Discoïdin and LamininG1 domains could be a major epitope in patients with LE. To precisely map the epitopes, we generated additional constructs, Caspr2-Discoïdin-LamininG1, Caspr2-Discoïdin, and Caspr2-LamininG1 as depicted in **Figure 2A** and showed that all the seven sera and CSF tested recognized both the Discoïdin and LamininG1 modules, whereas the 30 amino-acids linker between these two modules was not recognized. The specific function of this N-terminal region is still unknown.

GABAergic Neurons are the Main Target of Anti-Caspr2 Autoantibodies in Patients with LE

Since only a subpopulation of axons was labeled using anti-Caspr2 LE1 serum IgGs, we further investigated whether excitatory or inhibitory subpopulation of neurons may be differentially targeted. DIV4 neurons were analyzed to study the somato-dendritic expression of Caspr2 at early stage. We first determined that 22% of MAP2-positive neurons were GABAergic using glutamate decarboxylase GAD65 as a marker (**Figures 3A,B**). Next using immunolabeling with LE1 serum IgGs, we estimated that 58% of the inhibitory neurons in contrast to only 4% of excitatory neurons (negative for GAD65, arrows) expressed Caspr2 at DIV4 (**Figures 3A,B**; **Table 3**). Thus, most of the Caspr2-positive neurons (81%) were inhibitory neurons as illustrated in **Figure 3C**. In the same manner, quantitative analyses were performed using LE2–LE5 serum IgGs and indicated that 51–68% of GAD65-positive neurons and only 4–8% of GAD65-negative neurons were targeted by these patients IgGs (**Table 3**).

We also examined how Caspr2 was distributed along axons and pre-synaptic sites at DIV14 and DIV21 later stages. The

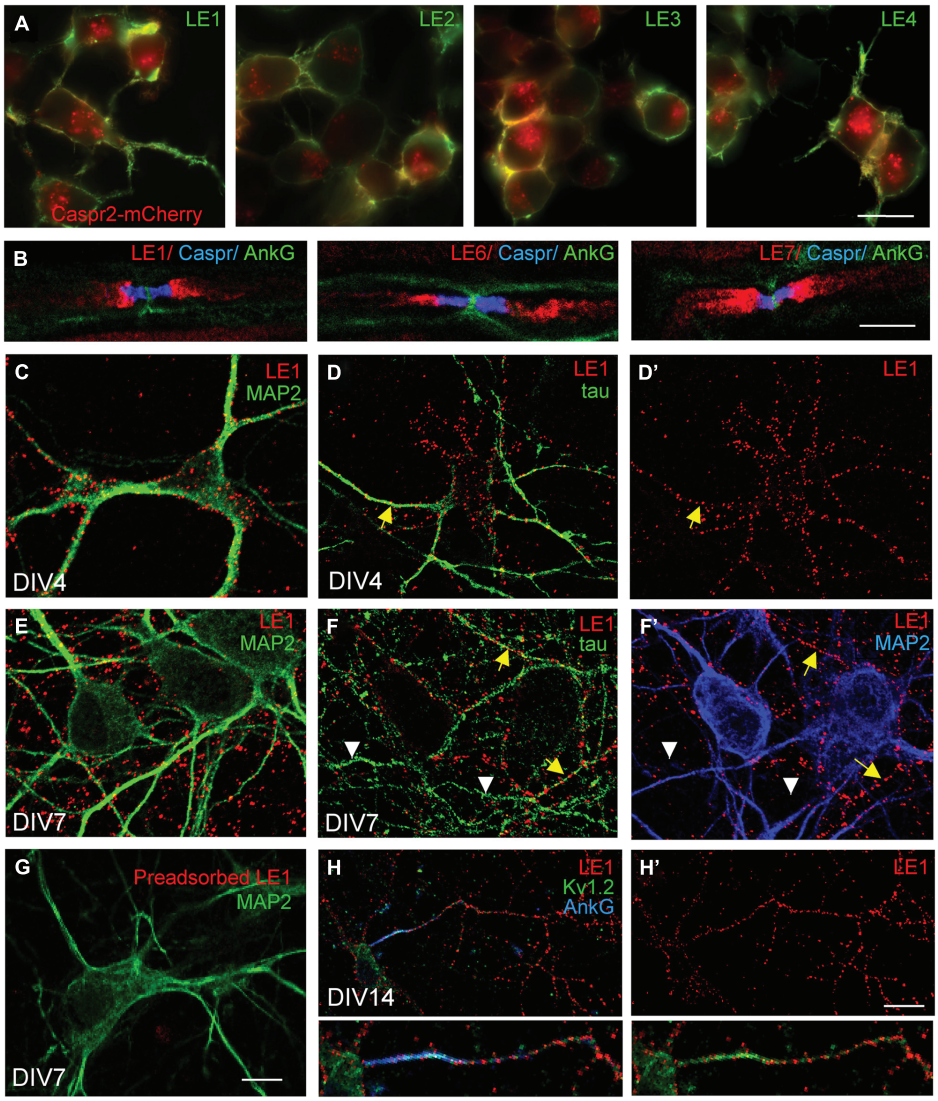

FIGURE 1 | Limbic encephalitis autoantibodies directed against Caspr2 bind hippocampal neurons in culture. (A) Neuroblastoma N2a cells were transfected with Caspr2-mcherry (red) and surface labeled with IgGs from LE1–LE4 patients (green). **(B)** Teased sciatic nerve of adult mice were fixed with methanol and immunostained for Contactin-associated protein Caspr (blue) and AnkyrinG (AnkG) (green) as markers of the paranodal and nodal regions of the nodes of Ranvier, respectively. Note that autoantibodies of patients LE1, LE6 and LE7 bound the juxtaparanodes (red). **(C–H)** Rat hippocampal neurons at DIV4 **(C,D,D')**, DIV7 **(E–G)**, and DIV14 **(H,H')** were surface labeled with LE1 IgGs (red). Cells were fixed with 4% paraformaldehyde, permeabilized, and double-stained for the somato-dendritic marker MAP2 (green in **C,E,G**; blue in **F'**) or axonal tau (green in **D,F**). Caspr2 surface staining was detected on the somato-dendritic and axonal compartments at DIV4 **(C,D,D')** but was mainly associated with axonal processes at DIV7 **(E,F,F')**. In **(F)**, yellow arrows indicate axons that were double-stained for Caspr2 and tau, whereas white arrowheads indicate unlabeled tau-positive axons. **(G)** LE1 IgGs were pre-adsorbed using incubation with Caspr2-transfected HEK cells and did not bind hippocampal neurons. **(H,H')** Hippocampal neurons at DIV14 were surface labeled for Caspr2 using LE1 IgGs (red) and fixed and permeabilized before immunostaining with mouse-anti-Kv1.2 mAb (green) and rabbit anti-AnkyrinG antibodies (blue). The Kv1.2 channels were enriched at the axonal initial segment stained for AnkyrinG, whereas surface Caspr2 was distributed along the axon. Insets are twofold magnification images. Fluorescence microscopy **(A)** and confocal images **(B–H)**. Bar is in **(A)**, 20 μm; in **(B)**, 5 μm; in **C–G**, 15 μm; in **(H,H')**, 30 μm.

vesicular glutamate transporter-1 vGLUT1 was used as a marker for glutamatergic axons and synapses. As shown in **Figure 4A**, some of the vGLUT1-positive axons at DIV14 were labeled for Caspr2 using LE1 serum IgGs. High magnification images show that Caspr2 co-localized with vGLUT1 at pre-synaptic sites (**Figure 4A'**, arrowheads). Next we used GAD65, which synthesizes GABA for neurotransmission as a marker for inhibitory axons and synapses. Caspr2 strongly co-localized with GAD65-positive axons as observed using serum IgGs of all the patients analyzed (**Supplementary Figure S2**). In particular, the GAD65-positive axons were surrounding the MAP2-labeled large pyramidal neurons and were heavily stained for Caspr2 at DIV14 and DIV21 as shown using LE1 serum IgGs (arrows in **Figures 4B,C**). The presynaptic sites labeled for GAD65

TABLE 2 | Isotyping and domain mapping of serum and CSF IgGs from LE patients using flow cytometry and cell binding assays.

Patient	Serum		CSF	
	Isotypes	**Domain mapping**	**Isotypes**	**Domain mapping**
LEI	IgGI, IgG2 > IgG3, IgG4	Multiple	IgGI, IgG4	Multiple
LE2	IgGI > IgG4	Multiple	IgGI > IgG4	Multiple
LE3	IgG4	Discoidin-LNGI	IgG4	Discoidin-LNGI
LE4	IgG2 > IgGI, IgG4	Multiple	IgGI	Discoidin-LNGI
LE5	IgG4 > IgGI	Multiple	IgG4 > IgGI	Multiple
LE6	IgG4	Discoidin-LNGI	IgG4	Discoidin-LNGI
LE7	IgG4 > IgGI	Discoidin-LNGI	IgGI, IgG4	Discoidin-LNGI

HEK cells were transfected with full-length or Δ1-, Δ2-, Δ3-, and Δ4-deleted Caspr2 constructs and were surface-labeled for the HA epitope. Sera at 1:500 dilution were analyzed for IgG1–IgG4 isotypes and CSF at 1:20 dilution for IgG1 and IgG4.

were intensely stained for Caspr2 at the contact with the soma (arrowheads in **Figure 4C"**) or dendrites (arrowheads in **Figures 4B',C"'**). We estimated that 51% of the GABAergic pre-synaptic contacts on dendrites were labeled for Caspr2 (5.9 ± 0.5 Caspr2-positive of 11.6 ± 0.5 total GABAergic contacts/25 μm dendritic length; $n = 14$ dendrites). As illustrated in **Figure 4C'**, Caspr2 was distributed along inhibitory axons partially overlapping with GAD65 puncta. We estimated that 34 % of the Caspr2-positive clusters contacting dendrites were GAD65-positive (13.7 ± 2 Caspr2-positive clusters among which 4.7 ± 0.8 were GABAergic/25 μm).

Hippocampal neurons were transfected at DIV14 with Gephyrin-GFP to visualize the post-synaptic clusters facing pre-synaptic inhibitory contacts at DIV21 (**Figure 5A**). Gephyrin is the major post-synaptic scaffolding protein at inhibitory synapses (Craig et al., 1996). As shown in **Figure 5A'**, pre-synaptic terminals positive for both GAD65 and Caspr2 were apposed to Gephyrin-GFP clusters (arrowheads). In addition, surface Caspr2 colocalized with the inhibitory presynaptic terminals that were labeled for VGAT (**Figures 5E,E'**). We asked whether the LE patient's autoantibodies directed against Caspr2 could display functional blocking activity by destabilizing inhibitory synaptic contacts. The LE5 and LE6 autoantibodies were tested which are mainly of the IgG4 isotype. LE5 IgGs are directed against multiple domains of Caspr2 and LE6 IgGs only target the N-terminal modules. Hippocampal neurons were transfected with Gephyrin-GFP at DIV14 and incubated at DIV17 with the culture medium, control IgGs, LE5, or LE6 IgGs diluted 1:100 for 1 h at 37°C. Using automatic spot detection of the Imaris software, we determined under each condition the number of total Gephyrin-GFP clusters and the number of Gephyrin-GFP clusters apposed to GAD65-positive presynaptic terminals (**Figure 5B**, white arrows). The ratio of synaptic versus total Gephyrin-GFP clusters was not significantly affected by incubation during 1 h with LE autoantibodies (**Figure 5C**). However, a significant decrease in the number of synaptic Gephyrin clusters per neuron was observed for LE5 and LE6 (24.5 and 30%, respectively, $P < 0.05$ using ANOVA and Fisher's test) but not for control IgGs (10%) by comparison with culture medium incubation (**Figure 5D**). The number of GAD65-positive clusters contacting the somato-dendritic compartment per Gephyrin-GFP transfected neuron was not significantly decreased (284 ± 41 with culture medium, 230 ± 18 with control IgGs, 218 ± 21 with LE5, 210 ± 30 with LE6). Since Caspr2 was only expressed in 60% of GAD65-positive neurons, the functional effect of LE autoantibodies may be underestimated. In conclusion, we observed that Caspr2 is selectively localized along GABAergic axons and at the inhibitory pre-synaptic terminals in cultured hippocampal neurons. In addition, the perturbating assays of post-synaptic Gephyrin clusters suggest that anti-Caspr2 autoantibodies of LE patients may be pathogenic by altering the inhibitory synaptic contacts.

The Caspr2-Fc Binding Sites are Localized on the Somato-Dendritic Compartment

Caspr2 belongs to the family of neurexins, which are pre-synaptic CAMs. Studies in culture indicate that neurexins are implicated in synaptogenesis by inducing the clustering of post-synaptic neuroligins (Dean et al., 2003; Craig and Kang, 2007). Neurexin/neuroligin association promotes the formation of excitatory and inhibitory synapses by interacting with PSD95 or Gephyrin, respectively. We asked whether Caspr2 might be also involved in trans-synaptic contacts. With this aim, we generated a Caspr2-Fc chimera to detect Caspr2 binding sites in hippocampal neuronal culture. Caspr2-Fc plasmid was transfected in HEK cells and the recombinant protein purified from the culture supernatant using Protein A-affinity chromatography. The chimera pre-clustered with fluorescent anti-Fc IgG was incubated with hippocampal neurons at DIV4 (**Figure 6**). We observed that Caspr2 binding sites were present on both GAD65-negative (arrow in **Figure 6A**) and GAD65-positive neurons (green arrow in **Figure 6B**). Quantitative analysis indicated that Caspr2-Fc bound 36% of the total neurons (**Figure 6C**). Caspr2-Fc bound to the somato-dendritic compartment of DIV7 neurons as determined using double-staining for MAP2 (**Figures 6D,D'**). In contrast, Caspr2-Fc was not co-localized with axons immunostained with anti-tau mAb (**Figures 6E,E'**). Caspr2-Fc binding sites were distributed on the somato-dendritic compartment of both inhibitory (26 ± 6%) and excitatory (38 ± 5%) neurons as analyzed at DIV4 ($n = 504$ neurons, three coverslips; **Figure 6C**).

Next, we analyzed whether the Caspr2 binding sites may be distributed at the post-synaptic sites. Neurons were transfected with GFP at DIV14 to clearly visualize dendrites and spines of isolated neurons at DIV21 (**Figure 7A**). Synaptic contacts on dendritic shafts (arrowheads) or spines (arrow) were detected using Synaptophysin as a pre-synaptic marker. As shown in high magnification pictures, Caspr2 binding sites (red) were detected on shafts at the contact with the pre-synaptic marker (blue; **Figures 7A',A"**). Quantitative analysis indicated that 58% of post-synapses on shafts and 48% on spines were labeled

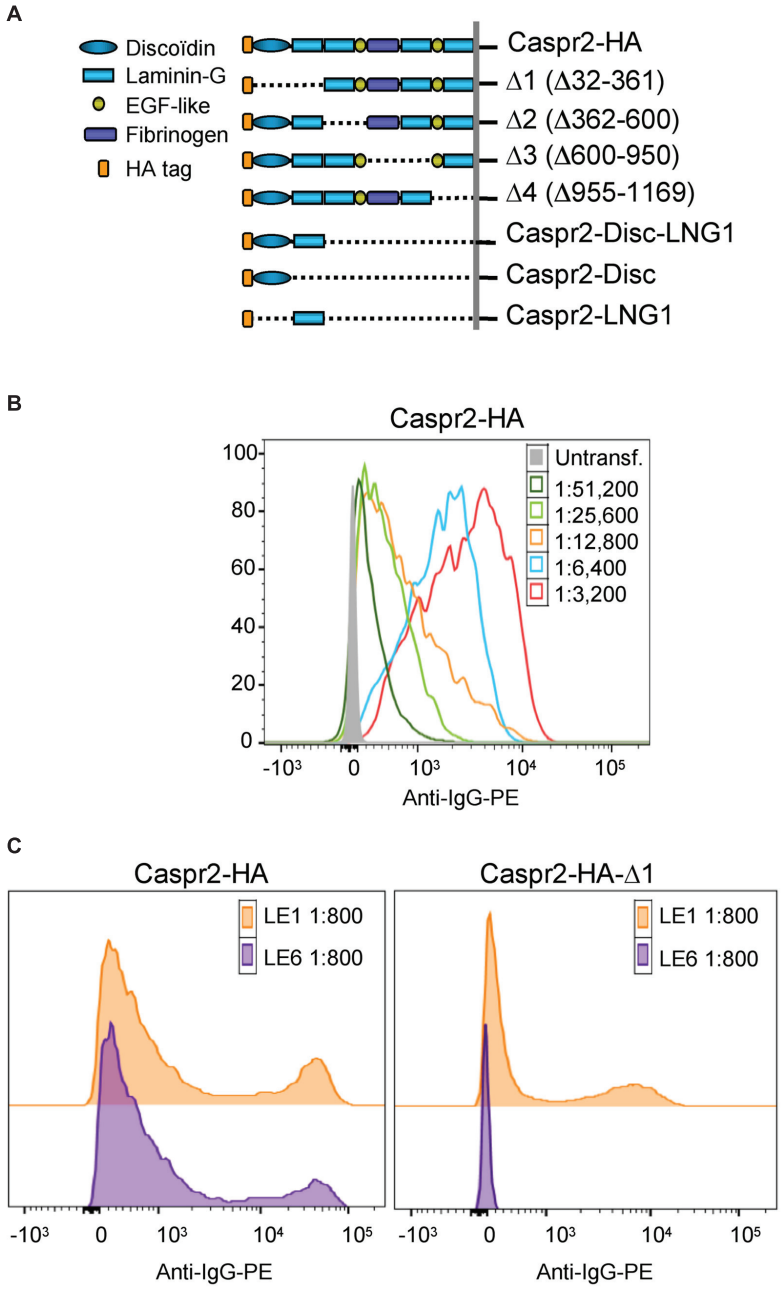

FIGURE 2 | Epitope mapping of anti-Caspr2 autoantibodies in LE patients. (A) Caspr2-HA constructs encompassing sequential deletions: Δ1 deleted of the N-terminal discoïdin and Laminin-G1 domains, Δ2 deleted of the Laminin-G2 and EGF-like1 domains, Δ3 deleted of the central fibrinogen and Laminin-G3 domains, Δ4 deleted of the EGF-like2, and Laminin-G4 domains, Caspr2-Disc-LNG1, Caspr2-Disc, and Caspr2-LNG1 only including the Discoïdin and/or LaminG1 modules in the ectodomain. **(B)** Flow cytometry analysis of anti-Caspr2 IgG titer of LE1 serum. Untransfected and Caspr2-HA-transfected HEK cells were incubated with serial dilutions of LE1 serum (1/3,200–1/51,200) and phycoerythrin-conjugated anti-human IgG (Anti-IgG-PE). **(C)** Flow cytometry analysis of anti-Caspr2 serum IgGs of LE1 and LE6 on HEK cells transfected with full-length or Δ1 deleted Caspr2-HA construct.

with Caspr2-Fc chimera ($n = 21$ images; **Figure 7B**). Thus, the receptors of Caspr2 were present both at inhibitory and excitatory post-synaptic sites on shafts and spines, respectively. The Caspr2-binding sites at the inhibitory post-synapses were complementary to the distribution of Caspr2 at inhibitory pre-synaptic sites.

The Somato-Dendritic Binding Sites of Caspr2 Depends on TAG-1 but not on LGI1, ADAM22, and ADAM23

Contactin 2/TAG-1 is an Ig-CAM that associates with Caspr2 and the VGKC complex at juxtaparanodes (Poliak et al., 2003;

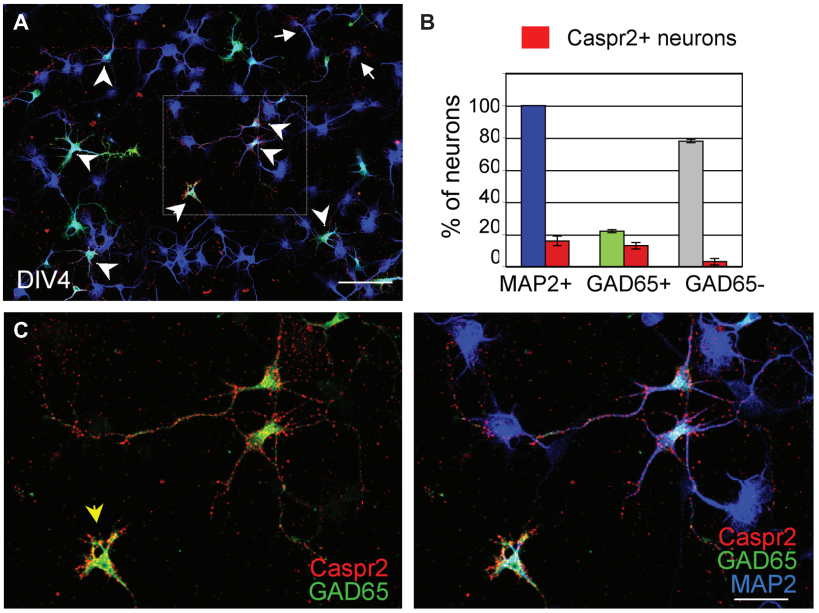

FIGURE 3 | GAD65-positive neurons are the main target of anti-Caspr2 LE1 autoantibodies. DIV4 hippocampal neurons were surface labeled with LE1 IgGs (red), fixed and permeabilized before immunostaining for MAP2 (blue) as a neuronal marker and GAD65 (green) to identify inhibitory neurons. **(A)** Low magnification image showing neurons that were surface labeled for Caspr2 (red). Most of them were GAD65-positive (green, arrowheads) and few were GAD65-negative (arrows). The box enlarged in C shows GAD65-positive neurons in green that were surface labeled for Caspr2. The arrowhead points to an isolated inhibitory neuron strongly labeled for Caspr2 on the soma **(B)** Quantitative analysis of the percentage of total neurons, GAD65-positive and GAD65-negative neurons that were surface labeled for Caspr2. Means ± SEM of three independent experiments. **(A)** Tiling of 5 × 4 confocal images acquired with the 63x objective, *z*-stack of 6 confocal sections with *z*-step of 0.5 μm. Bar is in A, 80 μm; in **(C)**, 35 μm.

TABLE 3 | The anti-Caspr2 autoantibodies in LE patients target inhibitory neurons.

			% Caspr2-positive neurons		
	(n)	% inhibitory neurons GAD65-positive	Total MAP2-positive	Inhibitory GAD65-positive	Excitatory GAD65-negative
LEI	434	22 ± 1	16 ± 3	58 ± 5	4 ± 2
LE2	480	17.4 ± 4	15 ± 3.8	51.2 ± 3.7	7.2 ± 3.7
LE3	374	23.9 ± 1	18.9 ± 4.5	57.4 ± 8.9	6.7 ± 3.2
LE4	354	19.9 ± 3.5	19.1 ± 3.9	64.3 ± 4.8	8.3 ± 3.3
LE5	358	21.5 ± 1.2	19.9 ± 2.7	68.5 ± 8.2	6.5 ± 1.2

After four days in vitro hippocampal neurons were surface labeled with LE1–LE5 IgGs and double-stained for MAP2 as a neuronal marker and GAD65 to identify inhibitory neurons. (n) indicates the total number of neurons analyzed on three different coverslips.

Traka et al., 2003). It was previously reported that TAG-1 strongly associates in cis with Caspr2 whereas the trans-interaction remains elusive, since TAG-1-Fc does not bind to Caspr2 expressed at the cell membrane of HEK cells (Traka et al., 2003). Conversely, we observed that the pre-clustered Caspr2-Fc chimera bound N2a cells transfected with GPI-anchored TAG-1 fused with GFP downstream the signal peptide (**Figure 8A**). In addition, Caspr2-Fc binding was strongly enhanced on neurons transfected with TAG-1 when compared with untransfected neurons (**Figures 8B,C**), indicating that the trans-interaction with TAG-1 strongly occurs in neuronal cells. Next, we tested whether Caspr2-Fc bound on hippocampal neurons from *Tag-1*$^{-/-}$ mice. Caspr2-Fc binding was faintly detected on TAG-1-deficient neurons (**Figure 8D**). In contrast, Caspr2-Fc strongly labeled hippocampal neurons from *Tag-1*$^{-/-}$ mice that were transfected with TAG-1-GFP in contrast with untransfected neurons (**Figure 8E**).

We also tested whether the binding of Caspr2-Fc may depend on LGI1/ADAM22 that are members of the VGKC complex and are recruited at the post-synapse (Fukata et al., 2006; Owuor et al., 2009; Ogawa et al., 2010). We did not observe any binding of Caspr2-Fc on N2a cells transfected with LGI1 alone or co-transfected with LGI1 and ADAM22 or ADAM23 (not shown). In addition, Caspr2-Fc binding was not increased on hippocampal neurons transfected with LGI1 and ADAM22 or ADAM23 by comparison with untransfected neurons (**Figures 8F,G**).

To analyze the subcellular targeting of transfected TAG-1, neurons were double-transfected with TAG-1-GFP and mCherry to visualize the dendritic arborisation (**Figures 8H,H'**). Using live immunostaining with anti-GFP antibodies, we observed that

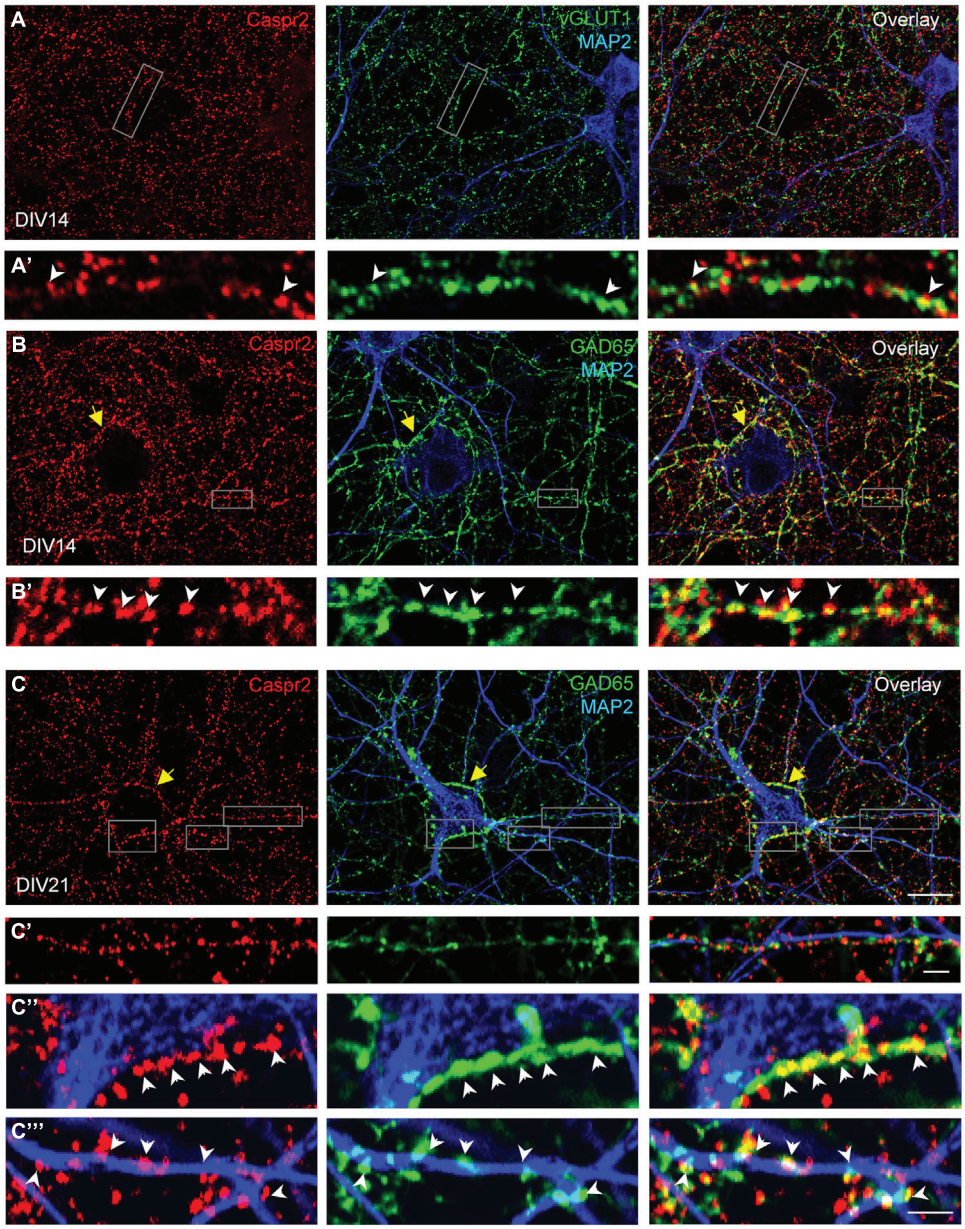

FIGURE 4 | Distribution of Caspr2 at pre-synaptic sites of excitatory and inhibitory axons. Confocal images of hippocampal neurons at DIV14 **(A,B)** or DIV21 **(C)** that were surface labeled for Caspr2 using LE1 IgGs (red). Cells were fixed and permeabilized before double-staining for MAP2 (blue), vGLUT1 (**A**, green) or GAD65 (**B,C**, green). **(A')** Enlarged areas shows glutamatergic pre-synaptic sites stained for Caspr2. **(B',C'–C''')** Inhibitory pre-synaptic sites labeled for GAD65 (arrowheads) were intensely stained for Caspr2 at the contact with the soma **(C'')** or dendrites **(B',C''')**. Note that GAD65-positive axons surrounding the soma of pyramidal neurons were heavily stained for Caspr2 (yellow arrows). **(C')** This enlarged area shows Caspr2 punctate immunostaining along a GAD65-positive axon apposed to a dendrite. Bar is in **(A–C)**, 9 μm; in insets, 1.5 μm.

TAG-1 was addressed to the surface of dendritic arborisation including at the dendritic spines at DIV17. TAG-1-GFP clusters were facing presynaptic sites labeled for synaptophysin both on shafts and spines (**Figures 8H,H'**, respectively). These data indicated that transfected TAG-1 was detected post-synaptically as observed for Caspr2-Fc binding sites. We concluded that TAG-1 may be critically required for Caspr2-Fc binding on the post-synaptic compartment of hippocampal neurons.

Discussion

In the present study, we analyzed autoantibodies against Caspr2 in a series of patients with LE. First, we determined that IgGs in the CSF of four out seven patients selectively react against the Discoïdin and LamininG1 N-terminal modules of Caspr2. Second, using live staining of hippocampal neurons in culture, we showed that autoimmunity to Caspr2 mainly

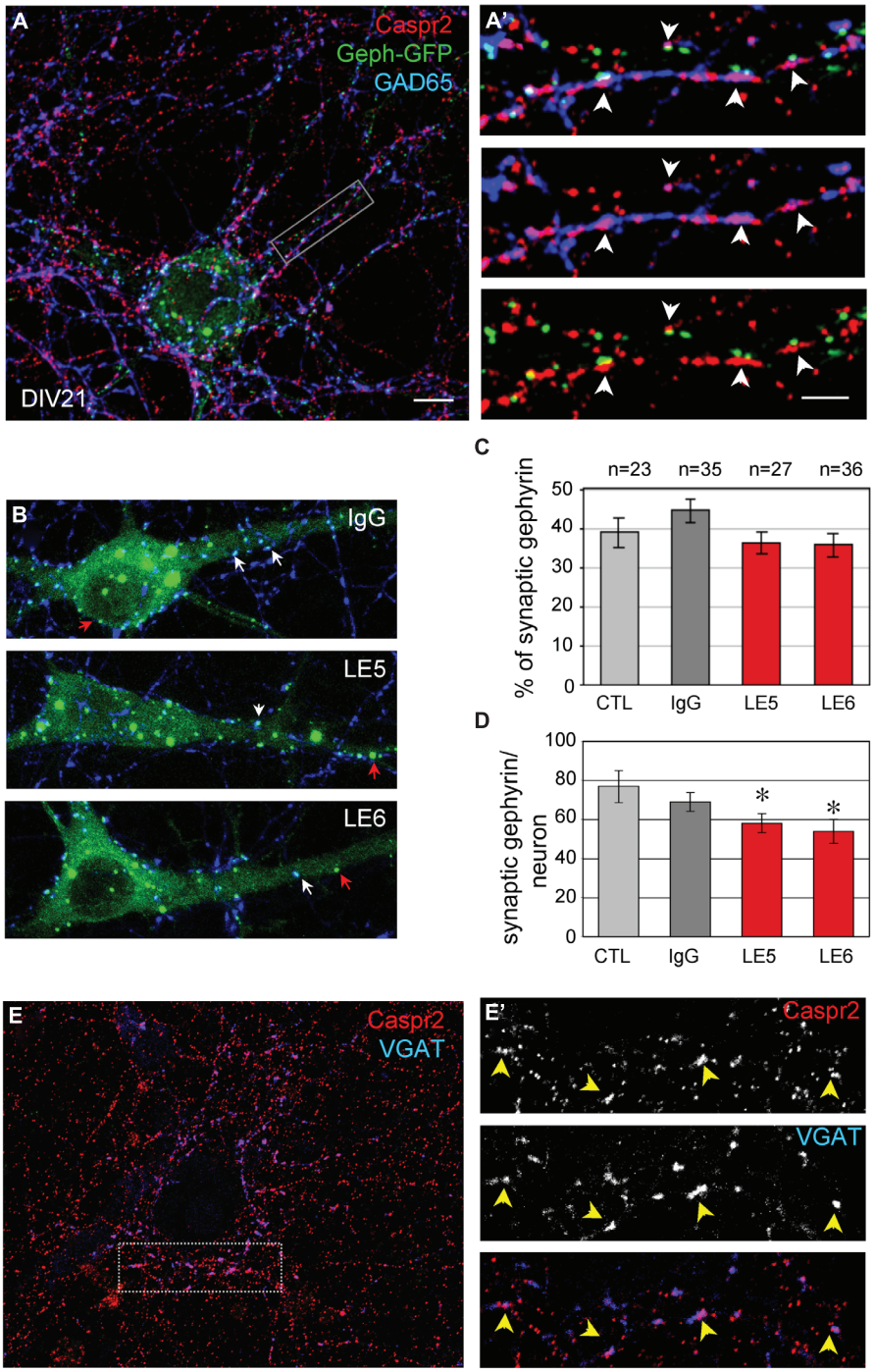

FIGURE 5 | (A) Neurons were transfected with Gephyrin-GFP (Geph-GFP, green) at DIV14 and labeled at DIV21 for surface Caspr2 (red) and GAD65 (blue). **(A')** The insets show the pre-synaptic sites double-labeled for Caspr2 and GAD65 facing post-synaptic clusters of Gephyrin-GFP (arrowheads). **(B)** Hippocampal neurons were transfected with Gephyrin-GFP (green) at DIV14 and incubated at DIV17 with control, LE5 or LE6 IgGs (1/100 dilution) for 1 h at 37°C. Clusters of post-synaptic Gephyrin in contact with presynaptic GAD65 are indicated with white arrows and non-synaptic Gephyrin with red arrows. **(C)** Quantitative analysis of the ratio of synaptic relative to total Gephyrin clusters under the different experimental conditions: incubation with culture medium (CTL), or with control, LE5 or LE6 IgGs. **(D)** Number of synaptic Gephyrin-GFP clusters per neuron. Means ± SEM, n indicates the number of neurons analyzed. *indicates significant difference ($P < 0.05$) with the culture medium condition using ANOVA followed by Fischer's test. **(E)** Double-staining for surface Caspr2 (red) and VGAT as a marker of inhibitory pre-synaptic terminals with the box enlarged in **(E')**. Note the colocalisation of Caspr2 and VGAT indicated with arrowheads. **(A,A', B,E)**: *Z*-stack of five confocal sections with *z*-step of 0.5 μm. **(E')** is a single confocal section. Bar is in **(A,B,E)**, 10 μm; in insets **(A',E')**, 1.5 μm.

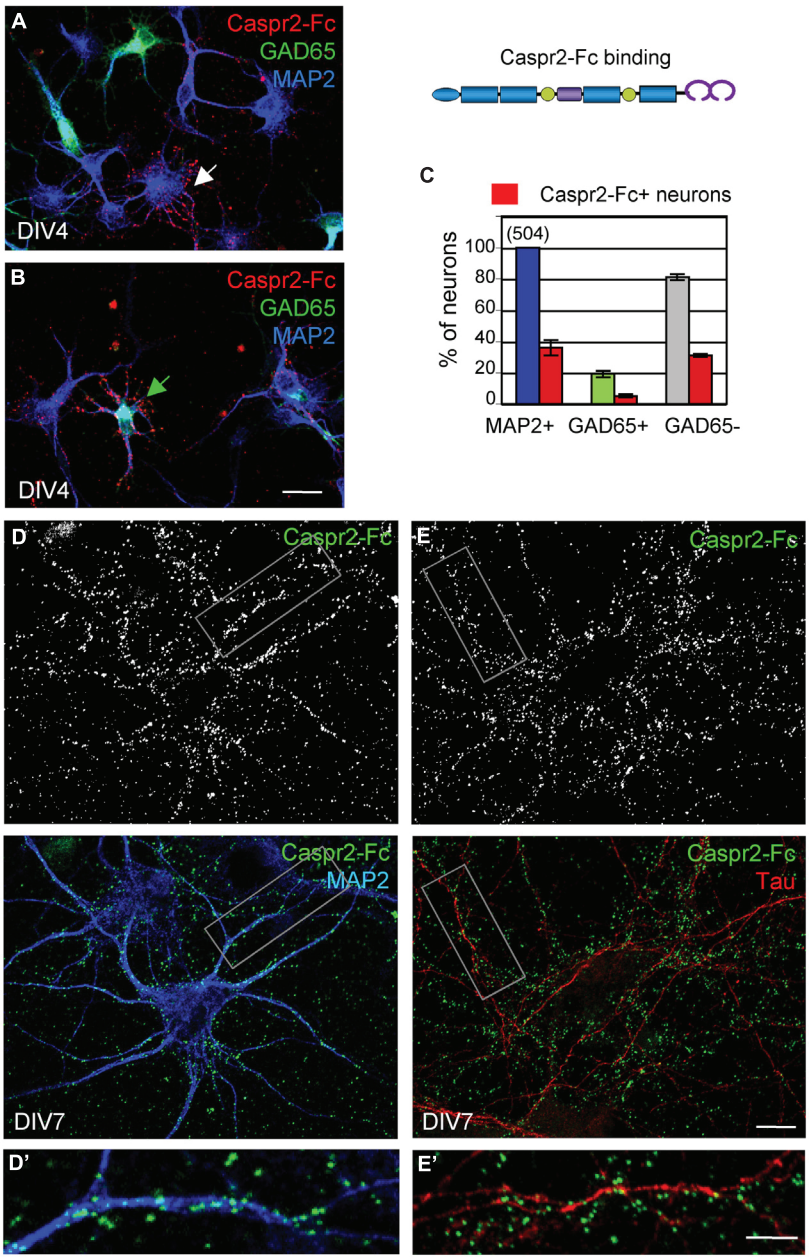

FIGURE 6 | The binding sites of Caspr2-Fc are localized on the somato-dendritic compartment. Hippocampal neurons at DIV4 **(A–C)** and DIV7 **(D,E)** were incubated with 10 μg/ml Caspr2-Fc preclustered with Alexa-conjugated anti-Fc IgGs for 30 min at 37°C. **(A,B)** DIV4 neurons bound with Caspr2-Fc (red). Cells were fixed and permeabilized before double-staining for MAP2 (blue) and GAD65 (green). **(A,B)** show representative images of GAD65-negative neurons (white arrow, **A**) and GAD65-positive neurons (green arrow, **B**) labeled with Caspr2-Fc. **(C)** Quantitative analysis of the percentage of total neurons, GAD65-positive and GAD65-negative neurons that were surface labeled for Caspr2-Fc. Means ± SEM of three independent experiments, $n = 504$ neurons. **(D,E)** DIV7 neurons bound with Caspr2-Fc (green) were double-stained for MAP2 (**D**, blue) or tau (**E**, red). The insets in **(D',E')** show that Caspr2-Fc preferentially bound on MAP2-positive dendrites and not on tau-positive axons. **(A,B)** *z*-stacks of six confocal sections with *z*-step of 0.5 μm. **(D,E)** Single optical sections of confocal images. Bar is in **(A,B)**, 20 μm; in **(D,E)**, 10 μm; in insets, 7 μm.

targets hippocampal inhibitory interneurons (**Figure 9A**). Anti-Caspr2 IgGs label GAD65-positive pre-synaptic sites apposed to Gephyrin post-synaptic clusters. Functional assays indicated that LE autoantibodies may induce alteration of inhibitory synaptic contacts. Third, we used a Caspr2-Fc chimera to reveal Caspr2 receptors on hippocampal neurons. Caspr2 binding sites are distributed on the somato-dendritic compartment at post-synaptic sites. We showed that TAG-1 expression is essential for Caspr2-Fc binding on hippocampal neurons (**Figure 9B**). These results indicate that Caspr2 may participate as a cell recognition

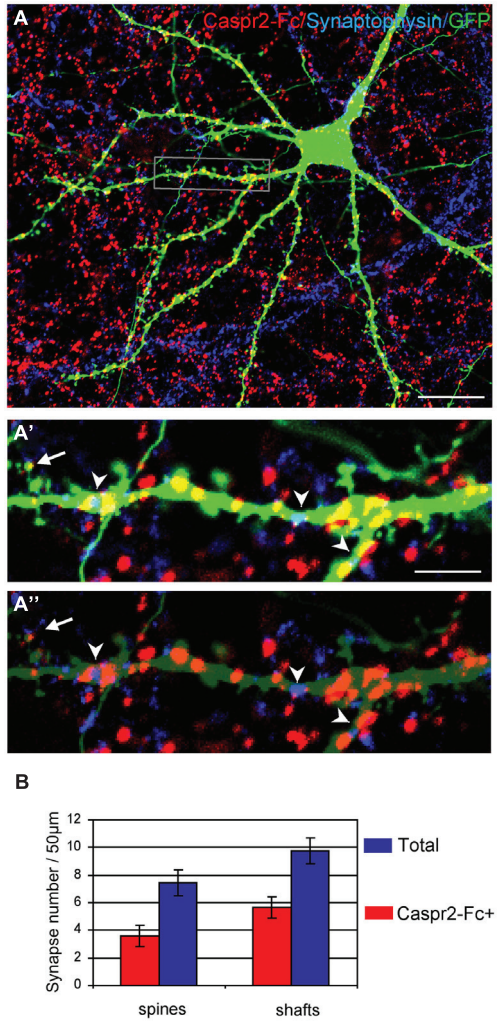

FIGURE 7 | The Caspr2-Fc binding sites are localized at post-synaptic contacts. (A) Hippocampal neurons were transfected at DIV14 with GFP and incubated at DIV21 with preclustered Caspr2-Fc (red). Cells were fixed, permeabilized and immunostained for Synaptophysin (blue). **(A',A")** Insets show the distribution of Caspr2-Fc binding sites (red) on the dendritic shaft (arrowheads) or on spines (arrow) that were contacting Synaptophysin pre-synaptic sites (blue). The green channel is turned down in **(A")** to visualize Synaptophysin clusters. **(B)** Quantitative analysis of the number of post-synaptic sites bound with Caspr2-Fc on spines and shaft. Means ± SEM, $n = 21$ dendrites of seven neurons. Single confocal sections. Bar is in **(A,B)**, 20 µm; in insets, 4 µm.

molecule in the dynamics of inhibitory networks. In addition, they point out to the immune targeting of inhibitory synapses as a critical clue for understanding the physiopathological role of Caspr2.

Distinct Axonal Distributions of Caspr2 and Kv1 Channels in Hippocampal Neurons

We previously reported that transfected Caspr2 is preferentially addressed to the axon and strongly internalized in the somato-dendritic compartment in cultured hippocampal neurons at DIV7 (Bel et al., 2009). The surface expression of Caspr2 is controlled via a Protein Kinase C-regulated motif of endocytosis in its cytoplasmic tail (Bel et al., 2009) that might also interfere with availability of the VGKC-complexes. In the present study, we used anti-Caspr2 IgGs of LE patients, which display very high titer, to label endogenous Caspr2. We showed that Caspr2 is preferentially expressed at the axonal surface, but not enriched at the axon initial segment as observed for Kv1 channels and contactin 2/TAG-1 at DIV14. The Kv1.1/1.2 channels display axonal distribution and are tethered at the axon initial segments in pyramidal cortical neurons and also in inhibitory neurons in hippocampal cell culture and slices (Sanchez-Ponce et al., 2012; Campanac et al., 2013). The recruitment of Caspr2 at the initial segment might be regulated or its antigenicity masked when associated with the VGKC complex. However, we showed that anti-Caspr2 IgGs of several patients bound to VGKC complex at juxtaparanodes of myelinated axons in culture and were reactive for dendrotoxin-precipitated VGKC.

Caspr2 is a Pre-Synaptic CAM Trans-Interacting with TAG-1

Caspr2 functional role may be partly independent from its association with the VGKC-complexes. Indeed, Caspr2 may participate in cell adhesive processes and play a morphogenetic role in neurite outgrowth and synaptogenesis (Anderson et al., 2012). The phenotypic analysis of Caspr2 knockout mice points to its involvement in the migration of cortical neurons and generation or positioning of interneurons (Penagarikano et al., 2011). The number of parvalbumin-positive interneurons is reduced in Caspr2 mutant mice associated with decreased synchronous firing of cortical neurons. However, evidence for synaptic alterations has not been reported. Alteration of developmental events may underlie the spontaneous seizures and behavioral disorders observed in adult Caspr2 knockout mice (Penagarikano et al., 2011).

Our data suggest a cell adhesive or cell-recognition function of pre-synaptic Caspr2 interacting with TAG-1 at the post-synaptic compartment. TAG-1 is the single interacting partner already identified for Caspr2 ectodomain, and their cis-association has been clearly evidenced (Poliak et al., 2003; Traka et al., 2003). We showed here that pre-clustered Caspr2-Fc binds TAG-1 anchored at the membrane of N2a cells indicating *trans*-interaction between the two CAMs. In contrast, the reciprocal interaction is not occurring between soluble TAG-1-Fc and Caspr2-expressed at the cell membrane (Traka et al., 2003). Our recent data indicate that the two molecules expressed at the membrane of opposing cells can mediate trans-adhesive interaction as determined by co-immunoprecipitation (Savvaki et al., 2010).

Both Caspr2 and TAG-1 are present in the fraction containing synaptic plasma membranes (Bakkaloglu et al., 2008) with Caspr2 highly depleted in the post-synaptic density fraction (Chen et al., 2015). TAG-1 is faintly expressed at the surface of cultured hippocampal neurons and detected at axon initial segment (Ogawa et al., 2008) and it is also released as a soluble form (Karagogeos et al., 1991). Strikingly, we observed that Caspr2-Fc binds the somato-dendritic compartment of wild-type but not of TAG-1-deficient hippocampal neurons. We showed

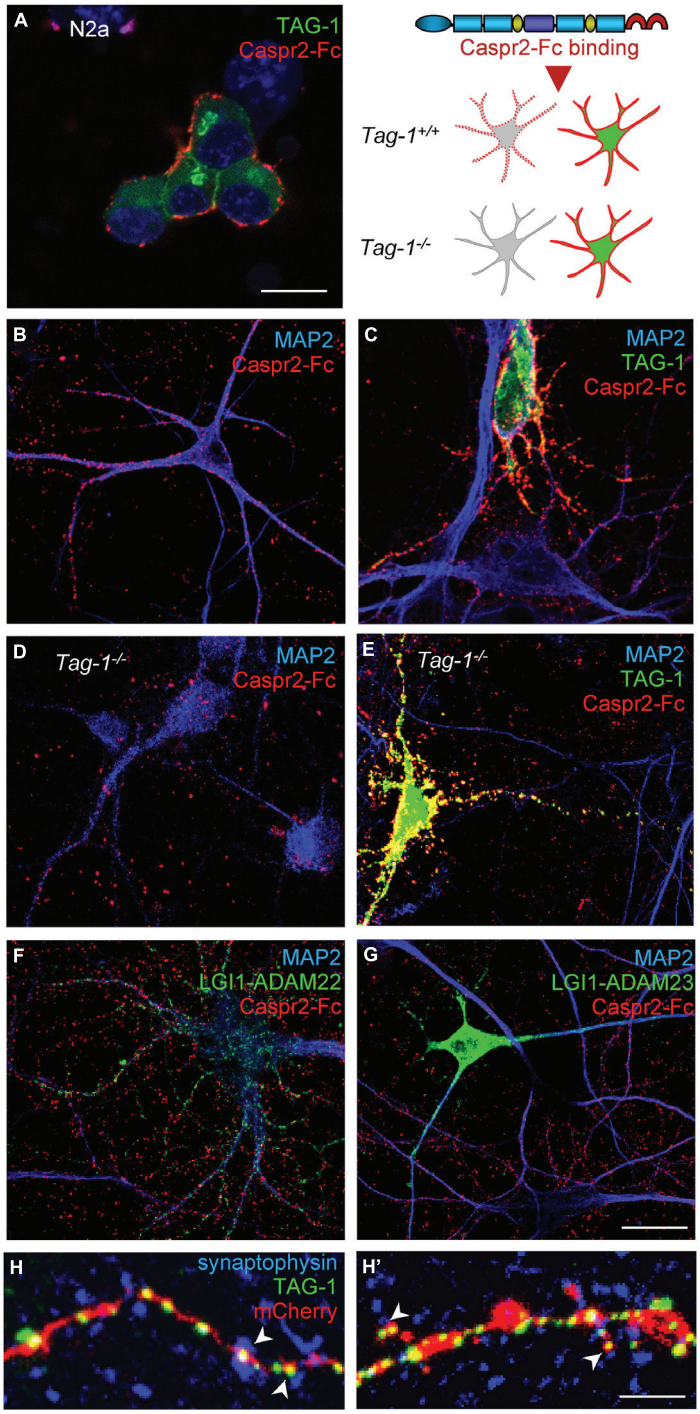

FIGURE 8 | TAG-1 is required for Caspr2-Fc binding on hippocampal neurons. (A) N2a neuroblastoma cells were transfected with TAG-1-GFP (green) and incubated with preclustered Caspr2-Fc (red). Caspr2-Fc only bound on TAG-1-GFP expressing N2a cells. **(B–G)** DIV8 hippocampal neurons were incubated with pre-clustered Caspr2-Fc (red) and cells were fixed and permeabilized before immunostaining for MAP2 (blue). Wild-type neurons were untransfected **(B)** or transfected with TAG-1-GFP **(C)**, or double-transfected with LGI1-GFP and ADAM22 **(F)** or LGI1-GFP and ADAM23 **(G)**. Caspr2-Fc strongly bound the TAG-1-GFP-expressing neuron (green) by comparison with untransfected neurons **(C)**. Transfection of LGI-GFP and ADAM22 or ADAM23 had no effect. **(D,E)** DIV8 hippocampal neurons from *Tag-1*$^{-/-}$ mice were untransfected **(D)** or transfected with TAG-1-GFP **(E)**. Caspr2-Fc strongly bound the TAG-1-GFP-expressing neuron (green) and did not bind untransfected *Tag1*$^{-/-}$ neurons. **(H,H')** DIV14 hippocampal neurons were co-transfected with TAG-1-GFP and mCherry. At DIV17, neurons were surface labeled with anti-GFP antibodies, fixed, and permeabilized before immunostaining for Synaptophysin (blue). Note that TAG-1-GFP clusters indicated with arrowheads on the shaft **(H)** or spines **(H')** were facing Synaptophysin presynaptic sites. **(A–G)** Single confocal sections. **(H,H')** z-stacks of four confocal sections with *z*-step of 0.5 μm Bars: 10 μm, in **(A–G)**, 4 μm in **(H,H')**.

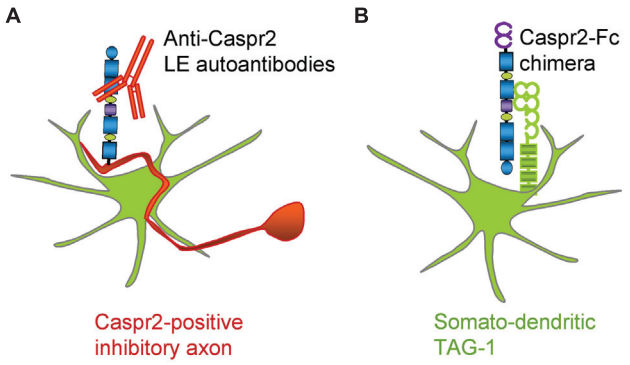

FIGURE 9 | Schematic representation of Caspr2 and Caspr2-Fc complementary distribution in hippocampal neurons. (A) Anti-Caspr2 autoantibodies target preferentially the axons of inhibitory neurons. **(B)** TAG-1 is required as a post-synaptic receptor of Caspr2.

that Caspr2-Fc binding was strongly increased on TAG-1-transfected neurons. LGI1 was also considered as a possible post-synaptic receptor for Caspr2 as it is recruited within the VGKC complex where it interacts with ADAM22 and ADAM23 (Ogawa et al., 2008) and LGI1 is also involved in some autoimmune encephalitis (Lai et al., 2010). However, we did not detect any trans-interaction of Caspr2-Fc with any of these components. We showed that both Caspr2-Fc binding sites and transfected TAG-1-GFP were localized at post-synaptic sites on dendritic shafts and spines facing synaptophysin-positive clusters. Thus, taken together these data suggest that TAG-1 may be critically involved as a post-synaptic partner of Caspr2. We observed that half of excitatory post-synapses on spines were labeled with Caspr2-Fc chimera, whereas Caspr2 was mainly expressed by inhibitory neurons. Indeed, TAG-1 has been reported to interact with several members of the L1 family (Felsenfeld et al., 1994; Pavlou et al., 2002) and may interplay with other partners at the excitatory synapse.

Caspr2 and LGI1 may be Differentially Implicated in LE Autoimmunity

Both LGI1 and Caspr2 are targeted in some patients with autoimmune LE (Irani et al., 2010; Lai et al., 2010). LGI1 is also implicated in inherited forms of epilepsy (Morante-Redolat et al., 2002). Like Caspr2, LGI1 is an element of the VGKC-complex and may induce alteration of axonal excitability. LGI1 colocalizes at axonal terminals with Kv1.1 and Kv1.4 and is strongly expressed on mossy fibers in the hippocampus (Schulte et al., 2006). Interestingly, anti-LGI1 autoantibodies of patients with LE have been reported to induce epileptiform activity by increasing the release probability on mossy fibers-CA3 pyramidal cell synapses, an effect that is mimicked by antagonists of Kv1 channels (Lalic et al., 2010). Other works demonstrated that LGI1 associated with ADAM22 is also implicated in regulating synaptic transmission (Fukata et al., 2006) and that anti-LGI1 autoantibodies of patients with LE are able to neutralize LGI1-ADAM22 interaction and to reduce synaptic clusters of AMPA receptors in cultured hippocampal neurons (Ohkawa et al., 2013). Since LGI1 is expressed by inhibitory interneurons as well as excitatory neurons in hippocampus, epileptic activity may be induced by function blocking of LGI1 on interneurons. However, the selective deletion of *Lgi1* in GABAergic parvalbumin neurons does not induce spontaneous seizures or increased seizure susceptibility. In contrast, depletion of LGI1 in pyramidal neurons is sufficient to generate seizures suggesting that LGI1 plays a pathological role in specific neurons (Boillot et al., 2014). Thus, it may be important to identify the subtypes of neurons expressing Caspr2 to decipher the role of this CAM in LE.

In the present study, we showed that Caspr2 is strongly expressed by inhibitory neurons in hippocampal cell culture including at their presynaptic terminals. Gephyrin is a main constituent of the inhibitory post-synaptic densities that anchors $GABA_A$ receptors. The dynamic exchange between pools of extrasynaptic and synaptic Gephyrin is implicated $GABA_AR$ stabilization and synaptic strength (Petrini et al., 2014) and the clustering of Gephyrin can be affected during inhibitory synapse remodeling through CaMKII-dependent phosphorylation (Flores et al., 2015). Our functional assays using Gephyrin-GFP transfected hippocampal neurons indicated that short-term incubation with anti-Caspr2 LE IgGs induced a significant decrease in the density of synaptic Gephyrin clusters. However, the ratio of synaptic versus total Gephyrin-GFP clusters was not modified. We hypothesize that autoantibodies to Caspr2 may induce alterations of inhibitory synaptic contact and Gephyrin clustering at the post-synapse. Because of the dynamic exchange between the pools of synaptic and total Gephyrin, the clustering of total Gephyrin may be also perturbed. Thus our data suggest that Caspr2 autoantibodies from LE patients might induce structural alteration of the inhibitory post-synaptic scaffold by neutralizing Caspr2 function.

Selectivity of Anti-Caspr2 Autoantibodies in the CSF and Serum of LE Patients

Autoantibodies have been reported to target selective modules of CAMs in peripheral neuropathies. For example, CIDP autoantibodies to Contactin are directed against functional modules implicated in its interaction with its glial partner Neurofascin155 and may thereby induce alteration of the paranodal complex (Ng et al., 2012; Labasque et al., 2014). Strikingly, in the present study, we showed that immunoreactivity of anti-Caspr2 CSF IgGs was restricted to the N-terminal discoïdin and LamininG1 domains in four out of seven LE patients suggesting that these two domains may play a major role in the physiopathology. The specific function of these N-terminal modules is still unknown, but they contain point mutations or deletions described in psychiatric, autism spectrum and language disorders associated with the Caspr2 gene, *cntnap2* (Zweier et al., 2009; O'Roak et al., 2011; Al-Murrani et al., 2012). We may hypothesize that these domains of Caspr2 could be implicated in its synaptic function. Indeed, we showed that the LE6 IgGs that selectively target the N-terminal modules display perturbing activity of the synaptic Gephyrin clusters. We may also notice that the anti-Caspr2 serum IgGs

of LE patients bound the juxtaparanodes of mouse sciatic nerves whereas these patients did not present neuromyotonia. This may be either due to the restricted accessibility of juxtaparanodes or to the selectivity of the targeted N-terminal epitopes.

Conclusion

This study highlights the role of inhibitory neurons as the main target for anti-Caspr2 autoantibodies and the potential role of the N-terminal discoïdin and LamininG1 domains. In patients with LE, anti-Caspr2 autoantibodies may alter Gephyrin clusters at inhibitory synaptic contacts possibly by disruption of Caspr2/TAG-1 interactions. All these data provide a clue to understand the central hyperexcitability observed in patients with autoimmune LE.

Acknowledgments

We wish to thank Dominique Debanne for helpful discussions, Laurence Goutebroze, Fabrice Ango for reagents and discussions. We wish to thank Marie-Pierre Blanchard of the CRN2M imaging core facility for image analysis. We are indebted to Florence Pelletier and Natalia Popa for flow cytometry. Serum and CSF samples were collected with the help of Neurobiotec Bank and the Hospices Civils de Lyon. This work was supported by the Association pour la Recherche sur la Sclérose en Plaques to CF-S and DK.

Supplementary Material

The Supplementary Material for this article can be found online at: http://journal.frontiersin.org/article/10.3389/fncel.2015.00265

FIGURE S1 | Anti-Caspr2 IgGs of LE patients bind axons of hippocampal neurons in culture. DIV7 hippocampal neurons were surface labeled with IgGs of LE2 **(A,B)**, LE3 **(C,D)**, LE4 **(E,F)**, LE5 **(G,H)** patients (red). Cells were fixed with 4% paraformaldehyde, permeabilized and double-stained for the somato-dendritic marker MAP2 (blue) or axonal tau (green). The LE IgGs did not bind hippocampal neurons when pre-adsorbed using incubation with Caspr2-transfected HEK cells **(B,D,F,H)**. Surface staining for Caspr2 using LE2–LE5 IgGs was restricted to tau-positive axons as indicated with yellow arrowheads in **(A,C,E,G)**. Single optical sections of confocal images. Bar is 7 μm.

FIGURE S2 | Anti-Caspr2 autoantibodies in LE patients label inhibitory axons in hippocampal cell culture. Hippocampal neurons at DIV21 were surface labeled with IgGs of LE2 **(A)**, LE3 **(B)**, LE4 **(C)**, or LE5 **(D)** patients (red). Cells were fixed and permeabilized before double-staining for MAP2 (blue) and GAD65 (green). The overlay images and insets show that inhibitory axons and pre-synaptic terminals were immunostained with all patient's autoantibodies. Single optical sections of confocal images. Bar is 10 μm; in insets, 3 μm.

References

Al-Murrani, A., Ashton, F., Aftimos, S., George, A. M., and Love, D. R. (2012). Amino-Terminal Microdeletion within the CNTNAP2 gene associated with variable expressivity of speech delay. *Case Rep. Genet.* 2012:172408. doi: 10.1155/2012/172408

Anderson, G. R., Galfin, T., Xu, W., Aoto, J., Malenka, R. C., and Sudhof, T. C. (2012). Candidate autism gene screen identifies critical role for cell-adhesion molecule CASPR2 in dendritic arborization and spine development. *Proc. Natl. Acad. Sci. U.S.A.* 109, 18120–18125. doi: 10.1073/pnas.1216398109

Bakkaloglu, B., O'Roak, B. J., Louvi, A., Gupta, A. R., Abelson, J. F., Morgan, T. M., et al. (2008). Molecular cytogenetic analysis and resequencing of contactin associated protein-like 2 in autism spectrum disorders. *Am. J. Hum. Genet.* 82, 165–173. doi: 10.1016/j.ajhg.2007.09.017

Bel, C., Oguievetskaia, K., Pitaval, C., Goutebroze, L., and Faivre-Sarrailh, C. (2009). Axonal targeting of Caspr2 in hippocampal neurons via selective somatodendritic endocytosis. *J. Cell Sci.* 122, 3403–3413. doi: 10.1242/jcs.050526

Boillot, M., Huneau, C., Marsan, E., Lehongre, K., Navarro, V., Ishida, S., et al. (2014). Glutamatergic neuron-targeted loss of LGI1 epilepsy gene results in seizures. *Brain* 137, 2984–2996. doi: 10.1093/brain/awu259

Campanac, E., Gasselin, C., Baude, A., Rama, S., Ankri, N., and Debanne, D. (2013). Enhanced intrinsic excitability in basket cells maintains excitatory-inhibitory balance in hippocampal circuits. *Neuron* 77, 712–722. doi: 10.1016/j.neuron.2012.12.020

Chen, N., Koopmans, F., Gordon, A., Paliukhovich, I., Klaassen, R. V., Van der Schors, R. C., et al. (2015). Interaction proteomics of canonical Caspr2 (CNTNAP2) reveals the presence of two Caspr2 isoorms with overlapping interactomes. *Biochim. Biophys. Acta* 1854, 827–833. doi: 10.1016/j.bbapap.2015.02.008

Cifuentes-Diaz, C., Chareyre, F., Garcia, M., Devaux, J., Carnaud, M., Levasseur, G., et al. (2011). Protein 4.1B contributes to the organization of peripheral myelinated axons. *PLoS ONE* 6:e25043. doi: 10.1371/journal.pone.0025043

Craig, A. M., Banker, G., Chang, W., McGrath, M. E., and Serpinskaya, A. S. (1996). Clustering of gephyrin at GABAergic but not glutamatergic synapses in cultured rat hippocampal neurons. *J. Neurosci.* 16, 3166–3177.

Craig, A. M., and Kang, Y. (2007). Neurexin-neurolingin signaling in synapse development. *Curr. Opin. Neurobiol.* 17, 43–52. doi: 10.1016/j.conb.2007.01.011

Dean, C., Scholl, F. G., Choih, J., DeMaria, S., Berger, J., Isacoff, E., et al. (2003). Neurexin mediates the assembly of presynaptic terminals. *Nat. Neurosci.* 6, 708–716. doi: 10.1038/nn1074

Devaux, J., and Gow, A. (2008). Tight junctions potentiate the insulative properties of small CNS myelinated axons. *J. Cell Biol.* 183, 909–921. doi: 10.1083/jcb.200808034

Duflocq, A., Chareyre, F., Giovannini, M., Couraud, F., and Davenne, M. (2011). Characterization of the axon initial segment (AIS) of motor neurons and identification of a para-AIS and a juxtapara-AIS, organized by protein 4.1B. *BMC Biol.* 9:66. doi: 10.1186/1741-7007-9-66

Felsenfeld, D. P., Hynes, M. A., Skoler, K. M., Furley, A. J., and Jessell, T. M. (1994). TAG-1 can mediate homophilic binding, but neurite outgrowth on TAG-1 requires an L1-like molecule and beta 1 integrins. *Neuron* 12, 675–690. doi: 10.1016/0896-6273(94)90222-4

Flores, C. E., Nikonenko, I., Mendez, P., Fritschy, J. M., Tyagarajan, S. K., and Muller, D. (2015). Activity-dependent inhibitory synapse remodeling through gephyrin phosphorylation. *Proc. Natl. Acad. Sci. U.S.A.* 112, E65–E72. doi: 10.1073/pnas.1411170112

Fukata, Y., Adesnik, H., Iwanaga, T., Bredt, D. S., Nicoll, R. A., and Fukata, M. (2006). Epilepsy-related ligand/receptor complex LGI1 and ADAM22 regulate synaptic transmission. *Science* 313, 1792–1795. doi: 10.1126/science.1129947

Horresh, I., Poliak, S., Grant, S., Bredt, D., Rasband, M. N., and Peles, E. (2008). Multiple molecular interactions determine the clustering of Caspr2 and Kv1 channels in myelinated axons. *J. Neurosci.* 28, 14213–14222. doi: 10.1523/JNEUROSCI.3398-08.2008

Huijbers, M. G., Zhang, W., Klooster, R., Niks, E. H., Friese, M. B., Straasheijm, K. R., et al. (2013). MuSK IgG4 autoantibodies cause myasthenia gravis by

inhibiting binding between MuSK and Lrp4. *Proc. Natl. Acad. Sci. U.S.A.* 110, 20783–20788. doi: 10.1073/pnas.1313944110

Inda, M. C., DeFelipe, J., and Munoz, A. (2006). Voltage-gated ion channels in the axon initial segment of human cortical pyramidal cells and their relationship with chandelier cells. *Proc. Natl. Acad. Sci. U.S.A.* 103, 2920–2925. doi: 10.1073/pnas.0511197103

Irani, S. R., Bien, C. G., and Lang, B. (2010). Autoimmune epilepsies. *Curr. Opin. Neurol.* 24, 146–153. doi: 10.1097/WCO.0b013e3283446f05

Karagogeos, D., Morton, S. B., Casano, F., Dodd, J., and Jessell, T. M. (1991). Developmental expression of the axonal glycoprotein TAG-1: differential regulation by central and peripheral neurons *in vitro*. *Development* 112, 51–67.

Labasque, M., Devaux, J. J., Leveque, C., and Faivre-Sarrailh, C. (2011). Fibronectintype III-like domains of neurofascin-186 protein mediate gliomedin binding and its clustering at the developing nodes of Ranvier. *J. Biol. Chem.* 286, 42426–42434. doi: 10.1074/jbc.M111.266353

Labasque, M., Hivert, B., Nogales-Gadea, G., Querol, L., Illa, I., and Faivre-Sarrailh, C. (2014). Specific contactin N-glycans are implicated in neurofascin binding and autoimmune targeting in peripheral neuropathies. *J. Biol. Chem.* 289, 7907–7918. doi: 10.1074/jbc.M113.528489

Lai, M., Huijbers, M. G., Lancaster, E., Graus, F., Bataller, L., Balice-Gordon, R., et al. (2010). Investigation of LGI1 as the antigen in limbic encephalitis previously attributed to potassium channels: a case series. *Lancet Neurol.* 9, 776–785. doi: 10.1016/S1474-4422(10)70137-X

Lalic, T., Pettingill, P., Vincent, A., and Capogna, M. (2010). Human limbic encephalitis serum enhances hippocampal mossy fiber-CA3 pyramidal cell synaptic transmission. *Epilepsia* 52, 121–131. doi: 10.1111/j.1528-1167.2010.02756.x

Lancaster, E., Huijbers, M. G., Bar, V., Boronat, A., Wong, A., Martinez-Hernandez, E., et al. (2011). Investigations of caspr2, an autoantigen of encephalitis and neuromyotonia. *Ann. Neurol.* 69, 303–311. doi: 10.1002/ana.22297

Morante-Redolat, J. M., Gorostidi-Pagola, A., Piquer-Sirerol, S., Saenz, A., Poza, J. J., Galan, J., et al. (2002). Mutations in the LGI1/Epitempin gene on 10q24 cause autosomal dominant lateral temporal epilepsy. *Hum. Mol. Genet.* 11, 1119–1128. doi: 10.1093/hmg/11.9.1119

Ng, J. K., Malotka, J., Kawakami, N., Derfuss, T., Khademi, M., Olsson, T., et al. (2012). Neurofascin as a target for autoantibodies in peripheral neuropathies. *Neurology* 79, 2241–2248. doi: 10.1212/WNL.0b013e31827689ad

Ogawa, Y., Horresh, I., Trimmer, J. S., Bredt, D. S., Peles, E., and Rasband, M. N. (2008). Postsynaptic density-93 clusters Kv1 channels at axon initial segments independently of Caspr2. *J. Neurosci.* 28, 5731–5739. doi: 10.1523/JNEUROSCI.4431-07.2008

Ogawa, Y., Oses-Prieto, J., Kim, M. Y., Horresh, I., Peles, E., Burlingame, A. L., et al. (2010). ADAM22, a Kv1 channel-interacting protein, recruits membrane-associated guanylate kinases to juxtaparanodes of myelinated axons. *J. Neurosci.* 30, 1038–1048. doi: 10.1523/JNEUROSCI.4661-09.2010

Ohkawa, T., Fukata, Y., Yamasaki, M., Miyazaki, T., Yokoi, N., Takashima, H., et al. (2013). Autoantibodies to epilepsy-related LGI1 in limbic encephalitis neutralize LGI1-ADAM22 interaction and reduce synaptic AMPA receptors. *J. Neurosci.* 33, 18161–18174. doi: 10.1523/JNEUROSCI.3506-13.2013

O'Roak, B. J., Deriziotis, P., Lee, C., Vives, L., Schwartz, J. J., Girirajan, S., et al. (2011). Exome sequencing in sporadic autism spectrum disorders identifies severe de novo mutations. *Nat. Genet.* 43, 585–589. doi: 10.1038/ng.835

Owuor, K., Harel, N. Y., Englot, D. J., Hisama, F., Blumenfeld, H., and Strittmatter, S. M. (2009). LGI1-associated epilepsy through altered ADAM23-dependent neuronal morphology. *Mol. Cell. Neurosci.* 42, 448–457. doi: 10.1016/j.mcn.2009.09.008

Pavlou, O., Theodorakis, K., Falk, J., Kutsche, M., Schachner, M., Faivre-Sarrailh, C., et al. (2002). Analysis of interactions of the adhesion molecule TAG-1 and its domains with other immunoglobulin superfamily members. *Mol. Cell. Neurosci.* 20, 367–381. doi: 10.1006/mcne.2002.1105

Penagarikano, O., Abrahams, B. S., Herman, E. I., Winden, K. D., Gdalyahu, A., Dong, H., et al. (2011). Absence of CNTNAP2 leads to epilepsy, neuronal migration abnormalities, and core autism-related deficits. *Cell* 147, 235–246. doi: 10.1016/j.cell.2011.08.040

Peñagarikano, O., and Geschwind, D. H. (2012). What does CNTNAP2 reveal about autism spectrum disorder? *Trends Mol. Med.* 18, 156–163. doi: 10.1016/j.molmed.2012.01.003

Petrini, E. M., Ravasenga, T., Hausrat, T. J., Iurilli, G., Olcese, U., Racine, V., et al. (2014). Synaptic recruitment of gephyrin regulates surface GABAA receptor dynamics for the expression of inhibitory LTP. *Nat. Commun.* 4, 39211–39219. doi: 10.1038/ncomms4921

Poliak, S., Salomon, D., Elhanany, H., Sabanay, H., Kiernan, B., Pevny, L., et al. (2003). Juxtaparanodal clustering of Shaker-like K^+ channels in myelinated axons depends on Caspr2 and TAG-1. *J. Cell Biol.* 162, 1149–1160. doi: 10.1083/jcb.200305018

Querol, L., Nogales-Gadea, G., Rojas-Garcia, R., Diaz-Manera, J., Pardo, J., Ortega-Moreno, A., et al. (2014). Neurofascin IgG4 antibodies in CIDP associate with disabling tremor and poor response to IVIg. *Neurology* 82, 879–886. doi: 10.1212/WNL.0000000000000205

Rasband, M. N. (1998). Clustered K^+ channel complexes in axons. *Neurosci. Lett.* 486, 101–106. doi: 10.1016/j.neulet.2010.08.081

Rodenas-Cuadrado, P., Ho, J., and Vernes, S. C. (2013). Shining a light on CNTNAP2: complex functions to complex disorders. *Eur. J. Hum. Genet.* 22, 171–178. doi: 10.1038/ejhg.2013.100

Sanchez-Ponce, D., DeFelipe, J., Garrido, J. J., and Munoz, A. (2012). Developmental expression of Kv potassium channels at the axon initial segment of cultured hippocampal neurons. *PLoS ONE* 7:e48557. doi: 10.1371/journal.pone.0048557

Savvaki, M., Theodorakis, K., Zoupi, L., Stamatakis, A., Tivodar, S., Kyriacou, K., et al. (2010). The expression of TAG-1 in glial cells is sufficient for the formation of the juxtaparanodal complex and the phenotypic rescue of tag-1 homozygous mutants in the CNS. *J. Neurosci.* 30, 13943–13954. doi: 10.1523/JNEUROSCI.2574-10.2010

Schulte, U., Thumfart, J. O., Klocker, N., Sailer, C. A., Bildl, W., Biniossek, M., et al. (2006). The epilepsy-linked Lgi1 protein assembles into presynaptic Kv1 channels and inhibits inactivation by Kvbeta1. *Neuron* 49, 697–706. doi: 10.1016/j.neuron.2006.01.033

Strauss, K. A., Puffenberger, E. G., Huentelman, M. J., Gottlieb, S., Dobrin, S. E., Parod, J. M., et al. (2006). Recessive symptomatic focal epilepsy and mutant contactin-associated protein-like 2. *N. Engl. J. Med.* 354, 1370–1377. doi: 10.1056/NEJMoa052773

Traka, M., Goutebroze, L., Denisenko, N., Bessa, M., Nifli, A., Havaki, S., et al. (2003). Association of TAG-1 with Caspr2 is essential for the molecular organization of juxtaparanodal regions of myelinated fibers. *J. Cell Biol.* 162, 1161–1172. doi: 10.1083/jcb.200305078

Viaccoz, A., Desestret, V., Ducray, F., Picard, G., Cavillon, G., Rogemond, V., et al. (2014). Clinical specificities of adult male patients with NMDA receptor antibodies encephalitis. *Neurology* 82, 556–563. doi: 10.1212/WNL.0000000000000126

Vincent, A., Buckley, C., Schott, J. M., Baker, I., Dewar, B. K., Detert, N., et al. (2004). Potassium channel antibody-associated encephalopathy: a potentially immunotherapy-responsive form of limbic encephalitis. *Brain* 127, 701–712. doi: 10.1093/brain/awh077

Zweier, C., de Jong, E. K., Zweier, M., Orrico, A., Ousager, L. B., Collins, A. L., et al. (2009). CNTNAP2 and NRXN1 are mutated in autosomal-recessive Pitt-Hopkins-like mental retardation and determine the level of a common synaptic protein in *Drosophila*. *Am. J. Hum. Genet.* 85, 655–666. doi: 10.1016/j.ajhg.2009.10.004

Conflict of Interest Statement: The authors declare that the research was conducted in the absence of any commercial or financial relationships that could be construed as a potential conflict of interest.